

**Characterization of the  
regulation of DNA joint molecule resolution  
during cell cycle and in response to replication fork stalling**

**Kumulative Dissertation**

**zur Erlangung des Doktorgrades**

der Fakultät für Biologie  
Ludwig-Maximilians-Universität München



vorgelegt von

**Lissa Princz**

aus Weißenburg i. Bay.

München 2017

### **Eidesstattliche Erklärung**

Hiermit erkläre ich an Eides statt, dass ich die vorliegende Dissertation selbstständig und ohne unerlaubte Hilfe angefertigt habe. Ich habe weder anderweitig versucht, eine Dissertation einzureichen oder eine Doktorprüfung durchzuführen, noch habe ich diese Dissertation oder Teile derselben einer anderen Prüfungskommission vorgelegt.

Lissa Princz

München, den 30.11.2017

Promotionsgesuch eingereicht:

Tag der mündlichen Prüfung:

Erstgutachter:

Zweitgutachter:

02.08.2017

30.11.2017

Prof. Dr. Heinrich Leonhardt

Prof. Dr. Peter Becker

# Table of Contents

Abbreviations .....	III
List of Publications .....	IV
<b>I. Summary .....</b>	<b>1</b>
<b>II. Introduction.....</b>	<b>2</b>
<b>A. Homologous Recombination.....</b>	<b>2</b>
1. Formation of DSBs .....	2
2. Repair decision: NHEJ or HR .....	3
3. Mechanism of recombination.....	3
<b>B. Regulation of Recombination .....</b>	<b>6</b>
1. HR-antagonizing factors.....	6
2. HR-promoting factors and means to regulate HR .....	7
a) Transcriptional regulation of HR.....	7
b) Regulation by localization .....	7
c) Regulation by post-translational modifications.....	8
d) Regulation by histone modifications and nucleosome remodellers .....	10
e) Regulation by the DNA damage checkpoint .....	11
<b>C. Recombination and Replication .....</b>	<b>12</b>
1. Replication-dependent repair.....	12
2. Involvement of recombination in template-switching .....	13
3. Regulation of DNA damage tolerance .....	14
4. The Dpb11-Slx4-Rtt107 complex .....	16
<b>D. Disentanglement of Recombination Intermediates .....</b>	<b>17</b>
1. Dissolution .....	17
2. Resolution .....	18
<b>E. Regulation of Resolution .....</b>	<b>21</b>
1. Regulation by the cell cycle .....	21
2. Regulation by the DNA damage checkpoint .....	22
<b>III. Aims of Study.....</b>	<b>24</b>

<b>IV. Results: Publications .....</b>	<b>25</b>
<b>A. Gritenaite <i>et al.</i>, 2014.....</b>	<b>25</b>
A cell cycle-regulated Slx4-Dpb11 complex promotes the resolution of DNA repair intermediates linked to stalled replication	
<b>B. Princz <i>et al.</i>, 2017 .....</b>	<b>42</b>
Dbf4-dependent kinase and the Rtt107 scaffold promote Mus81-Mms4 resolvase activation during mitosis	
<b>C. Lee <i>et al.</i>, 2015.....</b>	<b>58</b>
The structure of human Holliday junction resolvase GEN1 reveals a chromodomain for efficient DNA recognition and cleavage	
<b>V. Discussion .....</b>	<b>83</b>
<b>A. Regulation of Mus81-Mms4 resolvase activation in mitosis .....</b>	<b>83</b>
1. Mus81 activity is regulated by cell cycle phase-dependent kinases .....	84
2. The Dpb11-Slx4-Rtt107 complex promotes resolution by Mus81-Mms4 .....	86
3. Kinases and scaffolds form a multi-protein complex with Mus81-Mms4 .....	89
4. Evolutionary conserved features of JM resolution by Mus81-Mms4.....	90
<b>B. The Dpb11-Slx4-Rtt107 complex after replication fork stalling.....</b>	<b>92</b>
1. Complex formation is regulated by CDK and checkpoint kinases .....	92
2. Dpb11-Slx4-Rtt107 dampen DNA damage checkpoint signalling.....	93
3. Multiple functions of Dpb11-Slx4-Rtt107 after replication stress in S-phase ....	94
<b>C. Dpb11 as a regulator of the DNA damage response.....</b>	<b>95</b>
1. BRCT domains bind phosphorylated proteins .....	95
2. Dpb11 complexes regulate multiple cellular pathways.....	96
<b>VI. References .....</b>	<b>97</b>
<b>VII. Acknowledgements .....</b>	<b>108</b>

#### Appendix: Publications including Supplementary Information

<b>A. Gritenaite <i>et al.</i>, 2014.....</b>	<b>Appendix page 1</b>
<b>B. Princz <i>et al.</i>, 2017 .....</b>	<b>Appendix page 62</b>
<b>C. Lee <i>et al.</i>, 2015.....</b>	<b>Appendix page 109</b>
<b>D. Princz <i>et al.</i>, 2015 (Review).....</b>	<b>Appendix page 148</b>

## Abbreviations

BIR	break-induced replication
BRCT	BRCA1 C-terminal
BTR	BLM-TopoIIIa-RMI1-RMI2
C-terminal	carboxy-terminal
CDK	cyclin-dependent kinase
ChIP	chromatin immuno-precipitation
CO	crossover
CPT	camptothecin
DDK	Dbf4-dependent kinase
DDT	DNA damage tolerance
DNA	deoxyribonucleic acid
DSB	double-strand break
F	phenylalanine
G1-phase	gap 1 phase of the cell cycle
G2-phase	gap 2 phase of the cell cycle
(d)HJ	(double) Holliday junction
HR	homologous recombination
HU	hydroxyurea
JM	joint molecule
LOH	loss of heterozygosity
M-phase	mitosis phase of the cell cycle
MMS	methyl methanesulphonate
MRX	Mre11-Rad50-Xrs2
N-terminal	amino-terminal
NCO	non-crossover
NES	nuclear export signal
NHEJ	non-homologous end joining
nHJ	nicked Holliday junction
NLS	nuclear localization signal/sequence
NPC	nuclear pore complex
PLK	Polo-like kinase
pS	phosphorylated serine
PTM	post-translational modifications
RNA	ribonucleic acid
S	serine
S-phase	synthesis phase of the cell cycle
<i>S. cerevisiae / pombe</i>	<i>Saccharomyces cerevisiae / pombe</i>
SDSA	synthesis-dependent strand annealing
SIM	SUMO-interacting motif
SSA	single-strand annealing
ssDNA / dsDNA	single-stranded / double-stranded DNA
STR	Sgs1-Top3-Rmi1
STUbL	SUMO-targeted ubiquitin ligase
T	threonine
TLS	translesion synthesis
X	any amino acid

## List of Publications

The current cumulative dissertation was conducted under the supervision of Dr. Boris Pfander at the Max Planck Institute of Biochemistry in Martinsried, Germany.

Essential parts of this work have been published in following publications.

Gritenaite D\*, **Princz LN\***, Szakal B, Bantele SCS, Wendeler L, Schilbach S, Habermann BH, Matos J, Lisby M, Branzei D, Pfander B (2014) A cell cycle-regulated Slx4-Dpb11 complex promotes the resolution of DNA repair intermediates linked to stalled replication. *Genes Dev* 28:1604-1619

**Princz LN\***, Gritenaite D\*, Pfander B (2015) The Slx4-Dpb11 scaffold complex: coordinating the response to replication fork stalling in S-phase and the subsequent mitosis. *Cell Cycle* 14(4):488-494

Lee S-H, **Princz LN**, Klügel MF, Habermann B, Pfander B, Biertümpfel C (2015) Human Holliday junction resolvase GEN1 uses a chromodomain for efficient DNA recognition and cleavage. *eLife* 4:e12256

**Princz LN**, Wild P, Bittmann J, Aguado FJ, Blanco MG, Matos J, Pfander B (2017) Dbf4-dependent kinase and the Rtt107 scaffold promote Mus81-Mms4 resolvase activation during mitosis. *EMBO J* 36(5):664-678

\* equal contribution

# I. Summary

The DNA is the central cellular information carrier, but its stability is constantly challenged by DNA-damaging incidents. As DNA lesions may elicit genomic instability – in mammalian cells the cause of cancer – DNA repair processes are indispensable for cellular integrity. DNA lesions during S-phase are a particular detriment as they interfere with replication fork progression and faithful chromosome duplication. Fork stalling at DNA damage sites is a common perturbation during replication, but may be bypassed by recombination-based mechanisms. These pathways involve the undamaged sister chromatid as a recombination template and as such formation of intermediate DNA structures, so-called DNA joint molecules (JMs) between both chromatids. Such covalent DNA linkages need to be disentangled before chromatid separation in anaphase to avoid chromosome breakage. Two principle mechanisms have been described to disentangle DNA JMs: dissolution, comprising collaborative helicase-topoisomerase activity, and resolution, comprising cleavage by endonucleases such as Mus81-Mms4 or Yen1. Previous research has revealed that JM resolvase activity by Mus81-Mms4 is under stringent cell cycle control, and up-regulated specifically in mitosis upon CDK- and Cdc5-dependent phosphorylation. Yet, we are only beginning to unravel the molecular mechanism of this temporal regulation.

In this study, we identify distinct means how cell cycle signals can be integrated into the activity of the JM resolvase Mus81-Mms4 using *Saccharomyces cerevisiae* as a model organism. First, we discovered a third cell cycle kinase, which is crucial for Mus81 nuclease activation in mitosis: Cdc7-Dbf4 (DDK, Dbf4-dependent kinase) targets Mus81-Mms4 together with Cdc5. Both kinases bind and phosphorylate Mus81-Mms4 inter-dependently in order to promote full Mus81 activation. A second layer of the temporal control of Mus81 is mediated by scaffold proteins. Cell cycle-dependent phosphorylation induces the formation of a multi-protein complex comprising the scaffold proteins Dpb11, Slx4, and Rtt107. Already in S-phase during the response to replication fork stalling, those proteins interact with each other upon evolutionary conserved CDK phosphorylation of Slx4 that mediates binding to Dpb11. This S-phase complex has been implicated in the regulation of the DNA damage checkpoint after replication fork stalling and may have a potential DNA repair function. In M-phase, the scaffold complex associates with Mus81-Mms4 dependent on cell cycle kinase activity. We could show that the scaffold protein Rtt107 recruits the DDK-Cdc5 kinase complex to Mus81-Mms4 via a direct interaction between Rtt107 and Cdc7, enabling Mus81-Mms4 hyper-phosphorylation and Mus81 activation. Future research will need to identify additional regulation factors that may influence substrate specificity or targeting.

Taken together, my PhD work described several regulatory mechanisms of mitotic DNA JM resolution by Mus81-Mms4 that involve the cell cycle kinases CDK, Cdc5 and DDK as well as the scaffold proteins Dpb11, Slx4, and Rtt107. These control mechanisms are highly inter-connected as association of the scaffold proteins depends on cell cycle kinase activity, but in turn stable multi-protein complex formation is required for efficient interaction with the DDK-Cdc5 kinases, full phosphorylation of Mus81-Mms4 and timely JM resolution.

## II. Introduction

### A. Homologous Recombination

DNA repair mechanisms are indispensable to all organisms as DNA damage constantly challenges the integrity of a cell's genome (Lindahl and Barnes, 2000; Hoeijmakers, 2009). DNA is the essential molecule to code genetic information. However, it is limited in its stability and prone to damage and degradation. Resulting lesions may interfere with DNA-related processes like replication and transcription evoking genomic instability (reviewed in Aguilera, 2002; Gottipati and Helleday, 2009; Lin and Pasero, 2012). Several intricate pathways to repair DNA damage have evolved, three of which were honoured with awarding the Nobel Prize in Chemistry in 2015 (T. Lindahl for base-excision repair, A. Sanchar for nucleotide-excision repair, and P. Modrich for mismatch-repair).

#### 1. Formation of DSBs

A DNA double-strand break (DSB) is a very severe threat to cell viability as it can lead to deletions, translocations or loss of whole chromosome arms. DSBs can arise from exogenous factors like  $\gamma$ -irradiation (van Gent *et al.*, 2001) or chemicals (e.g., the topoisomerase inhibitor camptothecin, CPT) (Nitiss and Wang, 1988; Kaiser *et al.*, 2011), but may also happen endogenously as a consequence of replication perturbations or even purposely as part of normal cell physiology. Such deliberate breakage of chromosomes occurs in processes like meiotic recombination (reviewed in de Massy, 2013), mating type switching in yeast (reviewed in Haber, 2012), or V(D)J recombination (reviewed in Soulas-Sprauel *et al.*, 2007).

Most endogenous DSBs occur in the context of DNA replication, for instance as a response to replication fork stalling, likely by nucleolytic processing of replication intermediates (Schwartz and Heyer, 2011; Rass, 2013; Syeda *et al.*, 2014). Such fork slow-down or pausing may take place at sites of DNA lesions or arise upon collision of the replisome with DNA-binding proteins or with the transcription machinery loaded onto DNA (Dutta *et al.*, 2011; Merrikh *et al.*, 2011; Wahba *et al.*, 2011; Duch *et al.*, 2013; Yan *et al.*, 2016; reviewed in Lin and Pasero, 2012; Brambati *et al.*, 2015). Extrinsically, replication fork stalling can be evoked genome-wide by inhibition of ribonucleotide reductase with hydroxyurea (HU) (Reichard, 1988; Galli and Schiestl, 1996; Lopes *et al.*, 2001), by DNA-alkylating agents such as methyl methanesulfonate (MMS) (Groth *et al.*, 2010), or site-specifically by introduction of replication fork-blocking sequences (Horiuchi and Fujimura, 1995).

Additionally, very common sources of DSBs are DNA nicks (Cowan *et al.*, 1987). They might arise from oxidative stress or ionizing radiation, but are also intermediates of nicking endonuclease activity during regulation of super-helicity by topoisomerases or during DNA repair reactions (e.g., nucleotide-excision repair, base-excision repair, or mismatch repair) (Bradley and Kohn, 1979; Pogozelski and Tullius, 1998; Demple and DeMott, 2002; Wang, 2002; Pommier *et al.*, 2003; reviewed in Caldecott, 2008). If left unrepaired, DNA replication can convert those nicks to ssDNA gaps or DSBs (Milligan *et al.*, 1995). Independent of the source of a DSB – if exogenously introduced or endogenously occurred – its repair is indispensable for genome integrity.

## 2. Repair decision: NHEJ or HR

After the occurrence of DNA damage, the decision for an appropriate repair pathway has to be reached. In the case of DSBs, direct ligation of the DNA ends by DNA ligases with little or no end processing is one potential repair pathway called non-homologous end-joining (NHEJ). As it may introduce deletions by rejoining two DSB ends, NHEJ is considered a low-fidelity repair pathway. In contrast, the most accurate pathway to repair DSBs is by exchange of genetic information between homologous DNA molecules (homologous recombination, HR). This homology-dependent transfer of genetic information is not only crucial for DNA repair and thereby for genome maintenance, but also assures faithful replication, chromosome segregation, and programmed cell developmental events.

The preferred repair template is the sister chromatid. Therefore, homologous recombination is restricted to S-, G2-, and M-phases of the cell cycle when an unbroken sister chromatid is available that can be used as repair template. In G1-phase, i.e. in the absence of a sister chromatid, NHEJ is the preferred pathway for DSB repair to avoid error-prone recombination from homologous sequences at non-allelic positions (Karathanasis and Wilson, 2002).

HR is also regulated by ploidy. In diploid budding yeast, NHEJ is down-regulated due to repression of its key factor Nej1 (Frank-Vaillant and Marcand, 2001; Kegel *et al.*, 2001; Valencia *et al.*, 2001), which makes HR the predominant DSB repair pathway. However, HR events in diploid cells come at the cost of loss of heterozygosity (LOH) if they take place with the homologous chromosome. Lastly, in meiotic cell cycles, recombination occurs in a programmed, highly regulated manner, and is essential for accurate chromosome segregation. During this process down-regulation of NHEJ is essential to avoid *de novo* mutations.

Besides cell cycle stage and ploidy, also the chromatin environment of the DNA lesion is integrated into the repair pathway choice since histones, DNA modifications as well as the accessibility of the lesion can have an impact on the repair pathway and the proteins involved.

## 3. Mechanism of recombination

In 1964, Robin Holliday proposed a model to elucidate DNA strand exchange mechanisms of meiotic gene conversion events and chromosome crossovers (Holliday, 1964; 1965; 1966). Together with subsequent models of branch migration (e.g., Broker and Lehman, 1971; Meselson and Radding, 1975; Orr-Weaver, Szostak and Rothstein, 1981; Szostak *et al.*, 1983), this work had a profound impact on our understanding of the mechanism of recombination. Apart from some variations and sub-pathways, canonical HR coincides in five essential steps (Figure 1, middle box):

- 1) **Recognition of the damage**
- 2) **DNA end resection**
- 3) **Homologous pairing and strand invasion**
- 4) **DNA synthesis**
- 5) **Disentanglement of recombination intermediates**

With the mechanism of HR being highly conserved among eukaryotes, in the following, I will mainly refer to proteins and nomenclature from *S. cerevisiae* as it was the model system of this study.

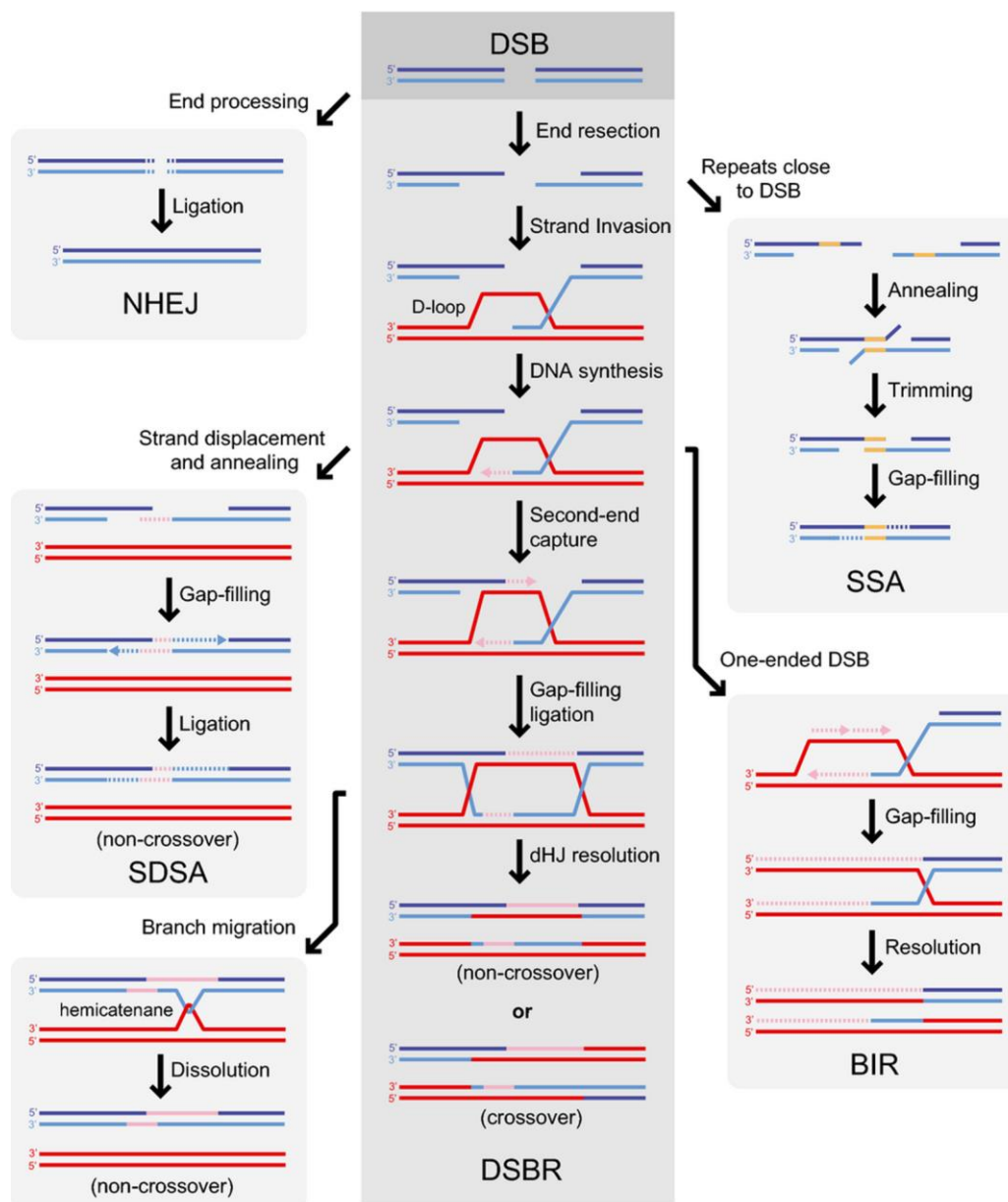


**Figure 1. Schematic mechanisms of DNA DSB repair and pathways of homologous recombination.** Occurring DNA DSBs can be repaired by NHEJ – i.e. simple ligation of the DNA ends – or by HR, which comprises DNA end processing by resection. In case the DSBs are flanked by direct repeat sequences, they can be repaired by SSA involving deletion of the sequence in-between. During the canonical HR pathway (middle box) one free ssDNA strand invades a homologous duplex DNA sequence (D-loop formation). The exposed 3' hydroxyl group primes for DNA synthesis to restore the genetic information. After second-end capture, the resulting dHJ needs to be disentangled by either dissolution or resolution. Alternative HR pathways are SDSA, which involves incipient DNA synthesis and gap filling, and BIR for one-ended DSBs (adapted from Mathiasen and Lisby, 2014).

During the first step of HR, the **recognition of the damage**, the broken DNA ends are sensed. In the case of a DSB, the DNA ends are bound by the Ku complex (Yku70-Yku80) and the MRX complex (Mre11-Rad50-Xrs2) (Ivanov *et al.*, 1994; Clerici *et al.*, 2008; Wu *et al.*, 2008). In G1-phase Ku-mediated end protection promotes NHEJ and simultaneously suppresses HR (Barlow *et al.*, 2008;

Zierhut and Diffley, 2008; Mimitou and Symington, 2010). The MRX complex is able to bridge two DNA ends by the zinc-hook of its subunit Rad50 (de Jager *et al.*, 2001; Hopfner *et al.*, 2002; Lobachev *et al.*, 2004; Wiltzius *et al.*, 2005; Hohl *et al.*, 2011). In cell cycle phases with high CDK activity, Ku binding is inhibited and Mre11 endonuclease activity is stimulated. Subsequently, both DNA ends are processed by **DNA end resection**. Resection is initiated by endonucleolytic cleavage by Mre11 in the proximity of the break and subsequent exonucleolytic cleavage in 3'-5' direction (towards the break) to reveal 3' ssDNA ends (Garcia *et al.*, 2011). This is followed by long-range resection (extension of the short 3' overhangs) in 5'-3' direction catalysed by Exo1 or the Sgs1-Top3-Rmi1/Dna2 complex (Mimitou and Symington, 2008; Zhu *et al.*, 2008; Shim *et al.*, 2010). The resulting 3' ssDNA tails are bound by ssDNA-binding protein RPA, which is subsequently replaced by Rad51 to form Rad51 nucleofilaments, the crucial intermediate of HR (Klapstein *et al.*, 2004; Chen *et al.*, 2008). This filament probes the genome for homologous DNA sequences (homology search) (Alani *et al.*, 1992; Shinohara *et al.*, 1992; Sugiyama *et al.*, 1997). One free Rad51-coated ssDNA end **invades** a homologous duplex DNA sequence forming a displacement loop (D-loop). Upon **strand annealing**, Rad51 mediates the exposure of a 3' hydroxyl group in order to prime for **DNA synthesis** templated by the donor DNA. *In vitro*, Rad51 alone is able to mediate strand exchange (Sung, 1994). However, efficient reaction *in vivo* – including Rad51 loading, filament stabilization, and strand exchange itself – involves mediator proteins such as Rad52, Rad54, Rad55 and Rad57 (Sung, 1997a; 1997b; New *et al.*, 1998; Sugawara *et al.*, 2003; Sung *et al.*, 2003).

In the classical DSB repair model by Jack Szostak the second 3' end anneals to the donor DNA to prime for another DNA synthesis round in similar fashion (second end capture) (Szostak *et al.*, 1983). The newly synthesized strands are ligated to the adjacent 5' ends, resulting in a DNA joint molecule (JM), a double Holliday junction (dHJ). Recombinational repair is finished with the **disentanglement of repair intermediates** to segregate those covalent DNA linkages. Disentanglement can occur either by combined helicase-topoisomerase activity (dissolution), or by endonucleolytic cleavage (resolution) (in detail in chapter D) (Kaliraman *et al.*, 2001; Wu and Hickson, 2003; Ip *et al.*, 2008; Cejka *et al.*, 2010a; 2010b).

Beside the canonical pathway via a dHJ, several sub-pathways of HR have been described (Figure 1): synthesis-dependent strand annealing (SDSA), break-induced replication (BIR), or single-strand annealing (SSA).

In the SDSA model, the 3' ssDNA ends invade the homologous donor DNA, but are then displaced after incipient DNA synthesis (Nassif *et al.*, 1994). Subsequent gap filling and ligation reactions complete the repair.

For one-ended DSBs, repair is mediated via BIR by formation of a migrating D-loop and initiation of replication, which can continue until the chromosome end (Kraus *et al.*, 2001; Llorente *et al.*, 2008). As this reaction is highly error-prone and leads to extensive LOH, BIR is apparently suppressed when both ends of the DSB are present (Malkova *et al.*, 1996, 2005; Bosco and Haber, 1998).

Moreover, in case DSBs are flanked by direct repeats, they can be repaired by SSA. Here, DNA end resection exposes the complementary ssDNA sequences of the repeats, which subsequently anneal and form heterologous flaps. Nucleolytic cleavage removes the flaps, and gap filling and ligation complete the repair (Fishman-Lobell *et al.*, 1992; Ivanov and Haber, 1995). SSA is counted among the HR pathways, even though it does not include a strand invasion event.

## B. Regulation of Recombination

The tight regulation of homologous recombination is of tremendous importance for genome integrity and cell viability. First, coordination of all DNA-associated processes, including replication, transcription and chromosome segregation, is crucial to avoid interference and maintain genomic stability (reviewed for example in Aguilera, 2002; Gottipatti and Helleday, 2009; Lin and Pasero, 2012). Second, regulation of concentration, association and activity of HR proteins defines the choice of the repair pathway as well as the fidelity of the repair itself. Overall, HR regulation is complex and involves the interplay between antagonizing and promoting factors that will be addressed in the following.

### 1. HR-antagonizing factors

As mentioned earlier, HR is restricted to S-, G<sub>2</sub>-, and M-phases of the cell cycle. In G<sub>1</sub>-phase HR is inhibited, and DSBs will be repaired predominantly by NHEJ (Karathanasis and Wilson, 2002). In this case, DNA end binding by the Ku complex is the rate-limiting step as it represents a barrier for DNA end resection factors, and thereby blocks HR initiation (Clerici *et al.*, 2008; Wasko *et al.*, 2009; Mimitou and Symington, 2010; Shim *et al.*, 2010). Accordingly, a *YKU80* deletion causes an increased HR/NHEJ ratio (Palmbos *et al.*, 2005). Prevention of recombinogenic events in G<sub>1</sub>-phase is central to impede repair from homologous sequences at non-allelic positions, which is error-prone and can lead to deletions and other mutagenic repair events (Karathanasis and Wilson, 2002).

A second major type of HR-counteracting factors are DNA-dependent translocases/helicases that disrupt HR intermediates, such as the anti-recombinase Srs2. Srs2 is a direct antagonist of the strand exchange protein Rad51 and recruited to resected DNA ends by the NHEJ factor Nej1 (Carter *et al.*, 2009). By disrupting the Rad51 nucleoprotein filament, Srs2 is able to block recombination initiation. Srs2 also binds to the replication factor PCNA (proliferating cell nuclear antigen; encoded by *POL30* in budding yeast), and was suggested to be crucial for inhibition of unwanted recombination in the context of DNA replication and stalled forks (Pfander *et al.*, 2005; Burgess *et al.*, 2009). A second helicase, Sgs1, is able to disrupt Rad51-mediated D-loops in a topoisomerase-dependent fashion in order to counteract HR (Bachrati *et al.*, 2006; Bugreev *et al.*, 2007; Fasching *et al.*, 2015).

Besides those direct means against recombination, also rather indirect cellular characteristics, such as the availability of a sister chromatid, play a role. In mammals for example, recombination is impaired not only in G<sub>1</sub>-phase, but also at a late stage of mitotic cell cycle when chromosomes are highly condensed. Concomitantly, Rad51 loading was shown to be blocked specifically in mammalian M-phase (Ayoub *et al.*, 2009; Peterson *et al.*, 2011).

## 2. HR-promoting factors and means to regulate HR

HR can be promoted by two principle mechanisms: first, by directly stimulating recombination proteins – which is regulated by the level of transcription, by their recruitment to damage sites, or by post-translational activation, and second by mediating access to the DNA substrate – which is regulated by the cell cycle phase and by chromatin structure. The following chapter summarizes the different mechanisms, by which HR can be regulated.

### a) Transcriptional regulation of HR

In bacteria, a rapid response to DNA damage is ensured by transcriptional activation of more than 20 DNA repair genes (“SOS response”) (Radman, 1975). One of those genes encodes the protein RecA, which is the prokaryotic orthologue of Rad51. In contrast, transcriptional regulation of HR in eukaryotic cells is less wide-spread and less distinct.

Both, DNA damage as well as the cell cycle, have an impact on the transcription of some recombination proteins. DNA damage-induced genes are for example *RFA1-3*, *RAD50*, *SRS2*, *RAD54*, *RAD51* as well as the DNA damage checkpoint genes *MEC1* and *RAD53*. The latter two establish a positive feedback loop enhancing their own expression, and Mec1 additionally stimulates the expression of HR genes. However, the overall induction of these genes on transcriptional level is mild (Cole *et al.*, 1987; Elledge and Davis, 1989,1990; Basile *et al.*, 1992; Kiser and Weinert, 1996; Vallen and Cross, 1999; Gasch *et al.*, 2001; Mercier *et al.*, 2001; Benton *et al.*, 2006).

Furthermore, transcriptional regulation contributes to the temporal regulation of NHEJ and HR during the cell cycle. At the G1-S boundary, levels of the NHEJ factor Yku70 decline and several HR genes get transcriptionally activated. In total, genome-wide transcriptional data sets identified 26 HR-linked genes with a cell cycle-regulated expression in budding yeast such as *EXO1*, *SGS1*, *TOP3*, *SAE2*, *RFA1-3*, *RAD51*, *RDH54*, and *SRS2* (Cho *et al.*, 1998; Spellman *et al.*, 1998; de Lichtenberg *et al.*, 2003; Jensen *et al.*, 2006).

### b) Regulation by localization

A more prevalent mode of HR regulation is via specific sub-cellular localization of recombination factors and in particular via an increase in their local concentration at the site of the DNA damage. Relocalization of different proteins occurs with distinct kinetics and can often be microscopically visualized as DNA damage focus. Foci detection has therefore been used to elucidate temporal order and inter-dependencies of recombination proteins during the damage response. After treatment with different DNA-damaging agents, for example, the formation of Rad51 foci can be detected whereupon other recombination proteins such as Rad52, Rad54 and RPA co-localize (Gasior *et al.*, 1998; Lisby *et al.*, 2001; Miyazaki *et al.*, 2004).

Besides the localization of recombination proteins, also the localization of the DNA within the nucleus plays an important role during HR. DNA sequences prone to deleterious recombination – such as centromeres or telomeres harbouring repetitive sequences, but also highly transcribed rDNA and tRNA genes – need to be protected from untimely recombination. Compartmentalization of the

nucleus therefore generates regions that are permissive to HR and others where HR is – at least in part – suppressed. Spontaneous recombination of rDNA is for example prevented by its localization to the nucleolus, from which HR and checkpoint proteins such as RPA, Rad52, Rad51, Rad55, Ddc1, Ddc2, and Rad9 are excluded (Torres-Rosell *et al.*, 2007). Another HR-suppressive environment is the nuclear periphery, where for example telomeres are found to localize in clusters (Gotta *et al.*, 1996; Antoniacchi *et al.*, 2007; Bupp *et al.*, 2007; Schober *et al.*, 2009). Nuclear pores, in contrast, seem to represent a compartment which stimulates HR. Possibly for this reason, persistent DSBs, collapsed replication forks, and damaged telomeres were found to re-localize and be tethered to NPCs (Nagai *et al.*, 2008; Khadaroo *et al.*, 2009). Several genes, including *MEC1/TEL1*, *SWR1*, and *RAD9/RAD24*, were found to be necessary for DSB localization to NPCs, probably by alteration of DNA mobility after damage induction (Dion *et al.*, 2012; Mine-Hattab and Rothstein, 2012; Horigome *et al.*, 2014).

### c) Regulation by post-translational modifications

Regulation of HR, but also of the DNA damage response in general, is to a large extent achieved by post-translational modifications (PTMs) of the involved proteins. PTMs affect the recruitment of proteins to DNA damage sites, facilitate the interaction with other factors, elicit changes in activity (positively or negatively) or stability. Common PTMs are phosphorylation, ubiquitylation, SUMOylation, and acetylation. This type of control generally allows a precise and often switch-like regulation of repair pathways as well as the coupling to concurrent processes like DNA replication.

Especially the cell cycle and the prevailing cell cycle phase highly influence PTMs, particularly phosphorylation, of recombination proteins. Cell cycle progression itself is established by the action of cyclin-dependent kinases (CDKs), and Cdc28 – the sole CDK of budding yeast – is regulated by association with one of nine specific co-factors, the cyclins Cln1-3 and Clb1-6, whose expression levels vary cyclically throughout the cell cycle (Richardson *et al.*, 1992; Schwob and Nasmyth, 1993; Tyers *et al.*, 1993). Notably, conditional alleles of Cdc28 result in chromosome instability (Devin *et al.*, 1990), defects in DSB resection and HR (Ira *et al.*, 2004; Barlow *et al.*, 2008; Huertas *et al.*, 2008), increased sensitivity to radiation (Koltovaya *et al.*, 1998) and accumulation of chronic DNA damage (Enserink *et al.*, 2009). Previous research has identified several means by which CDK stimulate HR directly or indirectly.

Following a DSB, the first choice to be made is between repair by HR and NHEJ. This repair pathway choice is made at the level of DNA end resection. It was shown that CDK-dependent phosphorylation is crucial for DNA end resection at several levels by stimulating resection enzymes on the one hand, and impeding negative regulators on the other hand. Accordingly, disruption of Cdc28 activity in budding yeast by an analogue-sensitive allele or by over-expression of the Cdc28 inhibitor *SIC1* leads to reduced resection (Aylon *et al.*, 2004; Ira *et al.*, 2004). In budding yeast, Cdc28-dependent phosphorylation of Sae2 (homologue of human CtIP) in S-, G<sub>2</sub>-, and M-phases results in activation of the Mre11 endonuclease and promotes resection initiation (Huertas *et al.*, 2008).

Long-range resection of DSBs is performed by Exo1 and/or Sgs1-Dna2, and is again regulated by PTMs: Cdc28-dependent phosphorylation of Dna2 causes its transport from the cytoplasm to the nucleus and its recruitment to DSBs, positively regulating long-range DNA end resection (Kosugi *et al.*, 2009; Chen *et al.*, 2011).

Another CDK-regulated resection enzyme is Fun30 (Ubersax *et al.*, 2003; Chen *et al.*, 2012, 2016; Costelloe *et al.*, 2012; Eapen *et al.*, 2012; Bantele *et al.*, 2017). Phosphorylation of Fun30 was described to stimulate its recruitment to damaged chromatin where it promotes long-range resection by antagonizing Rad9 (Chen *et al.*, 2012; Bantele *et al.*, 2017). Rad9 (orthologue of human 53BP1) is recruited to damaged DNA via different pathways, and blocks resection at the break site (Lazzaro *et al.*, 2008). Interestingly, both proteins, Rad9 and Fun30, bind the same interaction site of the scaffold protein Dpb11 (TopBP1 in humans) in a cell cycle-dependent manner (Pfander and Diffley, 2011; Bantele *et al.*, 2017). Similar to a *FUN30* deletion, mutation of the corresponding CDK sites on Fun30 (*fun30-SS20,28AA*) showed increased hyper-sensitivity to CPT that could be suppressed by additional *RAD9* deletion. This rescue suggests that inhibition of Rad9, and thereby promotion of resection, is mediated by the Fun30-Dpb11 complex. However, the exact mechanism of this antagonism is still subject to future research.

Following resection, the resulting 3' ssDNA stretches are covered by RPA (Alani *et al.*, 1992), whereupon Rad52 gets recruited. Both, Rad52 and RPA, are CDK targets, but the exact role in Rad52 recruitment is still unknown (Plate *et al.*, 2008; Barlow and Rothstein, 2009).

Modification by ubiquitin and SUMO was also implicated in the regulation of HR and the response to DNA damage (particular in post-replication repair (see chapter C)). The connection between ubiquitination and the DNA damage response was first established when Rad6 – known to be involved in post-replication repair – was identified as ubiquitin-conjugating enzyme (Jentsch *et al.*, 1987).

To date, two general functions of ubiquitin conjugation have been revealed: mediating proteasomal degradation and facilitating protein-protein interactions. Ubiquitination of RAD51 in fission yeast and human cells was suggested to regulate its cellular stability and subsequent degradation (Kovalenko *et al.*, 1996; Tsutsui *et al.*, 2014). However, many ubiquitin modifications influence their substrate by non-proteolytic mechanisms. A recent study in mammalian cells implicated RAD51 mono-ubiquitination with its cellular localization, thereby preventing re-association with DNA and suppressing inappropriate recombination (Chu *et al.*, 2015). Involvement of proteasomal degradation in DNA DSB repair is not well understood as deregulation of the proteasome was implicated in pro- as well as anti-recombinogenic mechanisms (Krogan *et al.*, 2004; Karpov *et al.*, 2013).

Furthermore, many recombination proteins, such as RPA, Rad52, Rad59, or Srs2, have been identified to be targets for SUMO conjugation (Sacher *et al.*, 2006; Burgess *et al.*, 2007; Ohuchi *et al.*, 2008; Saponaro *et al.*, 2010; Cremona *et al.*, 2012; Psakhye and Jentsch, 2012). In budding yeast, SUMOylated RPA triggers SUMOylation of Rad52 and Rad59 by recruitment of the SUMO ligase Siz2 (Chung and Zhao, 2015). Rad52 SUMOylation was shown to protect the protein from proteasomal degradation, as well as to inhibit recombination by interfering with its ssDNA binding capacity (Sacher *et al.*, 2006; Altmannova *et al.*, 2010). Interestingly, Psakhye and Jentsch established a model for SUMO conjugation during the response to DNA damage, in which SUMO does not target individual proteins, but rather a group of proteins involved in the same pathway. Proteins involved in HR where the first example for this type of modification (Psakhye and Jentsch, 2012).

A cooperative activity of SUMOylation and ubiquitination is demonstrated by so-called SUMO-targeted ubiquitin ligases (STUbLs). Those enzymes harbour SUMO-interacting motifs (SIMs) that allow binding to SUMOylated target proteins and subsequent ubiquitination (Psakhye and Jentsch, 2012). The Slx5-Slx8 STUbL localizes to replication forks and ensures the suppression of recombination during DNA replication (Burgess *et al.*, 2007). Deletion of either *SLX5* or *SLX8* results in an increase in gross chromosomal rearrangements as well as in spontaneous mutation rates (Zhang *et al.*, 2006).

In summary, PTMs change protein properties, be it activity, interaction capability, stability or localization. These changes can be made fast, and their reversibility turns PTMs into very adaptive regulation measures.

#### **d) Regulation by histone modifications and nucleosome remodellers**

Various histone modifications (e.g., phosphorylation, acetylation, methylation, ubiquitination, SUMOylation, ADP ribosylation) were described to occur in response to different types of DNA damage (reviewed in House *et al.*, 2014). These modifications show that chromatin is not just a simple barrier to DNA repair processes, but rather an important regulator, with modified histones representing interaction surfaces for associating proteins of the corresponding pathway.

The first damage-associated histone modification identified was phosphorylation of serine 129 of histone H2A ( $\gamma$ -H2A), which occurs within minutes after the occurrence of a DSB in the surrounding chromatin (Rogakou *et al.*, 1998; Downs *et al.*, 2000). H2A-S129 phosphorylation was described to recruit several repair factors and chromatin-remodelling complexes to the damage site (Downs *et al.*, 2004; Morrison *et al.*, 2004; van Attikum *et al.*, 2004). However, recent studies found remodeller recruitment to be independent of  $\gamma$ -H2A during HR in G2 cells, and rather reliant upon the Rad51 filament itself, linking chromatin remodelling to early stages of recombination (Bennett *et al.*, 2013).

Furthermore, chromatin structure and compactness play a central role in all DNA-related processes, such as gene regulation, replication, DNA repair and recombination, as involved factors need to access the DNA. Means to regulate the degree of condensation are, first, covalent histone modifications and, second, active deposition and removal of nucleosomal barriers by nucleosome remodellers. Nucleosome remodellers catalyse the alteration of nucleosome-DNA interactions in order to promote ATP-dependent sliding of nucleosomes, subunit exchange or eviction.

Chromatin folding can further be stimulated or repressed by histone modifications, which may have a distinct impact on DNA structure or on the nucleosomes themselves. Acetylation of histone H4 (H4-K16ac), for example, results in a reduced interaction between H4 and H2A, and thereby in a less condensed chromatin conformation (Shogren-Knaak *et al.*, 2006; Robinson *et al.*, 2008). Also modification of histone H2B by ubiquitin was shown to diminish chromatin compaction in yeast and human cells (Fierz *et al.*, 2011; Moyal *et al.*, 2011). Additionally, H2B ubiquitination was proposed to promote the assembly of repair factors, as well as to activate the checkpoint effector kinase Rad53 in *S. cerevisiae* (Giannattasio *et al.*, 2005). These findings do not only associate histone modifications with regulation of chromatin structure, but also with regulation of repair pathways and the DNA damage checkpoint.

### e) Regulation by the DNA damage checkpoint

Checkpoint signalling regulates the response to replication stress and DNA damage in order to coordinate cell cycle progression to cellular processes, such as accurate replication and repair. DNA lesions are recognized by sensors that transduce the signal to effectors orchestrating a signal transduction cascade. Consequently, cell cycle progression and chromosome segregation are delayed, and the DNA damage response is initiated.

In budding yeast, checkpoint activation is critically mediated by recruitment of the checkpoint kinases Mec1 and Tel1 (ATR and ATM in humans, respectively) to DNA lesions. Tel1 binds to break sites via the MRX complex (Lisby *et al.*, 2004; Fukunaga *et al.*, 2011), whereas Mec1 binds to RPA-coated ssDNA via its co-factor Ddc2, e.g. to ssDNA exposed by DNA end resection or to ssDNA exposed at stalled replication forks (Rouse and Jackson, 2002; Zou and Elledge, 2003; Ball *et al.*, 2005; 2007; Jazayeri *et al.*, 2006). In case of Mec1 signalling, the 9-1-1 complex (Rad17-Mec3-Ddc1 in *S. cerevisiae*) serves as a co-sensor, as it is loaded onto ssDNA-dsDNA junctions where the Ddc1 subunit can activate Mec1 directly, as well as indirectly by binding a second activator of Mec1, Dpb11 (Wang and Elledge, 2002; Majka *et al.*, 2006; Mordes *et al.*, 2008; Navadgi-Patil and Burgers 2008; 2009; Puddu *et al.*, 2008; Pfander and Diffley, 2011).

In the context of HR, checkpoint kinases have several targets, such as the strand annealing proteins Rad51 – phosphorylation of which stimulates its ATP hydrolysis and DNA binding activity (Flott *et al.*, 2011) – and Rad55 (Bashkurov *et al.*, 2000). Phosphorylation of histone H2A by Mec1 is involved in binding of the checkpoint mediator protein Rad9, which promotes the activation of the effector kinase Rad53 (CHK2 in humans) coordinating the downstream signalling cascade together with Chk1 (Navas *et al.*, 1996; Emili, 1998; Sun *et al.*, 1998; Vialard *et al.*, 1998; Gilbert *et al.*, 2001; Sweeney *et al.*, 2005). With the checkpoint coordinating cell cycle progression to recombinational repair, it is an essential part of HR regulation.

## C. Recombination and Replication

### 1. Replication-dependent repair

DNA replication has to occur with high fidelity in order to allow stable inheritance of genetic information. Considering the comparatively low error rate in the context of constant challenges, such fidelity is remarkable. In addition, the replication machinery has to overcome impediments such as DNA-bound proteins, repetitive sequences, RNA-DNA hybrids or DNA secondary structures – obstacles that can hamper the progression of replication forks. On the other hand, DNA replication can also be viewed as an opportunity to completely scan the genome for DNA lesions. This principle has already been described for transcription where RNA polymerase-blocking DNA lesions induce DNA repair (Mellon *et al.*, 1987; Selby and Sancar, 1993). Likewise, fork stalling induces the recruitment of repair factors and initiation of the DNA damage response (see below).

Cells need efficient ways to deal with polymerase stalling in order to avoid that stalled forks collapse, resulting in chromosome breaks and genomic instability (Branzei and Foiani, 2010). Replication-coupled repair therefore has three distinct tasks: to overcome DNA lesions such as base modifications in order to avoid fork stalling, to rescue stalled replication forks from collapsing and causing DNA ruptures, and to repair lesions and separate covalently linked DNA structures before cell division.

Eukaryotes have evolved several mechanisms to bypass DNA lesions during replication, combined under the term DNA damage tolerance (DDT) or post-replication repair. DDT consists of two branching pathways: translesion synthesis (TLS) and template-switching. Both pathways are initiated upon the occurrence of RPA-bound ssDNA stretches at stalled replication forks.

Translesion synthesis allows DNA to be replicated past lesions that affect the template strand. This occurs by replacing the replicative polymerase with specialized polymerases (“polymerase switch”). TLS polymerases possess an increased tolerance for distorted DNA in their active site, but in parallel also a reduced fidelity (Prakash *et al.*, 2005). Due to this low fidelity, TLS is error-prone, i.e. mutagenic. However, it assures continuation of replication in order to avoid prolonged fork stalling and collapse. By this mechanism, the replisome can be released from the block and replication can be completed.

In contrast, template-switching is error-free in principle as it utilizes the newly synthesized, undamaged DNA strand as replication template. As such, template-switching involves recombination, but the detailed molecular mechanism is not understood in full detail. In yeast, mutations in genes involved in the error-free pathway of DDT lead to an elevated sensitivity to DNA-damaging agents compared to mutations in TLS, suggesting that template-switching is the preferred pathway for lesion bypass (Xiao *et al.*, 1999; Brusky *et al.*, 2000).

## 2. Involvement of recombination in template-switching

First experimental evidence for a connection between recombination and error-free DDT was shown in a plasmid-based assay, in which accurate plasmid replication over a lesion required the presence of proteins from both processes (Zhang and Lawrence, 2005). Recent studies have furthermore employed 2D gel electrophoresis to visualize the progression of replication forks as well as the formation of X-shaped molecules, such as HJs. Intriguingly, the establishment of X-shaped structures was dependent on proteins of the error-free DDT pathway (Rad18, Rad5, Ubc13-Mms2) and on the HR protein Rad51 (Branzei *et al.*, 2008; Minca and Kowalski, 2010). Concomitantly, recombination-deficient mutants were found to be sensitive to agents such as HU or MMS that induce replication fork stalling (Bjergbaek *et al.*, 2005), further emphasizing the cooperation between the two processes.

During replication-coupled repair, homologous recombination is thought to play two distinct roles: first, HR promotes template-switching by enabling strand invasion into the already replicated DNA molecule. Second, HR is crucial for the recovery of DNA sequences after stalled replication forks have collapsed into a DSB. Common to both scenarios is the formation of covalently linked JMs, mostly dHJs or pseudo-HJs containing ssDNA (Figure 2).

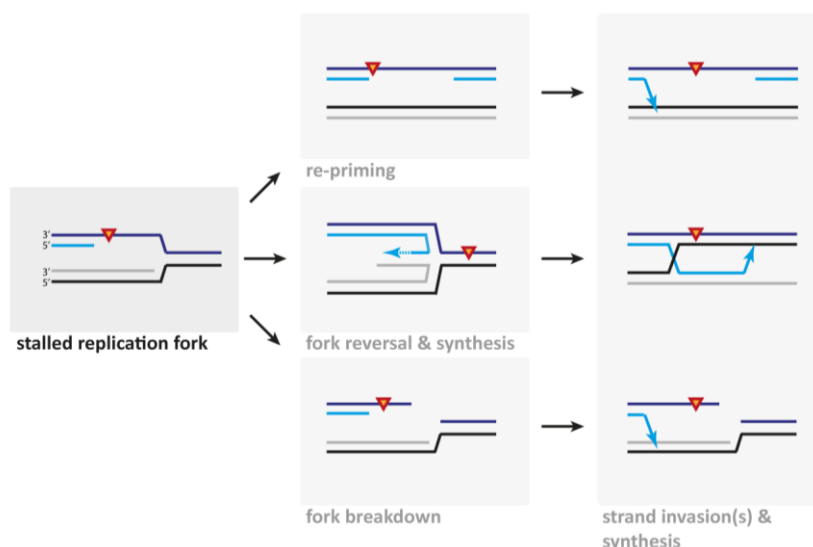


**Figure 2. Template-switching mechanisms after replication fork stalling.** Parental DNA strands are shown in black and dark blue; newly synthesized DNA strands are shown in grey and light blue. After replication fork stalling by a DNA lesion (depicted as red triangle) different recombination-based mechanisms can be initialized to bypass the replication block: re-priming downstream of the lesion site, fork reversal and DNA synthesis across the lesion, and cleavage resulting in a one-ended DSB. Strand invasion events leads to the formation of JMs. (analogous to Princz *et al.*, 2015).

Template-switch mechanisms after replication fork stalling can be mediated by re-priming or deliberate fork reversal. Re-priming downstream of the DNA lesion leaves a ssDNA gap behind, which then has to be filled employing TLS or template-switching mechanisms. As this mechanism allows continuation of DNA replication, it is unclear whether post-replication repair occurs in the context of replication forks.

Besides, a stalled replication fork can be rescued by fork regression: Upon DNA damage in the leading strand, replication of the lagging (or even the leading) strand may continue resulting in a ssDNA stretch. Helicase activity leads to reversal of the replication fork and to the formation of a four-way DNA junction, also referred to as “chicken foot”. This moves the DNA lesion back into the duplex DNA where it can be removed in an excision repair reaction. Recently, evidence was provided that fork regression and restoration can be promoted *in vitro* by incubation with the human recombination proteins RAD51 and RAD54 (Bugreev *et al.*, 2011). However, it is currently unclear whether the template-switch and fork regression models are mutually exclusive or act sequentially.

### 3. Regulation of DNA damage tolerance

The regulation of recombination-based tolerance pathways is pivotal for cell survival as unscheduled recombinational events during replication may lead to aberrant fork structures and unstable chromosomal rearrangements, and thus to potential genomic instability and loss of genetic information (Sogo *et al.*, 2002; Branzei and Foiani, 2010; Ghosal and Chen, 2013; Branzei and Szakal, 2016).

During DNA damage tolerance, the alternation of covalent modifications of the replication factor PCNA, also known as “PCNA switch”, plays a central role (Figure 3). PCNA forms a homotrimeric structure around DNA, which travels as polymerase processivity factor with the replication fork (Moldovan *et al.*, 2007). Its general function lies in providing a protein interaction surface at replicating DNA. During S-phase, PCNA is constitutively SUMOylated (Hoegge *et al.*, 2002). SUMO-modified PCNA was shown to recruit the anti-recombinase Srs2 to the fork suppressing inappropriate recombination events during replication. In agreement with that, mitotic recombination rates are elevated in a background, in which the E3 SUMO ligase Siz1 is mutated (Papouli *et al.*, 2005; Pfander *et al.*, 2005).

Ubiquitination of PCNA is triggered upon generation of ssDNA and association of the E3 ligase Rad18 (Hoegge *et al.*, 2002). Importantly, this modification determines the pathway choice in DDT: Mono-ubiquitination of PCNA promotes TLS by recruiting TLS polymerases (Bienko *et al.*, 2005), whereas elongation to a poly-ubiquitin chain induces the error-free pathway of DDT (Ulrich and Jentsch, 2000). Notably, ubiquitination of PCNA and its connected role in directing DDT is highly conserved among eukaryotes (Ulrich and Walden, 2010).

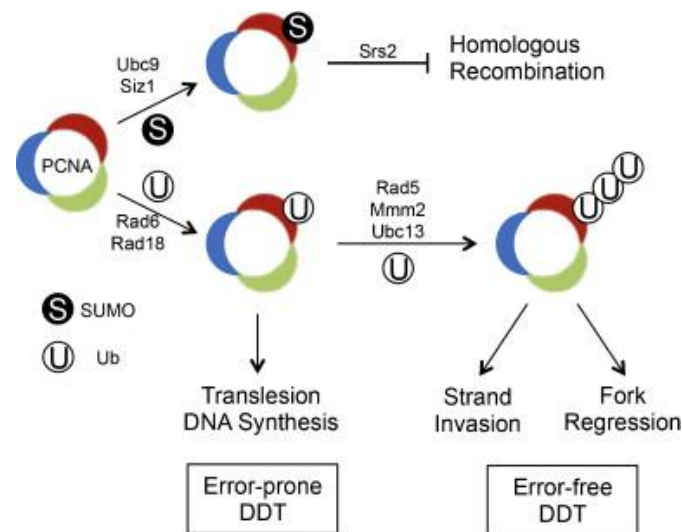


**Figure 3. Regulation of DNA damage tolerance by PCNA modification.** SUMO conjugation of PCNA leads to recruitment of the anti-recombinase Srs2, disruption of Rad51 nucleofilaments and inhibition of inappropriate recombination during replication. Ubiquitin conjugation of PCNA determines the pathway choice during DNA damage tolerance: Mono-ubiquitination recruits TLS polymerases, and poly-ubiquitination via a K63-linked chain initiates the error-free pathway of DDT involving template-switch mechanisms (adapted from Xu *et al.*, 2015)

A second regulatory layer of the response to replication fork stalling is mediated by the checkpoint. After fork disturbance the checkpoint gets activated and interferes with cell cycle progression during S-phase by, for example, Rad53-mediated phosphorylation of the replicative primase Pol $\alpha$  (Pelliccioli *et al.*, 1999). Rad53 also targets Dbf4, which is the regulatory subunit of DDK (Dbf4-dependent kinase with catalytic subunit Cdc7) and essential for replication fork progression and origin firing (Weinreich and Stillman, 1999; Lopez-Mosqueda *et al.*, 2010; Zegerman and Diffley, 2010). Checkpoint-mediated delay of cell cycle progression allows repair and concurrently prevents segregation of damaged DNA strands. Additionally, the checkpoint kinase Mec1 targets various substrates resulting in preservation of fork stability (Tercero and Diffley, 2001; Boddy and Russell, 2001; Lopes *et al.* 2001; Sogo *et al.*, 2002) and stabilization of the association between fork and replisome (Cobb *et al.*, 2003; Lucca *et al.*, 2004).

Although recombination-based mechanisms are required for the rescue of stalled and collapsed replication forks, recombination is in parallel inhibited by the checkpoint after replication fork stalling. The checkpoint is thought to delay HR to G2-phase to prevent abnormal recombination-dependent structures at stalled forks (Meister *et al.*, 2005). How these HR-promoting and -antagonizing means intertwine to mediate accurate damage signalling during DNA replication still has to be elucidated.

#### 4. The Dpb11-Slx4-Rtt107 complex

Scaffold proteins such as PCNA exhibit a crucial function during many cellular processes by displaying docking sites for additional factors. Other scaffold proteins are for example the checkpoint proteins Rad9, Mrc1, and the 9-1-1 complex.

One complex to highlight in regard to the response to replication fork stalling is the Dpb11-Slx4-Rtt107 complex consisting of three scaffold proteins with Slx4 bridging between Dpb11 and Rtt107 (Ohouo *et al.*, 2010). Extensive phosphorylation by Mec1 is crucial for complex formation as well as for the response to replication fork stalling by the DNA-alkylating drug MMS (Rouse, 2004; Flott and Rouse, 2005; Roberts *et al.*, 2006). Interestingly, Dpb11 also forms a complex with the checkpoint proteins Rad9, Ddc1 and Mec1 (Mordes *et al.*, 2008; Navadgi-Patil and Burgers, 2008; Puddu *et al.*, 2008; Pfander and Diffley, 2011). Probably due to competition between binding partners, it could be shown that the Dpb11-Slx4-Rtt107 complex counteracts the checkpoint complex upon fork stalling (Ohouo *et al.*, 2013; Cussiol *et al.*, 2015).

Dpb11 as well as Rtt107 both harbour multiple BRCT (BRCA1 C-terminal homology) domains that are known to bind phosphorylated proteins (Yu *et al.*, 2003; Garcia *et al.*, 2005; Li *et al.*, 2012). Scaffold proteins function by bringing together factors with catalytic activity or by recruiting enzymes to certain loci. For instance, Rtt107 binds to the ubiquitin ligase complex Rtt101-Mms1-Mms22 to mediate stabilization of stressed forks (Luke *et al.*, 2006; Roberts *et al.*, 2008; Vaisica *et al.*, 2011). Moreover, Rtt107 interaction with phosphorylated histone H2A was proposed to be important for its DNA association and for cell survival in the presence of DNA damaging agents, such as MMS, CPT and HU (Williams *et al.*, 2010; Li *et al.*, 2012). The scaffold protein Slx4 interacts with structure-specific endonucleases such as Rad1-Rad10 or Slx1: In case of Rad1-Rad10, Slx4 was shown to stimulate the activity to remove 3' ssDNA overhangs in the process of single-strand annealing (Toh *et al.*, 2010). In case of Slx1, Slx4 was implicated in the stability of rDNA loci by cleaving branched DNA structures (Coulon *et al.*, 2004; Fricke and Brill, 2003). In mammals, SLX1-SLX4 forms a complex with the resolution enzyme MUS81-EME1 suggesting a cooperative activity of the two nucleases in HJ resolution (Fekairi *et al.*, 2009; Svendsen *et al.*, 2009). So far, a similar cooperativity in yeast HJ resolution has not been identified.

## D. Disentanglement of Recombination Intermediates

In mitosis, sister chromatids are distributed to the cell poles to form two daughter nuclei. During that process, all covalent linkages between sister chromatids have to be cleared. As described in the previous chapters, DNA JMs are intermediates that can arise from recombination-based DSB repair, but also from replication stress or fork regression. Besides, also replication of certain loci late in the cell cycle or replication of common fragile sites (CFSs) entails DNA structures that often need to be processed before chromosome segregation (Lemoine *et al.*, 2005; Azvolinsky *et al.*, 2009; Fachinetti *et al.*, 2010; Feng *et al.*, 2011; Paeschke *et al.*, 2011; Casper *et al.*, 2012; Franchitto, 2013; Kim and Mirkin, 2013; Song *et al.*, 2014).

Indications of persistent JMs hampering segregation of chromosomes are anaphase bridges and lagging chromosomes (Garner *et al.*, 2013; Wyatt *et al.*, 2013; Sarbajna *et al.*, 2014). To avoid these perturbations and imminent mitotic catastrophe, it is pivotal to untie any DNA linkages before chromosome separation.

Disentanglement of DNA linkages that have arisen by HR can be mediated by two distinct mechanisms: **dissolution**, a helicase- and topoisomerase-based mechanism, or **resolution**, an endonuclease-based mechanism by so-called resolvases. While different in mechanism, both pathways exhibit functional overlap.

### 1. Dissolution

Dissolution is mediated by the Sgs1-Top3-Rmi1 complex in budding yeast (STR complex; BLM-TopoIIIa-RMI1-RMI2, BTR complex in mammals), and involves the combined activity of a RecQ family DNA helicase (Sgs1) and a topoisomerase (Top3) to decatenate JMs (Wu and Hickson, 2003; Cejka *et al.*, 2010a; b). Mechanistically, dHJs are first transformed to hemicatenanes, and are subsequently dissociated to give rise to non-crossover (NCO) products only (Wu and Hickson, 2003; Cejka *et al.*, 2010b). In this reaction, Sgs1 displays an ATP-dependent motor activity to mediate the convergent migration of the two HJs, whereas Top3 is a type1A topoisomerase that catalyses strand passage by a transesterification reaction in an ATPase-independent manner. The Rmi1 subunit stimulates Top3 DNA binding and catalytic activity (Chen and Brill, 2007) (Figure 4).

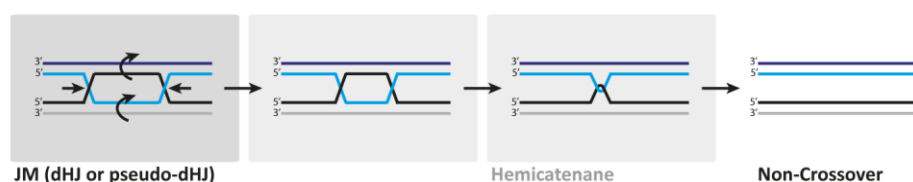


**Figure 4. Model for Sgs1-Top3-Rmi1-catalyzed dissolution of dHJs.** Two Holliday junctions are converted to a hemicatenane by Sgs1 helicase and Top3 topoisomerase activity. The Rmi1 subunit is dispensable during the initial reaction, but stimulates dissolution at the later stage.

The dissolution complex is associated with a rare human genetic disorder – Bloom’s syndrome – which is characterized by short stature, skin lesions, immunodeficiency as well as an increased risk of cancer development in the affected persons (summarized in Sanz *et al.*, 2006, updated 2016). On the molecular level, mutations in the BLM protein cause increased occurrence of sister chromatid exchanges (Chaganti *et al.*, 1974; Ray and German, 1984; Ellis *et al.*, 1995; Hickson, 2003), indicative of increased crossovers (COs) between sister chromatids. Alongside, mutant backgrounds of *sgs1Δ* and *top3Δ* in yeast exhibit elevated levels of COs in the context of spontaneous and DSB-induced recombination (Wallis *et al.*, 1989; Watt *et al.*, 1996; Ira *et al.*, 2003). Also, late-forming replication-dependent JMs persist in an *sgs1Δ* background after MMS treatment (Liberi *et al.*, 2005; Branzei *et al.*, 2008). The fact that CO formation is increased in the absence of Sgs1/BLM is commonly interpreted by the fact that a second pathway to disentangle JMs – resolution – takes over, which involves the formation of CO products.

## 2. Resolution

An alternative mechanism to disentangle JMs is their cleavage by structure-selective endonucleases, termed resolution. This mechanism generates both, NCO and CO products (Figure 5). In *S. cerevisiae*, the endonucleases Slx1-Slx4, Mus81-Mms4, and Yen1 (SLX1-SLX4, MUS81-EME1, and GEN1 in mammals) have been implicated in resolution. However, these enzymes differ partially in their mode of action as well as in their respective DNA substrates (Boddy *et al.*, 2001; Kaliraman *et al.*, 2001; Fricke and Brill, 2003; Ip *et al.*, 2008). Interestingly, both *SLX1-SLX4* and *MUS81-MMS4* mutants were discovered to be essential for cell survival in the absence of *SGS1* (Mullen *et al.*, 2001), suggesting functional overlap.

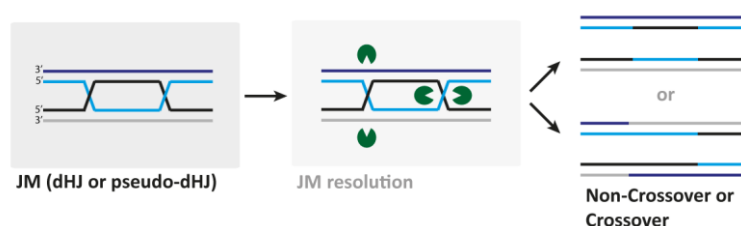


**Figure 5. Resolution of JMs by structure-selective endonucleases.** JMs can be resolved by endonucleolytic cleavage resulting in non-crossover and crossover products (analogous to Princz *et al.*, 2015).

Slx1 contains a conserved UvrC-intron-endonuclease domain in the amino-terminal region of the protein as well as a carboxy-terminal RING/PHD-type zinc finger domain. Thereby, Slx1 belongs to the GIY-YIG superfamily of endonucleases (Dunin-Horkawicz *et al.*, 2006). When bound to Slx4, it is a versatile 5' flap endonuclease able to cleave a variety of branched DNA structures, such as replication forks or HJs (Fricke and Brill, 2003; Coulon *et al.*, 2004; Wyatt *et al.*, 2013).

Mus81-Mms4 cuts intact HJs with low efficiency, and prefers nicked HJs, 3' flaps or replication forks as substrates (Kaliraman *et al.*, 2001; Whitby *et al.*, 2003; Ciccina *et al.*, 2003; Gaillard *et al.*, 2003; Fricke *et al.*, 2005; Ehmsen and Heyer, 2008; Taylor and McGowan, 2008; Wyatt *et al.*, 2013). Structurally, Mus81 belongs to the ERCC4/XPF family of structure-selective endonucleases harbouring a tandem helix-hairpin-helix motif for DNA binding and an endonuclease domain with a catalytic G-D-X<sub>n</sub>-E-R-K-X<sub>3</sub>-D motif (Ciccina *et al.*, 2008).

Interestingly, in human cells, single deletion of *SLX4*, *SLX1*, or *MUS81* genes in cells lacking *BLM* shows a comparable reduction of sister chromatid exchanges as the combined deletion of *MUS81* with *SLX4* or *SLX1*, suggesting a collaborative activity of the nucleases (Wyatt *et al.*, 2013; Castor *et al.*, 2013). In agreement with those findings, it was shown that SLX1-SLX4 and MUS81-EME1 endonuclease complexes cooperatively target HJs in human cells (SLX-MUS complex), and even physically interact with each other (Fekairi *et al.*, 2009; Svendsen *et al.*, 2009; Wyatt *et al.*, 2013). Although the MUS81-binding SAP domain in SLX4 is conserved among eukaryotes (Fekairi *et al.*, 2009), a direct interaction of Mus81 and Slx4 in budding yeast has not been described. Within the human multi-protein complex, SLX1 catalyses the initial, rate-limiting cut introducing a nick, following a second cut by MUS81 on the opposing strand (Wyatt *et al.*, 2013). Recently, interaction and functional cooperation with even a third endonuclease, XPF-ERCC1, (forming an SMX complex) was described (Wyatt *et al.*, 2017). In this connection, SLX4 was described to harbour binding sites for all three nucleases, suggesting a function as common docking platform. XPF-ERCC1 is thought to further stimulate the resolution reaction of SLX1 and MUS81. Yet, an involvement of its catalytic activity is still unknown. Whether a comparable combination of enzymatic activities is evolutionary conserved in other organisms outside of the mammalian kingdom is still subject of ongoing research.

In yeast, *MUS81* or *MMS4* deletion was associated with sensitivity to genotoxic agents (such as MMS or UV), the occurrence of persistent recombination intermediates and genomic instability (Boddy *et al.*, 2000; 2001; Interthal and Heyer 2000; de los Santos *et al.*, 2001; Kaliraman *et al.*, 2001; Mullen *et al.*, 2001; Doe *et al.*, 2002; Smith *et al.*, 2003; Ho *et al.*, 2010; Dayani *et al.*, 2011). Absence of Slx1 in budding yeast, on the other hand, does not have a defect in chromosome segregation, but cells are sensitive to MMS and display increased spontaneous recombination rates (Mullen *et al.*, 2001; Fricke and Brill, 2003; Zhang *et al.*, 2006). Intriguingly, *slx4Δ* but not *slx1Δ* displays a reduction in spontaneous mitotic crossovers (Ho *et al.*, 2010; de Muyt *et al.*, 2012; Zakharyevich *et al.*, 2012). In contrast to *mus81Δ*, the synthetic lethality of *slx1Δ* with *sgs1Δ* cannot be rescued in *rad52Δ* or *rad51Δ* recombination-deficient backgrounds suggesting diverging substrates or functions of Mus81 and Slx1 endonucleases (Fabre *et al.*, 2002; Bastin-Shanower *et al.*, 2003; Fricke and Brill, 2003).

The third resolvase of *S. cerevisiae* is the Yen1 endonuclease (GEN1 in vertebrates; absent in *S. pombe*). As part of a subclass of the Rad2/XPG family of endonucleases Yen1 contains three characteristic motifs: An amino-terminal XPG-type domain, a conserved nuclease domain in the central region of the protein, and a flanking helix-hairpin-helix domain (Harrington and Lieber, 1994; Johnson *et al.*, 1998). Yen1 preferably targets 5' flap structures, replication forks and HJs (intact or nicked) (Ip *et al.*, 2008; Rass *et al.*, 2010).

*YEN1* deletion does neither affect resistance to DNA-damaging agents, nor viability or crossover formation, when *SGS1* and *MUS81-MMS4* are present (Blanco *et al.*, 2010; Ho *et al.*, 2010; Matos *et al.*, 2011; de Muyt *et al.*, 2012; Zakharyevich *et al.*; 2012). Additionally, lethality of the *sgs1Δ mus81Δ* double mutant indicates that Yen1 alone is not capable of clearing all DNA recombination intermediates. Suppression of the *sgs1Δ mus81Δ* lethality can only be evoked by constitutive activation of Yen1 (Blanco *et al.*, 2010; Ho *et al.*, 2010; Tay *et al.*, 2010; Matos *et al.*, 2013). Furthermore, a *mus81Δ yen1Δ* double mutant shows an additive effect on reduction of CO formation compared to a *mus81Δ* single mutant, suggesting that the two nucleases function in parallel resolution pathways, with Mus81-Mms4 displaying the primary resolvase (Blanco *et al.*, 2010; Ho *et al.*, 2010; Matos *et al.*, 2011; 2013).

Overall, the described enzymes to separate linked DNA molecules seem to operate partially redundantly and also hierarchically.

## E. Regulation of Resolution

With dissolution generating solely NCOs, it prevents sister chromatid exchanges and potential loss of heterozygosity (Ellis *et al.*, 1995; Chaganti *et al.*, 1974; Ray and German, 1984; Wallis *et al.*, 1989; Watt *et al.*, 1996; Hickson, 2003; Ira *et al.*, 2003). Thereby, it is thought to be the preferred pathway to disperse DNA joint molecules in contrast to resolution, which will generate CO products. Furthermore, resolvases cleave branched DNA structures, which intrinsically occur during the process of DNA replication (Kaliraman *et al.*, 2001; Ciccia *et al.*, 2003; Fricke and Brill, 2003; Gaillard *et al.*, 2003; Whitby *et al.*, 2003; Coulon *et al.*, 2004; Fricke *et al.*, 2005; Ehmsen and Heyer, 2008; Ip *et al.*, 2008; Taylor and McGowan, 2008; Rass *et al.*, 2010; Wyatt *et al.*, 2013). Cleavage of replication fork structures will interfere with S-phase, giving a second reason why resolution may have to be temporally restrained. Overall, it is therefore thought that resolution is temporally restricted from early stages of the cell cycle in order to prioritize dissolution over resolution and to safeguard replication forks from nucleases.

### 1. Regulation by the cell cycle

Dissolution is independent of the cell cycle, while temporal control of resolvases is mainly mediated by the action of cell cycle-dependent kinases and phosphatases. At the onset of mitosis, yeast Mus81-Mms4 is activated by phosphorylating events by Cdc28 and Cdc5 kinases, primarily on the non-catalytic subunit Mms4 (Matos *et al.*, 2011, 2013; Gallo-Fernandez *et al.*, 2012; Schwartz *et al.*, 2012; Szakal and Branzei, 2013). Cdc5 seems to be temporally limiting for Mus81-Mms4 activation as over-expression of *CDC5* was shown to be sufficient for premature activation in earlier cell cycle phases (Matos *et al.*, 2011; 2013). Phosphatase treatment of immuno-purified Mus81-Mms4 in an *in vitro* resolution assay with a model HJ showed that phosphorylation and stimulation of catalytic activity are directly linked, but so far it is unknown by which mechanism this stimulation occurs (Matos *et al.*, 2011).

Mammalian cells regulate resolution in a manner that is comparable to yeast: MUS81-MMS4 activity is enhanced at the G2/M-phase transition in dependence of CDK1 and, to a lesser extent, PLK1 (Cdc5 homologue). Notably, a resolvase complex containing SLX1-SLX4 and MUS81-MMS4 forms in dependency of this phosphorylation (Wyatt *et al.*, 2013).

Also Yen1/GEN1 resolution activity is dependent on the cell cycle and on phosphorylation by cell cycle phase-specific kinases. However, in this case phosphorylation leads to inactivation of the enzyme. At the G1/S-phase transition, yeast Yen1 gets inhibited by Cdc28 phosphorylation, whereupon it stays inactive throughout S- and G2-phases until metaphase, and only gets activated upon dephosphorylation mediated by Cdc14 in anaphase (Matos *et al.*, 2011; Blanco *et al.*, 2014; Eissler *et al.*, 2014). A constitutively active form of Yen1 was generated by mutating selected phosphorylation sites to non-phosphorylatable residues or by ectopically expressing Cdc14 phosphatase. In this scenario, precocious activation of Yen1 nuclease activity results in increased DNA damage sensitivity to replication-perturbing agents (MMS, HU) as well as in increased CO formation. Mechanistically, phosphorylation controls Yen1 in two ways: first, extensive CDK-mediated phosphorylation enhances negative charges on the surface of Yen1 and concurrently reduces its binding affinity to DNA (Blanco *et al.*, 2014). Second, modification of amino acid S679

blocks its nuclear localization signal (NLS) restricting phosphorylated Yen1 locally to the cytoplasm (Kosugi *et al.* 2009; Blanco *et al.*, 2014; Eissler *et al.*, 2014). As yeast performs a closed mitosis where the nuclear envelope stays intact, Yen1 from *S. cerevisiae* requires active import to the nucleus.

In contrast, its mammalian homologue GEN1 is specifically regulated by exclusion from the nucleus (Chan and West, 2014; Matos and West, 2014). Harboring a nuclear export signal (NES), GEN1 can target its DNA substrates not before the nuclear membrane has broken down during late prophase of mitosis. Mutant versions of GEN1, which contain an inactivated NES and several artificial NLS sequences, could be forced to constitutively localize in the nucleus and resolve DNA intermediates as indicated by an increased CO formation (Chan and West, 2014).

Taken together, the temporal regulation of the disentanglement of DNA recombination intermediates establishes a hierarchy between dissolution and resolution, but also between the different resolution enzymes (Figure 6): The STR complex separates early DNA recombination intermediates that may have arisen in the context of replication. Upon mitotic entry, kinase activity stimulates Mus81-Mms4 to resolve remaining DNA joint molecules before anaphase, especially in the absence of Sgs1 (Ira *et al.*, 2003; Dayani *et al.*, 2011; Matos *et al.*, 2011, 2013; Szakal and Branzei, 2013). Consecutively, declining kinase activity and increasing phosphatase activity at the mitotic exit inactivates Mus81-Mms4 and concomitantly activates Yen1 to ensure resolution of any residual DNA linkages.

## 2. Regulation by the DNA damage checkpoint

Beside regulation by kinase-mediated phosphorylation, also the checkpoint has been implicated in influencing the resolution of DNA JMs. In the absence of a functional checkpoint, mitotic processing of recombination intermediates was found to occur as a conditional depletion of the checkpoint protein Ddc2 in an *sgs1Δ* background did not abolish late JM resolution (Szakal and Branzei, 2013). Notably, this checkpoint defect even triggered precocious resolution of X-shaped DNA molecules by Mus81-Mms4 (Szakal and Branzei, 2013). As mentioned in an earlier chapter, checkpoint activation during DNA damage bypass in S-phase ensures fork stability by counteracting recombination-associated processes (Meister *et al.*, 2005; Barlow and Rothstein, 2009). Above data therefore suggest that one purpose of fork protection by the checkpoint is to antagonize Mus81-Mms4 endonuclease activation during DNA damage bypass processes. On a molecular level, it was proposed that effector checkpoint kinases inhibit Mus81 function, either indirectly by repressing Cdc5 phosphorylation (budding yeast, Rad53), or directly by Mus81 targeting (fission yeast, Cds1) (Szakal and Branzei, 2013; Cussiol *et al.*, 2015; Kai *et al.*, 2005). In fission yeast, checkpoint-dependent phosphorylation of Mus81 leads to dissociation from chromatin (Kai *et al.*, 2005).

Taken together, checkpoint activation displays a second layer of resolution regulation and thereby preserves genomic stability during replication stress (Figure 6).

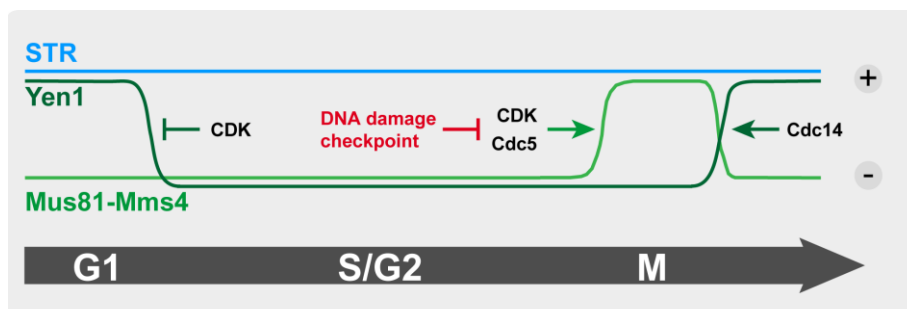


**Figure 6. Regulation of JM disentanglement pathways by cell cycle kinases and the DNA damage checkpoint.** Dissolution by Sgs1-Top3-Rmi1 (STR) is independent of the cell cycle, while resolution by Mus81-Mms4 or Yen1 is temporally regulated throughout the cell cycle. At a molecular level, cell cycle-dependent kinases specifically target resolvases to promote their activation (Mus81-Mms4) or inhibition (Yen1). In the presence of DNA damage, checkpoint kinases indirectly repress Mus81-Mms4 phosphorylation and resolution activity (analogous to Princz *et al.*, 2015).

### III. Aims of Study

The starting point of this thesis work was a characterization of protein complexes with Dpb11 in *Saccharomyces cerevisiae*. Interestingly, Dpb11 – and in analogy its human homolog TopBP1 – is a scaffold protein that was found to regulate different processes, all related to genome integrity. Specifically, Dpb11 displays interaction surfaces for phosphorylated proteins via its tandem BRCT domains (Yu, 2003; Garcia *et al.*, 2005), and has been described to bind several factors implicated in DNA replication, checkpoint, or repair. At the beginning of this work three Dpb11 complexes had been identified: When binding Sld3 and Sld2, Dpb11 regulates replication initiation (Tanaka *et al.*, 2007; Zegerman and Diffley, 2007); when binding Rad9, the 9-1-1 complex and Mec1-Ddc2, it coordinates the checkpoint signaling cascade (Mordes *et al.*, 2008; Navadgi-Patil and Burger, 2008; Puddu *et al.*, 2008; Pfander and Diffley, 2011); and when binding Slx4 together with Rtt107, Dpb11 forms a complex that was suggested to counteract the DNA damage checkpoint complex (Ohouo *et al.*, 2010; 2012). However, the complex with Slx4 had not been characterized in detail in its regulation and function.

The first aim was therefore to elucidate the prerequisites of complex formation between Dpb11 and Slx4, i.e. cell cycle- or DNA damage-specific conditions as well as identifying the kinases mediating the phosphorylation events. As both, Dpb11 and Slx4, are known to bind several proteins of independent function, we furthermore aimed to generate an *slx4* separation-of-function mutant that is specifically defective in binding to Dpb11 and thus could be used to analyze the function of the interaction.

The second aim was to characterize a novel interaction between Dpb11 and the Mus81-Mms4 nuclease, which was revealed in an initial two-hybrid screen. As both, Slx4 and Mus81-Mms4 were strongly implicated to function in the processing of recombination intermediates, we aimed to reveal whether Dpb11 may form a physical and functional link between these factors. *In vivo* binding assays and quantitative proteomics performed in the first two years of the thesis work not only confirmed the mitosis-specific interactions of Dpb11 with Mus81-Mms4, Slx4 and Rtt107, but also identified cell cycle kinases as partners in this interaction network.

Therefore, the third aim became to analyze this multi-protein complex regarding its architecture and biochemical requirements such as target sites for phosphorylations. As the complex formation temporally coincides with Mus81 nuclease activation, our objective was to understand the interplay between kinases and scaffolds, and how they build up the described temporal regulation of Mus81-Mms4 to efficiently resolve DNA JMs.

## IV. Results: Publications

- A. **Gritenaite D\*, Princz LN\*, Szakal B, Bantele SCS, Wendeler L, Schilbach S, Habermann BH, Matos J, Lisby M, Branzei D, Pfander B (2014)**

**A cell cycle-regulated Slx4-Dpb11 complex promotes the resolution of DNA repair intermediates linked to stalled replication**

***Genes Dev* 28:1604-1619**

**\* equal contribution**

# A cell cycle-regulated Slx4–Dpb11 complex promotes the resolution of DNA repair intermediates linked to stalled replication

Dalia Gritenaite,<sup>1,7</sup> Lissa N. Prinz,<sup>1,7</sup> Barnabas Szakal,<sup>2</sup> Susanne C.S. Bantele,<sup>1</sup> Lina Wendeler,<sup>1</sup> Sandra Schilbach,<sup>1,6</sup> Bianca H. Habermann,<sup>3</sup> Joao Matos,<sup>4</sup> Michael Lisby,<sup>5</sup> Dana Branzei,<sup>2</sup> and Boris Pfander<sup>1,8</sup>

<sup>1</sup>DNA Replication and Genome Integrity, Max-Planck Institute of Biochemistry, 82152 Martinsried, Germany; <sup>2</sup>Fondazione IFOM, Istituto FIRC di Oncologia Molecolare, 20139 Milan, Italy; <sup>3</sup>Computational Biology, Max-Planck Institute of Biochemistry, 82152 Martinsried, Germany; <sup>4</sup>Institute of Biochemistry, Eidgenössische Technische Hochschule Zürich, 8093 Zürich, Switzerland; <sup>5</sup>Department of Biology, University of Copenhagen, 2200 Copenhagen, Denmark

**A key function of the cellular DNA damage response is to facilitate the bypass of replication fork-stalling DNA lesions. Template switch reactions allow such a bypass and involve the formation of DNA joint molecules (JMs) between sister chromatids. These JMs need to be resolved before cell division; however, the regulation of this process is only poorly understood. Here, we identify a regulatory mechanism in yeast that critically controls JM resolution by the Mus81–Mms4 endonuclease. Central to this regulation is a conserved complex comprising the scaffold proteins Dpb11 and Slx4 that is under stringent control. Cell cycle-dependent phosphorylation of Slx4 by Cdk1 promotes the Dpb11–Slx4 interaction, while in mitosis, phosphorylation of Mms4 by Polo-like kinase Cdc5 promotes the additional association of Mus81–Mms4 with the complex, thereby promoting JM resolution. Finally, the DNA damage checkpoint counteracts Mus81–Mms4 binding to the Dpb11–Slx4 complex. Thus, Dpb11–Slx4 integrates several cellular inputs and participates in the temporal program for activation of the JM-resolving nuclease Mus81.**

[*Keywords:* DNA damage response; cell cycle; post-replicative repair; homologous recombination; joint molecule resolution]

Supplemental material is available for this article.

Received February 24, 2014; revised version accepted June 4, 2014.

Intrinsically and extrinsically induced DNA lesions can compromise the integrity of the genetic information and threaten cell viability. DNA lesions are particularly dangerous during S phase, when faithful DNA replication relies on two intact DNA strands. DNA lesions hamper the progression of replication forks and thereby the complete duplication of chromosomes. Moreover, replication forks that are stalled at DNA lesion sites can collapse and cause chromosome breaks and genome instability (Branzei and Foiani 2010).

Eukaryotes possess two fundamentally different mechanisms to bypass DNA lesions that affect one of the parental DNA strands: translesion synthesis (TLS) and template

switching. TLS employs specialized polymerases (translesion polymerases) that in many cases are able to replicate the damaged strand but with a reduced fidelity (Prakash et al. 2005). On the other hand, during template switching, the genetic information is copied from the newly synthesized, undamaged sister chromatid. This mechanism is therefore error-free in principle, yet its precise mechanism remains poorly understood. Template switching is a complex process that can be initiated by different recombination-based mechanisms (homologous recombination [HR] and error-free post-replicative repair [PRR]) (Branzei et al. 2008). The choice between the different bypass mechanisms is regulated by ubiquitin and SUMO modifications

<sup>6</sup>Present address: Max-Planck Institute of Biophysical Chemistry, Molecular Biology, 37077 Göttingen, Germany.

<sup>7</sup>These authors contributed equally to this work.

<sup>8</sup>Corresponding author

E-mail [bpfander@biochem.mpg.de](mailto:bpfander@biochem.mpg.de)

Article is online at <http://www.genesdev.org/cgi/doi/10.1101/gad.240515.114>.

© 2014 Gritenaite et al. This article is distributed exclusively by Cold Spring Harbor Laboratory Press for the first six months after the full-issue publication date (see <http://genesdev.cshlp.org/site/misc/terms.xhtml>). After six months, it is available under a Creative Commons License (Attribution-NonCommercial 4.0 International), as described at <http://creativecommons.org/licenses/by-nc/4.0/>.

of the replication protein PCNA at sites of stalled replication forks (Pfander et al. 2005).

Template switch mechanisms involve the formation of DNA joint molecules (JMs; also referred to as sister chromatid junctions [SCJs] or X molecules) as repair intermediates (Branzei et al. 2008). In order to allow completion of DNA replication and faithful chromosome segregation, these X-shaped DNA structures need to be disentangled before sister chromatids are separated during mitosis. To date, three enzymatic activities—the topoisomerase-containing Sgs1–Top3–Rmi1 complex (STR) as well as the Mus81–Mms4 and Yen1 structure-specific endonucleases—were shown to process JMs in budding yeast (Liberi et al. 2005; Blanco et al. 2010; Mankouri et al. 2011; Szakal and Branzei 2013). These three activities can be distinguished by their mechanism (termed dissolution for STR and resolution for Mus81–Mms4 and Yen1) (Gaillard et al. 2003; Ip et al. 2008; Cejka et al. 2010) but show a partial functional overlap. Moreover, they are differentially regulated during the cell cycle: Whereas the STR activity appears to be cell cycle-independent, the activity of Mus81–Mms4 is stimulated by CDK-mediated and Cdc5 (budding yeast Polo-like kinase)-mediated phosphorylation and peaks in mitosis (Matos et al. 2011, 2013; Gallo-Fernández et al. 2012; Szakal and Branzei 2013). Accordingly, the Mus81 regulation is assumed to create a hierarchy, with STR acting as a primary resolution pathway and Mus81–Mms4 acting as a salvage pathway. How Mus81–Mms4 phosphorylation by cell cycle kinases facilitates this temporal regulation of JM resolution pathways remains hardly understood.

The bypass of DNA lesions during replication is additionally regulated by the DNA damage checkpoint, the main cellular signaling pathway in response to DNA damage (Harrison and Haber 2006). As the primary purpose of the checkpoint is the stabilization of stalled replication forks (Branzei and Foiani 2010), its activation is a fundamental requirement for all fork repair and reactivation reactions. Notably, the checkpoint has been suggested to be involved in the choice of the JM resolution pathway, since precocious activation of the Mus81–Mms4 endonuclease is observed in checkpoint-deficient mutants (Szakal and Branzei 2013). However, it remains to be clarified how this second layer of regulation of JM resolution is achieved on a molecular level and how it is linked to cell cycle regulation.

Here, we identify an evolutionarily conserved protein complex comprising two scaffold proteins, Slx4 and Dpb11/TopBP1, as an important regulator of JM resolution by Mus81–Mms4. We show that the formation of the Slx4–Dpb11 complex is regulated by the cell cycle stage. An *slx4* mutant, compromised specifically in Dpb11 binding, exhibits hypersensitivity to the replication fork-stalling drug MMS, a delay in the resolution of X-shaped DNA JMs, and a reduced propensity to form crossovers (COs). The function of the Slx4–Dpb11 scaffold in JM resolution correlates with the finding that Dpb11 binds to the Mus81–Mms4 endonuclease. This association is restricted to mitosis, since it is dependent on the mitotic kinase Cdc5. Moreover, the checkpoint acts antagonistically to the regulation of JM

resolution by Slx4 and Dpb11, as we found that partial inactivation of the DNA damage checkpoint can compensate for defects in formation of the Slx4–Dpb11 scaffold complex.

## Results

### *An evolutionarily conserved and phosphorylation-dependent interaction between Slx4 and Dpb11/TopBP1*

Dpb11 and its human homolog, TopBP1, are critical regulators of the cellular DNA damage response and interact with several DNA replication, repair, and checkpoint proteins (Garcia et al. 2005; Germann et al. 2011). In these protein complexes, Dpb11/TopBP1 specifically binds to phosphorylated proteins via its tandem BRCT domains (Yu 2003; Garcia et al. 2005). A key role of Dpb11/TopBP1 is to function as a scaffold, bringing together specific sets of proteins via several interaction surfaces. In budding yeast, two Dpb11 complexes have been described in detail, which regulate replication initiation (with Sld3 and Sld2) (Tanaka et al. 2007; Zegerman and Diffley 2007) and the DNA damage checkpoint (with Rad9, the 9-1-1 complex, and Mec1–Ddc2) (Mordes et al. 2008; Navadgi-Patil and Burgers 2008; Puddu et al. 2008; Pfander and Diffley 2011), respectively (Fig. 1A). Recently, a third Dpb11 complex with Slx4 and Rtt107 was identified (Ohouo et al. 2010, 2012). In this latter complex, Slx4 appears to inhibit the formation of the Dpb11 DNA damage checkpoint complex (Ohouo et al. 2012).

In the course of our studies of Dpb11 function, we identified an interaction between a Dpb11 fragment that includes the tandem BRCT repeats 3 and 4 (BRCT3+4) and Slx4 using a two-hybrid screen. To confirm this finding, we tested the binding of different Dpb11 constructs to Slx4 and known Dpb11 binders. As observed before (Puddu et al. 2008; Pfander and Diffley 2011), we found that Rad9 binds to BRCT1+2 of Dpb11, whereas Ddc1 binds to BRCT3+4 (Fig. 1B). For Slx4, we found an interaction with full-length Dpb11 and the BRCT3+4 fragment but not with the BRCT1+2 domain (Fig. 1B). When we tested binding of Slx4 from cell extracts to recombinant, purified fragments of Dpb11, Slx4 also bound to BRCT3+4, albeit weaker than to the full-length protein (Supplemental Fig. S1A). Moreover, ablation of Dpb11 Thr451, which is predicted to be part of the BRCT3+4 phospho-protein-binding surface (Rappas et al. 2011), partially inhibited the Slx4–Dpb11 interaction (Supplemental Fig. S1B). A recent report suggested that the Dpb11 BRCT1+2 domain is involved in Slx4 binding (Ohouo et al. 2012). However, although our data do not rule out a contribution of BRCT1+2 in overall binding, our two independent lines of evidence clearly demonstrate that BRCT3+4 of Dpb11 significantly contributes to Slx4 binding.

Next, we mapped the Dpb11-binding site on Slx4 starting from a fragment (amino acids 461–738) that was common to all Slx4 clones identified in our initial Dpb11 two-hybrid screen. Truncated variants that begin at amino acid 490 failed to interact with Dpb11 (Supplemental Fig. S1C),

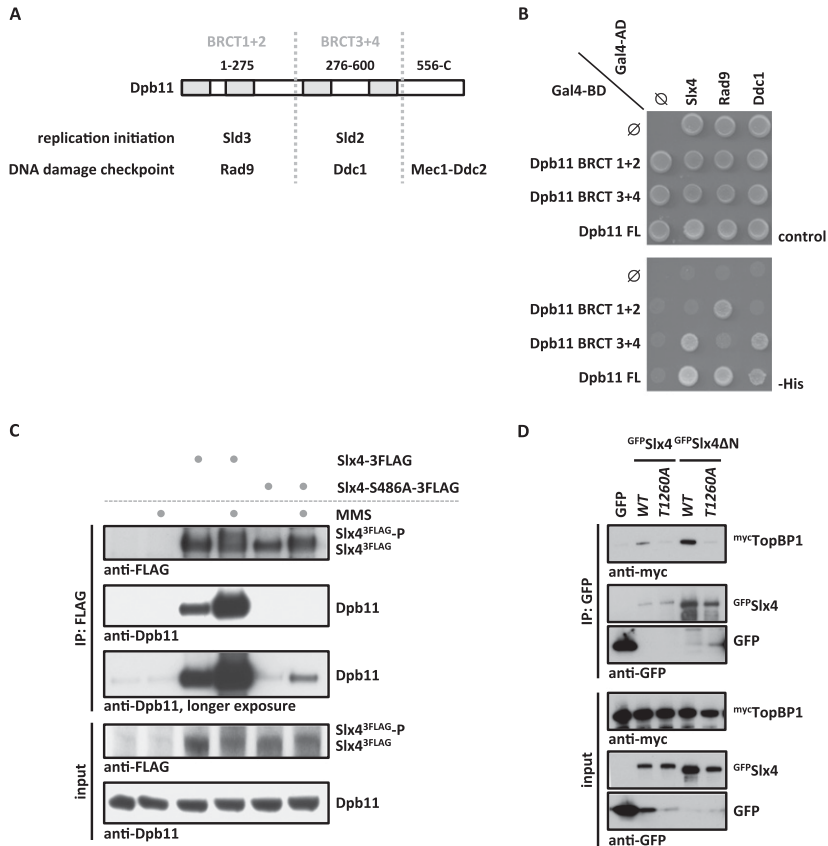


**Figure 1.** An evolutionarily conserved, phosphorylation-dependent interaction between Slx4 and Dpb11/TopBP1. (A) Schematic diagram of Dpb11 domain structure depicted with its interaction partners in replication initiation and DNA damage checkpoint. (B) Slx4 binds to the BRCT3+4 domain of Dpb11. Two-hybrid analysis of GAL4-BD fused to full-length Dpb11 or to BRCT1+2 and BRCT3+4 fragments and of GAL4-AD fusions with Slx4, Rad9, and Ddc1. (C) The Slx4–Dpb11 interaction is reduced by mutation of Slx4 Ser486 and is regulated by DNA damage. Coimmunoprecipitation of endogenous Dpb11 with Slx4<sup>3Flag</sup> or phosphorylation-deficient Slx4-S486A<sup>3Flag</sup> from undamaged cells or cells treated for 30 min with 0.033% MMS. (D) Human TopBP1 and Slx4 interact dependent on Thr1260 of Slx4. Coimmunoprecipitation of human mycTopBP1 with GFP-Slx4 or N-terminally truncated GFP-Slx4ΔN after transient overexpression in HEK293T cells. Slx4 or Slx4ΔN was expressed either as wild type (WT) or a T1260A phosphorylation-deficient variant.

indicating that the region between amino acid 461 and amino acid 490 is important for Dpb11 interaction. As several examples indicate that Dpb11 binds phosphorylated S/TP motifs, we tested all S/TP motifs within the C-terminal part of Slx4 for their ability to mediate Dpb11 binding. Indeed, we found that alteration of Ser486 in Slx4 into a nonphosphorylatable alanine residue (*slx4-S486A* mutant) reduced Dpb11 binding in a two-hybrid system (Supplemental Fig. S1D). Moreover, whereas immunoprecipitation of wild-type Slx4 efficiently copurified endogenous Dpb11 from cell extracts, in particular following MMS treatment, the Slx4–Dpb11 interaction was strongly decreased in extracts from cells expressing the *slx4-S486A* mutant, even after induction of DNA damage (Fig. 1C; see also Ohouo et al. 2012). Furthermore, the phospho-S486-containing peptide was specifically enriched (17-fold), when Dpb11 immunoprecipitations were analyzed by quantitative mass spectrometry (MS) (Supplemental Fig. S4A). We therefore conclude that the Slx4–Dpb11 interaction involves the BRCT3+4 region of Dpb11 and a region of Slx4 harboring the phosphorylated residue S486.

We further tested whether also the human homologs TopBP1 and Slx4 are binding partners. Indeed, we detected a specific interaction of TopBP1 and Slx4 or an N-terminally truncated version of Slx4 after transient transfection in human embryonic kidney (HEK) 293T cells (Fig. 1D). In contrast to the yeast proteins, we did not observe a stimulation of TopBP1 binding to Slx4 by DNA damage (Supplemental Fig. S1E). Human Slx4 is substantially larger than

yeast Slx4, with an overall sequence conservation of only 17.9%. Nonetheless, we identified a conserved short linear motif present in Slx4 proteins from different eukaryotes that comprises Ser486 in budding yeast and Thr1260 in humans (Supplemental Fig. S2). Mutation of Thr1260 to a nonphosphorylatable alanine (T1260A) in human Slx4 reduced the interaction with TopBP1 (Fig. 1D), suggesting that this residue may function analogously to Ser486 in budding yeast. These data suggest the presence of a novel, evolutionarily conserved motif in Slx4 that functions in Dpb11/TopBP1 binding.

#### *Cdk1-dependent phosphorylation of Slx4 regulates binding to Dpb11*

In order to unravel the regulation of the Slx4–Dpb11-binding surface, we quantified the relative amount of Ser486 phosphorylation under different cellular conditions using SILAC-based quantitative MS. We observed a specific increase of Ser486 phosphorylation in G2/M-arrested cells compared with G1-arrested cells, indicating that the analyzed Slx4 phosphorylation is cell cycle-regulated (Fig. 2A). In agreement with Ser486 matching the consensus target sequence for phosphorylation by cyclin-dependent kinase Cdk1 (S/TPxK) (Holt et al. 2009), we observed a marked reduction of Ser486 phosphorylation in G2/M-arrested cells when Cdk1 activity was abrogated using the *cdc28-as1* allele (Bishop et al. 2000) in combination with 1NM-PP1 inhibitor treatment (Fig. 2B). Notably, we also detected

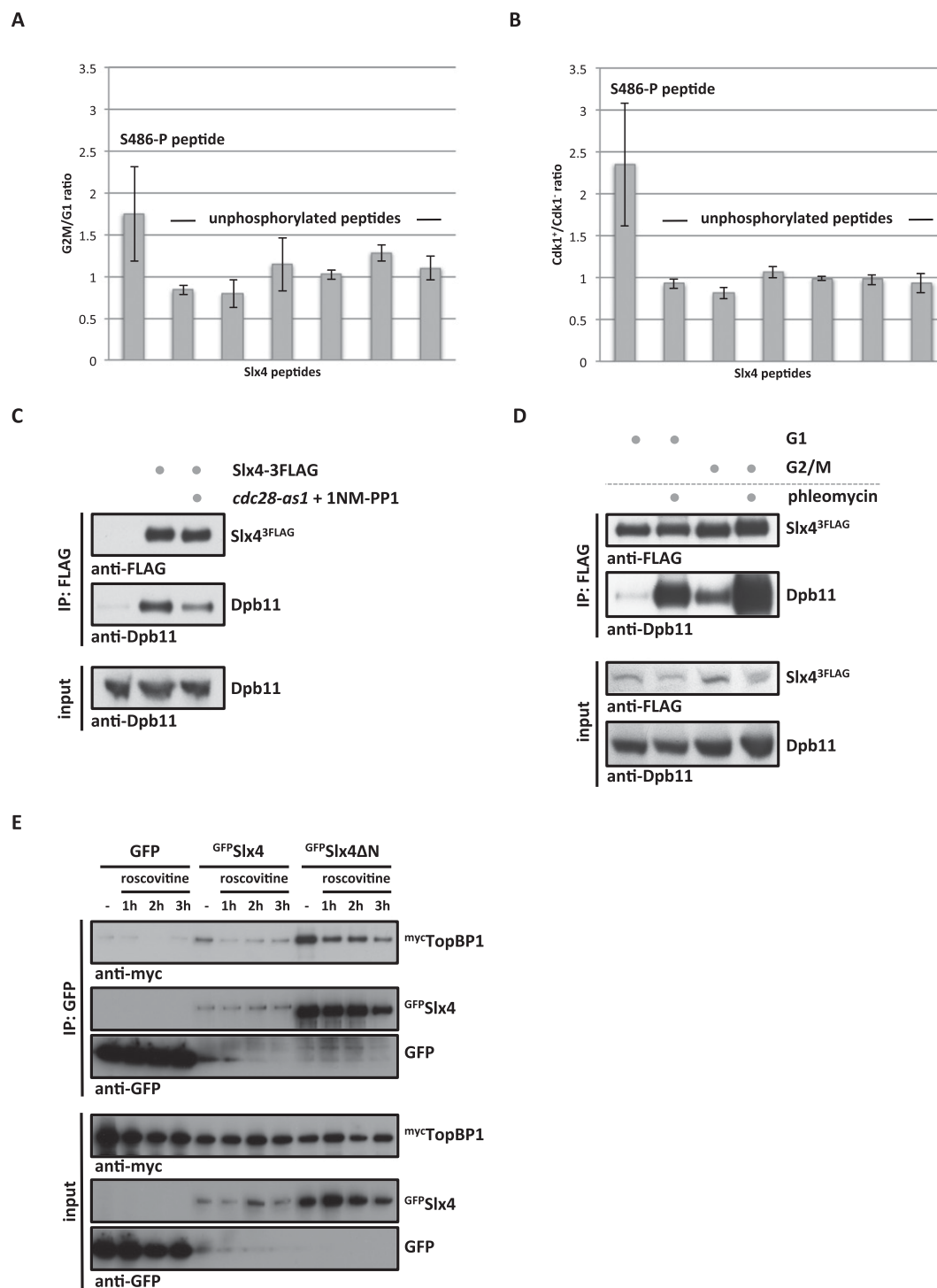


**Figure 2.** The Slx4–Dpb11/TopBP1-binding interface is cell cycle-regulated by Cdk1 phosphorylation of Slx4. (A) Ser486 phosphorylation is cell cycle-regulated. Relative abundance of the Slx4 480–489 phospho-peptide and six unmodified Slx4 peptides was measured by SILAC-based quantitative MS using  $^{15}\text{N}_2^{13}\text{C}_6$  lysine (Lys8) and compared between Slx4 isolated from G1- and G2/M-arrested cells. H/L ratios for individual peptides were normalized to total Slx4 ratios. Error bars represent standard deviations from two independent experiments, including label switch. (B) S486 phosphorylation depends on Cdk1. Analysis as in A but comparing Slx4 from G2/M-arrested cells with normal Cdk1 activity with cells in which Cdk1 has been inactivated using the *cdc28-as1* allele and 500 nM 1NM-PP1. (C) The Slx4–Dpb11 interaction is regulated by CDK. Coimmunoprecipitation of Dpb11 and Slx4<sup>3FLAG</sup> from G2/M-arrested cells or G2/M-arrested cells in which Cdk1 has been inactivated as in B. (D) The Slx4–Dpb11 interaction is regulated by cell cycle phase and DNA damage. Experiment as in C but with G1- and G2/M-arrested cells, which were either damaged by 50  $\mu\text{g}/\text{mL}$  phleomycin or left untreated. (E) Binding of human Slx4 and TopBP1 is regulated by CDK phosphorylation. Coimmunoprecipitation of mycTopBP1 with GFP<sup>Slx4</sup> and GFP<sup>Slx4ΔN</sup> after transient overexpression in HEK293T cells. Cells were left untreated or treated with 10  $\mu\text{g}/\text{mL}$  roscovitine for the indicated times to inhibit CDK activity.

reduced Slx4 binding to Dpb11 when Cdk1 was inhibited (Fig. 2C).

In addition to cell cycle-dependent regulation, we also observed a stimulation of Slx4–Dpb11 binding by DNA damage (Figs. 1C, 2D, Supplemental Fig. S1F). When Slx4 binding to recombinant GST–Dpb11 was tested, the DNA damage-dependent stimulation was less pronounced (Supplemental Fig. S1A), substantiating the notion that the Slx4–Dpb11 interaction may be additionally regulated by a damage-induced post-translational modification of Dpb11. On the other hand, Slx4 harbors several sites that can be targeted by kinases of the DNA damage checkpoint pathway. Mutation of seven sites in Slx4 partially inhibits its binding to Dpb11 (Ohouo et al. 2010), and the corresponding mutant shows phenotypes similar to those of *slx4-S486A* (Supplemental Fig. S3). As we cannot fully exclude pleiotropic defects for this mutant, we focused our analysis on *slx4-S486A*.

Taken together, our findings suggest that the Slx4–Dpb11 complex integrates at least two cellular signals: (1) cell cycle state through Cdk1 phosphorylation of Slx4 at Ser486 and (2) the presence of DNA damage through checkpoint kinase phosphorylation of several sites on Slx4 and perhaps on Dpb11.

Interestingly, the CDK regulation of this interaction is conserved between yeast and humans, since addition of the CDK inhibitor roscovitine reduced binding of Slx4 and TopBP1 (Fig. 2E).

#### *The Slx4–Dpb11 complex is required for the response to replication fork stalling*

Budding yeast Slx4 is known to bind to several DNA repair proteins (Slx1, Rtt107, and Rad1–Rad10) (Mullen et al. 2001; Roberts et al. 2006; Flott et al. 2007; Ohouo et al. 2010). However, whether these interaction partners are part of only one or several distinct complexes is unknown. While Slx4 has several independent DNA repair functions in budding yeast (Flott et al. 2007), until now, a detailed phenotypic characterization has only been conducted for *slx4Δ* deletion mutants. To test the specificity of the Dpb11-binding-deficient *slx4-S486A* phosphorylation site mutant, we compared its binding partners with those of wild-type Slx4 using quantitative proteomics. Indeed, we found that the mutant protein (Slx4-S486A<sup>3Flag</sup>) displayed eightfold reduced binding to Dpb11 (Fig. 3A). This variant still bound Slx1 and Rtt107 as efficiently as wild-type Slx4, indicating that Ser486 phosphorylation is specifically relevant for the Dpb11 interaction (Fig. 3A; see Supplemental Fig. S4A for specific Slx4 interactors). We thus took advantage of the *slx4-S486A* separation-of-function mutant to reveal a specific role of the Slx4–Dpb11 complex.

Using different DNA-damaging agents, we observed that the *slx4-S486A* mutant is particularly sensitive to MMS and, to a lesser extent, 4-NQO (Fig. 3B; Supplemental Fig. S4B), two reagents that create toxicity through replication fork stalling. Notably, the mutant was not sensitive to reagents that generate DNA strand breaks or interstrand cross-links, consistent with a recombination rate that was similar to wild type (Supplemental Fig. S4B,C). Remarkably,

expression of a fusion protein of the phospho-site mutant variant of Slx4 with Dpb11 (Dpb11–Slx4-S486A) rescued the MMS hypersensitivity phenotype almost to wild-type levels (Fig. 3B), suggesting that binding of Slx4 to Dpb11 is crucial for tolerance of replication fork-stalling lesions.

Next, we tested whether the response to stalled replication forks is aberrant in the *slx4-S486A* mutant. To this end, we treated synchronized cells with a pulse of MMS in early S phase. Under these conditions, the *slx4-S486A* mutant completed DNA replication with slightly slower kinetics compared with wild-type cells (Fig. 3C, 1-h time point). Also, the appearance of fully replicated and repaired chromosomes, as visualized by pulsed-field gel electrophoresis, was delayed (Fig. 3D, 1-h time point). This finding indicates that stalled replication fork structures or repair intermediates persist longer in the absence of the Slx4–Dpb11 complex. Additionally, the DNA damage checkpoint activation was prolonged in *slx4-S486A* cells (Fig. 3E), as determined by the phosphorylation status of the checkpoint kinase Rad53. This effect was specific for MMS treatment and could not be observed in cells in which double-strand breaks were induced by zeocin or phleomycin inside or outside of S phase (Supplemental Fig. S4D).

Defects in a checkpoint-antagonistic pathway (checkpoint “dampening”) (Ohouo et al. 2012) in *slx4* mutants could, in principle, lead to prolonged checkpoint activation and could thereby indirectly lead to slow S-phase kinetics and DNA damage hypersensitivity. Alternatively, persistence of unrepaired DNA lesions or DNA repair intermediates could lead to very similar phenotypes. In order to discriminate between the two possibilities, we examined the DNA damage levels during recovery from an MMS pulse in wild-type and *slx4-S486A* cells. To this end, we investigated the appearance and disappearance of nuclear foci formed by the ssDNA-binding protein RPA after MMS treatment in S phase. Indeed, *slx4-S486A* cells contained more RPA foci, which persisted longer than in wild-type cells (Fig. 3F). Therefore, we conclude that unrepaired DNA lesions or DNA repair intermediates that contain ssDNA persist in *slx4-S486A* mutants. This finding does not necessarily exclude a role of Slx4 as a regulator of the DNA damage checkpoint yet strongly suggests an additional direct function of the Slx4–Dpb11 complex in the repair of replication fork structures.

#### *The Slx4–Dpb11 complex promotes Mus81–Mms4-dependent JM resolution*

As our findings pointed to a function of the Slx4–Dpb11 complex in the response and repair of MMS-induced lesions, we next investigated whether the complex is involved in the DNA damage bypass. Therefore, we tested possible functions in HR and error-prone or error-free PRR. From several lines of genetic evidence, we conclude that the Slx4–Dpb11 complex is not exclusively involved in either PRR or HR (Supplemental Fig. S5). First, the *slx4-S486A* mutation enhanced the MMS hypersensitivity of mutants defective in error-free PRR (double mutant with either *mms2Δ*, *rad5-KT538,539AA*,

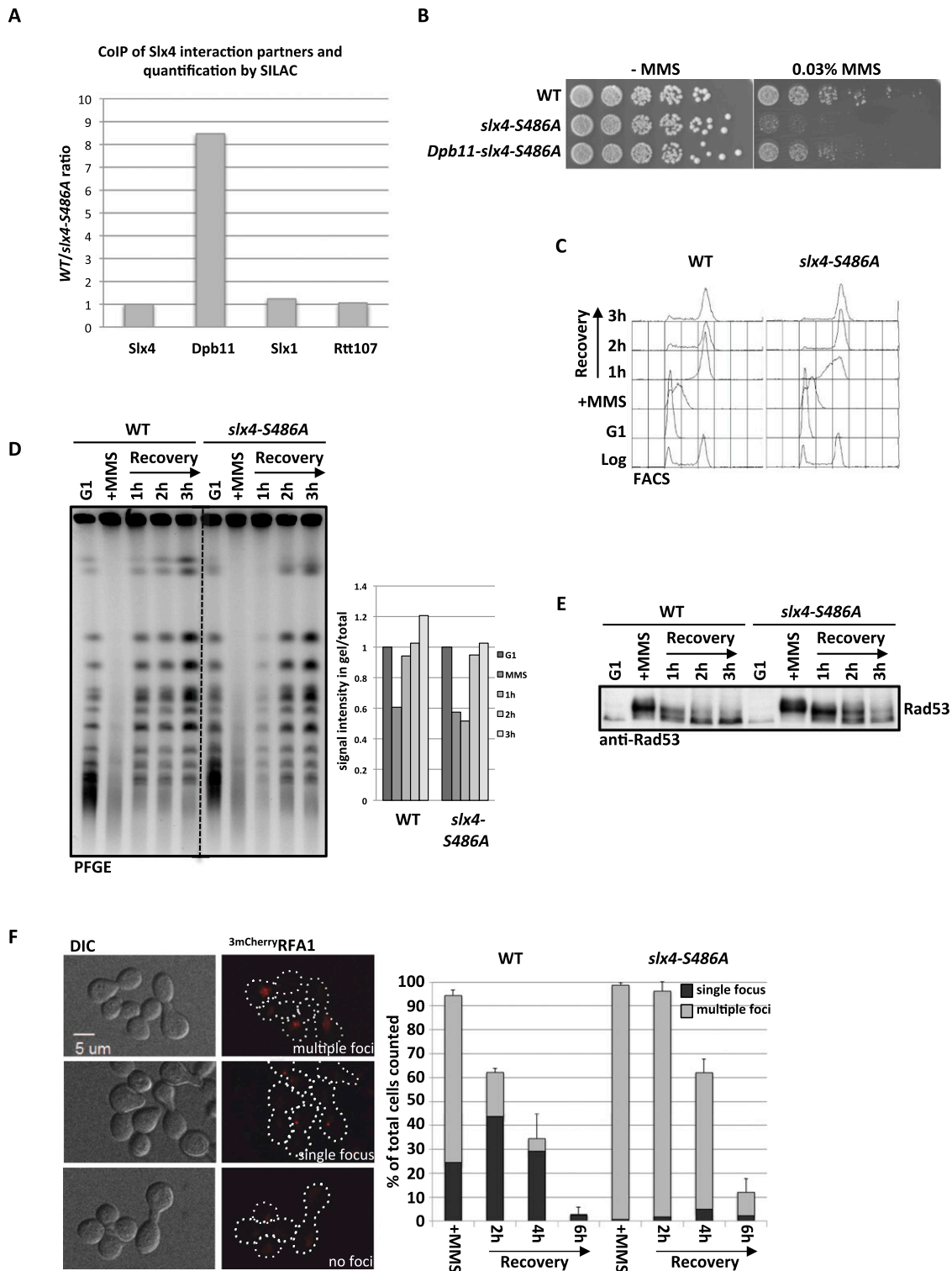


**Figure 3.** Mutation of *slx4-S486A* results in a specific defect in binding to Dpb11 and the response to stalled replication forks. (A) The *slx4-S486A* mutant leads to a specific defect in binding to Dpb11. Relative enrichment of Slx4 interactors (see Supplemental Fig. S4A) found in purifications of wild-type (WT) Slx4<sup>3Flag</sup> versus Slx4-S486A<sup>3Flag</sup> as determined by SILAC-based quantitative MS. Values >1 indicate a reduced binding to the Slx4-S486A relative to wild-type Slx4. (B) The *slx4-S486A* mutant, but not a *Dpb11-slxA4-S486A*-fusion, is hypersensitive to MMS. Wild type or strains expressing *slxA4-S486A* or the *Dpb11-slxA4-S486A*-fusion from the *SLX4* promoter as only a copy of *SLX4* were spotted in fivefold serial dilutions on MMS-containing medium and assayed for growth after 2 d. (C,D) Replication fork stalling is prolonged in the *slxA4-S486A* mutant. Cells were treated with a pulse of MMS during S phase, and recovery was analyzed by FACS (C; to measure cellular DNA content) and pulsed-field gel electrophoresis (D; to measure intact, fully replicated chromosomes). (D) For quantification, the fluorescence signal of chromosomes that migrated into the gel was divided by the total signal, including the pocket, and all signals were normalized to the G1 sample from each strain. (E) The DNA damage checkpoint is inactivated with reduced kinetics in the *slxA4-S486A* mutant. Cells were treated as in C, and checkpoint activity was determined by anti-Rad53 Western blot. (F) The *slxA4-S486A* mutant shows increased DNA damage foci and delayed recovery after transient MMS treatment in S phase. DNA damage sites were visualized by the ssDNA-binding RFA1<sup>3mCherry</sup> after transient MMS treatment during S phase. Cells were sorted into three categories: multiple, dispersed RFA1 foci; one RFA1 focus; and no RFA1 foci. Values are from two independent experiments, counting 100–150 cells per strain and time point. Error bars represent standard deviations.

or *rad5-C914S*), error-prone PRR (double mutant with either *rev1Δ*, *rev3Δ*, or *rad30Δ*), or HR (double mutant with *rad51Δ*) (Supplemental Fig. S5A). Second, spontaneous mutagenesis, a hallmark of error-prone PRR, was not significantly altered in *slx4-S486A* mutants (Supplemental Fig. S5B). Third, recombination rates, as determined by a direct repeat recombination assay, were similar between wild-type and *slx4-S486A* strains (Supplemental Fig. S4C). Fourth, *siz1Δ* or *srs2ΔC* mutations, which cause an up-regulation of HR at stalled replication forks (Pfander et al. 2005), did not alleviate the MMS hypersensitivity of *slx4-S486A* mutants (Supplemental Fig. S5C).

The nonepistatic relationship of the *slx4-S486A* mutant to PRR or HR pathways could be explained if Slx4 and Dpb11 participated in a step common to both error-free PRR and HR because, in such a scenario, both pathways would be affected by the *slx4-S486A* mutation. Both HR and error-free PRR operate via template switching in order to bypass the replication fork-stalling lesion by copying the undamaged information from the sister chromatid. A critical step in template switching is the final removal of X-shaped DNA intermediates (JMs) that link the two sister chromatids (Mankouri et al. 2013). JM removal pathways act, in principle, independently of the pathway by which JMs have been created (Branzei et al. 2008; for *mus81Δ* phenotypes, see Interthal and Heyer 2000; Li and Brill 2005). To test whether the Slx4–Dpb11 complex is involved in this late step, we visualized these DNA intermediates in a *sgs1Δ* mutant (deficient in JM dissolution) by two-dimensional (2D) gel electrophoresis (Liberi et al. 2005; Mankouri et al. 2011). In this mutant, MMS treatment in S phase leads to enhanced levels of JMs, which subsequently disappear during late S, G2, and M phase (Szakal and Branzei 2013). The additional mutation of *slx4-S486A* in the *sgs1Δ* background does not alter the formation of JMs, indicating that the Slx4–Dpb11 complex is not required at early steps (Supplemental Fig. S6A). Interestingly, however, during the recovery from the MMS treatment, JMs are more slowly resolved in the *sgs1Δ slx4-S486A* double mutant compared with the *sgs1Δ* single mutant (Fig. 4A). A similar effect can be observed using an *slx4Δ* mutant and conditionally inactivated *SGS1* in the same experimental setup (Supplemental Fig. S6B). Consistently, we observed an enhanced MMS sensitivity for the *sgs1Δ slx4-S486A* double mutant compared with the respective single mutants (Fig. 4B). From these experiments, we conclude that the Slx4–Dpb11 complex is involved in the resolution of JMs that are supposedly intermediates arising from a template switch reaction and that this complex functions in a pathway parallel to dissolution by the STR complex.

To elucidate a potential role of the Slx4–Dpb11 complex in a resolution mechanism, we investigated the genetic interaction with Mus81–Mms4. Indeed, the MMS sensitivities of *slx4-S486A mms4Δ* or *slx4-S486A mus81Δ* double mutants were identical to those of *mms4Δ* or *mus81Δ* single mutants (Fig. 4C). This suggests that the Slx4–Dpb11 complex acts in the Mus81–Mms4 pathway. The same epistatic relationship was seen between *mms4Δ* and *slx4-S486A* when we investigated JM resolution by 2D gel

electrophoresis when the STR complex was inactivated using the *Tc-sgs1* allele (Supplemental Fig. S6C). We note that the MMS hypersensitivity and the JM resolution defect of the *slx4-S486A* mutant are less pronounced compared with the deletion mutants that fully abolish Mus81 function (Fig. 4C; Supplemental Fig. S6C), suggesting that not all functions of the Mus81–Mms4 endonuclease depend on the Slx4–Dpb11 complex.

We also tested the involvement of other structure-specific endonucleases (Slx1, Rad1–Rad10, and Yen1) (Tomkinson et al. 1993; Fricke and Brill 2003; Coulon 2006; Ip et al. 2008), specifically of Slx1, as it associates with the Slx4–Dpb11 complex (Supplemental Fig. S4A). We found that *rad1Δ* showed an additive phenotype with *slx4-S486A*, while *slx1Δ* and *yen1Δ* mutants were not hypersensitive to MMS (Supplemental Fig. S6D; Fricke and Brill 2003; Coulon 2006; Blanco et al. 2010). We therefore conclude that these factors either are not involved in the resolution of template switch intermediates by Mus81 and the Slx4–Dpb11 complex or (in case of Slx1 and Yen1) have a function that can be taken over by a redundant pathway in the respective deletion mutant. Interestingly, the *yen1Δ* mutation caused an increase of MMS sensitivity specifically of the *sgs1Δ slx4-S486A* double mutant (Supplemental Fig. S6E), suggesting that Yen1 function becomes specifically important if the STR complex is inactive and function of the Slx4–Dpb11 complex is reduced.

The balance between STR-dependent JM dissolution and Mus81-dependent JM resolution is reflected in the ratio of CO to non-CO (NCO) products (Ira et al. 2003; Ho et al. 2010; Mankouri et al. 2013), since STR-mediated dissolution will not yield COs, while Mus81-mediated resolution can generate CO products. We therefore analyzed the rates of CO formation in the *slx4-S486A* mutant with a recombination assay using interchromosomal *arg4* heteroalleles (Robert et al. 2006; Szakal and Branzei 2013). Despite a slight increase in overall recombination rates, we measured a reduction in CO rates in the *slx4-S486A* mutant compared with wild-type cells (Fig. 4D). We therefore conclude that the Slx4–Dpb11 complex is an important regulator of JM removal pathways and that it acts by stimulating JM resolution, inhibiting JM dissolution, or both.

Persistent JMs interfere with the separation of sister chromatids in mitosis. Under circumstances in which JMs are not resolved before anaphase, these repair intermediates are thought to give rise to anaphase bridges between the dividing DNA masses (Chan et al. 2007; Mankouri et al. 2013). Consistent with a role in the resolution of JMs, Dpb11 localizes to DNA bridges between the separated chromosome masses in anaphase (Germann et al. 2014). Dpb11-containing anaphase bridges can be observed with a low frequency in undamaged cells (<5%) and are induced upon MMS treatment, suggesting that they arise from replication fork stalling (Germann et al. 2014). Interestingly, the occurrence of Dpb11 bridges is increased in *sgs1Δ* cells (Germann et al. 2014), indicating that the localization of Dpb11 to chromatin bridges reflects its action in a resolution mechanism. We observed a pro-

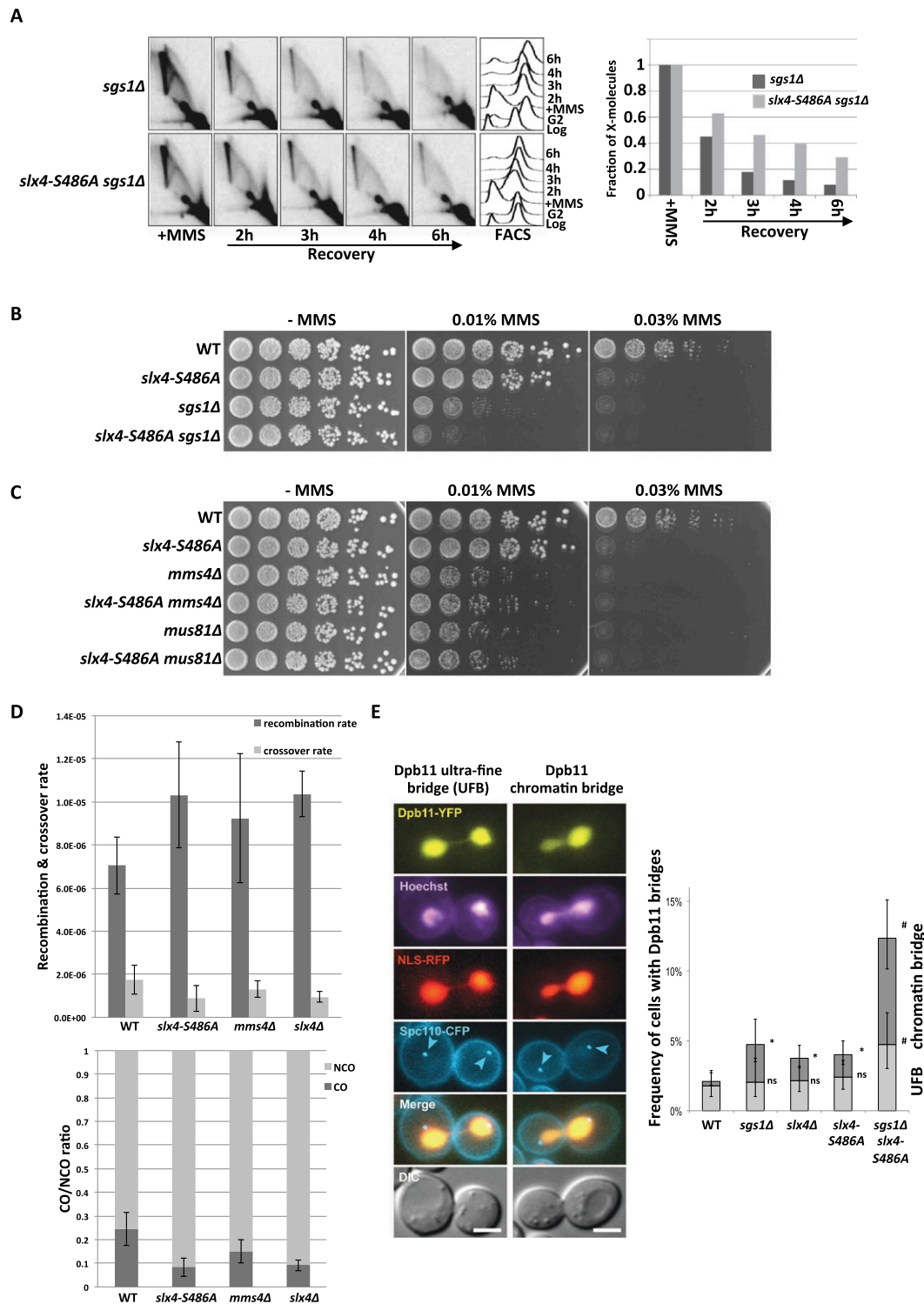


**Figure 4.** The Dpb11 binding-deficient *slx4-S486A* mutant causes defects in the Mus81–Mms4-dependent JM resolution. (A) JM structures are resolved slower in *sgs1Δ slx4-S486A* cells. X-shaped JMs were visualized as spike signal in 2D gels in *sgs1Δ* and *sgs1Δ slx4-S486A* cells that have been treated with a pulse of MMS in S phase. (B) MMS sensitivity is enhanced in the *sgs1Δ slx4-S486A* double mutant compared with each single mutant. Analysis of the MMS hypersensitivity phenotype as in Figure 3B. (C) The MMS hypersensitivity of *mms4Δ* and *mus81Δ* mutants is not further enhanced by an additional *slx4-S486A* mutation. Experiment as in B. (D) The *slx4-S486A* mutation leads to a reduced CO formation. COs and NCOs from an interchromosomal recombination assay using *arg4* heteroalleles on chromosome V and VIII (Robert et al. 2006) were determined using a PCR-based strategy. (Top panel) Recombination and CO rates were determined by fluctuation analysis using a maximum likelihood approach. (Bottom panel) CO ratio is quotient of CO rate and overall recombination rate. Error bars represent standard deviations of two to 11 independent experiments. (E) Dpb11 anaphase bridge structures occur more frequently when JM dissolution and the Dpb11–Slx4 interaction are defective. (Right panel) Quantification of Dpb11 ultrafine bridges (UFBs) or chromatin bridges in wild-type (WT), *sgs1Δ*, *slx4Δ*, *slx4-S486A*, and *slx4-S486A sgs1Δ* strains. Cells express Dpb11-YFP, NLS-RFP as a marker of the nucleoplasm and Spc110-CFP as a marker of the spindle pole body. DNA is stained with Hoechst. (Left panel) Images of representative anaphase cells are shown. Bar, 3  $\mu$ m. Error bars indicate 95% confidence intervals. Significance is as follows: (\*)  $P < 0.01$  (compared with wild type); (#)  $P < 0.01$  (compared with the single mutants); (ns) not significantly different from wild type.

nounced increase of cells containing Dpb11 bridges when the *sgs1Δ* and *slx4-S486A* mutants were combined (Fig. 4E). The genetic requirements for Dpb11 bridges are therefore highly similar to those for persistent JMs (Fig. 4A), supporting a role for Dpb11 and Slx4 in JM resolution. In line with this model, we observed frequent colocalization of either Slx4<sup>YFP</sup> or Mus81<sup>YFP</sup> with Dpb11<sup>CFP</sup>-positive bridges that is further enhanced in *sgs1Δ* cells (Supplemental Fig. S7A). We also noticed a colocalization of Slx4, Mus81, and Dpb11 in DNA damage foci yet to a lesser extent (Supplemental Fig. S7B). Overall, the data in Figure 4 provide strong support for an involvement of the Slx4–Dpb11 complex in JM resolution by Mus81–Mms4.

#### *Mus81–Mms4 interacts with the Slx4–Dpb11 complex during mitosis in a Cdc5-dependent fashion*

To elucidate how the Slx4–Dpb11 complex regulates Mus81 function, we investigated a possible physical interaction. In previous studies using asynchronously growing yeast cells, no binding of Slx4 to Mus81–Mms4 was detectable (Schwartz et al. 2012). However, we detected Mms4 as a cell cycle-specific interactor if Slx4<sup>3Flag</sup> immunoprecipitations were investigated by SILAC MS (such as in Fig. 2A). Moreover, when we arrested cells in G2/M by nocodazole treatment, immunopurification of Mms4<sup>3Flag</sup> copurified Dpb11 and Slx4 (Fig. 5A). Notably, this interaction is highly cell cycle-specific, as it could not be observed in G1- or S-phase cells (Fig. 5A). We determined, using an unbiased SILAC MS approach, that Dpb11, Slx4, and Rtt107 are among the best interactors of Mus81–Mms4 in G2/M-arrested cells (Supplemental Fig. S8A).

Next, we tested whether Dpb11, Slx4, and Mus81–Mms4 form a single protein complex. Indeed, the three proteins comigrated at a size of ~33 S (Supplemental Fig. S8B, fractions 18–20, apparent molecular weight 1.1–1.2 MDa) when the eluate of an Mms4<sup>3Flag</sup> purification from G2/M cells was subjected to a glycerol gradient centrifugation. When we analyzed the complex architecture by a two-hybrid approach, we detected a direct interaction of Dpb11 and Mms4 that is independent of Slx4 (Supplemental Fig. S8C). Moreover, when we immunoprecipitated Mms4<sup>3Flag</sup> in the *slx4-S486A* background, we observed a reduction of Slx4, but not Dpb11, binding to Mms4<sup>3Flag</sup> (Fig. 5B). These findings thus suggest that Dpb11, Slx4, and Mus81–Mms4 are part of a multiprotein complex in which Dpb11 acts as a bridge between Slx4 and Mus81–Mms4.

We observed that Dpb11 and Slx4 could be partially eluted from Mms4-containing beads using λ-phosphatase treatment (Supplemental Fig. S8D), suggesting that the binding is at least in part dependent on protein phosphorylation. Previous work has established that Mus81 activity is decisively up-regulated in mitosis in response to a sequential phosphorylation of Mms4 by CDK and the Polo-like kinase Cdc5 (Matos et al. 2011; Gallo-Fernández et al. 2012; Saugar et al. 2013; Szakal and Branzei 2013). We therefore used two systems to interfere with Cdc5 activity: the *cdc5-as1* analog-sensitive allele, which we inhibited using chloromethylketone (CMK) (Snead et al. 2007), and transcriptional shutoff of *pGAL-CDC5* using

glucose repression. Both types of Cdc5 inactivation resulted in a loss of the slower-migrating species of Mms4 in gels and at the same time diminished the binding of Dpb11 and Slx4 to Mms4<sup>3Flag</sup> (Fig. 5C; Supplemental Fig. S9A). In order to rule out indirect effects, we tested whether Cdk1 activity was uninfluenced under conditions of Cdc5 inhibition/shutoff and saw that neither the interaction between Slx4 and Dpb11 nor phosphorylation of a CDK target site on Rad9 (T474) (Pfander and Diffley 2011) was influenced by Cdc5 inactivation (Supplemental Fig. S9B,C). Together with our results on the architecture of the Slx4–Dpb11–Mms4–Mus81 complex, these experiments suggest that binding of Mms4 to Dpb11 is regulated by Cdc5 phosphorylation.

We also tested whether the formation of the Slx4–Dpb11–Mms4–Mus81 was regulated upon DNA damage. We found that Mms4<sup>3Flag</sup> bound similar amounts of Dpb11 and Slx4 after phleomycin or mock treatment of G2/M-arrested cells (Supplemental Fig. S9D). Moreover, we could also observe formation of the Slx4–Dpb11–Mms4–Mus81 complex during recovery from MMS pulse treatment during S phase (Fig. 5D). However, this binding occurred only once Cdc5 became active, as visualized by the slower-migrating form of Mms4, indicating that even after DNA damage, the Dpb11–Mms4 interaction is dependent on Cdc5 (Fig. 5D).

Given that the cell cycle regulation of Mus81 activity and the cell cycle regulation of the Slx4–Dpb11–Mms4–Mus81 complex formation have the same requirements, we tested whether the up-regulation of Mus81 nuclease activity requires Slx4 and Dpb11. We analyzed in vitro resolution of nicked Holliday junctions, Holliday junctions, and model replication fork structures on immunopurified Mus81–Mms4 and found that the enhanced activity of mitotic Mus81 is similar, independently of whether Mus81 was purified from wild-type or *slx4-S486A* cells (Fig. 5E; Supplemental Fig. S9E). Therefore, we conclude that cell cycle kinases regulate Mus81 by at least two mechanisms: direct up-regulation of the catalytic activity, which can be reconstituted in vitro, and an up-regulation through formation of an Slx4–Dpb11–Mms4–Mus81 complex, which could be seen in vivo.

#### *The DNA damage checkpoint regulates the Slx4–Dpb11-dependent Mus81 function*

The DNA damage checkpoint prevents collapse of stalled replication forks and thereby is fundamentally required for all aspects of the response to stalled replication forks (Branzei and Foiani 2010). Moreover, the checkpoint was also suggested to counteract Cdc5-dependent Mus81 activation, since premature Mms4 phosphorylation by Cdc5 was observed after MMS treatment of checkpoint-deficient cells (Szakal and Branzei 2013). Possible explanations for this phenomenon are a faster S-phase progression in the checkpoint mutants or a direct inhibition of Cdc5 activity by the checkpoint (Zhang et al. 2009).

To address these possibilities, we investigated the influence of the DNA damage checkpoint on Slx4–Dpb11–Mms4–Mus81 complex function. Interestingly, we found

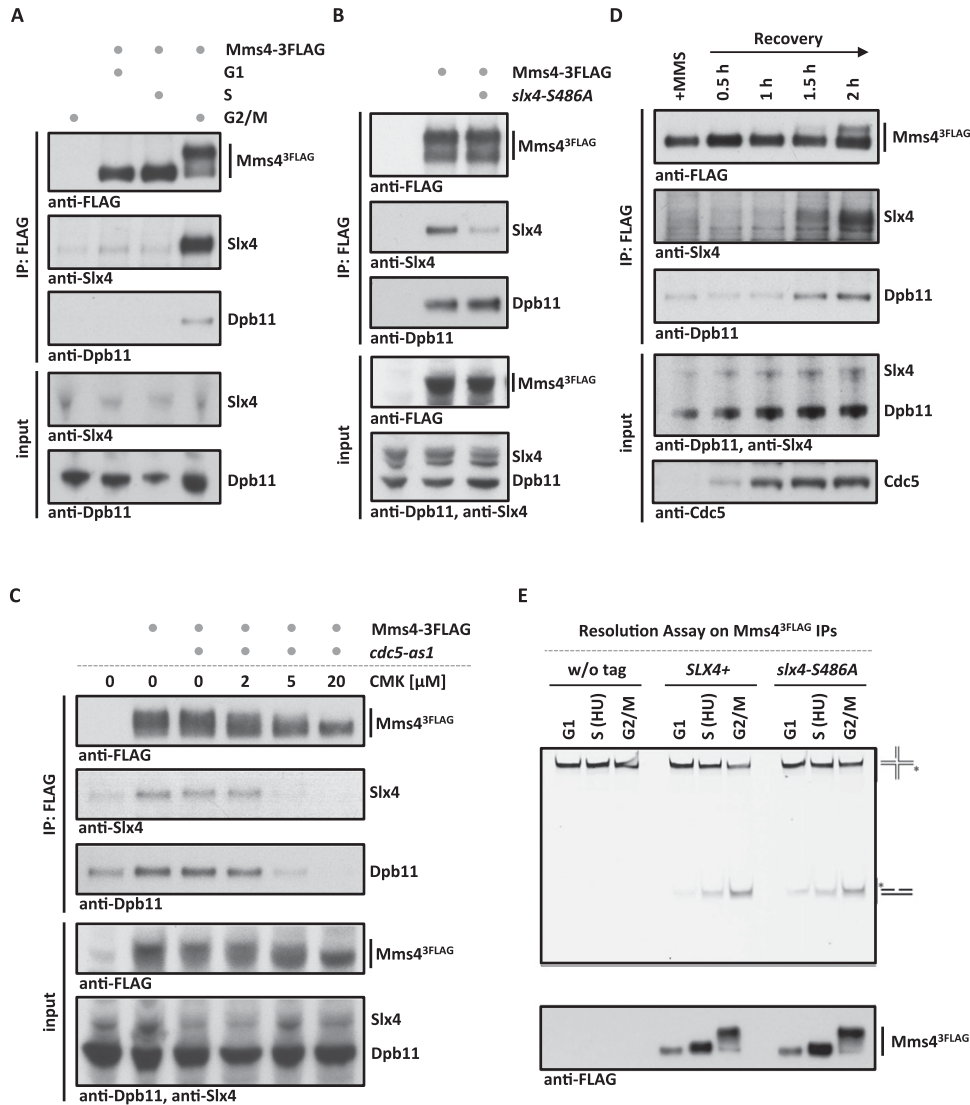


**Figure 5.** Slx4, Dpb11, and Mus81–Mms4 form a Cdc5-dependent complex at the G2/M cell cycle stage. (A) Mms4 binds to Dpb11 and Slx4 specifically in G2/M. Coimmunoprecipitation samples of Mms4<sup>3FLAG</sup> from G1, S, or G2/M cells were tested for binding to Dpb11 and Slx4. (B) Slx4-S486A is partially lost from the Slx4–Dpb11–Mms4–Mus81 complex, suggesting that Dpb11 bridges the interaction between Mms4 and Slx4. Mms4<sup>3FLAG</sup> coimmunoprecipitation were carried out as in A but from G2/M-arrested wild-type (WT) or *slx4-S486A* mutant cells. (C) The Dpb11–Mms4 interaction is dependent on the Polo-like kinase Cdc5. *cdc5-as1* was inhibited by 2, 5, and 20  $\mu$ M CMK in G2/M-arrested cells. Mms4<sup>3FLAG</sup> coimmunoprecipitation was performed as in A. (D) Cdc5 hyperphosphorylated Mus81–Mms4 binds to Slx4 and Dpb11 during recovery from MMS damage. Cells were treated with a 30-min pulse of 0.03% MMS. Mms4<sup>3FLAG</sup> coimmunoprecipitations were performed from samples after 0, 30, 60, 90, and 120 min of recovery in nocodazole-containing medium. (E) Cell cycle regulation of Mus81–Mms4 nuclease activity remains intact in the *slx4-S486A* mutant. Mms4<sup>3FLAG</sup> and control immunoprecipitations (see the *bottom* panel for immunoprecipitation samples) from cells arrested in their cell cycle by  $\alpha$  factor, HU, or nocodazole were incubated with a fluorescence-labeled nicked Holliday junction substrate.

that a partial defect in DNA damage checkpoint signaling alleviated the phenotypes of the *slx4-S486A* mutant (Fig. 6A,B; Supplemental Fig. S10A,B; see also Ohouo et al. 2012). In these experiments, we used three distinct mutants, which were partially impaired in checkpoint signaling: *ddc1-T602A* (defective in Dpb11-dependent Rad9 recruitment (Puđu et al. 2008), *dot1 $\Delta$*  (defective in chromatin-dependent Rad9 recruitment) (Giannattasio et al. 2005), and *rad53-3HA* (a hypomorphic Rad53 allele) (Cordon-Preciado et al. 2006). All three mutants partially

suppressed the hypersensitivity of *slx4-S486A* to chronic exposure of MMS (Fig. 6A; Supplemental Fig. S10A). Furthermore, the recovery from MMS treatment as judged by the reappearance of fully replicated chromosomes in PFGE and reappearance of unphosphorylated Rad53 was enhanced in *slx4-S486A ddc1-T602A* cells compared with *slx4-S486A* cells (Fig. 6B; Supplemental Fig. S10B).

A plausible interpretation of these results is that a partial inactivation of the checkpoint may compensate for a reduced or delayed formation of the Slx4–Dpb11–Mms4–

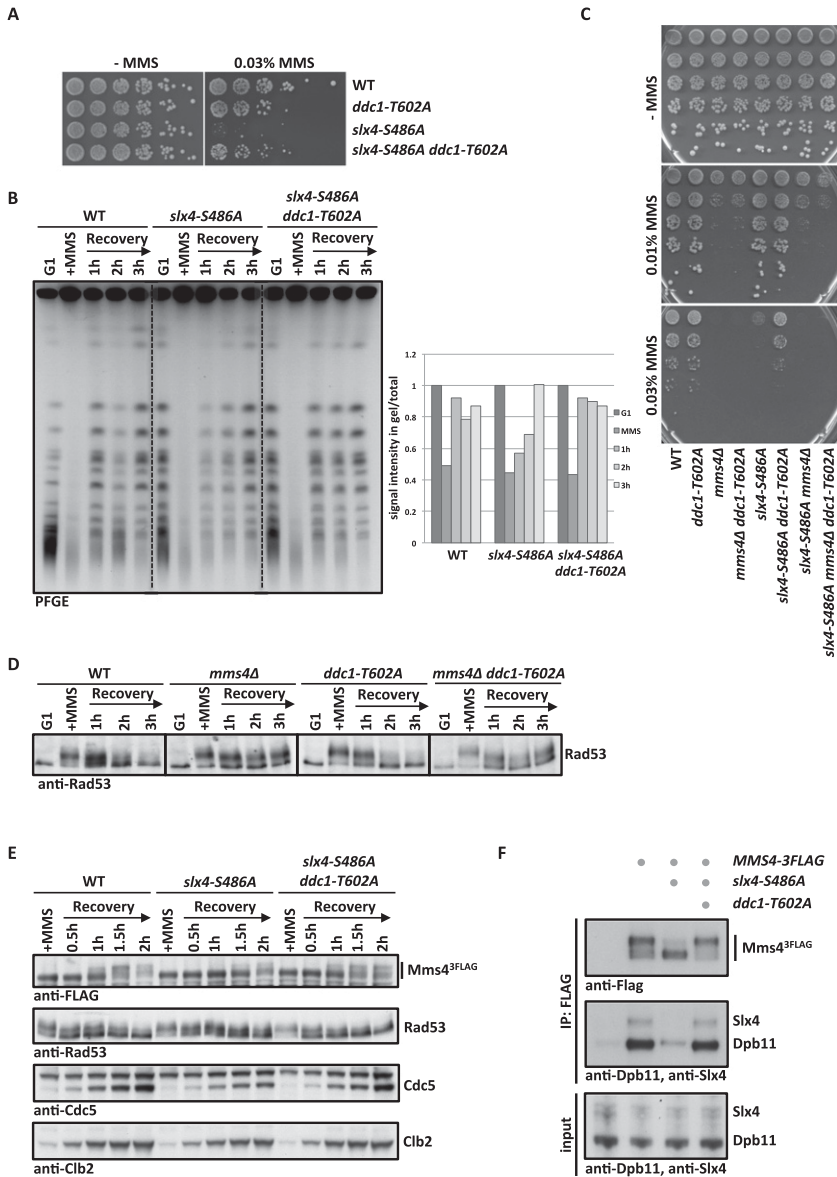


**Figure 6.** Partial inactivation of the DNA damage checkpoint rescues *slx4-S486A* phenotypes in an *MMS4*-dependent manner. (A) The DNA damage checkpoint defect of *slx4-S486A* is suppressed by partial inactivation of the DNA damage checkpoint. Wild type (WT), *slx4-S486A*, the partial checkpoint mutant *ddc1-T602A*, and the *slx4-S486A ddc1-T602A* double mutant were spotted in fivefold serial dilutions on MMS-containing plates. (B) The prolonged replication fork stalling of the *slx4-S486A* mutant is rescued by the *ddc1-T602A* mutation. Cells were cell cycle-synchronized and treated with a 30-min pulse of 0.033% MMS in S phase. Recovery of fully replicated chromosomes was analyzed by pulsed-field gel electrophoresis. Quantification as in Figure 3D. (C) A complete defect in Mus81 activity (*mms4Δ*) cannot be rescued by checkpoint inactivation. The MMS hypersensitivity phenotypes of *slx4-S486A*, *mms4Δ*, and *ddc1-T602A* mutants and double and triple mutant combinations were analyzed as in A. (D) The checkpoint recovery defect of *mms4Δ* mutants is not rescued by a partial checkpoint mutant. Cells were treated as in B, and checkpoint activity was measured by Rad53 phosphorylation. (E,F) Cdc5-dependent hyperphosphorylation of Mms4 and concomitant binding to Dpb11 and Slx4 occur earlier during recovery from replication fork stalling in *slx4-S486A ddc1-T602A* double mutants compared with *slx4-S486A* mutants. (E) Cells were treated with a 40-min pulse of 0.033% MMS in S phase. The Cdc5-dependent Mms4<sup>3FLAG</sup> phosphorylation shift was measured by anti-Flag Western blot, checkpoint activity was measured by Rad53 phosphorylation, and cell cycle progression was followed by anti-Clb2 and anti-Cdc5 Westerns. (F) Wild-type, *slx4-S486A*, and *slx4-S486A ddc1-T602A* cells that contain MMS4<sup>3FLAG</sup> were harvested during the recovery phase (2.5 h after MMS removal) and subjected to anti-Flag immunoprecipitation. Coimmunoprecipitation samples were tested for binding to Dpb11 and Slx4.

Mus81 complex. Such compensation may occur by either a direct up-regulation of the Slx4–Dpb11–Mms4–Mus81 complex or hyperactivation of a Mus81-independent salvage pathway. We therefore tested whether the observed rescue would depend on Mms4. Consistent with a direct influence of the checkpoint on the Slx4–Dpb11–Mms4–Mus81 complex, a partial inactivation of the checkpoint did not rescue the MMS hypersensitivity of the *mms4Δ* or *mms4Δ slx4-S486A* mutants (Fig. 6C). In contrast, the *sgs1Δ slx4-S486A* or *yen1Δ slx4-S486A* double mutants could be rescued by additional mutation of *ddc1-T602A* (Supplemental Fig. S10C), suggesting that neither STR nor Yen1 activity is required for the rescue. Furthermore, *mms4Δ ddc1-T602A* mutants show a slow checkpoint recovery after a pulse of MMS in S phase that is similar to *mms4Δ* cells (Fig. 6D). These results suggest that the

rescue of *slx4-S486A* mutants upon partial checkpoint inactivation is due to the action of Mms4–Mus81.

Furthermore, when we transiently exposed cells to MMS during S phase and released them into a G2/M arrest, we observed that the Cdc5-dependent phosphorylation shift of Mms4, which in this experiment serves as a marker for the interaction with Slx4–Dpb11, was slightly delayed in *slx4-S486A* cells compared with wild-type cells (Fig. 6E), probably because of a slower S-phase progression (see Fig. 3C). Importantly, the additional partial inactivation of the checkpoint (*slx4-S486A ddc1-T602A*) (Fig. 6E,F) allowed Cdc5-dependent Mms4 phosphorylation to occur earlier. Concomitantly, the binding of Mms4 to Dpb11 and Slx4 was rescued by partial checkpoint inactivation when immunoprecipitations were performed during the recovery phase (Fig. 6F). The occurrence of Mms4 phosphorylation

in the two mutants inversely correlated with DNA damage checkpoint activation (Rad53 phosphorylation) (Fig. 6E). It needs to be emphasized that Slx4–Dpb11 interaction is reduced, but not abolished, in the *slx4-S486A* mutant (Figs. 1B, 3A). The results in Figure 6, E and F, therefore suggest that the Slx4–Dpb11–Mms4–Mus81 complex can form earlier and potentially to a larger extent in the *slx4-S486A ddc1-T602A* mutant compared with the *slx4-S486A* single mutant. This offers a straightforward explanation for the rescue of the *slx4-S486A* mutant phenotypes by partial inactivation of the DNA damage checkpoint.

Taken together, we therefore identified an intricate regulatory mechanism of the Mus81 endonuclease, which critically depends on the formation of an Slx4–Dpb11–Mms4–Mus81 complex. The formation of this complex is activated by cell cycle stage-specific signaling and antagonized by the DNA damage checkpoint. Remarkably, complex formation and the direct control of Mus81 catalytic activity occur with similar timing, at the G2/M transition (Fig. 7).

## Discussion

In this study, we describe a new facet of JM resolution following the bypass of DNA damage via template switch recombination. We describe a multiprotein complex containing Slx4, Dpb11, and Mus81–Mms4. This complex is cell cycle-controlled by at least two mechanisms: Cdk1-dependent phosphorylation of Slx4 and Cdc5-dependent phosphorylation of Mms4, and Dpb11 acts as a reader of both modifications. The conservation of the Slx4–Dpb11/TopBP1 interaction and its cell cycle regulation suggests that a similar complex may be involved in JM resolution in human cells. Importantly, the inhibition of Slx4 binding to Dpb11 causes phenotypes that are indicative of JM resolution defects, and we therefore infer that the association with Slx4 and Dpb11 promotes Mus81 function.

### Temporal regulation of the response to replication fork stalling

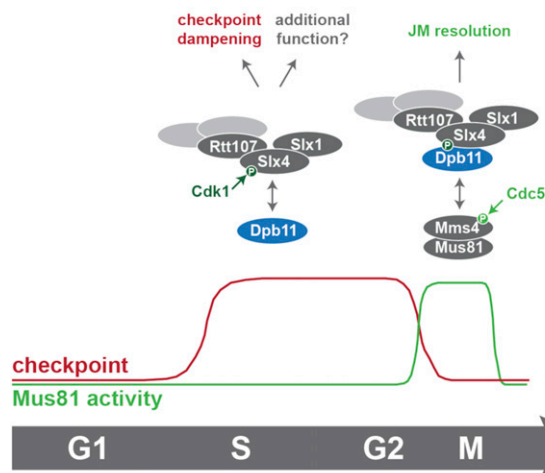


**Figure 7.** Model of the temporal response to replication fork stalling and its regulation by Slx4–Dpb11 complexes.

### *Slx4–Dpb11 multiprotein complex formation correlates with DNA JM resolution*

The starting point of our analysis was a multiprotein complex containing Slx4, Dpb11, Slx1, and Rtt107 (Ohouo et al. 2010, 2012). In order to characterize a putative function of this complex in DNA repair, we tested whether the Slx4–Dpb11 complex would transiently interact with DNA repair enzymes and found an interaction with the Mus81–Mms4 structure-specific endonuclease specifically in mitotic cells. Based on the findings that the *slx4-S486A* mutant impairs complex formation and results in JM resolution defects, we propose that the Slx4–Dpb11 complex regulates Mus81–Mms4 activity. Our binding studies furthermore indicate a direct Dpb11–Mms4 interaction. Given the nature of Dpb11 as a scaffold protein, it appears likely that Dpb11 operates by tethering Mus81 to other activities that collaborate in the resolution reaction or targeting Mus81 to JM structures.

An intricate feature of the Slx4–Dpb11 complex is its complexity, as it involves four scaffold proteins: Dpb11, Slx4, Rtt107, and Mms4. An obvious advantage of such a multiscaffold complex is that its formation depends on several interaction surfaces, which offer numerous possibilities for regulation. The assembly of the complex therefore allows the integration of different cellular signals (for example, cell cycle and DNA damage), or one specific signal may control complex assembly by several mechanisms. Such a setup includes features of multisite phosphorylation systems, which have the ability to create switch-like transitions (Nash et al. 2001). Moreover, a multiscaffold complex may allow the assembly and coordination of different enzymatic activities (see below).

Our work has identified Mus81 as one catalytically active component of the Slx4–Dpb11 complex; a second one could potentially be Slx1. Recently, the Mus81 and Slx1 endonucleases from humans and mice have been shown to cooperate in the resolution of Holliday junctions in an Slx4-dependent manner (Wyatt et al. 2013). While our results suggest that also in budding yeast, Mus81 and Slx1 may be part of the same complex, we did not observe any specific defects in the response to MMS-induced replication fork stalling for *slx1Δ* cells (Supplemental Fig. S6D). Therefore, we conclude that either Slx1 is not involved in Mus81-dependent JM resolution in budding yeast or a functionally redundant nuclease compensates for the defects of the *slx1Δ* mutant.

### *Cell cycle regulation of the response to replication fork stalling and JM resolution*

The cellular response to replication fork-stalling DNA lesions is intimately linked to the progression of the cell cycle. First, the primary problem, fork stalling, arises specifically in S phase. Moreover, the cells are required to finish the repair/bypass process at the latest in mitosis, when sister chromatids need to be accurately separated, and any remaining links between the chromatids have to be resolved.

In this study, we characterized two Dpb11 interactors: Slx4 and Mms4. Both proteins are phosphorylation tar-

gets of CDKs; however, Mms4 is additionally phosphorylated by the Polo-like kinase Cdc5 (Matos et al. 2011; Gallo-Fernández et al. 2012; Szakal and Branzei 2013). Interestingly, the Slx4–Dpb11 and Mms4–Dpb11 interactions display distinct cell cycle specificities: We observed a strong Slx4–Dpb11 interaction in asynchronous cultures as well as in S-phase and mitotic cells (Figs. 1C, 2C), while the Mms4–Dpb11 interaction was highly specific for mitosis (Fig. 5A). Accordingly, we found that the Mms4–Dpb11 interaction requires Cdc5, suggesting that Dpb11 can act as a reader of phosphorylation events that are initiated by different cell cycle kinases.

The cell cycle regulation of the Mus81–Mms4 association with the Slx4–Dpb11 complex correlates exactly with the known activity profile of Mus81 (Matos et al. 2011). Notably, the multiprotein complex is not the only mechanism of cell cycle regulation: Our *in vitro* resolution assays suggest that Cdc5 phosphorylation of Mus81–Mms4 directly stimulates Mus81 independently of complex formation. Therefore, we conclude that at least two parallel pathways of cell cycle regulation exist that promote appropriate Mus81 function in mitosis.

To date, it remains uncertain why cells restrict the activity of Mus81 until mitosis. The temporal regulation of Mus81 channels a large proportion of JMs into the Sgs1–Top3–Rmi1 dissolution pathway (Matos et al. 2011; Szakal and Branzei 2013). It has therefore been speculated that Sgs1-dependent dissolution, which leads to a NCO outcome (Ira et al. 2003), may be beneficial for cells dividing by a mitotic cell cycle. A second reason for restricting Mus81 activity may be the necessity to achieve temporal separation of the lesion bypass reaction and the JM resolution reaction (Saugar et al. 2013). Mus81 could impede the bypass reaction, given its relatively broad substrate specificity to a range of DNA structures (e.g., replication forks, D-loop structures, and Holliday junctions).

Intriguingly, the differences in the temporal regulation of the Slx4–Dpb11 and Mms4–Dpb11 interactions suggest that the composition of the Slx4–Dpb11 complex changes from the replication-associated template switch to the resolution reaction. Supporting the idea of several distinct Slx4–Dpb11 complexes is the fact that not all features of the Slx4–Dpb11 interaction (for example, enhanced binding after DNA damage) are seen in the Slx4–Dpb11–Mms4–Mus81 complex. It therefore appears plausible that Slx4–Dpb11 may associate with stalled replication forks already in S phase, while Mus81–Mms4 joins the complex in mitosis. It is tempting to speculate that the Slx4–Dpb11 complex may chaperone the DNA lesion site/repair intermediates until resolution (Fig. 7).

#### *Regulation of JM resolution by the DNA damage checkpoint*

The DNA damage checkpoint antagonizes JM resolution by Mus81 (Fig. 6; Szakal and Branzei 2013), and it has been suggested that Slx4 may act as negative regulator (“dampener”) of the checkpoint by competing with binding of the checkpoint mediator Rad9 to Dpb11 (Ohouo et al. 2012). The JM resolution phenotypes of the *slx4-S486A* mutant

could therefore, in principle, be explained by an indirect effect arising from checkpoint hyperactivation. Given the extensive ties between checkpoint and DNA repair pathways, the presented *in vivo* experiments cannot rule out a contribution of checkpoint misregulation to the observed JM resolution phenotypes.

We favor, however, a more direct role of Slx4 and Dpb11 in JM resolution for two reasons. First, the formation of the Slx4–Dpb11–Mms4–Mus81 complex and its regulation correlate with the temporal activation of Mus81. Second, the “dampener” model cannot account for all observed phenotypes. For example, the rescue of the MMS hypersensitivity of the *slx4-S486A* mutant by a covalent fusion with Dpb11 cannot be explained by competition, since in the fusion mutant, cells express two copies of full-length Dpb11 (one endogenous, one fused to Slx4), and therefore even more Dpb11 molecules (not less) are able to engage in checkpoint signaling complexes. Moreover, our analysis of RPA foci suggests that DNA lesions or repair intermediates persist and accumulate in the absence of a functional Slx4–Dpb11 complex, indicative of a role for Slx4 and Dpb11 in DNA repair.

Importantly, we found that the checkpoint regulates the formation of the Slx4–Dpb11–Mms4–Mus81 complex: Partial inhibition of the checkpoint enables Cdc5-dependent hyperphosphorylation of Mms4, which allows Dpb11 binding to occur earlier during the recovery from an MMS pulse and thereby reverses the effect of the *slx4* mutant. These findings suggest that at least in the *slx4-S486A* mutant background, the DNA damage checkpoint antagonizes the Slx4–Dpb11–Mms4–Mus81 complex. Partial inactivation of the checkpoint may therefore extend the temporal window during which Mus81 is active, which we propose to be beneficial in mutants with reduced JM resolution activity such as *slx4-S486A*. Whether this inhibitory mechanism takes place on the level of Cdc5 regulation in general (Zhang et al. 2009; Matos et al. 2013) or by specifically regulating Mms4 phosphorylation by Cdc5 remains to be determined. The important implication of this finding is that the activation of Mus81 is temporally restricted by two pathways: activation by cell cycle kinases and inhibition by the DNA damage checkpoint.

#### *The Slx4–Dpb11 complex is conserved among eukaryotes*

In addition to the mechanistic studies of the budding yeast Slx4–Dpb11 complex, we also provide the first evidence that at least parts of this complex may be found in human cells as well, since Slx4 and TopBP1 interact in a manner that depends on CDK phosphorylation of Slx4. It is worth noting that not all aspects of the protein network that controls resolution of JMs are conserved through evolution: While in human cells, Slx4 binds directly to Mus81–Eme1, this interaction appears to be absent in budding yeast (Fekairi et al. 2009; Muñoz et al. 2009; Svendsen et al. 2009; Schwartz et al. 2012). Given that both Slx4 and Mms4 bind to Dpb11, our data suggest that Dpb11 may serve as a bridge between the two proteins. Although a direct interaction between Slx4 and Mus81–Mms4 cannot be definitively

excluded, it appears as if the bridging interaction with Dpb11 in yeast may replace the direct interaction of Slx4 and Mus81 in human cells. Importantly, similar to our results in yeast, a stimulation of Slx4 binding to Mus81–Eme1 after phosphorylation by CDK and Polo-like kinase was observed in mitotic human cells as well (Wyatt et al. 2013). At this point, it seems therefore very likely that in both systems, JM resolution is promoted by a cell cycle-regulated complex containing several scaffold proteins.

## Materials and methods

### Yeast strains

All yeast strains are based on W303. Genotypes are listed in Supplemental Material.

### Interaction assays

Coimmunoprecipitations of yeast extracts were performed using anti-Flag agarose resin (Sigma). Bound proteins were eluted with 3× Flag-peptide (Sigma).

For GST pull-downs, GST-Dpb11 or GST-tagged protein fragments were recombinantly expressed and purified as described (Pfander and Diffley 2011). Pull-downs were performed with ammonium sulphate-precipitated (57%) yeast extracts on glutathione sepharose 4B (GE Healthcare).

For coimmunoprecipitations from HEK293T, GFP-tagged proteins were transiently overexpressed and precipitated using GFP-Trap magnetic beads (Chromotek).

### Nuclease activity assays

Nuclease assays on Mms4<sup>3Flag</sup> immunoprecipitations were done as described (Matos et al. 2011).

### DNA gel electrophoresis

PFGE and 2D gel analysis of DNA intermediates were performed as previously described (Karras and Jentsch 2010; Szakal and Branzei 2013).

### Mutation and recombination assays

Mutation rates were determined using a *CAN1* forward mutation assay. Interchromosomal recombination rates were determined using a direct repeat system using *leu2* heteroalleles (Aguilera and Klein 1988). CO rates were determined using a system harboring two *arg4* alleles on chromosome V and VIII (Robert et al. 2006; Szakal and Branzei 2013). In all, rates were determined by fluctuation analysis using a maximum likelihood approximation (Pfander et al. 2005).

### Microscopy and immunofluorescence

Microscopy experiments were carried out as described (Germann et al. 2014).

A detailed methods description is provided in the Supplemental Material.

## Acknowledgments

We thank U. Kagerer for excellent technical assistance, and C. Biertümpfel, J. Diffley, and H. Klein for providing plasmids, strains, and antibodies. We are grateful to Z. Storchova for help

with microscopy analysis of RPA foci and thank S. Jentsch, M. Räschele, Z. Storchova, and members of the Jentsch and Pfander laboratories for stimulating discussion and critical reading of the manuscript. We thank the Max-Planck Institute of Biochemistry core facility for MS analysis. This work was supported by the Max-Planck Society and the German Research Council (Deutsche Forschungsgemeinschaft) to B.P.; the European Research Council, the Italian Association for International Cancer Research, and The Italian Foundation for Cancer Research (FIRC) to D.B.; and the Danish Agency for Science, Technology, and Innovation, the Villum Kann Rasmussen Foundation, the Lundbeck Foundation, and the European Research Council to M.L. S.C.S.B. is supported by a fellowship from the German Chemical Industry Association (VCI). B.S and D.B. performed the 2D gel experiments of Figure 4A and Supplemental Figure S6A–C and analyzed the data. M.L. performed the imaging experiments of Figure 4E and Supplemental Figure S7 and analyzed the data. J.M. performed the in vitro nuclease assays of Figure 5E and Supplemental Figure S9E and analyzed the data. B.H.H. did the bioinformatics analysis of Supplemental Figure S2. All other experiments were performed and analyzed by D.G., L.N.P., S.C.S.B, L.W., S.S., and B.P. B.P. wrote the paper, and all authors commented on the manuscript.

## References

- Aguilera A, Klein HL. 1988. Genetic control of intrachromosomal recombination in *Saccharomyces cerevisiae*. I. Isolation and genetic characterization of hyper-recombination mutations. *Genetics* **119**: 779–790.
- Bishop AC, Ubersax JA, Petsch DT, Matheos DP, Gray NS, Blethrow J, Shimizu E, Tsien JZ, Schultz PG, Rose MD, et al. 2000. A chemical switch for inhibitor-sensitive alleles of any protein kinase. *Nature* **407**: 395–401.
- Blanco MG, Matos J, Rass U, Ip SCY, West SC. 2010. Functional overlap between the structure-specific nucleases Yen1 and Mus81–Mms4 for DNA-damage repair in *S. cerevisiae*. *DNA Repair (Amst)* **9**: 394–402.
- Branzei D, Foiani M. 2010. Maintaining genome stability at the replication fork. *Nat Rev Mol Cell Biol* **11**: 208–219.
- Branzei D, Vanoli F, Foiani M. 2008. SUMOylation regulates Rad18-mediated template switch. *Nature* **456**: 915–920.
- Cejka P, Plank JL, Bachrati CZ, Hickson ID, Kowalczykowski SC. 2010. Rmi1 stimulates decatenation of double Holliday junctions during dissolution by Sgs1–Top3. *Nat Struct Mol Biol* **17**: 1377–1382.
- Chan K-L, North PS, Hickson ID. 2007. BLM is required for faithful chromosome segregation and its localization defines a class of ultrafine anaphase bridges. *EMBO J* **26**: 3397–3409.
- Cordon-Preciado V, Ufano S, Bueno A. 2006. Limiting amounts of budding yeast Rad53 S-phase checkpoint activity results in increased resistance to DNA alkylation damage. *Nucleic Acids Res* **34**: 5852–5862.
- Coulon S. 2006. Rad22Rad52-dependent repair of ribosomal DNA repeats cleaved by Slx1–Slx4 endonuclease. *Mol Biol Cell* **17**: 2081–2090.
- Fekairi S, Scaglione S, Chahwan C, Taylor ER, Tissier A, Coulon S, Dong M-Q, Ruse C, Yates JR, Russell P, et al. 2009. Human SLX4 is a Holliday junction resolvase subunit that binds multiple DNA repair/recombination endonucleases. *Cell* **138**: 78–89.
- Flott S, Alabert C, Toh GW, Toth R, Sugawara N, Campbell DG, Haber JE, Pasero P, Rouse J. 2007. Phosphorylation of Slx4 by Mec1 and Tel1 regulates the single-strand annealing mode of DNA repair in budding yeast. *Mol Cell Biol* **27**: 6433–6445.

- Fricke WM, Brill SJ. 2003. Slx1–Slx4 is a second structure-specific endonuclease functionally redundant with Sgs1–Top3. *Genes Dev* **17**: 1768–1778.
- Gaillard P-HL, Noguchi E, Shanahan P, Russell P. 2003. The endogenous Mus81–Eme1 complex resolves Holliday junctions by a nick and counternick mechanism. *Mol Cell* **12**: 747–759.
- Gallo-Fernández M, Saugar I, Ortiz-Bazán MÁ, Vázquez MV, Tercero JA. 2012. Cell cycle-dependent regulation of the nuclease activity of Mus81–Eme1/Mms4. *Nucleic Acids Res* **40**: 8325–8335.
- García V, Furuya K, Carr AM. 2005. Identification and functional analysis of TopBP1 and its homologs. *DNA Repair (Amst)* **4**: 1227–1239.
- Germann SM, Oestergaard VH, Haas C, Salis P, Motegi A, Lisby M. 2011. Dpb11/TopBP1 plays distinct roles in DNA replication, checkpoint response and homologous recombination. *DNA Repair (Amst)* **10**: 210–224.
- Germann SM, Schramke V, Pedersen RT, Gallina I, Eckert-Boulet N, Oestergaard VH, Lisby M. 2014. TopBP1/Dpb11 binds DNA anaphase bridges to prevent genome instability. *J Cell Biol* **204**: 45–59.
- Giannattasio M, Lazzaro F, Plevani P, Muzi-Falconi M. 2005. The DNA damage checkpoint response requires histone H2B ubiquitination by Rad6–Bre1 and H3 methylation by Dot1. *J Biol Chem* **280**: 9879–9886.
- Harrison JC, Haber JE. 2006. Surviving the breakup: the DNA damage checkpoint. *Annu Rev Genet* **40**: 209–235.
- Ho CK, Mazón G, Lam AF, Symington LS. 2010. Mus81 and Yen1 promote reciprocal exchange during mitotic recombination to maintain genome integrity in budding yeast. *Mol Cell* **40**: 988–1000.
- Holt LJ, Tuch BB, Villén J, Johnson AD, Gygi SP, Morgan DO. 2009. Global analysis of Cdk1 substrate phosphorylation sites provides insights into evolution. *Science* **325**: 1682–1686.
- Interthal H, Heyer WD. 2000. MUS81 encodes a novel helix–hairpin–helix protein involved in the response to UV- and methylation-induced DNA damage in *Saccharomyces cerevisiae*. *Mol Gen Genet* **263**: 812–827.
- Ip SCY, Rass U, Blanco MG, Flynn HR, Skehel JM, West SC. 2008. Identification of Holliday junction resolvases from humans and yeast. *Nature* **456**: 357–361.
- Ira G, Malkova A, Liberi G, Foiani M, Haber JE. 2003. Srs2 and Sgs1–Top3 suppress crossovers during double-strand break repair in yeast. *Cell* **115**: 401–411.
- Karras GI, Jentsch S. 2010. The RAD6 DNA damage tolerance pathway operates uncoupled from the replication fork and is functional beyond S phase. *Cell* **141**: 255–267.
- Li M, Brill SJ. 2005. Roles of SGS1, MUS81, and RAD51 in the repair of lagging-strand replication defects in *Saccharomyces cerevisiae*. *Curr Genet* **48**: 213–225.
- Liberi G, Maffioletti G, Lucca C, Chiolo I, Baryshnikova A, Cotta-Ramusino C, Lopes M, Pelliccioli A, Haber JE, Foiani M. 2005. Rad51-dependent DNA structures accumulate at damaged replication forks in sgs1 mutants defective in the yeast ortholog of BLM RecQ helicase. *Genes Dev* **19**: 339–350.
- Mankouri HW, Ashton TM, Hickson ID. 2011. Holliday junction-containing DNA structures persist in cells lacking Sgs1 or Top3 following exposure to DNA damage. *Proc Natl Acad Sci* **108**: 4944–4949.
- Mankouri HW, Huttner D, Hickson ID. 2013. How unfinished business from S-phase affects mitosis and beyond. *EMBO J* **32**: 2661–2671.
- Matos J, Blanco MG, Maslen S, Skehel JM, West SC. 2011. Regulatory control of the resolution of DNA recombination intermediates during meiosis and mitosis. *Cell* **147**: 158–172.
- Matos J, Blanco MG, West SC. 2013. Cell-cycle kinases coordinate the resolution of recombination intermediates with chromosome segregation. *Cell Rep* 1–11.
- Mordes DA, Nam EA, Cortez D. 2008. Dpb11 activates the Mec1–Ddc2 complex. *Proc Natl Acad Sci* **105**: 18730–18734.
- Mullen JR, Kaliraman V, Ibrahim SS, Brill SJ. 2001. Requirement for three novel protein complexes in the absence of the Sgs1 DNA helicase in *Saccharomyces cerevisiae*. *Genetics* **157**: 103–118.
- Muñoz IM, Hain K, Déclais A-C, Gardiner M, Toh GW, Sanchez-Pulido L, Heuckmann JM, Toth R, Macartney T, Eppink B, et al. 2009. Coordination of structure-specific nucleases by human SLX4/BTBD12 is required for DNA repair. *Mol Cell* **35**: 116–127.
- Nash P, Tang X, Orlicky S, Chen Q, Gertler FB, Mendenhall MD, Sicheri F, Pawson T, Tyers M. 2001. Multisite phosphorylation of a CDK inhibitor sets a threshold for the onset of DNA replication. *Nature* **414**: 514–521.
- Navadgi-Patil VM, Burgers PM. 2008. Yeast DNA replication protein Dpb11 activates the Mec1/ATR checkpoint kinase. *J Biol Chem* **283**: 35853–35859.
- Ohou PY, Bastos de Oliveira FM, Almeida BS, Smolka MB. 2010. DNA damage signaling recruits the Rtt107–Slx4 scaffolds via Dpb11 to mediate replication stress response. *Mol Cell* **39**: 300–306.
- Ohou PY, de Oliveira FMB, Liu Y, Ma CJ, Smolka MB. 2012. DNA-repair scaffolds dampen checkpoint signalling by counteracting the adaptor Rad9. *Nature* **493**: 120–124.
- Pfander B, Diffley JFX. 2011. Dpb11 coordinates Mec1 kinase activation with cell cycle-regulated Rad9 recruitment. *EMBO J* **30**: 4897–4907.
- Pfander B, Moldovan GL, Sacher M, Hoegge C, Jentsch S. 2005. SUMO-modified PCNA recruits Srs2 to prevent recombination during S phase. *Nature* **436**: 428–433.
- Prakash S, Johnson RE, Prakash L. 2005. Eukaryotic translesion synthesis DNA polymerases: specificity of structure and function. *Annu Rev Biochem* **74**: 317–353.
- Puddu F, Granata M, Di Nola L, Balestrini A, Piergiovanni G, Lazzaro F, Giannattasio M, Plevani P, Muzi-Falconi M. 2008. Phosphorylation of the budding yeast 9-1-1 complex is required for Dpb11 function in the full activation of the UV-induced DNA damage checkpoint. *Mol Cell Biol* **28**: 4782–4793.
- Rappas M, Oliver AW, Pearl LH. 2011. Structure and function of the Rad9-binding region of the DNA-damage checkpoint adaptor TopBP1. *Nucleic Acids Res* **39**: 313–324.
- Robert T, Dervins D, Fabre F, Gangloff S. 2006. Mrc1 and Srs2 are major actors in the regulation of spontaneous crossover. *EMBO J* **25**: 2837–2846.
- Roberts TM, Kobor MS, Bastin-Shanower SA, Ii M, Horte SA, Gin JW, Emili A, Rine J, Brill SJ, Brown GW. 2006. Slx4 regulates DNA damage checkpoint-dependent phosphorylation of the BRCT domain protein Rtt107/Esc4. *Mol Biol Cell* **17**: 539–548.
- Saugar I, Vazquez MV, Gallo-Fernandez M, Ortiz-Bazan MA, Segurado M, Calzada A, Tercero JA. 2013. Temporal regulation of the Mus81–Mms4 endonuclease ensures cell survival under conditions of DNA damage. *Nucleic Acids Res* **41**: 8943–8958.
- Schwartz EK, Wright WD, Ehmsen KT, Evans JE, Stahlberg H, Heyer WD. 2012. Mus81–Mms4 functions as a single heterodimer to cleave nicked intermediates in recombinational DNA repair. *Mol Cell Biol* **32**: 3065–3080.
- Snead JL, Sullivan M, Lowery DM, Cohen MS, Zhang C, Randle DH, Taunton J, Yaffe MB, Morgan DO, Shokat KM. 2007. A coupled chemical-genetic and bioinformatic approach to

- Polo-like kinase pathway exploration. *Chem Biol* **14**: 1261–1272.
- Svendsen JM, Smogorzewska A, Sowa ME, O'Connell BC, Gygi SP, Elledge SJ, Harper JW. 2009. Mammalian BTBD12/SLX4 assembles a Holliday junction resolvase and is required for DNA repair. *Cell* **138**: 63–77.
- Szakal B, Branzei D. 2013. Premature Cdk1/Cdc5/Mus81 pathway activation induces aberrant replication and deleterious crossover. *EMBO J* **32**: 1155–1167.
- Tanaka S, Umemori T, Hirai K, Muramatsu S, Kamimura Y, Araki H. 2007. CDK-dependent phosphorylation of Sld2 and Sld3 initiates DNA replication in budding yeast. *Nature* **445**: 328–332.
- Tomkinson AE, Bardwell AJ, Bardwell L, Tappe NJ, Friedberg EC. 1993. Yeast DNA repair and recombination proteins Rad1 and Rad10 constitute a single-stranded-DNA endonuclease. *Nature* **362**: 860–862.
- Wyatt HDM, Sarbajna S, Matos J, West SC. 2013. Coordinated actions of SLX1–SLX4 and MUS81–EME1 for Holliday junction resolution in human cells. *Mol Cell* **52**: 234–247.
- Yu X. 2003. The BRCT domain is a phospho-protein binding domain. *Science* **302**: 639–642.
- Zegerman P, Diffley JFX. 2007. Phosphorylation of Sld2 and Sld3 by cyclin-dependent kinases promotes DNA replication in budding yeast. *Nature* **445**: 281–285.
- Zhang T, Nirantar S, Lim HH, Sinha I, Surana U. 2009. DNA damage checkpoint maintains Cdh1 in an active state to inhibit anaphase progression. *Dev Cell* **17**: 541–551.

- B. Princz LN, Wild P, Bittmann J, Aguado FJ, Blanco MG, Matos J, Pfander B (2017)**

**Dbf4-dependent kinase and the Rtt107 scaffold promote Mus81-Mms4 resolvase activation during mitosis**

***EMBO J* 36(5):664-678**

# Dbf4-dependent kinase and the Rtt107 scaffold promote Mus81-Mms4 resolvase activation during mitosis

Lissa N Princz<sup>1</sup>, Philipp Wild<sup>2</sup>, Julia Bittmann<sup>1</sup>, F Javier Aguado<sup>3</sup>, Miguel G Blanco<sup>3</sup> , Joao Matos<sup>2</sup> & Boris Pfander<sup>1,\*</sup> 

## Abstract

DNA repair by homologous recombination is under stringent cell cycle control. This includes the last step of the reaction, disentanglement of DNA joint molecules (JMs). Previous work has established that JM resolving nucleases are activated specifically at the onset of mitosis. In case of budding yeast Mus81-Mms4, this cell cycle stage-specific activation is known to depend on phosphorylation by CDK and Cdc5 kinases. Here, we show that a third cell cycle kinase, Cdc7-Dbf4 (DDK), targets Mus81-Mms4 in conjunction with Cdc5—both kinases bind to as well as phosphorylate Mus81-Mms4 in an interdependent manner. Moreover, DDK-mediated phosphorylation of Mms4 is strictly required for Mus81 activation in mitosis, establishing DDK as a novel regulator of homologous recombination. The scaffold protein Rtt107, which binds the Mus81-Mms4 complex, interacts with Cdc7 and thereby targets DDK and Cdc5 to the complex enabling full Mus81 activation. Therefore, Mus81 activation in mitosis involves at least three cell cycle kinases, CDK, Cdc5 and DDK. Furthermore, tethering of the kinases in a stable complex with Mus81 is critical for efficient JM resolution.

**Keywords** cell cycle; genome stability; homologous recombination; joint molecule resolution; post-translational modification

**Subject Categories** Cell Cycle; DNA Replication, Repair & Recombination

**DOI** 10.15252/embj.201694831 | Received 22 May 2016 | Revised 15 December 2016 | Accepted 19 December 2016 | Published online 18 January 2017

**The EMBO Journal (2017) 36: 664–678**

## Introduction

Many DNA transactions are under cell cycle control to adjust them to cell cycle phase-specific features of chromosomes (Branzei & Foiani, 2008). Homologous recombination (HR) is cell cycle-regulated at several steps including the first, DNA end resection, and the

last, JM removal (Heyer *et al*, 2010; Ferretti *et al*, 2013; Mathiasen & Lisby, 2014; Matos & West, 2014). Given that JMs provide stable linkages between sister chromatids, they will interfere with chromosome segregation and therefore need to be disentangled before sister chromatid separation during mitosis. Accordingly, JM resolvases, such as budding yeast Mus81-Mms4 (Interthal & Heyer, 2000; Schwartz *et al*, 2012) or Yen1 (Ip *et al*, 2008), become activated during mitosis (Matos *et al*, 2011, 2013; Gallo-Fernández *et al*, 2012; Szakal & Branzei, 2013; Blanco *et al*, 2014; Eissler *et al*, 2014). In contrast, the alternative JM removal pathway, JM dissolution by the Sgs1-Top3-Rmi1 complex, is thought to be constantly active throughout the cell cycle (Mankouri *et al*, 2013; Bizard & Hickson, 2014). The activation of JM resolvases in mitosis therefore leads to a shift in the balance between JM removal pathways, with dissolution being preferred outside of mitosis, but JM resolution becoming increasingly important in mitosis (Matos *et al*, 2011, 2013; Gallo-Fernández *et al*, 2012; Dehé *et al*, 2013; Saugar *et al*, 2013; Szakal & Branzei, 2013; Wyatt *et al*, 2013). It has been hypothesized that JM resolvases are downregulated at cell cycle stages other than mitosis in order to counteract crossover-induced loss of heterozygosity or to prevent over-active resolvases from interfering with S phase by, for example, cleaving stalled replication forks (Gallo-Fernández *et al*, 2012; Szakal & Branzei, 2013; Blanco *et al*, 2014).

Budding yeast Mus81-Mms4 has previously been shown to be targeted by two cell cycle kinases, cyclin-dependent kinase Cdc28 (CDK) and the yeast polo-kinase Cdc5 (Matos *et al*, 2011, 2013; Gallo-Fernández *et al*, 2012; Szakal & Branzei, 2013). The corresponding Mms4 phosphorylation events were shown to correlate with and to be required for activation of Mus81-Mms4 in mitosis. In 2014, we showed that in mitosis Mus81-Mms4 also forms a complex with Slx4-Slx1 and the scaffold proteins Dpb11 and Rtt107 (Gritenaite *et al*, 2014). Interestingly, mass spectrometric analysis of this complex (Gritenaite *et al*, 2014) revealed that Cdc5 and a third cell cycle kinase Dbf4-Cdc7 (Dbf4-dependent kinase, DDK) are also a stable part of this protein assembly (see Appendix Fig S1A). Here,

<sup>1</sup> Max Planck Institute of Biochemistry, DNA Replication and Genome Integrity, Martinsried, Germany

<sup>2</sup> Institute of Biochemistry, Eidgenössische Technische Hochschule, Zürich, Switzerland

<sup>3</sup> Department of Biochemistry and Molecular Biology, Center for Research in Molecular Medicine and Chronic Diseases, Universidade de Santiago de Compostela, Santiago de Compostela, Spain

\*Corresponding author. Tel: +49 89 85783050; Fax: +49 89 85783022; E-mail: bpfander@biochem.mpg.de

we investigate the role of DDK in Mus81-Mms4 regulation and find that DDK can phosphorylate Mms4 and that DDK and Cdc5 target Mus81-Mms4 in an interdependent manner. Moreover, we show that Rtt107 promotes the association of both kinases with the Mus81-Mms4 complex. The DDK-dependent regulation of Mus81-Mms4 is critical for Mus81 activity thus revealing DDK as a novel regulator of homologous recombination.

## Results

### Mus81-Mms4 is a DDK phosphorylation target

The cell cycle regulation of JM resolution by Mus81-Mms4 is intricate and involves phosphorylation by the cell cycle kinases CDK

and Cdc5 (Matos *et al*, 2011, 2013; Gallo-Fernández *et al*, 2012; Szakal & Branzei, 2013) as well as complex formation with the scaffold proteins Dpb11, Slx4 and Rtt107 (Gritenaite *et al*, 2014). To study this protein complex, we performed an analysis of Mms4<sup>3FLAG</sup> interactors in mitosis by SILAC-based quantitative mass spectrometry (Gritenaite *et al*, 2014) and found in addition to Dpb11, Slx4, Rtt107 and Cdc5, also Cdc7 and Dbf4 as specific interactors of Mms4 (Appendix Fig S1A). We verified that Cdc7 binds to Mus81-Mms4 in an Mms4<sup>3FLAG</sup> pull down from mitotic cells analysed by Western blots (Fig 1A). The fact that Mus81-Mms4 binds to DDK suggested that it might be involved in the phosphorylation cascade that occurs on Mms4 and controls Mus81 activity in mitosis. Accordingly, we found that purified DDK was able to phosphorylate both subunits of purified Mus81-Mms4 *in vitro* (Fig 1B, lane 3). When we furthermore compared the DDK-dependent

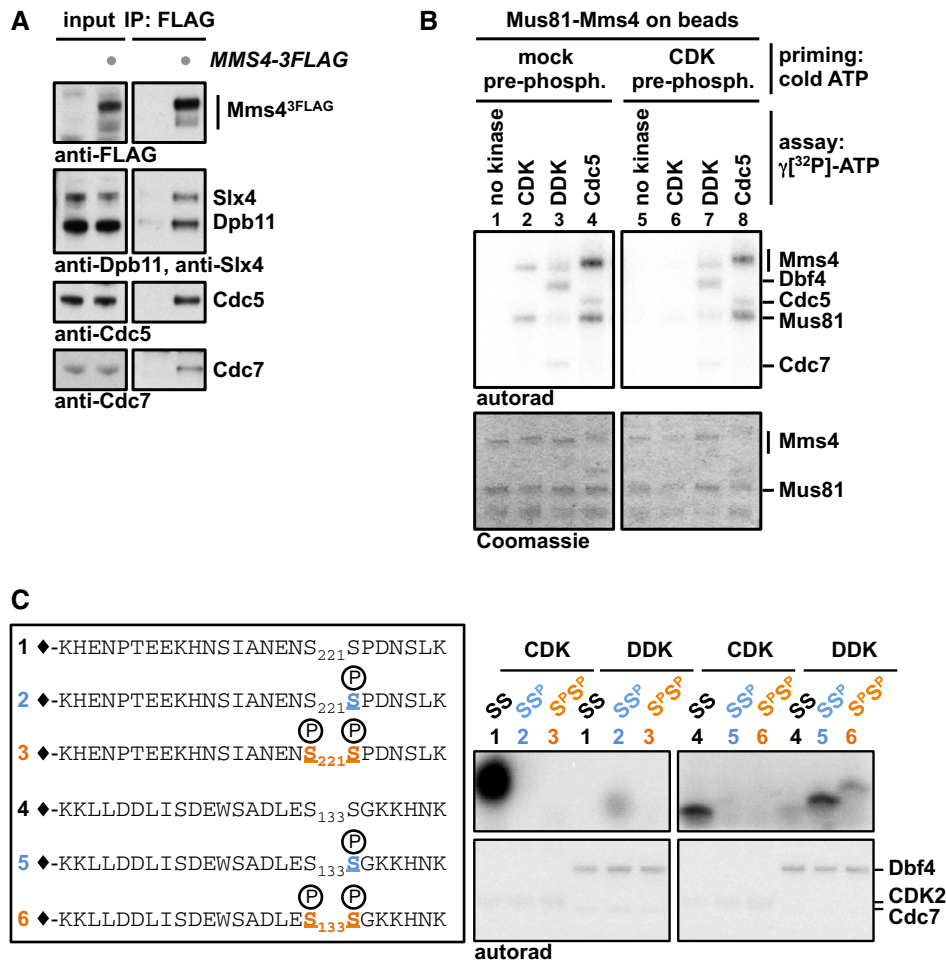


**Figure 1. Dbf4-dependent kinase (DDK) binds to the Mus81-Mms4 complex in mitosis and can phosphorylate Mms4 at (S/T)(S/T) motifs.**

A Cdc7 and Cdc5 are specifically enriched in Mms4<sup>3FLAG</sup> co-IPs from cells arrested in mitosis (with nocodazole). Under the same conditions, Mus81-Mms4 associates with scaffold proteins such as Dpb11 and Slx4 (Appendix Fig S1A and Gritenaite *et al*, 2014).

B DDK can phosphorylate Mus81-Mms4 *in vitro*. Purified, immobilized Mus81-Mms4 is incubated in an *in vitro* kinase assay with purified CDK2/cycA<sup>N170</sup> (a model CDK), DDK or Cdc5 (lanes 1–4). Additionally, Mus81-Mms4 is incubated with respective kinases after a non-radioactive priming step with CDK (lanes 5–8).

C DDK phosphorylates Mms4 peptides at (S/T)(S/T) motifs and is enhanced by priming phosphorylation. Mms4 peptides including (S/T)(S/T) motifs (221/222; 133/134) were synthesized in different phosphorylation states (depicted in left panel) and incubated in an *in vitro* kinase assay with either CDK or DDK. CDK targets unphosphorylated Mms4 peptides 1 and (to a weaker extent) 4 consistent with its substrate specificity (Mok *et al*, 2010), while DDK primarily targets Mms4 peptides 2 and 5, which harbour a priming phosphorylation at the C-terminal (S/T) site (see Appendix Fig S1B for in-gel running behaviour of peptides).

phosphorylation signal to Mms4 phosphorylation by CDK and Cdc5 (Fig 1B, lanes 2–4), we observed different degrees of phosphorylation shifts indicating that the three kinases phosphorylate Mms4 at distinct sites and/or to different degrees. DDK target sites on other proteins have been studied in detail, and in several cases, DDK was found to target (S/T)(S/T) motifs, where phosphorylation was stimulated by a priming phosphorylation usually on the second (S/T) (Masai *et al*, 2006; Montagnoli *et al*, 2006; Randell *et al*, 2010; Lyons *et al*, 2013). Intriguingly, Mms4 contains 15 of these motifs and we therefore tested whether these could be targeted by DDK and would depend on priming phosphorylation. We therefore turned to a peptide-based assay where Mms4 phosphorylation states are precisely defined. To this end, we synthesized peptides corresponding to two (S/T)(S/T) motifs of Mms4. We chose two representative motifs: S222, as it harbours a minimal CDK consensus motif (S/T)P, and S134, as it contains a non-(S/T)P consensus for CDK [(S/T)X(K/R)(K/R) (Suzuki *et al*, 2015)]. For each of these motifs, we generated peptides in three different phosphorylation states: non-phosphorylated, phosphorylated at the second serine and doubly phosphorylated (Fig 1C and Appendix Fig S1B). When using such peptides as substrates in *in vitro* kinase reactions, we saw that CDK targeted specifically only the second serine in each peptide, although much stronger for S222 than for S134, consistent with these residues matching CDK consensus motifs (Fig 1C). In contrast, DDK showed only little activity towards the non-phosphorylated peptides, but was strongly stimulated when the second residue in the (S/T)(S/T) motif was in a phosphorylated state (Fig 1C). DDK may thus be stimulated by priming phosphorylation in order to efficiently phosphorylate Mms4 on (S/T)(S/T) sites. However, using the full-length protein as a phosphorylation substrate, we did not obtain evidence for a stimulatory effect on DDK by prior CDK phosphorylation (Fig 1B and Appendix Fig S1C), perhaps because over the whole 15 (S/T)(S/T) motifs CDK phosphorylation plays a minor role. We also did not reveal any priming activity of either CDK or DDK for Mms4 phosphorylation by Cdc5 (Fig 1B and Appendix Fig S1D). Overall, the data in Fig 1 thus identify Mus81-Mms4 as an interaction partner and potential substrate of DDK.

### Mus81-Mms4 is phosphorylated by a mitotic Cdc5-DDK complex

DDK is present and active throughout S phase and mitosis until anaphase when the Dbf4 subunit is degraded by APC/C<sup>Cdc20</sup> (Cheng *et al*, 1999; Weinreich & Stillman, 1999; Ferreira *et al*, 2000). We therefore tested at which cell cycle stage DDK would associate with Mus81-Mms4 using cells synchronously progressing through the cell cycle. Figure 2A shows that DDK did not associate with Mus81-Mms4 in S phase, but only once cells had reached mitosis. Strikingly, DDK binding therefore coincided with binding of Cdc5, Slx4 and Dpb11 and most notably the appearance of the hyperphosphorylated form of Mms4<sup>3FLAG</sup> (Fig 2A).

Given this late timing of the association, we tested in co-immunoprecipitation (co-IP) experiments whether DDK binding to Mus81-Mms4 would depend on CDK or Cdc5 activity. Using analog-sensitive mutant yeast strains for CDK [*cdc28-as1* (Bishop *et al*, 2000)] and for Cdc5 [*cdc5-as1* (Snead *et al*, 2007)], we observed that inhibition of these kinases in mitotically arrested cells strongly reduced the hyperphosphorylation shift of Mms4 (see also Matos

*et al*, 2013) and compromised the association with DDK (Fig 2B and C, and Appendix Fig S2A–C). Notably, both conditions also interfered with Cdc5 binding (Fig 2B and C, and Appendix Fig S2A), suggesting that the association of DDK may follow a similar regulation as Cdc5.

Next, we tested whether conversely DDK is involved in Mms4 phosphorylation. To bypass the essential function of DDK in DNA replication, we used the *mcm5<sup>bob1-1</sup>* allele (Hardy *et al*, 1997), which allowed us to test a *cdc7Δ* mutant. Using Western blot and SILAC-based mass spectrometry as a read-out of Mms4<sup>3FLAG</sup> co-IPs from cells arrested in mitosis, we found that Cdc5 association with Mus81-Mms4 was strongly reduced in the *cdc7Δ* mutant strain (Fig 2D and E). Moreover, we observed that Mms4<sup>3FLAG</sup> phosphorylation as indicated by mobility shift was decreased in the absence of DDK, although not to the same extent as upon CDK or Cdc5 inhibition (Fig 2D and Appendix Fig S2C). Additionally, as an alternative way to deregulate DDK, we used the *cdc7-1* temperature-sensitive mutant. Even with WT cells, we observed that elevated temperature (38°C) leads to a slight reduction in Cdc5 binding to Mus81-Mms4. However, in *cdc7-1* mutant cells, incubation at 38°C leads to the complete disappearance of Cdc5 binding to Mus81-Mms4 (Appendix Fig S2D). Therefore, we conclude from these data that DDK and Cdc5 bind to Mus81-Mms4 in an interdependent fashion.

Interestingly, Cdc5 was previously shown to interact with DDK via a non-consensus polo-box binding site within Dbf4 (Miller *et al*, 2009; Chen & Weinreich, 2010). The proposed model based on genetic experiments suggested that DDK binding antagonizes mitotic functions of Cdc5. However, the catalytic activity of Cdc5 was not inhibited in this complex (Miller *et al*, 2009) and we reason that DDK may simply target Cdc5 to a specific set of substrates. Since the Cdc5 binding site was mapped to the N-terminal portion of Dbf4 (Miller *et al*, 2009), we tested whether N-terminal truncations of Dbf4 would affect DDK or Cdc5 association with Mus81-Mms4. While the *dbf4-ΔN66* truncation lacking the first 66 amino acids (including a D-box motif) did not influence DDK or Cdc5 binding to Mms4<sup>3FLAG</sup>, the *dbf4-ΔN109* truncation, which additionally lacks the Cdc5 binding motif (Miller *et al*, 2009), showed strongly decreased DDK and Cdc5 binding to Mus81-Mms4 (Fig 2F). Additionally, also mitotic hyperphosphorylation of Mms4 was diminished when DDK and Cdc5 could not interact with each other (Fig 2F). Overall, these data strongly suggest that Cdc5 and DDK interact with and target Mus81-Mms4 in an interdependent manner. Furthermore, it is currently unclear whether collaboration of DDK and Cdc5 is a widespread phenomenon that may affect other Cdc5 substrates as well, given that mitotic phosphorylation of two candidate Cdc5 substrates, Ulp2 and Scc1 (Alexandru *et al*, 2001), was affected to varying degree by the *cdc7Δ* mutation (Appendix Fig S2E).

Given the known cell cycle regulation of Cdc5 and DDK (Shirayama *et al*, 1998; Cheng *et al*, 1999; Weinreich & Stillman, 1999; Ferreira *et al*, 2000; Mortensen *et al*, 2005), the limiting factor for the temporal regulation of this complex and its restriction to mitosis is expected to be Cdc5 and not DDK, which is present already throughout S phase. Consistently, we observed that forced expression of Cdc5 (using the galactose-inducible *GAL* promoter) in cells that were arrested in S phase by hydroxyurea (HU) led to the premature occurrence of Mms4

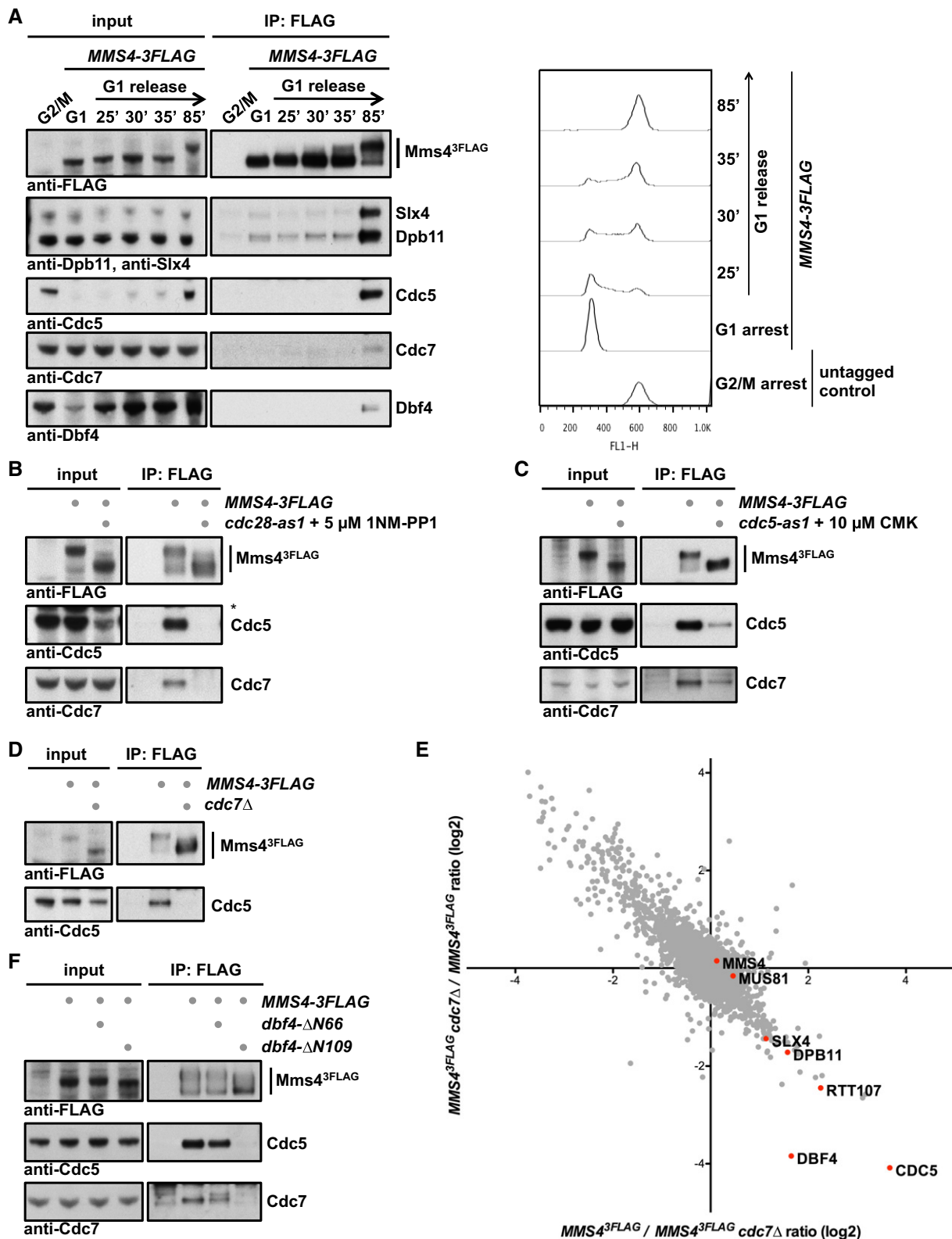


Figure 2.

hyperphosphorylation (Fig EV1A; Matos *et al*, 2013), suggesting that S-phase DDK is in principle competent for Cdc5 binding and joint substrate phosphorylation.

Furthermore, we performed additional experiments that addressed the regulation of Mus81-Mms4 by the DNA damage response. In M-phase-arrested cells, association of DDK and

**Figure 2. DDK and Cdc5 target Mus81-Mms4 in an interdependent manner.**

- A DDK stably associates with Mus81-Mms4 in mitosis, but not in S phase or G1. Mms4<sup>3FLAG</sup> pull down experiment (left panel, as in Fig 1A) from cells arrested in G1 (with alpha-factor) or in cells progressing synchronously through S phase until mitosis (arrest with nocodazole) reveals that DDK binds specifically in mitosis concomitant with the raise in Cdc5 levels and Cdc5 binding to Mus81-Mms4. A nocodazole-arrested untagged strain was used as a control. Right panel shows measurements of DNA content by FACS from the respective samples.
- B CDK activity is required for DDK and Cdc5 association with Mus81-Mms4. Mms4<sup>3FLAG</sup> pull down as in (A), but in mitotic WT or *cdc28-as1* mutant cells treated with 5  $\mu$ M 1NM-PP1 for 1 h. Additional Western blots of this experiment are shown in Appendix Fig S5B, including as a control the identical anti-FLAG Western blot.
- C Cdc5 activity is required for DDK association with Mus81-Mms4. Mms4<sup>3FLAG</sup> pull down as in (A), but with mitotically arrested WT or *cdc5-as1* mutant cells treated with 10  $\mu$ M CMK for 1 h.
- D, E DDK is required for Cdc5 binding to Mus81-Mms4 in mitosis and the mitotic Mms4 phospho-shift. (D) Mms4<sup>3FLAG</sup> pull down using mitotically arrested cells as in (A), but using a *bob1-1* background (all samples), where the DDK subunit Cdc7 could be deleted. (E) SILAC-based quantification of Mms4<sup>3FLAG</sup> pull downs in mitotically arrested *bob1-1* vs. *bob1-1 cdc7 $\Delta$*  cells. Plotted are the H/L ratios of two independent experiments including label switch.
- F The Cdc5 binding region on Dbf4 is required for interaction of DDK and Cdc5 with Mus81-Mms4 and for efficient Mms4 phosphorylation. Mms4<sup>3FLAG</sup> pull down as in (A), but using mitotically arrested cells expressing N-terminal truncation mutants of Dbf4 lacking aa2–66 (including a D-box motif) or 2–109 [additionally including the Cdc5 binding site (Miller *et al.*, 2009)].

Cdc5 with Mus81-Mms4 was reduced after induction of DNA damage with phleomycin (Appendix Fig S2F), but this treatment was not sufficient to induce a significant reduction in the Mms4 phosphorylation shift. Interestingly, when we forced Cdc5 expression in S-phase cells and compared normal S-phase cells to cells treated with hydroxyurea (HU), we observed that the Mms4 phosphorylation shift was less pronounced in the presence of hydroxyurea (HU) (Fig EV1B). These data are therefore consistent with the current view that DNA damage, specifically the DNA damage checkpoint, negatively influences Mus81 resolution activity (Szakal & Branzei, 2013; Gritenaite *et al.*, 2014). Since DDK is known to be targeted and inhibited by the DNA damage checkpoint (Weinreich & Stillman, 1999; Lopez-Mosqueda *et al.*, 2010; Zegerman & Diffley, 2010), it could become particularly critical to regulate Mms4 phosphorylation after DNA damage.

Even though DDK and Cdc5 seem to target Mus81-Mms4 in unison, we tested whether it was possible to resolve differences on the level of individual phosphorylation sites. Therefore, we analysed Mms4 phosphorylation sites in M-phase cells after Cdc5 inhibition (Fig 3A and C) or *CDC7* deletion (Fig 3B and D) by SILAC-based mass spectrometry. We also applied two different experimental set-ups that used either endogenously expressed Mus81-Mms4 (Fig 3A and B) or overexpressed Mus81-Mms4 (Fig 3C and D), as the latter set-up allowed much better coverage of Mms4 phosphopeptides in higher order phosphorylation states (peptides harbouring > 1 phosphorylated site). Cdc5 inhibition or lack of DDK led to overlapping, but distinct changes in Mms4 phosphorylation sites, suggesting that each kinase phosphorylates specific sites on Mms4. After Cdc5 inhibition, phosphorylation of many sites was reduced and among those were sites that match to a putative Cdc5 consensus [(D/E/N)X(S/T), blue, Fig 3A and C; Mok *et al.*, 2010]. Overall, *CDC7* affected Mms4 phosphorylation less than Cdc5 inhibition, but nonetheless, we found widespread changes in the phosphorylation of (S/T)(S/T) motifs (Fig 3B and D). (S/T)(S/T) motifs were found less abundantly in the doubly phosphorylated state (Fig 3D, red), while conversely these motifs were found more abundantly in the state where only the second (S/T) was singly phosphorylated (Fig 3B and D, yellow), as expected for a substrate–product relation. These data are thus consistent with phosphorylation of the second (S/T) priming for phosphorylation at the preceding (S/T) (Appendix Table S1 and Appendix Fig S3).

### DDK phosphorylation is required for activation of Mus81-Mms4 during mitosis

Phosphorylation of Mms4 by CDK and Cdc5 has previously been shown to be required for the upregulation of Mus81-Mms4 activity during mitosis (Matos *et al.*, 2011, 2013; Gallo-Fernández *et al.*, 2012; Szakal & Branzei, 2013). Based on our finding that hyperphosphorylation of Mms4 was impaired in the absence of DDK (Fig 2D and Appendix Fig S2C), we predicted that also Mus81-Mms4 activity would be influenced. Therefore, we tested the activity of endogenous Mus81<sup>9myc</sup>-Mms4<sup>3FLAG</sup> immunopurified from G2/M arrested cells (approx. 5 fmol) on a nicked Holliday junction (nHJ) substrate (500 fmol) using an assay related to those in (Matos *et al.*, 2011, 2013; Gritenaite *et al.*, 2014). Notably, the activity of the endogenous purified Mus81-Mms4 from G2/M cells exceeded the activity of recombinant Mus81-Mms4 (subjected to a dephosphorylation step during the purification), indicating that it is the mitotically activated form (Appendix Fig S4A). Moreover, the activity of endogenous purified Mus81-Mms4 was not influenced by 350 mM NaCl salt washes. This indicates that the presence of accessory, salt-labile factors such as Rtt107 or Cdc5 in the reaction is unlikely to contribute to Mus81 activity (Appendix Fig S4B and C).

Importantly, when we used this assay to test immunopurified Mus81<sup>9myc</sup>-Mms4<sup>3FLAG</sup> from mitotic cells lacking DDK (*cdc7 $\Delta$*  or *dbf4 $\Delta$* ), we observed a reduced activity compared to Mus81<sup>9myc</sup>-Mms4<sup>3FLAG</sup> from WT cells (Fig 4A and Appendix Fig S4D; also observed with an RF substrate, Appendix Fig S4E). In order to exclude that indirect effects of the *CDC7* deletion may cause the reduction in Mus81 activity, we furthermore created an Mms4 mutant that specifically lacks candidate DDK phosphorylation sites. We chose to mutate (S/T)(S/T) motifs (SS motifs in particular) and created an *mms4-8A* mutant that harboured eight S to A exchanges at the N-terminal (S/T) of the motifs (see Appendix Fig S3A). This mutant appeared less phosphorylated in mitosis as judged by a less pronounced phosphorylation shift (Fig 4B). Furthermore, we observed a reduction in the association of DDK and Cdc5 with the Mus81-Mms4-8A complex in pull-down experiments (Fig 4B), suggesting that phosphorylation of Mms4 also plays a role in tethering these kinases. Notably, Mus81<sup>9myc</sup>-Mms4<sup>3FLAG</sup>-8A from mitotic cells showed a moderate but reproducible reduction in resolution activity on nHJ substrates compared to WT Mus81<sup>9myc</sup>-Mms4<sup>3FLAG</sup> (Fig 4C and Appendix Fig

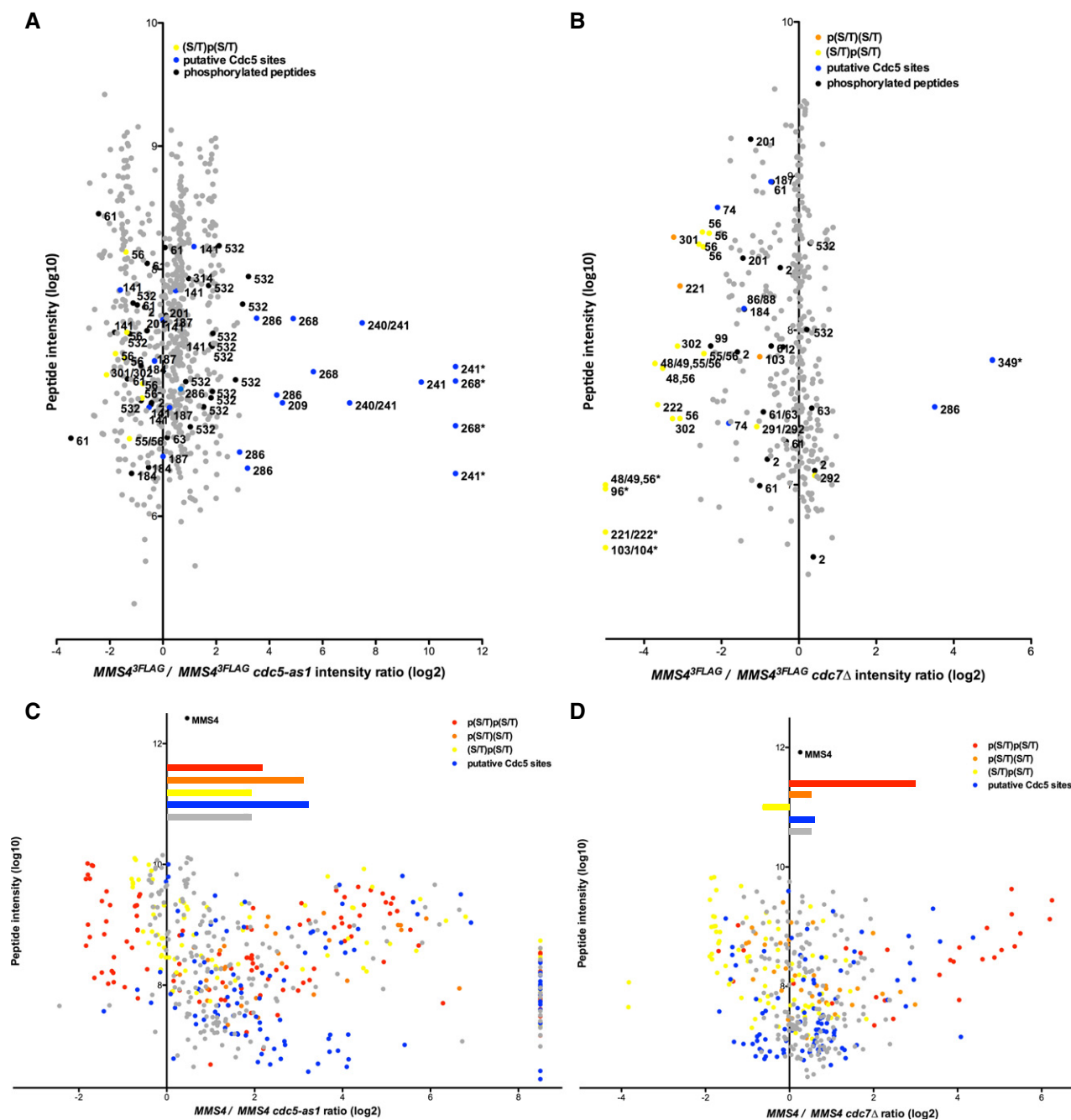


**Figure 3. Analysis of Mms4 phosphorylation sites reveals Cdc5 and DDK target sites, as well as the interdependence between the two.**

Changes of the abundance of phosphorylated Mms4 peptides after Cdc5 inhibition (as in Fig 2C) (A, C) or in the absence of Cdc7 (B, D) in mitotically arrested cells.

A, B Depicted are SILAC-based intensity ratios of individual MS evidences for peptides of endogenously expressed Mms4. Evidences of non-phosphorylated Mms4 peptides are shown in grey; evidences of phosphorylated peptides are shown in black, yellow, orange or blue. Blue colour indicates putative Cdc5 phosphorylation as defined by the (D/E/N)X(S/T) consensus (and additionally S268, which was also very strongly deregulated upon Cdc5 inhibition). Yellow or orange colours mark singly phosphorylated (S/T)(S/T) motifs, with orange marking p(S/T)(S/T) and yellow marking (S/T)p(S/T). Numbers indicate the phosphorylated residue in the depicted peptide. An asterisk marks peptide evidences that contained measured intensity values exclusively in the heavy or light sample. For doubly phosphorylated peptides, the two phospho-sites are separated by a comma. For singly phosphorylated (S/T)(S/T) motifs, peptide ion fragmentation was in some cases unable to unambiguously identify the phosphorylated residue. In these cases, possible phosphorylation sites are indicated as "a/b". Note that doubly phosphorylated (S/T)(S/T) sites were not reproducibly identified under conditions of endogenous Mus81-Mms4 expression.

C, D As in panels (A, B) but using Mus81-Mms4 expressed from a high-copy promoter. Depicted are SILAC-based H/L ratios of individual MS evidences for phosphorylated peptides only. Peptides were sorted into categories according to their phosphorylation status: putative DDK target sites ((S/T)(S/T) motifs) were differentiated into the categories p(S/T)p(S/T) (red), p(S/T)(S/T) (orange) or (S/T)p(S/T) (yellow). Phosphorylated peptides matching the Cdc5 consensus site are coloured in blue. All other phosphorylated peptides are marked in grey. Bars depict the mean of the ratios of the respective category. Overall, Mms4 H/L ratio is shown on top.

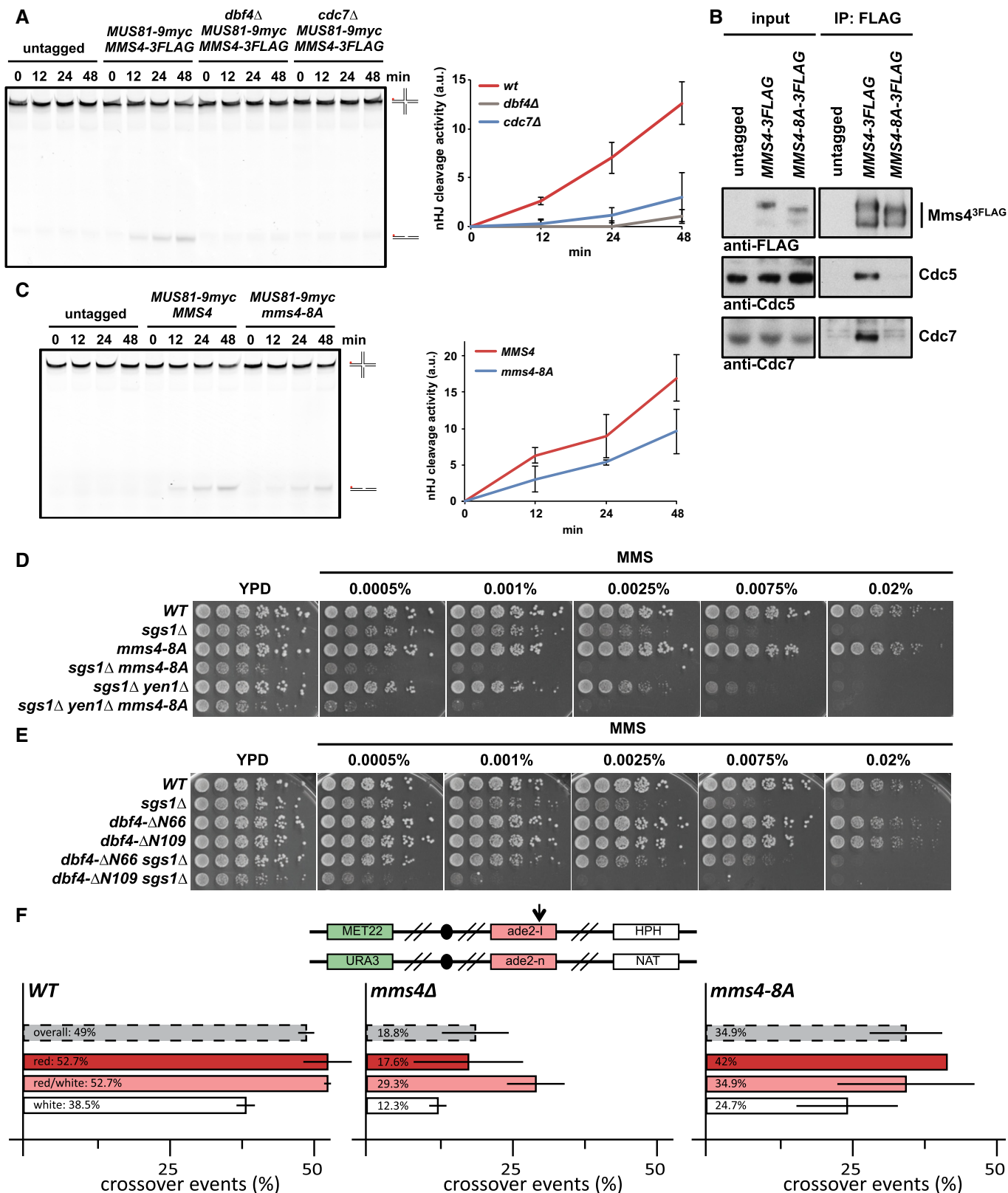


Figure 4.

S4F). These data thus indicate that DDK targets Mus81-Mms4 and that (S/T)(S/T) phosphorylation events are essential for full activation of Mus81 in mitosis.

Additionally, we investigated the relevance of the *mms4-8A* mutation *in vivo*. In comparison with *mus81Δ* or *mms4Δ* mutants, the *mms4-8A* mutant showed a hypomorphic phenotype. For

**Figure 4. DDK phosphorylation controls activation of Mus81-Mms4 resolvase activity in mitosis.**

- A DDK is required for mitotic activation of Mus81-Mms4. Resolution assay using a nicked Holliday junction (nHJ) substrate and Mus81<sup>9myc</sup>-Mms4<sup>3FLAG</sup> purified from mitotically arrested *bob1-1* (DDK-WT<sup>+</sup>), *bob1-1 dbf4Δ* and *bob1-1 cdc7Δ* strains or untagged control cells. Right panel: quantification of cleavage products. See Appendix Fig S4D for Western blots samples of anti-myc IPs. Left panel: representative gel image.
- B A defect in the phosphorylation of Mms4 (S/T)(S/T) sites causes reduced association of Cdc5 and DDK with Mus81-Mms4 and reduced phosphorylation of Mms4. Mms4<sup>3FLAG</sup> pull down as in Fig 1A, but using mitotically arrested WT and *mms4-8A* mutant cells, which harbour 8 serine to alanine exchanges at (S/T)(S/T) motifs (detailed in Appendix Fig S3).
- C Reduced (S/T)(S/T) phosphorylation of Mms4 generates a defect in Mus81-Mms4 activity. Resolution assay as in (A), but comparing mitotic Mus81-Mms4 from untagged, WT and *mms4-8A* strains (see Appendix Fig S4F for Western blot samples of anti-myc IPs).
- D, E The *mms4-8A* mutation and lack of the Cdc5-DDK interaction (*dbf4-ΔN109*) lead to hypersensitivity towards MMS specifically in the *sgs1Δ* background. Shown is the growth of indicated strains in fivefold serial dilution on plates containing MMS at indicated concentrations after 2 days at 30°C.
- F The *mms4-8A* mutant leads to a reduction in crossover formation. Recombination assay between heterologous *ade2* alleles in diploid cells as described in Ho et al (2010). The top panel indicates markers on both copies of chromosome XV that are used to determine genetic outcomes of DSB repair. Arrow indicates the I-SceI cut site. Bottom panel indicates rates of crossover events (%) overall (grey) and in the individual classes (red, red/white, white) that differ in gene conversion tract length. Error bars indicate standard deviation of two independent experiments, each scoring 400–600 colonies per strain.

Data information: (A, C) Depicted are means from three independent experiments, error bars correspond to standard deviation.

example, it did neither significantly increase the MMS hypersensitivity of a *yen1Δ* mutant, nor did it confer synthetic lethality with mutants defective in STR function, such as *sgs1Δ*, even though the *mms4-8A sgs1Δ* double mutant displayed a slow growth phenotype (Figs 4D and EV2A). Importantly, however, we did observe a strongly increased hypersensitivity towards MMS, when we tested an *mms4-8A sgs1Δ* double mutant and compared it to an *sgs1Δ* single mutant (Fig 4D). The *mms4-8A* mutation thus leads to a phenotype that is very similar to other activation-deficient *MMS4* mutants in budding and fission yeast (Gallo-Fernández et al, 2012; Dehé et al, 2013; Matos et al, 2013). Remarkably, the MMS hypersensitivity phenotype of the *mms4-8A* mutant was highly similar to that of the Cdc5 binding-deficient *dbf4-ΔN109* mutant (Figs 4E and EV2B), which also showed reduced survival when combined with *sgs1Δ* (Fig 4E). These data are therefore consistent with DDK functioning to stimulate JM resolution via Mms4 hyperphosphorylation.

It is likely that the *mms4-8A* mutant is only partially deficient in DDK phosphorylation, since Mms4 contains overall 15 (S/T)(S/T) sites and DDK may phosphorylate the protein on non-(S/T)(S/T) sites as well. We therefore note that an *mms4-12A* mutant, harbouring four additional S to A exchanges on (S/T)(S/T) motifs, showed further increased MMS sensitivity in the *mms4-12A sgs1Δ* mutant, when compared to the *mms4-8A sgs1Δ* mutant, even though there were only minor additional effects on either the Mms4 mitotic phosphorylation shift or JM resolution activity (Fig EV2C–E).

In order to directly assess whether DDK phosphorylation was required for Mus81 function during JM resolution, we tested the influence of the *mms4-8A* mutant in a genetic crossover assay (Ho et al, 2010). In this system, a site-specific DSB is induced in diploid cells and repair products can be measured by the arrangement of markers and colony sectoring (Fig 4F, upper panel). In this assay, *mus81Δ* and *mms4Δ* mutants show a reduction in CO products and a proportional increase in NCO products (Fig 4F; Ho et al, 2010), as would be expected from a defect in JM resolution and the accompanying shift of repair pathways towards JM dissolution. The *mms4-8A* mutant shows a similar, albeit weaker defect in the formation of CO products (Fig 4F), suggesting that the defect in Mus81 activation in mitosis results in an overall defect in JM resolution. We therefore conclude that DDK—in conjunction with Cdc5—acts directly on Mms4 and that these phosphorylation events are required for efficient Mus81-dependent JM resolution in mitosis.

**The Dpb11-Mms4 interaction is not required for DDK-Cdc5-dependent activation of Mus81-Mms4**

It is noteworthy that the association of DDK and Cdc5 with Mus81-Mms4 coincides with the formation of the Mus81-Mms4 complex with scaffold proteins such as Slx4, Dpb11 and Rtt107, which come together in mitosis (Fig 2A). Therefore, we asked whether the scaffold proteins Dpb11, Slx4 or Rtt107 would be required to target DDK and Cdc5 to Mus81-Mms4. In order to investigate the influence of Dpb11, we searched for an *MMS4* mutant that was deficient in the interaction with Dpb11. When we used a two-hybrid approach to map the Dpb11 interaction site on Mms4, we found that Mms4 constructs comprising aa 1–212 or 101–230 interacted with Dpb11, while constructs comprising aa 1–195 or 176–230 showed no or reduced interaction (Appendix Fig S5A). This suggested that the Dpb11 binding site may be located between aa 101–212 of Mms4. Consistently, we observed that the Mms4-S201A mutation abolished binding to Dpb11 in yeast two-hybrid and co-IP (Fig 5A and B), while the Mms4-S184A mutation reduced it (Fig 5A). Serine 201 and 184 are therefore likely candidates for phospho-sites bound and read by Dpb11. Serine 201 matches the full CDK consensus motif (S/T)PxK, while serine 184 matches the minimal CDK consensus motif (S/T)P. Indeed, we find that CDK inhibition reduced the Dpb11 interaction with Mus81-Mms4 (Appendix Fig S5B) consistent with a requirement of CDK phosphorylation for a robust interaction between Dpb11 and Mms4.

When we investigated the phenotype of the *mms4-SS184,201AA* mutant, we found that it showed enhanced hypersensitivity to MMS specifically in the *sgs1Δ* mutant background, consistent with a role of Dpb11 in JM resolution after MMS damage (Fig 5C). We also noted that the phenotype of this *MMS4* variant differed from that induced by Dpb11 binding-deficient version of Slx4 [*slx4-S486A* (Gritenaite et al, 2014; Ohouo et al, 2012)]. This could suggest that these mutants are able to separate different Dpb11 functions such as a mitotic function in conjunction with Mus81-Mms4 and an S-phase function, which Slx4 and Dpb11 might have independently of Mus81-Mms4 (Ohouo et al, 2012; Gritenaite et al, 2014; Cussiol et al, 2015; Princz et al, 2015). However, it also needs to be considered that Slx4 and Mus81-Mms4 may be connected by more than one scaffold protein (see below).

Importantly, however, we did not observe a defect in the association of DDK or Cdc5 with Mus81-Mms4, when we performed

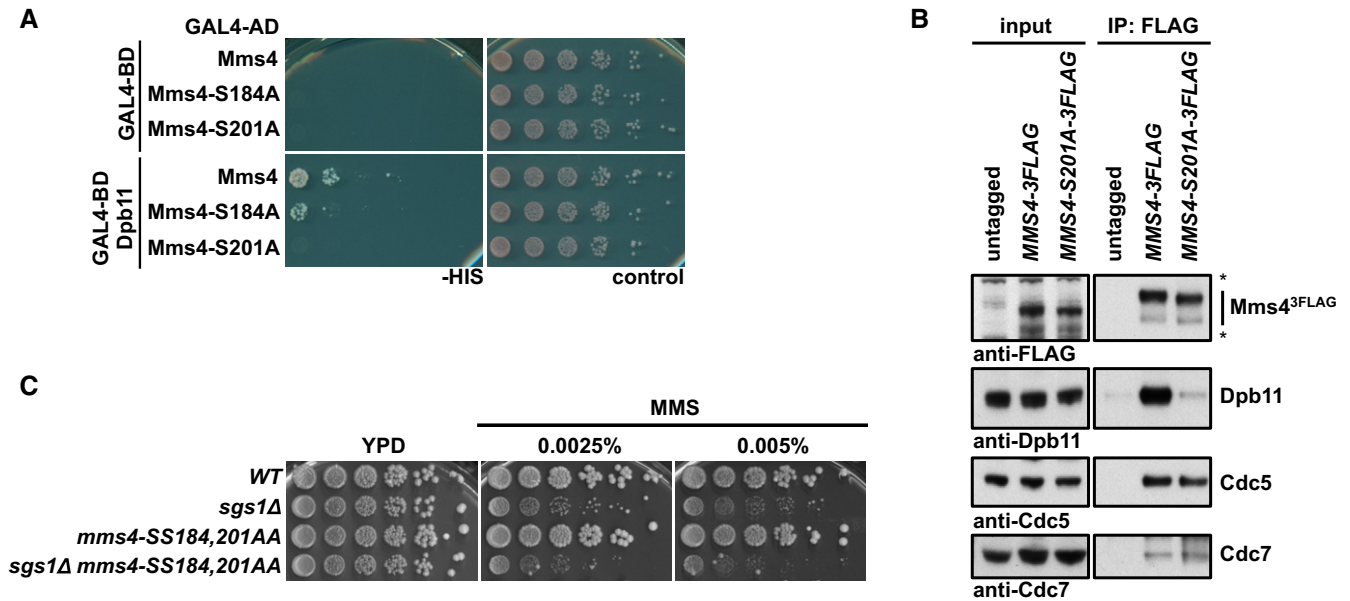


**Figure 5. The interaction between Mms4 and Dpb11 is dispensable for binding of Cdc5 and DDK and mitotic Mus81-Mms4 activation.**

A, B Serine 201 of Mms4 is required for Dpb11 binding, but not for interaction with DDK and Cdc5. (A) Two-hybrid interaction analysis using Gal4-BD-Dpb11 with Gal4-AD-Mms4, Gal4-AD-Mms4-S184A and Gal4-AD-Mms4-S201A constructs. (B) Mms4<sup>3FLAG</sup> pull downs from mitotically arrested cells as in Fig 1A, but using WT or S201A variants of Mms4<sup>3FLAG</sup>. Asterisks mark cross-reactive bands.

C The Dpb11 binding-deficient allele *mms4-SS184,201AA* leads to a MMS hypersensitivity specifically in the *sgs1Δ* background. Spotting assay as in Fig 4D.

Mms4-S201A<sup>3FLAG</sup> pull downs and compared them to a WT Mms4<sup>3FLAG</sup> pull down (Fig 5B). Furthermore, we only observed a very minor defect in the *in vitro* resolution of nHJ substrates, when we purified Mus81-Mms4 from mitotically arrested *mms4-S201A* cells (Appendix Fig S5C). We therefore reason that Dpb11 is most likely not involved in promoting Mms4 phosphorylation or DDK-Cdc5-dependent activation of Mus81-Mms4.

#### The Rtt107 scaffold recruits DDK and Cdc5 to Mus81-Mms4

Having excluded a role of Dpb11 in the recruitment of DDK and Cdc5, we next tested a possible involvement of the Rtt107 scaffold protein. Indeed, when we used an *rtt107Δ* mutant in IP and SILAC-based IP-MS experiments, we observed that DDK and Cdc5 binding to Mus81-Mms4 was strongly reduced (Fig 6A and Appendix Fig S6A). Interestingly, Rtt107 bound to DDK and Cdc5 even under conditions where Rtt107 binding to Mus81-Mms4 was abolished (*mus81Δ*, Appendix Fig S6B). This suggests that Rtt107 may form a subcomplex with DDK and Cdc5. Consistently, we found that Rtt107 bound to Cdc7 in a two-hybrid assay (Fig 6B). These data therefore suggest that Rtt107 mediates binding of DDK and Cdc5 to the Mus81-Mms4 complex, most likely via a Cdc7 interaction site on Rtt107.

During our co-IP studies, we furthermore found that the location of Rtt107 in the mitotic Mus81-Mms4 complex was different than expected. Given that Slx4 was required to bridge between Rtt107 and Dpb11 (Ohouo *et al*, 2010) and that Mms4 and Dpb11 seemingly interact directly (Gritenaite *et al*, 2014 and Fig 5A and B), we initially expected that Slx4 and Dpb11 would be required to mediate the interaction between Rtt107 and Mus81-Mms4. Surprisingly, we found that an *slx4Δ* mutant did not influence DDK or Cdc5 binding

to Mus81-Mms4 and thereby differed from *rtt107Δ* (Fig 6A). Therefore, we tested if Rtt107 could bind to Mus81-Mms4 independently of Slx4 or Dpb11. Indeed, we found that the Mus81-Mms4 interaction to Rtt107 was not influenced by the *slx4Δ* mutant (Fig 6C) or the Dpb11 binding-deficient *mms4-S201A* allele (Fig 6D), indicating that Rtt107 binding to the Mus81-Mms4 complex occurs independently of the other scaffold proteins. In contrast, our data also show that its binding is strongly dependent on kinases and Mms4 phosphorylation, since Rtt107 binding was strongly reduced in the absence of DDK (Fig 2E), after Cdc5 inhibition (Appendix Fig S2A) or in the *mms4-8A* phosphorylation site mutant (Fig EV3).

Therefore, these data provide novel insight into the role of Rtt107 in Mus81-Mms4 regulation. First, it shows that Rtt107 mediates the association of DDK and Cdc5 kinases with Mus81-Mms4. Second, it also suggests that Rtt107 may bind directly to Mus81-Mms4 and that this binding is dependent on Mms4 phosphorylation and the cell cycle kinases DDK and Cdc5, although an alternative model whereby Rtt107 indirectly promotes DDK and Cdc5 to tightly associate with Mus81-Mms4 cannot be ruled out entirely. The fact that Rtt107 promotes the interaction of Mus81-Mms4 with the kinases, yet in turn requires the kinases and Mms4 phosphorylation for interaction, suggests that Rtt107 may be acting after initial Mms4 phosphorylation has occurred and at this late stage tethers the kinases, thus promoting phosphorylation of otherwise inefficiently phosphorylated sites.

#### Rtt107 stimulates Mms4 hyperphosphorylation in order to enhance Mus81-Mms4 activity in mitosis

Given Rtt107's involvement in tethering DDK and Cdc5 to the Mus81-Mms4 complex, we asked whether Rtt107 would mediate

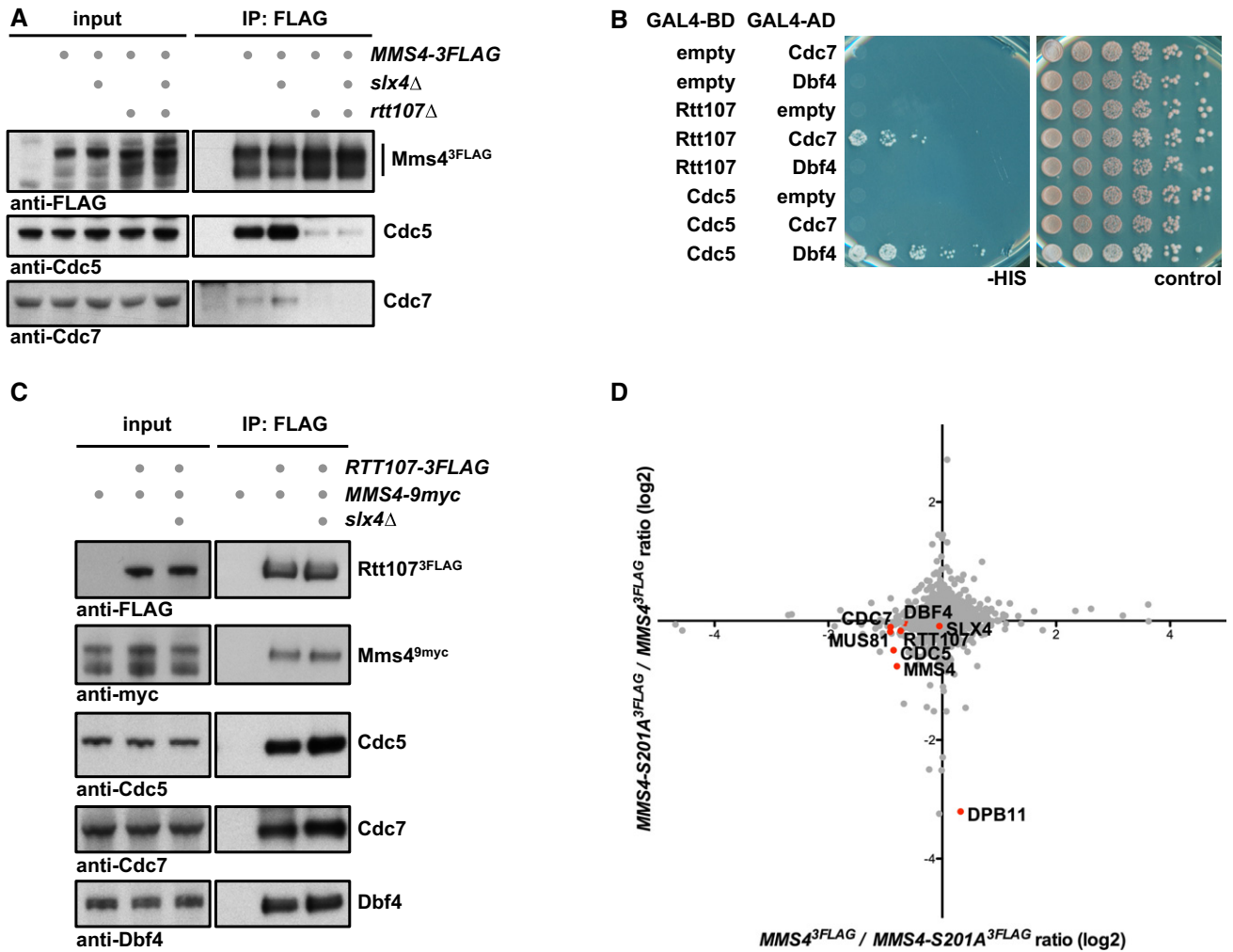


**Figure 6. The Rtt107 scaffold tethers DDK and Cdc5 to Mus81-Mms4 independently of Slx4 and Dpb11.**

- A Rtt107, but not Slx4, is required for DDK and Cdc5 interaction with Mus81-Mms4. Mms4<sup>3FLAG</sup> pull downs from mitotically arrested cells as in Fig 1A, but specifically comparing interactions of Mus81-Mms4 in WT, *slx4Δ*, *rtt107Δ* and *slx4Δ rtt107Δ* mutant backgrounds.
- B Rtt107 interacts with Cdc7. Two-hybrid interaction was tested using Gal4-BD-Rtt107 constructs and Gal4-AD-Cdc7 or Gal4-AD-Dbf4 constructs. Interaction between Gal4-BD-Cdc5 and Gal4-AD-Dbf4 serves as positive control.
- C Rtt107 interacts with Mus81-Mms4, DDK and Cdc5 independently of Slx4. Rtt107<sup>3FLAG</sup> co-IPs from untagged control, WT or *slx4Δ* cells arrested in mitosis were probed for indicated proteins.
- D Rtt107 interacts with Mus81-Mms4 independently of the Mms4-Dpb11 interaction. SILAC-based Mms4<sup>3FLAG</sup> pull down in WT and *mms4-S201A* cells reveals changes in the Dpb11 association, but not in Rtt107, Slx4, Cdc5 or DDK binding. Plotted are the H/L ratios of two experiments including label switch.

mitotic hyperphosphorylation of Mms4 and concomitant activation of the Mus81 nuclease. We observed only a minor effect on the mitotic phospho-shift of Mms4 when using *rtt107Δ* mutants (Fig 6A and Appendix Fig S2C). However, as it is still unclear which phosphorylation sites contribute to the Mms4 phospho-shift, we investigated the effect of *rtt107Δ* on individual phosphorylation sites in our mass spectrometry data. Appendix Fig S7A and B shows SILAC-based comparisons of Mms4 phosphorylation sites in WT and *rtt107Δ* cells, expressing Mus81-Mms4 from endogenous (Appendix Fig S7A) or high-copy promoters (Appendix Fig S7B). The overexpression set-up allowed us to quantify phosphorylation at (S/T)(S/T) motifs, and we found that double phosphorylation of several of these sites was reduced (Appendix Fig S7B), although the change was much smaller compared to cells lacking DDK. On the

other hand, while we could not detect higher order phosphorylated Mms4 peptides using endogenous Mus81-Mms4, we could detect an effect of Rtt107 on several other sites (T209, S241 and S268, and to a lesser extent S286; Appendix Fig S7A), which were also deregulated after Cdc5 inhibition (Fig 3A and C). These data are thus consistent with Rtt107 promoting efficient DDK and Cdc5 phosphorylation of Mms4.

Therefore, we tested whether Rtt107 would affect the mitotic activation of Mus81-Mms4. We immunopurified Mus81<sup>9myc</sup>-Mms4<sup>3FLAG</sup> from WT and *rtt107Δ* cells that were arrested in mitosis and found that Mus81-Mms4 activity on a nHJ substrate was reduced in the *rtt107Δ* background (Fig 7A and Appendix Fig S7C). Furthermore, in the background of deficient DDK (*cdc7Δ bob1-1*), additional mutation of *rtt107Δ* did not lead to a further defect in

Mus81-mediated cleavage (Appendix Fig S7D). Therefore, we conclude that Rtt107 is required for full mitotic activation of Mus81-Mms4 and that it works at least in part through cell cycle kinases such as DDK.

In order to test whether such a defect in Mus81-Mms4 activation would translate into a shifted balance of JM removal pathways, we measured rates of crossover and non-crossover formation in the absence of Rtt107. We observed a reduction in crossover rates in the *rtt107Δ* mutant indicating a shift in the balance of JM removal pathways (Fig 7B). The decrease was mostly visible in one class of recombinants (Fig 7B, “red”) and is smaller compared to the phenotype of a *mus81Δ* or a *mms4-8A* mutant (Ho et al, 2010; Fig 4F), consistent with a stimulatory but non-essential role of the Rtt107

scaffold in Mus81-Mms4 function. These data thus provide the first mechanistic insight of how the interaction of the mitotic Mus81-Mms4 complex with the scaffold proteins influences Mus81 function, as Rtt107 facilitates DDK and Cdc5 tethering, full mitotic phosphorylation of Mms4 and activation of Mus81-Mms4.

### Discussion

Activation of Mus81-Mms4 during mitosis is critical for the response to DNA damage, in particular to process repair intermediates that may arise from DSBs and stalled replication forks (Matos et al, 2011, 2013; Gallo-Fernández et al, 2012; Saugar et al, 2013; Szakal

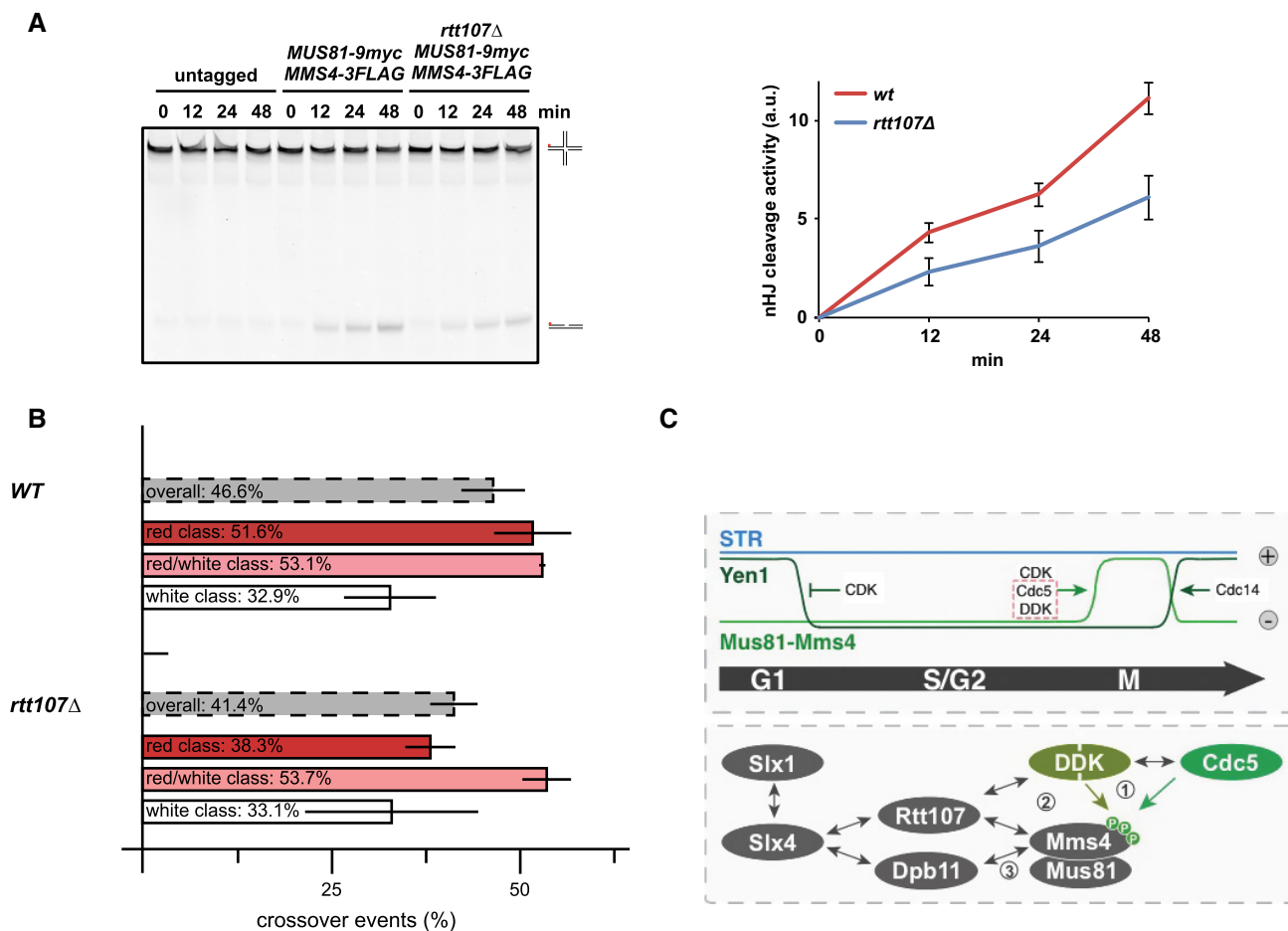


**Figure 7. Rtt107 is required for efficient Mus81-Mms4 activation in mitosis.**

**A** Mus81-Mms4 purified from mitotic *rtt107Δ* cells is less active compared to Mus81-Mms4 from WT cells. *In vitro* resolution activity of Mus81<sup>9myc</sup>-Mms4<sup>3FLAG</sup> purified from WT or *rtt107Δ* cells is tested on a nHJ substrate (see Appendix Fig S7C for control Western blot). Right panel: quantification of cleavage products from three independent experiments (mean ± SD). Left panel: representative gel picture.

**B** The *rtt107Δ* mutant leads to a reduction in crossover formation. Recombination assay as in Fig 4F. Note that the *rtt107Δ* mutant particularly affects crossover formation in the red class (long conversion tracts), while no significant defect could be observed in the red/white and white class (mean ± SD).

**C** Hypothetical model of Mus81-based JM resolution. Upper panel: cell cycle regulation of JM removal pathways, indicating Mus81 activation in mitosis. Lower panel: physical interactions of Mus81-Mms4 and its regulatory complex in mitotic cells. Grey arrows indicate physical interactions; green arrows specifically indicate kinase-substrate interactions. Genetic data indicate a hierarchy of molecular events leading to Mus81 activation. (1) DDK, Cdc5 and CDK (not shown) phosphorylate Mms4. (2) Rtt107 binds to DDK and Cdc5 and—in a phosphorylation-dependent manner—associates with Mus81-Mms4. This interaction is either direct or could potentially depend on bridging effects by DDK and Cdc5. Rtt107 promotes the stable interaction of DDK and Cdc5 with Mus81-Mms4 and thus full phosphorylation of Mms4 and Mus81 activation. (3) Upon Mms4 phosphorylation, two scaffold proteins, Rtt107 and Dpb11, bind independently to Mus81-Mms4. Both proteins can also bind to Slx4 enabling two alternative connections of Slx4 with Mus81-Mms4.

& Branzei, 2013). Previously, this regulation was shown to critically depend on phosphorylation by the cell cycle kinases CDK and Cdc5 (Matos *et al*, 2011, 2013; Gallo-Fernández *et al*, 2012; Saugar *et al*, 2013; Szakal & Branzei, 2013), but also involve the formation of a multi-protein complex comprising several scaffold proteins (Gritenaite *et al*, 2014). Here, we not only identify a new cell cycle kinase to be crucial for this regulation—DDK—but moreover show that the two regulatory pathways—cell cycle kinase phosphorylation and scaffold complex formation—are connected by Rtt107 (see Fig 7C for a hypothetical model). Rtt107 association depends on active cell cycle kinases and Mms4 phosphorylation, but in turn Rtt107 is required for stable DDK and Cdc5 association with the Mus81-Mms4 complex, as well as full phosphorylation of Mms4 and mitotic activation of Mus81. This study thus extends our mechanistic understanding of the regulatory framework that controls cell cycle-regulated JM resolution.

Interestingly, our work shows that for its function as a regulator of Mus81-Mms4 DDK must act interdependently and as a complex with Cdc5. DDK and Cdc5 have been shown to interact physically (Miller *et al*, 2009; Chen & Weinreich, 2010), but until now DDK was viewed to antagonize mitotic functions of Cdc5 (Miller *et al*, 2009). In contrast, in meiosis I DDK and Cdc5 are known to cooperate in order to promote chromosome segregation and jointly phosphorylate the monopolin and cohesin subunits Lrs4 and Rec8, respectively, as well as the meiotic regulator Spo13 (Matos *et al*, 2008). We now provide the first example for a joint DDK and Cdc5 substrate in the mitotic cell cycle, suggesting that cooperation between DDK and Cdc5 could be a more widespread phenomenon than previously anticipated. The apparent antagonism between DDK and Cdc5 in the regulation of mitotic exit (Miller *et al*, 2009), a canonical Cdc5 function, could be explained if DDK targeted Cdc5 to a specialized subset of substrates rather than to substrates involved in mitotic exit. It is also interesting to note that we could detect significant DDK binding to Mus81-Mms4 only after cells finished S phase (Fig 2A). Therefore, the role of DDK in Mms4 phosphorylation is clearly post-replicative and further challenges a simplified view of DDK as an S-phase kinase (Matos *et al*, 2008). It will therefore be interesting to see whether additional DDK substrates during mitosis can be identified and whether DDK collaborates with Cdc5 for their phosphorylation as well.

Mus81-Mms4 has previously been shown to be cell cycle-regulated and Mms4 to be a critical CDK and Cdc5 phosphorylation target (Matos *et al*, 2011; Gallo-Fernández *et al*, 2012). We add DDK to this already complex regulation. Our data clearly show that phosphorylation of (S/T)(S/T) motifs is critical for Mus81-Mms4 function. The hypomorphic phenotype of the *mms4-8A* mutant (Fig 4C, D and F) is likely due to additional DDK phosphorylation sites either on Mms4 or perhaps even on Mus81. Importantly, DDK does not appear to establish the timing of Mms4 phosphorylation in mitosis, as Cdc5 still seems to be the limiting factor for this temporal control in undisturbed cell cycles (Fig EV1B). However, the fact that activation of Mus81-Mms4 depends on the activity of several kinases makes it a coincidence detector that integrates the activity of several cell cycle regulators. Therefore, it can be envisioned that there are specific cellular conditions under which DDK activity becomes limiting for Mus81-Mms4 activation. Notably, DNA damage checkpoint kinases are known to phosphorylate DDK and counteract its function during S phase (Weinreich & Stillman, 1999; Lopez-Mosqueda *et al*, 2010; Zegerman & Diffley, 2010). Therefore,

it can be speculated that the checkpoint acts as a negative regulator of Mus81-Mms4 activation via inhibition of DDK. Such regulation could therefore explain how the presence of DNA damage restricts Mus81 activity towards replication intermediates (Matos *et al*, 2011, 2013; Saugar *et al*, 2013; Szakal & Branzei, 2013; Gritenaite *et al*, 2014), suggesting that cell cycle and checkpoint pathways converge in the regulation of Mus81.

A second layer of Mus81 regulation relies on the formation of a multi-protein complex, which assembles specifically in mitosis and contains Mus81-Mms4, DDK, Cdc5 and Slx4 as well as the scaffold proteins Dpb11 and Rtt107 (Gritenaite *et al*, 2014). We are only beginning to understand the mechanism whereby this scaffold complex influences Mus81 function. Here, we show that Rtt107, but not Dpb11 or Slx4, promotes the stable association of DDK and Cdc5 with Mus81-Mms4 (Fig 6), suggesting that one function of the multi-protein complex is to promote efficient Mus81-Mms4 phosphorylation. Conversely, our new data as well as our previous work (Gritenaite *et al*, 2014) show that phosphorylation by cell cycle kinases also regulates the formation of the multi-protein complex. In particular, Rtt107 association with Mus81-Mms4 depends strongly on DDK and Cdc5 (Fig 2E and Appendix Fig S2A). A direct interaction of Rtt107 with Mus81-Mms4 seems the most plausible interpretation of our data, although we currently cannot exclude that Rtt107 may facilitate the interaction of DDK and Cdc5 with Mus81-Mms4 without a direct interaction. A possible phosphorylation dependence of Rtt107 binding to the complex could thus originate from Mms4 phosphorylation generating a binding site for Rtt107 [e.g. for Rtt107 BRCT domains (Li *et al*, 2012)].

Importantly, Rtt107 is in turn required for stable binding of DDK and Cdc5 (Fig 6A and Appendix Fig S6A). Via tethering the kinases, Rtt107 regulates the phosphorylation of specific Mms4 sites and is required for full Mus81 activation (Fig 7A and Appendix Fig S7A and B). The interdependence between Rtt107 and Cdc5/DDK phosphorylation therefore suggests that Rtt107 may be part of a signal amplification mechanism, which ensures efficient Mus81-Mms4 phosphorylation and activation. Mechanistically, Rtt107-dependent stimulation of Mms4 phosphorylation thus resembles a kinase priming mechanism. It is entirely possible that other kinase priming mechanisms for either Cdc5 or DDK are at work in the Mms4 phosphorylation cascade, although the *in vitro* kinase assays with full-length proteins did not provide support for such a mechanism (Fig 1B, and Appendix Fig S1C and D). Altogether, it seems plausible to speculate that Rtt107-dependent and Rtt107-independent amplification mechanisms are involved in generating a switch-like activation of Mus81 in mitosis.

Furthermore, Rtt107 can also bind to Slx4 (Ohouo *et al*, 2010). There are thus two BRCT-containing scaffold proteins—Dpb11 (Gritenaite *et al*, 2014) and Rtt107—that could bridge between Mus81-Mms4 and Slx4. Interestingly, our data with different *mms4* mutants suggest that either one of these BRCT scaffold proteins is sufficient to connect Slx4 and Mus81-Mms4 [Figs 6D and EV3; note that the *rtt107Δ* mutant (Appendix Fig S6A) is difficult to interpret in this regard as it also leads to defects in Slx4 phosphorylation and the Slx4-Dpb11 interaction (Ohouo *et al*, 2010)]. This redundancy may thus explain the modest phenotype of the *mms4-S201A* mutant that is deficient in the Mms4-Dpb11 interaction (Fig 5C).

Several aspects of Mus81-Mms4 regulation are conserved throughout eukaryotic evolution. The HJ resolution activity of

Mus81-Eme1 in mammalian cells is cell cycle-regulated (Matos *et al*, 2011; Wyatt *et al*, 2013). Mus81-Eme1 furthermore binds to Slx4 and forms multi-protein complexes (Fekairi *et al*, 2009; Muñoz *et al*, 2009; Svendsen *et al*, 2009; Castor *et al*, 2013; Wyatt *et al*, 2013), albeit these complexes may have a different organization to that in yeast. Therefore, it will be interesting to explore in the future if in human cells DDK is also required for activation of Mus81-Eme1 and if this mechanism may contribute to the anti-tumorigenic activity of DDK inhibitors (Montagnoli *et al*, 2008).

## Materials and Methods

All yeast strains are based on W303 and were constructed using standard methods. Plasmids were constructed using the In-Fusion HD cloning kit (Clontech Laboratories), and mutations were introduced by site-directed mutagenesis. A summary of all yeast strains used in this study can be found in the Appendix Table S2.

Cell cycle synchronization was achieved using alpha-factor (G1), hydroxyurea (S), or nocodazole (mitosis). DNA content was measured by flow cytometry with a BD FACSCalibur system using SYTOX green to stain DNA.

Co-immunoprecipitations of yeast extracts were performed on anti-FLAG agarose resin (Sigma) for 2 h with head-over-tail rotation at 4°C as previously described (Gritenaite *et al*, 2014). After bead washing, proteins were eluted by 3X FLAG-peptide (Sigma), precipitated and separated on 4–12% Bis-Tris gels. For SILAC-based mass spectrometry, cells were labelled with heavy-isotope-labelled lysine (Lys6 or Lys8), and proteins were digested with Lys-C. Mass spectrometry data were analysed using MaxQuant (Cox & Mann, 2008).

Yeast two-hybrid assays, genetic interaction assays, *in vitro* kinase assays and peptide binding assays were performed as described previously (Pfander & Diffley, 2011; Gritenaite *et al*, 2014).

Nuclease assays were done as described (Matos *et al*, 2011, 2013). Briefly, Mus81<sup>9myc</sup> was immunopurified from mitotically arrested cells and mixed with 5'-Cy3-end-labelled nicked Holliday junctions. After incubation at 30°C for the indicated times, the reaction was stopped by proteinase K and SDS for 1 h at 37°C. Products were separated by 10% PAGE, and cleavage efficiency was normalized to the level of immunoprecipitated Mus81<sup>9myc</sup>. Unspecific nHJ cleavage in untagged controls was subtracted in the quantifications.

DSB-induced recombination assays were performed as described (Ho *et al*, 2010). Diploids harbouring I-SceI under the control of the GAL promoter were grown in adenine-rich raffinose medium and arrested in mitosis. Nuclease expression was induced by addition of galactose for 2.5 h. Cells were plated on YPAD and replica plated on YPAD + Hyg + Nat, YPAD + Hyg, YPAD + Nat, SC-Met, SC-Ura and SCR-ADE + Gal media after 3–4 days to classify recombination events.

Detailed experimental procedures are available in the Appendix.

### Data availability

Mass spectrometric datasets are available at EBI PRIDE. DDK and the Rtt107 scaffold promote Mus81-Mms4 resolvase activation during mitosis (2015). PXD005356.

**Expanded View** for this article is available online.

## Acknowledgements

We thank U. Kagerer for technical assistance, D. Gritenaite for early contributions to the project, N. Nagaraj and the proteomics laboratory of the MPIB core facility for proteomics analysis, the MPIB core facility for peptide synthesis and sequencing, J. Diffley and L. Symington for antibodies, plasmid constructs and strains, S. Jentsch, Z. Storchova, C. Biertümpfel and members of the Jentsch and Pfander labs for stimulating discussion and critical reading of the manuscript. Work in the Pfander laboratory is supported by the Max-Planck Society and the German Research Council (DFG). Work in the Matos laboratory is supported by ETH Zürich and the Swiss National Science Foundation (Grants 31003A\_153058 and 155823). Work in the Blanco laboratory is co-financed by Ministerio de Economía y Competitividad and FEDER (RYC-2012-10835 and BFU2013-41554-P). Philipp Wild is supported by an EMBO long-term fellowship (ALTF 475-2015). F. Javier Aguado is supported by a PhD fellowship from the I2C Program of Xunta de Galicia (ED481A-2015/011).

## Author contributions

PW and JM performed *in vitro* resolution assays of Figs 4A and C, 7A, and EV2E, and Appendix Figs S4A, C, E, and S7D and analysed the data. FJA and MGB provided recombinant purified Mus81-Mms4 used in Fig 1B, and Appendix Figs S1C and D, and S4A. All other experiments were performed and analysed by LNP, JB and BP. BP wrote the paper and all authors commented on the manuscript.

## Conflict of interest

The authors declare that they have no conflict of interest.

## References

- Alexandru G, Uhlmann F, Mechtler K, Poupard MA, Nasmyth K (2001) Phosphorylation of the cohesin subunit Scc1 by Polo/Cdc5 kinase regulates sister chromatid separation in yeast. *Cell* 105: 459–472
- Bishop AC, Ubersax JA, Petsch DT, Matheos DP, Gray NS, Blethrow J, Shimizu E, Tsien JZ, Schultz PG, Rose MD, Wood JL, Morgan DO, Shokat KM (2000) A chemical switch for inhibitor-sensitive alleles of any protein kinase. *Nature* 407: 395–401
- Bizard AH, Hickson ID (2014) The dissolution of double Holliday junctions. *Cold Spring Harb Perspect Biol* 6: a016477
- Blanco MG, Matos J, West SC (2014) Dual control of Yen1 nuclease activity and cellular localization by Cdk and Cdc14 prevents genome instability. *Mol Cell* 54: 94–106
- Branzei D, Foiani M (2008) Regulation of DNA repair throughout the cell cycle. *Nat Rev Mol Cell Biol* 9: 297–308
- Castor D, Nair N, Déclais A-C, Lachaud C, Toth R, Macartney TJ, Lilley DMJ, Arthur JSC, Rouse J (2013) Cooperative control of Holliday junction resolution and DNA repair by the SLX1 and MUS81-EME1 nucleases. *Mol Cell* 52: 221–233
- Chen YC, Weinreich M (2010) Dbf4 regulates the Cdc5 polo-like kinase through a distinct non-canonical binding interaction. *J Biol Chem* 285: 41244–41254
- Cheng L, Collyer T, Hardy CF (1999) Cell cycle regulation of DNA replication initiator factor Dbf4p. *Mol Cell Biol* 19: 4270–4278
- Cox J, Mann M (2008) MaxQuant enables high peptide identification rates, individualized p.p.b.-range mass accuracies and proteome-wide protein quantification. *Nat Biotechnol* 26: 1367–1372

- Cussiol JR, Jablonowski CM, Yimit A, Brown GW, Smolka MB (2015) Dampening DNA damage checkpoint signalling via coordinated BRCT domain interactions. *EMBO J* 34: 1704–1717
- Dehé P-M, Coulon S, Scaglione S, Shanahan P, Takedachi A, Wohlschlegel JA, Yates JR, Llorente B, Russell P, Gaillard P-HL (2013) Regulation of Mus81–Eme1 Holliday junction resolvase in response to DNA damage. *Nat Struct Mol Biol* 20: 598–603
- Eissler CL, Mazón G, Powers BL, Savinov SN, Symington LS, Hall MC (2014) The Cdk/Cdc14 module controls activation of the Yen1 Holliday junction resolvase to promote genome stability. *Mol Cell* 54: 80–93
- Fekairi S, Scaglione S, Chahwan C, Taylor ER, Tissier A, Coulon S, Dong M-Q, Ruse C, Yates JR, Russell P, Fuchs RP, McGowan CH, Gaillard P-HL (2009) Human SLX4 is a Holliday junction resolvase subunit that binds multiple DNA repair/recombination endonucleases. *Cell* 138: 78–89
- Ferreira MF, Santocanale C, Drury LS, Diffley JF (2000) Dbf4p, an essential S phase-promoting factor, is targeted for degradation by the anaphase-promoting complex. *Mol Cell Biol* 20: 242–248
- Ferretti LP, Lafranchi L, Sartori AA (2013) Controlling DNA-end resection: a new task for CDKs. *Front Genet* 4: 1–7
- Gallo-Fernández M, Saugar I, Ortiz-Bazán MÁ, Vázquez MV, Tercero JA (2012) Cell cycle-dependent regulation of the nuclease activity of Mus81–Eme1/Mms4. *Nucleic Acids Res* 40: 8325–8335
- Gritenaite D, Princz LN, Szakal B, Bantele SCS, Wendeler L, Schilbach S, Habermann BH, Matos J, Lisby M, Branzei D, Pfander B (2014) A cell cycle-regulated Slx4–Dpb11 complex promotes the resolution of DNA repair intermediates linked to stalled replication. *Genes Dev* 28: 1604–1619
- Hardy CF, Dryga O, Seematter S, Pahl PM, Sclafani RA (1997) mcm5/cdc46-bob1 bypasses the requirement for the S phase activator Cdc7p. *Proc Natl Acad Sci USA* 94: 3151–3155
- Heyer W-D, Ehmsen KT, Liu J (2010) Regulation of homologous recombination in eukaryotes. *Annu Rev Genet* 44: 113–139
- Ho CK, Mazón G, Lam AF, Symington LS (2010) Mus81 and Yen1 promote reciprocal exchange during mitotic recombination to maintain genome integrity in budding yeast. *Mol Cell* 40: 988–1000
- Interthal H, Heyer WD (2000) MUS81 encodes a novel helix-hairpin-helix protein involved in the response to UV- and methylation-induced DNA damage in *Saccharomyces cerevisiae*. *Mol Gen Genet* 263: 812–827
- Ip SCY, Rass U, Blanco MG, Flynn HR, Skehel JM, West SC (2008) Identification of Holliday junction resolvases from humans and yeast. *Nature* 456: 357–361
- Li X, Liu K, Li F, Wang J, Huang H, Wu J, Shi Y (2012) Structure of C-terminal tandem BRCT repeats of Rtt107 protein reveals critical role in interaction with phosphorylated histone H2A during DNA damage repair. *J Biol Chem* 287: 9137–9146
- Lopez-Mosqueda J, Maas NL, Jonsson ZO, DeFazio-Eli LG, Wohlschlegel J, Toczyski DP (2010) Damage-induced phosphorylation of Sld3 is important to block late origin firing. *Nature* 467: 479–483
- Lyons NA, Fonslow BR, Diedrich JK, Yates JR, Morgan DO (2013) Sequential primed kinases create a damage-responsive phosphodegron on Eco1. *Nat Struct Mol Biol* 20: 194–201
- Mankouri HW, Huttner D, Hickson ID (2013) How unfinished business from S-phase affects mitosis and beyond. *EMBO J* 32: 2661–2671
- Masai H, Taniyama C, Ogino K, Matsui E, Kakusho N, Matsumoto S, Kim JM, Ishii A, Tanaka T, Kobayashi T, Tamai K, Ohtani K, Arai K-I (2006) Phosphorylation of MCM4 by Cdc7 kinase facilitates its interaction with Cdc45 on the chromatin. *J Biol Chem* 281: 39249–39261
- Mathiasen DP, Lisby M (2014) Cell cycle regulation of homologous recombination in *Saccharomyces cerevisiae*. *FEMS Microbiol Rev* 38: 172–184
- Matos J, Lipp JJ, Bogdanova A, Guillot S, Okaz E, Junqueira M, Shevchenko A, Zachariae W (2008) Dbf4-dependent CDC7 kinase links DNA replication to the segregation of homologous chromosomes in meiosis I. *Cell* 135: 662–678
- Matos J, Blanco MG, Maslen S, Skehel JM, West SC (2011) Regulatory control of the resolution of DNA recombination intermediates during meiosis and mitosis. *Cell* 147: 158–172
- Matos J, Blanco MG, West SC (2013) Cell-cycle kinases coordinate the resolution of recombination intermediates with chromosome segregation. *Cell Rep* 4: 76–86
- Matos J, West SC (2014) Holliday junction resolution: regulation in space and time. *DNA Repair (Amst)* 19: 176–181
- Miller CT, Gabrielse C, Chen Y-C, Weinreich M (2009) Cdc7p-Dbf4p regulates mitotic exit by inhibiting polo kinase. *PLoS Genet* 5: 1–13
- Mok J, Kim PM, Lam HYK, Piccirillo S, Zhou X, Jeschke GR, Sheridan DL, Parker SA, Desai V, Jwa M, Camerini E, Niu H, Good M, Remenyi A, Ma J-LN, Sheu Y-J, Sassi HE, Sopko R, Chan CSM, De Virgilio C et al (2010) Deciphering protein kinase specificity through large-scale analysis of yeast phosphorylation site motifs. *Sci Signal* 3: ra12
- Montagnoli A, Valsasina B, Brotherton D, Troiani S, Rainoldi S, Tenca P, Molinari A, Santocanale C (2006) Identification of Mcm2 phosphorylation sites by S-phase-regulating kinases. *J Biol Chem* 281: 10281–10290
- Montagnoli A, Valsasina B, Croci V, Menichincheri M, Rainoldi S, Marchesi V, Tibolla M, Tenca P, Brotherton D, Albanese C, Patton V, Alzani R, Ciavolella A, Sola F, Molinari A, Volpi D, Avanzi N, Fiorentini F, Cattoni M, Healy S et al (2008) A Cdc7 kinase inhibitor restricts initiation of DNA replication and has antitumor activity. *Nat Chem Biol* 4: 357–365
- Mortensen EM, Haas W, Gygi M, Gygi SP, Kellogg DR (2005) Cdc28-dependent regulation of the Cdc5/Polo kinase. *Curr Biol* 15: 2033–2037
- Muñoz IM, Hain K, Déclais A-C, Gardiner M, Toh GW, Sanchez-Pulido L, Heuckmann JM, Toth R, Macartney T, Eppink B, Kanaar R, Ponting CP, Lilley DMJ, Rouse J (2009) Coordination of structure-specific nucleases by human SLX4/BTBD12 is required for DNA repair. *Mol Cell* 35: 116–127
- Ohouo PY, de Oliveira FMB, Almeida BS, Smolka MB (2010) DNA damage signaling recruits the Rtt107-Slx4 scaffolds via Dpb11 to mediate replication stress response. *Mol Cell* 39: 300–306
- Ohouo PY, de Oliveira FMB, Liu Y, Ma CJ, Smolka MB (2012) DNA-repair scaffolds dampen checkpoint signalling by counteracting the adaptor Rad9. *Nature* 493: 120–124
- Pfander B, Diffley JFX (2011) Dpb11 coordinates Mec1 kinase activation with cell cycle-regulated Rad9 recruitment. *EMBO J* 30: 4897–4907
- Princz LN, Gritenaite D, Pfander B (2015) The Slx4–Dpb11 scaffold complex: coordinating the response to replication fork stalling in S-phase and the subsequent mitosis. *Cell Cycle* 14: 488–494
- Randell JCW, Fan A, Chan C, Francis LI, Heller RC, Galani K, Bell SP (2010) Mec1 is one of multiple kinases that prime the Mcm2–7 helicase for phosphorylation by Cdc7. *Mol Cell* 40: 353–363
- Saugar I, Vazquez MV, Gallo-Fernandez M, Ortiz-Bazan MA, Segurado M, Calzada A, Tercero JA (2013) Temporal regulation of the Mus81–Mms4 endonuclease ensures cell survival under conditions of DNA damage. *Nucleic Acids Res* 41: 8943–8958
- Schwartz EK, Wright WD, Ehmsen KT, Evans JE, Stahlberg H, Heyer WD (2012) Mus81–Mms4 functions as a single heterodimer to cleave nicked intermediates in recombinational DNA repair. *Mol Cell Biol* 32: 3065–3080

- Shirayama M, Zachariae W, Ciosk R, Nasmyth K (1998) The Polo-like kinase Cdc5p and the WD-repeat protein Cdc20p/fizzy are regulators and substrates of the anaphase promoting complex in *Saccharomyces cerevisiae*. *EMBO J* 17: 1336–1349
- Snead JL, Sullivan M, Lowery DM, Cohen MS, Zhang C, Randle DH, Taunton J, Yaffe MB, Morgan DO, Shokat KM (2007) A coupled chemical-genetic and bioinformatic approach to polo-like kinase pathway exploration. *Chem Biol* 14: 1261–1272
- Suzuki K, Sako K, Akiyama K, Isoda M, Senoo C, Nakajo N, Sagata N (2015) Identification of non-Ser/Thr-Pro consensus motifs for Cdk1 and their roles in mitotic regulation of C2H2 zinc finger proteins and Ect2. *Sci Rep* 5: 7929
- Svensden JM, Smogorzewska A, Sowa ME, O'Connell BC, Gygi SP, Elledge SJ, Harper JW (2009) Mammalian BTBD12/SLX4 assembles a Holliday junction resolvase and is required for DNA repair. *Cell* 138: 63–77
- Szakal B, Branzei D (2013) Premature Cdk1/Cdc5/Mus81 pathway activation induces aberrant replication and deleterious crossover. *EMBO J* 32: 1155–1167
- Weinreich M, Stillman B (1999) Cdc7p-Dbf4p kinase binds to chromatin during S phase and is regulated by both the APC and the RAD53 checkpoint pathway. *EMBO J* 18: 5334–5346
- Wyatt HDM, Sarbajna S, Matos J, West SC (2013) Coordinated actions of SLX1-SLX4 and MUS81-EME1 for Holliday junction resolution in human cells. *Mol Cell* 52: 234–247
- Zegerman P, Diffley JFX (2010) Checkpoint-dependent inhibition of DNA replication initiation by Sld3 and Dbf4 phosphorylation. *Nature* 467: 474–478



**License:** This is an open access article under the terms of the Creative Commons Attribution-NonCommercial-NoDerivs 4.0 License, which permits use and distribution in any medium, provided the original work is properly cited, the use is non-commercial and no modifications or adaptations are made.

- C. Lee S-H, Princz LN, Klügel MF, Habermann B, Pfander B, Biertümpfel C (2015)**

**The structure of human Holliday junction resolvase GEN1 reveals a chromodomain for efficient DNA recognition and cleavage**

***eLife* 4:e12256**

# Human Holliday junction resolvase GEN1 uses a chromodomain for efficient DNA recognition and cleavage

Shun-Hsiao Lee<sup>1</sup>, Lissa Nicola Princz<sup>2</sup>, Maren Felizitas Klügel<sup>1</sup>, Bianca Habermann<sup>3</sup>, Boris Pfander<sup>2</sup>, Christian Biertümpfel<sup>1\*</sup>

<sup>1</sup>Department of Structural Cell Biology, Molecular Mechanisms of DNA Repair, Max Planck Institute of Biochemistry, Martinsried, Germany; <sup>2</sup>Department of Molecular Cell Biology, DNA Replication and Genome Integrity, Max Planck Institute of Biochemistry, Martinsried, Germany; <sup>3</sup>Computational Biology, Max Planck Institute of Biochemistry, Martinsried, Germany

**Abstract** Holliday junctions (HJs) are key DNA intermediates in homologous recombination. They link homologous DNA strands and have to be faithfully removed for proper DNA segregation and genome integrity. Here, we present the crystal structure of human HJ resolvase GEN1 complexed with DNA at 3.0 Å resolution. The GEN1 core is similar to other Rad2/XPG nucleases. However, unlike other members of the superfamily, GEN1 contains a chromodomain as an additional DNA interaction site. Chromodomains are known for their chromatin-targeting function in chromatin remodelers and histone(de)acetylases but they have not previously been found in nucleases. The GEN1 chromodomain directly contacts DNA and its truncation severely hampers GEN1's catalytic activity. Structure-guided mutations *in vitro* and *in vivo* in yeast validated our mechanistic findings. Our study provides the missing structure in the Rad2/XPG family and insights how a well-conserved nuclease core acquires versatility in recognizing diverse substrates for DNA repair and maintenance.

DOI: [10.7554/eLife.12256.001](https://doi.org/10.7554/eLife.12256.001)

\*For correspondence:

[biertuempfel@biochem.mpg.de](mailto:biertuempfel@biochem.mpg.de)

**Competing interests:** The authors declare that no competing interests exist.

**Funding:** See page 20

**Received:** 12 October 2015

**Accepted:** 17 December 2015

**Published:** 18 December 2015

**Reviewing editor:** Volker Dötsch, Goethe University, Germany

© Copyright Lee et al. This article is distributed under the terms of the [Creative Commons Attribution License](https://creativecommons.org/licenses/by/4.0/), which permits unrestricted use and redistribution provided that the original author and source are credited.

## Introduction

Homologous recombination (HR) is a fundamental pathway ensuring genome integrity and genetic variability (Heyer, 2015). In mitotic cells, double-strand breaks (DSBs) can be repaired by HR using the sister chromatid as a template to restore the information in the complementary double strand. In meiosis, the repair of programmed DSBs by HR and the formation of crossovers are crucial to provide physical linkages between homologs and to segregate homologous chromosomes. Furthermore, HR during meiosis creates sequence diversity in the offspring through the exchange between homologs (Petronczki et al., 2003; Sarbajna and West, 2014).

HR proceeds by pathways that may lead to the formation of DNA four-way junctions or Holliday junctions (HJs) that physically link two homologous DNA duplexes (Heyer, 2015; Holliday, 1964; Schwacha and Kleckner, 1995; Szostak et al., 1983). Faithful removal of HJs is critical to avoid chromosome aberrations (Wechsler et al., 2011) and cells have evolved sophisticated measures to disentangle joint molecules. One basic mechanism is resolution mediated by HJ resolvases that introduce precise symmetrical nicks into the DNA at the branch point. Nicked DNA strands are then rejoined by endogenous ligases leading to fully restored or recombined DNA strands. This mechanism is well studied for bacterial and bacteriophage resolvases such as *Escherichia coli* RuvC, T7 endonuclease I, T4 endonuclease VII (Benson and West, 1994; Lilley and White, 2001). These resolvases operate as dimers and show a large degree of conformational flexibility in substrate

**eLife digest** Factors like ultraviolet radiation and harmful chemicals can damage DNA inside living cells, which can lead to breaks that form across both strands in the DNA double helix. “Homologous recombination” is one of the major mechanisms by which cells repair these double-strand breaks. During this process, the broken DNA interacts with another undamaged copy of the DNA to form a special four-way structure called a “Holliday junction”. The intact DNA strands are then used as templates to repair the broken strands. However, once this has occurred the Holliday junction needs to be ‘resolved’ so that the DNA strands can disentangle.

One way in which Holliday junctions are resolved is through the introduction of precise symmetrical cuts in the DNA at the junction by an enzyme that acts like a pair of molecular scissors. Re-joining these cut strands then fully restores the DNA. Enzymes that generate the cuts in DNA are called nucleases, and the nuclease GEN1 is crucial for resolving Holliday junctions in organisms such as fungi, plants and animals. GEN1 belongs to a family of enzymes that act on various types of DNA structures that are formed either during damage repair, DNA duplication or cell division. However, GEN1 is the only enzyme in the family that can also recognize a Holliday junction and it was unclear why this might be.

Lee et al. have now used a technique called X-ray crystallography to solve the three-dimensional structure of the human version of GEN1 bound to a Holliday junction. This analysis revealed that many features in GEN1 resemble those found in other members of the same nuclease family. These features include two surfaces of the protein that bind to DNA and are separated by a wedge, which introduces a sharp bend in the DNA. However, Lee et al. also found that GEN1 contains an additional region known as a “chromodomain” that further anchors the enzyme to the DNA. The chromodomain allows GEN1 to correctly position itself against DNA molecules, and without the chromodomain, GEN1’s ability to cut DNA in a test tube was severely impaired. Further experiments showed that the chromodomain was also important for GEN1’s activity in yeast cells growing under stressed conditions.

The discovery of a chromodomain in this human nuclease may provide many new insights into how GEN1 is regulated, and further work could investigate if this chromodomain is also involved in binding to other proteins.

DOI: [10.7554/eLife.12256.002](https://doi.org/10.7554/eLife.12256.002)

recognition and in aligning both active sites for coordinated cleavage. Interestingly, T4 endonuclease VII and RuvC reach into and widen the DNA junction point whereas T7 endonuclease I binds DNA by embracing HJs at the branch point (*Biertümpfel et al., 2007; Górecka et al., 2013; Hadden et al., 2007*).

In eukaryotes, HR is more complex and tightly regulated. In somatic cells, HJ dissolution by a combined action of a helicase and a topoisomerase (BLM-TOPIII $\alpha$ -RMI1-RMI2 complex in humans) is generally the favored pathway, possibly to restore the original (non-crossover) DNA arrangement (*Cejka et al., 2010, 2012; Ira et al., 2003; Putnam et al., 2009; Wu and Hickson, 2003*). In contrast, HJ resolution generates crossover and non-crossover arrangements depending on cleavage direction. Several endonucleases such as GEN1, MUS81-EME1, and SLX1-SLX4 have been implicated as HJ resolvases in eukaryotes (*Andersen et al., 2011; Castor et al., 2013; Fekairi et al., 2009; Garner et al., 2013; Ip et al., 2008; Muñoz et al., 2009; Svendsen and Harper, 2010; Svendsen et al., 2009; Wyatt et al., 2013*). Interestingly, these resolvases are not structurally related and have different domain architectures, giving rise to variable DNA recognition and regulation mechanisms. The interplay between resolution and dissolution mechanisms is not fully understood yet, however, cell cycle regulation of resolvases seems to play an important role (*Blanco et al., 2014; Chan and West, 2014; Eissler et al., 2014; Matos et al., 2011*).

GEN1 belongs to the Rad2/XPG family of structure-selective nucleases that are conserved from yeast to humans (*Ip et al., 2008; Lieber, 1997; Yang, 2011*). The Rad2/XPG family has four members with different substrate preferences that function in DNA maintenance (*Nishino et al., 2006; Tsutakawa et al., 2014*). They share a conserved N-terminal domain (XPG-N), an internal domain (XPG-I) and a 5’->3’ exonuclease C-terminal domain containing a conserved helix-hairpin-helix motif.

C-terminal to the nuclease core is a regulatory region that is diverse in sequence and predicted to be largely unstructured. Although the catalytic cores are well conserved in the superfamily, substrate recognition is highly diverse: XPG/Rad2/ERCC5 recognizes bubble/loop structures during nucleotide-excision repair (NER), FEN1 cleaves flap substrates during Okazaki fragment processing in DNA replication, EXO1 is a 5'→3' exonuclease that is involved in HR and DNA mismatch repair (MMR) and GEN1 recognizes Holliday junctions (*Grasby et al., 2012; Ip et al., 2008; Nishino et al., 2006; Tomlinson et al., 2010; Tsutakawa et al., 2014*). A common feature of the superfamily is their inherent ability to recognize flexible or bendable regions in the normally rather stiff DNA double helix. Interestingly, GEN1 shows versatile substrate recognition accommodating 5' flaps, gaps, replication fork intermediates and Holliday junctions (*Ip et al., 2008; Ishikawa et al., 2004; Kanai et al., 2007*). According to the current model, however, the primary function of GEN1 is HJ resolution (*Garner et al., 2013; Sarbajna and West, 2014; West et al., 2015*) and it is suggested to be a last resort for the removal of joint molecules before cytokinesis (*Matos et al., 2011*).

To date, structural information is available for all members of the family but GEN1 (*Miętus et al., 2014; Orans et al., 2011; Tsutakawa et al., 2011*). A unified feature of these structures is the presence of two DNA-binding interfaces separated by a hydrophobic wedge. This wedge is composed of two protruding helices that induce a sharp bend into flexible DNA substrates. Rad2/XPG family members also share a helix-two-turn-helix (H2TH) motif that binds and stabilizes the uncleaved DNA strand downstream of the catalytic center. However, the comparison of DNA recognition features within the Rad2/XPG family has been hampered because of the lack of structural information on GEN1.

To understand the molecular basis of GEN1's substrate recognition, we determined the crystal structure of human GEN1 in complex with HJ DNA. In combination with mutational and functional analysis using *in vitro* DNA cleavage assays and *in vivo* survival assays with mutant yeast strains, we highlight GEN1's sophisticated DNA recognition mechanism. We found that GEN1 does not only have the classical DNA recognition features of Rad2/XPG nucleases, but also contains an additional DNA interaction site mediated by a chromodomain. In the absence of the chromodomain, GEN1's catalytic activity was severely impaired. This is the first example showing the direct involvement of a chromodomain in a nuclease. Our structural analysis gives implications for a safety mechanism using an adjustable hatch for substrate discrimination and to ensure coordinated and precise cleavage of Holliday junctions.

## Results

### Structure determination and architecture of the GEN1-DNA complex

In order to structurally characterize human GEN1, we crystallized the catalytically inactive variant GEN1<sup>2-505 D30N</sup>, denoted GEN1 for simplicity, in complex with an immobile Holliday junction having arm lengths of 10 bp (*Figure 1*). The structure was determined experimentally and refined up to 3.0 Å resolution with an  $R_{\text{free}}$  of 0.25 (*Table 1*). The HJ crystallized bridging between two protein monomers in the asymmetric unit (*Figure 1—figure supplement 1*). The overall structure of GEN1 resembles the shape of a downwards-pointing right hand with a 'thumb' extending out from the 'palm' and the DNA is packed against the ball of the thumb (*Figure 1*). The palm contains the catalytic core, which is formed by intertwined XPG-N and XPG-I domains (*Figure 1A/B*, green). They consist of a seven-stranded  $\beta$ -sheet in the center surrounded by nine helices harboring the conserved active site (*Figure 1B/D*, orange). The catalytic residues form a cluster of negatively charged residues (D30, E75, E134, E136, D155, D157, D208) that were originally identified by mutational analysis (*Ip et al., 2008; Lee et al., 2002; Wakasugi et al., 1997*) and are conserved in other Rad2/XPG family members (*Figure 1B/C* and *Figure 2*). The XPG-I domain is followed by a 5'→3' exonuclease C-terminal domain (EXO; *Figure 1B/D*, blue). The EXO domain consists of a helix-two-turn-helix (H2TH) motif (helices  $\alpha$ 10- $\alpha$ 11) accompanied by several  $\alpha$ -hairpins ( $\alpha$ 12- $\alpha$ 13 and  $\alpha$ 14- $\alpha$ 15). A similar arrangement is also found in other proteins, which use a H2TH motif for non-sequence specific DNA recognition (*Tomlinson et al., 2010*). The EXO domain in GEN1 has a 78 amino acid insertion (residues 245–322), of which only helix  $\alpha$ 12b (residues 308–322) is ordered in the structure (*Figure 1A*, gray and *Figure 2*). Helix  $\alpha$ 12b packs loosely with the H2TH helices ( $\alpha$ 10- $\alpha$ 11) and helix  $\alpha$ 12 at the 'finger' part of GEN1. Yeast Rad2, a homolog of human XPG, also contains helix  $\alpha$ 12b,

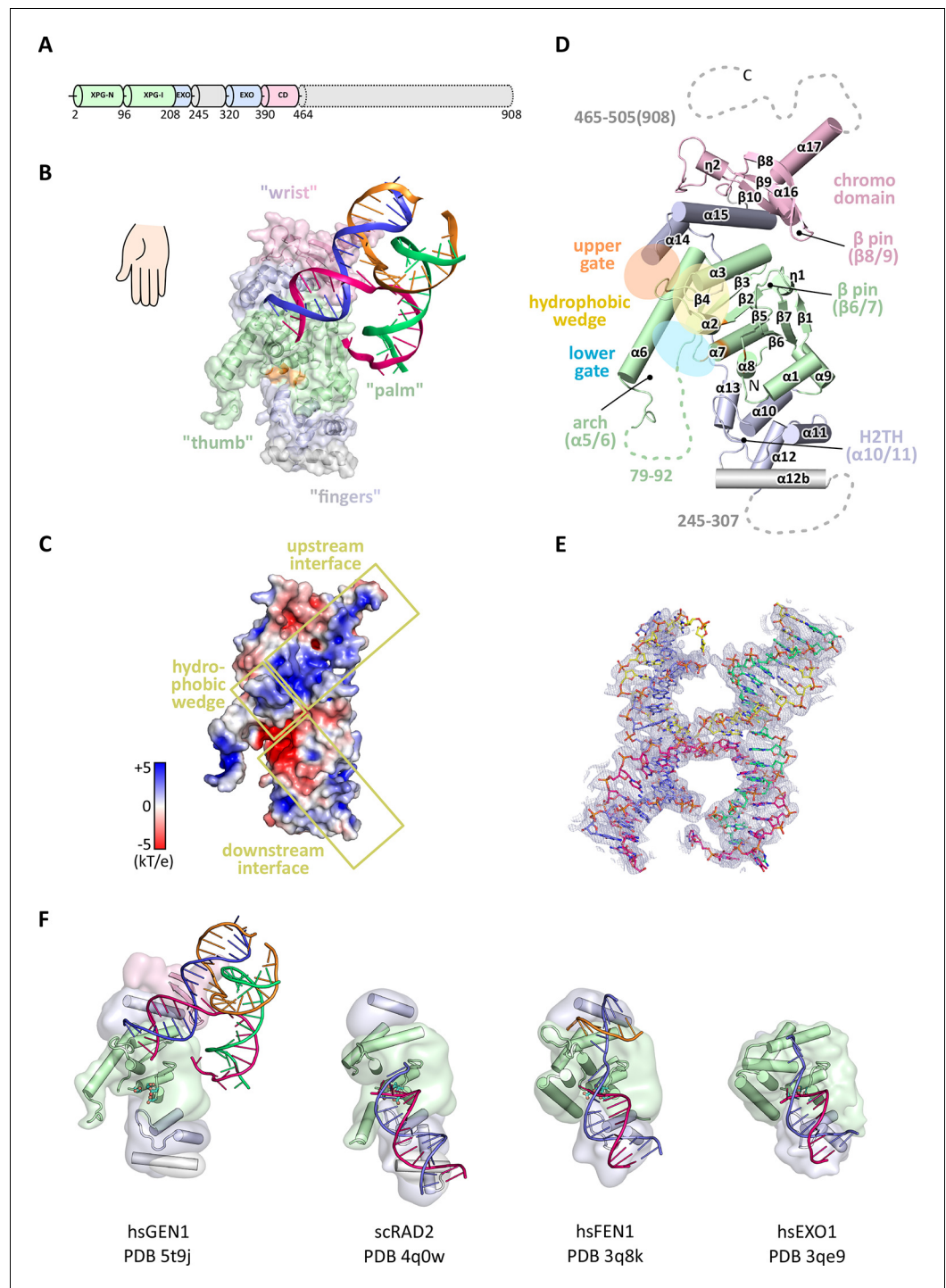


**Figure 1.** Architecture of human GEN1. (A) Domain architecture of human GEN1. The structurally unknown regulatory domain (residues 465–908) is shown with dotted lines. (B) Overview of the catalytic core of GEN1 in complex with HJ DNA. The protein resembles the shape of a downwards-pointing right hand with helix  $\alpha 6$  as the thumb. The protein is depicted in half transparent surface representation with secondary structure elements underneath. The DNA is shown in ladder representation with individual strands in different colors. The coloring of GEN1 follows domain boundaries: intertwining XPG-N and XPG-I in green, 5'→3' exonuclease C-terminal domain (EXO) in blue, chromodomain in pink, unassigned regions in gray. Active site residues (E134, E136, D155, D157) are highlighted in orange. (C) Electrostatic surface potential of GEN1. The coloring follows the potential from -5 (red) to +5 kT/e (blue). The DNA-binding interfaces and the position of the hydrophobic wedge are marked in yellow. (D) Secondary structure elements of the catalytic core of GEN1 in cartoon representation with the same coloring as in (B). (E) Ribbon representation of the catalytic core of GEN1. (F) Comparison of GEN1 complexes: hsGEN1 (PDB 5t9j), scRAD2 (PDB 4q0w), hsFEN1 (PDB 3q8k), and hsEXO1 (PDB 3qe9).

Figure 1 continued

colors as before. Dotted lines represent parts that are not resolved in the crystal structure. The numbering follows a unified scheme for the Rad2/XPG family (compare **Figure 2**) for  $\alpha$ -helices,  $\beta$ -sheets and  $3_{10}$ -helices ( $\eta$ ). (E) Experimental electron density map (autoSHARP, solvent flattened, contoured at  $1\sigma$ ) drawn around the HJ in the GEN1 complex. The DNA model is shown in ball-stick representation with carbon atoms of individual strands in different colors (yellow, light blue, magenta, green) and oxygen atoms in red, phosphor atoms in orange, nitrogen atoms in dark blue. (F) Structural comparison of Rad2/XPG family nucleases. Proteins are shown in a simplified surface representation with important structural elements in cartoon representation and DNA in ladder representation. The color scheme is the same as in **B. Figure 1—figure supplement 1** shows the content of the asymmetric unit.

DOI: [10.7554/eLife.12256.003](https://doi.org/10.7554/eLife.12256.003)

The following figure supplement is available for figure 1:

**Figure supplement 1.** Content of the asymmetric unit of the GEN1-HJ crystal.

DOI: [10.7554/eLife.12256.004](https://doi.org/10.7554/eLife.12256.004)

and it shows a similar arrangement as in GEN1 (**Figure 1F**). The EXO domain sandwiches the XPG-N/I domains with a long linker reaching from the bottom ‘fingers’ ( $\alpha 10$ - $\alpha 13$ ) along the backside of GEN1 to the top of the XPG-N/I domains at the ‘wrist’ ( $\alpha 14$ - $\alpha 15$ ). A structure-based sequence alignment of the nuclease core of human GEN1, FEN1, EXO1 and yeast Rad2 proteins with functional annotations relates sequence conservation to features in the Rad2/XPG family (**Figure 2**). The comparison with members in the Rad2/XPG identified two DNA binding interfaces and a hydrophobic wedge (ball of the thumb) that separates the upstream and the downstream interface (**Figure 1C/D** and compare **Figure 1F**). GEN1 has two prominent grooves close to the hydrophobic wedge, which we termed upper and lower gate or gateway for comparison (**Figure 1D**, orange and blue ellipses, respectively).

Notably, a small globular domain (residues 390–464) was found extending the GEN1 nuclease core at the wrist (**Figure 1**, pink). A DALI search (**Holm and Rosenström, 2010**) against the Protein Data Bank (PDB) identified this domain as a chromodomain (chromatin organization modifier domain). The domain has a chalice-shaped structure with three antiparallel  $\beta$ -strands packed against a C-terminal  $\alpha$ -helix and it forms a characteristic aromatic cage. The opening of the chalice abuts helix  $\alpha 15$  from the EXO domain.

### GEN1 has a conserved chromodomain with a closed aromatic cage

Chromodomains are found in many chromatin-associated proteins that bind modified histone tails for chromatin targeting (reviewed in **Blus et al., 2011; Eissenberg, 2012; Yap and Zhou, 2011**), but it has not previously been associated with nucleases. To understand the significance of the chromodomain for the function of GEN1, we first examined if the chromodomain is conserved in GEN1 homologs using HMM-HMM (Hidden Markov Models) comparisons in HHPRED (**Söding et al., 2005**). We found that the chromodomain in GEN1 is conserved from yeast (Yen1) to humans (**Figure 3A**). The only exception is *Caenorhabditis elegans* GEN1, which has a much smaller protein size of 443 amino acids compared to yeast Yen1 (759 aa) or human GEN1 (908 aa).

To further compare the structural arrangement of the aromatic cage in human GEN1 with other chromodomains, we analyzed the best matches from the DALI search (**Figure 3B**). We found many hits for different chromo- and chromo-shadow domains with root mean square deviations between 1.9 and 2.8 Å (compare **Figure 3—source data 1**). A superposition of the aromatic cage of the five structurally most similar proteins with GEN1 (**Figure 3C**) showed that residues W418, T438, and E440 are well conserved, whereas two residues at the rim of the canonical binding cleft are changed from phenylalanine/tyrosine to a leucine (L397) in one case and a proline (P421) in another (**Figure 3C**). Instead, Y424 occupies the space proximal to P421, which is about 1.5 Å outwards of the canonical cage and widens the GEN1 cage slightly. The substitution of phenylalanine/tyrosine to leucine is also found in CBX chromo-shadow domains (see below); however, the rest of the GEN1 aromatic cage resembles rather chromodomains.

Chromodomains often recognize modified lysines through their aromatic cage thus targeting proteins to chromatin (reviewed in **Blus et al., 2011; Eissenberg, 2012; Yap and Zhou, 2011**). Given the conserved aromatic cage in GEN1, we tested the binding to modified histone tail peptides

**Table 1.** Data collection and refinement statistics.

Data Set	G505-4w006native	G505-4w006Ta peak	G505-4w006SeMet peak
<b>Diffraction Data Statistics</b>			
Synchrotron Beamline	SLS PXII	SLS PXII	SLS PXII
Wavelength	0.99995	1.25473	0.97894
Resolution (Å)	75-3.0	75.4-3.8	43.6-4.4
Space Group	P 3 <sub>2</sub>	P 3 <sub>2</sub>	P 3 <sub>2</sub>
Cell dimensions			
a (Å)	86.94	87.06	87.11
b (Å)	86.94	87.06	87.11
c (Å)	200.72	201.30	199.69
α (°)	90	90	90
β (°)	90	90	90
γ (°)	120	120	120
I/σI*	18.4 (1.9)	27.49 (5.83)	16.58 (3.82)
Completeness (%)*	99.8 (98.8)	99.6 (97.3)	97.3 (83.3)
Redundancy*	6.3	10.2	5.1
R <sub>sym</sub> (%)*	6.2 (90.7)	7.7 (42.2)	6.9 (43.4)
<b>Refinement Statistics</b>			
Resolution (Å)	75-3.0		
Number of Reflections	33933		
R <sub>work</sub> /R <sub>free</sub>	0.199/0.241		
Number of Atoms			
Protein	6298		
DNA	1589		
Water/Solutes	27		
B-factors			
Protein	123.4		
DNA	150.2		
Water/Solutes	92.6		
R.M.S Deviations			
Bond lengths (Å)	0.010		
Bond Angles (°)	0.623		
Ramachandran Plot			
Preferred	753 (97.9 %)		
Allowed	16 (2.1%)		

\*Values for the highest resolution shell are shown in parenthesis

DOI: [10.7554/eLife.12256.005](https://doi.org/10.7554/eLife.12256.005)

(**Figure 3C/D**). However, we did not detect any binding despite extensive efforts using various histone tail peptides in pull-down assays, microscale-thermophoresis (MST) or fluorescence anisotropy measurements (compare **Figure 3—source data 2** and **Figure 3—figure supplement 2**). Our structure shows that the aromatic cage is closed by helix α15 (**Figure 3E** blue/pink), which has a hydrophobic interface towards the aromatic cage with residues L376, T380, and M384 reaching into it (compare **Figure 4F**). This potentially hampers the binding of the tested peptides in this conformation under physiological conditions.

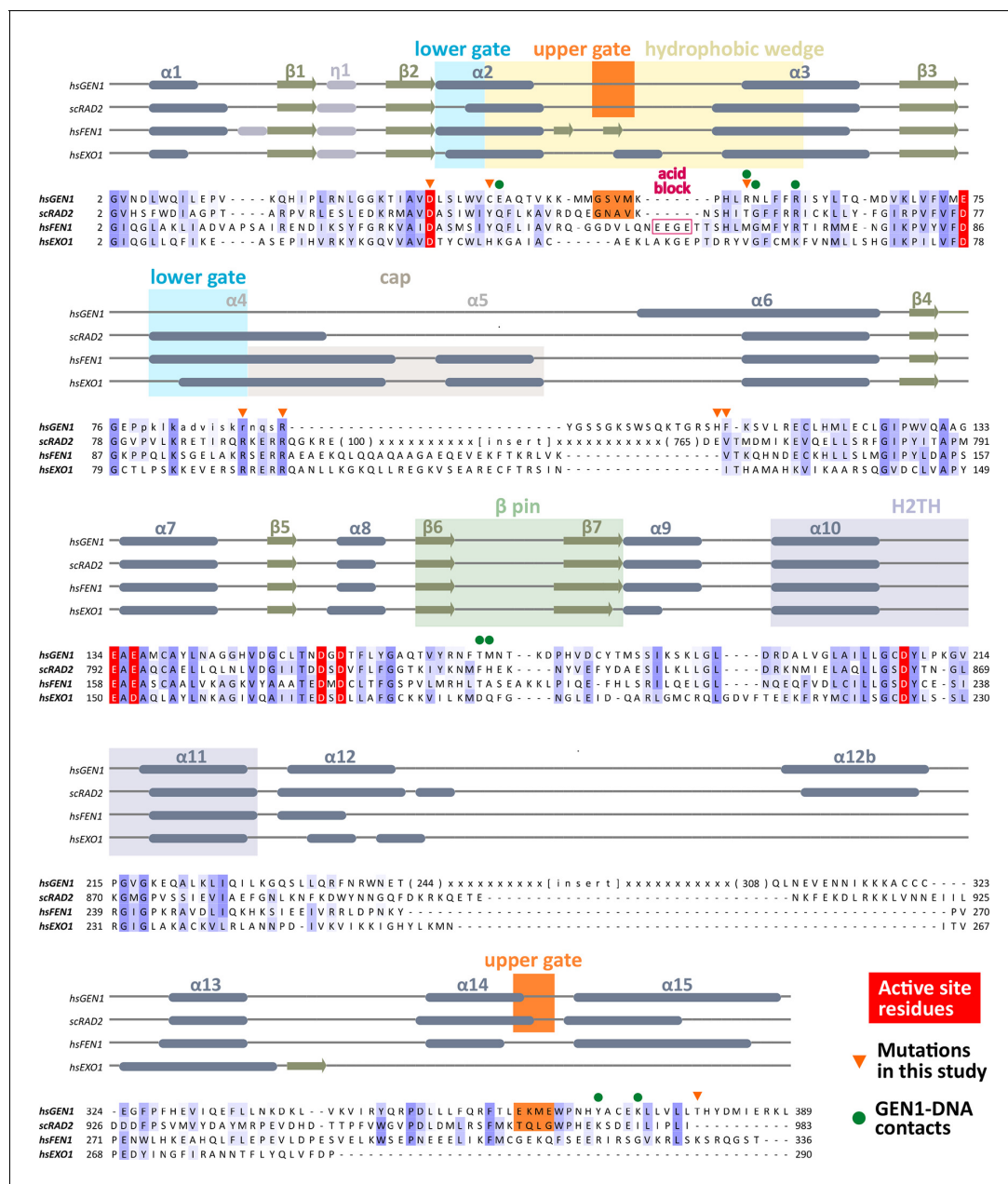


**Figure 2.** Alignment of the nuclease cores of Rad2/XPG-family proteins. The alignment is based on known crystal structures: human GEN1 (PDB 5t9j), this study), yeast Rad2 (PDB 4q0w), human FEN1 (PDB 3q8k), human EXO1 (3qe9). Secondary structure elements are depicted on top of the sequence with dark blue bars for  $\alpha$ -helices, light blue bars for  $3_{10}$ -helices and green arrows for  $\beta$ -sheets. The numbering follows a unified scheme for the superfamily. Functional elements are labeled and described in the main text. Sequences are colored by similarity (BLOSUM62 score) and active site residues are marked in red. Mutations analyzed in this study are marked with an orange triangle and DNA contacts found in the human GEN1-HJ structure have a dark green dot. Disordered or missing parts in the structures are labeled in small letters or with x.  
DOI: 10.7554/eLife.12256.006

## The GEN1 chromodomain is distantly related to CBX and CDY chromodomains

To explore the functional role of the GEN1 chromodomain, we evaluated its similarity to other chromodomains by comparing all of the 46 known human chromodomains from 34 different proteins. We made pairwise comparisons with HHPRED, PSIBLAST, combined the alignments and generated a phylogenetic tree (Figure 3F and Figure 3—figure supplement 1). The analysis showed a tree

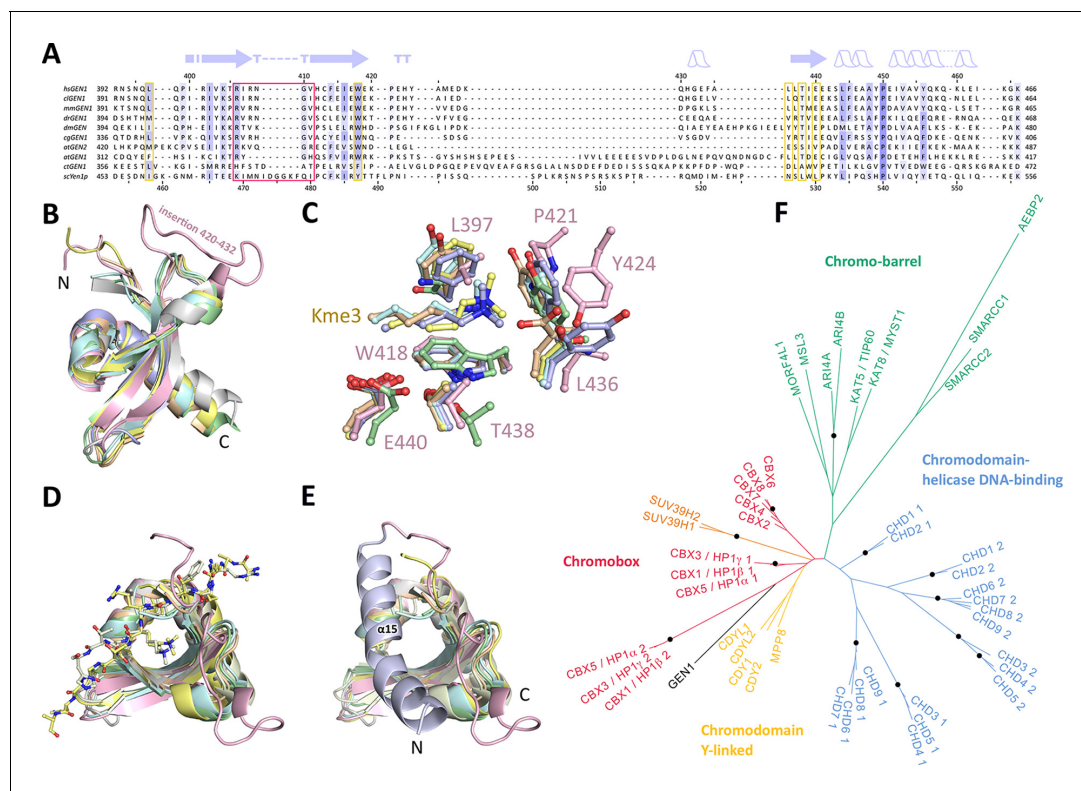


**Figure 3.** Chromodomain comparison. (A) Sequence alignment of GEN1 chromodomains from different organisms: hsGEN1 (*Homo sapiens*), clGEN1 (*Canis lupus*), mmGEN1 (*Mus musculus*), drGEN1 (*Danio rerio*), atGEN1/2 (*Arabidopsis thaliana*), cgGEN1 (*Crassostrea gigas*), scYEN1 (*Saccharomyces cerevisiae*). The presence of a chromodomain is conserved from yeast to human with *Caenorhabditis elegans* as an exception. Secondary structure elements of the GEN1 chromodomain are shown on top. The sequence coloring is based on a similarity matrix (BLOSUM62). The corresponding positions of the DNA-interaction site in human GEN1 is marked with a red box and residues of the aromatic cage are highlighted with a yellow box. (B) GEN1 has a canonical chromodomain fold of three antiparallel beta-sheets packed against an  $\alpha$ -helix. (C) The arrangement of the aromatic cage in GEN1 is comparable to other chromodomains but less aromatic and slightly larger. (D) The superposition of different chromodomains places cognate binding peptides of hsMPP8 and mmCBX7 (and others) into the aromatic cage. (E) The aromatic cage of GEN1 is closed by helix  $\alpha$ 15. Panels B–D show the chromodomains of hsGEN1 (pink, PDB 5t9j), hsCBX3 (gray, PDB 3kup), hsSUV39H1 (green, PDB 3mts), hsMPP8 (yellow, PDB 3lwe), dmHP1a (orange, chromo shadow PDB 3p7j), dmRHINO (cyan, PDB 4qvc/3r93), mmCBX7 (light blue, PDB 4x3s; compare **Figure 3—source data 1**). (F) Phylogenetic tree of all known human chromodomains. GEN1 is distantly related to the CBX chromo-shadow domains and CDY chromodomains. The corresponding alignment for calculating the phylogenetic tree is shown in **Figure 3—figure supplement 1**. GEN1 is colored in black, chromobox (CBX) proteins are colored in red, interspersed by SUV39H histone acetylases (orange) and chromodomain Y-linked (CDY) proteins (yellow). Chromo-barrel domain proteins are colored in green and chromodomain-helicase DNA-binding (CHD) proteins are in blue. Chromodomains and chromo-shadow domains from the same protein are labeled with 1 and 2, respectively. Stable branches with bootstrap values equal or higher than 0.8 are marked with a black dot. The binding of the GEN1 chromodomain to a set of histone peptides was tested but no interaction was detected (**Figure 3—source data 2** and **Figure 3—figure supplement 2**).

DOI: 10.7554/eLife.12256.007

The following source data and figure supplements are available for figure 3:

**Source data 1.** Proteins found in a DALI search.

DOI: 10.7554/eLife.12256.008

**Source data 2.** N-terminally fluorescein-labeled peptides used for chromodomain binding assays.

DOI: 10.7554/eLife.12256.009

**Figure supplement 1.** Sequence alignment of all known human chromodomains.

DOI: 10.7554/eLife.12256.010

**Figure supplement 2.** Histone peptide pull-down assay.

DOI: 10.7554/eLife.12256.011

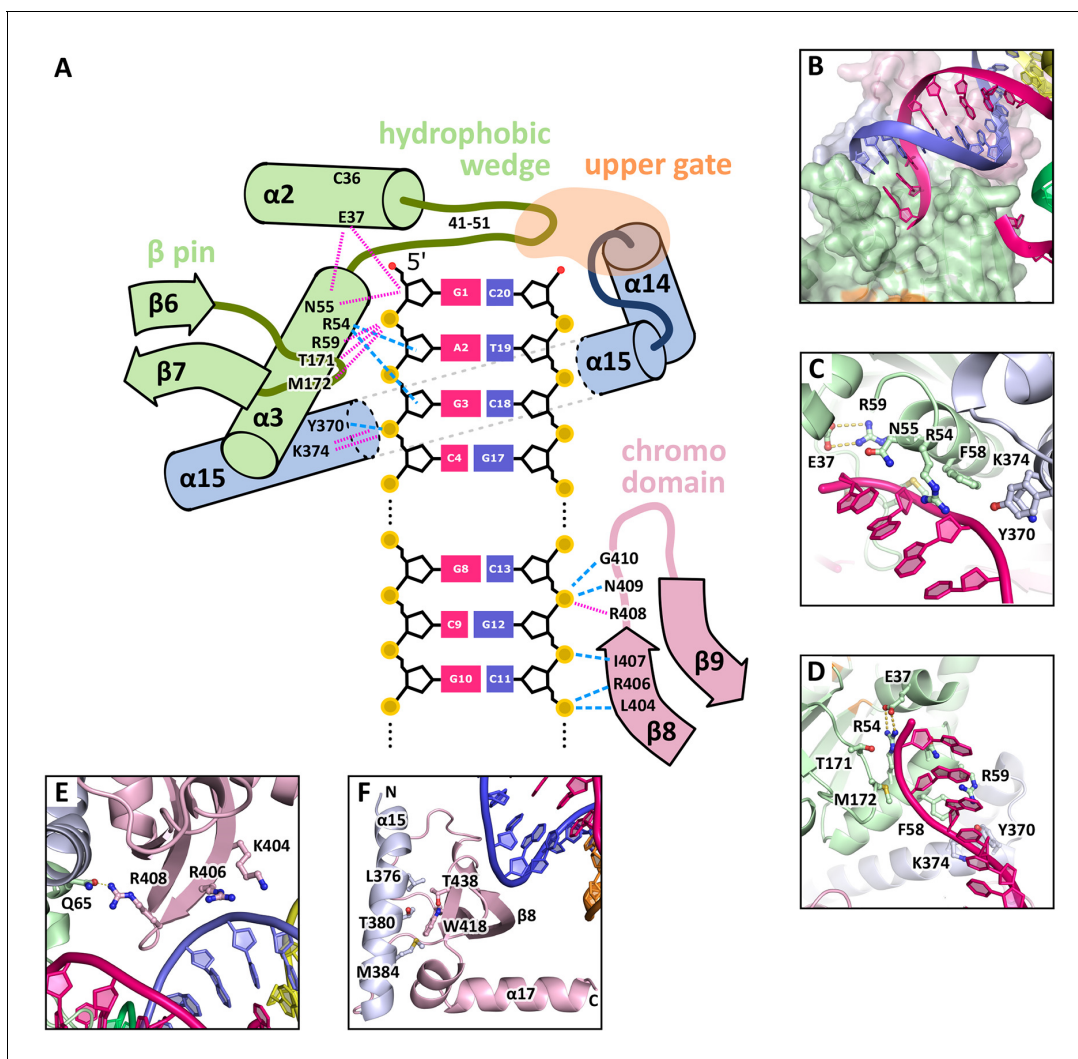


**Figure 4.** DNA interactions in the GEN1-DNA complex. (A) Schematic of the GEN1-DNA interactions at the upstream interface. The coloring is the same as in **Figure 1**. The nuclease core (green and blue) interacts with the uncleaved strand and the chromodomain (pink) contacts the complementary strand. Hydrogen bonds are shown with blue dashed lines and van-der-Waals contacts are in red dotted lines. (B) Interactions at the hydrophobic wedge. The end of the DNA double helix docks onto the hydrophobic wedge formed by helices  $\alpha 2$  and  $\alpha 3$ . (C/D) Interactions with the uncleaved strand in two views. All key residues form sequence-independent contacts to the DNA backbone. R54 reaches into the minor groove of the DNA. The complementary DNA strand has been removed for clarity (E/F) Interactions of the chromodomain with the complementary strand in two views. The backbone of residues 406–410 ( $\beta$ -hairpin  $\beta 8$ – $\beta 9$ ) abuts the DNA backbone. R406 has a supporting role in the interaction and R408 forms a polar interaction with Q65, which establishes a connection between the chromodomain and the nuclease core. Helix  $\alpha 15$  makes hydrophobic interactions with the aromatic cage and thus blocks it.

DOI: [10.7554/eLife.12256.012](https://doi.org/10.7554/eLife.12256.012)

branching into known subfamilies: chromobox proteins (CBX, red), chromodomain Y-linked proteins (CDY, yellow), chromodomain-helicase DNA-binding proteins (blue) and chromo-barrel domain proteins (green). The GEN1 chromodomain was found to be distantly related to the CDY chromodomains and chromobox proteins, particularly to the chromo-shadow domains of CBX1, CBX3 and CBX5. This agrees with the result from the DALI search, in which CBX chromo-shadow domains and homologs thereof were among the closest structural matches. Together with the observed differences in residues forming the aromatic cage, it indicates that the GEN1 chromodomain forms a new subgroup with features from chromo- and chromo-shadow domains that emerged from a common ancestor within CBX/CDY proteins.

## GEN1-DNA interactions

The GEN1-HJ structure revealed that the upstream DNA-binding interface acts as a docking site for double-stranded DNA and that the chromodomain secures its position. The DNA is bound at the upstream interface and the hydrophobic wedge but does not extend into the active site or to the downstream interface (**Figure 1B/C/D**). Comparison of the structure of GEN1 to related structures of FEN1, Rad2 and EXO1 (*Miqtus et al., 2014; Orans et al., 2011; Tsutakawa et al., 2011*) suggests that a DNA substrate has to extend to the downstream interface to position a DNA strand for cleavage by the active site of GEN1 (**Figure 1B/C** and **Figure 1F**). In the GEN1 structure, the end of the DNA arm attaches to the hydrophobic wedge provided by parts of helices  $\alpha 2$ - $\alpha 3$  and their connecting loop (**Figure 4A/B**), forming van-der-Waals contacts with the first base pair, which docks perfectly onto the protruding curb of residues 41–51 (**Figure 4B**). The uncleaved DNA strand is further stabilized and its geometrical arrangement is fixed by the upstream DNA-binding interface. Particularly, the DNA is contacted by a  $\beta$ -pin (strands  $\beta 6$ - $\beta 7$ ; **Figure 4A/C**) from one side and by R54 and F58 (**Figure 4A/D**) from helix  $\alpha 3$  together with Y370 and K374 (helix  $\alpha 15$ ) from the opposite side (**Figure 4A/C**). The key residues in the  $\beta$ -pin are T171 that forms a hydrogen bridge to the phosphate of the first base (**Figure 4A**, 'G1') and M172 that makes a van-der-Waals contact to the DNA backbone at the second base (**Figure 4A**, 'A2'). R54 reaches into the DNA minor groove and forms a hydrogen bond with the ribose ring oxygen at the third base of the uncleaved strand and F58 packs against the same ribose moiety (**Figure 4C/D**). Y370 and K374 in  $\alpha 15$  form hydrogen bonds to the backbone of the third base of the uncleaved DNA strand (**Figure 4D**, 'G3').

An additional interaction point is provided by a  $\beta$ -hairpin from the chromodomain (strands  $\beta 8$ - $\beta 9$ ), one DNA turn upstream of the hydrophobic wedge (**Figure 4A/E/F**). This  $\beta$ -hairpin interacts with the complementary DNA strand by matching the protein backbone (residues 406–411) to the contour of the DNA backbone in a sequence unspecific manner (**Figure 4A/E**). The side chains of K404 and R406 project out, and they are in hydrogen bonding distance to the DNA (**Figure 4E**). Remarkably, R408 forms a polar interaction with Q65, which establishes a connection between the DNA contact point at the chromodomain and the nuclease core (**Figure 4E**). The interactions at the chromodomain extend the upstream DNA-binding interface to cover a full DNA turn, reinforcing the binding.

The downstream binding interface can be inferred from other Rad2/XPG structures (**Figure 1C/F**) as the nuclease core is well conserved in GEN1, FEN1, Rad2 and EXO1 (root mean square deviations of 0.9–1.1 Å for 161 C $\alpha$  atoms, respectively). The residues corresponding to the tip of the thumb (residues 79–92), which are disordered in the GEN1 structure, likely form helix  $\alpha 4$  upon DNA binding to the downstream interface as seen in human FEN1 and EXO1 (*Orans et al., 2011; Tsutakawa et al., 2011*). The missing residues in GEN1 have 35.7% identity and 78.6% similarity (BLOSUM62 matrix) to the corresponding residues in FEN1 (90–103), which form helix  $\alpha 4$  in the FEN1-DNA complex (compare **Figure 2**). The same region is disordered in FEN1 when no DNA is bound (*Sakurai et al., 2005*). This indicates that also GEN1 undergoes such a disorder-to-order transition to form an arch with helices  $\alpha 4$  and  $\alpha 6$  upon substrate binding (*Patel et al., 2012*) and similar to the arrangement in T5 FEN (*Ceska et al., 1996*).

## The activity of GEN1 depends on correct DNA positioning

GEN1 has versatile substrate recognition features, ranging from gaps, flaps, replication fork intermediates to HJs (*Ip et al., 2008; Ishikawa et al., 2004; Kanai et al., 2007*). To understand the functional relevance of the GEN1 structure for DNA recognition we performed a series of mutagenesis studies with single point mutations and truncated protein variants (**Figure 5** and **Figure 5—figure supplement 1/2**) to investigate the effect on the active site (D30N), upstream DNA binding (R54E), downstream DNA binding (C36E), arch at the downstream interface (R89E, R93E, H109E, F110E), and chromodomain ( $\Delta$ chromo, K404E, R406E). We performed nuclease assays by titrating different amounts of GEN1 to a fixed DNA concentration of 40 nM for 15 min and DNA cleavage products were analyzed by native electrophoresis (**Figure 5A** and **Figure 5—figure supplement 1/2**). We used an immobile HJ and a 5' flap substrate side-by-side to facilitate the comparison of the effects on separate GEN1 functions. Notably, stoichiometric amounts of GEN1 were required to cleave HJ substrates whereas 5' flaps were readily processed with catalytic amounts (**Figure 5A**).

The active site modification D30N showed that the cleavage activity on both HJ and 5' flap substrates was lost in agreement with previously published data (*Ip et al., 2008*). According to our

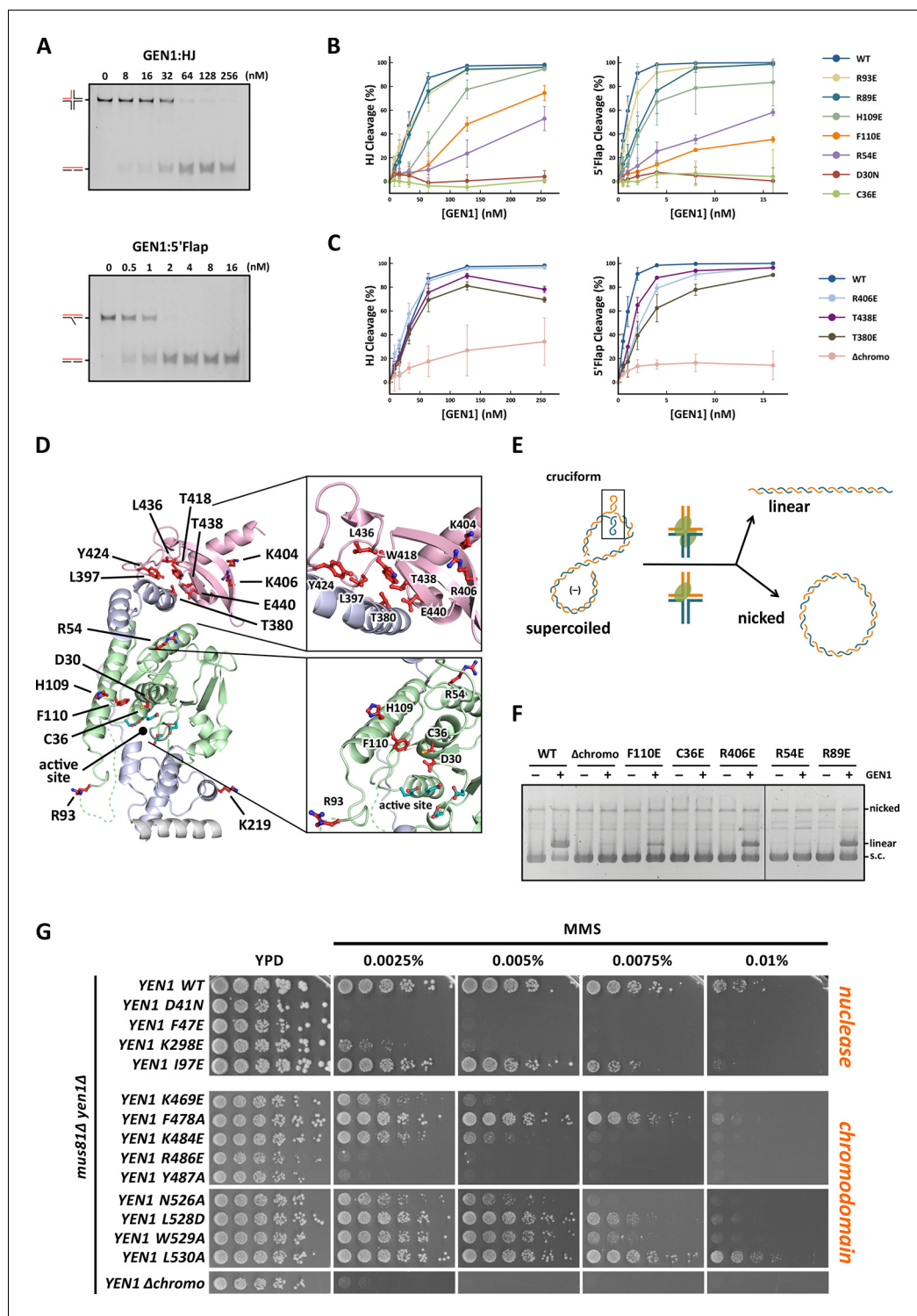


**Figure 5.** Functional analysis of GEN1. (A) Nuclease activity of GEN1 with HJ and 5' flap DNA. 40 nM 5' 6FAM-labeled substrates were mixed with indicated amounts of GEN1. Reactions were carried out at 37°C for 15 min, products were separated by native PAGE and analyzed with a phosphoimager. **Figure 5—source data 1** gives the sequences of DNA oligos used in biochemical assays and **Figure 5—source data 3** shows activity measurements. (B) Quantification of nuclease assays of wild type GEN1 and variants with mutated residues located at the protein-DNA interfaces. Percentage of cleavage was plotted against the enzyme concentration. Error bars depict the standard deviation calculated from at least three independent experiments. **Figure 5—figure supplement 1** shows representative gels from the PAGE analysis. (C) Quantification of nuclease assays of wild type GEN1 and **Figure 5 continued on next page**

Figure 5 continued

variants with mutated residues located at the chromodomain. Error bars depict the standard deviation calculated from at least three independent experiments. **Figure 5—figure supplement 2** shows representative gels from the PAGE analysis. (D) GEN1 mutations used in this study. Locations of human GEN1 mutations used in biochemical assays and corresponding residues in yeast MMS survival assays are highlighted in red. Active site residues E134, E136, D155, D157 are marked in turquoise. (E) Schematic of the cruciform plasmid cleavage assay. A cruciform structure can be formed in plasmid pIRbke8<sup>mut</sup>, which harbors an inverted-repeat sequence and is stabilized by negative supercoiling. Introducing two cuts across the junction point within the lifetime of the resolvase-junction complex yields linear products whereas sequential cleavage generates nicked products and the relaxed plasmid cannot be a substrate for the next cleavage. (F) Cruciform plasmid cleavage assay with different GEN1 variants. Plasmid pIRbke8<sup>mut</sup> was treated with 256 nM GEN1 each and reactions were carried out at 37°C for 15 min. Supercoiled, linear and nicked plasmids were separated by native agarose gel electrophoresis and visualized with SYBR safe under UV light. (G) MMS survival assays with yeast *yen1* variants. The survival of *yen1* mutants was tested under a *yen1Δ mus81Δ* background with indicated amounts of MMS. The top part shows mutations at GEN1-DNA interfaces and the bottom part mutations at the chromodomain (compare **Figure 5—figure supplement 3** for all controls and expression tests). **Figure 5—source data 2** gives a list of all yeast strains. DOI: [10.7554/eLife.12256.013](https://doi.org/10.7554/eLife.12256.013)

The following source data and figure supplements are available for figure 5:

**Source data 1.** Oligonucleotides used in biochemical assays.

DOI: [10.7554/eLife.12256.014](https://doi.org/10.7554/eLife.12256.014)

**Source data 2.** Yeast strains used for MMS survival assays.

DOI: [10.7554/eLife.12256.015](https://doi.org/10.7554/eLife.12256.015)

**Source data 3.** In vitro activity measurements of different GEN1<sup>2-505</sup> variants.

DOI: [10.7554/eLife.12256.016](https://doi.org/10.7554/eLife.12256.016)

**Figure supplement 1.** DNA cleavage assays of different GEN1 mutations.

DOI: [10.7554/eLife.12256.017](https://doi.org/10.7554/eLife.12256.017)

**Figure supplement 2.** DNA cleavage assays of different GEN1 fragments.

DOI: [10.7554/eLife.12256.018](https://doi.org/10.7554/eLife.12256.018)

**Figure supplement 3.** MMS survival assays with yeast *yen1* mutants.

DOI: [10.7554/eLife.12256.019](https://doi.org/10.7554/eLife.12256.019)

---

structure, R54 in helix  $\alpha 3$  at the upstream interface fixes the substrate position by reaching into the minor DNA groove and we observed that R54E had a strongly reduced cleavage activity (~50%; **Figure 5B**), indicating a key role in substrate positioning.

Residue C36 in helix  $\alpha 2$  points towards the downstream interface and likely contacts the DNA upon binding (compare **Figure 5D**). The corresponding FEN1 Y40, is a key residue stacking with the -1 base of the 5' flap at the FEN1 active site (*Tsutakawa et al., 2011*). Therefore, we tested the cleavage ability of a GEN1<sup>C36E</sup> and found that the mutant protein had completely lost its enzymatic activity for both, HJ and 5' flap cleavage, to the same degree as the active site modification D30N (**Figure 5B**). This effect is stronger than for FEN1<sup>Y40A</sup>, which showed only a partial loss in activity (*Tsutakawa et al., 2011*). Our results suggest that C36 provides a polar interface for orienting and guiding the cleaved strand towards the active site and the lower gateway.

We further tested a glutamate modification of the superfamily-conserved R89 and R93 located in the disordered part continuing to helix  $\alpha 6$ , presumably forming an arch (see above). The arch was shown to facilitate cleavage by clamping flap substrates in FEN1 and the modification R100A showed a strong decrease in the cleavage activity (*Patel et al., 2012*). The GEN1 R89E mutation, corresponding to residue R100 in FEN1, showed that the activity of GEN1 with a HJ substrate was not altered. In the case of a 5' flap substrate, cleavage was slightly reduced and it reached to the full level at enzyme concentrations higher than 10 nM. The effect of the R93E modification was even less pronounced compared to R89E. In contrast, the cleavage of both 5' flap and HJ substrates depended strongly on F110 at helix  $\alpha 6$  (thumb), which points towards the active site. An F110E modification showed a reduction in cleavage by 25% for HJ substrates, and the effect was even stronger for 5' flap substrates, where the activity is reduced by 65%. The equivalent position in FEN1 is V133 showing a critical involvement in stabilizing 5' flap DNA by orienting the -1 nucleotide for catalysis (*Tsutakawa et al., 2011*). We have also tested the effect of modifying H109, which neighbors the critical F110. Even though it points away from the active site, a glutamate at this

position reduced 5' flap cleavage to 83% and HJ cleavage recovered only at high substrate concentrations of 256 nM. Overall, the results suggest that F110 has a key position for DNA recognition and processing.

### Coordinated cleavage of HJs

Classical HJ resolvases introduce two symmetrical incisions across the junction point by coordinating the action of two active sites. The first nick is rate-limiting and the second one takes place near-simultaneously and within the lifetime of the resolvase-DNA complex. This mechanism has been well studied for bacterial and bacteriophage HJ resolvases (Fogg and Lilley, 2000; Giraud-Panis and Lilley, 1997; Pottmeyer and Kemper, 1992; Shah et al., 1997). Hence, it is thought that also GEN1 dimerizes upon binding to HJ substrates as indicated by coordinated cleavage and by an increase in hydrodynamic radius compared to protein alone (Chan and West, 2015; Rass et al., 2010). In order to further examine the effect of GEN1 modifications on HJ cleavage, we used a cruciform plasmid cleavage assay to evaluate GEN1's nicking function, as illustrated in Figure 5E. Here, the plasmid pIRbke8<sup>mut</sup> served as a substrate that contains an inverted-repeat sequence extruding a cruciform structure when supercoiled (Chan and West, 2015; Lilley, 1985; Rass et al., 2010). Coordinated dual incision of the cruciform (by a dimer) leads to linear duplex products with slow migration, whereas uncoordinated cleavage (by monomeric enzymes) results in nicked plasmids that migrate even slower (Figure 5F). Cruciform structures are reabsorbed when the superhelical stress is released upon single nicking and the DNA cannot serve as a substrate anymore.

We observed that wild type GEN1 resolved cruciform structures into linear products (Figure 5F) in agreement with previous reports (Chan and West, 2015; Rass et al., 2010). GEN1<sup>C36E</sup> (downstream interface) and GEN1<sup>R54E</sup> (upstream interface) showed only residual activity confirming their importance for HJ cleavage. The cruciform cleavage by F110E (thumb) was strongly reduced in line with our nuclease assays using small DNA substrates (Figure 5B). GEN1<sup>R89E</sup> (disordered part of the arch) did not show any appreciable effect, which suggests that this part of the arch is not directly involved in HJ recognition. Taken together, our results suggest that the positioning of HJ junction substrates both at the upper and the lower gateway is critical for productive cleavage. Furthermore, none of the tested modifications at the different DNA interaction interfaces was able to uncouple the coordinated HJ cleavage.

### The chromodomain of GEN1 facilitates efficient substrate cleavage

Agreeing with the structural significance for DNA binding, the truncation of the chromodomain ( $\Delta$ chromo, residues 2-389) showed a severe reduction (~3-fold) in HJ cleavage activity whereas all longer GEN1 fragments containing the chromodomain (2-464, 2-505 and 2-551) showed full activity (Figure 5—figure supplement 2). Interestingly, the effect of the chromodomain truncation is even more pronounced for 5' flap DNA cleavage than for HJs, showing a 7-fold reduction compared to wild type (Figure 5C). The activity of GEN1 in the plasmid-based cruciform cleavage assay was also severely hampered in the absence of the chromodomain (Figure 5F) showing only a weak band for linear products and no increase for nicked plasmid, emphasizing the importance of the chromodomain for GEN1 activity.

Further, to test the influence of the positively charged side chains K404 and R406 on DNA binding, we introduced charge-reversal mutations to glutamates and assessed their nuclease activities. Even though K404 and R406 are within hydrogen-bonding distance to the DNA, K404E, and R406E showed no appreciable influence on GEN1's nuclease activity. Only a slight reduction in cleavage of 5' flap substrates was observed for GEN1<sup>R406E</sup>, whereas the processing of HJ substrates was not altered significantly (Figure 5C). This reinforces the conclusion from our structural observations that the chromodomain and the DNA interact through their backbones via van-der-Waals interactions.

### Influence of phosphorylation-mimicking chromodomain modifications

PhosphoSitePlus (Hornbeck et al., 2014) lists two phosphorylation sites at residues T380 and T438 in GEN1 that were found in a T-cell leukemia and a glioblastoma cell line. These residues are located in helix  $\alpha$ 15 and at the rim of the aromatic cage, respectively. Both phosphorylation sites are positioned to interrupt hydrophobic interactions between helix  $\alpha$ 15 and the chromodomain (Figure 5D and Figure 4F). Therefore, we tested if the phosphorylation-mimicking modifications T380E and

T438E had an effect on GEN1's activity. At low enzyme concentrations (<50 nM) HJ cleavage was similar to that of wild-type protein but at high concentrations the activity declined to less than 80% (**Figure 5C**). For a 5' flap substrate, the assay showed consistently lower activity than wild type, recovering to about 80% cleavage at the highest enzyme concentration (**Figure 5C**). These results suggest that phosphorylation of GEN1 chromodomain residues may regulate DNA recognition and cleavage.

## Physiological relevance of GEN1 interactions

To test the physiological relevance of the identified GEN1-DNA interactions, we investigated the survival of *Saccharomyces cerevisiae* mutant strains expressing variants of Yen1 (GEN1 homolog) after treatment with the DNA-damaging agent MMS (**Figure 5G** and **Figure 5—figure supplement 3/source data 2**). All Yen1 variants were expressed to a similar degree as endogenous Yen1, which was confirmed by Western Blot analysis (**Figure 5—figure supplement 3**). Because of the functional overlap of Mus81 and Yen1 in HR (**Blanco et al., 2010**) a double knockout (*yen1Δ mus81Δ*) was used and complemented with different variants of Yen1.

The control strain, complemented with wild type Yen1, survived MMS concentrations of up to 0.01%, consistent with the described hypersensitivity of *mus81Δ* mutants (**Blanco et al., 2010; Interthal and Heyer, 2000**). In stark contrast, cells containing either the active site mutant Yen1-D41N (corresponding to GEN1<sup>D30N</sup>) or the downstream interface mutant Yen1-F47E (corresponding to GEN1<sup>C36E</sup>) did not grow even at an MMS concentration as low as 0.0025% (**Figure 5G**). After the expression of the upstream interface mutant Yen1-I97E (corresponding to GEN1<sup>R54E</sup>) cells showed a slight but significant growth defect at high MMS concentrations (see panels for 0.0075% and 0.01% MMS in **Figure 5G**). These results are therefore consistent with the in vitro cleavage results carried out with GEN1 mutants and showing a reduction in activity for R54E and no activity for C36E (see **Figure 5C**). As a last mutant in the nuclease core, we tested the K298E mutation which is located in helix  $\alpha$ 10 of the H2TH motif in the downstream DNA-binding interface, and for which we were unable to obtain the corresponding GEN1<sup>K219E</sup> modification for cleavage assays (compare **Figure 5D**). This mutant displayed a strong sensitivity towards MMS but lower than the one observed for the catalytic mutant, indicating that the mutant was partially functional in yeast (**Figure 5G**).

We next investigated the effect of mutations in the aromatic cage of Yen1's chromodomain (compare **Figure 3**) and found that their severity was strongly position dependent. Mutation of R486E and Y487A in Yen1, both of which are located near the base of the cage, corresponding to the W418 position in GEN1 (see **Figure 3C**), showed a strong effect on MMS sensitivity (see **Figure 5G**), similar to the one observed for the catalytic mutant, presumably due to a dysfunctional chromodomain. In contrast, mutations located further outside of the core (F478A and K484E) led to a less pronounced MMS sensitivity. The same was true for the K469E variant, which corresponds to position R406 at the chromodomain-DNA interface in GEN1 (see **Figure 3A** and **5F**), and for residues at the rim of the chromodomain (*yen1-N526A*, *yen1-L528D* and *yen1-W529A*), consistent with our in vitro observation for GEN1<sup>T438E</sup> (slightly reduced activity, **Figure 5C**). No effect on MMS sensitivity was detected for *yen1-L530A*, which corresponds to a conserved glutamate in chromodomains (E440 in GEN1). Lastly, we found that the deletion of the chromodomain (Yen1- $\Delta$ 452–560) lead to a severe phenotype comparable to the active site mutant Yen1-D41N (**Figure 5G** and **Figure 5—source data 2**). The Yen1 variant lacking the chromodomain was expressed to levels similar to the full-length protein and we therefore conclude that the chromodomain is crucial for the function of Yen1. Taken together, the functional data of Yen1 mutants in vivo and GEN1 mutants in vitro point towards an essential and evolutionary conserved role of the chromodomain in GEN1/Yen1 proteins.

## Discussion

### Implications of the chromodomain

The structure of the human GEN1 catalytic core provides the missing structural information in the Rad2/XPG family. The GEN1 structure complements recent reports on the structures of Rad2, EXO1 and FEN1, (**Miętus et al., 2014; Orans et al., 2011; Tsutakawa et al., 2011**). Thereby, it gives insights how relatively conserved nuclease domains recognize diverse substrates in a structure-

selective manner and act in different DNA maintenance pathways. In comparison with other Rad2/XPG nucleases, GEN1 shows many modifications on common structural themes that give the ability to recognize a diverse set of substrates including replication fork intermediates and HJs. The upstream DNA interface of GEN1 lacks the 'acid block' found in FEN1, instead it has a prominent groove at the same position (compare **Figure 1**, 'upper gate') with a strategically positioned R54 nearby. Furthermore, the helical arch in GEN1 misses helix  $\alpha 5$ , which forms a cap structure in FEN1 and EXO1 that stabilizes 5' overhangs for cleavage. These features have implications for the recognition and cleavage of HJ substrates (see below). The most striking difference to other Rad2/XPG family members is that the GEN1 nuclease core is extended by a chromodomain, which provides an additional DNA anchoring point for the upstream DNA-binding interface. The evolutionarily conserved chromodomain is important for efficient substrate cleavage as we showed using truncation and mutation analyses. This finding opens new perspectives for the regulation of GEN1 and for its interactions with other proteins. Chromodomains serve as chromatin-targeting modules (reviewed in **Blus et al., 2011; Eissenberg, 2012; Yap and Zhou, 2011**), general protein interaction elements (**Smother and Henikoff, 2000**) as well as dimerization sites (**Canzio et al., 2011; Cowieson et al., 2000; Li et al., 2011**). These possibilities are particularly interesting, as chromatin targeting of proteins via chromodomains has been implicated in the DNA damage response. The chromatin remodeler CHD4 is recruited in response to DNA damage to decondense chromatin (reviewed in **O'Shaughnessy and Hendrich, 2013; Stanley et al., 2013**). The chromodomains in CHD4 distinguish the histone modifications H3K9me3 and H3K9ac and determine the way how downstream DSB repair takes place (**Ayrapetov et al., 2014; Price and D'Andrea, 2013**). It is plausible that GEN1 uses its chromodomain not only as a structural module to securely bind DNA but also for targeting or regulatory purposes. Even though it was not possible to find any binding partner with a series of tested histone tail peptides, we cannot exclude that the chromodomain is used as an interaction motif or chromatin reader. It will therefore be interesting to extend our interaction analysis to a larger number of peptides and proteins. Interestingly, the modifications GEN1<sup>L397E</sup> and GEN1<sup>Y424A</sup> at the rim of the chromodomain did not alter DNA cleavage activity (**Figure 5—figure supplement 1**), however, mutations of residues at the rim of Yen1's chromodomain show a phenotype, suggesting an additional role like binding to an endogenous factor.

Another intriguing aspect of the chromodomain is that the conserved T438 at the rim of the aromatic cage and T380 at the closing helix  $\alpha 15$  are both part of a casein kinase II consensus sequence for phosphorylation (Ser/Thr-X-X-Asp/Glu). **Ayoub et al., 2008** showed that the analogous threonine in the chromodomain of CBX1 is phosphorylated in response to DNA damage and phosphorylation disrupts the binding to H3K9me. We observed a reduction in DNA cleavage activity for the phosphorylation mimicking mutations T380E and T438E, which may suggest a regulatory role. They might function together and in combination with other modifications to provide a way of functional switching at the chromodomain. Furthermore, **Blanco et al., 2014** and **Eissler et al., 2014** recently identified several CDK phosphorylation sites in an insertion in the Yen1 chromodomain which affects HJ cleavage and together with phosphorylation of a nuclear localization signal (NLS) in the regulatory domain restricts Yen1's activity to anaphase. The insertion is not found in other chromodomains and it is extended in Yen1 compared to GEN1, which is lacking these phosphorylation sites (compare **Figure 3A/B**). Notably, the activity of Yen1 is negatively regulated by CDK-dependent phosphorylation (**Blanco et al., 2014; Chan and West, 2014; Eissler et al., 2014; Matos et al., 2011**), suggesting that the chromodomain is targeted by cell cycle kinases. It also provides a likely explanation for the different regulatory mechanisms found in GEN1 and Yen1 (**Blanco and Matos, 2015; Chan and West, 2014; Matos and West, 2014**). Exploration of the regulatory function of the GEN1 chromodomain will be an important topic to follow up, and this may lead to the understanding of the precise regulation mechanism of GEN1 as well as its substrate recognition under physiological conditions.

It is noteworthy that our analysis also revealed that the human transcription modulator AEBP2, which is associated with the polycomb repression complex 2 (PRC2), contains a chromo-barrel domain, which, to our knowledge, has not been reported so far.

## Recognition of DNA substrates

The GEN1-DNA structure showed a considerable similarity to the other members of the Rad2/XPG family, and this facilitated the generation of a combined model to understand substrate recognition

of GEN1 (**Figure 6**). This was done by superimposing the protein part of the FEN1-DNA complex (PDB 3q8k) onto our GEN1 structure and extending the DNA accordingly (**Figure 6A/B**). Remarkably, the superimposition of the proteins aligns the DNA from the FEN1 structure in the same register as the DNA in the GEN1 complex at the upstream interface (**Figure 6A and 6B insert**). Furthermore, the free 5' and 3' ends of the double flap DNA from the FEN1 structure point towards the lower and the upper gateway in GEN1, respectively (**Figure 6B**). We extended the GEN1 structure by homology modeling of the disordered residues 79-92 (helix  $\alpha 4$ ) in GEN1 (**Figure 6B**). In addition to the similarity of this part to FEN1, the model readily showed the arrangement forming an arch structure. This would explain why GEN1 recognizes 5' flap substrates efficiently, analogous to FEN1, as the arch can clamp a single-stranded DNA overhang for productive cleavage. This also explains why the F110E modification in the arch at helix  $\alpha 6$  hampered 5' flap cleavage severely. The

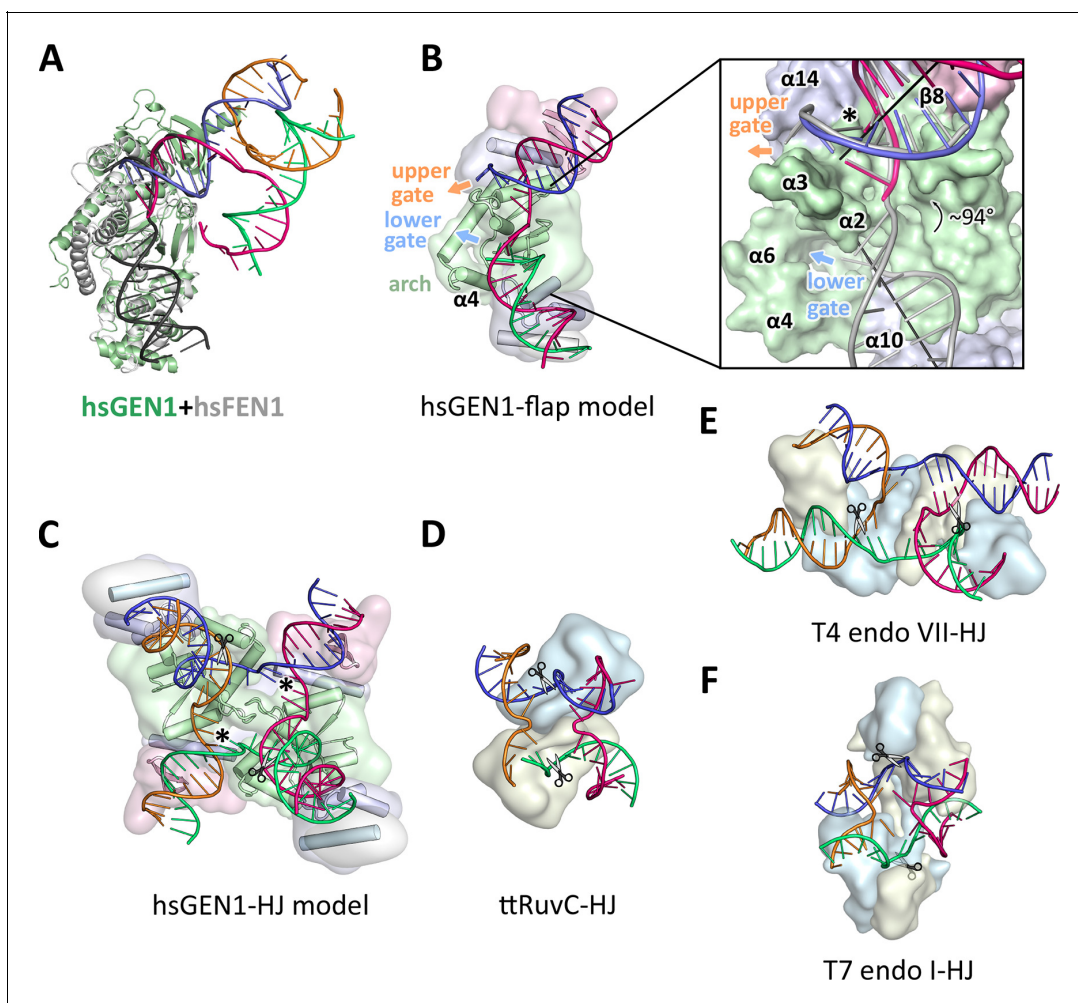


**Figure 6.** Substrate recognition features of GEN1. (A) Superposition of the protein part of the FEN1-DNA complex (PDB 3q8k, protein in gray, DNA in black) onto the GEN1-HJ complex (protein in green and the DNA strands in different colors). The FEN1-DNA aligns with the same register as the GEN1-DNA at the upstream interface. (B) Model for the recognition of a 5' flap substrate by GEN1. The DNA was extended using the superimposition from A. Homology modeling suggests an additional helix  $\alpha 4$  (disordered residues 79–92) forming an arch with helix  $\alpha 6$ . The protein is shown in a simplified surface representation with the same colors as in **Figure 1** and structural elements are highlighted. The insert shows a zoomed in view of the hydrophobic wedge with the modeled FEN1-DNA in gray. (C) Model for the dimerization of GEN1 upon binding to a HJ substrate based on the 5' flap model in B. The monomers interlock via both arches ( $\alpha 4$ - $\alpha 6$ ) and the hydrophobic wedges ( $\alpha 2$ - $\alpha 3$ ) contact each other. (D) Structure of the *Thermus thermophilus* RuvC-HJ complex (PDB 4ld0). (E) Structure of the T4 endonuclease VII-HJ complex (PDB 2qnc). (F) Structure of the T7 endonuclease I-HJ complex (PDB 2pfj). Individual monomers are in surface representation, colored in light blue and beige, respectively. DNA strands are shown as ladders in different colors.

DOI: 10.7554/eLife.12256.020

side chain points directly towards the active site and likely disturbs the stabilization of a 5' overhang for catalysis by charge repulsion. However, there are two features in GEN1 that vary from the arrangement in FEN1 and EXO1 considerably. Helix  $\alpha 6$  is longer (24 instead of 15 residues) and helix  $\alpha 5$  is missing in GEN1. As a result the arch points away from the DNA rather than forming a 'cap' structure as it is observed in FEN1 and EXO1 (Orans *et al.*, 2011; Tsutakawa *et al.*, 2011). Furthermore, the modified arch in GEN1 provides an opening, marked as 'lower gate' in **Figure 6B**. These differences are likely the basis for GEN1's versatile DNA recognition features.

### Implications of an adjustable hatch in GEN1 for substrate discrimination

The diverging orientation of the arch (helices  $\alpha 4$  and  $\alpha 6$ ) in GEN1 compared to the one in FEN1 and EXO1 (helices  $\alpha 4$ ,  $\alpha 5$ , and  $\alpha 6$ ) may have thus significance for the recognition of HJ substrates. By pointing away from the active site the arch provides an opening to accommodate unpaired, single-stranded DNA to pass along the arch at the lower gate (groove between  $\alpha 2$  and  $\alpha 4$ ) (**Figure 6B** 'lower gate') from one GEN1 monomer to the upper gate (groove between  $\alpha 2$ - $\alpha 3$  and  $\alpha 14$ ) (**Figure 6B** 'upper gate') of the other within a GEN1 dimer (**Figure 6B/C**). R54 is perfectly positioned at the minor groove to guide the second cleavage strand to pass through the upper gate (compare **Figure 4** and **Figure 6B/C**, marked with an asterisk). In FEN1, this position is occupied by the 'acid block', which stabilizes a single 3' flap of the unpaired substrate (Tsutakawa *et al.*, 2011) and it would not accommodate longer 3' DNA overhangs. In our model, two GEN1 monomers come together crosswise upon HJ binding (**Figure 6C**). The helical arches of both proteins likely provide additional protein-protein interactions as well as protein-DNA contacts by packing against the backbone of opposite DNA arms (**Figure 6C**). As a result, the GEN1 dimer orients both active sites symmetrically across the junction point resembling the situation in bacterial RuvC (**Figure 6D**; Bennett and West, 1995a; Górecka *et al.*, 2013). This arrangement would ensure that both incisions are introduced within the lifetime of the GEN1-HJ complex as observed biochemically by us and others (Chan and West, 2015; Rass *et al.*, 2010). The mechanism likely works in a coordinated nick-and-counter-nick fashion, as shown for bacterial or bacteriophage HJ resolvases (Fogg and Lilley, 2000; Giraud-Panis and Lilley, 1997; Pottmeyer and Kemper, 1992; Shah *et al.*, 1997) and recently for GEN1 (Chan and West, 2015).

The distance between both gates is bridged by unpaired bases in our GEN1-HJ model. This view is supported by the observation that FEN1 unpairs two bases near the active site through interactions with the hydrophobic wedge leading to strongly bent DNA arms between the upstream and downstream DNA interfaces. This mechanism seems to be a common feature of Rad2/XPG nucleases (Finger *et al.*, 2013; Grasby *et al.*, 2012; Tsutakawa *et al.*, 2011). Consistent with this view, the bacterial RuvC resolvase (**Figure 6D**) has also been shown to unfold HJ junctions (Bennett and West, 1995b; Górecka *et al.*, 2013). In the case of GEN1, the critical step would be the assembly of the dimer around the junction point in a highly restraint way and the introduction of the first nick. This releases the tension on the complex like a spring leading to an immediate second cut and subsequent disassembly of the GEN1-HJ complex. Furthermore, a HJ does not provide free DNA ends and adopts a structure that intrinsically restrains its degrees of freedom, thus inhibiting cleavage by a single GEN1 monomer. Altogether we speculate that the arch (helix  $\alpha 4$ - $\alpha 6$ ) acts like a lever or hatch switching between flap and HJ recognition modes. When a free 5' end is available it closes and clamps the flap, thus positions the DNA for cleavage. For the case of a HJ substrate, the arch adopts an open conformation, allowing unpaired, single-stranded DNA to pass, while preventing the correct positioning of the DNA for catalysis at first. HJ cleavage is inhibited until a second GEN1 monomer binds. This mechanism differs from the one used by bacterial or bacteriophage HJ resolvases, which act as obligate dimers binding to DNA substrates in a concerted way (compare **Figure 6D-F**). Our model for DNA cleavage by GEN1 describes a conformational switch provided by a flexible arch that can discriminate between substrates containing free 5' ends or those with a restraint structure like HJs. This aspect may explain our observation that GEN1 cleaves 5' flap DNA catalytically while stoichiometric amounts are required for HJ substrates (**Figure 5A-C**). Using a switchable hatch in a spring-loaded mechanism would be an efficient way of preventing a single cut at a HJ junction while allowing GEN1 to adapt to recognize various DNA substrates and perform different functional roles. Thus, GEN1 may have an intrinsic safety mechanism that ensures symmetrical dual incision across a branch point. Further studies have to address the exact engagement mechanism.

## GEN1 in a biological context

GEN1's biological role is not fully understood yet. Yeast cells are viable without the GEN1 homolog Yen1 even in the presence of DNA damaging agents as the Mus81-Eme1 complex can complement the defect (compare **Figure 5—figure supplement 3**; [Blanco et al., 2010](#)). Consistently, both proteins can cleave 5' flaps and HJ substrates in vitro. However, GEN1 can cleave intact HJs symmetrically whereas MUS81-EME1 is much more efficient with nicked DNA four-way junctions ([Castor et al., 2013](#); [Wyatt et al., 2013](#)). [Matos et al., 2011](#) suggested that Yen1/GEN1 might serve as a backup enzyme to resolve persistent HJs that have eluded other mechanisms of joint molecule removal before cytokinesis.

Our analysis infers that HJ cleavage is slower than 5' flap cleavage (**Figure 5B/C**), bringing interesting implications for a safety control of GEN1's activity. GEN1 may have to assemble in an accurate way before it can cleave a HJ. Likewise, it increases GEN1's persistence time on HJs and opens a window for branch migration for extending the length of recombined stretches of DNA. Moreover, GEN1 recognizes various DNA substrates, which may point towards a general role in processing substrates in different DNA maintenance pathways. GEN1 has been shown to cleave replication fork intermediates, and it is implicated in the resolution of replication-induced HJs ([Garner et al., 2013](#); [Sarbjana et al., 2014](#)). Like MUS81-EME1, it might also be important for the processing of fragile sites to ensure proper chromosome segregation ([Ying et al., 2013](#)). These functions have to be tested systematically to understand GEN1's biological role. In this context, the regulation of GEN1 is an important factor and needs to be explored. Our study identified a chromodomain extending the GEN1 nuclease core that might have a role in regulating the enzyme. An open question is the function and architecture of the remaining 444 amino acids at the C-terminus of GEN1. They are thought to regulate the nuclease activity and control subcellular localization ([Blanco et al., 2014](#); [Chan and West, 2014](#); [García-Luis et al., 2014](#)). It is very likely that new interaction sites and post-translational modifications in this region will be discovered in future. The presented structure together with additional studies will help to unravel these questions and to obtain a comprehensive view of the functions of the Rad2/XPG nucleases.

## Materials and methods

### Experimental procedures

#### Protein expression and purification

Wild type human GEN1 and truncations thereof (residues 2-551, 2-505, 2-464, 2-389) were amplified by PCR from IMAGE clone 40125755 (Mammalian Gene collection, natural variant S92T, S310N, UniProtID Q17RS7) and cloned into a self-made ligation-independent cloning vector with various C-terminal tags followed by His8. Truncated versions were designed based on limited proteolysis in combination with domain prediction and functional assays to determine the smallest yet active fragment. The N-terminal methionine was cleaved by cellular methionyl-aminopeptidase, which is an essential requirement in the Rad2/XPG family as the N-terminus (conserved residue G2) folds towards the active site. Mutations were introduced by site-directed mutagenesis using Phusion Polymerase (NEB, Frankfurt/Main, Germany). All recombinant proteins were expressed in the *E. coli* BL21(DE3) pRIL strain (MerckMillipore, Darmstadt, Germany). Cells were grown at 37°C until mid-log phase and induced overnight with 0.2 mM IPTG at 16°C. Cells were harvested by centrifugation and resuspended in lysis buffer containing 1x phosphate buffered saline (PBS) with additional 500 mM NaCl, 10% (v/v) glycerol, 2 mM DTT, 1 mM EDTA, 1 μM leupeptin, 1 μM pepstatin A, 0.1 mM AEBSF and 2 μM aprotinin and lysed by sonication. Cell debris was removed by centrifugation (75 600 g for 45 min), the clarified lysate was applied onto Complete HisTag Nickel resin (Roche Diagnostics, Mannheim, Germany) and washed with buffer A consisting of 20 mM Tris-HCl pH 7.5, 500 mM NaCl, 10% (v/v) glycerol, 2 mM DTT and followed by a chaperone wash step with 20 mM Tris-HCl pH 7.5, 500 mM NaCl, 2 mM ATP, 5 mM MgCl<sub>2</sub>, 10% (v/v) glycerol and 2 mM DTT. The protein was eluted with buffer A containing 300 mM imidazole. The tag was cleaved, followed by cation exchange chromatography using a HiTrap SP HP column (GE Healthcare, Freiburg, Germany) with a linear gradient from 150 mM to 450 mM NaCl. Peak fractions were pooled and further purified by size-exclusion chromatography on a HiLoad 16/60 Superdex 200 (GE Healthcare) equilibrated with 20 mM Tris-HCl

pH 7.5, 100 mM NaCl, 5%(v/v) glycerol, 0.1 mM EDTA and 2 mM TCEP. Peak fractions were pooled, concentrated, flash-frozen in liquid nitrogen and stored at  $-80^{\circ}\text{C}$ .

### Crystallization and data collection

GEN1<sup>2-505 D30N</sup> and DNA (4w1010-1 GAATTCGGATTAGGGATGC, 4w1010-2 GCATCCCTAAGC TCCATCGT, 4w1010-3 ACGATGGAGCCGCTAGGCTC, 4w1010-4 GAGCCTAGCGTCCGGAATTC) were mixed at a molar ratio of 2:1.1 at a final protein concentration of 14 mg/ml including 1 mM  $\text{MgCl}_2$  and co-crystallized by sitting drop vapor diffusion. Drops were set up by mixing sample with mother liquor consisting of 100 mM MES-NaOH pH 6.5 and 200 mM NaCl at a 2:1 ratio at room temperature. Crystals grew within 2 days, and several iterations of streak seeding were needed for obtaining diffraction quality crystals. For data collection, crystals were stepwise soaked in 10%, 20%, and 30% (v/v) glycerol in 100 mM MES-NaOH pH 6.5, 200 mM NaCl and 5% PEG 8000 and flash-frozen in liquid nitrogen. Diffraction data were collected at beamline PXII of the Swiss Light Source (SLS, Villigen, Switzerland) at 100 K with a Pilatus 6M detector. In order to obtain phase information, crystals were soaked for 10–30 min in 1 mM  $[\text{Ta}_6\text{Br}_{12}]\text{Br}_2$ , flash-frozen and data were collected at the Ta L(III)-edge. In addition, seleno-methionine (SeMet)-substituted protein was expressed in M9 media supplemented with SeMet, purified, and crystallized according to the protocol above and data were collected at the Se K-edge.

### Structure determination and refinement

All data were processed with XDS (Table 1, Kabsch, 2010). HKL2MAP (Pape and Schneider, 2004) found 12 tantalum and 8 selenium positions, which were used in a combined MIRAS strategy (multiple isomorphous replacement with anomalous scattering) in autoSHARP (Vonrhein, et al., 2007) to determine the structure of the GEN1-HJ complex. The obtained solvent-flattened experimental map was used to build a model with PHENIX (Adams et al., 2010) combined with manual building. The structure was then further refined by iterative rounds of manual building in COOT (Emsley and Cowtan, 2004), refinement with PHENIX and assisted by the PDB\_REDO server (Joosten, et al., 2014). The structure was visualized and analyzed in PYMOL (Delano, 2002). Electrostatic surface potentials were calculated with PDB2PQR (Dolinsky et al., 2004) and APBS (Baker et al., 2001).

### Nuclease assay

All DNA substrates (Figure 5—source data 1) were synthesized by Eurofins/MWG (Ebersberg, Germany), resuspended in annealing buffer (20 mM Tris-HCl pH 8.0, 50 mM NaCl, 0.1 mM EDTA), annealed by heating to  $85^{\circ}\text{C}$  for 5 min and slow-cooling to room temperature. Different amounts of GEN1 proteins (as indicated) were mixed with 40 nM 6FAM-labeled DNA substrates in 20 mM Tris-HCl pH 8.0, 50 ng/ $\mu\text{l}$  bovine serum albumin (BSA) and 1 mM DTT. Reactions were initiated by adding 5 mM  $\text{MgCl}_2$ , incubated at  $37^{\circ}\text{C}$  for 15 min and terminated by adding 15 mM EDTA, 0.3% SDS and further, DNA substrates were deproteinized using 1 mg/ml proteinase K at  $37^{\circ}\text{C}$  for 15 min. Products were separated by 8% 1x TBE native polyacrylamide gel electrophoresis, the fluorescence signal detected with a Typhoon FLA 7000 phosphorimager (GE Healthcare), quantified with IMAGEJ (GE Healthcare) and visualized by GNU PLOT (Williams et al., 2015).

### Cruciform plasmid cleavage assay

The cruciform plasmid pIRbke8<sup>mut</sup> was a gift from Stephen West's lab (Rass et al., 2010), and it was originally prepared by David Lilley's lab (Lilley, 1985). 50 ng/ $\mu\text{l}$  plasmid were mixed with 20 mM Tris-HCl pH 8.0, 50 mM potassium glutamate, 5 mM  $\text{MgCl}_2$ , 50 ng/ $\mu\text{l}$  BSA and 1 mM DTT and pre-warmed at  $37^{\circ}\text{C}$  for 1 hr to induce the formation of a cruciform structure. Reactions were initiated by adding indicated amounts of GEN1, incubated at  $37^{\circ}\text{C}$  for 15 min and stopped as for DNA cleavage assays. The products were separated by 1% 1xTBE native agarose gel electrophoresis, stained with SYBR safe (Life Technologies, Darmstadt, Germany) and visualized under UV light.

### Sequence alignments and phylogenetic analysis

Sequences of GEN1 proteins from different organisms as well as all human chromodomain proteins were aligned to the human GEN1 sequence using the programs HHPRED (Söding et al., 2005), PSI-BLAST and further by manual adjustments. Alignments were tested by back-searches against RefSeq

or HMM databases. A phylogenetic tree was calculated by the program PHYML with 100 bootstraps using the alignment in **Figure 3—figure supplement 1** and a BLOSUM62 substitution model. The tree was displayed with DENDROSCOPE (*Huson and Scornavacca, 2012*).

### Histone peptide pull-down assay

The GEN1 chromodomain with a C-terminal His8-tag was immobilized on complete HisTag Nickel resin and washed twice with binding buffer consisting of 20 mM Tris-HCl pH 7.5, 200 mM NaCl, 5% glycerol, 0.1 mM EDTA, 0.05% (v/v) Tween-20 and 2 mM TCEP. Peptide mixtures containing 0.4  $\mu$ M fluorescein labeled histone peptides were incubated with beads at 4°C for 1 hr and washed twice with binding buffer. Immobilized proteins were eluted with binding buffer supplemented with 300 mM imidazole and separated on 20% SDS-PAGE. Fluorescein-labeled peptides were visualized by detecting the fluorescence signal with a Typhoon FLA 7000 phosphoimager (GE Healthcare).

### Yeast genetics and MMS survival assay in *Saccharomyces cerevisiae*

All yeast strains are based on W303 Rad5+ (see **Figure 5—source data 2** for a complete list). *yen1 $\Delta$*  or *yen1 $\Delta$  mus81 $\Delta$*  strains were transformed with an integrative plasmid expressing mutant versions of *YEN1*. Freshly grown over-night cultures were diluted to  $1 \times 10^7$  cells/ml. 5-fold serial dilutions were spotted on YPD plates with/without MMS (methyl methanesulphonate, concentrations as indicated) and incubated for 2 days at 30°C. The expression of 3FLAG-tagged Yen1 constructs was verified by SDS-PAGE and Western Blot analysis. Proteins were detected using a mouse monoclonal anti-FLAG M2-peroxidase (HRP) antibody (Sigma-Aldrich, München, Germany).

### Database entry

The coordinates of the human GEN1-Holliday junction complex have been deposited in the Protein Data Bank (PDB code 5t9j).

## Acknowledgements

We would like to thank Naoko Mizuno, Michael J. Taschner and Esben Lorentzen for many scientific discussions and critical reading of the manuscript. We are grateful for the support by the Department of Structural Cell Biology at the MPI of Biochemistry (MPIB), particularly for the help with screening by the Crystallization Facility and Claire Basquin for assistance with biophysical analysis. The Microchemistry Core Facility of the MPIB provided mass spectrometry analysis. We would like to thank Jürg Müller for providing histone tail peptides for binding tests and Stephen C. West for providing the plasmid pIRbke8<sup>mut</sup> for functional assays. Furthermore, we would like to acknowledge the professional assistance of the beamline staff at the Swiss Light Source, Villigen, Switzerland, during data collection. The Max Planck Society for the Advancement of Science supported this research through the Otto Hahn Program (BP) and the Max Planck Research Group Leader Program (CB).

## Additional information

### Funding

Funder	Grant reference number	Author
Max-Planck-Gesellschaft	Max Planck Research Group Leader Program	Shun-Hsiao Lee Maren Felizitas Klügel Christian Biertümpfel
Max-Planck-Gesellschaft	Otto Hahn Program	Lissa Nicola Princz Boris Pfander
Max-Planck-Gesellschaft	MPI of Biochemistry	Bianca Habermann

The funders had no role in study design, data collection and interpretation, or the decision to submit the work for publication.

**Author contributions**

S-HL, CB, Conception and design, Acquisition of data, Analysis and interpretation of data, Drafting or revising the article, Contributed unpublished essential data or reagents; LNP, MFK, Acquisition of data, Contributed unpublished essential data or reagents; BH, Acquisition of data, Analysis and interpretation of data; BP, Acquisition of data, Analysis and interpretation of data, Drafting or revising the article

**Additional files****Major datasets**

The following dataset was generated:

Author(s)	Year	Dataset title	Dataset URL	Database, license, and accessibility information
Lee S-H, Biertumpfel C	2016	Crystal Structure of human GEN1 in complex with Holliday junction DNA in the upper interface	<a href="http://www.rcsb.org/pdb/explore/explore.do?structureId=5T9J">http://www.rcsb.org/pdb/explore/explore.do?structureId=5T9J</a>	Publicly available at the RCSB Protein Data Bank (accession no. 5T9J)

**References**

- Adams PD**, Afonine PV, Bunkóczi G, Chen VB, Davis IW, Echols N, Headd JJ, Hung LW, Kapral GJ, Grosse-Kunstleve RW, McCoy AJ, Moriarty NW, Oeffner R, Read RJ, Richardson DC, Richardson JS, Terwilliger TC, Zwart PH. 2010. PHENIX: a comprehensive Python-based system for macromolecular structure solution. *Acta Crystallographica Section D Biological Crystallography* **66**:213–221. doi: [10.1107/S0907444909052925](https://doi.org/10.1107/S0907444909052925)
- Andersen SL**, Kuo HK, Savukoski D, Brodsky MH, Sekelsky J, Lichten M. 2011. Three structure-selective endonucleases are essential in the absence of BLM helicase in *Drosophila*. *PLoS Genetics* **7**:e1002315. doi: [10.1371/journal.pgen.1002315](https://doi.org/10.1371/journal.pgen.1002315)
- Ayoub N**, Jeyasekharan AD, Bernal JA, Venkitaraman AR. 2008. HP1-beta mobilization promotes chromatin changes that initiate the DNA damage response. *Nature* **453**:682–686. doi: [10.1038/nature06875](https://doi.org/10.1038/nature06875)
- Ayrapetov MK**, Gursoy-Yuzugullu O, Xu C, Xu Y, Price BD. 2014. DNA double-strand breaks promote methylation of histone H3 on lysine 9 and transient formation of repressive chromatin. *Proceedings of the National Academy of Sciences* **111**:9169–9174. doi: [10.1073/pnas.1403565111](https://doi.org/10.1073/pnas.1403565111)
- Baker NA**, Sept D, Joseph S, Holst MJ, McCammon JA. 2001. Electrostatics of nanosystems: application to microtubules and the ribosome. *Proceedings of the National Academy of Sciences* **98**:10037–10041. doi: [10.1073/pnas.181342398](https://doi.org/10.1073/pnas.181342398)
- Bennett RJ**, West SC. 1995a. RuvC protein resolves Holliday junctions via cleavage of the continuous (noncrossover) strands. *Proceedings of the National Academy of Sciences* **92**:5635–5639. doi: [10.1073/pnas.92.12.5635](https://doi.org/10.1073/pnas.92.12.5635)
- Bennett RJ**, West SC. 1995b. Structural analysis of the RuvC-Holliday junction complex reveals an unfolded junction. *Journal of Molecular Biology* **252**:213–226. doi: [10.1006/jmbi.1995.0489](https://doi.org/10.1006/jmbi.1995.0489)
- Benson FE**, West SC. 1994. Substrate specificity of the *Escherichia coli* RuvC protein. Resolution of three- and four-stranded recombination intermediates. *The Journal of Biological Chemistry* **269**:5195–5201.
- Biertumpfel C**, Yang W, Suck D. 2007. Crystal structure of T4 endonuclease VII resolving a Holliday junction. *Nature* **449**:616–620. doi: [10.1038/nature06152](https://doi.org/10.1038/nature06152)
- Blanco MG**, Matos J, Rass U, Ip SC, West SC. 2010. Functional overlap between the structure-specific nucleases Yen1 and Mus81-Mms4 for DNA-damage repair in *S. cerevisiae*. *DNA Repair* **9**:394–402. doi: [10.1016/j.dnarep.2009.12.017](https://doi.org/10.1016/j.dnarep.2009.12.017)
- Blanco MG**, Matos J, West SC. 2014. Dual control of Yen1 nuclease activity and cellular localization by Cdk and Cdc14 prevents genome instability. *Molecular Cell* **54**:94–106. doi: [10.1016/j.molcel.2014.02.011](https://doi.org/10.1016/j.molcel.2014.02.011)
- Blanco MG**, Matos J. 2015. Hold your horSSEs: controlling structure-selective endonucleases MUS81 and Yen1/GEN1. *Frontiers in Genetics* **6**:1–11. doi: [10.3389/fgene.2015.00253](https://doi.org/10.3389/fgene.2015.00253)
- Blus BJ**, Wiggins K, Khorasanizadeh S. 2011. Epigenetic virtues of chromodomains. *Critical Reviews in Biochemistry and Molecular Biology* **46**:507–526. doi: [10.3109/10409238.2011.619164](https://doi.org/10.3109/10409238.2011.619164)
- Canzio D**, Chang EY, Shankar S, Kuchenbecker KM, Simon MD, Madhani HD, Narlikar GJ, Al-Sady B. 2011. Chromodomain-mediated oligomerization of HP1 suggests a nucleosome-bridging mechanism for heterochromatin assembly. *Molecular Cell* **41**:67–81. doi: [10.1016/j.molcel.2010.12.016](https://doi.org/10.1016/j.molcel.2010.12.016)
- Castor D**, Nair N, Déclais AC, Lachaud C, Toth R, Macartney TJ, Lilley DM, Arthur JS, Rouse J. 2013. Cooperative control of holliday junction resolution and DNA repair by the SLX1 and MUS81-EME1 nucleases. *Molecular Cell* **52**:221–233. doi: [10.1016/j.molcel.2013.08.036](https://doi.org/10.1016/j.molcel.2013.08.036)
- Cejka P**, Plank JL, Bachrati CZ, Hickson ID, Kowalczykowski SC. 2010. Rmi1 stimulates decatenation of double Holliday junctions during dissolution by Sgs1-Top3. *Nature Structural & Molecular Biology* **17**:1377–1382. doi: [10.1038/nsmb.1919](https://doi.org/10.1038/nsmb.1919)

- Cejka P, Plank JL, Dombrowski CC, Kowalczykowski SC. 2012. Decatenation of DNA by the *S. cerevisiae* Sgs1-Top3-Rmi1 and RPA complex: a mechanism for disentangling chromosomes. *Molecular Cell* **47**:886–896. doi: [10.1016/j.molcel.2012.06.032](https://doi.org/10.1016/j.molcel.2012.06.032)
- Ceska TA, Sayers JR, Stier G, Suck D. 1996. A helical arch allowing single-stranded DNA to thread through T5 5'-exonuclease. *Nature* **382**:90–93. doi: [10.1038/382090a0](https://doi.org/10.1038/382090a0)
- Chan YW, West S. 2015. GEN1 promotes Holliday junction resolution by a coordinated nick and counter-nick mechanism. *Nucleic Acids Research* **43**:10882–10892. doi: [10.1093/nar/gkv1207](https://doi.org/10.1093/nar/gkv1207)
- Chan YW, West SC. 2014. Spatial control of the GEN1 Holliday junction resolvase ensures genome stability. *Nature Communications* **5**:4844. doi: [10.1038/ncomms5844](https://doi.org/10.1038/ncomms5844)
- Cowieson NP, Partridge JF, Allshire RC, McLaughlin PJ. 2000. Dimerisation of a chromo shadow domain and distinctions from the chromodomain as revealed by structural analysis. *Current Biology* **10**:517–525. doi: [10.1016/S0960-9822\(00\)00467-X](https://doi.org/10.1016/S0960-9822(00)00467-X)
- Delano WL. *The PyMOL molecular graphics system*. 2002.
- Dolinsky TJ, Nielsen JE, McCammon JA, Baker NA. 2004. PDB2PQR: an automated pipeline for the setup of Poisson-Boltzmann electrostatics calculations. *Nucleic Acids Research* **32**:W665–W667. doi: [10.1093/nar/gkh381](https://doi.org/10.1093/nar/gkh381)
- Eissenberg JC. 2012. Structural biology of the chromodomain: form and function. *Gene* **496**:69–78. doi: [10.1016/j.gene.2012.01.003](https://doi.org/10.1016/j.gene.2012.01.003)
- Eissler CL, Mazón G, Powers BL, Savinov SN, Symington LS, Hall MC. 2014. The Cdk/cDc14 module controls activation of the Yen1 holliday junction resolvase to promote genome stability. *Molecular Cell* **54**:80–93. doi: [10.1016/j.molcel.2014.02.012](https://doi.org/10.1016/j.molcel.2014.02.012)
- Emsley P, Cowtan K. 2004. Coot: model-building tools for molecular graphics. *Acta Crystallographica Section D Biological Crystallography* **60**:2126–2132. doi: [10.1107/S0907444904019158](https://doi.org/10.1107/S0907444904019158)
- Fekairi S, Scaglione S, Chahwan C, Taylor ER, Tissier A, Coulon S, Dong MQ, Ruse C, Yates JR, Russell P, Fuchs RP, McGowan CH, Gaillard PH. 2009. Human SLX4 is a Holliday junction resolvase subunit that binds multiple DNA repair/recombination endonucleases. *Cell* **138**:78–89. doi: [10.1016/j.cell.2009.06.029](https://doi.org/10.1016/j.cell.2009.06.029)
- Finger LD, Patel N, Beddows A, Ma L, Exell JC, Jardine E, Jones AC, Grasby JA. 2013. Observation of unpaired substrate DNA in the flap endonuclease-1 active site. *Nucleic Acids Research* **41**:9839–9847. doi: [10.1093/nar/gkt737](https://doi.org/10.1093/nar/gkt737)
- Fogg JM, Lilley DM. 2000. Ensuring productive resolution by the junction-resolving enzyme RuvC: large enhancement of the second-strand cleavage rate. *Biochemistry* **39**:16125–16134. doi: [10.1021/bi001886m](https://doi.org/10.1021/bi001886m)
- García-Luis J, Clemente-Blanco A, Aragón L, Machín F. 2014. Cdc14 targets the Holliday junction resolvase Yen1 to the nucleus in early anaphase. *Cell Cycle* **13**:1392–1399. doi: [10.4161/cc.28370](https://doi.org/10.4161/cc.28370)
- Garner E, Kim Y, Lach FP, Kottemann MC, Smogorzewska A. 2013. Human GEN1 and the SLX4-associated nucleases MUS81 and SLX1 are essential for the resolution of replication-induced Holliday junctions. *Cell Reports* **5**:207–215. doi: [10.1016/j.celrep.2013.08.041](https://doi.org/10.1016/j.celrep.2013.08.041)
- Giraud-Panis MJ, Lilley DM. 1997. Near-simultaneous DNA cleavage by the subunits of the junction-resolving enzyme T4 endonuclease VII. *The EMBO Journal* **16**:2528–2534. doi: [10.1093/emboj/16.9.2528](https://doi.org/10.1093/emboj/16.9.2528)
- Górecka KM, Komorowska W, Nowotny M. 2013. Crystal structure of RuvC resolvase in complex with Holliday junction substrate. *Nucleic Acids Research* **41**:9945–9955. doi: [10.1093/nar/gkt769](https://doi.org/10.1093/nar/gkt769)
- Grasby JA, Finger LD, Tsutakawa SE, Atack JM, Tainer JA. 2012. Unpairing and gating: sequence-independent substrate recognition by FEN superfamily nucleases. *Trends in Biochemical Sciences* **37**:74–84. doi: [10.1016/j.tibs.2011.10.003](https://doi.org/10.1016/j.tibs.2011.10.003)
- Hadden JM, Déclais AC, Carr SB, Lilley DM, Phillips SE. 2007. The structural basis of Holliday junction resolution by T7 endonuclease I. *Nature* **449**:621–624. doi: [10.1038/nature06158](https://doi.org/10.1038/nature06158)
- Heyer WD. 2015. Regulation of recombination and genomic maintenance. *Cold Spring Harbor Perspectives in Biology* **7**:a016501. doi: [10.1101/cshperspect.a016501](https://doi.org/10.1101/cshperspect.a016501)
- Holliday R. 1964. A mechanism for gene conversion in fungi. *Genetical Research* **5**:282–304. doi: [10.1017/S0016672300001233](https://doi.org/10.1017/S0016672300001233)
- Holm L, Rosenström P. 2010. Dali server: conservation mapping in 3D. *Nucleic Acids Research* **38**:W545–W549. doi: [10.1093/nar/gkq366](https://doi.org/10.1093/nar/gkq366)
- Hornbeck PV, Zhang B, Murray B, Kornhauser JM, Latham V, Skrzypek E. 2014. PhosphoSitePlus, 2014: mutations, PTMs and recalibrations. *Nucleic Acids Research* **43**:D512–D520. doi: [10.1093/nar/gku1267](https://doi.org/10.1093/nar/gku1267)
- Huson DH, Scornavacca C. 2012. Dendroscope 3: an interactive tool for rooted phylogenetic trees and networks. *Systematic Biology* **61**:1061–1067. doi: [10.1093/sysbio/sys062](https://doi.org/10.1093/sysbio/sys062)
- Interthal H, Heyer WD. 2000. MUS81 encodes a novel helix-hairpin-helix protein involved in the response to UV- and methylation-induced DNA damage in *Saccharomyces cerevisiae*. *Molecular and General Genetics MGG* **263**:812–827. doi: [10.1007/s004380000241](https://doi.org/10.1007/s004380000241)
- Ip SC, Rass U, Blanco MG, Flynn HR, Skehel JM, West SC. 2008. Identification of Holliday junction resolvases from humans and yeast. *Nature* **456**:357–361. doi: [10.1038/nature07470](https://doi.org/10.1038/nature07470)
- Ira G, Malkova A, Liberi G, Foiani M, Haber JE. 2003. Srs2 and Sgs1-Top3 suppress crossovers during double-strand break repair in yeast. *Cell* **115**:401–411. doi: [10.1016/S0092-8674\(03\)00886-9](https://doi.org/10.1016/S0092-8674(03)00886-9)
- Ishikawa G, Kanai Y, Takata K, Takeuchi R, Shimanouchi K, Ruike T, Furukawa T, Kimura S, Sakaguchi K. 2004. DmGEN, a novel RAD2 family endo-exonuclease from *Drosophila melanogaster*. *Nucleic Acids Research* **32**:6251–6259. doi: [10.1093/nar/gkh962](https://doi.org/10.1093/nar/gkh962)
- Joosten RP, Long F, Murshudov GN, Perrakis A. 2014. The PDB\_REDO server for macromolecular structure model optimization. *IUCrJ* **1**:213–220. doi: [10.1107/S2052252514009324](https://doi.org/10.1107/S2052252514009324)

- Kabsch W.** 2010. Integration, scaling, space-group assignment and post-refinement. *Acta Crystallographica Section D Biological Crystallography* **66**:133–144. doi: [10.1107/S0907444909047374](https://doi.org/10.1107/S0907444909047374)
- Kanai Y, Ishikawa G, Takeuchi R, Ruike T, Nakamura R, Ihara A, Ohashi T, Takata K, Kimura S, Sakaguchi K, Nakamura Ryo-ichi, Takata Kei-ichi.** 2007. DmGEN shows a flap endonuclease activity, cleaving the blocked-flap structure and model replication fork. *FEBS Journal* **274**:3914–3927. doi: [10.1111/j.1742-4658.2007.05924.x](https://doi.org/10.1111/j.1742-4658.2007.05924.x)
- Lee Bi BI, Nguyen LH, Barsky D, Fernandes M, Wilson DM.** 2002. Molecular interactions of human Exo1 with DNA. *Nucleic Acids Research* **30**:942–949. doi: [10.1093/nar/30.4.942](https://doi.org/10.1093/nar/30.4.942)
- Li J, Li Z, Ruan J, Xu C, Tong Y, Pan PW, Tempel W, Crombet L, Min J, Zang J, Gay N.** 2011. Structural basis for specific binding of human MPP8 chromodomain to histone H3 methylated at lysine 9. *PLoS ONE* **6**:e25104. doi: [10.1371/journal.pone.0025104](https://doi.org/10.1371/journal.pone.0025104)
- Lieber MR.** 1997. The FEN-1 family of structure-specific nucleases in eukaryotic DNA replication, recombination and repair. *BioEssays* **19**:233–240. doi: [10.1002/bies.950190309](https://doi.org/10.1002/bies.950190309)
- Lilley DM, White MF.** 2001. The junction-resolving enzymes. *Nature Reviews Molecular Cell Biology* **2**:433–443. doi: [10.1038/35073057](https://doi.org/10.1038/35073057)
- Lilley DM.** 1985. The kinetic properties of cruciform extrusion are determined by DNA base-sequence. *Nucleic Acids Research* **13**:1443–1465. doi: [10.1093/nar/13.5.1443](https://doi.org/10.1093/nar/13.5.1443)
- Matos J, Blanco MG, Maslen S, Skehel JM, West SC.** 2011. Regulatory control of the resolution of DNA recombination intermediates during meiosis and mitosis. *Cell* **147**:158–172. doi: [10.1016/j.cell.2011.08.032](https://doi.org/10.1016/j.cell.2011.08.032)
- Matos J, West SC.** 2014. Holliday junction resolution: regulation in space and time. *DNA Repair* **19**:176–181. doi: [10.1016/j.dnarep.2014.03.013](https://doi.org/10.1016/j.dnarep.2014.03.013)
- Miętus M, Nowak E, Jaciuk M, Kustos P, Studnicka J, Nowotny M.** 2014. Crystal structure of the catalytic core of Rad2: insights into the mechanism of substrate binding. *Nucleic Acids Research* **42**:10762–10775. doi: [10.1093/nar/gku729](https://doi.org/10.1093/nar/gku729)
- Muñoz IM, Hain K, Déclais AC, Gardiner M, Toh GW, Sanchez-Pulido L, Heuckmann JM, Toth R, Macartney T, Eppink B, Kanaar R, Ponting CP, Lilley DM, Rouse J.** 2009. Coordination of structure-specific nucleases by human SLX4/BTBD12 is required for DNA repair. *Molecular Cell* **35**:116–127. doi: [10.1016/j.molcel.2009.06.020](https://doi.org/10.1016/j.molcel.2009.06.020)
- Nishino T, Ishino Y, Morikawa K.** 2006. Structure-specific DNA nucleases: structural basis for 3D-scissors. *Current Opinion in Structural Biology* **16**:60–67. doi: [10.1016/j.sbi.2006.01.009](https://doi.org/10.1016/j.sbi.2006.01.009)
- Orans J, McSweeney EA, Iyer RR, Hast MA, Hellinga HW, Modrich P, Beese LS.** 2011. Structures of human exonuclease 1 DNA complexes suggest a unified mechanism for nuclease family. *Cell* **145**:212–223. doi: [10.1016/j.cell.2011.03.005](https://doi.org/10.1016/j.cell.2011.03.005)
- O'Shaughnessy A, Hendrich B.** 2013. CHD4 in the DNA-damage response and cell cycle progression: not so NuRDy now. *Biochemical Society Transactions* **41**:777–782. doi: [10.1042/BST20130027](https://doi.org/10.1042/BST20130027)
- Pape T, Schneider TR.** 2004. HKL2MAP: a graphical user interface for macromolecular phasing with SHELX programs. *Journal of Applied Crystallography* **37**:843–844. doi: [10.1107/S0021889804018047](https://doi.org/10.1107/S0021889804018047)
- Patel N, Atack JM, Finger LD, Exell JC, Thompson P, Tsutakawa S, Tainer JA, Williams DM, Grasby JA.** 2012. Flap endonucleases pass 5'-flaps through a flexible arch using a disorder-thread-order mechanism to confer specificity for free 5'-ends. *Nucleic Acids Research* **40**:4507–4519. doi: [10.1093/nar/gks051](https://doi.org/10.1093/nar/gks051)
- Petronczki M, Siomos MF, Nasmyth K.** 2003. Un ménage à quatre: the molecular biology of chromosome segregation in meiosis. *Cell* **112**:423–440. doi: [10.1016/S0092-8674\(03\)00083-7](https://doi.org/10.1016/S0092-8674(03)00083-7)
- Pottmeyer S, Kemper B.** 1992. T4 endonuclease VII resolves cruciform DNA with nick and counter-nick and its activity is directed by local nucleotide sequence. *Journal of Molecular Biology* **223**:607–615. doi: [10.1016/0022-2836\(92\)90977-R](https://doi.org/10.1016/0022-2836(92)90977-R)
- Price BD, D'Andrea AD.** 2013. Chromatin remodeling at DNA double-strand breaks. *Cell* **152**:1344–1354. doi: [10.1016/j.cell.2013.02.011](https://doi.org/10.1016/j.cell.2013.02.011)
- Putnam CD, Hayes TK, Kolodner RD.** 2009. Specific pathways prevent duplication-mediated genome rearrangements. *Nature* **460**:984–989. doi: [10.1038/nature08217](https://doi.org/10.1038/nature08217)
- Rass U, Compton SA, Matos J, Singleton MR, Ip SC, Blanco MG, Griffith JD, West SC.** 2010. Mechanism of Holliday junction resolution by the human GEN1 protein. *Genes & Development* **24**:1559–1569. doi: [10.1101/gad.585310](https://doi.org/10.1101/gad.585310)
- Sakurai S, Kitano K, Yamaguchi H, Hamada K, Okada K, Fukuda K, Uchida M, Ohtsuka E, Morioka H, Hakoshima T.** 2005. Structural basis for recruitment of human flap endonuclease 1 to PCNA. *The EMBO Journal* **24**:683–693. doi: [10.1038/sj.emboj.7600519](https://doi.org/10.1038/sj.emboj.7600519)
- Sarbajna S, Davies D, West SC.** 2014. Roles of SLX1-SLX4, MUS81-EME1, and GEN1 in avoiding genome instability and mitotic catastrophe. *Genes & Development* **28**:1124–1136. doi: [10.1101/gad.238303.114](https://doi.org/10.1101/gad.238303.114)
- Sarbajna S, West SC.** 2014. Holliday junction processing enzymes as guardians of genome stability. *Trends in Biochemical Sciences* **39**:409–419. doi: [10.1016/j.tibs.2014.07.003](https://doi.org/10.1016/j.tibs.2014.07.003)
- Schwacha A, Kleckner N.** 1995. Identification of double Holliday junctions as intermediates in meiotic recombination. *Cell* **83**:783–791. doi: [10.1016/0092-8674\(95\)90191-4](https://doi.org/10.1016/0092-8674(95)90191-4)
- Shah R, Cosstick R, West SC.** 1997. The RuvC protein dimer resolves Holliday junctions by a dual incision mechanism that involves base-specific contacts. *The EMBO Journal* **16**:1464–1472. doi: [10.1093/emboj/16.6.1464](https://doi.org/10.1093/emboj/16.6.1464)
- Smothers JF, Henikoff S.** 2000. The HP1 chromo shadow domain binds a consensus peptide pentamer. *Current Biology* **10**:27–30. doi: [10.1016/S0960-9822\(99\)00260-2](https://doi.org/10.1016/S0960-9822(99)00260-2)
- Söding J, Biegert A, Lupas AN.** 2005. The HHpred interactive server for protein homology detection and structure prediction. *Nucleic Acids Research* **33**:W244–W248. doi: [10.1093/nar/gki408](https://doi.org/10.1093/nar/gki408)

- Stanley FKT**, Moore S, Goodarzi AA. 2013. CHD chromatin remodelling enzymes and the DNA damage response. *Mutation Research/Fundamental and Molecular Mechanisms of Mutagenesis* **750**:31–44. doi: [10.1016/j.mrfmmm.2013.07.008](https://doi.org/10.1016/j.mrfmmm.2013.07.008)
- Svendsen JM**, Harper JW. 2010. GEN1/Yen1 and the SLX4 complex: Solutions to the problem of Holliday junction resolution. *Genes & Development* **24**:521–536. doi: [10.1101/gad.1903510](https://doi.org/10.1101/gad.1903510)
- Svendsen JM**, Smogorzewska A, Sowa ME, O'Connell BC, Gygi SP, Elledge SJ, Harper JW. 2009. Mammalian BTBD12/SLX4 assembles a Holliday junction resolvase and is required for DNA repair. *Cell* **138**:63–77. doi: [10.1016/j.cell.2009.06.030](https://doi.org/10.1016/j.cell.2009.06.030)
- Szostak JW**, Orr-Weaver TL, Rothstein RJ, Stahl FW. 1983. The double-strand-break repair model for recombination. *Cell* **33**:25–35. doi: [10.1016/0092-8674\(83\)90331-8](https://doi.org/10.1016/0092-8674(83)90331-8)
- Tomlinson CG**, Atack JM, Chapados B, Tainer JA, Grasby JA. 2010. Substrate recognition and catalysis by flap endonucleases and related enzymes. *Biochemical Society Transactions* **38**:433–437. doi: [10.1042/BST0380433](https://doi.org/10.1042/BST0380433)
- Tsutakawa SE**, Classen S, Chapados BR, Arvai AS, Finger LD, Guenther G, Tomlinson CG, Thompson P, Sarker AH, Shen B, Cooper PK, Grasby JA, Tainer JA. 2011. Human flap endonuclease structures, DNA double-base flipping, and a unified understanding of the FEN1 superfamily. *Cell* **145**:198–211. doi: [10.1016/j.cell.2011.03.004](https://doi.org/10.1016/j.cell.2011.03.004)
- Tsutakawa SE**, Lafrance-Vanasse J, Tainer JA. 2014. The cutting edges in DNA repair, licensing, and fidelity: DNA and RNA repair nucleases sculpt DNA to measure twice, cut once. *DNA Repair* **19**:95–107. doi: [10.1016/j.dnarep.2014.03.022](https://doi.org/10.1016/j.dnarep.2014.03.022)
- Vonrhein C**, Blanc E, Roversi P, Bricogne G. 2007. Automated structure solution with autoSHARP. *Methods in Molecular Biology* **364**:215–245. doi: [10.1385/1-59745-266-1:215](https://doi.org/10.1385/1-59745-266-1:215)
- Wakasugi M**, Reardon JT, Sancar A. 1997. The non-catalytic function of XPG protein during dual incision in human nucleotide excision repair. *Journal of Biological Chemistry* **272**:16030–16034. doi: [10.1074/jbc.272.25.16030](https://doi.org/10.1074/jbc.272.25.16030)
- Wechsler T**, Newman S, West SC. 2011. Aberrant chromosome morphology in human cells defective for Holliday junction resolution. *Nature* **471**:642–646. doi: [10.1038/nature09790](https://doi.org/10.1038/nature09790)
- West SC**, Blanco MG, Chan YW, Matos J, Sarbajna S, Wyatt HDM. 2015. Resolution of Recombination Intermediates: Mechanisms and Regulation. *Cold Spring Harbor Symposia on Quantitative Biology* **80**:103–109. doi: [10.1101/sqb.2015.80.027649](https://doi.org/10.1101/sqb.2015.80.027649)
- Williams T**, Kelley C, Campbell J, Cunningham R, Denholm D, Elber G, Fearick R, Grammes C, Hart L, Hecking L. *Gnuplot 5.0.0*. 2015.
- Wu L**, Hickson ID. 2003. The Bloom's syndrome helicase suppresses crossing over during homologous recombination. *Nature* **426**:870–874. doi: [10.1038/nature02253](https://doi.org/10.1038/nature02253)
- Wyatt HDM**, Sarbajna S, Matos J, West SC. 2013. Coordinated Actions of SLX1-SLX4 and MUS81-EME1 for Holliday Junction Resolution in Human Cells. *Molecular Cell* **52**:234–247. doi: [10.1016/j.molcel.2013.08.035](https://doi.org/10.1016/j.molcel.2013.08.035)
- Yang W**. 2011. Nucleases: diversity of structure, function and mechanism. *Quarterly Reviews of Biophysics* **44**:1–93. doi: [10.1017/S0033583510000181](https://doi.org/10.1017/S0033583510000181)
- Yap KL**, Zhou MM. 2011. Structure and mechanisms of lysine methylation recognition by the chromodomain in gene transcription. *Biochemistry* **50**:1966–1980. doi: [10.1021/bi101885m](https://doi.org/10.1021/bi101885m)
- Ying S**, Minocherhomji S, Chan KL, Palmal-Pallag T, Chu WK, Wass T, Mankouri HW, Liu Y, Hickson ID. 2013. MUS81 promotes common fragile site expression. *Nature Cell Biology* **15**:1001–1007. doi: [10.1038/ncb2773](https://doi.org/10.1038/ncb2773)

## V. Discussion

### A. Regulation of Mus81-Mms4 resolvase activation in mitosis

Repair of DNA damage sites by homologous recombination comprises the formation of covalently linked DNA intermediates. Processing of those DNA JMs is pivotal for the response to DNA damage and segregation of chromosomes in mitosis. Disentanglement of DNA JMs can be catalysed either by dissolution, which includes helicase and topoisomerase activity, or by resolution, which includes the action of structure-selective endonucleases. Previous work has shown that resolvases, such as Mus81-Mms4 or Yen1, underlie a tight regulation throughout the cell cycle. This temporal program establishes a hierarchy between dissolution and resolution as well as between the different resolution pathways, and thereby guarantees efficient disentanglement of DNA repair intermediates coordinated with cell cycle progression. At a molecular level, cell cycle-dependent kinases specifically target resolution enzymes, which promotes their activation (Mus81-Mms4) or inhibition (Yen1) to a distinct time during cell cycle.

Our study broadened the understanding regarding the different regulatory layers of resolution. We not only identified and characterized DDK (Dbf4-dependent kinase) as an additional cell cycle kinase besides CDK and Cdc5 to be decisive for Mus81 activation, but also connected the control by phosphorylation to a second layer of regulation, the formation of a multi-protein complex involving the scaffold proteins Dpb11, Slx4, and Rtt107 (Figure 7).

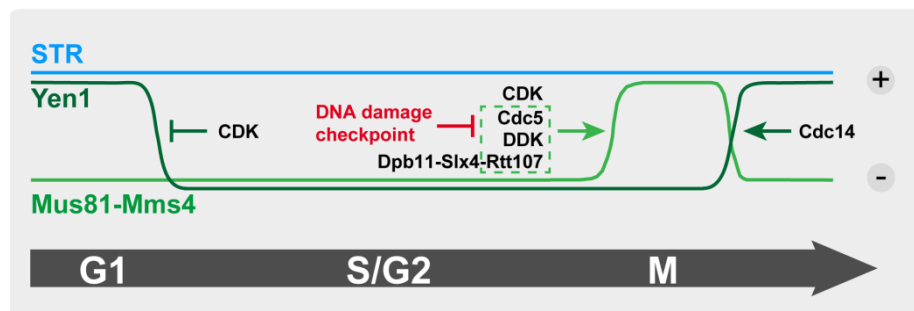


**Figure 7. Novel facets in the cell cycle regulation of JM resolution by Mus81-Mms4.** Dissolution by Sgs1-Top3-Rmi1 (STR) is independent of the cell cycle, while resolution by Mus81-Mms4 or Yen1 is temporally regulated throughout the cell cycle. At a molecular level, cell cycle-dependent kinases specifically target resolvases to promote their activation (Mus81-Mms4) or inhibition (Yen1). Here, we identified DDK as a third cell cycle kinase – besides CDK and Cdc5 – to be crucial for Mus81 nuclease activation in mitosis, and additionally linked kinase targeting to the formation of a multi-protein complex with the scaffold proteins Dpb11, Slx4, and Rtt107. Notably, DDK and Cdc5 target Mus81-Mms4 in conjunction, and Rtt107 likely mediates their recruitment to the nuclease complex. In the presence of DNA damage, checkpoint kinases indirectly repress Mus81-Mms4 phosphorylation and resolution activity, possibly by inhibiting the non-catalytic subunit of DDK, Dbf4 (adapted from Princz *et al.*, 2015).

## 1. Mus81 activity is regulated by cell cycle phase-dependent kinases

Mus81 endonuclease activity is specifically up-regulated at the G2/M-phase transition, which has been associated with CDK- and Cdc5-dependent hyper-phosphorylation of its non-catalytic subunit Mms4 (Matos *et al.*, 2011, 2013; Gallo-Fernandez *et al.*, 2012; Szakal and Branzei, 2013; Matos and West, 2014). *In vitro* dephosphorylation and concomitant declining activity, as well as expression of phospho-mimetic Mms4 mutants and concomitant increased CO formation have linked phosphorylation directly to Mus81 nuclease activity (Matos *et al.*, 2011; Szakal and Branzei, 2013).

Here, our work revealed that a third cell cycle kinase – DDK – is crucial for Mus81 activation in mitosis. Consistent with its consensus sequence, DDK targets Mms4 on the N-terminal residue of (S/T)(S/T) sites (Fig. 1C, Princz *et al.*, 2017). In line with this finding, mutation of 8 candidate sites to non-phosphorylatable alanines displayed a reduction in overall Mms4 phosphorylation, in survival in the *sgs1Δ* background of defective dissolution (especially upon DNA damage treatment), and in Mus81 resolution activity (Fig. 4B-D and EV2C-E, Princz *et al.*, 2017). Activation-deficient *mms4* mutants from previous studies that interfered with CDK and/or Cdc5 targeting showed comparable (*mms4-np*, Gallo-Fernandez *et al.*, 2012) or stronger phenotypes (*mms4-14A*, Matos *et al.*, 2013; *mms4-7A*, Szakal and Branzei, 2013). These differences may be reasoned by diverging impact of individual phosphorylation sites on Mus81 activity as well as by the existence of additional (DDK) target sites on Mms4 or even on Mus81 influencing the activity. Notably, deletion of *CDC7* or *DBF4* reduced resolution activity much more strongly than the *mms4-8A* mutant, consistent with the idea that more than 8 target sites exist on Mus81-Mms4 (Fig. 4A, C, Princz *et al.*, 2017).

With three kinases targeting Mus81-Mms4, elucidating the contribution of each of the kinases to Mus81 activation in mitosis was one of our main research interests. CDK as well as DDK are both activated at the onset of S-phase, where they regulate DNA replication and cell cycle progression. However, Cdc5 seems to be the kinase that establishes the temporal control of Mus81 activity as Cdc5 activation and targeting coincides with nuclease activation at the G2/M-phase transition. Consistently, ectopic expression of *CDC5* in S-phase resulted in premature hyper-phosphorylation of Mms4 (Fig. EV1A, Princz *et al.*, 2017; Matos *et al.*, 2013), suggesting that the S-phase kinases are in principle competent to phosphorylate Mms4, but that Cdc5 activity is crucial for full Mms4 phosphorylation.

Interestingly, we could show that DDK does not bind to Mms4 in S-phase, but rather in conjunction with Cdc5 at the G2/M transition (Fig. 1A, 2A and Appendix Fig. S1A, Princz *et al.*, 2017). This binding is strictly inter-dependent as, on the one hand, Cdc5 association with Mus81-Mms4 relies on the presence of DDK, and on the other hand, DDK association relies on Cdc5 activity (Fig. 2C-E and Appendix Fig. S2A, S2D, Princz *et al.*, 2017). Cdc5 has been previously described to interact with DDK, specifically with an N-terminal non-consensus polo-box binding motif of Dbf4 (Miller *et al.*, 2009; Chen and Weinreich, 2010). Notably, a truncation of Dbf4 lacking this Cdc5 binding motif (*dbf4-ΔN109*) displayed a strong reduction of DDK and Cdc5 binding to Mus81-Mms4, illustrating that binding of DDK-Cdc5 to the nuclease is dependent on their mutual interaction (Fig. 2F, Princz *et al.*, 2017). Overall, this suggests that two major cell cycle kinases – Cdc5 and DDK – form a functional unit.

So far, a cooperative action of DDK and Cdc5 has only been described in meiosis I, where they mediate accurate chromosome segregation (Matos *et al.*, 2008). In mitosis in contrast, DDK was suggested to counteract Cdc5 function in releasing Cdc14 and promoting mitotic exit – however, not by inhibiting Cdc5 catalytic activity (Miller *et al.*, 2009; Chen and Weinreich, 2010). To this, our findings now add a novel function for DDK in mitosis. With identifying a substrate of the DDK-Cdc5 complex we propose that DDK may target Cdc5 to a specialized subset of mitotic substrates. In this regard, it could be reasoned that DDK recruits Cdc5 to Mus81-Mms4 in order to ensure efficient JM resolution before Cdc5 initiates mitotic exit. It will therefore be crucial to identify additional substrates of the DDK-Cdc5 complex and to categorize Cdc5 phosphorylation substrates into DDK-dependent and -independent groups.

Intriguingly, the DDK consensus sequence matches the Cdc5 binding site – a (S/T)(S/T) motif, in which the C-terminal residue is pre-phosphorylated (Elia *et al.*, 2003a; b; Masai *et al.*, 2006; Montagnoli *et al.*, 2006; Randell *et al.*, 2010; Lyons *et al.*, 2013). This fact does not only explain the *mms4-8A* defect in kinase binding (Fig. 4B and EV2C, Princz *et al.*, 2017), but also suggests that cooperation of the two kinases may be more widespread than previously anticipated. Additionally, it is striking that both kinases seem to require a priming phosphorylation event. CDK has previously been implicated in mediating the priming phosphorylation that stimulates DDK during DNA replication and meiotic recombination (Wan *et al.*, 2008; Reuβwig *et al.*, 2016). The temporal succession of activity and association of the kinases involved in Mus81-Mms4 activation also qualified CDK as priming kinase for our purposes. Indeed, we detected such stimulation *in vitro* using Mms4 peptides (Fig. 1C, Princz *et al.*, 2017), although we could not confirm this type of stimulation with the full-length protein (Fig. 1B and Appendix Fig. S1C, D, Princz *et al.*, 2017). Whether this is a technical limitation of the applied *in vitro* assay still needs to be elucidated. With CDK being furthermore involved in Cdc5 activation (Mortensen *et al.*, 2005; Rodriguez-Rodriguez *et al.*, 2016), overall, Mus81-Mms4 activation displays an example for an elaborate, highly inter-twined kinase network.

This network becomes even more intricate in the context of DNA damage, when additionally checkpoint kinases are activated. Checkpoint effector kinases were proposed to counteract Mus81 function, either indirectly by repressing kinase activity (budding yeast, Rad53), or directly by phosphorylating Mus81 (fission yeast, Cds1) (Kai *et al.*, 2005; Szakal and Branzei, 2013; Cussiol *et al.*, 2015). Furthermore, the checkpoint effector kinase Rad53 is known to target Dbf4 and to inhibit DDK activity (Weinreich and Stillman, 1999; Lopez-Mosqueda *et al.*, 2010; Zegerman and Diffley, 2010). On this basis, we overexpressed *CDC5* in S-phase and compared untreated to HU-treated cells simulating a condition, in which DDK becomes limiting over Cdc5. In the presence of Cdc5, S-phase kinases were able to hyper-phosphorylate Mms4 (see above), but HU treatment resulted in checkpoint activation and in concurrent reduction of Mms4 phosphorylation (Fig. EV1B, Princz *et al.*, 2017). Therefore, cell cycle and DNA damage checkpoint kinases collaborate in regulating of Mus81-mediated resolution.

Mechanistically, it is not yet understood how hyper-phosphorylation of Mms4 facilitates activation of Mus81. Assumptions that phosphorylation might induce dimerization or multimerisation to accomplish the dual cleavage necessary for complete resolution of JMs (Gaskell *et al.*, 2007) could not be confirmed (Schwartz *et al.*, 2012). Also the interaction between the nuclease components Mus81 and Mms4 seems to be phosphorylation-independent as phosphorylation site mutants have no effect on the association (Matos *et al.*, 2011). Alternatively, phosphorylation might result in

structural changes of the nuclease, which may enhance activity or substrate binding, or even trigger association with additional factors. Yeast as well as human Mus81-Mms4/MUS81-EME1 have been described to undergo substrate-induced conformational changes on DNA that are distinct from initial DNA binding and induce bending of the DNA substrate (Gwon *et al.*, 2014; Mukherjee *et al.*, 2014). However, a possible influence of phosphorylation on nuclease structure has not been assessed yet.

Resolvase activity is not only dependent on post-translational modifications, but may be influenced also by other factors such as the binding to its DNA substrates. This particular question we addressed for another resolvase – Yen1/GEN1. In collaboration with the Biertümpfel group we investigated the DNA binding of the resolvase Yen1/GEN1, especially via its newly described chromo-domain, and tested how mutations in this domain may affect its activity (Lee *et al.*, 2015). Notably, we identified specific residues in the chromo-domain of GEN1, which are crucial for chromatin contact and *in vitro* activity (Lee *et al.*, 2015). Mutation of the respective sites in the yeast homologue Yen1 resulted in a sensitivity to the DNA-alkylating agent MMS in a *mus81Δ* background that was highly similar to a catalytically inactive mutant (Lee *et al.*, 2015), suggesting that the chromo-domain mediates Yen1 resolution function, likely by recognizing its DNA substrates. These findings hint towards a conserved involvement of the chromo-domain in Yen1/GEN1 activity, and indicate further that HJ resolvase activity is dependent on more than phosphorylation.

## 2. The Dpb11-Slx4-Rtt107 complex promotes resolution by Mus81-Mms4

Our studies also identified a mitosis-specific interaction of Mus81-Mms4 and the Dpb11-Slx4-Rtt107 scaffold complex, mediated by a direct binding between Mms4 and Dpb11 (Fig. 5A and Appendix Fig. S8A-C, Gritenaite *et al.*, 2014; Fig. 1A, 2A, 5A and Appendix Fig. S1A, S5A, Princz *et al.*, 2017). This interaction coincided with activation of Mus81, revealing a second layer of Mus81 regulation. Notably, an *slx4* separation-of-function mutant that specifically interferes with Dpb11-Slx4 binding causes defects that suggest an impairment in JM resolution. These defects include accumulation of X-shaped structures, decreased CO formation, and interference with sister chromatid separation, all observed after DNA damage induction and in a dissolution-deficient background (Fig. 4A, D-E, Gritenaite *et al.*, 2014).

A central question of my PhD work was how association of the Dpb11-Slx4-Rtt107 complex would promote Mus81-Mms4-mediated resolution. Previous studies have already described the principal concept that physical interaction with other factors could promote Mus81 stimulation. For example, both the recombination protein Rad54 as well as the anti-recombinase Srs2 have been associated with Mus81-Mms4 recruitment via direct interaction to Mus81 (Matulova *et al.*, 2009; Chavdarova *et al.*, 2015). Rad54 binds to Mus81 specifically in the presence of dsDNA and enhances Mus81-Mms4 nuclease activity in *in vitro* resolution assays (Mazina and Mazin, 2008; Matulova *et al.*, 2009). Similarly, Srs2 was shown to co-localize with Mus81 in G2-phase upon DNA damage and to stimulate its activity in mitosis by suppressing the inhibitory function of Rad51 on Mus81-mediated resolution (Chavdarova *et al.*, 2015; Keyamura *et al.*, 2016). Both Srs2 and Rad54 display enzymatic activities as well as DNA contact sites on their own, which predestines them for a targeting function in JM resolution.

The scaffold proteins Dpb11, Slx4, and Rtt107, in contrast, do not possess catalytic activity. Within the known complexes they function by assembling and coordinating various proteins or enzymatic entities. Although Slx4 has already been associated with the stimulation of several structure-selective endonucleases in different species, so far, Mus81 is the only DNA-processing enzyme that we identified in the context of the mitotic Slx4-Dpb11-Mus81-Mms4 multi-protein complex. A potential candidate might be Slx1 – an endonuclease, which binds Slx4 directly, and which we also found to physically interact with Slx4 and Dpb11 upon MMS treatment and in mitosis (Fig. S4A, Gritenaite *et al.*, 2014; Princz and Pfander, unpublished data). Whether Slx1 is part of the Mus81-Mms4 complex, or whether there are separate complexes with Dpb11-Slx4 could not be confirmed so far.

Intriguingly, human SLX1 has even been implicated in HJ resolution together with MUS81 in an SLX4-dependent manner in vertebrate cells (Wyatt *et al.*, 2013). Recently, first evidence was given for a cooperative activity of Slx1 and Mus81 in yeast (Thu *et al.*, 2015). Yet, the cooperativity of the two resolvases seems to be pathway- and substrate-specific as stimulation was detected on 3' flaps, but not on HJs (Schwartz *et al.*, 2012; Thu *et al.*, 2015). Furthermore, an involvement in mammalian replication-related phenotypes could be detected for SLX4 and MUS81, but not for SLX1, suggesting divergent functions of SLX4 and SLX1 during replication fork recovery (Sarbjana *et al.*, 2014). Consistently, we did not observe any defects in response to MMS-induced DNA damage in an *slx1Δ* background, in contrast to what was observed with the *slx4* separation-of-function mutant. Therefore, we reasoned that either Slx1 may not have an active role in Mus81-mediated resolution after replication fork stalling, or that a protein of redundant function takes over in the absence of Slx1.

Next to Slx1, also the endonuclease Rad27/Fen1 was described to interact with Mus81 in budding yeast, whereupon they mutually stimulate their endonucleolytic activity (Kang *et al.*, 2010; Thu *et al.*, 2015). Interestingly, Rad27 and Srs2 in yeast, as well as SLX4 in vertebrate cells all bind to the N-terminus of Mus81/MUS81 (Nair *et al.*, 2014; Chavdarova *et al.*, 2015; Thu *et al.*, 2015) – a region that has recently been implied in DNA binding (Wyatt *et al.*, 2017). Although interaction sites were not mapped, the N-terminus of Mus81 was also crucial for Slx1-mediated stimulation in yeast (Thu *et al.*, 2015). It would therefore be interesting to test in the future whether an N-terminal truncation of Mus81 affects protein interactions to Mus81-Mms4 within the Slx4-Dpb11-Mus81-Mms4 complex.

Still open is the question how Dpb11 and Slx4 stimulate Mus81-Mms4 resolution activity. Although the interaction between Dpb11 and Slx4 is crucial for JM resolution, neither of the two proteins is important for efficient hyper-phosphorylation of Mms4 (Fig. 4A, D-E, Gritenaite *et al.*, 2014; Fig. 5B, 6A, Princz *et al.*, 2017). Therefore, we envision two possibilities for the role of Dpb11-Slx4 in Mus81-mediated resolution, both involving tethering to additional factors. First, interaction with DNA-associated proteins could recruit Mus81-Mms4 specifically to repair intermediates that have arisen from DSBs or stalled replication forks. Such a recruitment function would be in agreement with unperturbed *in vitro* resolution in the absence of binding to Dpb11 or Slx4 (Fig. 5E, Gritenaite *et al.*, 2014; Appendix Fig. 5C, Princz *et al.*, 2017), a setup where recruitment is likely dispensable. Second, interaction with an additional nuclease could stimulate Mus81 activity as was shown for Mus81-Slx1 or Mus81-Fen1 (Kang *et al.*, 2010; Thu *et al.*, 2015). A coordinated action of two nucleases was described to be beneficial during resolution as two symmetrical incisions are needed to efficiently resolve a HJ (Pottmeyer and Kemper, 1992; Giraud-Panis and Lilley, 1997; Shah *et al.*, 1997; Fogg and Lilley, 2000). As no direct binding between Mus81-Mms4 and Slx4 was detected, Dpb11 might function as mediator linking the enzymatic moieties.

Recently, we have specifically focused our attention towards the third scaffold protein within the Dpb11-Slx4-Rtt107 complex – Rtt107 (Ohouo *et al.*, 2010). Like Dpb11, Rtt107 comprises phospho-protein binding BRCT domains, and was shown to directly interact with Slx4 (Rouse *et al.*, 2004; Roberts *et al.*, 2006). Interestingly, despite Slx4 is known to bridge Rtt107 and Dpb11 (Ohouo *et al.*, 2010), association of Rtt107 (as well as Dpb11) to Mus81-Mms4 is unchanged in an *SLX4* deletion background (Appendix Fig. S8C, Gritenaite *et al.*, 2014; Fig. 6C, Princz *et al.*, 2017; Princz and Pfander, unpublished data). Concomitantly, our analysis with two specific binding-deficient mutants (*mms4-8A*, *mms4-S201A*) revealed that either of the two BRCT scaffold proteins is sufficient to link Slx4 to Mus81-Mms4 (Fig. 6D and EV3, Princz *et al.*, 2017), suggesting that Rtt107 provides a second interaction site with Mus81-Mms4, likely by direct binding or perhaps via an additional component of the complex.

*In vitro* resolution assays on a nHJ substrate revealed a striking result that suggested Rtt107 to be involved in Mus81-Mms4 activation by cell cycle kinase phosphorylation: While interference with Dpb11-Slx4 binding did not result in a defect in Mus81 activity, deletion of *RTT107* did (Fig. 5E, Gritenaite *et al.*, 2014; Fig. 7A, Princz *et al.*, 2017). Additionally, we detected a reduction in Mms4 hyper-phosphorylation as well as a decrease in CO rates in the *rtt107Δ* background (Fig. 6A, 7B and Appendix Fig. S2C, Princz *et al.*, 2017). Intriguingly, we were able to show that Rtt107, but not Slx4 or Dpb11, was required for stable DDK-Cdc5 binding to the nuclease complex, linking Rtt107 directly to kinase recruitment and Mus81-Mms4 hyper-phosphorylation (Fig. 5B, 6A, C-D, Princz *et al.*, 2017). In line with this, the Mus81 activation defect of a *cdc7Δ* mutant was not enhanced by additional deletion of *RTT107* (Fig. 4A and Appendix Fig. S7D, Princz *et al.*, 2017). Interestingly, Rtt107 directly binds to Cdc7 (Fig. 6B, Princz *et al.*, 2017), and interaction of Rtt107 with DDK and Cdc5 is independent of the presence of Mus81-Mms4 (Appendix Fig. S6B, Princz *et al.*, 2017), suggesting the formation of an Rtt107-DDK-Cdc5 sub-complex and a putative tethering function for Rtt107.

Given that Dpb11 and Rtt107 contain phospho-protein-binding BRCT domains, it seems reasonable that phosphorylation will induce protein-protein interactions within the complex. Indeed, a direct, phosphorylation-dependent interaction of Mms4 to the BRCT domains 3+4 of Dpb11 was identified, whereas a direct interaction to Rtt107 could not be verified so far (Fig. 5C and Appendix Fig. S8C-D, Gritenaite *et al.*, 2014; Appendix Fig. S5A, Princz *et al.*, 2017; Princz and Pfander, unpublished data; Cussiol *et al.*, 2015). However, it is conceivable that DDK- and Cdc5-dependent binding of Rtt107 to the nuclease is actually induced by newly generated binding sites on Mms4 or Mus81 (Fig. 2E and Appendix Fig. S2A, Princz *et al.*, 2017).

As Rtt107 can also bind several other enzymes (like Rtt101-Mms1-Mms22, Rtt109, or the Smc5/6 complex (Ho *et al.*, 2002; Baldwin *et al.*, 2005; Roberts *et al.*, 2008; Ohouo *et al.*, 2010; Leung *et al.*, 2011; Hang *et al.*, 2015)) or even mediate DNA contact via phosphorylated histone H2A (Leung *et al.*, 2011; Li *et al.*, 2012), it will be interesting to address additional roles of Rtt107 during JM resolution in future studies.

Taken together, these results indicate that two separate functional groups exist within the Dpb11-Slx4-Rtt107 complex, which regulate Mus81-dependent JM resolution: Dpb11-Slx4 on the one side, which are dispensable for Mus81 activity (as measured by *in vitro* assays), but which are required for efficient JM resolution in cell-based assays, and Rtt107 on the other side that has a direct effect on Mus81 activity by tethering DDK and Cdc5 kinases into a stable complex with Mus81-Mms4.

### 3. Kinases and scaffolds form a multi-protein complex with Mus81-Mms4

In this study, we describe a new facet of JM resolution by Mus81-Mms4, which is mediated by the formation of a multi-protein complex in mitosis. Notably, association of all involved proteins – i.e. the kinases DDK and Cdc5 as well as the scaffold proteins Dpb11, Slx4, and Rtt107 – coincides with hyperphosphorylation of Mms4 and activation of the resolvase Mus81 (Fig. 5A, D and Appendix Fig. S8A, C, Gritenaite *et al.*, 2014; Fig. 1A, 2A and Appendix Fig. S1A, Princz *et al.*, 2017).

Importantly, we could show that formation of this multi-protein complex involves intricate interdependencies as kinase activity mediates binding of the scaffold proteins, and the scaffold protein Rtt107 in turn promotes stable association of the kinases. Strikingly, Rtt107 is thereby part of both functional modules, and creates a positive feedback loop linking the control by cell cycle kinases and scaffold proteins (Figure 8).

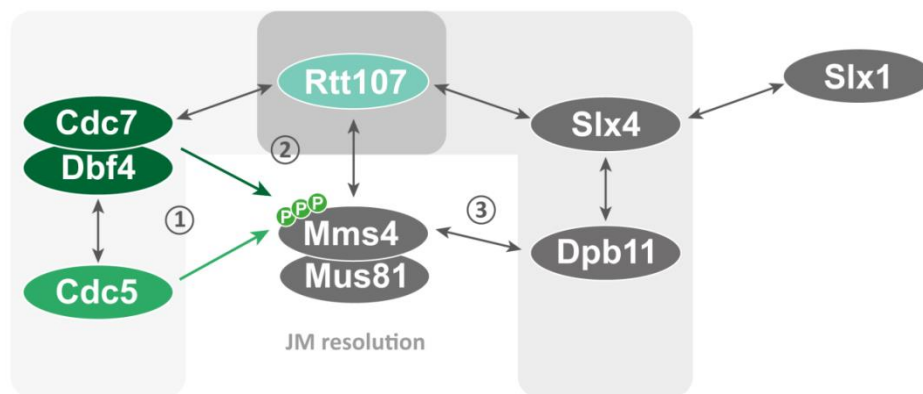


**Figure 8. Hypothetical model of the regulatory multi-protein complex that controls Mus81-Mms4-mediated JM resolution.** Grey arrows depict physical interactions; green arrows depict kinase-substrate connections. Genetic and biochemical data establish a hierarchy of events during Mus81 activation: (1) CDK (not shown), DDK and Cdc5 phosphorylate Mms4. (2) Rtt107 binds to DDK and Cdc5 and associates – directly or indirectly – with Mus81-Mms4 in a phosphorylation-dependent manner. Thereby, Rtt107 promotes stable binding of the kinases to Mus81-Mms4, full Mms4 phosphorylation, and Mus81 activation. (3) Upon Mms4 phosphorylation the BRCT domain-containing scaffold proteins Rtt107 and Dpb11 interact independently with Mus81-Mms4. Either of both proteins is sufficient to bind Slx4 to Mus81-Mms4 (adapted from Princz *et al.*, 2017).

The formation of a multi-protein complex in dependence of several kinases and scaffold proteins implies the possibility to integrate distinct cellular signals – such as cell cycle phase or the presence of DNA damage – into the regulation of Mus81-Mms4-mediated JM resolution. Mms4 is able to read those cellular inputs and permits a directed, switch-like activation of Mus81 at a certain time of the cell cycle. Thereby, Mus81 activation occurs via multi-site phosphorylation of Mms4 as well as via an Rtt107-mediated positive feedback – features that are characteristic for a switch-like transition (Nash *et al.*, 2001; Xiong and Ferrell, 2003; Liu *et al.*, 2010). Such switch-like mechanisms have been described earlier for other phosphorylation substrates, especially at cell cycle phase transitions (Matos *et al.*, 2008; Reußwig *et al.*, 2016;), and ensure rapid adaptation to cellular changes and even functional restriction of enzymes to specific cell cycle phases as in the case of Mus81-Mms4. Taken together, Mms4 connects kinase and scaffold signals via phosphorylation events, and thereby constitutes the temporal program for timely activation of Mus81 at the G2/M transition.

#### 4. Evolutionary conserved features of JM resolution by Mus81-Mms4

Several, but not all features of Mus81 regulation have been found to be conserved among eukaryotes. In contrast to Mus81 in yeast, human MUS81 exists in a complex with two alternative interaction partners, EME1 and EME2 (Ciccina *et al.*, 2003). Both complexes share the ability to resolve branched DNA structures *in vitro*, whereas they differ in substrate specificity (Ciccina *et al.*, 2007; Amangyeld *et al.*, 2014; Pepe and West, 2014). While MUS81-EME2 is thought to promote replication fork restart perhaps even in S-phase, MUS81-EME1 promotes resolution of recombination intermediates in G2- and M-phases (Pepe and West, 2014). Therefore, MUS81-EME1 represents the homologous counterpart of Mus81-Mms4 in budding yeast.

EME1 becomes phosphorylated in a CDK1-dependent manner at the G2/M transition, which correlates with an enhancement of MUS81 resolvase activity (Matos *et al.*, 2011; Wyatt *et al.*, 2013; Duda *et al.*, 2016). As MUS81 activity depends on CDK1, and to a lesser extent on PLK1 (Cdc5 homologue) activity, JM resolution by MUS81-EME1 in mammalian cells appears to be regulated by a temporal program that shows close resemblance to the one in budding yeast. Given that DDK is involved in replication-associated repair in vertebrates, it would be interesting to test if also mammalian JM resolution is influenced by DDK (reviewed in Yamada *et al.*, 2014). Additionally, the molecular mechanism of Mus81/MUS81-mediated resolution is highly similar among eukaryotes as both resolvases were described to cleave branched DNA structures by an initial bending step (Gwon *et al.*, 2014; Mukherjee *et al.*, 2014).

Data from mammalian cells showed a physical interaction between SLX1-SLX4 and MUS81-EME1 (SLX-MUS complex), as well as a cooperating function during resolution (Fekairi *et al.*, 2009; Svendsen *et al.*, 2009; Garner *et al.*, 2013; Wyatt *et al.*, 2013). Intriguingly, SLX4 is also targeted by CDK1-dependent phosphorylation and this modification mediates complex formation and cooperation (Wyatt *et al.*, 2013). Whether association with other endonucleases, such as Slx1 or Fen1, to promote HJ resolution is a conserved mode-of-action of Mus81 is currently still unclear. So far, data does not hint towards a cooperative function of Mus81 and Slx1 in the resolution of HJs in yeast: While *MUS81* or *MMS4* deletion accumulate persistent recombination intermediates and therefore cause genomic instability in mitosis and meiosis (Boddy *et al.*, 2001; Matos *et al.*, 2011; Szakal and Branzei, 2013), deletion of *SLX1* does not hamper chromosome segregation (Mullen *et al.*, 2001; Fricke and Brill, 2003; Zhang *et al.*, 2006). Furthermore, the synthetic lethality of *slx1Δ* with *sgs1Δ* cannot be rescued in *rad52Δ* or *rad51Δ* recombination-deficient backgrounds as was shown for *mus81Δ* (Fabre *et al.*, 2002; Bastin-Shanower *et al.*, 2003; Fricke and Brill, 2003). However, the synthetic lethality of *slx1Δ* and *sgs1Δ* is likely caused by defects in rDNA replication rather than by defective resolution (Coulon *et al.*, 2004; Fricke and Brill, 2003), which makes elucidating the involvement of Slx1 in JM resolution challenging. Therefore, construction of a specific Slx1 separation-of-function, such as the *slx4-S486A* mutant to separate Slx4 functions, would be indispensable to gain more insight into how Slx1 may contribute to resolution. Nevertheless, Slx4 evidently harbours Slx1-independent functions that are associated with resolution as *slx4Δ*, but not *slx1Δ*, reduces spontaneous mitotic crossovers (Ho *et al.*, 2010; de Muyt *et al.*, 2012; Zakharyevich *et al.*, 2012). Taken together, these findings suggest that Mus81 and Slx1 endonucleases probably do not cooperate in JM resolution during recombination-based DNA repair pathways in yeast, or that a redundant factor is able to take over in the absence of Slx1.

In mammals, the link between MUS81 and SLX1 endonucleases is SLX4. It was hypothesized that SLX4 displays a platform for several nucleases thereby coordinating their activities (Kim *et al.*, 2013; Wyatt *et al.*, 2017). However, despite conservation of the MUS81-binding SAP domain in SLX4 throughout eukaryotes (Fekairi *et al.*, 2009), a direct interaction of Mus81 and Slx4 in budding yeast has not been described. In contrast, we discovered a conserved interaction in human cells between SLX4 and TopBP1, the homologue of Dpb11 (Fig. 1D, 2E and Appendix Fig. S2, Gritenaite *et al.*, 2014). While it still has to be validated whether TopBP1 is part of the SLX-MUS complex, its role in yeast to bridge Mus81-Mms4 to Slx4 (and associated factors) may not be necessary in mammals due to the direct MUS81-SLX4 interface.

Interestingly however, TopBP1 was associated with the induction of chromatin bridges, which largely depend on HR (Germann *et al.*, 2014), as well as with SLX4 foci formation in mitosis in chicken DT40 cells (Pederson *et al.*, 2015). These findings let to the hypothesis that TopBP1 may restrain chromatin bridge formation by mediating SLX4-dependent resolution of HJ intermediates, and predestines TopBP1 as a potential regulator of resolution also in mammals.

Besides its mitotic function, TopBP1 might also have an SLX4-dependent role in S-phase, equivalent to the Dpb11-Slx4 complex we characterized after replication fork stalling (see following chapter).

## B. The Dpb11-Slx4-Rtt107 complex after replication fork stalling

Consistent with previous studies our data revealed that the scaffold proteins Dpb11, Slx4, and Rtt107 form a complex already in S-phase upon MMS-induced replication fork stalling (Ohouo *et al.*, 2010; Appendix Fig. S4A, Gritenaite *et al.*, 2014). Notably, deletion of *RTT107* or *SLX4* in *S. cerevisiae* results in genome instability and increased sensitivity to replication stress (Flott and Rouse, 2005; Flott *et al.*, 2007; Roberts *et al.*, 2006; 2008). This led us to propose a working model, whereby two types of complexes exist throughout the cell cycle: one mitosis-specific complex that promotes efficient JM resolution by Mus81-Mms4 (see above), and one S-phase-specific complex that regulates the response to replication stress. So far, it has not been validated whether both complexes co-exist in M-phase, or whether the S-phase complex is in fact a precursor, which later on associates with Mus81-Mms4 in mitosis.

### 1. Complex formation is regulated by CDK and checkpoint kinases

The interaction between Dpb11, Slx4, and Rtt107 is mediated by several phosphorylation events that integrate two cellular signals: the cell cycle phase – by CDK-dependent phosphorylation of Slx4-S486 (Fig. 1C, 2C, E, Gritenaite *et al.*, 2014; Ohouo *et al.*, 2013) – and the presence of DNA damage – by checkpoint kinase-dependent phosphorylation of Dpb11, Slx4, and Rtt107 (Rouse 2004; Flott and Rouse, 2005; Roberts *et al.*, 2006; Ohouo *et al.*, 2010; Balint *et al.* 2015; Fig. 2D, Gritenaite *et al.*, 2014). By characterizing specific phosphorylation-deficient *slx4* mutants and their phenotypes after replication fork stalling we and others have elucidated potential functions of the Dpb11-Slx4-Rtt107 complex in S-phase.

An *slx4-S486A* mutant, which is particularly defective in Dpb11 binding, as well as an *slx4-7A* mutant, in which seven putative Mec1 sites are substituted by non-phosphorylatable alanines, are hypersensitive specifically to DNA alkylation by MMS, and therefore to MMS-induced replication fork stalling (Ohouo *et al.*, 2013; Appendix Fig. S3A, Gritenaite *et al.*, 2014). Strikingly, *slx4* hypersensitivity can be rescued by a fusion of Dpb11 to Slx4-S486A (Fig. 3B, Gritenaite *et al.*, 2014), and even by a fusion of Dpb11 to Rtt107 (Cussiol *et al.*, 2015). These results therefore suggest that formation of a Dpb11-Slx4-Rtt107 complex after replication stress aims at connecting the two scaffold proteins Dpb11 and Rtt107, or their associated factors.

A recent study linked complex assembly to efficient Mec1 signalling distal to stalled replication forks: Genome-wide ChIP enrichment data revealed that Rtt107 contacts DNA via Mec1-phosphorylated histone H2A, and recruits Slx4 and (subsequently) Dpb11 behind replication forks upon MMS treatment (Leung *et al.*, 2011; Li *et al.*, 2012; Balint *et al.*, 2015). Dpb11 accumulation on chromatin enhances Mec1 activity (Puddu *et al.*, 2008), which in turn amplifies Dpb11, Slx4, Rtt107 and H2A phosphorylation and therefore Dpb11-Slx4-Rtt107 binding (Balint *et al.*, 2015). Consequently, Dpb11-Slx4-Rtt107 complex formation launches a positive feedback loop to promote full Mec1 activation.

## 2. Dpb11-Slx4-Rtt107 dampen DNA damage checkpoint signalling

DNA damage checkpoint signalling is initiated by formation of a multi-protein checkpoint complex, which triggers the activation of the effector kinase Rad53. Within this complex, Dpb11 engages three protein interaction surfaces to bind Rad9, Ddc1 and Mec1-Ddc2 (Wang and Elledge, 2002; Majka *et al.*, 2006; Mordes *et al.*, 2008; Navadgi-Patil and Burgers, 2008; 2009; Puddu *et al.*, 2008; Pfander and Diffley, 2011). This signalling complex localizes to DNA damage sites via Ddc1 (i.e., the 9-1-1 complex), and via Rad9 bound to  $\gamma$ -H2A and methylated histone H3 (Furuya *et al.*, 2004; Giannattasio *et al.*, 2005; Toh *et al.*, 2006; Delacroix *et al.*, 2007; Grenon *et al.*, 2007; Hammet *et al.*, 2007; Lee *et al.*, 2007; Puddu *et al.*, 2008). Upon Mec1-dependent phosphorylation, the checkpoint mediator protein Rad9 promotes activation of Rad53, thereby coordinating the downstream signalling cascade of the checkpoint response (Majka *et al.*, 2006; Mordes *et al.*, 2008; Navadgi-Patil and Burgers, 2008; 2009; Puddu *et al.*, 2008; Pfander and Diffley, 2011).

Hyper-activation of the checkpoint (as indicated by increased phosphorylation of the effector kinase Rad53) in MMS-treated *slx4-S486A* or *slx4-7A* cells that lack the Slx4-Dpb11 interaction led to a model whereby the Dpb11-Slx4-Rtt107 complex may counteract checkpoint signalling during the response to replication stalling (Ohouo *et al.*, 2013; Fig. 3E, Gritenaite *et al.*, 2014; Cussiol *et al.*, 2015; Dibitetto *et al.*, 2015). In agreement, checkpoint mutants (such as *ddc1-T602A* or *rad53-3HA*) can partially rescue the *slx4* phenotypes associated with replication stress (Fig. 6A-B and Appendix Fig. S10A-B, Gritenaite *et al.*, 2014; Ohouo *et al.*, 2013; Dibitetto *et al.*, 2015; Jablonowski *et al.*, 2015).

Recent studies related this checkpoint dampening function to a direct competition between the binding partners of the two Dpb11 complexes (Ohouo *et al.*, 2013; Balint *et al.*, 2015; Cussiol *et al.*, 2015; Dibitetto *et al.*, 2015): Slx4 and Rtt107 both counteract Rad9 binding to the N-terminal BRCT domains of Dpb11 as well as to phosphorylated histone H2A, respectively (Leung *et al.*, 2011; Li *et al.*, 2012; Ohouo *et al.*, 2013). Thereby, the Dpb11-Slx4-Rtt107 complex directly counteracts Rad9 in its binding to lesion sites as well as in its binding to both Mec1 activators, Dpb11 and Ddc1. This impedes Rad9 and Rad53 phosphorylation, and concurrently Rad53 activation.

Notably, the Dpb11-Slx4-Rtt107 complex does not only counteract chromatin binding of Rad9, but also its function in inhibiting DNA end resection (Lazzaro *et al.*, 2008). Alongside, checkpoint dampening by the Dpb11-Slx4-Rtt107 complex was associated with efficient long range resection as *slx4 $\Delta$* , *slx4-S486A* and *rtt107 $\Delta$*  mutants delay formation of long ssDNA tails (Dibitetto *et al.*, 2015).

Interestingly, binding of Ddc1 to Dpb11 is not impaired by the formation of the Dpb11-Slx4-Rtt107 complex after replication fork stalling. In contrast, Dpb11 was shown to bridge between Slx4 and Ddc1 proteins (Cussiol *et al.*, 2015). Thereby, the Dpb11-Slx4-Rtt107 complex and the checkpoint complex bear remarkable resemblance in their composition, with  $\gamma$ -H2A and Ddc1 mediating chromatin contact and Rtt107-Slx4 representing the counterpart to Rad9. Cussiol *et al.* proposed a spatio-temporal program, in which checkpoint complex formation occurs first upon replication stress activating Rad53 at proximal regions to stabilize stressed forks (Branzei and Foiani, 2010; Cussiol *et al.*, 2015). After fork bypass Slx4 and Rtt107 displace Rad9, presumably due to a stronger interaction to Dpb11, and dampen the DNA damage checkpoint signalling. During the recovery from replication stress, however, Mms4 was described to outcompete Ddc1 in binding to the BRCT domains 3+4 of Dpb11 (Cussiol *et al.*, 2015). This succession of interaction events would be consistent with our

hypothetical model for a transition from the S-phase-specific to the M-phase-specific Dpb11-Slx4-Rtt107 complex. Interestingly, we found that *slx4-S486A* mutation delayed Mms4 phosphorylation, and that partial checkpoint inactivation was able to alleviate this phenotype (Fig. 6E-F, Gritenaite *et al.*, 2014), consistent with an antagonizing function of the checkpoint on Mus81-Mms4 activity (see above). Additionally, the rescue of *slx4* mutants by partial checkpoint inactivation is dependent on Mus81 activity, but not on Sgs1-Top3-Rmi1 or Yen1 activity (Fig. 6C-D and Appendix Fig. S10C, Gritenaite *et al.*, 2014). Therefore, one function of the Dpb11-Slx4-Rtt107 complex might be to promote JM resolution indirectly by checkpoint dampening.

### 3. Multiple functions of Dpb11-Slx4-Rtt107 after replication stress in S-phase

Several recent studies implicated the Dpb11-Slx4-Rtt107 complex in counteracting the DNA damage checkpoint after replication fork stalling (Ohouo *et al.*, 2013; Balint *et al.*, 2015; Cussiol *et al.*, 2015; Dibitetto *et al.*, 2015). However, our data indicate that checkpoint dampening is not the only function of the scaffold complex in S-phase, but suggest an additional involvement in DNA repair.

Experimental evidence for this hypothesis was obtained in the *slx4-S486A* mutant background, where we observed accumulation of RPA nuclear foci after MMS treatment (Fig. 3F, Gritenaite *et al.*, 2014), which is consistent with the occurrence of persistent ssDNA structures such as stalled replication forks or perhaps repair intermediates thereof. Together with a delay in S-phase progression and in the reappearance of fully replicated, repaired chromosomes in MMS-treated *slx4-S486A* cells (Fig. 3C-D and Appendix Fig. S3B, Gritenaite *et al.*, 2014), these results hint towards a putative repair function of the Dpb11-Slx4-Rtt107 complex. Based on this model, Dpb11, Slx4, and Rtt107 are recruited to sites of stalled forks, where they display a platform for repair enzymes. However, so far, no repair enzymes have been associated with the complex during the response to replication fork stalling.

Taken together, the Dpb11-Slx4-Rtt107 complex seems to have various roles during the response to replication fork stalling. It was implicated in full activation of Mec1 uncoupled from Rad53 activation by recruiting Dpb11 behind stressed replication forks (Balint *et al.*, 2015), in a potential repair function (Gritenaite *et al.*, 2014), and in checkpoint dampening by counteracting Rad9 (Ohouo *et al.*, 2013). Resolving those different functions is challenging since they all include binding of Slx4 to Dpb11 (and likely also to Rtt107). Furthermore, it may not even be possible to study those functions in isolation as they are highly inter-twined: For example, checkpoint dampening will influence a putative DNA repair function as Rad9 inhibition fosters DNA end resection, which displays the initial step in recombination-based repair pathways. Additionally, the checkpoint dampening function of Dpb11-Slx4-Rtt107 complex in S-phase highly correlates with its mitotic function to promote Mus81 activation and JM resolution.

Future research needs to identify additional factors, especially repair factors, as well as to further elucidate the contributions of the Dpb11-Slx4-Rtt107 complex during the response to replication stress, and also with regard to the correlation between S- and M-phase complexes.

## C. Dpb11 as a regulator of the DNA damage response

The cellular response to DNA damage involves an elaborate network of signalling cascades that coordinates repair processes with cell cycle progression to preserve genomic integrity. Within this network, signal transduction depends on specific, regulated protein-protein interactions. One way to achieve this specificity and regulation is by timed phosphorylation events – catalysed by cell cycle-dependent kinases or checkpoint kinases. Several modular domains, such as 14-3-3, FHA or BRCT domains, have been described to specifically recognize phosphorylated proteins (Mohammad and Yaffe, 2009). With Dpb11, Rtt107, and Rad9 containing multiple BRCT domains, their characterization was of particular interest for our research.

### 1. BRCT domains bind phosphorylated proteins

Originally, BRCT (BRCA1 C-terminal homology) domains were identified to be 90-100 amino acid regions in the tumour suppressor protein BRCA1 as mutation of these regions causes increased occurrence of breast and ovarian cancers (Futreal *et al.*, 1994; Miki *et al.*, 1994). To date, additional BRCT domain-comprising proteins have been detected, most of which with functions during DNA-associated processes (Leung *et al.*, 2011; Gerloff *et al.*, 2012). In those proteins the number of BRCT domains can range from single isolated domains to tandem repeats and multiple BRCT domains like in Dpb11/TopBP1 or Rtt107/PTIP (Lechner *et al.*, 2000; Huo *et al.*, 2010; Rappas *et al.*, 2011). Tandem BRCT domains have been found to often allow binding to phosphorylated proteins. Besides, BRCT domains have been additionally linked to DNA binding and interaction with poly(ADP-ribose) (Pleschke *et al.*, 2000; Yamane *et al.*, 2000; Dhingra *et al.*, 2015).

Comparison of BRCT domains from different proteins revealed conserved residues in the target recognition site as well as in the hydrophobic core, whereas the connecting loops show more variety in sequence and structure (Glover *et al.*, 2004; Rodriguez and Songyang, 2008). Especially for BRCA1 binding partners, sequence alignments of target peptides identified a conserved pSXXF motif representing a bipartite interface to tandem BRCT repeats. Thereby, the phosphorylated residue interacts with the binding pocket of one BRCT domain (mostly the N-terminal), while the phenylalanine in position +3 interacts with the hydrophobic pocket of the second BRCT domain (Shiozaki *et al.*, 2004; Schreyer and Blundell, 2013). Whether this bipartite interaction pattern displays a widespread mode to bind tandem BRCT domains is currently not known. Apart from the two main interaction sites, variation of the X residues at the positions +1 and +2 might be responsible for protein-specific affinities. Particularly, a proline residue at the +1 position is thought to augment the binding properties by modulating the peptide structure with the intent that the phosphorylated and the hydrophobic residue face the same site (Lokesh *et al.*, 2007; Yuan *et al.*, 2011). Additional interaction sites outside of the motif seem to have an impact on binding as well adding further complexity to the BRCT domain interactome (Wu *et al.*, 2015).

During our studies we characterized the BRCT domain target sites in Slx4 (S486), Mms4 (S201) and other Dpb11 interaction partners. For the Dpb11 BRCT 1+2 domains, in particular, a composite binding surface for two phosphorylated residues was described (Tanaka *et al.*, 2007; Zegerman and Diffley, 2007; Zegerman and Diffley, 2010; Pfander and Diffley, 2011; Bantele *et al.*, 2017).

Interestingly, we did not identify a phenylalanine residue in the +3 position of respective motifs in Slx4 and Mms4, but several hydrophobic amino acids in the vicinity of the phosphorylated target site to influence binding affinities (Princz, Rühmann and Pfander, unpublished data). Therefore, a cooperative binding of phosphorylated and hydrophobic residues to a tandem BRCT repeat would be consistent with the bipartite interaction pattern described for BRCA1.

## 2. Dpb11 complexes regulate multiple cellular pathways

Especially during the last four years, research on Dpb11 and its eukaryotic homologues (Cut5/Rad4 in *S. pombe*, TopBP1 in mammals) has made significant progress in elucidating novel functions as well as in unravelling the underlying molecular mechanisms. It has become clear that Dpb11 and homologues are able to read phosphorylations via their BRCT domains, and to scaffold the respective proteins into multi-protein complexes. Thereby, they can specifically integrate various cellular inputs like cell cycle and DNA damage signals, and contribute to the regulation and coordination of cellular pathways.

Dpb11 is an essential protein and has been implicated in diverse DNA-associated processes, such as DNA replication (with Sld3 and Sld2), the DNA damage checkpoint (with Rad9, Ddc1 and Mec1) and DNA repair by recombination-based mechanisms (with Rtt107-Slx4 and Ddc1; with Rtt107-Slx4 and Mms4-Mus81; or with Fun30 and Ddc1). With many of Dpb11's functions showing conservation in higher eukaryotes, yeast has become a fundamental model organism to study the function of TopBP1 in multi-cellular organisms. Interestingly, TopBP1 harbours additional BRCT domains compared to Dpb11 and Cut5/Rad4, which may be connected to additional interaction partners and functions in higher eukaryotes (Garcia *et al.*, 2005; Rappas *et al.*, 2011). Alongside, TopBP1 has emerged as a potential regulator of transcription in recent studies (Wright *et al.*, 2006; Sjøttem *et al.*, 2007), and was also described to bind additional factors such as BLM and the MRN complex (Duursma *et al.*, 2013; Wang *et al.*, 2013; Blackford *et al.*, 2015).

A major aim of our research was to reveal coordination and potential crosstalk between the distinct Dpb11 complexes. Indeed, we performed profound characterization of a Dpb11 complex formed in S-phase after replication fork stalling (Gritenaite *et al.*, 2014), and functionally linked it to resolution of JMs in the subsequent mitosis, which is accompanied by further assembly into a multi-protein complex (Princz *et al.*, 2017).

In contrast to this kind of “handover” mechanism, other Dpb11 interactors seem to counteract each other. In line with this, Dpb11 has for example been associated with resection-promoting and -antagonizing factors (Fun30/Rtt107-Slx4 and Rad9, respectively) (Ohouo *et al.*, 2013; Cussiol *et al.*, 2015; Bantele *et al.*, 2017). Intriguingly, several Dpb11 interactions were shown to be mutually exclusive. With Dpb11 being present only by some hundred molecules per cell (Ghaemmaghami *et al.*, 2003; Kulak *et al.*, 2014), competition between the binding partners displays a versatile mode of action to regulate the corresponding complex functions. This ensures temporal separation of cellular events, such as replication and DNA damage checkpoint signalling (by Sld3-Rad9 competition) (Boos *et al.*, 2011), or checkpoint signalling and JM resolution (by competition of Ddc1 and Mms4) (Ohouo *et al.*, 2013). In conclusion, Dpb11 coordinates protein interactions in order to build up a safeguard mechanism to spatio-temporally separate opposing processes.

## VI. References

- Aguilera A (2002) The connection between transcription and genomic instability. *EMBO J* 21(3):195-201
- Alani E, Thresher R, Griffith JD, Kolodner RD (1992) Characterization of DNA-binding and strand-exchange stimulation properties of  $\gamma$ -RPA, a yeast single-strand-DNA-binding protein. *J Mol Biol* 227:54-71
- Altmannova V, Eckert-Boulet N, Arneric M, Kolesar P, Chaloupkova R, Damborsky J, Sung P, Zhao X, Lisby M, Krejci L (2010) Rad52 SUMOylation affects the efficiency of the DNA repair. *Nucleic Acids Res* 38(14):4708-4721
- Amangyeld T, Shin YK, Lee M, Kwon B, Seo YS (2014) Human MUS81-EME2 can cleave a variety of DNA structures including intact Holliday junction and nicked duplex. *Nucleic Acids Res* 42(9):5846-5862
- Antoniacci LM, Kenna MA, Skibbens RV (2007) The nuclear envelope and spindle pole body-associated Mps3 protein bind telomere regulators and function in telomere clustering. *Cell Cycle* 6:75-79
- Aylon Y, Liefshitz B, Kupiec M (2004) The CDK regulates repair of double-strand breaks by homologous recombination during the cell cycle. *EMBO J* 23:4868-4875
- Ayoub N, Rajendra E, Su X, Jeyasekharan AD, Mahen R, Venkitaraman AR (2009) The carboxyl terminus of Brca2 links the disassembly of Rad51 complexes to mitotic entry. *Curr Biol* 19(13):1075-1085
- Azvolinsky A, Giresi PG, Lieb JD, Zakian VA (2009) Highly transcribed RNA polymerase II genes are impediments to replication fork progression in *Saccharomyces cerevisiae*. *Mol Cell* 34(6):722-734
- Bachrati CZ, Borts RH, Hickson ID (2006) Mobile D-loops are a preferred substrate for the Bloom's syndrome helicase. *Nucleic Acids Res* 34(8):2269-2279
- Baldwin EL, Berger AC, Corbett AH, Osheroff N (2005) Mms22p protects *Saccharomyces cerevisiae* from DNA damage induced by topoisomerase II. *Nucleic Acids Res* 33(3):1021-1030
- Balint A, Kim T, Gallo D, Cussiol JR, Bastos de Oliveira FM, Yimit A, Ou J, Nakato R, Gurevich A, Katsuhiko S, Smolka MB, Zhang Z, Brown, GW (2015) Assembly of Slx4 signaling complexes behind DNA replication forks. *EMBO J* 34(16):2182-2197
- Ball HL, Ehrhardt MR, Mordes DA, Glick GG, Chazin WJ, Cortez D (2007) Function of a conserved checkpoint recruitment domain in ATRIP proteins. *Mol Cell Biol* 27:3367-3377
- Ball HL, Myers JS, Cortez D (2005) ATRIP binding to replication protein A-single-stranded DNA promotes ATR-ATRIP localization but is dispensable for Chk1 phosphorylation. *Mol Biol Cell* 16:2372-2381
- Bantele SC, Ferreira P, Gritenaite D, Boos D, Pfander B (2017) Targeting of the Fun30 nucleosome remodeller by the Dpb11 scaffold facilitates cell cycle-regulated DNA end resection. *eLife* 6:e21687
- Barlow JH and Rothstein R (2009) Rad52 recruitment is DNA replication independent and regulated by Cdc28 and the Mec1 kinase. *EMBO J* 28:1121-1130
- Barlow JH, Lisby M, Rothstein R (2008) Differential regulation of the cellular response to DNA double-strand breaks in G1. *Mol Cell* 30(1):73-85
- Bashkirov VI, King JS, Bashkirova EV, Schmuckli-Maurer J, Heyer WD (2000) DNA repair protein Rad55 is a terminal substrate of the DNA damage checkpoints. *Mol Cell Biol* 20(12):4393-4404
- Basile G, Aker M, Mortimer RK (1992) Nucleotide sequence and transcriptional regulation of the yeast recombinational repair gene RAD51. *Mol Cell Biol* 12:3235-3246
- Bastin-Shanower SA, Fricke WM, Mullen JR, Brill SJ (2003) The mechanism of Mus81-Mms4 cleavage site selection distinguishes it from the homologous endonuclease Rad1-Rad10. *Mol Cell Biol* 23:3487-3496
- Bennett G, Papamichos-Chronakis M, Peterson CL (2013) DNA repair choice defines a common pathway for recruitment of chromatin regulators. *Nat Commun* 4:2084
- Benton MG, Somasundaram S, Glasner JD, Palecek SP (2006) Analyzing the dose-dependence of the *Saccharomyces cerevisiae* global transcriptional response to methyl methanesulfonate and ionizing radiation. *BMC Genomics* 7:305
- Bienko M, Green CM, Crosetto N, Rudolf F, Zapart G, Coull B, Kannouche P, Wider G, Peter M, Lehmann AR, Hofmann K, Dikic I (2005) Ubiquitin-binding domains in Y-family polymerases regulate translesion synthesis. *Science* 310(5755):1821-1824
- Bjergbaek L, Cobb JA, Tsai-Pflugfelder M, Gasser SM (2005) Mechanistically distinct roles for Sgs1p in checkpoint activation and replication fork maintenance. *EMBO J* 24:405-417
- Blackford AN, Nieminuszczy J, Schwab RA, Galanty Y, Jackson SP, Niedzwiedz W (2015) TopBP1 Interacts with BLM to Maintain Genome Stability but Is Dispensable for Preventing BLM Degradation. *Mol Cell* 57(6):1133-1141
- Blanco MG, Matos J, Rass U, Ip SC, West SC (2010) Functional overlap between the structure-specific nucleases Yen1 and Mus81-Mms4 for DNA-damage repair in *S. cerevisiae*. *DNA Repair (Amst)* 9(4):394-402
- Blanco MG, Matos J, West SC (2014) Dual control of Yen1 nuclease activity and cellular localization by Cdk and Cdc14 prevents genome instability. *Mol Cell* 54(1):94-106
- Boddy MN and Russell P (2001) DNA replication checkpoint. *Curr Biol* 11(23):R953-956
- Boddy MN, Lopez-Girona A, Shanahan P, Interthal H, Heyer WD, Russell P (2000) Damage tolerance protein Mus81 associates with the FHA1 domain of checkpoint kinase Cds1. *Mol Cell Biol* 20:8758-8766
- Boos D, Sanchez-Pulido L, Rappas M, Pearl LH, Oliver AW, Ponting CP, Diffley JF (2011) Regulation of DNA replication through Sld3-Dpb11 interaction is conserved from yeast to humans. *Curr Biol* 21(13):1152-1157
- Bosco G and Haber JE (1998) Chromosome break-induced DNA resection leads to nonreciprocal translocations and telomere capture. *Genetics* 150(3):1037-1047
- Bradley MO and Kohn KW (1979) X-ray induced DNA double strand break production and repair in mammalian cells as measured by neutral filter elution. *Nucleic Acids Res* 7(3):793-804
- Brambati A, Colosio A, Zardoni L, Galanti L, Liberi G (2015) Replication and transcription on a collision course: eukaryotic regulation mechanisms and implications for DNA stability. *Front Genet* 6:166

- Branzei D and Foiani M (2010) Maintaining genome stability at the replication fork. *Nat Rev Mol Cell Biol* 11(3):208-219
- Branzei D and Szakal B (2016) DNA damage tolerance by recombination: Molecular pathways and DNA structures. *DNA Repair (Amst)* 44:68-75
- Branzei D, Vanoli F, Foiani M (2008) SUMOylation regulates Rad18-mediated template switch. *Nature* 456(7224):915-920
- Broker TR and Lehman IR (1971) Branched DNA molecules: intermediates in T4 recombination. *J Mol Biol* 60:131-149
- Brusky J, Zhu Y, Xiao W (2000) UBC13, a DNA-damage-inducible gene, is a member of the error-free postreplication repair pathway in *Saccharomyces cerevisiae*. *Curr Genet* 37(3):168-174
- Bugreev DV, Rossi MJ, Mazin AV (2011) Cooperation of RAD51 and RAD54 in regression of a model replication fork. *Nucleic Acids Res* 39:2153-2164
- Bugreev DV, Yu X, Egelman EH, Mazin AV (2007) Novel pro- and anti-recombination activities of the Bloom's syndrome helicase. *Gene Dev* 21(23):3085-3094
- Bupp JM, Martin AE, Stensrud ES, Jaspersen SL (2007) Telomere anchoring at the nuclear periphery requires the budding yeast Sad1-UNC-84 domain protein Mps3. *J Cell Biol* 179:845-854
- Burgess RC, Lisby M, Altmannova V, Krejci L, Sung P, Rothstein R (2009) Localization of recombination proteins and Srs2 reveals anti-recombinase function in vivo. *J Cell Biol* 185(6):969-981
- Burgess RC, Rahman S, Lisby M, Rothstein R, Zhao X (2007) The Slx5-Slx8 complex affects sumoylation of DNA repair proteins and negatively regulates recombination. *Mol Cell Biol* 27:6153-6162
- Caldecott KW (2008) Single-strand break repair and genetic disease. *Nat Rev Genet* 9(8):619-631
- Carter SD, Viganova D, Chen J, Chovanec M, Aström SU (2009) Nej1 recruits the Srs2 helicase to DNA double-strand breaks and supports repair by a single-strand annealing-like mechanism. *Proc Natl Acad Sci U S A* 106(29):12037-12042
- Casper AM, Rosen DM, Rajula KD (2012) Sites of genetic instability in mitosis and cancer. *Ann N Y Acad Sci* 1267:24-30
- Castor D, Nair N, Déclais AC, Lachaud C, Toth R, Macartney TJ, Lilley DM, Arthur JS, Rouse J (2013) Cooperative control of Holliday junction resolution and DNA repair by the SLX1 and MUS81-EME1 nucleases. *Mol Cell* 52(2):221-233
- Cejka P and Kowalczykowski SC (2010a) The full-length *Saccharomyces cerevisiae* Sgs1 protein is a vigorous DNA helicase that preferentially unwinds Holliday junctions. *J Biol Chem* 285:8290-8301
- Cejka P, Plank JL, Bachrati CZ, Hickson ID, Kowalczykowski SC (2010b) Rmi1 stimulates decatenation of double Holliday junctions during dissolution by Sgs1-Top3. *Nat Struct Mol Biol* 17:1377-1382
- Chaganti RSK, Schonberg S, German J (1974) A manifold increase in sister chromatid exchanges in Bloom's Syndrome lymphocytes. *Proc Natl Acad Sci U S A* 71(11):4508-4512
- Chan YW and West S (2015) GEN1 promotes Holliday junction resolution by a coordinated nick and counter-nick mechanism. *Nucleic Acids Res* 43(22):10882-10892
- Chavdarova M, Marini V, Sisakova A, Sedlackova H, Viganova D, Brill SJ, Lisby M, Krejci L (2015) Srs2 promotes Mus81-Mms4-mediated resolution of recombination intermediates. *Nucleic Acids Res* 43(7):3626-3642
- Chen CF and Brill SJ (2007) Binding and activation of DNA topoisomerase III by the Rmi1 subunit. *J Biol Chem* 282(39):28971-28979
- Chen X, Cui D, Papusha A, Zhang X, Chu CD, Tang J, Chen K, Pan X, Ira G (2012) The Fun30 nucleosome remodeler promotes resection of DNA double-strand break ends. *Nature* 489(7417):576-580
- Chen X, Niu H, Chung WH, Zhu Z, Papusha A, Shim EY, Lee SE, Sung P, Ira G (2011) Cell cycle regulation of DNA double-strand break end resection by Cdk1-dependent Dna2 phosphorylation. *Nat Struct Mol Biol* 18(9):1015-1019
- Chen X, Niu H, Yu Y, Wang J, Zhu S, Zhou J, Papusha A, Cui D, Pan X, Kwon Y, Sung P, Ira G (2016) Enrichment of Cdk1-cyclins at DNA double-strand breaks stimulates Fun30 phosphorylation and DNA end resection. *Nucleic Acids Res* 44(6):2742-2753
- Chen YC and Weinreich M (2010) Dbf4 regulates the Cdc5 polo-like kinase through a distinct non-canonical binding interaction. *J Biol Chem* 285: 41244-41254
- Chen Z, Yang H, Pavletich NP (2008) Mechanism of homologous recombination from the RecA-ssDNA/dsDNA structures. *Nature* 453:489-484
- Cho RJ, Campbell MJ, Winzeler EA, Steinmetz L, Conway A, Wodicka L, Wolfsberg TG, Gabrielian AE, Landsman D, Lockhart DJ, Davis RW (1998) A genome-wide transcriptional analysis of the mitotic cell cycle. *Mol Cell* 2(1):65-73
- Chu WK, Payne MJ, Beli P, Hanada K, Choudhary C, Hickson ID (2015) FBH1 influences DNA replication fork stability and homologous recombination through ubiquitylation of RAD51. *Nat Commun* 6:5931
- Chung I and Zhao X (2015) DNA break-induced sumoylation is enabled by collaboration between a SUMO ligase and the ssDNA-binding complex RPA. *Genes Dev* 29(15):1593-1598
- Ciccía A, Constantinou A, West SC (2003) Identification and characterization of the human MUS81-EME1 endonuclease. *J Biol Chem* 278:25172-25178
- Ciccía A, Constantinou A, West SC (2003) Identification and characterization of the human MUS81-EME1 endonuclease. *J Biol Chem* 278(27):25172-25178
- Ciccía A, Ling C, Coulthard R, Yan Z, Xue Y, Meetei AR, Laghmani H, Joenje H, McDonald N, de Winter JP (2007) Identification of FAAP24, a Fanconi anemia core complex protein that interacts with FANCM. *Mol Cell* 25:331-343
- Ciccía A, McDonald N, West SC (2008) Structural and functional relationships of the XPF/MUS81 family of proteins. *Annu Rev Biochem* 77:259-287
- Clerici M, Mantiero D, Guerini I, Lucchini G, Longhese MP (2008) The Yku70-Yku80 complex contributes to regulate double-strand break processing and checkpoint activation during the cell cycle. *EMBO Rep* 9(8):810-818
- Cobb JA, Bjergbaek L, Shimada K, Frei C, Gasser SM (2003) DNA polymerase stabilization at stalled replication forks requires Mec1 and the RecQ helicase Sgs1. *EMBO J* 22:4325-4336
- Cole GM, Schild D, Lovett ST, Mortimer RK (1987) Regulation of RAD54- and RAD52-lacZ gene fusions in *Saccharomyces cerevisiae* in response to DNA damage. *Mol Cell Biol* 7:1078-1084
- Costelloe T, Louge R, Tomimatsu N, Mukherjee B, Martini E, Khadaroo B, Dubois K, Wiegant WW, Thierry A, Burma S, van Attikum H, Llorente B (2012) The yeast Fun30 and human SMARCAD1 chromatin remodellers promote DNA end resection. *Nature* 489(7417):581-584
- Coulon S, Gaillard PH, Chahwan C, McDonald WH, Yates JR 3rd, Russell P (2004) Slx1-Slx4 are subunits of a structure-specific endonuclease that maintains ribosomal DNA in fission yeast. *Mol Biol Cell* 15(1):71-80
- Cowan R, Collis CM, Grigg GW (1987) Breakage of double-stranded DNA due to single-stranded nicking. *J Theor Biol* 127(2):229-245

- Cremona CA, Sarangi P, Yang Y, Hang LE, Rahman S, Zhao X (2012) Extensive DNA damage-induced sumoylation contributes to replication and repair and acts in addition to the mec1 checkpoint. *Mol Cell* 45(3):422-432
- Cussiol JR, Jablonowski CM, Yimit A, Brown GW, Smolka MB (2015) Dampening checkpoint signalling via coordinated BRCT-domain interactions. *EMBO J* 34:1704-1717
- Dayani Y, Simchen G, Lichten M (2011) Meiotic recombination intermediates are resolved with minimal crossover formation during return-to-growth, an analogue of the mitotic cell cycle. *PLoS Genet* 7:e1002083
- de Jager M, Dronkert MLG, Modesti M, Beerens CEMT, Kanaar R, van Gent DC (2001) DNA-binding and strand-annealing activities of human Mre11: implications for its roles in DNA double-strand break repair pathways. *Nucleic Acids Res* 29(6):1317-1325
- de Lichtenberg U, Jensen TS, Jensen LJ, Brunak S (2003) Protein feature based identification of cell cycle regulated proteins in yeast. *J Mol Biol* 329:663-674
- de los Santos T, Loidl J, Larkin B, Hollingsworth NM (2001) A role for MMS4 in the processing of recombination intermediates during meiosis in *Saccharomyces cerevisiae*. *Genetics* 159(4):1511-1525
- de Massy B (2013) Initiation of meiotic recombination: how and where? Conservation and specificities among eukaryotes. *Annu Rev Genet* 47:563-599
- de Muyt A, Jessop L, Kolar E, Sourirajan A, Chen J, Dayani Y, Lichten M (2012) BLM helicase ortholog Sgs1 is a central regulator of meiotic recombination intermediate metabolism. *Mol Cell* 46:43-53
- Delacroix S, Wagner JM, Kobayashi M, Yamamoto K, Karnitz LM (2007) The Rad9-Hus1-Rad1 (9-1-1) clamp activates checkpoint signaling via TopBP1. *Genes Dev* 21:1472-1477
- Demple B and DeMott MS (2002) Dynamics and diversions in base excision DNA repair of oxidized abasic lesions. *Oncogene* 21(58):8926-8934
- Devin AB, Prosvirova TYu, Peshekhonov VT, Chepurnaya OV, Smirnova ME, Koltovaya NA, Troitskaya EN, Arman IP (1990) The start gene CDC28 and the genetic stability of yeast. *Yeast* 6(3):231-243
- Dhingra N, Bruck I, Smith S, Ning B, Kaplan DL (2015) Dpb11 protein helps control assembly of the Cdc45-Mcm2-7-GINS replication fork helicase. *J Biol Chem* 290:7586-7601
- Dibitetto D, Ferrari M, Rawal CC, Balint A, Kim T, Zhang Z, Smolka MB, Brown GW, Marini F, Pellicoli A (2015) Slx4 and Rtt107 control checkpoint signalling and DNA resection at double-strand breaks. *Nucleic Acids Res* 44(2):669-682
- Dion V, Kalck V, Horigome C, Towbin BD, Gasser SM (2012) Increased mobility of double-strand breaks requires Mec1, Rad9 and the homologous recombination machinery. *Nat Cell Biol* 14:502-509
- Doe CL, Ahn JS, Dixon J, Whitby MC (2002) Mus81-Eme1 and Rqh1 involvement in processing stalled and collapsed replication forks. *J Biol Chem* 277:32753-32759
- Downs JA, Allard S, Jobin-Robitaille O, Javaheri A, Auger A, Bouchard N, Kron SJ, Jackson SP, Côté J (2004) Binding of chromatin-modifying activities to phosphorylated histone H2A at DNA damage sites. *Mol Cell* 16(6):979-990
- Downs JA, Lowndes NF, Jackson SP (2000) A role for *Saccharomyces cerevisiae* histone H2A in DNA repair. *Nature* 408(6815):1001-1004
- Duch A, Felipe-Abrío I, Barroso S, Yaakov G, García-Rubio M, Aguilera A, de Nadal E, Posas F (2012) Coordinated control of replication and transcription by a SAPK protects genomic integrity. *Nature* 493(7430):116-119
- Duda H, Arter M, Gloggnitzer J, Teloni F, Wild P, Blanco MG, Altmeyer M & Matos J (2016) A mechanism for controlled breakage of under-replicated chromosomes during mitosis. *Dev Cell* 39:740-755
- Dunin-Horkawicz S, Feder M, Bujnicki JM (2006) Phylogenomic analysis of the GIY-YIG nuclease superfamily. *BMC Genomics* 7:98
- Dutta D, Shatalin K, Epshtein V, Gottesman ME, Nudler E (2011) Linking RNA polymerase backtracking to genome instability. *Cell* 146(4): 533-543
- Duursma AM, Driscoll R, Elias JE, Cimprich KA (2013) A role for the MRN complex in ATR activation through TOPBP1 recruitment. *Mol Cell* 50(1):116-122
- Eapen VV, Sugawara N, Tsabar M, Wu WH, Haber JE (2012) The *Saccharomyces cerevisiae* chromatin remodeler Fun30 regulates DNA end resection and checkpoint deactivation. *Mol Cell Biol* 32:4727-4740
- Ehmsen KT and Heyer WD (2008) *Saccharomyces cerevisiae* Mus81-Mms4 is a catalytic, DNA structure-selective endonuclease. *Nucleic Acids Res* 36:2182-2195
- Eissler CL, Mazón G, Powers BL, Savinov SN, Symington LS, Hall MC (2014) The Cdk/cDc14 module controls activation of the Yen1 Holliday junction resolvase to promote genome stability. *Mol Cell* 54(1):80-93
- Elia AE, Cantley LC, Yaffe MB (2003a) Proteomic screen finds pSer/pThr-binding domain localizing Plk1 to mitotic substrates. *Science* 299(5610):1228-1231
- Elia AE, Rellos P, Haire LF, Chao JW, Ivins FJ, Hoepker K, Mohammad D, Cantley LC, Smerdon SJ, Yaffe MB (2003b) The molecular basis for phosphodependent substrate targeting and regulation of Plks by the Polo-box domain. *Cell* 115(1):83-95
- Elledge SJ and Davis RW (1989) DNA damage induction of ribonucleotide reductase. *Mol Cell Biol* 9:4932-4940
- Elledge SJ and Davis RW (1990) Two genes differentially regulated in the cell cycle and by DNA-damaging agents encode alternative regulatory subunits of ribonucleotide reductase. *Genes Dev* 4:740-751
- Ellis NA, Groden J, Ye T-Z, Straughen J, Lennon DJ, Ciccio S, Proytcheva M, German J (1995) The Bloom's syndrome gene product is homologous to RecQ helicases. *Cell* 83:655-666
- Emili A (1998) MEC1-dependent phosphorylation of Rad9p in response to DNA damage. *Mol Cell* 2:183-189
- Enserink JM, Hombauer H, Huang ME, Kolodner RD (2009) Cdc28/Cdk1 positively and negatively affects genome stability in *S. cerevisiae*. *J Cell Biol* 185(3):423-437
- Fabre F, Chan A, Heyer WD, Gangloff S (2002) Alternate pathways involving Sgs1/Top3, Mus81/Mms4, and Srs2 prevent formation of toxic recombination intermediates from single-stranded gaps created by DNA replication. *Proc Natl Acad Sci U S A* 99:16887-16892
- Fachinetti D, Bermejo R, Cocito A, Minardi S, Katou Y, Kanoh Y, Shirahige K, Azvolinsky A, Zakian VA, Foiani M (2010) Replication termination at eukaryotic chromosomes is mediated by Top2 and occurs at genomic loci containing pausing elements. *Mol Cell* 39(4):595-605
- Fasching CL, Cejka P, Kowalczykowski SC, Heyer W-D (2015) Top3-Rmi1 dissolve Rad51-mediated D-loops by a topoisomerase-based mechanism. *Mol Cell* 57(4):595-606
- Fekairi S, Scaglione S, Chahwan C, Taylor ER, Tissier A, Coulon S, Dong M-Q, Ruse C, Yates JR, Russell P, Fuchs RP, McGowan CH, Gaillard PHL (2009) Human SLX4 is a Holliday junction resolvase subunit that binds multiple DNA repair/recombination endonucleases. *Cell* 138:78-89

- Feng W, Di Rienzi SC, Raghuraman MK, Brewer BJ (2011) Replication stress-induced chromosome breakage is correlated with replication fork progression and is preceded by single-stranded DNA formation. *G3 (Bethesda)* 1(5):327-335
- Fierz B, Chatterjee C, McGinty RK, Bar-Dagan M, Raleigh DP, Muir TW (2011) Histone H2B ubiquitylation disrupts local and higher-order chromatin compaction. *Nat Chem Biol* 7:113-119
- Fishman-Lobell J, Rudin N, Haber JE (1992) Two alternative pathways of double-strand break repair that are kinetically separable and independently modulated. *Mol Cell Biol* 12(3):1292-1303
- Flott S and Rouse J (2005) Slx4 becomes phosphorylated after DNA damage in a Mec1/Tel1-dependent manner and is required for repair of DNA alkylation damage. *Biochem J* 391:325-333
- Flott S, Alabert C, Toh GW, Toth R, Sugawara N, Campbell DG, Haber JE, Pasero P, Rouse J (2007) Phosphorylation of Slx4 by Mec1 and Tel1 regulates the single-strand annealing mode of DNA repair in budding yeast. *Mol Cell Biol* 27(18):6433-6445
- Flott S, Kwon Y, Pigli YZ, Rice PA, Sung P, Jackson SP (2011) Regulation of Rad51 function by phosphorylation. *EMBO Rep* 12(8):833-839
- Fogg JM and Lilley DMJ (2000) Ensuring productive resolution by the junction-resolving enzyme RuvC: Large enhancement of the second-strand cleavage rate. *Biochemistry* 39:16125-16134
- Franchitto A (2013) Genome instability at common fragile sites: searching for the cause of their instability. *BioMed Res Int* 2013:730714
- Frank-Vaillant M and Marcand S (2001) NHEJ regulation by mating type is exercised through a novel protein, Lif2p, essential to the Ligase IV pathway. *Genes Dev* 15:3005-3012
- Fricke WM and Brill SJ (2003) Slx1-Slx4 is a second structure-specific endonuclease functionally redundant with Sgs1-Top3. *Genes Dev* 17(14):1768-1778
- Fricke WM, Bastin-Shanower SA, Brill SJ (2005) Substrate specificity of the *Saccharomyces cerevisiae* Mus81-Mms4 endonuclease. *DNA Repair (Amst)* 4:243-251
- Fukunaga K, Kwon Y, Sung P, Sugimoto K (2011) Activation of Protein Kinase Tel1 through Recognition of Protein-Bound DNA Ends. *Mol Cell Biol* 31(10):1959-1971
- Furuya K, Poitelea M, Guo L, Caspari T, Carr AM (2004) Chk1 activation requires Rad9 S/TQ-site phosphorylation to promote association with C-terminal BRCT domains of Rad4TOPBP1. *Genes Dev* 18:1154-1164
- Futreal PA, Liu Q, Shattuck-Eidens D, Cochran C, Harshman K, Tavtigian S, Bennett LM, Haugen-Strano A, Swensen J, Miki Y, Eddington K, McClure M, Frye C, Weaver-Feldhaus J, Ding W, Gholami Z, Soderkvist P, Terry L, Jhanwar S, Berchuck A, Iglehart JD, Marks J, Ballinger DG, Barrett JC, Skolnick MH, Kamb A, Wiseman A (1994) BRCA1 mutations in primary breast and ovarian carcinomas. *Science* 266(5182):120-122
- Gaillard P-HL, Noguchi E, Shanahan P, Russell P (2003) The endogenous Mus81-Eme1 complex resolves Holliday junctions by a nick and counternick mechanism. *Mol Cell* 12:747-759
- Galli A and Schiestl RH (1996) Hydroxyurea induces recombination in dividing but not in G1 or G2 cell cycle arrested yeast cells. *Mutat Res* 354(1):69-75
- Gallo-Fernández M, Saugar I, Ortiz-Bazán MÁ, Vázquez MV, Tercero JA (2012) Cell cycle-dependent regulation of the nuclease activity of Mus81-Eme1/Mms4. *Nucleic Acids Res* 40:8325-8335
- García V, Furuya K, Carr AM (2005) Identification and functional analysis of TopBP1 and its homologs. *DNA Repair* 4:1227-1239
- García V, Phelps SEL, Gray S, Neale MJ (2011) Bidirectional resection of DNA double-strand breaks by Mre11 and Exo1. *Nature* 479(7372):241-244
- Garner E, Kim Y, Lach FP, Kottemann MC, Smogorzewska A (2013) Human GEN1 and the SLX4-associated nucleases MUS81 and SLX1 are essential for the resolution of replication-induced Holliday junctions. *Cell Reports* 5(1):207-215
- Gasch AP, Huang M, Metzner S, Botstein D, Elledge SJ, Brown PO (2001) Genomic expression responses to DNA-damaging agents and the regulatory role of the yeast ATR homolog Mec1p. *Mol Biol Cell* 12(10):2987-3003
- Gasior SL, Wong AK, Kora Y, Shinohara A, Bishop DK (1998) Rad52 associates with RPA and functions with Rad55 and Rad57 to assemble meiotic recombination complexes. *Genes Dev* 12(14):2208-2221
- Gaskell LJ, Osman F, Gilbert RJ, Whitby MC (2007) Mus81 cleavage of Holliday junctions: a failsafe for processing meiotic recombination intermediates? *EMBO J* 26(7):1891-1901
- Gerloff DL, Woods NT, Farago AA, Monteiro ANA (2012) BRCT domains: A little more than kin, and less than kind. *FEBS Lett* 586:2711-2716
- Germann SM, Schramke V, Pedersen RT, Gallina I, Eckert-Boulet N, Oestergaard VH, Lisby M (2014) TopBP1/Dpb11 binds DNA anaphase bridges to prevent genome instability. *J Cell Biol* 204(1):45-59
- Ghaemmaghami S, Huh WK, Bower K, Howson RW, Belle A, Dephoure N, O'Shea EK, Weissman JS (2003) Global analysis of protein expression in yeast. *Nature* 425(6959):737-741
- Ghosal G and Chen J (2013) DNA damage tolerance: a double-edged sword guarding the genome. *Transl Cancer Res* 2(3):107-129
- Giannattasio M, Lazzaro F, Plevani P, Muzi-Falconi M (2005) The DNA damage checkpoint response requires histone H2B ubiquitination by Rad6-Bre1 and H3 methylation by Dot1. *J Biol Chem* 280:9879-9886
- Gilbert CS, Green CM, Lowndes NF (2001) Budding yeast Rad9 is an ATP-dependent Rad53 activating machine. *Mol Cell* 8:129-136
- Giraud-Panis MJE and Lilley DMJ (1997) Near simultaneous DNA cleavage by the subunits of the junction-resolving enzyme T4 endonuclease VII. *EMBO J* 16:2528-2534
- Glover JNM, Williams RS, Lee MS (2004) Interactions between BRCT repeats and phosphoproteins: tangled up in two. *Trends Biochem Sci* 29:579-585
- Gotta M, Laroche T, Formenton A, Maillet L, Scherthan H, Gasser SM (1996) The clustering of telomeres and colocalization with Rap1, Sir3, and Sir4 proteins in wild-type *Saccharomyces cerevisiae*. *J Cell Biol* 134(6):1349-1363
- Gottipati P and Helleday T (2009) Transcription-associated recombination in eukaryotes: link between transcription, replication and recombination. *Mutagenesis* 24(3):203-210
- Grenon M, Costelloe T, Jimeno S, O'Shaughnessy A, Fitzgerald J, Zgheib O, Degerth L, Lowndes NF (2007) Docking onto chromatin via the *Saccharomyces cerevisiae* Rad9 Tudor domain. *Yeast* 24:105-119
- Gritenaite D, Princz LN, Szakal B, Bantele SCS, Wendeler L, Schilbach S, Habermann BH, Matos J, Lisby M, Branzei D, Pfander B (2014) A cell cycle-regulated Slx4-Dpb11 complex promotes the resolution of DNA repair intermediates linked to stalled replication. *Genes Dev* 28:1604-1619

- Groth P, Ausländer S, Majumder MM, Schultz N, Johansson F, Petermann E, Helleday T (2010) Methylated DNA causes a physical block to replication forks independently of damage signalling, O<sup>6</sup>-methylguanine or DNA single-strand breaks and results in DNA damage. *J Mol Biol* 402(1):70-82
- Gwon GH, Jo A, Baek K, Jin KS, Fu Y, Lee JB, Kim Y, Cho Y (2014) Crystal structures of the structure-selective nuclease Mus81-Eme1 bound to flap DNA substrates. *EMBO J* 33(9):1061-1072
- Haber JE (2012) Mating-type genes and MAT switching in *Saccharomyces cerevisiae*. *Genetics* 191(1):33-64
- Hammet A, Magill C, Helerhorst J, Jackson SP (2007) Rad9 BRCT domain interaction with phosphorylated H2AX regulates the G1 checkpoint in budding yeast. *EMBO Rep* 8:851-857
- Hang LE, Peng J, Tan W, Szakal B, Menolfi D, Sheng Z, Lobachev K, Branzei D, Feng W, Zhao X (2015) Rtt107 is a multi-functional scaffold supporting replication progression with partner SUMO and ubiquitin ligases. *Mol Cell* 60(2):268-279
- Harrington JJ and Lieber MR (1994) Functional domains within FEN-1 and RAD2 define a family of structure-specific endonucleases: Implications for nucleotide excision repair. *Genes Dev* 8:1344-1355
- Hickson ID (2003) RECQ helicase: Caretakers of the genome. *Nat Rev Mol Cell Biol* 3:169-178
- Ho CK, Mazon G, Lam AF, Symington LS (2010) Mus81 and Yen1 promote reciprocal exchange during mitotic recombination to maintain genome integrity in budding yeast. *Mol Cell* 40:988-1000
- Ho Y, Gruhler A, Heilbut A, Bader GD, Moore L, Adams SL, Millar A, Taylor P, Bennett K, Boutillier K, Yang L, Wolting C, Donaldson I, Schandorff S, Shewnarane J, Vo M, Taggart J, Goudreaux M, Muskat B, Alfarano C, Dewar D, Lin Z, Michalickova K, Willems AR, Sassi H, Nielson PA, Rasmussen KJ, Andersen JR, Johansen LE, Hansen LH, Jespersen H, Podtelejnikov A, Nielsen E, Crawford J, Poulsen V, Sorensen BD, Matthiesen J, Hendrickson RC, Gleeson F, Pawson T, Moran MF, Durocher D, Mann M, Hoque CW, Figeys D, Tyers M (2002) Systematic identification of protein complexes in *Saccharomyces cerevisiae* by mass spectrometry. *Nature* 415:180-183
- Hoeghe C, Pfander B, Moldovan GL, Pyrowolakis G, Jentsch S (2002) RAD6-dependent DNA repair is linked to modification of PCNA by ubiquitin and SUMO. *Nature* 419(6903):135-141
- Hoeljmackers JH (2009) DNA damage, aging, and cancer. *N Engl J Med* 361:1475-1485
- Hohl M, Kwon Y, Galván SM, Xue X, Tous C, Aguilera A, Sung P, Petrini JH (2011) The Rad50 coiled coil domain is indispensable for Mre11 complex functions. *Nat Struct Mol Biol* 18(10):1124-1131
- Holliday R (1964) A mechanism for gene conversion in fungi. *Genet Res* 5:282-304
- Holliday R (1965) Induced mitotic crossing-over in relation to genetic replication in synchronously dividing cells of *Ustilago maydis*. *Genet Res* 6:104-120
- Holliday R (1966) Studies on mitotic gene conversion in *Ustilago*. *Genet Res* 8(3):323-337
- Hopfner KP, Craig L, Moncalian G, Zinkel RA, Usui T, Owen BA, Karcher A, Henderson B, Bodmer JL, McMurray CT, Carney JP, Petrini JH, Tainer JA (2002) The Rad50 zinc-hook is a structure joining Mre11 complexes in DNA recombination and repair. *Nature* 418(6897):562-566
- Horigome C, Oma Y, Konishi T, Schmid R, Marcomini I, Hauer MH, Dion V, Harata M, Gasser SM (2014) SWR1 and INO80 chromatin remodelers contribute to DNA double-strand break perinuclear anchorage site choice. *Mol Cell* 55(4):626-639
- Horiuchi T and Fujimura Y (1995) Recombinational rescue of the stalled DNA replication fork: a model based on analysis of an *Escherichia coli* strain with a chromosome region difficult to replicate. *J Bacteriol* 177(3):783-791
- House NCM, Koch MR, Freudenreich CH (2014) Chromatin modifications and DNA repair: beyond double-strand breaks. *Frontiers in Genetics* 5:296
- Huertas P, Cortes-Ledesma F, Sartori AA, Aguilera A, Jackson SP (2008) CDK targets Sae2 to control DNA-end resection and homologous recombination. *Nature* 455(7213):689-692
- Huo YG, Bai L, Xu M, Jiang T (2010) Crystal structure of the N-terminal region of human Topoisomerase II $\beta$  binding protein 1. *Biochem Biophys Res Commun* 401:401-405
- Interthal H and Heyer WD (2000) MUS81 encodes a novel helix-hairpin-helix protein involved in the response to UV- and methylation-induced DNA damage in *Saccharomyces cerevisiae*. *Mol Gen Genet* 263(5):812-827
- Ip SCY, Rass U, Blanco MG, Flynn HR, Skehel JM, West SC (2008) Identification of Holliday junction resolvases from humans and yeast. *Nature* 456:357-361
- Ira G, Malkova A, Liberi G, Foiani M, Haber JE (2003) Srs2 and Sgs1-Top3 suppress crossovers during double-strand break repair in yeast. *Cell* 115:401-411
- Ira G, Pelliccioli A, Balijja A, Wang X, Fiorani S, Carotenuto W, Liberi G, Bressan D, Wan L, Hollingsworth NM, Haber JE, Foiani M (2004) DNA end resection, homologous recombination and DNA damage checkpoint activation require CDK1. *Nature* 431(7011):1011-1017
- Ivanov EL and Haber JE (1995) RAD1 and RAD10, but not other excision repair genes, are required for double-strand break-induced recombination in *Saccharomyces cerevisiae*. *Mol Cell Biol* 15(4):2245-2251
- Ivanov EL, Sugawara N, White CI, Fabre F, Haber JE (1994) Mutations in XRS2 and RAD50 delay but do not prevent mating-type switching in *Saccharomyces cerevisiae*. *Mol Cell Biol* 14(5):3414-3425
- Jablonowski CM, Cussiol JR, Oberly S, Yimit A, Balint A, Kim T, Zhang Z, Brown GW, Smolka MB (2015) Termination of replication stress signaling via concerted action of the Slx4 scaffold and the PP4 phosphatase. *Genetics* 201(3):937-949
- Jazayeri A, Falck J, Lukas C, Bartek J, Smith GC, Lukas J, Jackson SP (2006) ATM- and cell cycle-dependent regulation of ATR in response to DNA double-strand breaks. *Nat Cell Biol* 8(1):37-45
- Jensen LJ, Jensen TS, de Lichtenberg U, Brunak S, Bork P (2006) Co-evolution of transcriptional and post-translational cell cycle regulation. *Nature* 443:594-597
- Jentsch S, McGrath JP, Varshavsky A (1987) The yeast DNA repair gene RAD6 encodes a ubiquitin-conjugating enzyme. *Nature* 329(6135):131-134
- Johnson RE, Kovvali GK, Prakash L, Prakash S (1998) Role of yeast Rth1 nuclease and its homologs in mutation avoidance, DNA repair, and DNA replication. *Curr Genet* 34:21-29
- Kai M, Boddy MN, Russell P, Wang TS-F (2005) Replication checkpoint kinase Cds1 regulates Mus81 to preserve genome integrity during replication stress. *Genes Dev* 19(8):919-932
- Kaiser GS, Germann SM, Westergaard T, Lisby M (2011) Phenylbutyrate inhibits homologous recombination induced by camptothecin and methyl methanesulfonate. *Mutat Res* 713:64-75
- Kaliraman V, Mullen JR, Fricke WM, Bastin-Shanower SA, Brill SJ (2001) Functional overlap between Sgs1-Top3 and the Mms4-Mus81 endonuclease. *Genes Dev* 15(20):2730-2740

- Kang MJ, Lee CH, Kang YH, Cho IT, Nguyen TA, Seo YS (2010) Genetic and functional interactions between Mus81-Mms4 and Rad27. *Nucleic Acids Res* 38(21):7611-7625
- Karathanasis E and Wilson TE (2002) Enhancement of *Saccharomyces cerevisiae* end-joining efficiency by cell growth stage but not by impairment of recombination. *Genetics* 161(3):1015-1027
- Karpov DS, Spasskaya DS, Tutyaeva VV, Mironov AS, Karpov VL (2013) Proteasome inhibition enhances resistance to DNA damage via upregulation of Rpn4-dependent DNA repair genes. *FEBS Lett* 587(18):3108-3114
- Kegel A, Sjostrand JOO, Astrom SU (2001) Nej1p, a cell type-specific regulator of nonhomologous end joining in yeast. *Curr Biol* 11:1611-1617
- Keyamura K, Arai K, Hishida T (2016) Srs2 and Mus81-Mms4 prevent accumulation of toxic inter-homolog recombination intermediates. *PLoS Genet* 12(7):e1006136
- Khadaroo B, Teixeira MT, Luciano P, Eckert-Boulet N, Germann SM, Simon MN, Gallina I, Abdallah P, Gilson E, Géli V, Lisby M (2009) The DNA damage response at eroded telomeres and tethering to the nuclear pore complex. *Nat Cell Biol* 11(8):980-987
- Kim JC and Mirkin SM (2013) The balancing act of DNA repeat expansions. *Curr Opin Genet Dev* 23(3):280-288
- Kim Y, Spitz GS, Veturi U, Lach FP, Auerbach AD, Smogorzewska A (2013) Regulation of multiple DNA repair pathways by the Fanconi anemia protein SLX4. *Blood* 121(1):54-63
- Kiser GL and Weinert TA (1996) Distinct roles of yeast MEC and RAD checkpoint genes in transcriptional induction after DNA damage and implications for function. *Mol Biol Cell* 7:703-718
- Klapstein K, Chou T, Bruinsma R (2004) Physics of RecA-mediated homologous recognition. *Biophys J* 87:1466-1477
- Koltovaya NA, Arman IP, Devin AB (1998) Mutations of the CDC28 gene and the radiation sensitivity of *Saccharomyces cerevisiae*. *Yeast* 14(2):133-146
- Kosugi S, Hasebe M, Tomita M, Yanagawa H (2009) Systematic identification of cell cycle-dependent yeast nucleocytoplasmic shuttling proteins by prediction of composite motifs. *Proc Natl Acad Sci U S A* 106:10171-10176
- Kovalenko OV, Plug AW, Haaf T, Gonda DK, Ashley T, Ward DC, Radding CM, Golub EI (1996) Mammalian ubiquitin-conjugating enzyme Ubc9 interacts with Rad51 recombination protein and localizes in synaptonemal complexes. *Proc Natl Acad Sci U S A* 93:2958-29263
- Kraus E, Leung WY, Haber JE (2001) Break-induced replication: a review and an example in budding yeast. *Proc Natl Acad Sci U S A* 98(15):8255-8262
- Krogan NJ, Lam MH, Fillingham J, Keogh MC, Gebbia M, Li J, Datta N, Cagney G, Buratowski S, Emili A, Greenblatt JF (2004) Proteasome involvement in the repair of DNA double-strand breaks. *Mol Cell* 16(6):1027-1034
- Kulak NA, Pichler G, Paron I, Nagaraj N, Mann M (2014) Minimal, encapsulated proteomic-sample processing applied to copy-number estimation in eukaryotic cells. *Nat Methods* 11(3):319-324
- Lazzaro F, Sapountzi V, Granata M, Pelliccioli A, Vaze M, Haber JE, Plevani P, Lydall D, Muzi-Falconi M (2008) Histone methyltransferase Dot1 and Rad9 inhibit single-stranded DNA accumulation at DSBs and uncapped telomeres. *EMBO J* 27(10):1502-1512
- Lechner MS, Levitan I, Dressler GR (2000) PTIP, a novel BRCT domain-containing protein interacts with Pax2 and is associated with active chromatin. *Nucleic Acids Research*, 28(14), 2741-2751
- Lee J, Kumagai A, Dunphy WG (2007) The Rad9-Hus1-Rad1 checkpoint clamp regulates interaction of TopBP1 with ATR. *J Biol Chem* 282:28036-28044
- Lee S-H, Princz LN, Klügel MF, Habermann B, Pfander B, Biertümpfel C (2015) Human Holliday junction resolvase GEN1 uses a chromodomain for efficient DNA recognition and cleavage. *eLife* 4:e12256
- Lemoine FJ, Degtyareva NP, Lobachev K, Petes TD (2005) Chromosomal translocations in yeast induced by low levels of DNA polymerase  $\alpha$  model for chromosome fragile sites. *Cell* 120(5):587-598
- Leung CCY and Glover JNM (2011) BRCT domains: easy as one, two, three. *Cell Cycle* 10:2461-2470
- Leung GP, Lee L, Schmidt TI, Shirahige K, Kobor MS (2011) Rtt107 is required for recruitment of the SMC5/6 complex to DNA double strand breaks. *J Biol Chem* 286(29):26250-26257
- Li X, Liu K, Li F, Wang J, Huang H, Wu J, Shi Y (2012) Structure of C-terminal tandem BRCT repeats of Rtt107 protein reveals critical role in interaction with phosphorylated histone H2A during DNA damage repair. *J Biol Chem* 287(12):9137-9146
- Liberi G, Maffioletti G, Lucca C, Chiolo I, Baryshnikova A, Cotta-Ramusino C, Lopes M, Pelliccioli A, Haber JE, Foiani M (2005) Rad51-dependent DNA structures accumulate at damaged replication forks in *sgs1* mutants defective in the yeast ortholog of BLM RecQ helicase. *Genes Dev* 19:339-350
- Lin YL and Pasero P (2012) Interference between DNA replication and transcription as a cause of genomic instability. *Curr Genomics* 13(1):65-73
- Lindahl T and Barnes DE (2000) Repair of endogenous DNA damage. *Cold Spring Harb Symp Quant Biol* 65:127-133
- Lisby M, Barlow JH, Burgess RC, Rothstein R (2004) Choreography of the DNA damage response: spatiotemporal relationships among checkpoint and repair proteins. *Cell* 118:699-713
- Lisby M, Rothstein R, Mortensen UH (2001) Rad52 forms DNA repair and recombination centers during S phase. *Proc Natl Acad Sci U S A* 98:8276-8282
- Liu X, Bardwell L, Nie Q (2010) A combination of multisite phosphorylation and substrate sequestration produces switch-like responses. *Biophys J* 98(8):1396-1407
- Llorente B, Smith CE, Symington LS (2008) Break-induced replication: what is it and what is it for? *Cell Cycle* 7(7):859-864
- Lobachev K, Vitriol E, Stemple J, Resnick MA, Bloom K (2004) Chromosome fragmentation after induction of a double-strand break is an active process prevented by the RMX repair complex. *Curr Biol* 14:2107-2112
- Lokesh GL, Muralidhara BK, Negi SS, Natarajan A (2007) Thermodynamics of phosphopeptide tethering to BRCT: the structural minima for inhibitor design. *J Am Chem Soc* 129:10658-10659
- Lopes M, Cotta-Ramusino C, Pelliccioli A, Liberi G, Plevani P, Muzi-Falconi M, Newlon CS, Foiani M (2001) The DNA replication checkpoint response stabilizes stalled replication forks. *Nature* 412(6846):557-561
- Lopez-Mosqueda J, Maas NL, Jonsson ZO, DeFazio Eli LG, Wohlschlegel J, Toczyski DP (2010) Damage-induced Phosphorylation of Sld3 is Important to Block Late Origin Firing. *Nature* 467(7314):479-483
- Lucca C, Vanoli F, Cotta-Ramusino C, Pelliccioli A, Liberi G, Haber J, Foiani M (2004) Checkpoint-mediated control of replisome-fork association and signalling in response to replication pausing. *Oncogene* 23(6):1206-1213

- Luke B, Versini G, Jaquenoud M, Zaidi IW, Kurz T, Pintard L, Pasero P, Peter M (2006) The cullin Rtt101p promotes replication fork progression through damaged DNA and natural pause sites. *Curr Biol* 16:786-792
- Lyons NA, Fonslow BR, Diedrich JK, Yates JR, Morgan DO (2013) Sequential primed kinases create a damage-responsive phosphodegron on Eco1. *Nat Struct Mol Biol* 20:194-201
- Majka J and Burgers PM (2003) Yeast Rad17/Mec3/Ddc1: a sliding clamp for the DNA damage checkpoint. *Proc Natl Acad Sci U S A* 100:2249-2254
- Majka J, Niedziela-Majka A, Burgers PM (2006) The checkpoint clamp activates Mec1 kinase during initiation of the DNA damage checkpoint. *Mol Cell* 24(6):891-901
- Malkova A, Ivanov EL, Haber JE (1996) Double-strand break repair in the absence of RAD51 in yeast: a possible role for break-induced DNA replication. *Proc Natl Acad Sci U S A* 93(14):7131-7136
- Malkova A, Naylor ML, Yamaguchi M, Ira G, Haber JE (2005) RAD51-dependent break-induced replication differs in kinetics and checkpoint responses from RAD51-mediated gene conversion. *Mol Cell Biol* 25(3):933-944
- Masai H, Taniyama C, Ogino K, Matsui E, Kakusho N, Matsumoto S, Kim JM, Ishii A, Tanaka T, Kobayashi T, Tamai K, Ohtani K, Arai K-I (2006) Phosphorylation of MCM4 by Cdc7 kinase facilitates its interaction with Cdc45 on the chromatin. *J Biol Chem* 281:39249-39261
- Mathiasen DP and Lisby M (2014) Cell cycle regulation of homologous recombination in *Saccharomyces cerevisiae*. *FEMS Microbiol Rev* 38(2):172-184
- Matos J and West SC (2014) Holliday junction resolution: regulation in space and time. *DNA Repair (Amst)* 19:176-181
- Matos J, Blanco MG, Maslen S, Skehel JM, West SC (2011) Regulatory control of the resolution of DNA recombination intermediates during meiosis and mitosis. *Cell* 147:158-172
- Matos J, Blanco MG, West SC (2013) Cell-cycle kinases coordinate the resolution of recombination intermediates with chromosome segregation. *Cell Reports* 4:76-86
- Matos J, Lipp JJ, Bogdanova A, Guillot S, Okaz E, Junqueira M, Shevchenko A, Zachariae W (2008) Dbf4-dependent CDC7 kinase links DNA replication to the segregation of homologous chromosomes in meiosis I. *Cell* 135:662-678
- Matulova P, Marini V, Burgess RC, Sisakova A, Kwon Y, Rothstein R, Sung P, Krejci L (2009) Cooperativity of Mus81-Mms4 with Rad54 in the Resolution of Recombination and Replication Intermediates. *J Biol Chem* 284(12):7733-7745
- Mazina OM and Mazin AV (2008) Human Rad54 protein stimulates human Mus81-Eme1 endonuclease. *Proc Natl Acad Sci U S A* 105(47):18249-18254
- Meister P, Taddei A, Vernis L, Poidevin M, Gasser SM, Baldacci G (2005) Temporal separation of replication and recombination requires the intra-S checkpoint. *J Cell Biol* 168:537-544
- Mellon I, Spivak G, Hanawalt PC (1987) Selective removal of transcription-blocking DNA damage from the transcribed strand of the mammalian DHFR gene. *Cell* 51(2):241-249
- Mercier G, Denis Y, Marc P, Picard L, Dutreix M (2001) Transcriptional induction of repair genes during slowing of replication in irradiated *Saccharomyces cerevisiae*. *Mutat Res* 487:157-172
- Merrick H, Machón C, Grainger WH, Grossman AD, Soultanas P (2011) Co-directional replication-transcription conflicts lead to replication restart. *Nature* 470(7335):554-557
- Meselson MM and Radding CM (1975) A general model for genetic recombination. *Proc Natl Acad Sci U S A* 72:358-361
- Miki Y, Swensen J, Shattuck-Eidens D, Futreal PA, Harshman K, Tavtigian S, Liu Q, Cochran C, Bennett LM, Ding W, Bell R, Rosenthal J, Hussey C, Tran T, McClure M, Frye C, Hattier T, Phelps R, Haugen-Strano A, Katcher H, Yakumo K, Gholami Z, Shaffer D, Stone S, Bayer S, Wray C, Bogden R, Dayananth P, Ward J, Tonin P, Narod S, Bristow PK, Norris FH, Helvering L, Morrison P, Rosteck P, Lai M, Barrett JC, Lewis C, Neuhausen S, Cannon-Albright L, Goldgar D, Wiseman R, Kamb A, Skolnick MH (1994) A strong candidate for the breast and ovarian cancer susceptibility gene BRCA1. *Science* 266(5182):66-71
- Miller CT, Gabrielse C, Chen Y-C, Weinreich M (2009) Cdc7p-Dbf4p regulates mitotic exit by inhibiting polo kinase. *PLoS Genet* 5:1-13
- Milligan JR, Ng JY, Wu CC, Aguilera JA, Fahey RC, Ward JF (1995) DNA repair by thiols in air shows two radicals make a double-strand break. *Radiat Res* 143:273-280
- Mimitou EP and Symington LS (2008) Sae2, Exo1 and Sgs1 collaborate in DNA double-strand break processing. *Nature* 455(7214):770-774
- Mimitou EP and Symington LS (2010) Ku prevents Exo1 and Sgs1-dependent resection of DNA ends in the absence of a functional MRX complex or Sae2. *EMBO J* 29(19):3358-3369
- Minca EC and Kowalski D (2010) Multiple Rad5 activities mediate sister chromatid recombination to bypass DNA damage at stalled replication forks. *Mol Cell* 38:649-661
- Mine-Hattab J and Rothstein R (2012) Increased chromosome mobility facilitates homology search during recombination. *Nat Cell Biol* 14:510-517
- Miyazaki T, Bressan DA, Shinohara M, Haber JE, Shinohara A (2004) In vivo assembly and disassembly of Rad51 and Rad52 complexes during double-strand break repair. *EMBO J* 23(4):939-949
- Mohammad DH, Yaffe MB (2009) 14-3-3 proteins, FHA domains and BRCT domains in the DNA damage response. *DNA Repair (Amst)* 8:1009-1017
- Moldovan GL, Pfander B, Jentsch S (2007) PCNA, the maestro of the replication fork. *Cell* 129(4):665-679
- Montagnoli A, Valsasina B, Brotherton D, Troiani S, Rainoldi S, Tenca P, Molinari A, Santocanale C (2006) Identification of Mcm2 phosphorylation sites by S-phase-regulating kinases. *J Biol Chem* 281:10281-10290
- Mordes DA, Glick GG, Zhao R, Cortez D (2008). TopBP1 activates ATR through ATRIP and a PIKK regulatory domain. *Genes Dev* 22(11):1478-1489
- Morrison AJ, Highland J, Krogan NJ, Arbel-Eden A, Greenblatt JF, Haber JE, Shen X (2004) INO80 and gamma-H2AX interaction links ATP-dependent chromatin remodeling to DNA damage repair. *Cell* 119(6):767-775
- Mortensen EM, Haas W, Gygi M, Gygi SP, Kellogg DR (2005) Cdc28-dependent regulation of the Cdc5/Polo kinase. *Curr Biol* 15(22):2033-2037
- Moyal L, Lerenthal Y, Gana-Weisz M, Mass G, So S, Wang SY, Eppink B, Chung YM, Shalev G, Shema E, Shkedy D, Smorodinsky NI, van Vliet N, Kuster B, Mann M, Ciechanover A, Dahm-Daphi J, Kanaar R, Hu MC, Chen DJ, Oren M, Shiloh Y (2011) Requirement of ATM-dependent monoubiquitylation of histone H2B for timely repair of DNA double-strand breaks. *Mol Cell* 41(5):529-542
- Mukherjee S, Wright WD, Ehmsen KT, Heyer WD (2014) The Mus81-Mms4 structure-selective endonuclease requires nicked DNA junctions to undergo conformational changes and bend its DNA substrates for cleavage. *Nucleic Acids Res* 42(10):6511-6522
- Mullen JR, Kaliraman V, Ibrahim SS, Brill SJ (2001) Requirement for three novel protein complexes in the absence of the Sgs1 DNA helicase in *Saccharomyces cerevisiae*. *Genetics* 157(1):103-118

- Nagai S, Dubrana K, Tsai-Pflugfelder M, Davidson MB, Roberts TM, Brown GW, Varela E, Hediger F, Gasser SM, Krogan NJ (2008) Functional targeting of DNA damage to a nuclear pore-associated SUMO-dependent ubiquitin ligase. *Science* 322(5901):597-602
- Nair N, Castor D, Macartney T, Rouse J (2014) Identification and characterization of MUS81 point mutations that abolish interaction with the SLX4 scaffold protein. *DNA Repair (Amst)* 24:131-137
- Nash P, Tang X, Orlicky S, Chen Q, Gertler FB, Mendenhall MD, Sicheri F, Pawson T, Tyers M (2001) Multisite phosphorylation of a CDK inhibitor sets a threshold for the onset of DNA replication. *Nature* 414(29):514-521
- Nassif N, Penney, Pal S, Engels WR, Gloor GB (1994) Efficient copying of nonhomologous sequences from ectopic sites via P-element-induced gap repair. *Mol Cell Biol* 14 (3):1613-1625
- Navadgi-Patil VM and Burgers PM (2008) Yeast DNA replication protein Dpb11 activates the Mec1/ATR checkpoint kinase. *J Biol Chem* 283:35853-35859
- Navadgi-Patil VM and Burgers PM (2009) The unstructured C-terminal tail of the 9-1-1 clamp subunit Ddc1 activates Mec1/ATR via two distinct mechanisms. *Mol Cell* 36:743-753
- Navas TA, Sanchez Y, Elledge SJ (1996) RAD9 and DNA polymerase epsilon form parallel sensory branches for transducing the DNA damage checkpoint signal in *Saccharomyces cerevisiae*. *Genes Dev* 10(20):2632-2643
- New JH, Sugiyama T, Zaitseva E, Kowalczykowski SC (1998) Rad52 protein stimulates DNA strand exchange by Rad51 and replication protein A. *Nature* 391: 407-410
- Nitiss J and Wang JC (1988) DNA topoisomerase-targeting antitumor drugs can be studied in yeast. *Proc Natl Acad Sci U S A* 85(20):7501-7505
- Ohouo PY, Bastos de Oliveira FM, Liu Y, Ma CJ, Smolka MB (2013) DNA Repair Scaffolds Dampen Checkpoint Signaling by Counteracting the Rad9 Adaptor. *Nature* 493(7430):120-124
- Ohouo PY, de Oliveira FMB, Almeida BS, Smolka MB (2010) DNA damage signaling recruits the Rtt107-Slx4 scaffolds via Dpb11 to mediate replication stress response. *Mol Cell* 39:300-306
- Ohuchi T, Seki M, Branzei D, Maeda D, Ui A, Ogiwara H, Tada S, Enomoto T (2008) Rad52 sumoylation and its involvement in the efficient induction of homologous recombination. *DNA Repair (Amst)* 7(6):879-889
- OrrWeaver TL, Szostak JW, Rothstein RJ (1981) Yeast transformation: a model system for the study of recombination. *Proc Natl Acad Sci U S A* 78:6354-6358
- Paeschke K, Capra JA, Zakian VA (2011) DNA replication through G-quadruplex motifs is promoted by the *S. cerevisiae* Pif1 DNA helicase. *Cell* 145(5):678-691
- Palmbos PL, Wu D, Daley JM, Wilson TE (2005) Mutations of the Yku80 C terminus and Xrs2 FHA domain specifically block yeast nonhomologous end joining. *Mol Cell Biol* 25(24):10782-10790
- Papouli E, Chen S, Davies AA, Huttner D, Krejci L, Sung P, Ulrich HD (2005) Crosstalk between SUMO and ubiquitin on PCNA is mediated by recruitment of the helicase Srs2p. *Mol Cell* 19(1):123-133
- Pedersen RT, Kruse T, Nilsson J, Oestergaard VH, Lisby M (2015) TopBP1 is required at mitosis to reduce transmission of DNA damage to G1 daughter cells. *J Cell Biol* 210(4):565-582
- Pellicoli A, Lucca C, Liberi G, Marini F, Lopes M, Plevani P, Romano A, Di Fiore PP, Foiani M (1999) Activation of Rad53 kinase in response to DNA damage and its effect in modulating phosphorylation of the lagging strand DNA polymerase. *EMBO J* 18(22):6561-6572
- Pepe A and West SC (2014) MUS81-EME2 promotes replication fork restart. *Cell Reports* 7(4):1048-1055
- Peterson SE, Li Y, Chait BT, Gottesman ME, Baer R, Gautier J (2011) Cdk1 uncouples CtIP-dependent resection and Rad51 filament formation during M-phase double-strand break repair. *J Cell Biol* 194(5):705-720
- Pfander B and Diffley JF (2011) Dpb11 coordinates Mec1 kinase activation with cell cycle-regulated Rad9 recruitment. *EMBO J* 30(24): 4897-4907
- Pfander B, Moldovan GL, Sacher M, Hoeghe C, Jentsch S (2005) SUMO-modified PCNA recruits Srs2 to prevent recombination during S phase. *Nature* 436(7049):428-433
- Plate I, Hallwyl SCL, Shi I, Krejci L, Müller C, Albertsen L, Sung P, Mortensen UH (2008) Interaction with RPA Is Necessary for Rad52 Repair Center Formation and for Its Mediator Activity. *J Biol Chem* 283(43):29077-29085
- Pleschke JM, Kleczkowska HE, Strohm M, Althaus FR (2000) Poly(ADP-ribose) binds to specific domains in DNA damage checkpoint proteins. *J Biol Chem* 275:40974-40980
- Pogozelski WK and Tullius TD (1998) Oxidative strand scission of nucleic acids: routes initiated by hydrogen abstraction from the sugar moiety. *Chem Rev* 98(3):1089-1108
- Pommier Y, Redon C, Rao VA, Seiler JA, Sordet O, Takemura H, Antony S, Meng L, Liao Z, Kohlhagen G, Zhang H, Kohn KW (2003) Repair of and checkpoint response to topoisomerase I-mediated DNA damage. *Mutat Res* 532(1-2):173-203
- Pottmeyer S and Kemper B (1992) T4 endonuclease VII resolves cruciform DNA with nick and counter-nick and its activity is directed by local nucleotide sequence. *J Mol Biol* 223(3):607-615
- Prakash S, Johnson RE, Prakash L (2005) Eukaryotic translesion synthesis DNA polymerases: specificity of structure and function. *Annu Rev Biochem* 74:317-353
- Princz LN, Gritenaite D, Pfander B (2015) The Slx4-Dpb11 scaffold complex: coordinating the response to replication fork stalling in S-phase and the subsequent mitosis. *Cell Cycle* 14(4):488-494
- Princz LN, Wild P, Bittmann J, Aguado FJ, Blanco MG, Matos J, Pfander B (2017) Dbf4-dependent kinase and the Rtt107 scaffold promote Mus81-Mms4 resolvase activation during mitosis. *EMBO J* 36(5):664-678
- Psakhye I and Jentsch S (2012) Protein group modification and synergy in the SUMO pathway as exemplified in DNA repair. *Cell* 151(4):807-820
- Puddu F, Granata M, Di Nola L, Balestrini A, Piergiovanni G, Lazzaro F, Giannattasio M, Plevani P, Muzi-Falconi M (2008) Phosphorylation of the budding yeast 9-1-1 complex is required for Dpb11 function in the full activation of the UV-induced DNA damage checkpoint. *Mol Cell Biol* 28:4782-4793
- Radman M (1975) SOS repair hypothesis: phenomenology of an inducible DNA repair which is accompanied by mutagenesis. *Basic Life Sci* 5A:355-367
- Randell JCW, Fan A, Chan C, Francis LI, Heller RC, Galani K, Bell SP (2010) Mec1 is one of multiple kinases that prime the Mcm2-7 helicase for phosphorylation by Cdc7. *Mol Cell* 40:353-363
- Rappas M, Oliver AW, Pearl LH (2011) Structure and function of the Rad9-binding region of the DNA-damage checkpoint adaptor TopBP1. *Nucleic Acids Res* 39:313-324
- Rass U (2013) Resolving branched DNA intermediates with structure-specific nucleases during replication in eukaryotes. *Chromosoma* 122(6):499-515

- Rass U, Compton SA, Matos J, Singleton MR, Ip SCY, Blanco MG, Griffith JD, West SC (2010) Mechanism of Holliday junction resolution by the human GEN1 protein. *Genes Dev* 24(14):1559-1569
- Ray JH and German J (1984) Bloom's syndrome and EM9 cells in BrdU-containing medium exhibit similarly elevated frequencies of sister chromatid exchange but dissimilar amounts of cellular proliferation and chromosome disruption. *Chromosoma* 90:383-388
- Reichard P (1988) Interactions between deoxyribonucleotide and DNA synthesis. *Annu Rev Biochem* 57:349-374
- Reußwig KU, Zimmermann F, Galanti L, Pfander B (2016) Robust replication control is generated by temporal gaps between licensing and firing phases and depends on degradation of firing factor Sld2. *Cell Reports* 17:556-569
- Richardson H, Lew DJ, Henze M, Sugimoto K, Reed SI (1992) Cyclin-B homologs in *Saccharomyces cerevisiae* function in S phase and in G2. *Genes Dev* 6:2021-2034
- Roberts TM, Kobor MS, Bastin-Shanower SA, Li M, Horte SA, Gin JW, Emili A, Rine J, Brill SJ, Brown GW (2006) Slx4 regulates DNA damage checkpoint-dependent phosphorylation of the BRCT domain protein Rtt107/Esc4. *Mol Biol Cell* 17:539-548
- Roberts TM, Zaidi IW, Vaisica JA, Peter M, Brown GW (2008) Regulation of Rtt107 recruitment to stalled DNA replication forks by the cullin Rtt101 and the Rtt109 acetyltransferase. *Mol Biol Cell* 19(1):171-180
- Robinson PJ, An W, Routh A, Martino F, Chapman L, Roeder RG, Rhodes D (2008) 30 nm chromatin fibre decompaction requires both H4-K16 acetylation and linker histone eviction. *J Mol Biol* 381(4):816-825
- Rodriguez MC and Songyang Z (2008) BRCT domains: phosphopeptide binding and signaling modules. *Front Biosci* 13:5905-5915
- Rodriguez-Rodriguez JA, Moyano Y, Játiva S, Queralt E (2016) Mitotic exit function of Polo-like kinase Cdc5 is dependent on sequential activation by Cdk1. *Cell Rep* 15(9):2050-2062
- Rogakou EP, Pilch DR, Orr AH, Ivanova VS, Bonner WM (1998) DNA double-stranded breaks induce histone H2AX phosphorylation on serine 139. *J Biol Chem* 273(10):5858-5868
- Rouse J (2004) Esc4p, a new target of Mec1p (ATR), promotes resumption of DNA synthesis after DNA damage. *EMBO J* 23:1188-1197
- Rouse J and Jackson SP (2002) Interfaces between the detection, signaling, and repair of DNA damage. *Science* 297(5581):547-551
- Sacher M, Pfander B, Hoegge C, Jentsch S (2006) Control of Rad52 recombination activity by double-strand break-induced SUMO modification. *Nat Cell Biol* 8:1284-1290
- Sanz MM, German J, Cunniff C (2006, updated 2016) Bloom's Syndrome. *GeneReviews*
- Saponaro M, Callahan D, Zheng X, Krejci L, Haber JE, Klein HL, Liberi G (2010) Cdk1 targets Srs2 to complete synthesis-dependent strand annealing and to promote recombinational repair. *PLoS Genet* 6(2):e1000858
- Sarbajna S, Davies D, West SC (2014) Roles of SLX1-SLX4, MUS81-EME1, and GEN1 in avoiding genome instability and mitotic catastrophe. *Genes Dev* 28(10):1124-1136
- Schober H, Ferreira H, Kalck V, Gehlen LR, Gasser SM (2009) Yeast telomerase and the SUN domain protein Mps3 anchor telomeres and repress subtelomeric recombination. *Genes Dev* 23:928-938
- Schreyer AM and Blundell TL (2013) CREDO: a Structural Interactomics Database for Drug Discovery. *Database (Oxford)*
- Schwartz EK and Heyer WD (2011) Processing of joint molecule intermediates by structure-selective endonucleases during homologous recombination in eukaryotes. *Chromosoma* 120:109-127
- Schwartz EK, Wright WD, Ehmsen KT, Evans JE, Stahlberg H, Heyer WD (2012) Mus81-Mms4 functions as a single heterodimer to cleave nicked intermediates in recombinational DNA repair. *Mol Cell Biol* 32:3065-3080
- Schwob E and Nasmyth K (1993) CLB5 and CLB6, a new pair of B cyclins involved in DNA replication in *Saccharomyces cerevisiae*. *Genes Dev* 7:1160-1175
- Selby CP and Sancar A (1993) Molecular mechanism of transcription-repair coupling. *Science* 260(5104):53-58
- Shah R, Cosstick R, West SC (1997) The RuvC dimer resolves Holliday junctions by a dual incision mechanism that involves base-specific contacts. *EMBO J* 16:1464-1472
- Shim EY, Chung WH, Nicolette ML, Zhang Y, Davis M, Zhu Z, Paull TT, Ira G, Lee SE (2010) *Saccharomyces cerevisiae* Mre11/Rad50/Xrs2 and Ku proteins regulate association of Exo1 and Dna2 with DNA breaks. *EMBO J* 29(19):3370-3380
- Shinohara A, Ogawa H, Ogawa T (1992) Rad51 protein involved in repair and recombination in *S. cerevisiae* is a RecA-like protein. *Cell* 69(3):457-470
- Shiozaki EN, Gu L, Yan N, Shi Y (2004) Structure of the BRCT repeats of BRCA1 bound to a BACH1 phosphopeptide: implications for signaling. *Mol Cell* 14:405-412
- Shogren-Knaak M, Ishii H, Sun JM, Pazin MJ, Davie JR, Peterson CL (2006) Histone H4-K16 acetylation controls chromatin structure and protein interactions. *Science* 311(5762):844-847
- Sjottem E, Rekdal C, Svineng G, Johnsen SS, Klenow H, Uglehus RD, Johansen T (2007) The ePHD protein SPBP interacts with TopBP1 and together they co-operate to stimulate Ets1-mediated transcription. *Nucleic Acids Res* 35:6648-6662
- Smith GR, Boddy MN, Russell P (2003) Fission yeast Mus81-Eme1 Holliday junction resolvase is required for meiotic crossing-over but not for gene conversion. *Genetics* 165(4):2289-2293
- Sogo JM, Lopes M, Foiani M (2002) Fork reversal and ssDNA accumulation at stalled replication forks owing to checkpoint defects. *Science* 297(5581):599-602
- Song W, Dominska M, Greenwell PW, Petes TD (2014) Genome-wide high-resolution mapping of chromosome fragile sites in *Saccharomyces cerevisiae*. *Proc Natl Acad Sci U S A* 111(21):E2210-E2218
- Soulas-Sprauel P, Rivera-Munoz P, Malivert L, Le Guyader G, Abramowski V, Revy P, de Villartay JP (2007) V(D)J and immunoglobulin class switch recombinations: a paradigm to study the regulation of DNA end-joining. *Oncogene* 26(56):7780-7791
- Spellman PT, Sherlock G, Zhang MQ, Iyer VR, Anders K, Eisen MB, Brown PO, Botstein D, Futcher B (1998) Comprehensive identification of cell cycle-regulated genes of the yeast *Saccharomyces cerevisiae* by microarray hybridization. *Mol Biol Cell* 9:3273-3297
- Sugawara N, Wang X, Haber JE (2003) In vivo roles of Rad52, Rad54, and Rad55 proteins in Rad51-mediated recombination. *Mol Cell* 12(1):209-219
- Sugiyama T, Zaitseva EM, Kowalczykowski SC (1997) A single-stranded DNA-binding protein is needed for efficient presynaptic complex formation by the *Saccharomyces cerevisiae* Rad51 protein. *J Biol Chem* 272(12):7940-7945
- Sun Z, Hsiao J, Fay DS, Stern DF (1998) Rad53 FHA domain associated with phosphorylated Rad9 in the DNA damage checkpoint. *Science* 281:272-274

- Sung P (1994) Catalysis of ATP-dependent homologous DNA pairing and strand exchange by yeast RAD51 protein. *Science* 265:1241-1243
- Sung P (1997a) Function of yeast Rad52 protein as a mediator between replication protein A and the Rad51 recombinase. *J Biol Chem* 272:28194-28197
- Sung P (1997b) Yeast Rad55 and Rad57 proteins form a heterodimer that functions with replication protein A to promote DNA strand exchange by Rad51 recombinase. *Genes Dev* 11:1111-1121
- Sung P, Krejci L, van Komen S, Sehorn MG (2003) Rad51 recombinase and recombination mediators. *J Biol Chem* 278(44):42729-42732
- Svendsen JM, Smogorzewska A, Sowa ME, O'Connell BC, Gygi SP, Elledge SJ, Harper JW (2009) Mammalian BTBD12/SLX4 assembles a Holliday junction resolvase and is required for DNA repair. *Cell* 138:63-77
- Sweeney FD, Yang F, Chi A, Shabanowitz J, Hunt DF, Durocher D (2005) *Saccharomyces cerevisiae* Rad9 acts as a Mec1 adaptor to allow Rad53 activation. *Curr Biol* 15(15):1364-1375
- Syeda AH, Hawkins M, McGlynn P (2014) Recombination and replication. *Cold Spring Harb Perspect Biol* 6(11): a016550
- Szkal B and Branzei D (2013) Premature Cdk1/Cdc5/Mus81 pathway activation induces aberrant replication and deleterious crossover. *EMBO J* 32:1155-1167
- Szostak JW, Orr WT, Rothstein RJ, Stahl FW (1983) The double-strand-break repair model for recombination. *Cell* 33:25-35
- Tanaka S, Umemori T, Hirai K, Muramatsu S, Kamimura Y, Araki H (2007) CDK-dependent phosphorylation of Sld2 and Sld3 initiates DNA replication in budding yeast. *Nature* 445:328-332
- Tay YD, Sidebotham JM, Wu L (2010) Mph1 requires mismatch repair-independent and -dependent functions of MutSalpha to regulate crossover formation during homologous recombination repair. *Nucleic Acids Res* 38:1889-1901
- Taylor ER and McGowan CH (2008) Cleavage mechanism of human Mus81-Eme1 acting on Holliday-junction structures. *Proc Natl Acad Sci U S A* 105:3757-3762
- Tercero JA and Diffley JF (2001) Regulation of DNA replication fork progression through damaged DNA by the Mec1/Rad53 checkpoint. *Nature* 412(6846):553-557
- Thu HPT, Nguyen TA, Munashingha PR, Kwon B, Dao Van Q, Seo YS (2015) A physiological significance of the functional interaction between Mus81 and Rad27 in homologous recombination repair. *Nucleic Acids Res* 43(3):1684-1699
- Toh GW, O'Shaughnessy AM, Jimeno S, Dobbie IM, Grenon M, Maffini S, O'Rorke A, Lowndes NF (2006) Histone H2A phosphorylation and H3 methylation are required for a novel Rad9 DSB repair function following checkpoint activation. *DNA Repair (Amst)* 5:693-703
- Toh GW, Sugawara N, Dong J, Toth R, Lee SE, Haber JE, Rouse J (2010) Mec1/Tel1-dependent phosphorylation of Slx4 stimulates Rad1-Rad10-dependent cleavage of non-homologous DNA tails. *DNA Repair (Amst)* 9(6):718-726
- Torres-Rosell J, Sunjevaric I, De Piccoli G, Sacher M, Eckert-Boulet N, Reid R, Jentsch S, Rothstein R, Aragón L, Lisby M (2007) The Smc5-Smc6 complex and SUMO modification of Rad52 regulates recombinational repair at the ribosomal gene locus. *Nat Cell Biol* 9(8):923-931
- Tsutsui Y, Kurokawa Y, Ito K, Siddique MS, Kawano Y, Yamao F, Iwasaki H (2014) Multiple regulation of Rad51-mediated homologous recombination by fission yeast Fbh1. *PLoS Genet* 10(8):e1004542
- Tyers M, Tokiwa G, Futcher B (1993) Comparison of the *Saccharomyces cerevisiae* G1 cyclins: Cln3 may be an upstream activator of Cln1, Cln2 and other cyclins. *EMBO J* 12:1955-1968
- Ubersax JA, Woodbury EL, Quang PN, Paraz M, Blethrow JD, Shah K, Shokat KM, Morgan DO (2003) Targets of the cyclin-dependent kinase Cdk1. *Nature* 425(6960):859-864
- Ulrich HD and Jentsch S (2000) Two RING finger proteins mediate cooperation between ubiquitin-conjugating enzymes in DNA repair. *EMBO J* 19(13):3388-3397
- Ulrich HD and Walden H (2010) Ubiquitin signalling in DNA replication and repair. *Nat Rev Mol Cell Biol* 11(7):479-489
- Vaisica JA, Baryshnikova A, Costanzo M, Boone C, Brown GW (2011) Mms1 and Mms22 stabilize the replisome during replication stress. *Mol Biol Cell* 22(13):2396-2408
- Valencia M, Bentele M, Vaze MB, Herrmann G, Kraus E, Lee SE, Schar P, Haber JE (2001) NEJ1 controls non-homologous end joining in *Saccharomyces cerevisiae*. *Nature* 414:666-669
- Vallen EA and Cross FR (1999) Interaction between the MEC1-dependent DNA synthesis checkpoint and G1 cyclin function in *Saccharomyces cerevisiae*. *Genetics* 151:459-471
- van Attikum H, Fritsch O, Hohn B, Gasser SM (2004) Recruitment of the INO80 complex by H2A phosphorylation links ATP-dependent chromatin remodeling with DNA double-strand break repair. *Cell* 119: 777-788
- van Gent DC, Hoijmakers JHJ, Kanaar R (2001) Chromosomal stability and the DNA double-stranded break connection. *Nat Rev Genet* 2:196-206
- Vialard JE, Gilbert CS, Green CM, Lowndes NF (1998) The budding yeast Rad9 checkpoint protein is subjected to Mec1/Tel1-dependent hyperphosphorylation and interacts with Rad53 after DNA damage. *EMBO J* 17:5679-5688
- Wahba L, Amon JD, Koshland D, Vuica-Ross M (2011) RNase H and multiple RNA biogenesis factors cooperate to prevent RNA-DNA hybrids from generating genome instability. *Mol Cell* 44(6): 978-988
- Wallis JW, Chrebet G, Brodsky G, Rolfe M, Rothstein R (1989) A hyper-recombination mutation in *S. cerevisiae* identifies a novel eukaryotic topoisomerase. *Cell* 58:409-419
- Wan L, Niu H, Futcher B, Zhang C, Shokat KM, Boulton SJ, Hollingsworth NM (2008) Cdc28-Clb5 (CDK-S) and Cdc7-Dbf4 (DDK) collaborate to initiate meiotic recombination in yeast. *Genes Dev* 22(3):386-397
- Wang H and Elledge SJ (2002) Genetic and physical interactions between DPB11 and DDC1 in the yeast DNA damage response pathway. *Genetics* 160(4):1295-1304
- Wang J, Chen J, Gong Z (2013) TopBP1 controls BLM protein level to maintain genome stability. *Mol Cell* 52:667-678
- Wang JC (2002) Cellular roles of DNA topoisomerases: a molecular perspective. *Nat Rev Mol Cell Biol* 3(6):430-440
- Wasko BM, Holland CL, Resnick MA, Lewis LK (2009) Inhibition of DNA double-strand break repair by the Ku heterodimer in *mrx* mutants of *Saccharomyces cerevisiae*. *DNA Repair* 8(2):162-169
- Watt PM, Hickson ID, Borts RH, Louis EJ (1996) Sgs1, a homolog of the Bloom's and Werner's syndrome genes, is required for maintenance of genome stability in *Saccharomyces cerevisiae*. *Genetics* 144:935-945
- Weinreich M and Stillman B (1999) Cdc7p-Dbf4p kinase binds to chromatin during S phase and is regulated by both the APC and the RAD53 checkpoint pathway. *EMBO J* 18(19):5334-5346

- Whitby MC, Osman F, Dixon J (2003) Cleavage of model replication forks by fission yeast Mus81-Eme1 and budding yeast Mus81-Mms4. *J Biol Chem* 278:6928-6935
- Williams JS, Williams RS, Dovey CL, Guenther G, Tainer JA, Russell P (2010) gammaH2A binds Brc1 to maintain genome integrity during S-phase. *EMBO J* 29:1136-1148
- Wiltzius JJ, Hohl M, Fleming JC, Petrini JH (2005) The Rad50 hook domain is a critical determinant of Mre11 complex functions. *Nat Struct Mol Biol* 12(5):403-407
- Wright RHG, Dornan ES, Donaldson MM, Morgan IM (2006) TopBP1 contains a transcriptional activation domain suppressed by two adjacent BRCT domains. *Biochem J* 400(Pt 3):573-582
- Wu D, Topper LM, Wilson TE (2008) Recruitment and dissociation of nonhomologous end joining proteins at a DNA double-strand break in *Saccharomyces cerevisiae*. *Genetics* 178(3):1237-1249
- Wu L and Hickson ID (2003) The Bloom's syndrome helicase suppresses crossing over during homologous recombination. *Nature* 426:870-874
- Wu Q, Jubb H, Blundell TL (2015) Phosphopeptide interactions with BRCA1 BRCT domains: More than just a motif. *Prog Biophys Mol Bio* 117:143-148
- Wyatt HDM, Laister RC, Martin SR, Arrowsmith CH, West SC (2017) The SMX DNA repair tri-nuclease. *Mol Cell* 65(5):848-860
- Wyatt HDM, Sarbajna S, Matos J, West SC (2013) Coordinated actions of SLX1-SLX4 and MUS81-EME1 for Holliday junction resolution in human cells. *Mol Cell* 52:234-247
- Xiao W, Chow BL, Fontanie T, Ma L, Bacchetti S, Hryciw T, Broomfield S (1999) Genetic interactions between error-prone and error-free postreplication repair pathways in *Saccharomyces cerevisiae*. *Mutat Res* 435(1):1-11
- Xiong W and Ferrell JE (2003) A positive-feedback-based bistable 'memory module' that governs a cell fate decision. *Nature* 426:460-465
- Xu X, Blackwell S, Lin A, Li F, Qin Z, Xiao W (2015) Error-free DNA-damage tolerance in *Saccharomyces cerevisiae*. *Mutat Res Rev* 764:43-50
- Yamada M, Masai H, Bartek J (2014) Regulation and roles of Cdc7 kinase under replication stress. *Cell Cycle* 13(12):1859-1866
- Yamane K, Katayama E, Tsuruo T (2000) The BRCT regions of tumor suppressor BRCA1 and of XRCC1 show DNA end binding activity with a multimerizing feature. *Biochem Biophys Res Commun* 279:678-684
- Yan H, Tammaro M, Liao S (2016) Collision of trapped topoisomerase 2 with transcription and replication: generation and repair of DNA double-strand breaks with 5' adducts. *Genes* 7(7):E32
- Yu X, Chini CC, He M, Mer G, Chen J (2003) The BRCT domain is a phospho-protein binding domain. *Science* 302(5645):639-642
- Yuan Z, Kumar EA, Kizhake S, Natarajan A (2011) Structure-activity relationship studies to probe the phosphoprotein binding site on the carboxy terminal domains of the breast cancer susceptibility gene 1. *J Med Chem* 54:4264-4268.
- Zakharyevich K, Tang S, Ma Y, Hunter N (2012) Delineation of joint molecule resolution pathways in meiosis identifies a crossover-specific resolvase. *Cell* 149:334-347
- Zegerman P and Diffley JF (2007) Phosphorylation of Sld2 and Sld3 by cyclin-dependent kinases promotes DNA replication in budding yeast. *Nature* 445:281-285
- Zegerman P and Diffley JF (2010) Checkpoint-dependent inhibition of DNA replication initiation by Sld3 and Dbf4 phosphorylation. *Nature* 467(7314):474-478
- Zhang C, Roberts TM, Yang J, Desai R, Brown GW (2006) Suppression of genomic instability by SLX5 and SLX8 in *Saccharomyces cerevisiae*. *DNA Repair (Amst)* 5(3):336-346
- Zhang H and Lawrence CW (2005) The error-free component of the RAD6/RAD18 DNA damage tolerance pathway of budding yeast employs sister-strand recombination. *Proc Natl Acad Sci U S A* 102(44):15954-15959
- Zhu Z, Chung WH, Shim EY, Lee SE, Ira G (2008) Sgs1 helicase and two nucleases Dna2 and Exo1 resect DNA double-strand break ends. *Cell* 134: 981-994
- Zierhut C and Diffley JF (2008) Break dosage, cell cycle stage and DNA replication influence DNA double strand break response. *EMBO J* 27(13):1875-1885
- Zou L and Elledge SJ (2003) Sensing DNA damage through ATRIP recognition of RPA-ssDNA complexes. *Science* 300(5625):1542-1548

## VII. Acknowledgements

First of all, I would like to thank Boris Pfander for giving me the opportunity to work in his research group on a most interesting topic during my master thesis and the subsequent PhD. I thank him for an outstanding supervision and support, for always having an open door and a sympathetic ear. His engagement and approach to solutions for scientific problems were very motivating and enriched my biochemical understanding. His constant interest contributed in a great measure to this work.

Besides, I would like to express my gratitude to Stefan Jentsch for his scientific support and inspiring career path. His unexpected passing leaves a huge void. Personally, I very much enjoyed being part of his research department thanks to his charismatic personality paired with that special sense of humour that I will always keep in memory.

Many thanks go to all members of my examination board for their time, and interest in my PhD work, especially to Heinrich Leonhardt, who came forward to assume Stefan's role as my thesis adviser.

Moreover, I would like to thank the members of my Thesis Advisory Committee, Karl-Peter Hopfner and Jürg Müller, for their helpful advice and suggestions on my project during the course of my PhD.

I would like to give huge thanks to the IMPRS coordination team, Hans-Jörg Schäffer, Ingrid Wolf, and Maxi Reif, who not only were helpful at all time in any matter, but who are also putting together an excellent programme for PhD students by combining scientific training with network and friendships.

During the first two years of my PhD, I worked together with my former colleague Dalia Gritenaite in close cooperation on the project, and would like to thank her for this teamwork.

Also our collaboration partners in the labs of Dana Brnzei, Joao Matos, Bianca Habermann, Michael Lisby, Miguel Blanco, and Christian Biertümpfel, I would like to thank for their significant contribution to the publications and the progression of our research.

Furthermore, I would like to acknowledge Nagarjuna Nagaraj and his predecessor Cyril Boulegue with their team in the core facility for their guidance through the myriads of mass spectrometry data.

Within the Pfander lab I want to thank, first of all, Uschi Kagerer for her excellent technical assistance and teamwork. Thank you a thousand times! Giulia DiCicco I want to thank for being the best bench and desk partner one could wish. Many thanks also go to Susi Bantele, Kalle Reußwig, Julia Bittmann, and Lorenzo Galanti, and to all for a cheerful atmosphere inside and outside of the lab as well as for their ideas and suggestions. I enjoyed the time working within the group very much.

Moreover, I would like to thank all my colleagues in the groups of Stefan Jentsch, Boris Pfander and Zuzana Storchova for the friendly atmosphere, company and help. Particularly, I want to thank Sven Schkölziger, Alex Strasser, Jochen Rech, and Ulla Cramer for their indispensable technical support, Massimo Bossi and Rosella Piroddi for making yeast culturing even easier, as well as Klara Schwander for her administrative help.

Last but not least, I would like to thank my family and friends, especially my parents and siblings for their infinite support. The knowledge that I can rely on them at all times gives me a lot of strength. Finally, I am thankful for Björn Helmholz being by my side and encouraging me with his love, patience and laughter.



# Appendix

# A cell cycle-regulated Slx4–Dpb11 complex promotes the resolution of DNA repair intermediates linked to stalled replication

Dalia Gritenaite,<sup>1,7</sup> Lissa N. Prinz,<sup>1,7</sup> Barnabas Szakal,<sup>2</sup> Susanne C.S. Bantele,<sup>1</sup> Lina Wendeler,<sup>1</sup> Sandra Schilbach,<sup>1,6</sup> Bianca H. Habermann,<sup>3</sup> Joao Matos,<sup>4</sup> Michael Lisby,<sup>5</sup> Dana Branzei,<sup>2</sup> and Boris Pfander<sup>1,8</sup>

<sup>1</sup>DNA Replication and Genome Integrity, Max-Planck Institute of Biochemistry, 82152 Martinsried, Germany; <sup>2</sup>Fondazione IFOM, Istituto FIRC di Oncologia Molecolare, 20139 Milan, Italy; <sup>3</sup>Computational Biology, Max-Planck Institute of Biochemistry, 82152 Martinsried, Germany; <sup>4</sup>Institute of Biochemistry, Eidgenössische Technische Hochschule Zürich, 8093 Zürich, Switzerland; <sup>5</sup>Department of Biology, University of Copenhagen, 2200 Copenhagen, Denmark

**A key function of the cellular DNA damage response is to facilitate the bypass of replication fork-stalling DNA lesions. Template switch reactions allow such a bypass and involve the formation of DNA joint molecules (JMs) between sister chromatids. These JMs need to be resolved before cell division; however, the regulation of this process is only poorly understood. Here, we identify a regulatory mechanism in yeast that critically controls JM resolution by the Mus81–Mms4 endonuclease. Central to this regulation is a conserved complex comprising the scaffold proteins Dpb11 and Slx4 that is under stringent control. Cell cycle-dependent phosphorylation of Slx4 by Cdk1 promotes the Dpb11–Slx4 interaction, while in mitosis, phosphorylation of Mms4 by Polo-like kinase Cdc5 promotes the additional association of Mus81–Mms4 with the complex, thereby promoting JM resolution. Finally, the DNA damage checkpoint counteracts Mus81–Mms4 binding to the Dpb11–Slx4 complex. Thus, Dpb11–Slx4 integrates several cellular inputs and participates in the temporal program for activation of the JM-resolving nuclease Mus81.**

[*Keywords:* DNA damage response; cell cycle; post-replicative repair; homologous recombination; joint molecule resolution]

Supplemental material is available for this article.

Received February 24, 2014; revised version accepted June 4, 2014.

Intrinsically and extrinsically induced DNA lesions can compromise the integrity of the genetic information and threaten cell viability. DNA lesions are particularly dangerous during S phase, when faithful DNA replication relies on two intact DNA strands. DNA lesions hamper the progression of replication forks and thereby the complete duplication of chromosomes. Moreover, replication forks that are stalled at DNA lesion sites can collapse and cause chromosome breaks and genome instability (Branzei and Foiani 2010).

Eukaryotes possess two fundamentally different mechanisms to bypass DNA lesions that affect one of the parental DNA strands: translesion synthesis (TLS) and template

switching. TLS employs specialized polymerases (translesion polymerases) that in many cases are able to replicate the damaged strand but with a reduced fidelity (Prakash et al. 2005). On the other hand, during template switching, the genetic information is copied from the newly synthesized, undamaged sister chromatid. This mechanism is therefore error-free in principle, yet its precise mechanism remains poorly understood. Template switching is a complex process that can be initiated by different recombination-based mechanisms (homologous recombination [HR] and error-free post-replicative repair [PRR]) (Branzei et al. 2008). The choice between the different bypass mechanisms is regulated by ubiquitin and SUMO modifications

<sup>6</sup>Present address: Max-Planck Institute of Biophysical Chemistry, Molecular Biology, 37077 Göttingen, Germany.

<sup>7</sup>These authors contributed equally to this work.

<sup>8</sup>Corresponding author

E-mail [bpfander@biochem.mpg.de](mailto:bpfander@biochem.mpg.de)

Article is online at <http://www.genesdev.org/cgi/doi/10.1101/gad.240515.114>.

© 2014 Gritenaite et al. This article is distributed exclusively by Cold Spring Harbor Laboratory Press for the first six months after the full-issue publication date (see <http://genesdev.cshlp.org/site/misc/terms.xhtml>). After six months, it is available under a Creative Commons License (Attribution-NonCommercial 4.0 International), as described at <http://creativecommons.org/licenses/by-nc/4.0/>.

of the replication protein PCNA at sites of stalled replication forks (Pfander et al. 2005).

Template switch mechanisms involve the formation of DNA joint molecules (JMs; also referred to as sister chromatid junctions [SCJs] or X molecules) as repair intermediates (Branzei et al. 2008). In order to allow completion of DNA replication and faithful chromosome segregation, these X-shaped DNA structures need to be disentangled before sister chromatids are separated during mitosis. To date, three enzymatic activities—the topoisomerase-containing Sgs1–Top3–Rmi1 complex (STR) as well as the Mus81–Mms4 and Yen1 structure-specific endonucleases—were shown to process JMs in budding yeast (Liberi et al. 2005; Blanco et al. 2010; Mankouri et al. 2011; Szakal and Branzei 2013). These three activities can be distinguished by their mechanism (termed dissolution for STR and resolution for Mus81–Mms4 and Yen1) (Gaillard et al. 2003; Ip et al. 2008; Cejka et al. 2010) but show a partial functional overlap. Moreover, they are differentially regulated during the cell cycle: Whereas the STR activity appears to be cell cycle-independent, the activity of Mus81–Mms4 is stimulated by CDK-mediated and Cdc5 (budding yeast Polo-like kinase)-mediated phosphorylation and peaks in mitosis (Matos et al. 2011, 2013; Gallo-Fernández et al. 2012; Szakal and Branzei 2013). Accordingly, the Mus81 regulation is assumed to create a hierarchy, with STR acting as a primary resolution pathway and Mus81–Mms4 acting as a salvage pathway. How Mus81–Mms4 phosphorylation by cell cycle kinases facilitates this temporal regulation of JM resolution pathways remains hardly understood.

The bypass of DNA lesions during replication is additionally regulated by the DNA damage checkpoint, the main cellular signaling pathway in response to DNA damage (Harrison and Haber 2006). As the primary purpose of the checkpoint is the stabilization of stalled replication forks (Branzei and Foiani 2010), its activation is a fundamental requirement for all fork repair and reactivation reactions. Notably, the checkpoint has been suggested to be involved in the choice of the JM resolution pathway, since precocious activation of the Mus81–Mms4 endonuclease is observed in checkpoint-deficient mutants (Szakal and Branzei 2013). However, it remains to be clarified how this second layer of regulation of JM resolution is achieved on a molecular level and how it is linked to cell cycle regulation.

Here, we identify an evolutionarily conserved protein complex comprising two scaffold proteins, Slx4 and Dpb11/TopBP1, as an important regulator of JM resolution by Mus81–Mms4. We show that the formation of the Slx4–Dpb11 complex is regulated by the cell cycle stage. An *slx4* mutant, compromised specifically in Dpb11 binding, exhibits hypersensitivity to the replication fork-stalling drug MMS, a delay in the resolution of X-shaped DNA JMs, and a reduced propensity to form crossovers (COs). The function of the Slx4–Dpb11 scaffold in JM resolution correlates with the finding that Dpb11 binds to the Mus81–Mms4 endonuclease. This association is restricted to mitosis, since it is dependent on the mitotic kinase Cdc5. Moreover, the checkpoint acts antagonistically to the regulation of JM

resolution by Slx4 and Dpb11, as we found that partial inactivation of the DNA damage checkpoint can compensate for defects in formation of the Slx4–Dpb11 scaffold complex.

## Results

### *An evolutionarily conserved and phosphorylation-dependent interaction between Slx4 and Dpb11/TopBP1*

Dpb11 and its human homolog, TopBP1, are critical regulators of the cellular DNA damage response and interact with several DNA replication, repair, and checkpoint proteins (Garcia et al. 2005; Germann et al. 2011). In these protein complexes, Dpb11/TopBP1 specifically binds to phosphorylated proteins via its tandem BRCT domains (Yu 2003; Garcia et al. 2005). A key role of Dpb11/TopBP1 is to function as a scaffold, bringing together specific sets of proteins via several interaction surfaces. In budding yeast, two Dpb11 complexes have been described in detail, which regulate replication initiation (with Sld3 and Sld2) (Tanaka et al. 2007; Zegerman and Diffley 2007) and the DNA damage checkpoint (with Rad9, the 9-1-1 complex, and Mec1–Ddc2) (Mordes et al. 2008; Navadgi-Patil and Burgers 2008; Puddu et al. 2008; Pfander and Diffley 2011), respectively (Fig. 1A). Recently, a third Dpb11 complex with Slx4 and Rtt107 was identified (Ohouo et al. 2010, 2012). In this latter complex, Slx4 appears to inhibit the formation of the Dpb11 DNA damage checkpoint complex (Ohouo et al. 2012).

In the course of our studies of Dpb11 function, we identified an interaction between a Dpb11 fragment that includes the tandem BRCT repeats 3 and 4 (BRCT3+4) and Slx4 using a two-hybrid screen. To confirm this finding, we tested the binding of different Dpb11 constructs to Slx4 and known Dpb11 binders. As observed before (Puddu et al. 2008; Pfander and Diffley 2011), we found that Rad9 binds to BRCT1+2 of Dpb11, whereas Ddc1 binds to BRCT3+4 (Fig. 1B). For Slx4, we found an interaction with full-length Dpb11 and the BRCT3+4 fragment but not with the BRCT1+2 domain (Fig. 1B). When we tested binding of Slx4 from cell extracts to recombinant, purified fragments of Dpb11, Slx4 also bound to BRCT3+4, albeit weaker than to the full-length protein (Supplemental Fig. S1A). Moreover, ablation of Dpb11 Thr451, which is predicted to be part of the BRCT3+4 phospho-protein-binding surface (Rappas et al. 2011), partially inhibited the Slx4–Dpb11 interaction (Supplemental Fig. S1B). A recent report suggested that the Dpb11 BRCT1+2 domain is involved in Slx4 binding (Ohouo et al. 2012). However, although our data do not rule out a contribution of BRCT1+2 in overall binding, our two independent lines of evidence clearly demonstrate that BRCT3+4 of Dpb11 significantly contributes to Slx4 binding.

Next, we mapped the Dpb11-binding site on Slx4 starting from a fragment (amino acids 461–738) that was common to all Slx4 clones identified in our initial Dpb11 two-hybrid screen. Truncated variants that begin at amino acid 490 failed to interact with Dpb11 (Supplemental Fig. S1C),

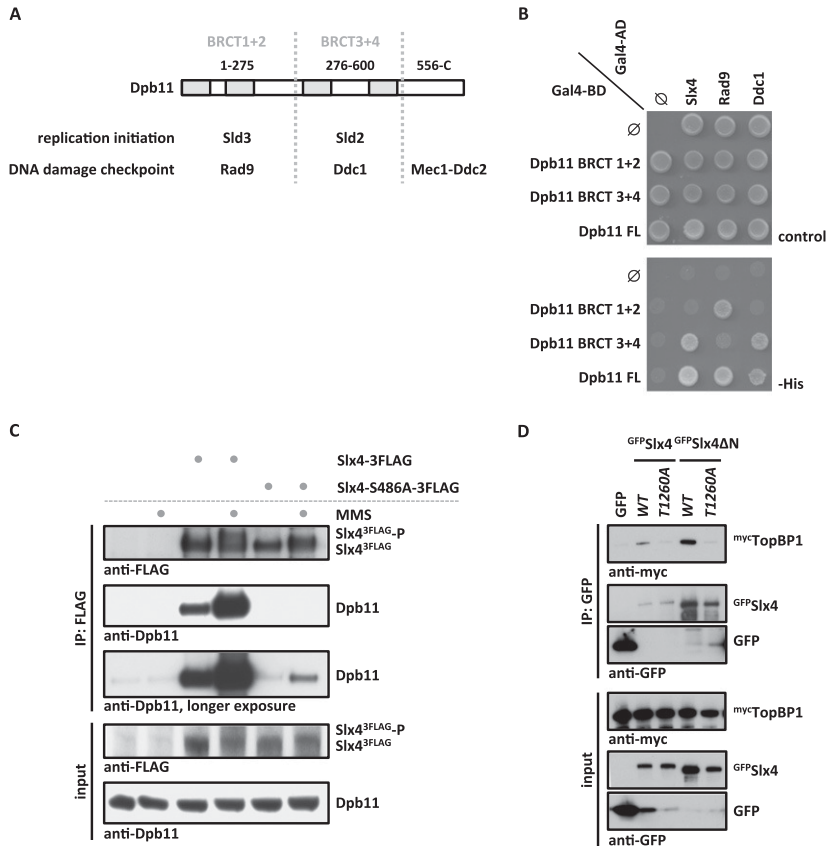


**Figure 1.** An evolutionarily conserved, phosphorylation-dependent interaction between Slx4 and Dpb11/TopBP1. (A) Schematic diagram of Dpb11 domain structure depicted with its interaction partners in replication initiation and DNA damage checkpoint. (B) Slx4 binds to the BRCT3+4 domain of Dpb11. Two-hybrid analysis of GAL4-BD fused to full-length Dpb11 or to BRCT1+2 and BRCT3+4 fragments and of GAL4-AD fusions with Slx4, Rad9, and Ddc1. (C) The Slx4–Dpb11 interaction is reduced by mutation of Slx4 Ser486 and is regulated by DNA damage. Coimmunoprecipitation of endogenous Dpb11 with Slx4<sup>3Flag</sup> or phosphorylation-deficient Slx4-S486A<sup>3Flag</sup> from undamaged cells or cells treated for 30 min with 0.033% MMS. (D) Human TopBP1 and Slx4 interact dependent on Thr1260 of Slx4. Coimmunoprecipitation of human myc<sup>c</sup>TopBP1 with GFP<sup>c</sup>Slx4 or N-terminally truncated GFP<sup>c</sup>Slx4ΔN after transient overexpression in HEK293T cells. Slx4 or Slx4ΔN was expressed either as wild type (WT) or a T1260A phosphorylation-deficient variant.

indicating that the region between amino acid 461 and amino acid 490 is important for Dpb11 interaction. As several examples indicate that Dpb11 binds phosphorylated S/TP motifs, we tested all S/TP motifs within the C-terminal part of Slx4 for their ability to mediate Dpb11 binding. Indeed, we found that alteration of Ser486 in Slx4 into a nonphosphorylatable alanine residue (*slx4-S486A* mutant) reduced Dpb11 binding in a two-hybrid system (Supplemental Fig. S1D). Moreover, whereas immunoprecipitation of wild-type Slx4 efficiently copurified endogenous Dpb11 from cell extracts, in particular following MMS treatment, the Slx4–Dpb11 interaction was strongly decreased in extracts from cells expressing the *slx4-S486A* mutant, even after induction of DNA damage (Fig. 1C; see also Ohouo et al. 2012). Furthermore, the phospho-S486-containing peptide was specifically enriched (17-fold), when Dpb11 immunoprecipitations were analyzed by quantitative mass spectrometry (MS) (Supplemental Fig. S4A). We therefore conclude that the Slx4–Dpb11 interaction involves the BRCT3+4 region of Dpb11 and a region of Slx4 harboring the phosphorylated residue S486.

We further tested whether also the human homologs TopBP1 and Slx4 are binding partners. Indeed, we detected a specific interaction of TopBP1 and Slx4 or an N-terminally truncated version of Slx4 after transient transfection in human embryonic kidney (HEK) 293T cells (Fig. 1D). In contrast to the yeast proteins, we did not observe a stimulation of TopBP1 binding to Slx4 by DNA damage (Supplemental Fig. S1E). Human Slx4 is substantially larger than

yeast Slx4, with an overall sequence conservation of only 17.9%. Nonetheless, we identified a conserved short linear motif present in Slx4 proteins from different eukaryotes that comprises Ser486 in budding yeast and Thr1260 in humans (Supplemental Fig. S2). Mutation of Thr1260 to a nonphosphorylatable alanine (T1260A) in human Slx4 reduced the interaction with TopBP1 (Fig. 1D), suggesting that this residue may function analogously to Ser486 in budding yeast. These data suggest the presence of a novel, evolutionarily conserved motif in Slx4 that functions in Dpb11/TopBP1 binding.

#### *Cdk1-dependent phosphorylation of Slx4 regulates binding to Dpb11*

In order to unravel the regulation of the Slx4–Dpb11-binding surface, we quantified the relative amount of Ser486 phosphorylation under different cellular conditions using SILAC-based quantitative MS. We observed a specific increase of Ser486 phosphorylation in G2/M-arrested cells compared with G1-arrested cells, indicating that the analyzed Slx4 phosphorylation is cell cycle-regulated (Fig. 2A). In agreement with Ser486 matching the consensus target sequence for phosphorylation by cyclin-dependent kinase Cdk1 (S/TPxK) (Holt et al. 2009), we observed a marked reduction of Ser486 phosphorylation in G2/M-arrested cells when Cdk1 activity was abrogated using the *cdc28-as1* allele (Bishop et al. 2000) in combination with 1NM-PP1 inhibitor treatment (Fig. 2B). Notably, we also detected

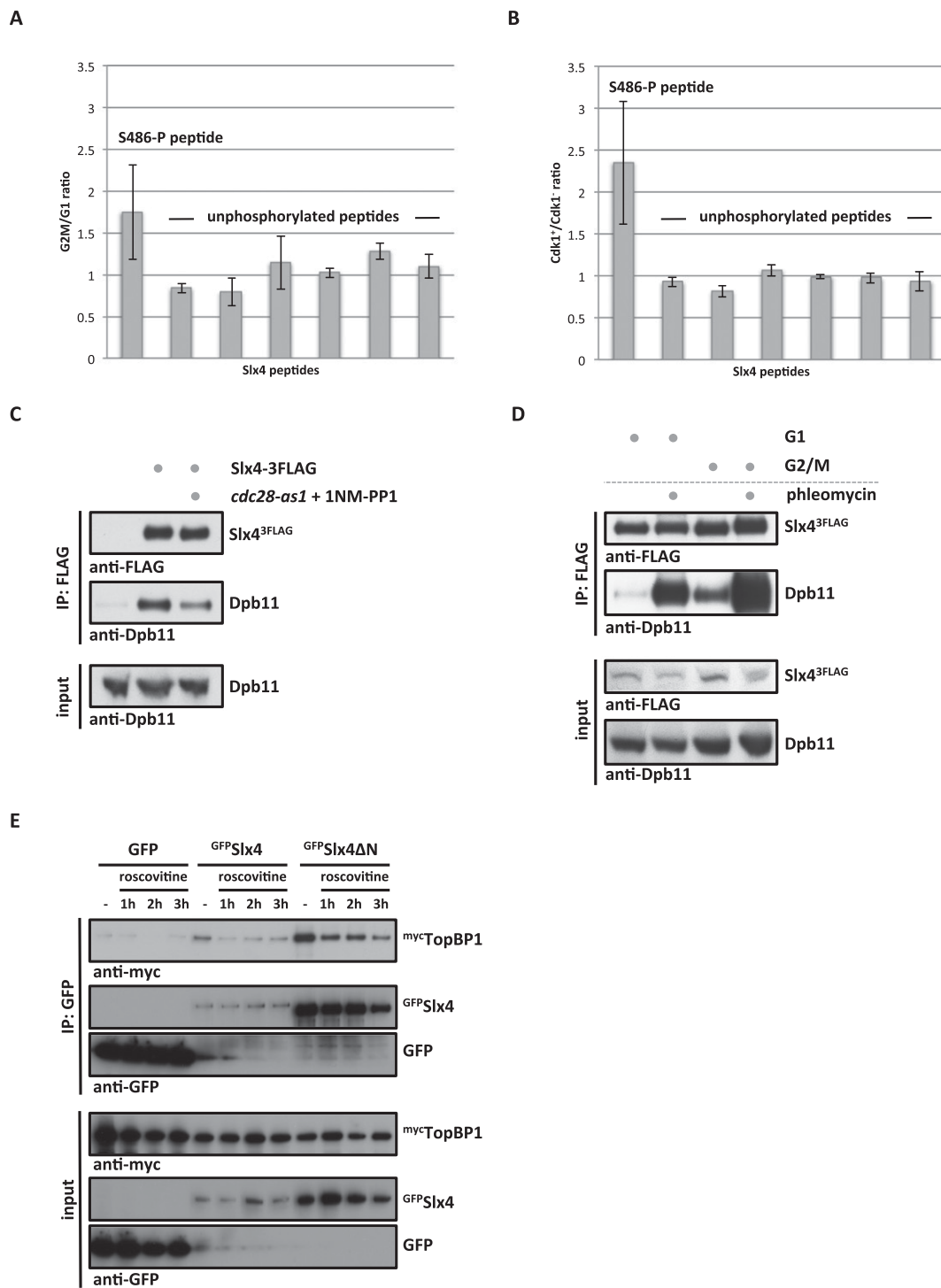


**Figure 2.** The Slx4–Dpb11/TopBP1-binding interface is cell cycle-regulated by Cdk1 phosphorylation of Slx4. (A) Ser486 phosphorylation is cell cycle-regulated. Relative abundance of the Slx4 480–489 phospho-peptide and six unmodified Slx4 peptides was measured by SILAC-based quantitative MS using  $^{15}\text{N}_2^{13}\text{C}_6$  lysine (Lys8) and compared between Slx4 isolated from G1- and G2/M-arrested cells. H/L ratios for individual peptides were normalized to total Slx4 ratios. Error bars represent standard deviations from two independent experiments, including label switch. (B) S486 phosphorylation depends on Cdk1. Analysis as in A but comparing Slx4 from G2/M-arrested cells with normal Cdk1 activity with cells in which Cdk1 has been inactivated using the *cdc28-as1* allele and 500 nM 1NM-PP1. (C) The Slx4–Dpb11 interaction is regulated by CDK. Coimmunoprecipitation of Dpb11 and Slx4<sup>3FLAG</sup> from G2/M-arrested cells or G2/M-arrested cells in which Cdk1 has been inactivated as in B. (D) The Slx4–Dpb11 interaction is regulated by cell cycle phase and DNA damage. Experiment as in C but with G1- and G2/M-arrested cells, which were either damaged by 50  $\mu\text{g}/\text{mL}$  phleomycin or left untreated. (E) Binding of human Slx4 and TopBP1 is regulated by CDK phosphorylation. Coimmunoprecipitation of mycTopBP1 with GFP<sup>Slx4</sup> and GFP<sup>Slx4ΔN</sup> after transient overexpression in HEK293T cells. Cells were left untreated or treated with 10  $\mu\text{g}/\text{mL}$  roscovitine for the indicated times to inhibit CDK activity.

reduced Slx4 binding to Dpb11 when Cdk1 was inhibited (Fig. 2C).

In addition to cell cycle-dependent regulation, we also observed a stimulation of Slx4–Dpb11 binding by DNA damage (Figs. 1C, 2D, Supplemental Fig. S1F). When Slx4 binding to recombinant GST–Dpb11 was tested, the DNA damage-dependent stimulation was less pronounced (Supplemental Fig. S1A), substantiating the notion that the Slx4–Dpb11 interaction may be additionally regulated by a damage-induced post-translational modification of Dpb11. On the other hand, Slx4 harbors several sites that can be targeted by kinases of the DNA damage checkpoint pathway. Mutation of seven sites in Slx4 partially inhibits its binding to Dpb11 (Ohouo et al. 2010), and the corresponding mutant shows phenotypes similar to those of *slx4-S486A* (Supplemental Fig. S3). As we cannot fully exclude pleiotropic defects for this mutant, we focused our analysis on *slx4-S486A*.

Taken together, our findings suggest that the Slx4–Dpb11 complex integrates at least two cellular signals: (1) cell cycle state through Cdk1 phosphorylation of Slx4 at Ser486 and (2) the presence of DNA damage through checkpoint kinase phosphorylation of several sites on Slx4 and perhaps on Dpb11.

Interestingly, the CDK regulation of this interaction is conserved between yeast and humans, since addition of the CDK inhibitor roscovitine reduced binding of Slx4 and TopBP1 (Fig. 2E).

#### *The Slx4–Dpb11 complex is required for the response to replication fork stalling*

Budding yeast Slx4 is known to bind to several DNA repair proteins (Slx1, Rtt107, and Rad1–Rad10) (Mullen et al. 2001; Roberts et al. 2006; Flott et al. 2007; Ohouo et al. 2010). However, whether these interaction partners are part of only one or several distinct complexes is unknown. While Slx4 has several independent DNA repair functions in budding yeast (Flott et al. 2007), until now, a detailed phenotypic characterization has only been conducted for *slx4Δ* deletion mutants. To test the specificity of the Dpb11-binding-deficient *slx4-S486A* phosphorylation site mutant, we compared its binding partners with those of wild-type Slx4 using quantitative proteomics. Indeed, we found that the mutant protein (Slx4-S486A<sup>3Flag</sup>) displayed eightfold reduced binding to Dpb11 (Fig. 3A). This variant still bound Slx1 and Rtt107 as efficiently as wild-type Slx4, indicating that Ser486 phosphorylation is specifically relevant for the Dpb11 interaction (Fig. 3A; see Supplemental Fig. S4A for specific Slx4 interactors). We thus took advantage of the *slx4-S486A* separation-of-function mutant to reveal a specific role of the Slx4–Dpb11 complex.

Using different DNA-damaging agents, we observed that the *slx4-S486A* mutant is particularly sensitive to MMS and, to a lesser extent, 4-NQO (Fig. 3B; Supplemental Fig. S4B), two reagents that create toxicity through replication fork stalling. Notably, the mutant was not sensitive to reagents that generate DNA strand breaks or interstrand cross-links, consistent with a recombination rate that was similar to wild type (Supplemental Fig. S4B,C). Remarkably,

expression of a fusion protein of the phospho-site mutant variant of Slx4 with Dpb11 (Dpb11–Slx4-S486A) rescued the MMS hypersensitivity phenotype almost to wild-type levels (Fig. 3B), suggesting that binding of Slx4 to Dpb11 is crucial for tolerance of replication fork-stalling lesions.

Next, we tested whether the response to stalled replication forks is aberrant in the *slx4-S486A* mutant. To this end, we treated synchronized cells with a pulse of MMS in early S phase. Under these conditions, the *slx4-S486A* mutant completed DNA replication with slightly slower kinetics compared with wild-type cells (Fig. 3C, 1-h time point). Also, the appearance of fully replicated and repaired chromosomes, as visualized by pulsed-field gel electrophoresis, was delayed (Fig. 3D, 1-h time point). This finding indicates that stalled replication fork structures or repair intermediates persist longer in the absence of the Slx4–Dpb11 complex. Additionally, the DNA damage checkpoint activation was prolonged in *slx4-S486A* cells (Fig. 3E), as determined by the phosphorylation status of the checkpoint kinase Rad53. This effect was specific for MMS treatment and could not be observed in cells in which double-strand breaks were induced by zeocin or phleomycin inside or outside of S phase (Supplemental Fig. S4D).

Defects in a checkpoint-antagonistic pathway (checkpoint “dampening”) (Ohouo et al. 2012) in *slx4* mutants could, in principle, lead to prolonged checkpoint activation and could thereby indirectly lead to slow S-phase kinetics and DNA damage hypersensitivity. Alternatively, persistence of unrepaired DNA lesions or DNA repair intermediates could lead to very similar phenotypes. In order to discriminate between the two possibilities, we examined the DNA damage levels during recovery from an MMS pulse in wild-type and *slx4-S486A* cells. To this end, we investigated the appearance and disappearance of nuclear foci formed by the ssDNA-binding protein RPA after MMS treatment in S phase. Indeed, *slx4-S486A* cells contained more RPA foci, which persisted longer than in wild-type cells (Fig. 3F). Therefore, we conclude that unrepaired DNA lesions or DNA repair intermediates that contain ssDNA persist in *slx4-S486A* mutants. This finding does not necessarily exclude a role of Slx4 as a regulator of the DNA damage checkpoint yet strongly suggests an additional direct function of the Slx4–Dpb11 complex in the repair of replication fork structures.

#### *The Slx4–Dpb11 complex promotes Mus81–Mms4-dependent JM resolution*

As our findings pointed to a function of the Slx4–Dpb11 complex in the response and repair of MMS-induced lesions, we next investigated whether the complex is involved in the DNA damage bypass. Therefore, we tested possible functions in HR and error-prone or error-free PRR. From several lines of genetic evidence, we conclude that the Slx4–Dpb11 complex is not exclusively involved in either PRR or HR (Supplemental Fig. S5). First, the *slx4-S486A* mutation enhanced the MMS hypersensitivity of mutants defective in error-free PRR (double mutant with either *mms2Δ*, *rad5-KT538,539AA*,

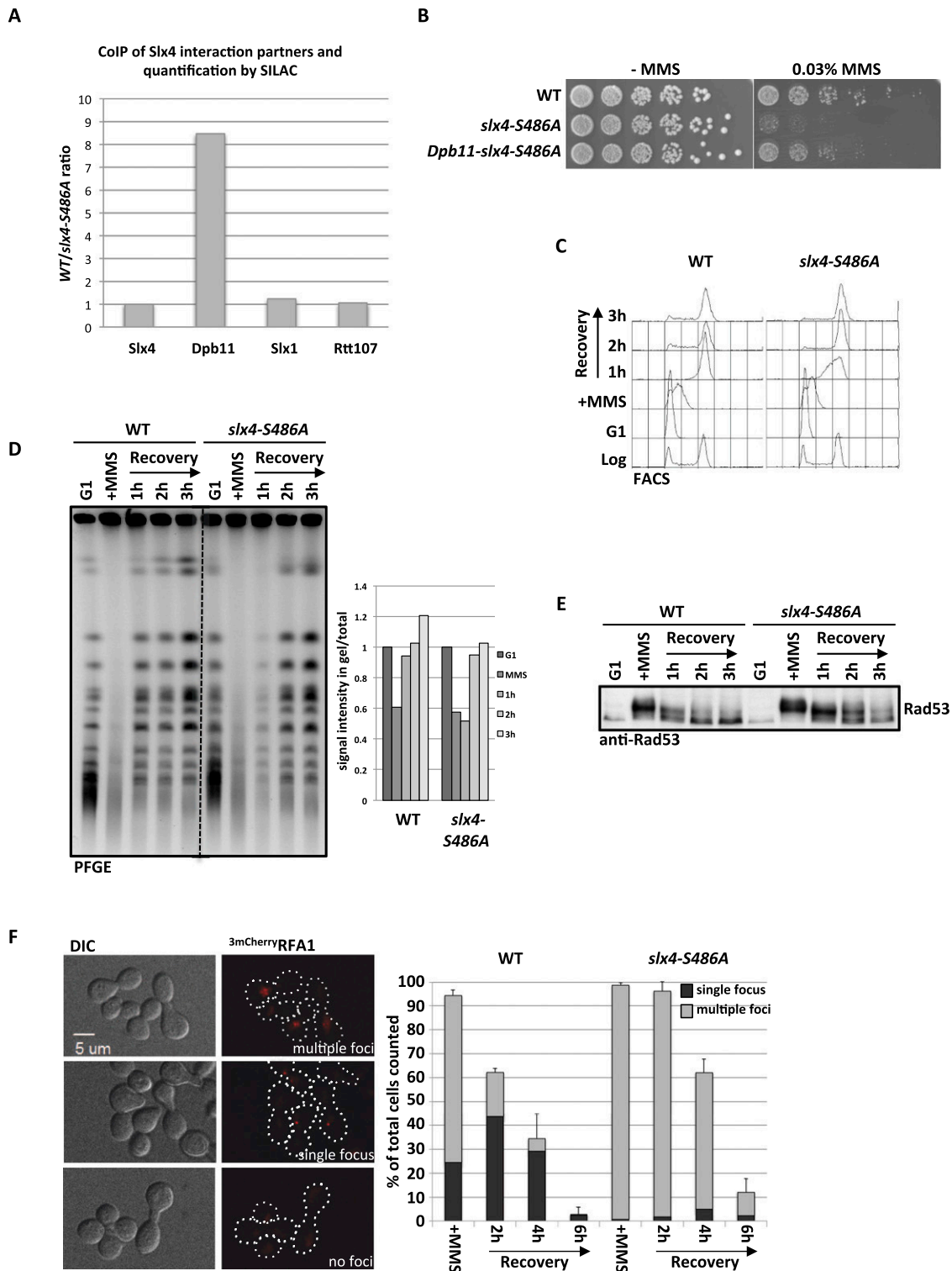


**Figure 3.** Mutation of *slx4-S486A* results in a specific defect in binding to Dpb11 and the response to stalled replication forks. (A) The *slx4-S486A* mutant leads to a specific defect in binding to Dpb11. Relative enrichment of Slx4 interactors (see Supplemental Fig. S4A) found in purifications of wild-type (WT) Slx4<sup>3Flag</sup> versus Slx4-S486A<sup>3Flag</sup> as determined by SILAC-based quantitative MS. Values >1 indicate a reduced binding to the Slx4-S486A relative to wild-type Slx4. (B) The *slx4-S486A* mutant, but not a *Dpb11-slxA4-S486A*-fusion, is hypersensitive to MMS. Wild type or strains expressing *slxA4-S486A* or the *Dpb11-slxA4-S486A*-fusion from the *SLX4* promoter as only a copy of *SLX4* were spotted in fivefold serial dilutions on MMS-containing medium and assayed for growth after 2 d. (C,D) Replication fork stalling is prolonged in the *slxA4-S486A* mutant. Cells were treated with a pulse of MMS during S phase, and recovery was analyzed by FACS (C; to measure cellular DNA content) and pulsed-field gel electrophoresis (D; to measure intact, fully replicated chromosomes). (D) For quantification, the fluorescence signal of chromosomes that migrated into the gel was divided by the total signal, including the pocket, and all signals were normalized to the G1 sample from each strain. (E) The DNA damage checkpoint is inactivated with reduced kinetics in the *slxA4-S486A* mutant. Cells were treated as in C, and checkpoint activity was determined by anti-Rad53 Western blot. (F) The *slxA4-S486A* mutant shows increased DNA damage foci and delayed recovery after transient MMS treatment in S phase. DNA damage sites were visualized by the ssDNA-binding RFA1<sup>3mCherry</sup> after transient MMS treatment during S phase. Cells were sorted into three categories: multiple, dispersed RFA1 foci; one RFA1 focus; and no RFA1 foci. Values are from two independent experiments, counting 100–150 cells per strain and time point. Error bars represent standard deviations.

or *rad5-C914S*), error-prone PRR (double mutant with either *rev1Δ*, *rev3Δ*, or *rad30Δ*), or HR (double mutant with *rad51Δ*) (Supplemental Fig. S5A). Second, spontaneous mutagenesis, a hallmark of error-prone PRR, was not significantly altered in *slx4-S486A* mutants (Supplemental Fig. S5B). Third, recombination rates, as determined by a direct repeat recombination assay, were similar between wild-type and *slx4-S486A* strains (Supplemental Fig. S4C). Fourth, *siz1Δ* or *srs2ΔC* mutations, which cause an up-regulation of HR at stalled replication forks (Pfander et al. 2005), did not alleviate the MMS hypersensitivity of *slx4-S486A* mutants (Supplemental Fig. S5C).

The nonepistatic relationship of the *slx4-S486A* mutant to PRR or HR pathways could be explained if Slx4 and Dpb11 participated in a step common to both error-free PRR and HR because, in such a scenario, both pathways would be affected by the *slx4-S486A* mutation. Both HR and error-free PRR operate via template switching in order to bypass the replication fork-stalling lesion by copying the undamaged information from the sister chromatid. A critical step in template switching is the final removal of X-shaped DNA intermediates (JMs) that link the two sister chromatids (Mankouri et al. 2013). JM removal pathways act, in principle, independently of the pathway by which JMs have been created (Branzei et al. 2008; for *mus81Δ* phenotypes, see Interthal and Heyer 2000; Li and Brill 2005). To test whether the Slx4–Dpb11 complex is involved in this late step, we visualized these DNA intermediates in a *sgs1Δ* mutant (deficient in JM dissolution) by two-dimensional (2D) gel electrophoresis (Liberi et al. 2005; Mankouri et al. 2011). In this mutant, MMS treatment in S phase leads to enhanced levels of JMs, which subsequently disappear during late S, G2, and M phase (Szakal and Branzei 2013). The additional mutation of *slx4-S486A* in the *sgs1Δ* background does not alter the formation of JMs, indicating that the Slx4–Dpb11 complex is not required at early steps (Supplemental Fig. S6A). Interestingly, however, during the recovery from the MMS treatment, JMs are more slowly resolved in the *sgs1Δ slx4-S486A* double mutant compared with the *sgs1Δ* single mutant (Fig. 4A). A similar effect can be observed using an *slx4Δ* mutant and conditionally inactivated *SGS1* in the same experimental setup (Supplemental Fig. S6B). Consistently, we observed an enhanced MMS sensitivity for the *sgs1Δ slx4-S486A* double mutant compared with the respective single mutants (Fig. 4B). From these experiments, we conclude that the Slx4–Dpb11 complex is involved in the resolution of JMs that are supposedly intermediates arising from a template switch reaction and that this complex functions in a pathway parallel to dissolution by the STR complex.

To elucidate a potential role of the Slx4–Dpb11 complex in a resolution mechanism, we investigated the genetic interaction with Mus81–Mms4. Indeed, the MMS sensitivities of *slx4-S486A mms4Δ* or *slx4-S486A mus81Δ* double mutants were identical to those of *mms4Δ* or *mus81Δ* single mutants (Fig. 4C). This suggests that the Slx4–Dpb11 complex acts in the Mus81–Mms4 pathway. The same epistatic relationship was seen between *mms4Δ* and *slx4-S486A* when we investigated JM resolution by 2D gel

electrophoresis when the STR complex was inactivated using the *Tc-sgs1* allele (Supplemental Fig. S6C). We note that the MMS hypersensitivity and the JM resolution defect of the *slx4-S486A* mutant are less pronounced compared with the deletion mutants that fully abolish Mus81 function (Fig. 4C; Supplemental Fig. S6C), suggesting that not all functions of the Mus81–Mms4 endonuclease depend on the Slx4–Dpb11 complex.

We also tested the involvement of other structure-specific endonucleases (Slx1, Rad1–Rad10, and Yen1) (Tomkinson et al. 1993; Fricke and Brill 2003; Coulon 2006; Ip et al. 2008), specifically of Slx1, as it associates with the Slx4–Dpb11 complex (Supplemental Fig. S4A). We found that *rad1Δ* showed an additive phenotype with *slx4-S486A*, while *slx1Δ* and *yen1Δ* mutants were not hypersensitive to MMS (Supplemental Fig. S6D; Fricke and Brill 2003; Coulon 2006; Blanco et al. 2010). We therefore conclude that these factors either are not involved in the resolution of template switch intermediates by Mus81 and the Slx4–Dpb11 complex or (in case of Slx1 and Yen1) have a function that can be taken over by a redundant pathway in the respective deletion mutant. Interestingly, the *yen1Δ* mutation caused an increase of MMS sensitivity specifically of the *sgs1Δ slx4-S486A* double mutant (Supplemental Fig. S6E), suggesting that Yen1 function becomes specifically important if the STR complex is inactive and function of the Slx4–Dpb11 complex is reduced.

The balance between STR-dependent JM dissolution and Mus81-dependent JM resolution is reflected in the ratio of CO to non-CO (NCO) products (Ira et al. 2003; Ho et al. 2010; Mankouri et al. 2013), since STR-mediated dissolution will not yield COs, while Mus81-mediated resolution can generate CO products. We therefore analyzed the rates of CO formation in the *slx4-S486A* mutant with a recombination assay using interchromosomal *arg4* heteroalleles (Robert et al. 2006; Szakal and Branzei 2013). Despite a slight increase in overall recombination rates, we measured a reduction in CO rates in the *slx4-S486A* mutant compared with wild-type cells (Fig. 4D). We therefore conclude that the Slx4–Dpb11 complex is an important regulator of JM removal pathways and that it acts by stimulating JM resolution, inhibiting JM dissolution, or both.

Persistent JMs interfere with the separation of sister chromatids in mitosis. Under circumstances in which JMs are not resolved before anaphase, these repair intermediates are thought to give rise to anaphase bridges between the dividing DNA masses (Chan et al. 2007; Mankouri et al. 2013). Consistent with a role in the resolution of JMs, Dpb11 localizes to DNA bridges between the separated chromosome masses in anaphase (Germann et al. 2014). Dpb11-containing anaphase bridges can be observed with a low frequency in undamaged cells (<5%) and are induced upon MMS treatment, suggesting that they arise from replication fork stalling (Germann et al. 2014). Interestingly, the occurrence of Dpb11 bridges is increased in *sgs1Δ* cells (Germann et al. 2014), indicating that the localization of Dpb11 to chromatin bridges reflects its action in a resolution mechanism. We observed a pro-

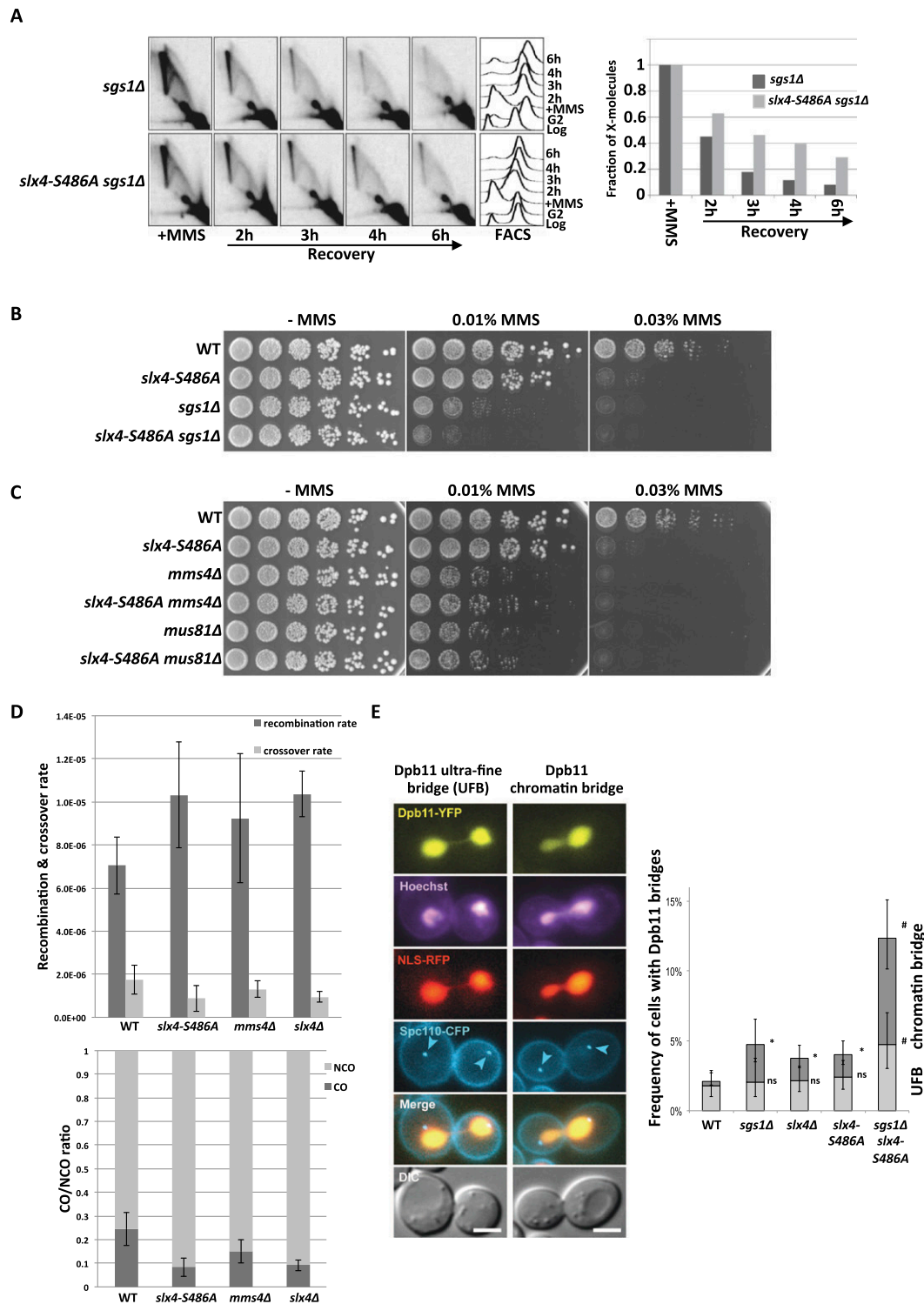


**Figure 4.** The Dpb11 binding-deficient *slx4-S486A* mutant causes defects in the Mus81–Mms4-dependent JM resolution. (A) JM structures are resolved slower in *sgs1Δ slx4-S486A* cells. X-shaped JMs were visualized as spike signal in 2D gels in *sgs1Δ* and *sgs1Δ slx4-S486A* cells that have been treated with a pulse of MMS in S phase. (B) MMS sensitivity is enhanced in the *sgs1Δ slx4-S486A* double mutant compared with each single mutant. Analysis of the MMS hypersensitivity phenotype as in Figure 3B. (C) The MMS hypersensitivity of *mms4Δ* and *mus81Δ* mutants is not further enhanced by an additional *slx4-S486A* mutation. Experiment as in B. (D) The *slx4-S486A* mutation leads to a reduced CO formation. COs and NCOs from an interchromosomal recombination assay using *arg4* heteroalleles on chromosome V and VIII (Robert et al. 2006) were determined using a PCR-based strategy. (Top panel) Recombination and CO rates were determined by fluctuation analysis using a maximum likelihood approach. (Bottom panel) CO ratio is quotient of CO rate and overall recombination rate. Error bars represent standard deviations of two to 11 independent experiments. (E) Dpb11 anaphase bridge structures occur more frequently when JM dissolution and the Dpb11–Slx4 interaction are defective. (Right panel) Quantification of Dpb11 ultrafine bridges (UFBs) or chromatin bridges in wild-type (WT), *sgs1Δ*, *slx4Δ*, *slx4-S486A*, and *slx4-S486A sgs1Δ* strains. Cells express Dpb11-YFP, NLS-RFP as a marker of the nucleoplasm and Spc110-CFP as a marker of the spindle pole body. DNA is stained with Hoechst. (Left panel) Images of representative anaphase cells are shown. Bar, 3  $\mu$ m. Error bars indicate 95% confidence intervals. Significance is as follows: (\*)  $P < 0.01$  (compared with wild type); (#)  $P < 0.01$  (compared with the single mutants); (ns) not significantly different from wild type.

nounced increase of cells containing Dpb11 bridges when the *sgs1Δ* and *slx4-S486A* mutants were combined (Fig. 4E). The genetic requirements for Dpb11 bridges are therefore highly similar to those for persistent JMs (Fig. 4A), supporting a role for Dpb11 and Slx4 in JM resolution. In line with this model, we observed frequent colocalization of either Slx4<sup>YFP</sup> or Mus81<sup>YFP</sup> with Dpb11<sup>CFP</sup>-positive bridges that is further enhanced in *sgs1Δ* cells (Supplemental Fig. S7A). We also noticed a colocalization of Slx4, Mus81, and Dpb11 in DNA damage foci yet to a lesser extent (Supplemental Fig. S7B). Overall, the data in Figure 4 provide strong support for an involvement of the Slx4–Dpb11 complex in JM resolution by Mus81–Mms4.

#### *Mus81–Mms4 interacts with the Slx4–Dpb11 complex during mitosis in a Cdc5-dependent fashion*

To elucidate how the Slx4–Dpb11 complex regulates Mus81 function, we investigated a possible physical interaction. In previous studies using asynchronously growing yeast cells, no binding of Slx4 to Mus81–Mms4 was detectable (Schwartz et al. 2012). However, we detected Mms4 as a cell cycle-specific interactor if Slx4<sup>3Flag</sup> immunoprecipitations were investigated by SILAC MS (such as in Fig. 2A). Moreover, when we arrested cells in G2/M by nocodazole treatment, immunopurification of Mms4<sup>3Flag</sup> copurified Dpb11 and Slx4 (Fig. 5A). Notably, this interaction is highly cell cycle-specific, as it could not be observed in G1- or S-phase cells (Fig. 5A). We determined, using an unbiased SILAC MS approach, that Dpb11, Slx4, and Rtt107 are among the best interactors of Mus81–Mms4 in G2/M-arrested cells (Supplemental Fig. S8A).

Next, we tested whether Dpb11, Slx4, and Mus81–Mms4 form a single protein complex. Indeed, the three proteins comigrated at a size of ~33 S (Supplemental Fig. S8B, fractions 18–20, apparent molecular weight 1.1–1.2 MDa) when the eluate of an Mms4<sup>3Flag</sup> purification from G2/M cells was subjected to a glycerol gradient centrifugation. When we analyzed the complex architecture by a two-hybrid approach, we detected a direct interaction of Dpb11 and Mms4 that is independent of Slx4 (Supplemental Fig. S8C). Moreover, when we immunoprecipitated Mms4<sup>3Flag</sup> in the *slx4-S486A* background, we observed a reduction of Slx4, but not Dpb11, binding to Mms4<sup>3Flag</sup> (Fig. 5B). These findings thus suggest that Dpb11, Slx4, and Mus81–Mms4 are part of a multiprotein complex in which Dpb11 acts as a bridge between Slx4 and Mus81–Mms4.

We observed that Dpb11 and Slx4 could be partially eluted from Mms4-containing beads using λ-phosphatase treatment (Supplemental Fig. S8D), suggesting that the binding is at least in part dependent on protein phosphorylation. Previous work has established that Mus81 activity is decisively up-regulated in mitosis in response to a sequential phosphorylation of Mms4 by CDK and the Polo-like kinase Cdc5 (Matos et al. 2011; Gallo-Fernández et al. 2012; Saugar et al. 2013; Szakal and Branzei 2013). We therefore used two systems to interfere with Cdc5 activity: the *cdc5-as1* analog-sensitive allele, which we inhibited using chloromethylketone (CMK) (Snead et al. 2007), and transcriptional shutoff of *pGAL-CDC5* using

glucose repression. Both types of Cdc5 inactivation resulted in a loss of the slower-migrating species of Mms4 in gels and at the same time diminished the binding of Dpb11 and Slx4 to Mms4<sup>3Flag</sup> (Fig. 5C; Supplemental Fig. S9A). In order to rule out indirect effects, we tested whether Cdk1 activity was uninfluenced under conditions of Cdc5 inhibition/shutoff and saw that neither the interaction between Slx4 and Dpb11 nor phosphorylation of a CDK target site on Rad9 (T474) (Pfander and Diffley 2011) was influenced by Cdc5 inactivation (Supplemental Fig. S9B,C). Together with our results on the architecture of the Slx4–Dpb11–Mms4–Mus81 complex, these experiments suggest that binding of Mms4 to Dpb11 is regulated by Cdc5 phosphorylation.

We also tested whether the formation of the Slx4–Dpb11–Mms4–Mus81 was regulated upon DNA damage. We found that Mms4<sup>3Flag</sup> bound similar amounts of Dpb11 and Slx4 after phleomycin or mock treatment of G2/M-arrested cells (Supplemental Fig. S9D). Moreover, we could also observe formation of the Slx4–Dpb11–Mms4–Mus81 complex during recovery from MMS pulse treatment during S phase (Fig. 5D). However, this binding occurred only once Cdc5 became active, as visualized by the slower-migrating form of Mms4, indicating that even after DNA damage, the Dpb11–Mms4 interaction is dependent on Cdc5 (Fig. 5D).

Given that the cell cycle regulation of Mus81 activity and the cell cycle regulation of the Slx4–Dpb11–Mms4–Mus81 complex formation have the same requirements, we tested whether the up-regulation of Mus81 nuclease activity requires Slx4 and Dpb11. We analyzed in vitro resolution of nicked Holliday junctions, Holliday junctions, and model replication fork structures on immunopurified Mus81–Mms4 and found that the enhanced activity of mitotic Mus81 is similar, independently of whether Mus81 was purified from wild-type or *slx4-S486A* cells (Fig. 5E; Supplemental Fig. S9E). Therefore, we conclude that cell cycle kinases regulate Mus81 by at least two mechanisms: direct up-regulation of the catalytic activity, which can be reconstituted in vitro, and an up-regulation through formation of an Slx4–Dpb11–Mms4–Mus81 complex, which could be seen in vivo.

#### *The DNA damage checkpoint regulates the Slx4–Dpb11-dependent Mus81 function*

The DNA damage checkpoint prevents collapse of stalled replication forks and thereby is fundamentally required for all aspects of the response to stalled replication forks (Branzei and Foiani 2010). Moreover, the checkpoint was also suggested to counteract Cdc5-dependent Mus81 activation, since premature Mms4 phosphorylation by Cdc5 was observed after MMS treatment of checkpoint-deficient cells (Szakal and Branzei 2013). Possible explanations for this phenomenon are a faster S-phase progression in the checkpoint mutants or a direct inhibition of Cdc5 activity by the checkpoint (Zhang et al. 2009).

To address these possibilities, we investigated the influence of the DNA damage checkpoint on Slx4–Dpb11–Mms4–Mus81 complex function. Interestingly, we found

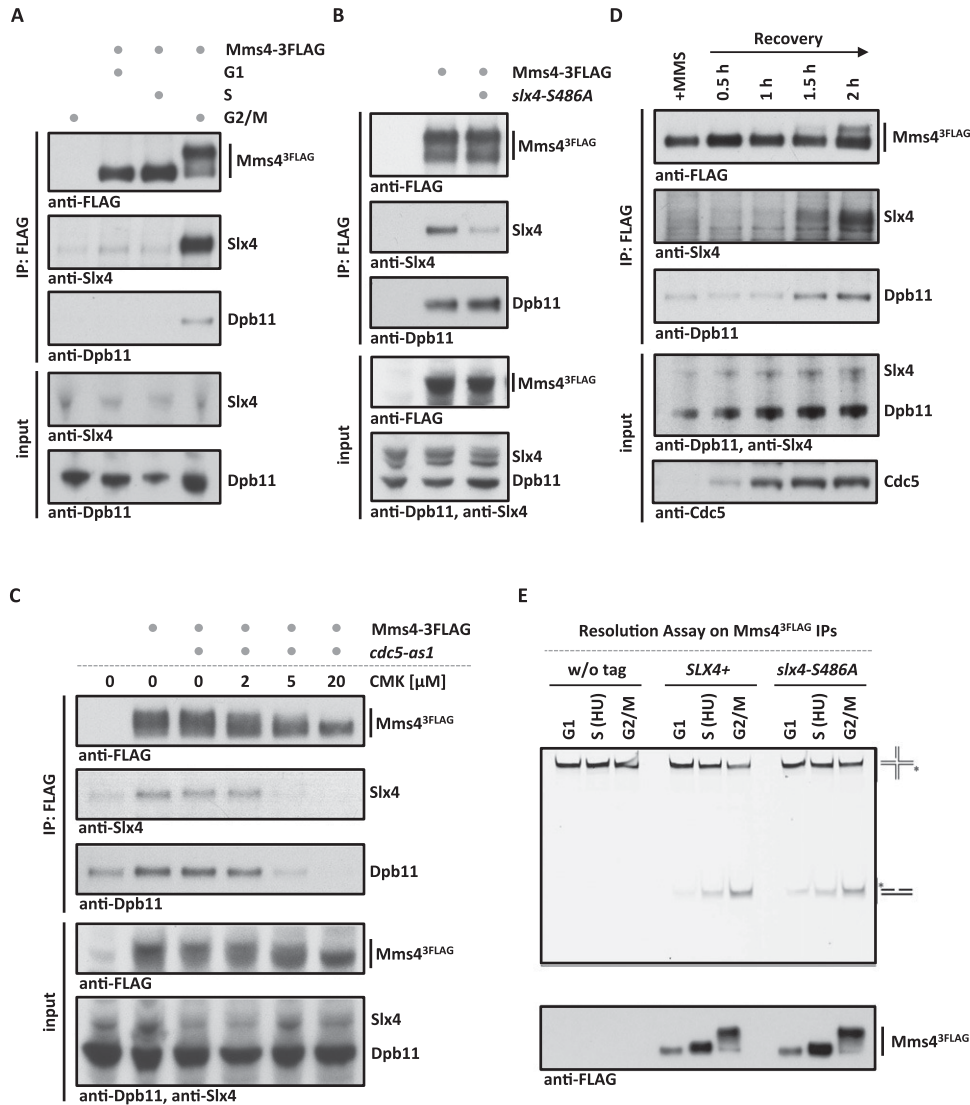


**Figure 5.** Slx4, Dpb11, and Mus81–Mms4 form a Cdc5-dependent complex at the G2/M cell cycle stage. (A) Mms4 binds to Dpb11 and Slx4 specifically in G2/M. Coimmunoprecipitation samples of Mms4<sup>3FLAG</sup> from G1, S, or G2/M cells were tested for binding to Dpb11 and Slx4. (B) Slx4-S486A is partially lost from the Slx4–Dpb11–Mms4 complex, suggesting that Dpb11 bridges the interaction between Mms4 and Slx4. Mms4<sup>3FLAG</sup> coimmunoprecipitation were carried out as in A but from G2/M-arrested wild-type (WT) or *slx4-S486A* mutant cells. (C) The Dpb11–Mms4 interaction is dependent on the Polo-like kinase Cdc5. *cdc5-as1* was inhibited by 2, 5, and 20  $\mu$ M CMK in G2/M-arrested cells. Mms4<sup>3FLAG</sup> coimmunoprecipitation was performed as in A. (D) Cdc5 hyperphosphorylated Mus81–Mms4 binds to Slx4 and Dpb11 during recovery from MMS damage. Cells were treated with a 30-min pulse of 0.03% MMS. Mms4<sup>3FLAG</sup> coimmunoprecipitations were performed from samples after 0, 30, 60, 90, and 120 min of recovery in nocodazole-containing medium. (E) Cell cycle regulation of Mus81–Mms4 nuclease activity remains intact in the *slx4-S486A* mutant. Mms4<sup>3FLAG</sup> and control immunoprecipitations (see the *bottom* panel for immunoprecipitation samples) from cells arrested in their cell cycle by  $\alpha$  factor, HU, or nocodazole were incubated with a fluorescence-labeled nicked Holliday junction substrate.

that a partial defect in DNA damage checkpoint signaling alleviated the phenotypes of the *slx4-S486A* mutant (Fig. 6A,B; Supplemental Fig. S10A,B; see also Ohouo et al. 2012). In these experiments, we used three distinct mutants, which were partially impaired in checkpoint signaling: *ddc1-T602A* (defective in Dpb11-dependent Rad9 recruitment (Puđu et al. 2008), *dot1 $\Delta$*  (defective in chromatin-dependent Rad9 recruitment) (Giannattasio et al. 2005), and *rad53-3HA* (a hypomorphic Rad53 allele) (Cordon-Preciado et al. 2006). All three mutants partially

suppressed the hypersensitivity of *slx4-S486A* to chronic exposure of MMS (Fig. 6A; Supplemental Fig. S10A). Furthermore, the recovery from MMS treatment as judged by the reappearance of fully replicated chromosomes in PFGE and reappearance of unphosphorylated Rad53 was enhanced in *slx4-S486A ddc1-T602A* cells compared with *slx4-S486A* cells (Fig. 6B; Supplemental Fig. S10B).

A plausible interpretation of these results is that a partial inactivation of the checkpoint may compensate for a reduced or delayed formation of the Slx4–Dpb11–Mms4–

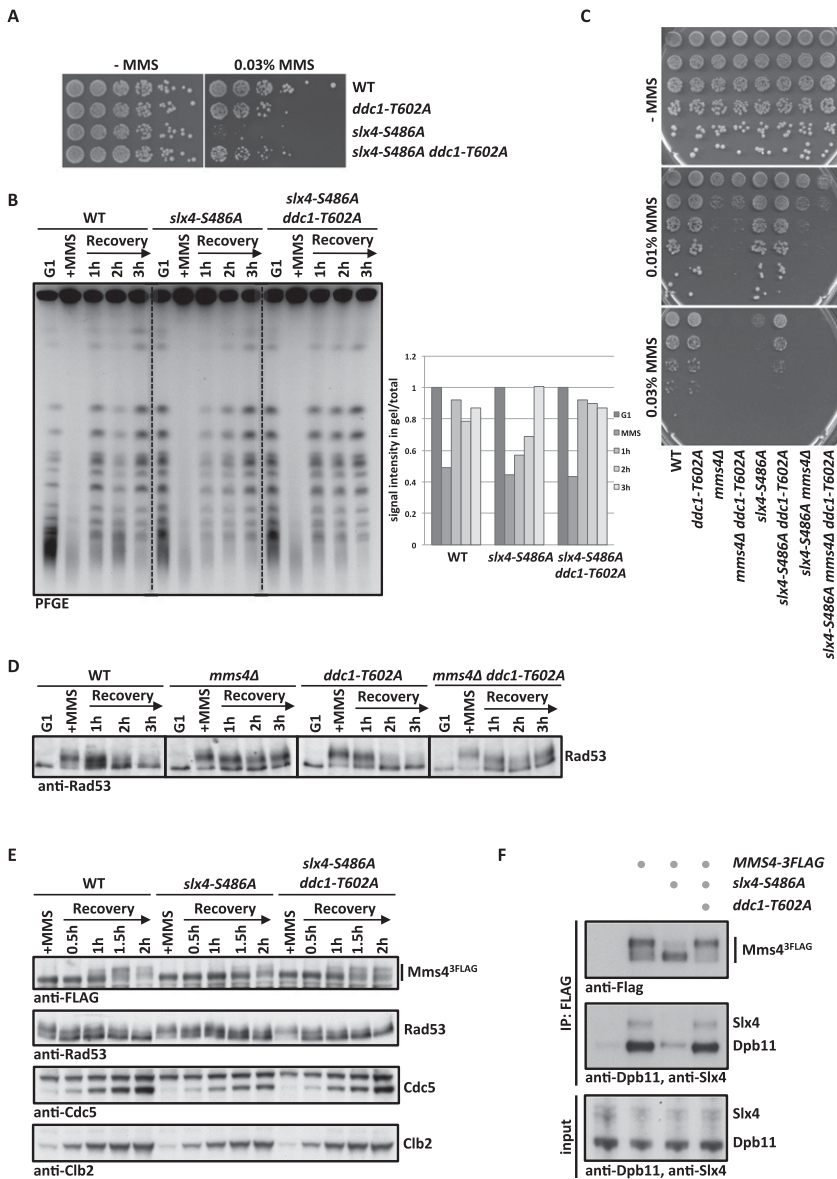


**Figure 6.** Partial inactivation of the DNA damage checkpoint rescues *slx4-S486A* phenotypes in an *MMS4*-dependent manner. (A) The DNA damage checkpoint defect of *slx4-S486A* is suppressed by partial inactivation of the DNA damage checkpoint. Wild type (WT), *slx4-S486A*, the partial checkpoint mutant *ddc1-T602A*, and the *slx4-S486A ddc1-T602A* double mutant were spotted in fivefold serial dilutions on MMS-containing plates. (B) The prolonged replication fork stalling of the *slx4-S486A* mutant is rescued by the *ddc1-T602A* mutation. Cells were cell cycle-synchronized and treated with a 30-min pulse of 0.033% MMS in S phase. Recovery of fully replicated chromosomes was analyzed by pulsed-field gel electrophoresis. Quantification as in Figure 3D. (C) A complete defect in Mus81 activity (*mms4Δ*) cannot be rescued by checkpoint inactivation. The MMS hypersensitivity phenotypes of *slx4-S486A*, *mms4Δ*, and *ddc1-T602A* mutants and double and triple mutant combinations were analyzed as in A. (D) The checkpoint recovery defect of *mms4Δ* mutants is not rescued by a partial checkpoint mutant. Cells were treated as in B, and checkpoint activity was measured by Rad53 phosphorylation. (E,F) Cdc5-dependent hyperphosphorylation of Mms4 and concomitant binding to Dpb11 and Slx4 occur earlier during recovery from replication fork stalling in *slx4-S486A ddc1-T602A* double mutants compared with *slx4-S486A* mutants. (E) Cells were treated with a 40-min pulse of 0.033% MMS in S phase. The Cdc5-dependent Mms4<sup>3Flag</sup> phosphorylation shift was measured by anti-Flag Western blot, checkpoint activity was measured by Rad53 phosphorylation, and cell cycle progression was followed by anti-Clb2 and anti-Cdc5 Westerns. (F) Wild-type, *slx4-S486A*, and *slx4-S486A ddc1-T602A* cells that contain *MMS4*<sup>3Flag</sup> were harvested during the recovery phase (2.5 h after MMS removal) and subjected to anti-Flag immunoprecipitation. Coimmunoprecipitation samples were tested for binding to Dpb11 and Slx4.

Mus81 complex. Such compensation may occur by either a direct up-regulation of the Slx4–Dpb11–Mms4–Mus81 complex or hyperactivation of a Mus81-independent salvage pathway. We therefore tested whether the observed rescue would depend on Mms4. Consistent with a direct influence of the checkpoint on the Slx4–Dpb11–Mms4–Mus81 complex, a partial inactivation of the checkpoint did not rescue the MMS hypersensitivity of the *mms4Δ* or *mms4Δ slx4-S486A* mutants (Fig. 6C). In contrast, the *sgs1Δ slx4-S486A* or *yen1Δ slx4-S486A* double mutants could be rescued by additional mutation of *ddc1-T602A* (Supplemental Fig. S10C), suggesting that neither STR nor Yen1 activity is required for the rescue. Furthermore, *mms4Δ ddc1-T602A* mutants show a slow checkpoint recovery after a pulse of MMS in S phase that is similar to *mms4Δ* cells (Fig. 6D). These results suggest that the

rescue of *slx4-S486A* mutants upon partial checkpoint inactivation is due to the action of Mms4–Mus81.

Furthermore, when we transiently exposed cells to MMS during S phase and released them into a G2/M arrest, we observed that the Cdc5-dependent phosphorylation shift of Mms4, which in this experiment serves as a marker for the interaction with Slx4–Dpb11, was slightly delayed in *slx4-S486A* cells compared with wild-type cells (Fig. 6E), probably because of a slower S-phase progression (see Fig. 3C). Importantly, the additional partial inactivation of the checkpoint (*slx4-S486A ddc1-T602A*) (Fig. 6E,F) allowed Cdc5-dependent Mms4 phosphorylation to occur earlier. Concomitantly, the binding of Mms4 to Dpb11 and Slx4 was rescued by partial checkpoint inactivation when immunoprecipitations were performed during the recovery phase (Fig. 6F). The occurrence of Mms4 phosphorylation

in the two mutants inversely correlated with DNA damage checkpoint activation (Rad53 phosphorylation) (Fig. 6E). It needs to be emphasized that Slx4–Dpb11 interaction is reduced, but not abolished, in the *slx4-S486A* mutant (Figs. 1B, 3A). The results in Figure 6, E and F, therefore suggest that the Slx4–Dpb11–Mms4–Mus81 complex can form earlier and potentially to a larger extent in the *slx4-S486A ddc1-T602A* mutant compared with the *slx4-S486A* single mutant. This offers a straightforward explanation for the rescue of the *slx4-S486A* mutant phenotypes by partial inactivation of the DNA damage checkpoint.

Taken together, we therefore identified an intricate regulatory mechanism of the Mus81 endonuclease, which critically depends on the formation of an Slx4–Dpb11–Mms4–Mus81 complex. The formation of this complex is activated by cell cycle stage-specific signaling and antagonized by the DNA damage checkpoint. Remarkably, complex formation and the direct control of Mus81 catalytic activity occur with similar timing, at the G2/M transition (Fig. 7).

## Discussion

In this study, we describe a new facet of JM resolution following the bypass of DNA damage via template switch recombination. We describe a multiprotein complex containing Slx4, Dpb11, and Mus81–Mms4. This complex is cell cycle-controlled by at least two mechanisms: Cdk1-dependent phosphorylation of Slx4 and Cdc5-dependent phosphorylation of Mms4, and Dpb11 acts as a reader of both modifications. The conservation of the Slx4–Dpb11/TopBP1 interaction and its cell cycle regulation suggests that a similar complex may be involved in JM resolution in human cells. Importantly, the inhibition of Slx4 binding to Dpb11 causes phenotypes that are indicative of JM resolution defects, and we therefore infer that the association with Slx4 and Dpb11 promotes Mus81 function.

### Temporal regulation of the response to replication fork stalling

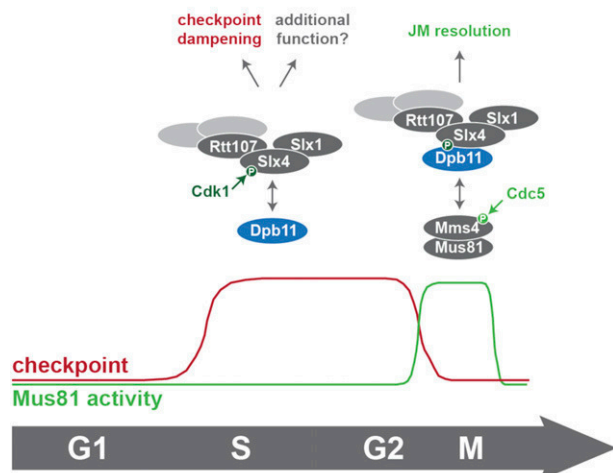


**Figure 7.** Model of the temporal response to replication fork stalling and its regulation by Slx4–Dpb11 complexes.

### *Slx4–Dpb11 multiprotein complex formation correlates with DNA JM resolution*

The starting point of our analysis was a multiprotein complex containing Slx4, Dpb11, Slx1, and Rtt107 (Ohouo et al. 2010, 2012). In order to characterize a putative function of this complex in DNA repair, we tested whether the Slx4–Dpb11 complex would transiently interact with DNA repair enzymes and found an interaction with the Mus81–Mms4 structure-specific endonuclease specifically in mitotic cells. Based on the findings that the *slx4-S486A* mutant impairs complex formation and results in JM resolution defects, we propose that the Slx4–Dpb11 complex regulates Mus81–Mms4 activity. Our binding studies furthermore indicate a direct Dpb11–Mms4 interaction. Given the nature of Dpb11 as a scaffold protein, it appears likely that Dpb11 operates by tethering Mus81 to other activities that collaborate in the resolution reaction or targeting Mus81 to JM structures.

An intricate feature of the Slx4–Dpb11 complex is its complexity, as it involves four scaffold proteins: Dpb11, Slx4, Rtt107, and Mms4. An obvious advantage of such a multiscaffold complex is that its formation depends on several interaction surfaces, which offer numerous possibilities for regulation. The assembly of the complex therefore allows the integration of different cellular signals (for example, cell cycle and DNA damage), or one specific signal may control complex assembly by several mechanisms. Such a setup includes features of multisite phosphorylation systems, which have the ability to create switch-like transitions (Nash et al. 2001). Moreover, a multiscaffold complex may allow the assembly and coordination of different enzymatic activities (see below).

Our work has identified Mus81 as one catalytically active component of the Slx4–Dpb11 complex; a second one could potentially be Slx1. Recently, the Mus81 and Slx1 endonucleases from humans and mice have been shown to cooperate in the resolution of Holliday junctions in an Slx4-dependent manner (Wyatt et al. 2013). While our results suggest that also in budding yeast, Mus81 and Slx1 may be part of the same complex, we did not observe any specific defects in the response to MMS-induced replication fork stalling for *slx1Δ* cells (Supplemental Fig. S6D). Therefore, we conclude that either Slx1 is not involved in Mus81-dependent JM resolution in budding yeast or a functionally redundant nuclease compensates for the defects of the *slx1Δ* mutant.

### *Cell cycle regulation of the response to replication fork stalling and JM resolution*

The cellular response to replication fork-stalling DNA lesions is intimately linked to the progression of the cell cycle. First, the primary problem, fork stalling, arises specifically in S phase. Moreover, the cells are required to finish the repair/bypass process at the latest in mitosis, when sister chromatids need to be accurately separated, and any remaining links between the chromatids have to be resolved.

In this study, we characterized two Dpb11 interactors: Slx4 and Mms4. Both proteins are phosphorylation tar-

gets of CDKs; however, Mms4 is additionally phosphorylated by the Polo-like kinase Cdc5 (Matos et al. 2011; Gallo-Fernández et al. 2012; Szakal and Branzei 2013). Interestingly, the Slx4–Dpb11 and Mms4–Dpb11 interactions display distinct cell cycle specificities: We observed a strong Slx4–Dpb11 interaction in asynchronous cultures as well as in S-phase and mitotic cells (Figs. 1C, 2C), while the Mms4–Dpb11 interaction was highly specific for mitosis (Fig. 5A). Accordingly, we found that the Mms4–Dpb11 interaction requires Cdc5, suggesting that Dpb11 can act as a reader of phosphorylation events that are initiated by different cell cycle kinases.

The cell cycle regulation of the Mus81–Mms4 association with the Slx4–Dpb11 complex correlates exactly with the known activity profile of Mus81 (Matos et al. 2011). Notably, the multiprotein complex is not the only mechanism of cell cycle regulation: Our *in vitro* resolution assays suggest that Cdc5 phosphorylation of Mus81–Mms4 directly stimulates Mus81 independently of complex formation. Therefore, we conclude that at least two parallel pathways of cell cycle regulation exist that promote appropriate Mus81 function in mitosis.

To date, it remains uncertain why cells restrict the activity of Mus81 until mitosis. The temporal regulation of Mus81 channels a large proportion of JMs into the Sgs1–Top3–Rmi1 dissolution pathway (Matos et al. 2011; Szakal and Branzei 2013). It has therefore been speculated that Sgs1-dependent dissolution, which leads to a NCO outcome (Ira et al. 2003), may be beneficial for cells dividing by a mitotic cell cycle. A second reason for restricting Mus81 activity may be the necessity to achieve temporal separation of the lesion bypass reaction and the JM resolution reaction (Saugar et al. 2013). Mus81 could impede the bypass reaction, given its relatively broad substrate specificity to a range of DNA structures (e.g., replication forks, D-loop structures, and Holliday junctions).

Intriguingly, the differences in the temporal regulation of the Slx4–Dpb11 and Mms4–Dpb11 interactions suggest that the composition of the Slx4–Dpb11 complex changes from the replication-associated template switch to the resolution reaction. Supporting the idea of several distinct Slx4–Dpb11 complexes is the fact that not all features of the Slx4–Dpb11 interaction (for example, enhanced binding after DNA damage) are seen in the Slx4–Dpb11–Mms4–Mus81 complex. It therefore appears plausible that Slx4–Dpb11 may associate with stalled replication forks already in S phase, while Mus81–Mms4 joins the complex in mitosis. It is tempting to speculate that the Slx4–Dpb11 complex may chaperone the DNA lesion site/repair intermediates until resolution (Fig. 7).

#### *Regulation of JM resolution by the DNA damage checkpoint*

The DNA damage checkpoint antagonizes JM resolution by Mus81 (Fig. 6; Szakal and Branzei 2013), and it has been suggested that Slx4 may act as negative regulator (“dampener”) of the checkpoint by competing with binding of the checkpoint mediator Rad9 to Dpb11 (Ohouo et al. 2012). The JM resolution phenotypes of the *slx4-S486A* mutant

could therefore, in principle, be explained by an indirect effect arising from checkpoint hyperactivation. Given the extensive ties between checkpoint and DNA repair pathways, the presented *in vivo* experiments cannot rule out a contribution of checkpoint misregulation to the observed JM resolution phenotypes.

We favor, however, a more direct role of Slx4 and Dpb11 in JM resolution for two reasons. First, the formation of the Slx4–Dpb11–Mms4–Mus81 complex and its regulation correlate with the temporal activation of Mus81. Second, the “dampener” model cannot account for all observed phenotypes. For example, the rescue of the MMS hypersensitivity of the *slx4-S486A* mutant by a covalent fusion with Dpb11 cannot be explained by competition, since in the fusion mutant, cells express two copies of full-length Dpb11 (one endogenous, one fused to Slx4), and therefore even more Dpb11 molecules (not less) are able to engage in checkpoint signaling complexes. Moreover, our analysis of RPA foci suggests that DNA lesions or repair intermediates persist and accumulate in the absence of a functional Slx4–Dpb11 complex, indicative of a role for Slx4 and Dpb11 in DNA repair.

Importantly, we found that the checkpoint regulates the formation of the Slx4–Dpb11–Mms4–Mus81 complex: Partial inhibition of the checkpoint enables Cdc5-dependent hyperphosphorylation of Mms4, which allows Dpb11 binding to occur earlier during the recovery from an MMS pulse and thereby reverses the effect of the *slx4* mutant. These findings suggest that at least in the *slx4-S486A* mutant background, the DNA damage checkpoint antagonizes the Slx4–Dpb11–Mms4–Mus81 complex. Partial inactivation of the checkpoint may therefore extend the temporal window during which Mus81 is active, which we propose to be beneficial in mutants with reduced JM resolution activity such as *slx4-S486A*. Whether this inhibitory mechanism takes place on the level of Cdc5 regulation in general (Zhang et al. 2009; Matos et al. 2013) or by specifically regulating Mms4 phosphorylation by Cdc5 remains to be determined. The important implication of this finding is that the activation of Mus81 is temporally restricted by two pathways: activation by cell cycle kinases and inhibition by the DNA damage checkpoint.

#### *The Slx4–Dpb11 complex is conserved among eukaryotes*

In addition to the mechanistic studies of the budding yeast Slx4–Dpb11 complex, we also provide the first evidence that at least parts of this complex may be found in human cells as well, since Slx4 and TopBP1 interact in a manner that depends on CDK phosphorylation of Slx4. It is worth noting that not all aspects of the protein network that controls resolution of JMs are conserved through evolution: While in human cells, Slx4 binds directly to Mus81–Eme1, this interaction appears to be absent in budding yeast (Fekairi et al. 2009; Muñoz et al. 2009; Svendsen et al. 2009; Schwartz et al. 2012). Given that both Slx4 and Mms4 bind to Dpb11, our data suggest that Dpb11 may serve as a bridge between the two proteins. Although a direct interaction between Slx4 and Mus81–Mms4 cannot be definitively

excluded, it appears as if the bridging interaction with Dpb11 in yeast may replace the direct interaction of Slx4 and Mus81 in human cells. Importantly, similar to our results in yeast, a stimulation of Slx4 binding to Mus81–Eme1 after phosphorylation by CDK and Polo-like kinase was observed in mitotic human cells as well (Wyatt et al. 2013). At this point, it seems therefore very likely that in both systems, JM resolution is promoted by a cell cycle-regulated complex containing several scaffold proteins.

## Materials and methods

### Yeast strains

All yeast strains are based on W303. Genotypes are listed in Supplemental Material.

### Interaction assays

Coimmunoprecipitations of yeast extracts were performed using anti-Flag agarose resin (Sigma). Bound proteins were eluted with 3× Flag-peptide (Sigma).

For GST pull-downs, GST-Dpb11 or GST-tagged protein fragments were recombinantly expressed and purified as described (Pfander and Diffley 2011). Pull-downs were performed with ammonium sulphate-precipitated (57%) yeast extracts on glutathione sepharose 4B (GE Healthcare).

For coimmunoprecipitations from HEK293T, GFP-tagged proteins were transiently overexpressed and precipitated using GFP-Trap magnetic beads (Chromotek).

### Nuclease activity assays

Nuclease assays on Mms4<sup>3Flag</sup> immunoprecipitations were done as described (Matos et al. 2011).

### DNA gel electrophoresis

PFGE and 2D gel analysis of DNA intermediates were performed as previously described (Karras and Jentsch 2010; Szakal and Branzei 2013).

### Mutation and recombination assays

Mutation rates were determined using a *CAN1* forward mutation assay. Interchromosomal recombination rates were determined using a direct repeat system using *leu2* heteroalleles (Aguilera and Klein 1988). CO rates were determined using a system harboring two *arg4* alleles on chromosome V and VIII (Robert et al. 2006; Szakal and Branzei 2013). In all, rates were determined by fluctuation analysis using a maximum likelihood approximation (Pfander et al. 2005).

### Microscopy and immunofluorescence

Microscopy experiments were carried out as described (Germann et al. 2014).

A detailed methods description is provided in the Supplemental Material.

## Acknowledgments

We thank U. Kagerer for excellent technical assistance, and C. Biertümpfel, J. Diffley, and H. Klein for providing plasmids, strains, and antibodies. We are grateful to Z. Storchova for help

with microscopy analysis of RPA foci and thank S. Jentsch, M. Räschle, Z. Storchova, and members of the Jentsch and Pfander laboratories for stimulating discussion and critical reading of the manuscript. We thank the Max-Planck Institute of Biochemistry core facility for MS analysis. This work was supported by the Max-Planck Society and the German Research Council (Deutsche Forschungsgemeinschaft) to B.P.; the European Research Council, the Italian Association for International Cancer Research, and The Italian Foundation for Cancer Research (FIRC) to D.B.; and the Danish Agency for Science, Technology, and Innovation, the Villum Kann Rasmussen Foundation, the Lundbeck Foundation, and the European Research Council to M.L. S.C.S.B. is supported by a fellowship from the German Chemical Industry Association (VCI). B.S. and D.B. performed the 2D gel experiments of Figure 4A and Supplemental Figure S6A–C and analyzed the data. M.L. performed the imaging experiments of Figure 4E and Supplemental Figure S7 and analyzed the data. J.M. performed the in vitro nuclease assays of Figure 5E and Supplemental Figure S9E and analyzed the data. B.H.H. did the bioinformatics analysis of Supplemental Figure S2. All other experiments were performed and analyzed by D.G., L.N.P., S.C.S.B., L.W., S.S., and B.P. B.P. wrote the paper, and all authors commented on the manuscript.

## References

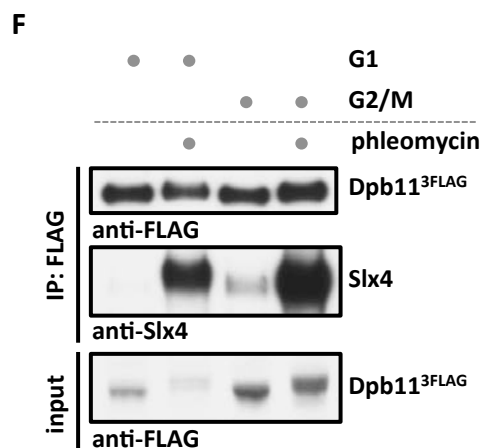
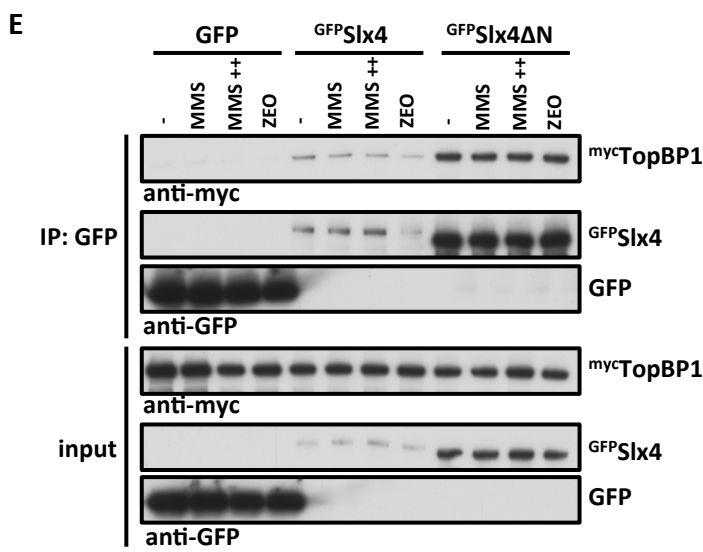
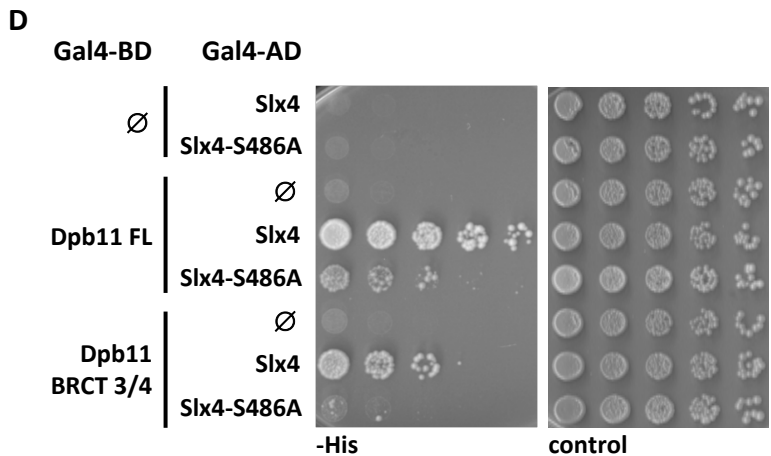
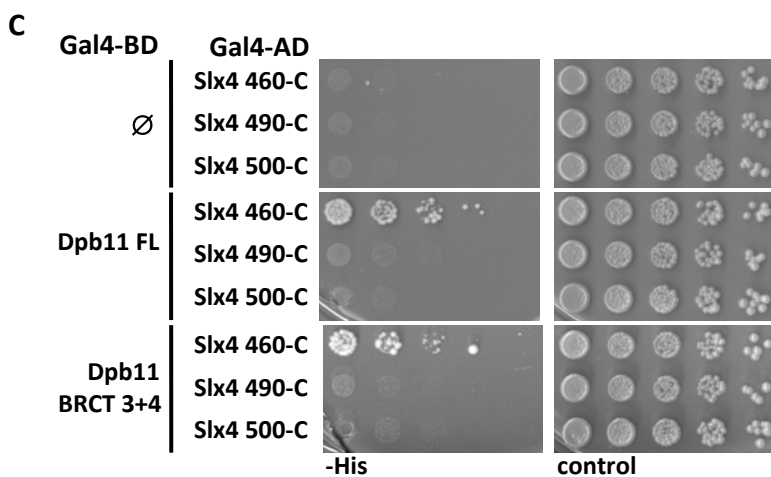
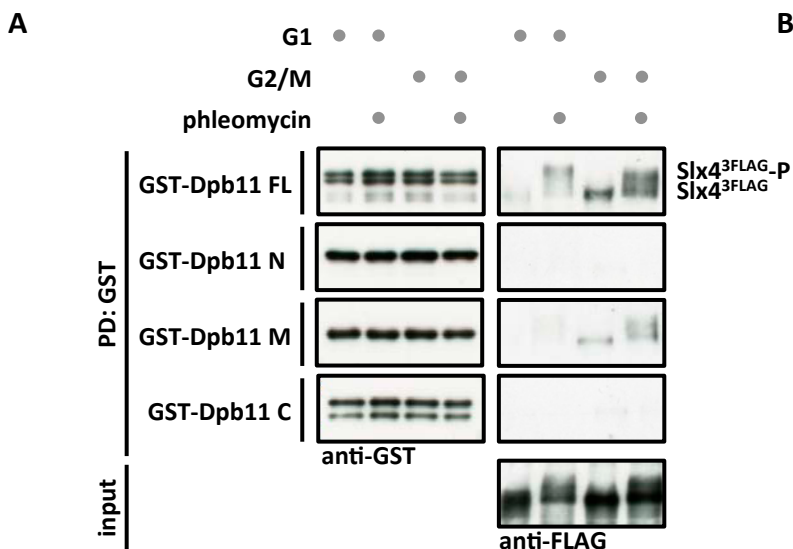
- Aguilera A, Klein HL. 1988. Genetic control of intrachromosomal recombination in *Saccharomyces cerevisiae*. I. Isolation and genetic characterization of hyper-recombination mutations. *Genetics* **119**: 779–790.
- Bishop AC, Ubersax JA, Petsch DT, Matheos DP, Gray NS, Blethrow J, Shimizu E, Tsien JZ, Schultz PG, Rose MD, et al. 2000. A chemical switch for inhibitor-sensitive alleles of any protein kinase. *Nature* **407**: 395–401.
- Blanco MG, Matos J, Rass U, Ip SCY, West SC. 2010. Functional overlap between the structure-specific nucleases Yen1 and Mus81–Mms4 for DNA-damage repair in *S. cerevisiae*. *DNA Repair (Amst)* **9**: 394–402.
- Branzei D, Foiani M. 2010. Maintaining genome stability at the replication fork. *Nat Rev Mol Cell Biol* **11**: 208–219.
- Branzei D, Vanoli F, Foiani M. 2008. SUMOylation regulates Rad18-mediated template switch. *Nature* **456**: 915–920.
- Cejka P, Plank JL, Bachrati CZ, Hickson ID, Kowalczykowski SC. 2010. Rmi1 stimulates decatenation of double Holliday junctions during dissolution by Sgs1–Top3. *Nat Struct Mol Biol* **17**: 1377–1382.
- Chan K-L, North PS, Hickson ID. 2007. BLM is required for faithful chromosome segregation and its localization defines a class of ultrafine anaphase bridges. *EMBO J* **26**: 3397–3409.
- Cordon-Preciado V, Ufano S, Bueno A. 2006. Limiting amounts of budding yeast Rad53 S-phase checkpoint activity results in increased resistance to DNA alkylation damage. *Nucleic Acids Res* **34**: 5852–5862.
- Coulon S. 2006. Rad22Rad52-dependent repair of ribosomal DNA repeats cleaved by Slx1–Slx4 endonuclease. *Mol Biol Cell* **17**: 2081–2090.
- Fekairi S, Scaglione S, Chahwan C, Taylor ER, Tissier A, Coulon S, Dong M-Q, Ruse C, Yates JR, Russell P, et al. 2009. Human SLX4 is a Holliday junction resolvase subunit that binds multiple DNA repair/recombination endonucleases. *Cell* **138**: 78–89.
- Flott S, Alabert C, Toh GW, Toth R, Sugawara N, Campbell DG, Haber JE, Pasero P, Rouse J. 2007. Phosphorylation of Slx4 by Mec1 and Tel1 regulates the single-strand annealing mode of DNA repair in budding yeast. *Mol Cell Biol* **27**: 6433–6445.

- Fricke WM, Brill SJ. 2003. Slx1–Slx4 is a second structure-specific endonuclease functionally redundant with Sgs1–Top3. *Genes Dev* **17**: 1768–1778.
- Gaillard P-HL, Noguchi E, Shanahan P, Russell P. 2003. The endogenous Mus81–Eme1 complex resolves Holliday junctions by a nick and counternick mechanism. *Mol Cell* **12**: 747–759.
- Gallo-Fernández M, Saugar I, Ortiz-Bazán MÁ, Vázquez MV, Tercero JA. 2012. Cell cycle-dependent regulation of the nuclease activity of Mus81–Eme1/Mms4. *Nucleic Acids Res* **40**: 8325–8335.
- García V, Furuya K, Carr AM. 2005. Identification and functional analysis of TopBP1 and its homologs. *DNA Repair (Amst)* **4**: 1227–1239.
- Germann SM, Oestergaard VH, Haas C, Salis P, Motegi A, Lisby M. 2011. Dpb11/TopBP1 plays distinct roles in DNA replication, checkpoint response and homologous recombination. *DNA Repair (Amst)* **10**: 210–224.
- Germann SM, Schramke V, Pedersen RT, Gallina I, Eckert-Boulet N, Oestergaard VH, Lisby M. 2014. TopBP1/Dpb11 binds DNA anaphase bridges to prevent genome instability. *J Cell Biol* **204**: 45–59.
- Giannattasio M, Lazzaro F, Plevani P, Muzi-Falconi M. 2005. The DNA damage checkpoint response requires histone H2B ubiquitination by Rad6–Bre1 and H3 methylation by Dot1. *J Biol Chem* **280**: 9879–9886.
- Harrison JC, Haber JE. 2006. Surviving the breakup: the DNA damage checkpoint. *Annu Rev Genet* **40**: 209–235.
- Ho CK, Mazón G, Lam AF, Symington LS. 2010. Mus81 and Yen1 promote reciprocal exchange during mitotic recombination to maintain genome integrity in budding yeast. *Mol Cell* **40**: 988–1000.
- Holt LJ, Tuch BB, Villén J, Johnson AD, Gygi SP, Morgan DO. 2009. Global analysis of Cdk1 substrate phosphorylation sites provides insights into evolution. *Science* **325**: 1682–1686.
- Interthal H, Heyer WD. 2000. MUS81 encodes a novel helix–hairpin–helix protein involved in the response to UV- and methylation-induced DNA damage in *Saccharomyces cerevisiae*. *Mol Gen Genet* **263**: 812–827.
- Ip SCY, Rass U, Blanco MG, Flynn HR, Skehel JM, West SC. 2008. Identification of Holliday junction resolvases from humans and yeast. *Nature* **456**: 357–361.
- Ira G, Malkova A, Liberi G, Foiani M, Haber JE. 2003. Srs2 and Sgs1–Top3 suppress crossovers during double-strand break repair in yeast. *Cell* **115**: 401–411.
- Karras GI, Jentsch S. 2010. The RAD6 DNA damage tolerance pathway operates uncoupled from the replication fork and is functional beyond S phase. *Cell* **141**: 255–267.
- Li M, Brill SJ. 2005. Roles of SGS1, MUS81, and RAD51 in the repair of lagging-strand replication defects in *Saccharomyces cerevisiae*. *Curr Genet* **48**: 213–225.
- Liberi G, Maffioletti G, Lucca C, Chiolo I, Baryshnikova A, Cotta-Ramusino C, Lopes M, Pelliccioli A, Haber JE, Foiani M. 2005. Rad51-dependent DNA structures accumulate at damaged replication forks in sgs1 mutants defective in the yeast ortholog of BLM RecQ helicase. *Genes Dev* **19**: 339–350.
- Mankouri HW, Ashton TM, Hickson ID. 2011. Holliday junction-containing DNA structures persist in cells lacking Sgs1 or Top3 following exposure to DNA damage. *Proc Natl Acad Sci* **108**: 4944–4949.
- Mankouri HW, Huttner D, Hickson ID. 2013. How unfinished business from S-phase affects mitosis and beyond. *EMBO J* **32**: 2661–2671.
- Matos J, Blanco MG, Maslen S, Skehel JM, West SC. 2011. Regulatory control of the resolution of DNA recombination intermediates during meiosis and mitosis. *Cell* **147**: 158–172.
- Matos J, Blanco MG, West SC. 2013. Cell-cycle kinases coordinate the resolution of recombination intermediates with chromosome segregation. *Cell Rep* 1–11.
- Mordes DA, Nam EA, Cortez D. 2008. Dpb11 activates the Mec1–Ddc2 complex. *Proc Natl Acad Sci* **105**: 18730–18734.
- Mullen JR, Kaliraman V, Ibrahim SS, Brill SJ. 2001. Requirement for three novel protein complexes in the absence of the Sgs1 DNA helicase in *Saccharomyces cerevisiae*. *Genetics* **157**: 103–118.
- Muñoz IM, Hain K, Déclais A-C, Gardiner M, Toh GW, Sanchez-Pulido L, Heuckmann JM, Toth R, Macartney T, Eppink B, et al. 2009. Coordination of structure-specific nucleases by human SLX4/BTBD12 is required for DNA repair. *Mol Cell* **35**: 116–127.
- Nash P, Tang X, Orlicky S, Chen Q, Gertler FB, Mendenhall MD, Sicheri F, Pawson T, Tyers M. 2001. Multisite phosphorylation of a CDK inhibitor sets a threshold for the onset of DNA replication. *Nature* **414**: 514–521.
- Navadgi-Patil VM, Burgers PM. 2008. Yeast DNA replication protein Dpb11 activates the Mec1/ATR checkpoint kinase. *J Biol Chem* **283**: 35853–35859.
- Ohouo PY, Bastos de Oliveira FM, Almeida BS, Smolka MB. 2010. DNA damage signaling recruits the Rtt107–Slx4 scaffolds via Dpb11 to mediate replication stress response. *Mol Cell* **39**: 300–306.
- Ohouo PY, de Oliveira FMB, Liu Y, Ma CJ, Smolka MB. 2012. DNA-repair scaffolds dampen checkpoint signalling by counteracting the adaptor Rad9. *Nature* **493**: 120–124.
- Pfander B, Diffley JFX. 2011. Dpb11 coordinates Mec1 kinase activation with cell cycle-regulated Rad9 recruitment. *EMBO J* **30**: 4897–4907.
- Pfander B, Moldovan GL, Sacher M, Hoegge C, Jentsch S. 2005. SUMO-modified PCNA recruits Srs2 to prevent recombination during S phase. *Nature* **436**: 428–433.
- Prakash S, Johnson RE, Prakash L. 2005. Eukaryotic translesion synthesis DNA polymerases: specificity of structure and function. *Annu Rev Biochem* **74**: 317–353.
- Puddu F, Granata M, Di Nola L, Balestrini A, Piergiovanni G, Lazzaro F, Giannattasio M, Plevani P, Muzi-Falconi M. 2008. Phosphorylation of the budding yeast 9-1-1 complex is required for Dpb11 function in the full activation of the UV-induced DNA damage checkpoint. *Mol Cell Biol* **28**: 4782–4793.
- Rappas M, Oliver AW, Pearl LH. 2011. Structure and function of the Rad9-binding region of the DNA-damage checkpoint adaptor TopBP1. *Nucleic Acids Res* **39**: 313–324.
- Robert T, Dervins D, Fabre F, Gangloff S. 2006. Mrc1 and Srs2 are major actors in the regulation of spontaneous crossover. *EMBO J* **25**: 2837–2846.
- Roberts TM, Kobor MS, Bastin-Shanower SA, Ii M, Horte SA, Gin JW, Emili A, Rine J, Brill SJ, Brown GW. 2006. Slx4 regulates DNA damage checkpoint-dependent phosphorylation of the BRCT domain protein Rtt107/Esc4. *Mol Biol Cell* **17**: 539–548.
- Saugar I, Vazquez MV, Gallo-Fernandez M, Ortiz-Bazan MA, Segurado M, Calzada A, Tercero JA. 2013. Temporal regulation of the Mus81–Mms4 endonuclease ensures cell survival under conditions of DNA damage. *Nucleic Acids Res* **41**: 8943–8958.
- Schwartz EK, Wright WD, Ehmsen KT, Evans JE, Stahlberg H, Heyer WD. 2012. Mus81–Mms4 functions as a single heterodimer to cleave nicked intermediates in recombinational DNA repair. *Mol Cell Biol* **32**: 3065–3080.
- Snead JL, Sullivan M, Lowery DM, Cohen MS, Zhang C, Randle DH, Taunton J, Yaffe MB, Morgan DO, Shokat KM. 2007. A coupled chemical-genetic and bioinformatic approach to

- Polo-like kinase pathway exploration. *Chem Biol* **14**: 1261–1272.
- Svendsen JM, Smogorzewska A, Sowa ME, O'Connell BC, Gygi SP, Elledge SJ, Harper JW. 2009. Mammalian BTBD12/SLX4 assembles a Holliday junction resolvase and is required for DNA repair. *Cell* **138**: 63–77.
- Szakal B, Branzei D. 2013. Premature Cdk1/Cdc5/Mus81 pathway activation induces aberrant replication and deleterious crossover. *EMBO J* **32**: 1155–1167.
- Tanaka S, Umemori T, Hirai K, Muramatsu S, Kamimura Y, Araki H. 2007. CDK-dependent phosphorylation of Sld2 and Sld3 initiates DNA replication in budding yeast. *Nature* **445**: 328–332.
- Tomkinson AE, Bardwell AJ, Bardwell L, Tappe NJ, Friedberg EC. 1993. Yeast DNA repair and recombination proteins Rad1 and Rad10 constitute a single-stranded-DNA endonuclease. *Nature* **362**: 860–862.
- Wyatt HDM, Sarbajna S, Matos J, West SC. 2013. Coordinated actions of SLX1–SLX4 and MUS81–EME1 for Holliday junction resolution in human cells. *Mol Cell* **52**: 234–247.
- Yu X. 2003. The BRCT domain is a phospho-protein binding domain. *Science* **302**: 639–642.
- Zegerman P, Diffley JFX. 2007. Phosphorylation of Sld2 and Sld3 by cyclin-dependent kinases promotes DNA replication in budding yeast. *Nature* **445**: 281–285.
- Zhang T, Nirantar S, Lim HH, Sinha I, Surana U. 2009. DNA damage checkpoint maintains Cdh1 in an active state to inhibit anaphase progression. *Dev Cell* **17**: 541–551.

## **Supplemental Information – Outline**

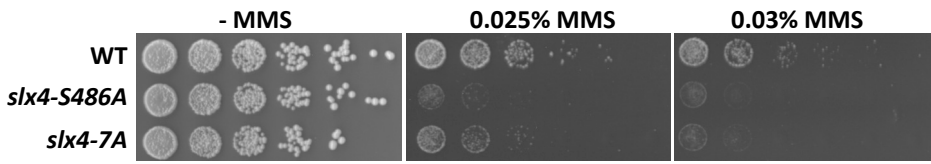
- Supplemental Figures
- Supplemental Figure Legends
- Supplemental Methods
- References



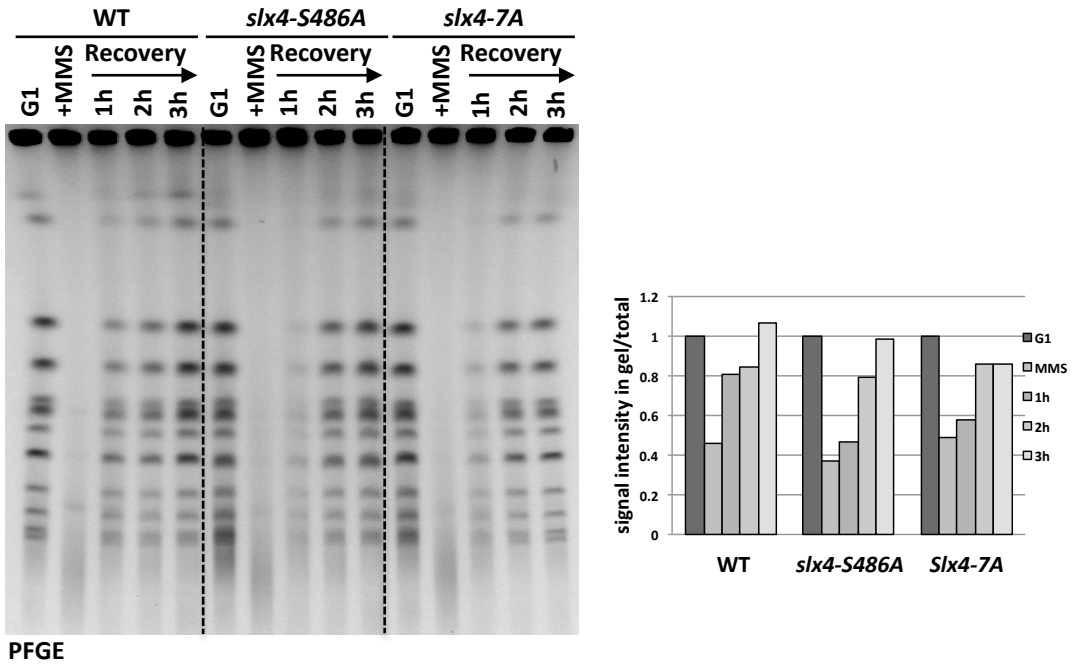
### Dpb11/TopBP1 interaction motif in Slx4 proteins from different eukaryotes

Sp	156	GFYYHR-----KPQLFEKSLLEKLGNK---SLEA-NR---SPLIKELC	190
Sc	458	QFFTPN--TSPLDGIIDLTQE-----SFKA-VRSLISPLKVENN	493 (S486)
Kl	372	KTKREYSRANINDQLINISQT-----SYDV-VSSIVSPMKAQRT	409
Ec	347	PDESPDNLPIHEDTVIDLTQE-----TFRA-VSNIASPVKATSR	384
Nc	494	SQSPTPGTSPQQDEIIDLTOE-----SFKA-VGRLISPVRPPTL	531
Ka	374	SIFSAHPSPEKPDNIIDLTVG-----SFKA-VKSLVSPKPDV	411
Td	282	QFYTPR--TPPDDEIIDLTOE-----SFKV-VKSLISPLKD---	314
Zr	305	DAGTPKTAHSPSDGVIDLTNG-----SFKV-VKSLISPLK----	338
Vp	391	QFFTADG--NMVDGVIDLTQG-----SFKA-VTKLFSPLKVDTL	426
Lt	385	HTYRTPSGLAGRDQLIDLTOE-----SFNA-VKSLISPLKS---	419
Hs	1236	WLFCDRESSPSEASTTDTSW-----LVPA-TP-LASRSRDCSS	1271 (T1260)
Sb	1196	WLFCDRESSPEEGSTTDTSW-----LVPA-TP-LAGRSRDCSS	1231
Mm	1038	WLLCSQKTSLEDESATDTSW-----LVPA-TP-GVRSRDCSS	1073
Rn	1242	WLFCSQTPSLGEDSATSSW-----LVPA-TP-GASKSRDRSS	1277
Sh	1214	RPVTRHE----ESSTTDTSW-----LVPA-TP-LTNRSHDCSS	1245
Tm	1250	QLFCKAESSP-EASTTDTSW-----LVPA-TP-LASRGCHRSS	1284
Oo	1244	QLFCDPKISGDESTTDTSW-----LVPA-TP-LASRSRDCSS	1279
Xt	1129	EVPQIST--IQSAFHYN-SLSPPL----LSPAKSP-AKPLSPPVSP	1166
Dr	1168	DVSRASTMGHLAQGVQPSSTP-----VHSVGS--LQRKILFDSP	1207
Dm	281	EGPIDLESYYVTDLFEVSRTPAHLLKNWAAI-QGRDFSPERETQK	326
Dg	283	EESLANLSAYYVQDLFEVSRTPAHLLKNWAAI-QGRDLSPKRPSKE	328
Dw	276	EDPIELN-VYYVKDLIEISYTPAEHLLKDWSAI-QGRDLSPKRLNPK	320
Cc	325	DEHRANLDEFYVRSLEEVANVQAGYLLKDWHAI-EGRDKSPKHRPNK	370
Ag	343	LPSEQLMEMYYPELLEANPAPVGCMLKDWSKI-PGRECTPERELDG	388

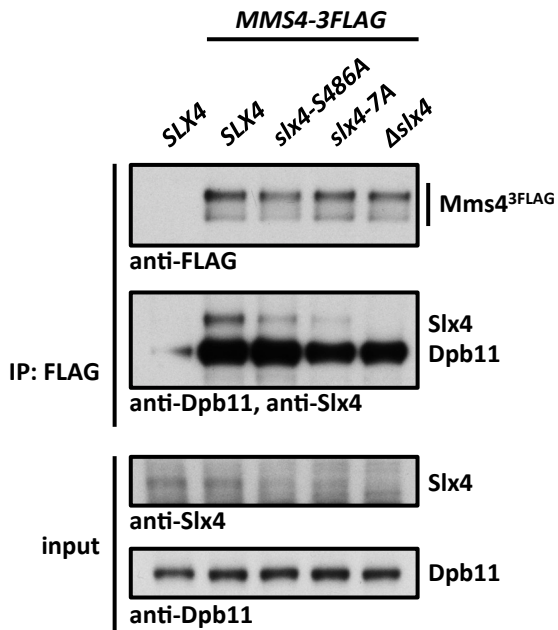
A



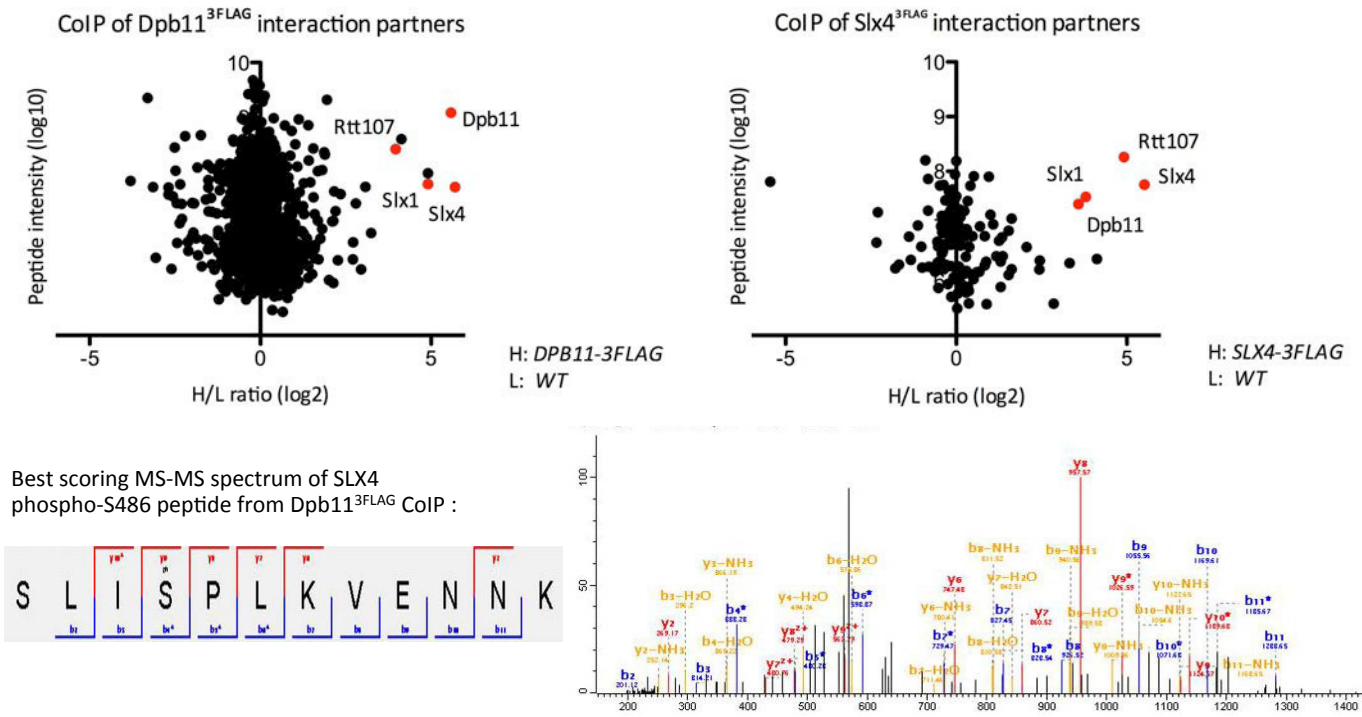
B



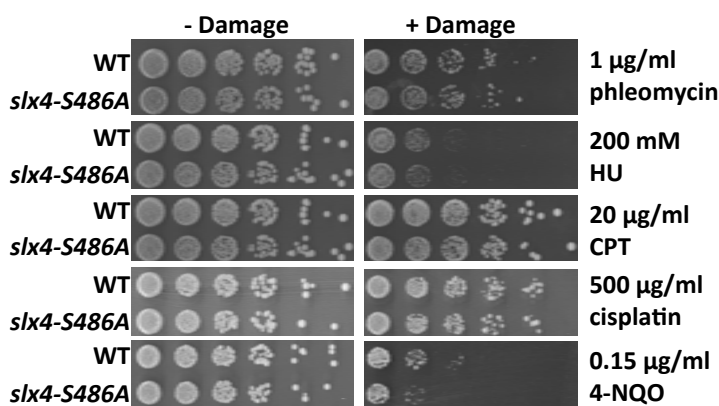
C



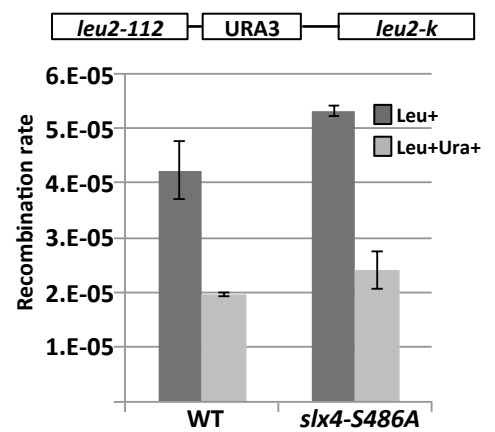
A



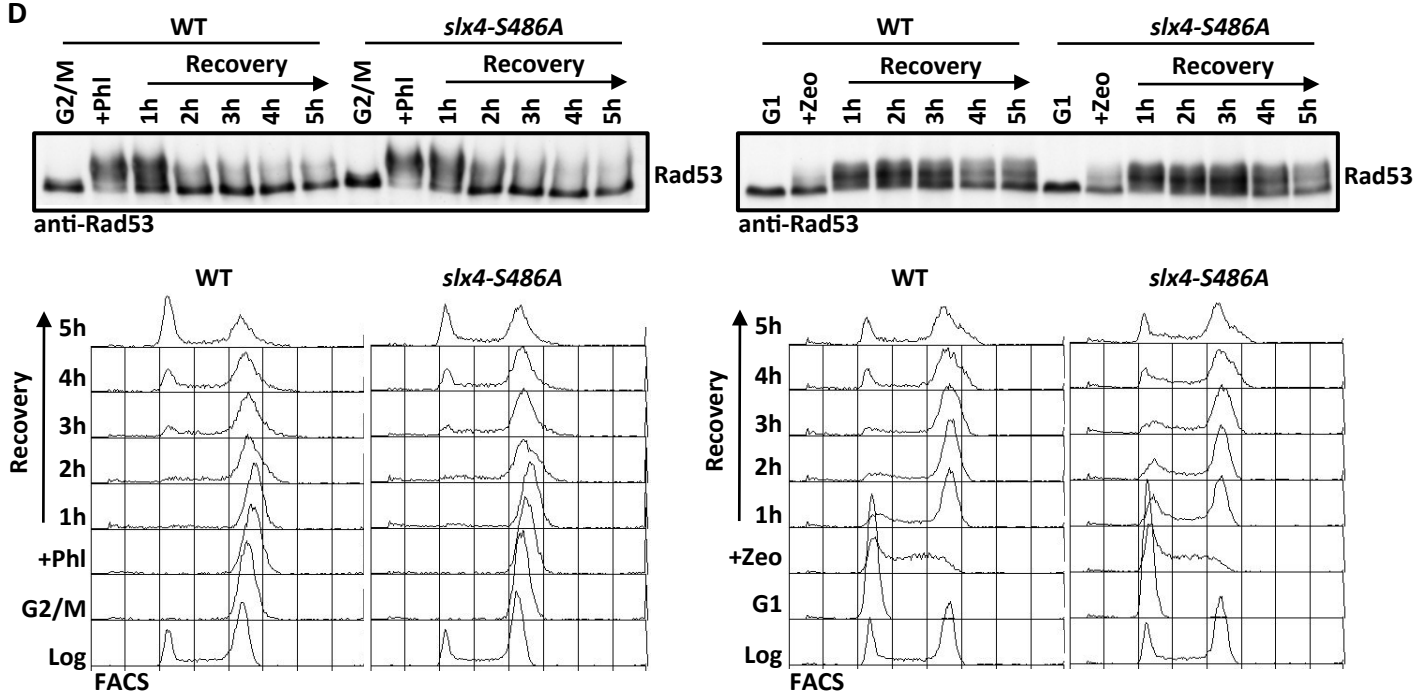
B



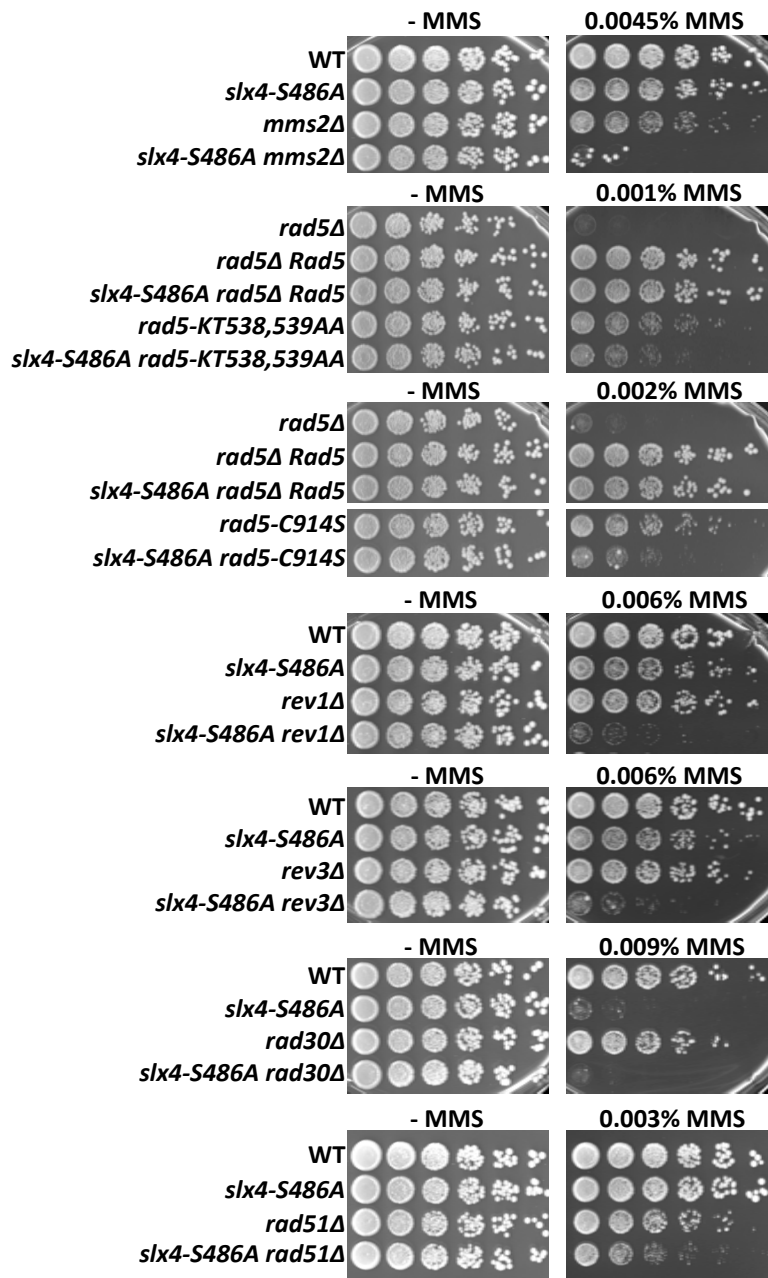
C



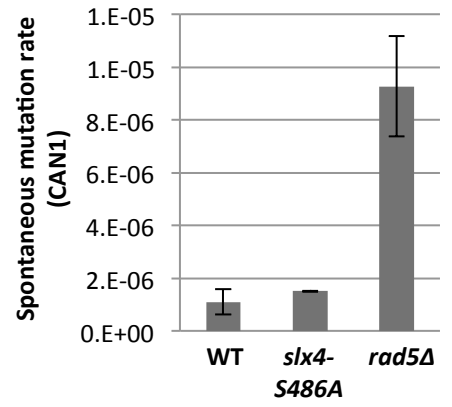
D



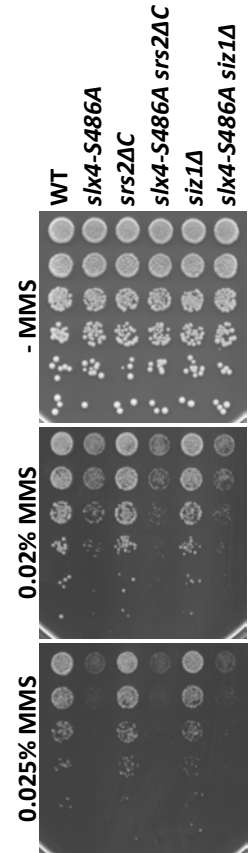
A



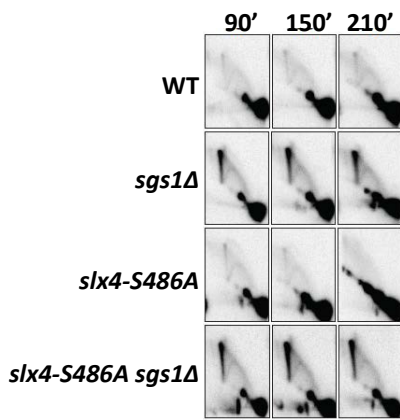
B



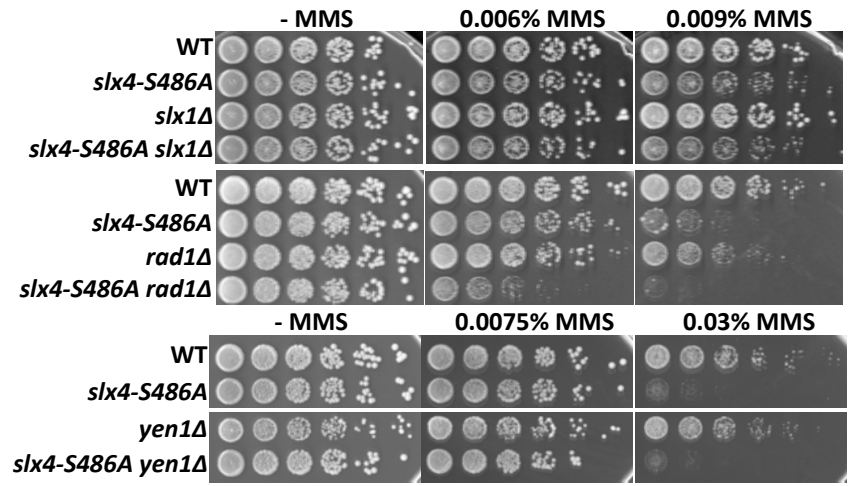
C



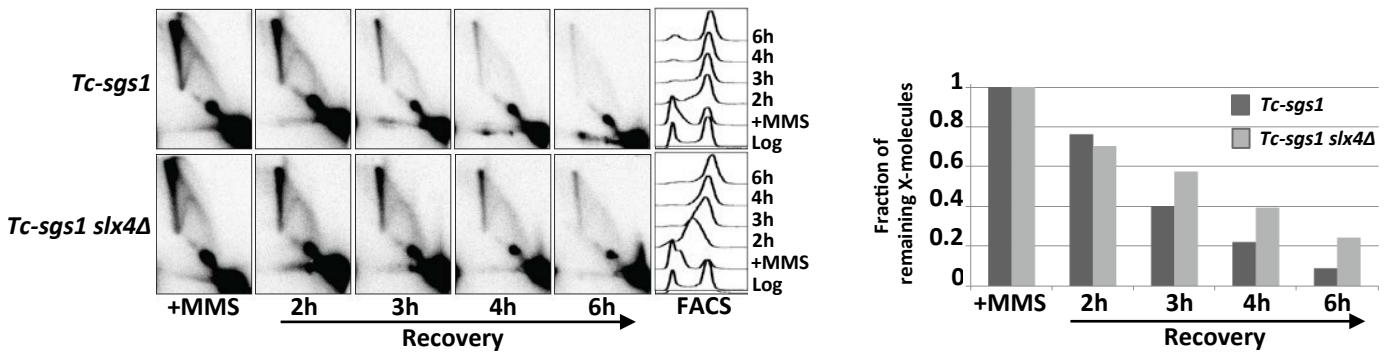
A



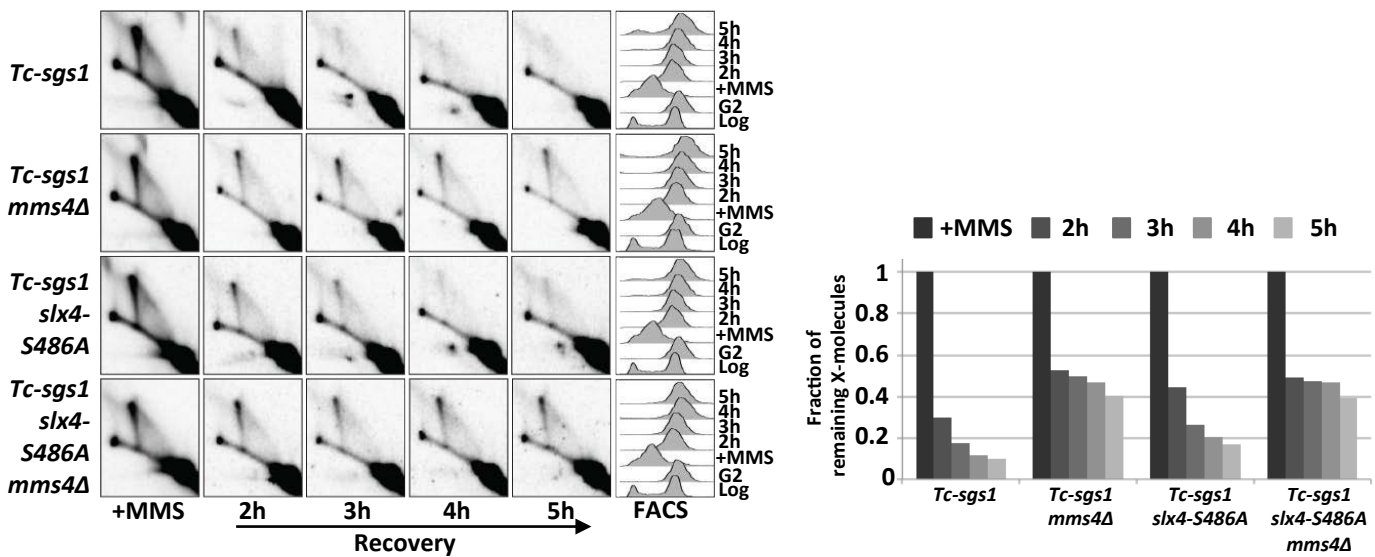
D



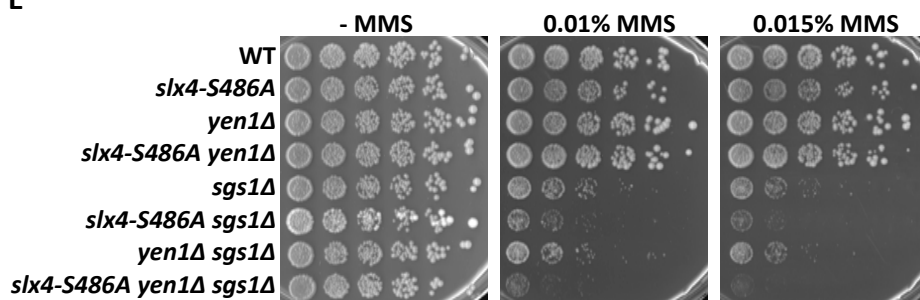
B



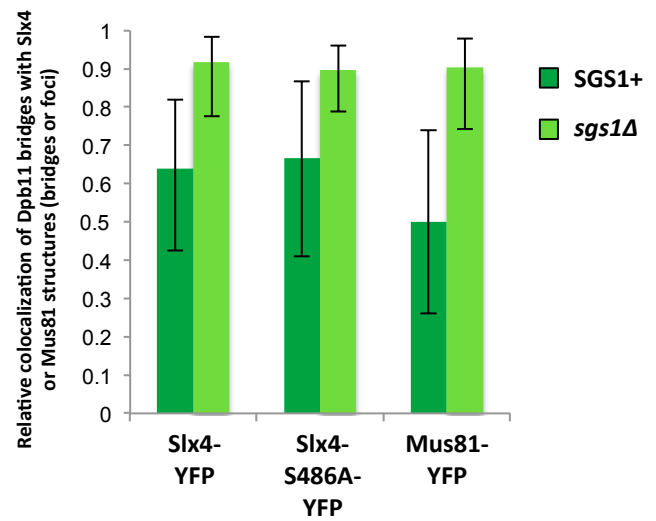
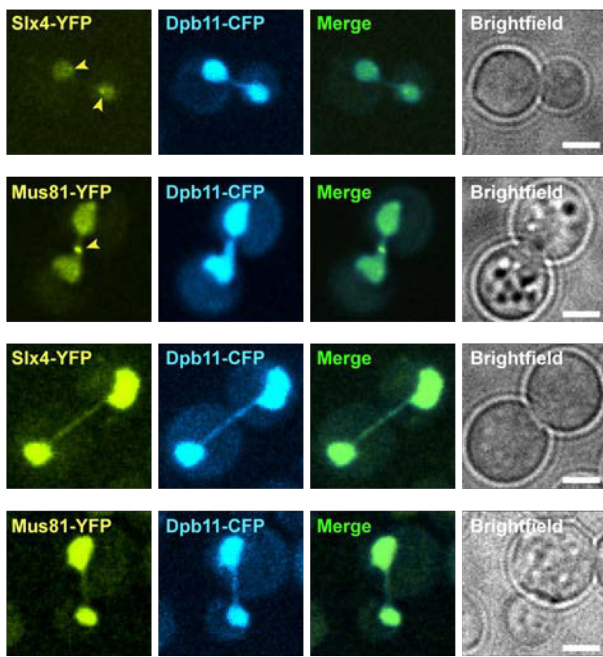
C



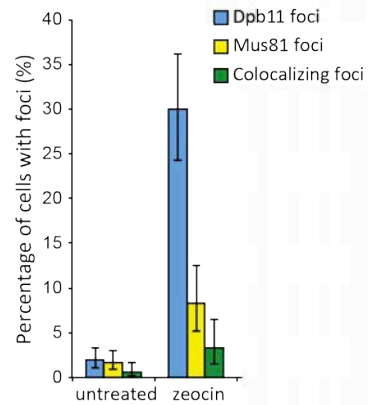
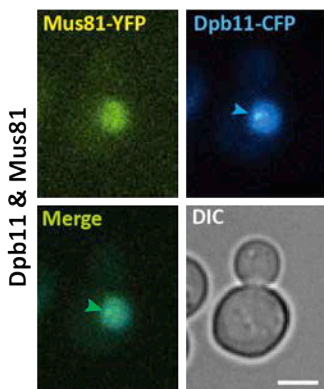
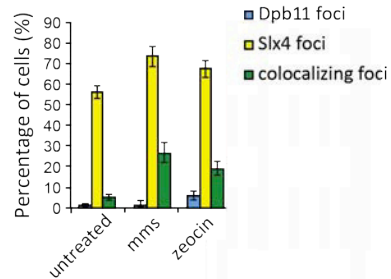
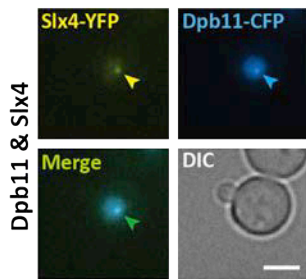
E



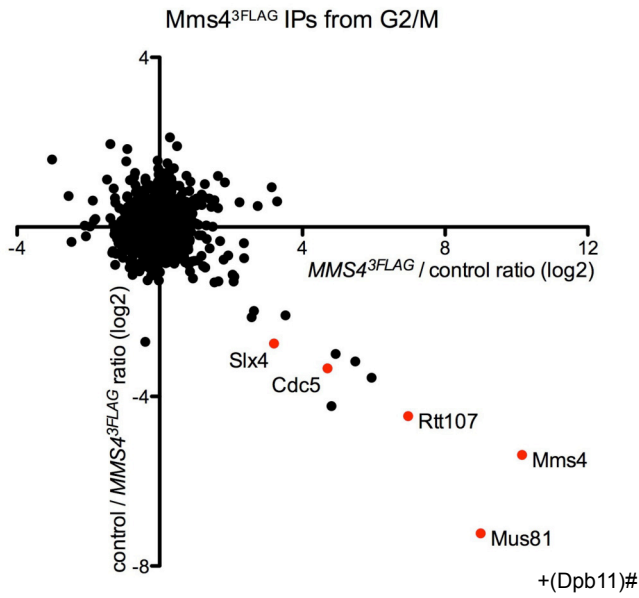
A



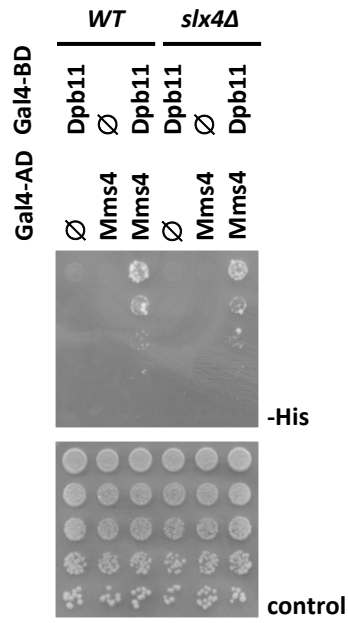
B



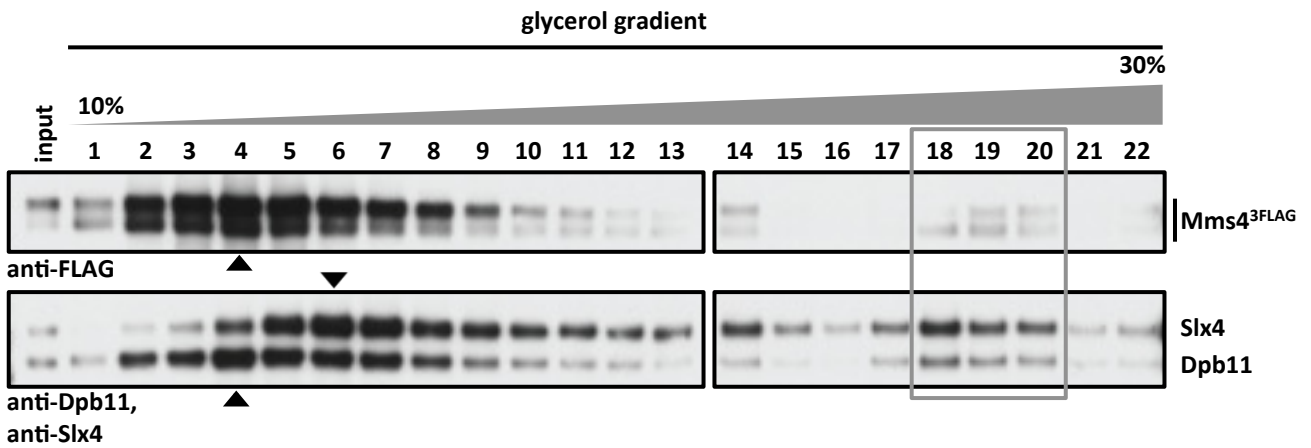
A



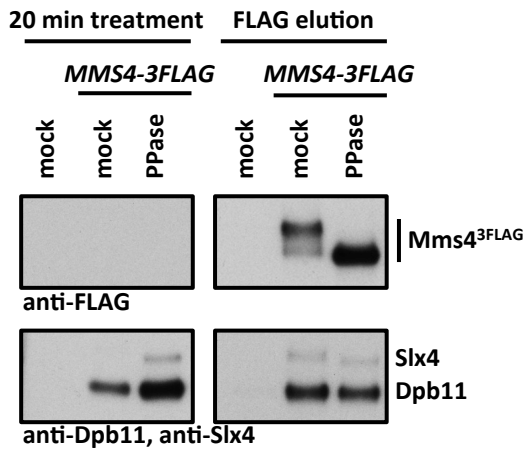
C



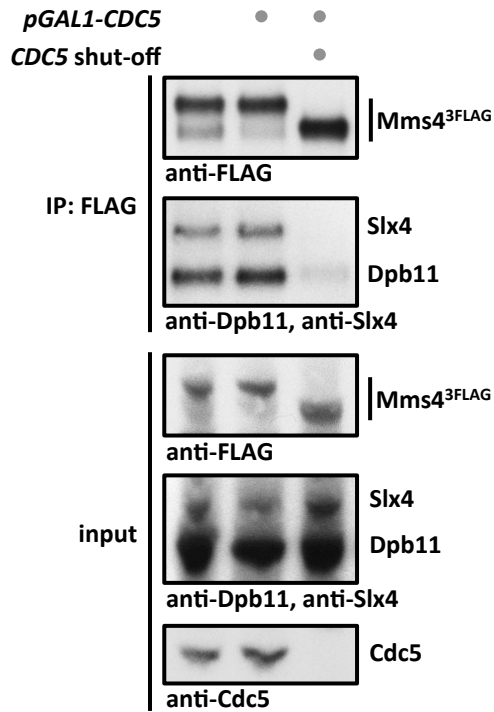
B



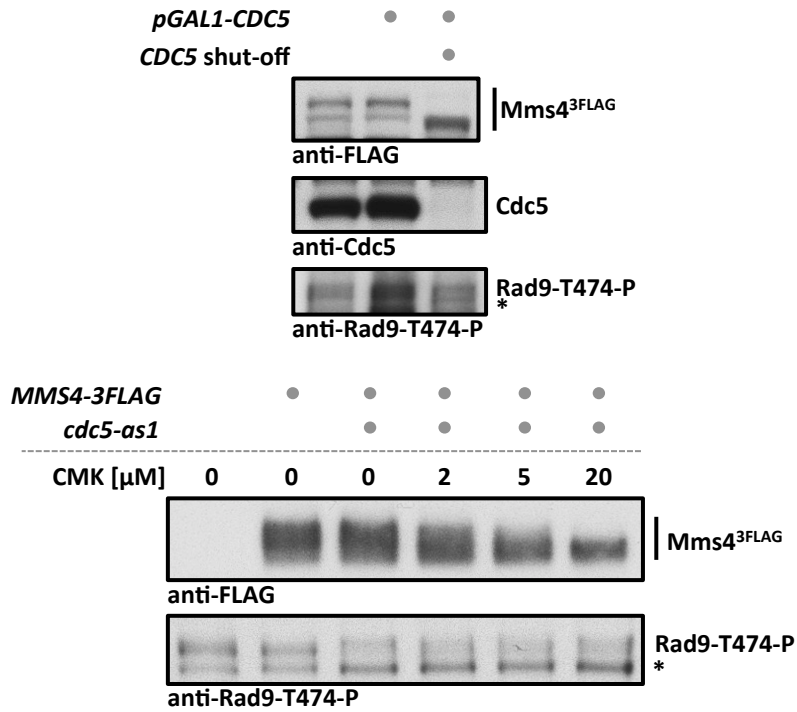
D



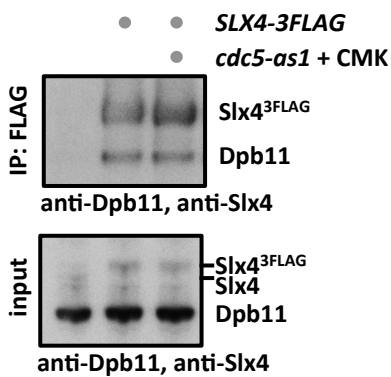
A



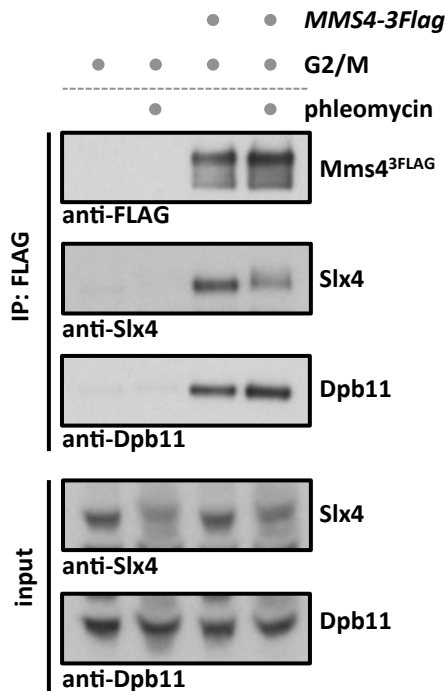
B



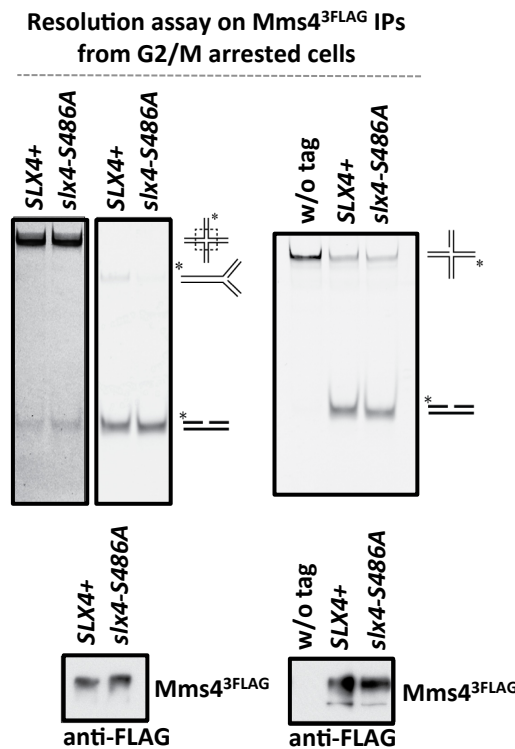
C



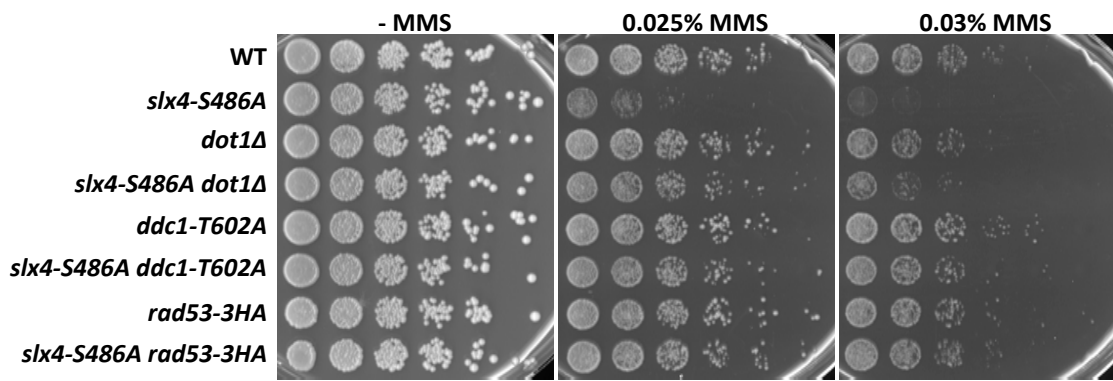
D



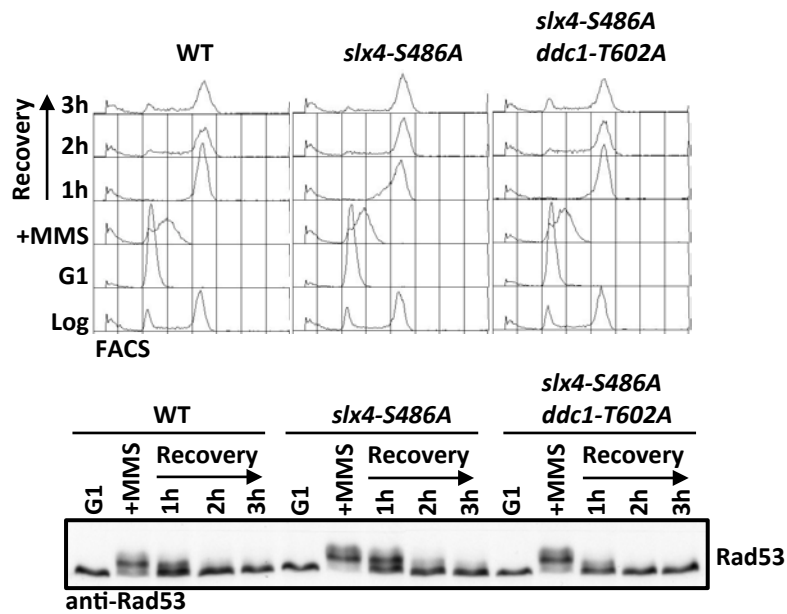
E



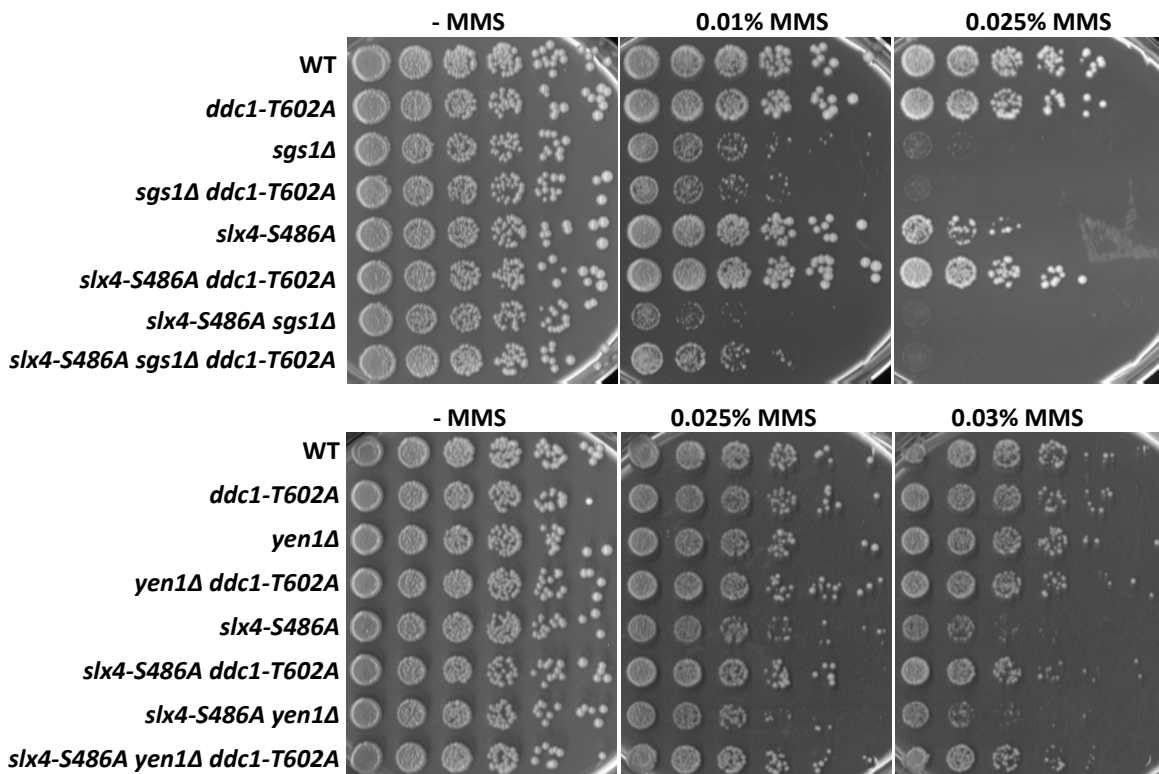
A



B



C



## Supplemental Figure Legends

### Figure S1.

**The binding surface of the evolutionary conserved Slx4 and Dpb11 complex contains BRCT3+4 of Dpb11 and S486 of Slx4 in *S. cerevisiae*.**

**A** Slx4 binds to Dpb11 fragments containing BRCT3+4. Pulldown of Slx4 from undamaged or phleomycin-treated G1 or G2/M cell extracts using GST-Dpb11 fragments (N: aa 1-275, M: aa 276-600, C: aa 556-764,  $\Delta$ C: aa 1-600).

**B** Mutation of the Dpb11 BRCT3+4 phospho-protein binding surface reduces Slx4 binding to Dpb11. Two-hybrid analysis of GAL4-BD fused to *WT* Dpb11 or to Dpb11-T451A, and GAL4-AD fusions with Slx4.

**C** A region in Slx4 sequence between aa 461 and aa 490 is important for Dpb11 interaction. Two-hybrid analysis of GAL4-BD (left panel) fused to *WT* Dpb11 or to the BRCT3+4 fragment, and GAL4-AD fusions with Slx4 C-terminal fragments. Expression of the constructs was verified by western blot analysis (right panel).

**D** Mutation of S486 in Slx4 to a non-phosphorylatable alanine residue reduces Dpb11 binding. Two-hybrid analysis of GAL4-BD (left panel) fused to *WT* Dpb11 or to the BRCT3+4 fragment, and GAL4-AD fusions with *WT* Slx4 or with Slx4-S486A. Expression of the constructs was verified by western blot analysis (right panel).

**E** The presence of DNA damage does not stimulate TopBP1 binding to Slx4 in human cells. Co-immunoprecipitation of <sup>myc</sup>TopBP1 with <sup>GFP</sup>Slx4 and <sup>GFP</sup>Slx4 $\Delta$ N after transient overexpression in HEK 293T cells.

Cells were left untreated or treated with 0.001% or 0.003% (++) MMS or 100  $\mu$ g/ml zeocin for 30 min to induce DNA damage.

**F** The Slx4-Dpb11 interaction is regulated by cell cycle phase and DNA damage. Co-

immunoprecipitation of Slx4 and Dpb11<sup>3FLAG</sup> from G1 or G2/M arrested cells, which were either damaged by 50 µg/ml phleomycin or left untreated.

### **Figure S2.**

#### **A phosphorylation-dependent Dpb11/TopBP1 binding motif in eukaryotic Slx4 proteins.**

Slx4 proteins from different eukaryotes comprise a conserved, short linear motif, which harbours serine 486 in budding yeast and threonine 1260 in humans. Multiple sequence alignment of the Dpb11/TopBP1 interaction motif. Conserved residues in more than one class are highlighted in yellow. Phosphorylation sites in *Saccharomyces cerevisiae* and *Homo sapiens*, as well as predicted sites as inferred from homology are indicated in red, alternative sites with unclear homology in light green. Species abbreviations, as well as accession numbers are listed in Supplementary Table 2.

### **Figure S3.**

#### **Mutation of seven SQ/TQ motifs in the C-terminus of Slx4 leads to similar phenotypes as the *slx4-S486A* mutation.**

**A** The *slx4-S486A* and *slx4-7A* mutants are hyper-sensitive to MMS. *WT* or strains expressing *slx4-S486A* or the *slx4-7A* as only copy of Slx4 from the *SLX4* promoter were spotted in 5-fold serial dilutions on MMS-containing media and assayed for growth after two days. **B** Replication fork stalling is prolonged in the *slx4-S486A* and *slx4-7A* mutant. Cells were treated with a pulse of MMS during S-phase and recovery was analysed by pulsed-field gel electrophoresis to measure intact, fully replicated chromosomes. For

quantification, the fluorescence signal of chromosomes that migrated into the gel was divided by the total signal including the pocket and all signals normalized to the G1 sample from each strain. **C** The *Slx4-7A* and *Slx4-S486A* mutant proteins show reduced binding to Mms4 and Dpb11. Co-immunoprecipitation of endogenous Dpb11 and Slx4 with Mms4<sup>3FLAG</sup> in combination with phosphorylation-deficient mutants of Slx4, S486A or 7A, or Slx4 deletion from G2/M arrested cells.

#### **Figure S4.**

##### **Analysis of composition and function of the Slx4-Dpb11 complex.**

**A** Slx4 and Dpb11 are part of a multi-protein complex containing Rtt107 and Slx1. Co-immunoprecipitations of Dpb11<sup>3FLAG</sup> (left panel) and Slx4<sup>3FLAG</sup> (right panel) were compared to purifications from untagged control strains using a SILAC setup. Cells were treated with 0.033% MMS, whereby strains containing Dpb11<sup>3FLAG</sup>/Slx4<sup>3FLAG</sup> were grown in heavy (<sup>15</sup>N<sub>2</sub> <sup>13</sup>C<sub>6</sub> lysine (Lys8) and <sup>15</sup>N<sub>4</sub> <sup>13</sup>C<sub>6</sub> arginine (Arg10)) medium, untagged control strains in light medium. Proteins shown in red are enriched in both purifications (Dpb11, Slx4, Rtt107, Slx1). The best scoring MS-MS spectra of the Slx4 peptide containing phosphorylated S486A from the Dpb11<sup>3FLAG</sup> CoIP is shown. This peptide showed an H/L ratio of 17 in the Dpb11<sup>3FLAG</sup> pulldown. **B** The *slx4-S486A* mutant is slightly sensitive to 4-NQO (in addition to MMS (Fig. 3B)), but not to other DNA damaging drugs. *WT* cells or the *slx4-S486A* mutant were spotted in 5-fold serial dilutions on media containing phleomycin, HU, CPT, cisplatin and 4-NQO and assayed for growth after two days. **C** The *slx4-S486A* mutant has a similar recombination rate compared to *WT*.

Recombination rates were measured using an intrachromosomal direct-repeat system (*leu2-112::URA3::leu2-k*, Aguilera and Klein 1988). Fluctuation analysis was performed using 10 independent cultures and recombinants were determined by plating on plates lacking leucine or leucine and uracil. Single colonies were counted and recombination rates were calculated using a maximum-likelihood method. The shown values represent means of three independent experiments. Error bars represent standard deviations. **D** The checkpoint response after treatment with DSB-inducing agents is similar in *WT* and *slx4-S486A* cells. Cells were treated with a 30 min pulse of 50 µg/ml phleomycin or zeocin during G2/M- or S-phase (see samples +Phl/+Zeo) and recovery was analysed by checkpoint activity as determined by anti-Rad53 western blot (upper panel) and by cellular DNA content as determined by FACS (lower panel).

### **Figure S5.**

**The Slx4-Dpb11 complex is not exclusively involved in either post-replicative repair (PRR) or homologous recombination (HR).**

**A** A defect in the Dpb11-Slx4 complex further enhances the hyper-sensitivity of PRR and HR mutants. Strains expressing *slx4-S486A* as endogenous copy of Slx4 alone or in combination with mutants defective in error-free PRR (*mms2Δ*, *rad5-KT538,539AA* and *rad5-C914S*), error-prone PRR (*rev1Δ*, *rev3Δ* and *rad30Δ*) or HR (*rad51Δ*) were spotted in 5-fold serial dilutions on MMS-containing media and assayed for growth after two days. **B** The spontaneous mutagenesis rate of the *slx4-S486A* mutant is similar to *WT*. A forward mutagenesis assay was performed using a *CAN1* tester strain and

resistance to canavanine. Fluctuation analysis was carried out with 10 independent cultures. Colonies on canavanine-containing plates were counted and mutation rates were determined using a maximum-likelihood approach. The mean from 2 independent experiments is shown. Error bars represent standard deviations. **C** Up-regulation of HR at replication forks does not rescue the MMS hyper-sensitivity of *slx4-S486A* mutants. Strains expressing *WT* Slx4 or *slx4-S486A* in combination with *siz1Δ* or *srs2ΔC* were spotted as in A.

### **Figure S6.**

**The Slx4-Dpb11 complex is involved in JM resolution by Mus81-Mms4 and functions separately from Sgs1, Yen1 and Rad1-Rad10.**

**A** DNA joint molecules form to a similar extent in *sgs1Δ* and *sgs1Δ slx4-S486A*. Cells were treated with 0.033% MMS in S-phase and after 90', 150' and 210' X-shaped JMs were visualized as spike signals in 2D gels. **B** JM structures are resolved slower in *slx4Δ tc-sgs1* cells. A conditional *sgs1* (*tc-sgs1*) allele was used because of *sgs1Δ slx4Δ* lethality (Mullen et al. 2001). In the *tc-sgs1* allele, Sgs1 translation is prevented upon addition of tetracycline (Gonzalez-Huici et al. 2014). Cells were treated with a pulse of MMS in S-phase and the profile of recombination intermediates was examined 0 h, 2 h, 3 h, 4 h and 6 h after release from MMS. X-shaped JMs were visualized as spike signal in 2D gels in *tc-sgs1* and *slx4Δ tc-sgs1* mutants. **C** The JM resolution defect in *slx4-S486A* mutants is weaker than in *mms4Δ* and both mutants show epistasis. *Tc-sgs1* inactivation and experiment as in B, but

samples were examined 0 h, 2 h, 3 h, 4 h and 5 h after release from MMS. **D** The Slx4-Dpb11 complex function in response to MMS is not related to the structure-specific endonucleases Rad1-Rad10, Slx1 or Yen1. Strains expressing *slx4-S486A* as endogenous copy of Slx4 alone or in combination with *rad1Δ*, *slx1Δ* and *yen1Δ* were spotted in 5-fold serial dilutions on MMS-containing media and assayed for growth after two days. **E** The *yen1Δ* increases MMS sensitivity of the *sgs1Δ slx4-S486A* double mutant, but not of either single mutant. *yen1Δ*, *sgs1Δ*, *slx4-S486A* mutants alone and double and triple mutant combinations were spotted as in D.

**Figure S7.**

**Slx4 and Mus81 structures co-localize with Dpb11 anaphase bridge. A**

Quantification of Slx4 and Mus81 foci and bridges at Dpb11 anaphase bridges. *WT* or *sgs1Δ* cells expressing Dpb11<sup>CFP</sup> and Slx4<sup>YFP</sup>, Slx4-S486A<sup>YFP</sup> or Mus81<sup>YFP</sup> were subjected to live cell fluorescence microscopy. Representative examples of Slx4 and Mus81 foci and bridges co-localizing with Dpb11 anaphase bridges are shown. Scale bar, 3 μm. Yellow arrowhead marks foci. Error bars correspond to 95% confidence intervals. **B** Slx4<sup>YFP</sup> and Mus81<sup>YFP</sup> show a partial co-localization with Dpb11<sup>CFP</sup> in spontaneous and DNA damage induced foci. Cells were treated with 0.03% MMS or 200 μg/ml zeocin for 1 h and co-localization (green arrow) of Dpb11<sup>CFP</sup> with Slx4<sup>YFP</sup> (top panel) and Mus81<sup>YFP</sup> (lower panel) in foci was scored manually. Error bars correspond to 95% confidence intervals. Arrowheads mark foci.

## Figure S8.

### **Mus81-Mms4 forms a complex with Dpb11 and Slx4.**

**A** Mus81-Mms4 from mitotic cells binds specifically to Dpb11, Slx4 and Rtt107. A SILAC MS experiment comparing an Mms4<sup>3FLAG</sup> IP to a control IP from an untagged strain using <sup>15</sup>N<sub>2</sub> <sup>13</sup>C<sub>6</sub> lysine (Lys8) and Lys-C digestion is shown. All cells were arrested in mitosis by nocodazole. H/L ratios from two label-switch experiments without ratio count cut-off are plotted. #, as the only protein of the analysis Dpb11 displayed exclusively peptides, which were derived from the Mms4<sup>3FLAG</sup> IP samples, but not the control samples, making Dpb11 a highly specific interactor of Mus81-Mms4. **B** Slx4, Dpb11 and Mus81-Mms4 are part of one multi-protein complex. Mms4<sup>3FLAG</sup> immunoprecipitates (as in A) from G2/M arrested cells were subjected to glycerol gradient (10%-30%) centrifugation. Slx4, Dpb11 and Mms4 co-migrate in fractions 18-20 (marked by box), corresponding to a multi-protein complex with an apparent molecular weight of 1-1.5 MDa. Arrowheads indicate elution peaks of single proteins. **C** The Dpb11-Mms4 interaction is independent of Slx4. Two-hybrid analysis in WT and *slx4Δ* cells with Gal4-BD-Dpb11 and Gal4-AD-Mms4. **D** Dpb11 and Slx4 binding to Mms4 is partially phosphatase-sensitive. Mms4<sup>3FLAG</sup> immunoprecipitates (as in A) from G2/M arrested cells were either mock treated or treated with 24,000 U/ml λ-phosphatase for 20 min at 4°C. Shown is the phosphatase eluate and a 3xFLAG peptide-eluate of the remaining bound material.

## Figure S9.

### **Mus81-Mms4 show a Cdc5-dependent association with Slx4-Dpb11 in mitosis.**

**A** Mms4 interaction with the Slx4-Dpb11 complex is dependent on Polo-like kinase Cdc5 activity. *CDC5* was expressed from a pGAL1-10 promoter. Cells were grown in raffinose-containing medium, arrested in G1, then expression was either induced in G1 by switching cells to galactose-containing medium prior to G2/M arrest (lane 2) or shut-off in G1 by switching cells to glucose-containing medium (lane 3). Co-immunoprecipitations of Mms4<sup>3FLAG</sup> were performed from the corresponding cell extracts and tested for binding to Dpb11 and Slx4. **B** CDK activity is not influenced by interfering with Cdc5 activity. TCA samples of experiments shown in Fig. 5C and Fig. S9A were tested for CDK-mediated phosphorylation of Rad9-T474 by using a phospho-specific antibody in western blot analysis. The asterisk denotes a cross-reactive band. **C** The Slx4-Dpb11 interaction is not dependent on the Polo-like kinase Cdc5. Co-immunoprecipitation of Dpb11 and Slx4<sup>3FLAG</sup> from G2/M arrested cells or G2/M arrested cells, in which Cdc5 has been inactivated by using the *cdc5-as1* allele and 10  $\mu$ M CMK. **D** The formation of the Slx4-Dpb11-Mms4-Mus81 complex is not influenced by the presence of DNA damage. Co-immunoprecipitation samples of Mms4<sup>3FLAG</sup> cell extracts from G2/M arrested cells, which were either damaged by 50  $\mu$ g/ml phleomycin or left untreated, were tested for binding to Dpb11 and Slx4. **E** Cell cycle regulation of Mus81-Mms4 nuclease activity remains intact in the *slx4-S486A* mutant. Mms4<sup>3FLAG</sup> and control IPs from cells arrested at G2/M with nocodazole (see lower panel for the inputs) were incubated with

fluorescence-labelled Holliday junction, replication fork and nicked Holliday junction substrates.

**Figure S10.**

**Partial inactivation of the DNA damage checkpoint rescues the defects of the *slx4-S486A* mutant in response to MMS.**

**A** A partial defect in DNA damage checkpoint signalling suppresses the *slx4-S486A* mutant hyper-sensitivity to MMS. Strains expressing *slx4-S486A* in combination with mutants defective in DNA damage checkpoint signalling (*dot1Δ*, *ddc1-T602A* and *rad53-3HA*) were spotted in 5-fold serial dilutions on MMS-containing media and assayed for growth after two days. **B** The *slx4-S486A* mutant recovers faster after a partial inactivation of the DNA damage checkpoint. *WT*, *slx4-S486A* and *slx4-S486A ddc1-T602A* mutant cells were treated with a pulse of 0.033% MMS during S-phase, and recovery was analysed by cellular DNA content as determined by FACS (upper panel) and by checkpoint activity as determined by anti-Rad53 western blot (lower panel). **C** Yen1 and Sgs1 are not required for the rescue of the *slx4-S486A* MMS hyper-sensitivity by partial checkpoint inactivation. MMS hyper-sensitivity phenotypes of *slx4-S486A*, *sgs1Δ*, *yen1Δ*, *ddc1-T602A* mutants and double or triple mutant combinations were spotted in 5-fold serial dilutions on MMS-containing media and assayed for growth after two (lower panel) or three (upper panel) days.

## Supplemental Methods

### Yeast strains

All yeast strains are based on W303 (Thomas and Rothstein 1989).

Genotypes are listed below. All biochemical experiments were performed in a W303-1A *pep4Δ* background. The genetic studies in Fig. 3B-E, 4, 6A-E and Fig. S3A-B, S4B-D, S5, S6, S10 were performed in a W303 *RAD5+* background to exclude any effect from a partial defect of the *rad5-535* allele, but similar results were obtained using W303-1A. Two-hybrid analyses were performed in the strain PJ69-7A (James et al. 1996).

*S. cerevisiae* strains were prepared by genetic crosses and transformation techniques. Deletion of particular genes and endogenous protein tagging were performed as described (Knop et al. 1999). Correct integrations were checked by genotyping PCR. Denaturing cell extracts were prepared by alkaline lysis and TCA precipitation (Knop et al. 1999). The *s/x4-S486A* allele was generated using site-directed mutagenesis and integrated as a linear plasmid at the TRP1 locus.

List of strains used in this study.

Strain	Full genotype	Relevant genotype	Source
1093-5A	MATa <i>ADE2+</i> <i>RAD5+</i> <i>CAN1+</i> <i>ura3-1 his3-11,15 trp1-1 leu2-3,112</i>	<i>CAN1+</i>	Klein lab
FY1060	MATa <i>RAD5+</i> <i>ade2-1 ura3-1 his3-11,15 trp1-1 leu2-3,112 can1-100 GAL PSI+ sgs1::HIS3</i>	<i>sgs1</i>	Branzei lab
HY4021	MATa <i>RAD5+</i> <i>ade2-1 trp1-1 leu2-3,112 his3-11,15 ura3-1 can1-100 sgs1::pADH1-tc3-3xHA-Sgs1</i>	<i>Tc-SGS1</i>	Branzei lab

	(NATMX)		
HY4072	MATa <i>RAD5+ ade2-1 trp1-1 leu2-3,112 his3-11,15 ura3-1 can1-100 slx4::HIS3 sgs1::pADH1-tc3-3xHA-Sgs1 (HPHMX4)</i>	<i>slx4 Tc-SGS1</i>	Branzei lab
ML664-10A	MATa <i>tTA(tetR-VP16)-tetO<sub>2</sub>-DPB11-4ala-YFP::KanMX NLS-yEmRFPrv::URA3 SPC110-CFP::KAN</i>	<i>DPB11-YFP SPC110-CFP</i>	Lisby lab
ML678-12B	MATa <i>tTA(tetR-VP16)-tetO<sub>2</sub>-DPB11-4ala-YFP::KanMX NLS-yEmRFPrv::URA3 SPC110-CFP::KanMX sgs1::HIS3</i>	<i>DPB11-YFP SPC110-CFP sgs1</i>	Lisby lab
ML779-4A	MATa <i>tTA(tetR-VP16)-tetO<sub>2</sub>-DPB11-4ala-YFP::KanMX NLS-yEmRFPrv::URA3 SPC110-CFP::KanMX slx4::KanMX</i>	<i>DPB11-YFP SPC110-CFP slx4</i>	Lisby lab
ML781-8D	MATa <i>tTA(tetR-VP16)-tetO<sub>2</sub>-DPB11-4ala-YFP::KanMX NLS-yEmRFPrv::URA3 SPC110-CFP::KanMX slx4::KanMX trp1-1::slx4-S486A::TRP1</i>	<i>DPB11-YFP SPC110-CFP slx4 slx4-S486A</i>	Lisby lab
ML798-4C	MATa <i>tTA(tetR-VP16)-tetO<sub>2</sub>-DPB11-4ala-YFP::KanMX NLS-yEmRFPrv::URA3 SPC110-CFP::KanMX slx4::KanMX trp1-1::slx4-S486A::TRP1 sgs1::HIS3</i>	<i>DPB11-YFP SPC110-CFP slx4 slx4-S486A sgs1</i>	Lisby lab
ML789-7D	MATa <i>ade2-1 ura3-1 his3-11,15 trp1-1 leu2-3,112 can1-100 tTA(tetR-VP16)-tetO<sub>2</sub>-DPB11-4ala-CFP::KanMX SLX4-4ala-YFP</i>	<i>DPB11-CFP SLX4-YFP</i>	Lisby lab
ML799-2C	MATa <i>tTA(tetR-VP16)-tetO<sub>2</sub>-DPB11-4ala-CFP::KanMX SLX4-YFP sgs1::HIS3</i>	<i>DPB11-CFP SLX4-YFP sgs1</i>	Lisby lab
ML806-3C	MATa <i>tTA(tetR-VP16)-tetO<sub>2</sub>-DPB11-4ala-CFP::KanMX slx4-S486A-YFP</i>	<i>DPB11-CFP slx4-S486A-YFP</i>	Lisby lab
ML806-3A	MATa <i>tTA(tetR-VP16)-tetO<sub>2</sub>-DPB11-4ala-CFP::KanMX slx4-S486A-YFP sgs1::HIS3</i>	<i>DPB11-CFP slx4-S486A-YFP sgs1</i>	Lisby lab
ML792-2D	MATa <i>ade2-1 ura3-1 his3-11,15 trp1-1 leu2-3,112 can1-100</i>	<i>DPB11-CFP MUS81-YFP</i>	Lisby lab

	<i>tTA(tetR-VP16)-tetO<sub>2</sub>-DPB11-4ala-CFP::KanMX MUS81-4ala-YFP</i>		
ML800-9A	<i>MATa tTA(tetR-VP16)-tetO<sub>2</sub>-DPB11-4ala-CFP::KanMX MUS81-YFP sgs1::HIS3</i>	<i>DPB11-CFP MUS81-YFP sgs1</i>	Lisby lab
Y2050	<i>MATα ade2-1 trp1-1 his3-11 his3-15 can1-100 leu2-112::URA3::leu2-k</i>	<i>leu2-112::URA3::leu2-k</i>	Jentsch lab
YBP388	<i>MATa ade2-1 ura3-1 his3-11,15 leu2-3,112 can1-100 leu2-3,112::pep4::LEU2</i>	<i>pep4</i>	This study
YBP392	<i>MATa ade2-1 ura3-1 his3-11,15 leu2-3,112 can1-100 trp1-1::bar1::TRP1 leu2-3,112::pep4::LEU2</i>	<i>bar1 pep4</i>	This study
YBP418-1	<i>MATa ade2-1 ura3-1 his3-11,15 can1-100 lys1::NAT-NT2 arg4::hph-NT1 trp1-1::bar1::TRP1 leu2-3,112::pep4::LEU2 SLX4-3FLAG::KanMx4</i>	<i>lys1 SLX4-3FLAG</i>	This study
YBP420	<i>MATa ade2-1 ura3-1 his3-11,15 can1-100 arg4::hph-NT2 lys1::NAT-NT1 leu2-3,112::pep4::LEU2 trp1-1::bar1::TRP1</i>	<i>lys1 arg4</i>	This study
YBP422	<i>MATa ade2-1 ura3-1 his3-11,15 can1-100 arg4::hph-NT2 lys1::NAT-NT1 leu2-3,112::pep4::LEU2 trp1-1::bar1::TRP1 DPB11-3FLAG::KanMx</i>	<i>lys1 arg4 DPB11-3FLAG</i>	This study
YDG40	<i>MATα ade2-1 ura3-1 his3-11,15 leu2-3,112 can1-100 slx4::kanMx4 trp1-1::slx4-S486A::TRP1</i>	<i>slx4-S486A</i>	This study
YDG66	<i>MATa ade2-1 ura3-1 his3-11,15 trp1-1 leu2-3,112 can1-100 rad51::natNT2</i>	<i>rad51</i>	This study
YDG96	<i>MATα ade2-1 trp1-1 his3-11 his3-15 can1-100 leu2-112::URA3::leu2-k slx4::kanMx slx4-S486A::TRP1</i>	<i>leu2-112::URA3::leu2-k slx4-S486A</i>	This study

YDG126	MATa <i>ade2-1 ura3-1 his3-11,15 trp1-1 leu2-3,112 can1-100 rad1::hphNTI</i>	<i>rad1</i>	This study
YDG134	MATa <i>ade2-1 ura3-1 his3-11,15 trp1-1 leu2-3,112 can1-100 slx1::hphNTI</i>	<i>slx1</i>	This study
YDG135	MATa <i>ade2-1 ura3-1 his3-11,15 leu2-3,112 can1-100 slx4::KanMx trp1-1::slx4-S486A::TRP1 slx1::hphNTI</i>	<i>slx4-S486A slx1</i>	This study
YDG150	MATa <i>ade2-1 ura3-1 his3-11,15 trp1-1 leu2-3,112 can1-100 mms2::hphNTI</i>	<i>mms2</i>	This study
YDG151	MAT $\alpha$ <i>ade2-1 ura3-1 his3-11,15 leu2-3,112 can1-100 slx4::kanMx trp1-1::slx4-S486A::TRP1 mms2::hphNTI</i>	<i>slx4-S486A mms2</i>	This study
YDG175	MATa <i>ade2-1 ura3-1 his3-11,15 trp1-1 leu2-3,112 can1-100 rad5::hphNTI</i>	<i>rad5</i>	This study
YDG182	MATa <i>ade2-1 ura3-1 his3-11,15 leu2-3,112 can1-100 slx4::kanMx trp1-1::slx4-S486A::TRP1 rad51::hphNT1</i>	<i>slx4-S486A rad51</i>	This study
YDG183	MATa <i>ade2-1 ura3-1 his3-11,15 trp1-1 leu2-3,112 can1-100 rev1::hphNT1</i>	<i>rev1</i>	This study
YDG184	MATa <i>ade2-1 ura3-1 his3-11,15 leu2-3,112 can1-100 slx4::kanMx trp1-1::slx4-S486A::TRP1 rev1::hphNT1</i>	<i>slx4-S486A rev1</i>	This study
YDG185	MATa <i>ade2-1 ura3-1 his3-11,15 trp1-1 leu2-3,112 can1-100 rev3::hphNT1</i>	<i>rev3</i>	This study
YDG186	MATa <i>ade2-1 ura3-1 his3-11,15 leu2-3,112 can1-100 slx4::kanMx trp1-1::slx4-S486A::TRP1 rev3::hphNT1</i>	<i>slx4-S486A rev3</i>	This study
YDG187	MATa <i>ade2-1 ura3-1 his3-11,15 trp1-1 leu2-3,112 can1-100 rad30::hphNT1</i>	<i>rad30</i>	This study
YDG188	MATa <i>ade2-1 ura3-1 his3-11,15 leu2-3,112 can1-100 slx4::kanMx</i>	<i>slx4-S486A rad30</i>	This study

	<i>trp1-1::slx4-S486A::TRP1</i> <i>rad30Δ::hphNT1</i>		
YDG189	MATa <i>RAD5+</i> <i>ade2-1 ura3-1</i> <i>leu2-3,112 can1-100 slx4::kanMx</i> <i>trp1-1::slx4-S486A::TRP1 his3-</i> <i>11,15::sgs1::HIS3</i>	<i>slx4-S486A sgs1</i>	This study
YDG190	MATa <i>RAD5+</i> <i>ade2-1 ura3-1</i> <i>his3-11,15 leu2-3,112 can1-100</i> <i>slx4::kanMx trp1-1::slx4-</i> <i>S486A::TRP1</i>	<i>slx4-S486A</i>	This study
YDG206	MATα <i>RAD5+</i> <i>CAN1+</i> <i>ADE2+</i> <i>ura3-1 his3-11,15 leu2-3,112</i> <i>slx4::kanMx4 trp1-1::slx4-</i> <i>S486A::TRP1</i>	<i>CAN1+ slx4-</i> <i>S486A</i>	This study
YDG207	MATa <i>CAN1+</i> <i>ADE2+</i> <i>ura3-1</i> <i>his3-11,15 trp1-1 leu2-3,112</i> <i>rad5::hphNT1</i>	<i>CAN1+ rad5</i>	This study
YDG209	MATa <i>ade2-1 his3-11,15 trp1-1</i> <i>leu2-3,112 can1-100</i> <i>rad5::hphNT1 ura3-</i> <i>1::RAD5+::URA3</i>	<i>rad5 RAD5+</i>	This study
YDG211	MATa <i>ade2-1 his3-11,15 trp1-1</i> <i>leu2-3,112 can1-100</i> <i>rad5::hphNT1 ura3-1::rad5+-</i> <i>C914S::URA3</i>	<i>rad5+-C914S</i>	This study
YDG212	MATa <i>ade2-1 his3-11,15 leu2-</i> <i>3,112 can1-100 slx4::kanMx4</i> <i>trp1-1::slx4-S486A::TRP1</i> <i>rad5::hphNT1 ura3-</i> <i>1::RAD5+::URA3</i>	<i>slx4-S486A rad5Δ</i> <i>RAD5+</i>	This study
YDG214	MATa <i>ade2-1 his3-11,15 leu2-</i> <i>3,112 can1-100 slx4::kanMx4</i> <i>trp1-1::slx4-S486A::TRP1</i> <i>rad5::hphNT1 ura3-1::rad5+-</i> <i>C914S::URA3</i>	<i>slx4-S486A rad5+-</i> <i>C914S</i>	This study
YDG217	MATa <i>RAD5+</i> <i>ade2-1 his3-11,15</i> <i>trp1-1 ura3-1 leu2-3,112 can1-</i> <i>100 srs2ΔC::hphNT1</i>	<i>srs2ΔC</i>	This study
YDG218	MATa <i>RAD5+</i> <i>ade2-1 his3-11,15</i> <i>ura3-1 leu2-3,112 can1-100</i> <i>slx4::kanMx4 trp1-1::slx4-</i> <i>S486A::TRP1 srs2ΔC::hphNT1</i>	<i>slx4-S486A</i> <i>srs2ΔC</i>	This study
YDG219	MATa <i>RAD5+</i> <i>ade2-1 his3-11,15</i>	<i>siz1</i>	This

	<i>trp1-1 ura3-1 leu2-3,112 can1-100 siz1::hphNT1</i>		study
YDG220	MATa <i>Rad5+ ade2-1 his3-11,15 ura3-1 leu2-3,112 can1-100 slx4::kanMx4 trp1-1::slx4-S486A::TRP1 siz1::hphNT1</i>	<i>slx4-S486A siz1</i>	This study
YDG240	MATa <i>ade2-1 his3-11,15 trp1-1 leu2-3,112 can1-100 rad5::hphNT1 ura3-1::rad5+-KT538,539AA::URA3</i>	<i>rad5+-KT538,539AA</i>	This study
YDG241	MATa <i>ade2-1 his3-11,15 leu2-3,112 can1-100 rad5::hphNT1 ura3-1:rad5+-KT538,539AA::URA3 slx4::kanMx4 trp1-1::slx4-S486A::TRP1</i>	<i>slx4-S486A rad5+-KT538,539AA</i>	This study
YDG251	MATa <i>RAD5+ ade2-1 leu2-3,112 ura3-1 trp1-1 can1-100 his3-11,15::rad53-3HA::HIS3</i>	<i>rad53-3HA</i>	This study
YDG252	MATa <i>RAD5+ ade2-1 leu2-3,112 ura3-1 can1-100 slx4Δ::kanMx4 trp1-1::slx4-S486A::TRP1 his3-11,15::rad53-3HA::HIS3</i>	<i>slx4-S486A rad53-3HA</i>	This study
YDG287	MATa <i>RAD5+ ade2-1 his3-11,15 leu2-3,112 ura3-1 can1-100 slx4::kanMx4 trp1-1::slx4-S486A::TRP1 dot1::natNT2</i>	<i>slx4-S486A dot1</i>	This study
YDG288	MATa <i>RAD5+ ade2-1 his3-11,15 leu2-3,112 ura3-1 can1-100 slx4::kanMx4 trp1-1::slx4-S486A::TRP1 ddc1-T602A::natNT2</i>	<i>slx4-S486A ddc1-T602A</i>	This study
YDG289	MATa <i>RAD5+ ade2-1 his3-11,15 leu2-3,112 trp1-1 ura3-1 can1-100 mms4::hphNT1</i>	<i>mms4</i>	This study
YDG290	MATa <i>RAD5+ ade2-1 his3-11,15 leu2-3,112 ura3-1 can1-100 slx4::kanMx4 trp1-1::slx4-S486A::TRP1 mms4::hphNT1</i>	<i>slx4-S486A mms4</i>	This study
YDG291	MATa <i>RAD5+ ade2-1 his3-11,15 leu2-3,112 trp1-1 ura3-1 can1-100 yen1::hphNT1</i>	<i>yen1</i>	This study
YDG292	MATa <i>RAD5+ ade2-1 his3-11,15</i>	<i>slx4-S486A yen1</i>	This

	<i>leu2-3,112 ura3-1 can1-100 slx4::kanMx4 trp1-1::slx4- S486A::TRP1 yen1::hphNT1</i>		study
YDG293	<i>MATa RAD5+ ade2-1 his3-11,15 leu2-3,112 ura3-1 can1-100 slx4::kanMx trp1-1::DPB11-slx4- S486A::TRP1</i>	<i>DPB11-slx4- S486A</i>	This study
YDG295	<i>MATa RAD5+ ade2-1 his3-11,15 leu2-3,112 ura3-1 can1-100 slx4::kanMx4 trp1-1::slx4- S486A::TRP1 ddc1- T602A::natNT2 yen1::hphNT1</i>	<i>slx4-S486A ddc1- T602A yen1</i>	This study
YDG296	<i>MATa RAD5+ ade2-1 his3-11,15 leu2-3,112 trp1-1 ura3-1 can1- 100 ddc1-T602A::natNT2 yen1::hphNT1</i>	<i>ddc1-T602A yen1</i>	This study
YDG329	<i>MATa RAD5+ ade2-1 ura3-1 his3-11,15 trp1-1 leu2-3,112 can1-100 sgs1::hphNT1</i>	<i>sgs1</i>	This study
YDG303	<i>MATa Rad5+ ade2-1 his3-11,15 leu2-3,112 trp1-1 ura3-1 can1- 100 ddc1-T602A::natNT2</i>	<i>ddc1-T602A</i>	This study
YDG304	<i>MATa RAD5+ ade2-1 his3-11,15 leu2-3,112 trp1-1 ura3-1 can1- 100 dot1::natNT2</i>	<i>dot1</i>	This study
YDG309	<i>MATa RAD5+ ade2-1 his3-11,15 leu2-3,112 ura3-1 can1-100 slx4::kanMx4 trp1-1::slx4- S486A::TRP1 ddc1- T602A::natNT2 mms4::hphNT1</i>	<i>slx4-S486A ddc1- T602A mms4</i>	This study
YDG310	<i>MATa RAD5+ ade2-1 his3-11,15 leu2-3,112 trp1-1 ura3-1 can1- 100 ddc1-T602A::natNT2 mms4::hphNT1</i>	<i>ddc1-T602A mms4</i>	This study
YDG313	<i>MATa RAD5+ ade2-1 his3-11,15 leu2-3,112 ura3-1 can1-100 slx4::kanMx4 trp1-1::slx4- S486A::TRP1 ddc1- T602A::natNT2 sgs1::hphNT1</i>	<i>slx4-S486A ddc1- T602A sgs1</i>	This study
YDG314	<i>MATa RAD5+ ade2-1 his3-11,15 leu2-3,112 trp1-1 ura3-1 can1- 100 ddc1-T602A::natNT2 sgs1::hphNT1</i>	<i>ddc1-T602A sgs1</i>	This study

YDG335	MATa <i>RAD5+</i> <i>ade2-1 ura3-1 his3-11,15 leu2-3,112 trp1-1 can1-100 mus81Δ::hphNT1</i>	<i>mus81</i>	This study
YDG336	MATa <i>RAD5+</i> <i>ade2-1 ura3-1 his3-11,15 leu2-3,112 can1-100 slx4::kanMx4 trp1-1::slx4-S486A::TRP1 mus81::hphNT1</i>	<i>slx4-S486A mus81</i>	This study
YDG339	MATa <i>RAD5+</i> <i>ade2-1 ura3-1 his3-11,15 trp1-1 leu2-3,112 can1-100 MMS4-3FLAG::hphNT1</i>	<i>MMS4-3FLAG</i>	This study
YDG340	MATa <i>RAD5+</i> <i>ade2-1 ura3-1 his3-11,15 leu2-3,112 can1-100 slx4::kanMx trp1-1::slx4-S486A::TRP1 MMS4-3FLAG::hphNT1</i>	<i>slx4-S486A MMS4-3FLAG</i>	This study
YDG355	MATa <i>RAD5+</i> <i>ade2-1 his3-11, 15 trp1-1 ura3-1 can1-100 mms4::hphNT1 leu2-3,112::mms4SS184,201AA::LEU2</i>	<i>mms4-SS184,201AA</i>	This study
YDG356	MATa <i>RAD5+</i> <i>ade2-1 trp1-1 ura3-1 can1-100 mms4::hphNT1 leu2-3,112::mms4SS184,201AA::LEU2 his3-11,15::sgs1::HIS3</i>	<i>mms4-SS184,201AA sgs1</i>	This study
YDG366	MATa <i>RAD5+</i> <i>ade2-1 his3-1,15 leu2-3,112 ura3-1 can1-100 slx4::kanMx trp1-1::slx4-S486A::TRP1 ddc1-T602A::natNT2 MMS4-3FLAG::hphNT1</i>	<i>slx4-S486A ddc1-T602A MMS4-3FLAG</i>	This study
YDG375	MATa <i>RAD5+</i> <i>ade2-1 ura3-1 his3-11,15 leu2-3,112 can1-100 slx4::NAT trp1-1::slx4-7A::TRP1</i>	<i>slx4-T457A, T474A, S499A, T597A, S627A, S659A, S725A</i>	This study
YDG376	MATa <i>RAD5+</i> <i>ade2-1 ura3-1 his3-11,15 trp1-1 leu2-3,112 can1-100 yen1::hphNT1 sgs1::natNT2</i>	<i>yen1 sgs1</i>	This study
YDG377	MATa <i>RAD5+</i> <i>ade2-1 ura3-1 his3-11,15 leu2-3,112 can1-100 slx4::kanMx trp1-1::slx4-S486A::TRP1 yen1Δ::hphNT1 sgs1::natNT2</i>	<i>slx4-S486A yen1 sgs1</i>	This study

YKR44	MATa <i>ade2-1 ura3-1 his3-11 his3-15 can1-100 trp1-1::bar1::TRP1 leu2-3,112::pep4::LEU2 DPB11-9myc::KanMX4</i>	<i>DPB11-9myc</i>	This study
YLP15	MATa <i>ade2-1 ura3-1 his3-11 his3-15 can1-100 trp1-1::bar1::TRP1 leu2-3,112::pep4::LEU2 lys1::nat-NT2</i>	<i>lys1</i>	This study
YLP18	MATa <i>ade2-1 ura3-1 can1-100 trp1-1::bar1::TRP1 leu2-3,112::pep4::LEU2 lys1::nat-NT2 his3-11,15::SLX4-3FLAG::HisMx</i>	<i>lys1 SLX4-3FLAG</i>	This study
YLP30	MATa <i>ade2-1 ura3-1 trp1-1 leu2-3,112 can1-100 pep4::NAT slx4::KanMx his3-11,15::slx4-S486A-3FLAG::HISMx</i>	<i>slx4-S486A-3FLAG</i>	This study
YLP41	MATa <i>ade2-1 ura3-1 trp1-1 leu2-3,112 can1-100 his3-11,15::slx4-S486A-3FLAG::HisMx pep4::NAT lys1::hph</i>	<i>lys1 slx4-S486A-3FLAG</i>	This study
YLP42	MATa <i>ade2-1 his3-11 his3-15 can1-100 trp1-1::bar1::TRP1 leu2-3,112::pep4::LEU2 SLX4-3FLAG::KanMx4 ura3-1::cdc28as-1 F88G::URA3</i>	<i>SLX4-3FLAG cdc28-as1</i>	This study
YLP43	MATa <i>ade2-1 his3-11,15 can1-100 lys1::hph trp1-1::bar1::TRP1 leu2-3,112::pep4::LEU2 SLX4-3FLAG::KanMx4 ura3-1::cdc28as-1 F88G::URA</i>	<i>lys1 SLX4-3FLAG cdc28-as1</i>	This study
YLP47	MATa <i>ade2-1 ura3-1 can1-100 trp1-1::bar1::TRP1 leu2-3,112::pep4::LEU2 his3-11,15::DPB11-3Flag::HIS3</i>	<i>DPB11-3FLAG</i>	This study
YLP57	MATa <i>RAD5+ ade2-1 ura3-1 trp1-1 leu2-3,112 can1-100 MMS4-3Flag::hphNT1 his3-11,15::pep4::HIS3</i>	<i>MMS4-3FLAG</i>	This study
YLP59	MATa <i>ade2-1 ura3-1 trp1-1 leu2-3,112 can1-100 MMS4-3Flag::hph-NT1 his3-11,15::pep4::HIS3Mx4 pGAL1-</i>	<i>MMS4-3FLAG pGal1-Cdc5</i>	This study

	<i>CDC5::KanMx</i>		
YLP62	MATa <i>ade2-1 ura3-1 leu2-3,112 can1-100 MMS4-3Flag::hph-NT1 his3-11,15::pep4::HIS3Mx4 slx4::KanMx trp1-1::slx4-S486A::TRP1</i>	<i>MMS4-3FLAG slx4-S486A</i>	This study
YLP63	MATa <i>RAD5+ ade2-1 ura3-1 trp1-1 leu2-3,112 can1-100 cdc5-as1 MMS4-3Flag::hph-NT1 his3-11,15::pep4::HIS3Mx4</i>	<i>MMS4-3FLAG cdc5-as1</i>	This study
YLP64	MATa <i>RAD5+ ade2-1 leu2-3,112 ura3-1 can1-100 slx4::kanMx trp1-1::slx4-S486A::TRP1 ddc1T602A:: natNT2 MMS4-3Flag::hphNTI his3-11,15::pep4::HIS3Mx4</i>	<i>MMS4-3FLAG slx4-S486A ddc1-T602A</i>	This study
YLP78	MATa <i>ade2-1 leu2-3,112 trp1-1 ura3-1 can1-100 MMS4-3Flag::hph-NT1 his3-11,15::pep4::HIS3Mx4 slx4::KanMx</i>	<i>MMS4-3FLAG slx4</i>	This study
YLP80	MATa <i>RAD5+ ade2-1 leu2-3,112 ura3-1 can1-100 MMS4-3Flag::hph-NT1 his3-11,15::pep4::HIS3Mx4 slx4::KanMx trp1-1::Slx4 T457A, T474A, S499A, T597A, S627A, S659A, S725A::TRP1</i>	<i>MMS4-3FLAG slx4-T457A, T474A, S499A, T597A, S627A, S659A, S725A</i>	This study
YLP83	MATa <i>RAD5+ ade2-1 his3-1,15 trp1-1 ura3-1 can1-100 leu2-3,112::pep4::LEU2 SLX4-3Flag::KanMx4 cdc5-as1</i>	<i>SLX4-3FLAG cdc5-as1</i>	This study
YLP87	MATa <i>RAD5+ ade2-1 leu2-3,112 trp1-1 ura3-1 can1-100 his3-11,15::pep4::HIS</i>	<i>pep4</i>	This study
YLP88	MATa <i>RAD5+ ade2-1 leu2-3,112 ura3-1 can1-100 slx4Δ::kanMx trp1-1::slx4-S486A::TRP1 MMS4-3Flag::hphNTI his3-11,15::pep4::HIS</i>	<i>MMS4-3FLAG slx4-S486A</i>	This study
YSB79	MATa <i>RAD5+ ade2-1 ura3-1 his3-11,15 leu2-3,112 trp1-1 can1-100 RFA1-</i>	<i>RFA1-3xmCherry</i>	This study

	<i>3xmCherry::hphNT1</i>		
YSB86	<i>MATa RAD5+ ade2-1 ura3-1 his3-11,15 leu2-3,112 trp1-1 can1-100 RFA1-3xmCherry::hphNT1 slx4::kanMx4 trp1-1:Slx4-S486A::TRP1</i>	<i>RFA1-3xmCherry slx4-S486A</i>	This study
YSS3	<i>MATa ade2-1 ura3-1 trp1-1 leu2-3,112 can1-100 MMS4-3Flag::hph-NT1 his3-11,15::pep4::HIS3Mx4</i>	<i>MMS4-3FLAG</i>	This study
YSS5	<i>MATa ade2-1 ura3-1 his3-11,15 can1-100 trp1-1::bar1::TRP1 leu2-3,112::pep4::LEU2 SLX4-3Flag::KanMx4</i>	<i>SLX4-3FLAG</i>	This study

### Synchronization by $\alpha$ -factor and nocodazole

Logarithmic growing cells were synchronized in G2/M-phase by nocodazole (5  $\mu$ g/ml), or in G1-phase by  $\alpha$ -factor (5-10  $\mu$ g/ml, or 167 ng/ml for *bar1* cells). The release from synchronization was performed by washing once in YPD, and suspending cells in YPD with 0.033% or 0.04% MMS. For recovery experiments, cells were washed after 30' (45' in Fig. 6E, S3B) of damage treatment, and suspended in drug free YPD media with (Fig. 5D, 6E-F) or without nocodazole.

### Drug treatment

DNA damage in liquid cultures was induced by MMS (final concentration 0.033%, or 0.04% (Fig. 3C-E, 6D)) or phleomycin/zeocin (final concentration 50  $\mu$ g/ml).

For solid media, concentrations of methyl methanesulfonate (MMS), hydroxyurea (HU), phleomycin, cisplatin, camptothecin (CPT) or 4-nitroquinoline 1-oxide (4-NQO) were as indicated in the figures.

### **FACS analysis**

$1 \times 10^7$  -  $2 \times 10^7$  cells were harvested by centrifugation and resuspended in 70% ethanol + 50 mM Tris pH 7.8. After centrifugation cells were washed with 1 ml 50 mM Tris pH 7.8 (Tris buffer) followed by resuspending in 520  $\mu$ l RNase solution (500  $\mu$ l 50 mM Tris pH 7.8 + 20  $\mu$ l RNase A (10 mg/ml in 10 mM Tris pH 7.5, 10 mM  $MgCl_2$ ) and incubation for 4 h at 37 °C. Next, cells were treated with proteinase K (200  $\mu$ l Tris buffer + 20  $\mu$ l proteinase K (10 mg/ml in 50% glycerol, 10 mM Tris pH 7.5, 25 mM  $CaCl_2$ ) and incubated for 30' at 50 °C. After centrifugation cells were resuspended in 500  $\mu$ l Tris buffer. Before measuring the DNA content, samples were sonified (5"; 50% CYCLE) and stained by SYTOX solution (999  $\mu$ l Tris buffer + 1  $\mu$ l SYTOX). Measurement was performed using FL1 channel 520 for SYTOX-DNA on a BD FACSCalibur system.

### **Interaction assays**

After cell growth under the indicated conditions, yeast extracts were obtained by freezer mill lysis in lysis buffer (100 mM Hepes, 200 mM KOAc, 0.1 % NP-40, 10 % glycerol, 2 mM b-ME, protease inhibitors, 100 mM octadecanoic acid, 10 mM NaF, 20 mM b-glycerophosphate). Co-IP was performed for 2 hours by head-over-tail rotation at 4 °C using anti-FLAG agarose resin (Sigma). Non-specific background was removed by six washes and bound proteins were

eluted by incubation with 0.5 mg/ml 3X FLAG-peptide (Sigma). The TCA precipitated eluates were resolved on 4-12% NuPAGE gradient gels (Invitrogen), and analyzed by standard Western blotting techniques. For GST pulldowns (Fig. S1A), GST-Dpb11 or GST-tagged protein fragments were recombinantly expressed and purified as described (Pfander and Diffley 2011). Proteins were immobilized on glutathione sepharose 4B (GE Healthcare) and incubated with ammonium sulphate-precipitated (57%) yeast extracts (lysis buffer as described above). Non-specific background was removed by five washes and bound proteins were eluted by Laemmli buffer. For Co-IP from HEK 293T cells were lysed in lysis buffer (see yeast lysates) for 30' on ice. Protein concentrations were determined by Bradford. GFP-tagged proteins were precipitated using GFP-Trap magnetic beads (Chromotek) and incubated for 1.5 h with head-over-tail rotation. Non-specifically bound proteins were removed by 6 washes with lysis buffer using a magnetic rack, and specifically bound proteins were eluted by Laemmli buffer.

### **Analysis of interacting proteins by SILAC**

For Co-IP experiments followed by mass spectrometry analysis, cells deficient in lysine biosynthesis were grown in synthetic complete (SC) medium supplemented with normal lysine ("light" medium) or heavy-isotope-labeled lysine (Lys8; "heavy" medium) from Cambridge Isotope Laboratories. For SILAC Co-IP experiments shown in Fig. S4A, cells deficient in lysine and arginine biosynthesis were grown in synthetic complete (SC) medium supplemented with normal lysine and arginine ("light" medium) or heavy-

isotope-labeled lysine and arginine (Lys8, Arg10; “heavy” medium) from Cambridge Isotope Laboratories. All other SILAC experiments were done using lysine-only labeling.

Lysates were prepared by harvesting cells in equal amounts after growth under the indicated conditions. After co-IP, eluted proteins from light and heavy cultures were pooled, TCA precipitated and separated on 4-12% NuPAGE Bis-Tris gel (Invitrogen). The gel was stained with GelCode Blue (Thermo Scientific). The gel lane was excised into ten slices and peptides were analyzed by LC-MS/MS after in-gel Lys-C or trypsin digestion. Samples were measured on an LTQ-Orbitrap and analyzed using MaxQuant (Cox and Mann 2008).

### **Antibodies**

Proteins were detected using specific antibodies: rabbit-anti-Rad53 (JD147, J. Diffley), rabbit-anti-Dpb11 (BPF19; Pfander and Diffley 2011), rabbit-anti-Rad9-T474-P (BPF25, Pfander and Diffley 2011), rabbit-anti-Slx4 (2057, Pfander lab), goat-anti-Cdc5 (sc-6733, Santa Cruz), rabbit-anti-Clb2 (sc-9071, Santa Cruz), rabbit-anti-FLAG (Sigma), rabbit-HRP-coupled-anti-GST (Z-5; sc-459, Santa Cruz), mouse-anti-myc (clone 4A6; Millipore), mouse-anti-GFP (B2; Santa Cruz), mouse-anti-Gal4-AD (TA-C10; Santa Cruz), mouse-anti-Gal4-BD (RK5C1; Santa Cruz).

### **Pulsed-field gel electrophoresis**

In the recovery experiments (Fig. 3D, 6B, S3B)  $8 \times 10^7$  of cells were taken for every time point and centrifuged at 5,000 x g 10 min at 4 °C. Cells were

resuspended in 1 ml cold 0.1% sodium azide and centrifuged at 3,000 rpm for 3 min. Remaining pellets were resuspended in 50 µl zymolyase buffer (50 mM EDTA, 10 mM Tris pH 8.0, 20 mM NaCl, 1 mg/ml zymolyase (T100)) and mixed with equal amount of 2% agarose. The samples were transferred to the plug mold. The plugs were incubated in zymolyase buffer at 37 °C for 1 h, followed by treatment with proteinase K (0.5 M EDTA pH 8.0, 1 mg/ml proteinase K, 10 mg/ml sodium lauryl sarcosine) at 50 °C for 24-48 h. Next, the plugs were washed 3 times with 50 mM EDTA and loaded.

Electrophoresis was performed using the CHEF-DRIII pulsed-field electrophoresis system (Bio-Rad) according to the manufacturer's instructions. The gel was stained with 1 µg/ml ethidium bromide and scanned under UV light. Quantification of PFGE signals was performed using ImageJ. For every time point the signal from the bands that have entered the gel was normalized to the total signal in the lane including that from the well, and the values from every time point were normalized relative to the G1 signal.

## **2D gel analysis and quantification of replication/recombination intermediates**

The experiments were conducted as described previously (Szakal and Branzei, 2013). The DNA samples were digested with HindIII and EcoRV and analysed with probes for ARS305. In all, 200 ml cultures ( $2-4 \times 10^9$  cells) were arrested by addition of sodium azide (final concentration 0.1%) and cooled down in ice. Cells were harvested by centrifugation, washed in cold water, and incubated in spheroplasting buffer (1 M sorbitol, 100 mM EDTA pH 8.0, 0.1% b-ME, and 50 U zymolase/ml) for 1.5 h at 30 °C. In all, 2 ml water, 200

$\mu$ l RNase A (10 mg/ml), and 2.5 ml Solution I (2% w/v cetyl-trimethyl-ammonium-bromide (CTAB), 1.4 M NaCl, 100 mM Tris-HCl pH 7.6, and 25 mM EDTA pH 8.0) were sequentially added to the spheroplast pellets and samples were incubated for 30 min at 50 °C. In all, 200  $\mu$ l proteinase K (20 mg/ml) was then added and the incubation was prolonged at 50 °C for 1 h 30 min, and at 30 °C overnight. The sample was then centrifuged at 4,000 rpm for 10 min: the cellular debris pellet was kept for further extraction, while the supernatant was extracted with 2.5 ml chloroform/isoamylalcohol (24/1) and the DNA in the upper phase was precipitated by addition of 2 volumes Solution II (1% w/v CTAB, 50 mM Tris-HCl pH 7.6, and 10 mM EDTA) and centrifugation at 8,500 rpm for 10 min. The pellet was resuspended in 2 ml Solution III (1.4 M NaCl, 10 mM Tris-HCl pH 7.6, and 1 mM EDTA). Residual DNA in the cellular debris pellet was also extracted by resuspension in 2 ml Solution III and incubation at 50 °C for 30 min, followed by extraction in 1 ml chloroform/isoamylalcohol (24/1). The upper phase was pooled together with the main DNA preparation. Total DNA was then precipitated with 1 volume isopropanol, washed with 70% ethanol, air dried, and finally resuspended in TE 1X. Quantification of X-shaped intermediate signals was performed using the Image Quant software as previously described (Liberi et al. 2005; Branzei et al. 2008; Vanoli et al. 2010). For each time point, areas corresponding to the monomer spot (M), the X-spike signal and a region without any replication intermediates as background reference were selected and the signal intensities (SIs) in percentage of each signal were obtained. The values for the X and monomer were corrected by subtracting from the SI value the background value after the latter was multiplied for the ratio between the

dimension of the area for the intermediate of interest and for background.

Thus, the values for X and M were calculated in the following way:

Value for X =  $\frac{SI(X_s) - SI(\text{background})}{SI(X_s) + SI(\text{background})}$  (area (Xs)/area (background));

Value for M =  $\frac{SI(M) - SI(\text{background})}{SI(M) + SI(\text{background})}$  (area (M)/area (background)).

The relative SI for the X was then determined by dividing the value for X with the sum of the total signals (the sum of the X and monomer values). The resulting values for X signals were then normalized. For instance, for recovery experiments the relative value of X obtained after MMS treatment was considered as 100% and the other X values were normalized to it.

### **Mutation and recombination assays**

Mutation rates were determined using a *CAN1* forward mutation assay (Klein 2001). Interchromosomal recombination rates were determined using a direct-repeat system using *leu2* heteroalleles (Aquilera and Klein 1988) and crossover rates were determined using a system harbouring two *arg4* alleles on chromosome V and VIII (Robert et al. 2006, Szakal and Branzei 2013). In all cases mutation/recombination rates were determined using fluctuation analysis and a maximum-likelihood approach. Therefore, for each strain ten independent cultures originated from the single cell were analyzed. To get single colonies 100 cells were plated or streaked out for single colonies on YPD media plates and incubated for 2 days at 30 °C. The frequency of mutants/recombinants in all cultures was determined by plating on selective media. The total cell number was determined by plating an appropriate dilution on non-selective media. For determination of CO rates, for each culture ten ARG+ colonies were picked, analyzed by PCR for CO or NCO

events (Szakal and Branzei 2013) and the overall number of crossover recombinants was extrapolated. From the number of mutants/recombinants/crossover recombinants the number of mutational/recombinational/crossover events was determined using a maximum-likelihood approach and rates were determined by dividing by the number of cell divisions (Pfander et al. 2005). For each strain 2-10 independent experiments were performed to determine mean and standard deviation.

### **Microscopy and immunofluorescence**

Yeast cells were grown in synthetic complete (SC) medium supplemented with 100 µg/ml adenine (SC+Ade) and processed for fluorescence microscopy as described (Eckert-Boulet et al. 2011). For staining of DNA in live yeast cells, 5 µg/ml of Hoechst 33258 (B2883, Sigma-Aldrich) were added to the culture 10-15 min prior to microscopy and washed out with fresh medium immediately prior to microscopy and imaged at 25 °C. Fluorophores used in yeast were cyan fluorescent protein (CFP, clone W7) (Heim and Tsien 1996) and yellow fluorescent protein (YFP, clone 10C) (Ormo et al. 1996).

Microscopy was performed using an AxioImager Z1 (Carl Zeiss MicroImaging, Inc) equipped with a 100x objective lens (Zeiss PLAN-APO, NA 1.4), a cooled Orca-ER CCD camera (Hamamatsu, Japan), differential interference contrast (DIC), and a Zeiss HXP120C illumination source, or on a Deltavision Elite microscope (Applied Precision, Inc) equipped with a 100x objective lens (Olympus U-PLAN S-APO, NA 1.4), a cooled Evolve 512 EMCCD camera (Photometrics, Japan), and a Insight solid state illumination source (Applied

Precision, Inc). Images were acquired using Volocity (PerkinElmer) or softWoRx (Applied Precision, Inc) software. Images were acquired and processed using Volocity (PerkinElmer) software. Images were pseudocoloured according to the approximate emission wavelength of the fluorophores.

For analysis of RPA foci (Fig. 3F) cells were grown in SC media, arrested with  $\alpha$ -factor and treated in S-phase with 0.033% MMS for 120 min, then released into the fresh SC media for recovery. For microscopy cells were fixed in FA for 30 min and quenched in 2.5 M glycine for 30 min. Cells were washed twice and resuspended in 50 mM Tris, pH 7.5. Images of cells were obtained using a fully automated Zeiss inverted microscope (AxioObserver Z1) equipped with a MS-2000 stage (Applied Scientific Instrumentation, USA), a CSU-X1 spinning disk confocal head (Yokogawa, Herrsching), LaserStack Launch with selectable laser lines (Intelligent Imaging Innovations, USA) and an X-CITE Fluorescent Illumination System. Images were captured using a CoolSnap HQ camera (Roper Scientific, Canada) under the control of the Slidebook software (Intelligent Imaging Innovations, USA). All fluorescence signals were imaged with a 63x oil objective.

### **Cell culture and transfection techniques**

HEK 293T cells were cultured at 37 °C at 7.5% CO<sub>2</sub> in DMEM (GIBCO-BRL) supplemented with 10% FCS. Transient transfections were performed in 6-well plates (HeLa) using the calcium phosphate method. In general 5x10<sup>5</sup> 293T cells per well were seeded and transfected the next day using 20  $\mu$ g

total DNA. After 4-6 h incubation the TF medium was replaced with fresh growth medium, and cells were cultured for another 18-20 h.

### **Nuclease assays**

5'-end-Cy3-labeled oligonucleotides were used to prepare synthetic DNA substrates as described (Rass & West 2006). Nuclease assays were carried out with immobilized Mms4-FLAG. The Anti-FLAG immunoprecipitates were extensively washed and mixed with 10  $\mu$ l reaction buffer (50 mM Tris-HCl pH 7.5, 3 mM MgCl<sub>2</sub>) containing ~2.5 nM 5'-Cy3-end-labeled substrate (Matos et al 2011). Reactions were incubated for 15-45 min with gentle rotation at 30 °C and stopped by addition of 4  $\mu$ l 10 mg/ml proteinase K and 2% SDS, and further incubation at 37 °C for 1 h. Loading buffer was added and radiolabeled products were separated by 10% PAGE, and analyzed using a Typhoon scanner.

### **Sequence analysis**

Close orthologues of budding yeast and human Slx4 were found by NCBI-BLAST (Altschul et al. 1997) and verified by reciprocal BLAST searches. Individual multiple sequence alignments of fungal and mammalian Slx4 were done using ClustalX (Chenna et al. 2003). The Profile Alignment feature was used in ClustalX to align the two profiles from mammalian and fungal Slx4 proteins. This identified the potential Dpb11/TopBP1 interaction motif in human Slx4. Slx4 proteins from further classes were identified by BLAST and first aligned with members of their individual class using ClustalX. Resulting multiple sequence alignments were manually analyzed for the occurrence of

the Dpb11/TopBP1 motif and subsequently manually aligned to the yeast and mammalian motif.

Species abbreviations and accession numbers for Figure S2.

Sp	Schizosaccharomyces pombe	NP_594064
Sc	Saccharomyces cerevisiae	NP_013236
Kl	Kluyveromyces lactis	XP_453790
Ec	Eremothecium cymbalariae	XP_003646141
Nc	Naumovozya castellii	XP_003928518
Ka	Kazachstania naganashii	CCK71307 (emb)
Td	Toluraspora delbrueckii	XP_003682477
Zr	Zygosaccharomyces rouxii	XP_002497655
Vp	Vanderwaltozyma polyspora	XP_001647185
Lt	Lachancea thermotolerans	XP_002555561
Hs	Homo sapiens	NP_115820
Sb	Samira b. boliviensis	XP_003928518
Mm	Mus musculus	NP_803423
Rn	Rattus norvegicus	XP_001079342
Sh	Sacrophilus harrisii	XP_003761955
Tm	Trichechus manatus latirostris	XP_004373478
Oo	Orcinus orca	XP_004270504
Xt	Xenopus tropicalis	XP_002932505
Dr	Danio rerio	XP_003201146
Dm	Drosophila melanogaster	NP_648104
Dg	Drosophila grimshawi	XP_001983575
Dw	Drosophila willistoni	XP_002062409
Cc	Ceratitidis capitata	XP_004526156
Ag	Anopheles gambiae	XP_001687887

## References

- Aguilera A, Klein HL. (1988). Genetic control of intrachromosomal recombination in *Saccharomyces cerevisiae*. I. Isolation and genetic characterization of hyper-recombination mutations. *Genetics*. 119, 779-790.
- Altschul SF, Madden TL, Schäffer AA, Zhang J, Zhang Z, Miller W, Lipman DJ. (1997). Gapped BLAST and PSI-BLAST: a new generation of protein database search programs. *Nucleic Acids Res*. 25, 3389-3402.
- Branzei D, Vanoli F, Foiani M. (2008). SUMOylation regulates Rad18-mediated template switch. *Nature*. 7224, 915-920.
- Chenna R, Sugawara H, Koike T, Lopez R, Gibson TJ, Higgins DG, Thompson JD. (2003). Multiple sequence alignment with the Clustal series of programs. *Nucleic Acids Res*. 31, 3497-3500.
- Cox J, Mann M. (2008). MaxQuant enables high peptide identification rates, individualized p.p.b.-range mass accuracies and proteome-wide protein quantification. *Nat Biotechnol*. 26, 1367-1372.
- Eckert-Boulet N, Rothstein R, Lisby M. (2011). Cell biology of homologous recombination in yeast. *Methods Mol Biol*. 745, 523-536.
- Gonzalez-Huici V, Szakal B, Urulangodi M, Psakhye I, Castellucci F, Menolfi D, Rajakumara E, Fumasoni M, Bermejo R, Jentsch S, Branzei D. (2014).

DNA bending facilitates the error-free DNA damage tolerance pathway and upholds genome integrity. *EMBO J.* (Epub ahead of print).

Heim R, Tsien RY. (1996). Engineering green fluorescent protein for improved brightness, longer wavelengths and fluorescence resonance energy transfer. *Curr Biol.* 6, 178-182.

James P, Halladay J, Craig EA. (1996). Genomic libraries and a host strain designed for highly efficient two-hybrid selection in yeast. *Genetics.* 144, 1425-1436.

Klein HL. (2001). Mutations in recombinational repair and in checkpoint control genes suppress the lethal combination of *srs2Delta* with other DNA repair genes in *Saccharomyces cerevisiae*. *Genetics.* 157, 557-565.

Knop M, Siegers K, Pereira G, Zachariae W, Winsor B, Nasmyth K, Schiebel E. (1999). Epitope tagging of yeast genes using a PCR-based strategy: more tags and improved practical routines. *Yeast.* 15, 963-972.

Liberi G, Maffioletti G, Lucca C, Chiolo I, Baryshnikova A, Cotta-Ramusino C, Lopes M, Pellicoli A, Haber JE, Foiani M. (2005). Rad51-dependent DNA structures accumulate at damaged replication forks in *sgs1* mutants defective in the yeast ortholog of BLM RecQ helicase. *Genes Dev.* 19, 339-350.

Matos J, Blanco MG, Maslen S, Skehel JM, West SC (2011) Regulatory control of the resolution of DNA recombination intermediates during meiosis and mitosis. *Cell* 147: 158-172

Mullen JR, Kaliraman V, Ibrahim SS, Brill SJ. (2001). Requirement for three novel protein complexes in the absence of the Sgs1 DNA helicase in *Saccharomyces cerevisiae*. *Genetics*. 157, 103-118.

Ormö M, Cubitt AB, Kallio K, Gross LA, Tsien RY, Remington SJ. (1996). Crystal structure of the *Aequorea victoria* green fluorescent protein. *Science*. 273, 1392-1395.

Pfander B, Moldovan GL, Sacher M, Hoege C, Jentsch S. (2005). SUMO-modified PCNA recruits Srs2 to prevent recombination during S phase. *Nature*. 7049, 428-433.

Rass U, West SC (2006) Synthetic junctions as tools to identify and characterise Holliday junction resolvases. In *Meth. Enzymol.*, Campbell JL, Modrich P (eds), Vol. 408, pp 485-501. San Diego: Elsevier

Robert T, Dervins D, Fabre F, Gangloff S. (2006). Mrc1 and Srs2 are major actors in the regulation of spontaneous crossover. *EMBO J*. 25, 2837-2846.

Szakal B, Branzei D. (2013). Premature Cdk1/Cdc5/Mus81 pathway activation induces aberrant replication and deleterious crossover. *EMBO J.* 32, 1155-1167.

Thomas BJ, Rothstein R. (1989). Elevated recombination rates in transcriptionally active DNA. *Cell.* 56, 619-630.

Vanoli F, Fumasoni M, Szakal B, Maloisel L, Branzei D. (2010). Replication and recombination factors contributing to recombination-dependent bypass of DNA lesions by template switch. *PLoS Genet.* 6: e1001205.

# Dbf4-dependent kinase and the Rtt107 scaffold promote Mus81-Mms4 resolvase activation during mitosis

Lissa N Princz<sup>1</sup>, Philipp Wild<sup>2</sup>, Julia Bittmann<sup>1</sup>, F Javier Aguado<sup>3</sup>, Miguel G Blanco<sup>3</sup> , Joao Matos<sup>2</sup> & Boris Pfander<sup>1,\*</sup> 

## Abstract

DNA repair by homologous recombination is under stringent cell cycle control. This includes the last step of the reaction, disentanglement of DNA joint molecules (JMs). Previous work has established that JM resolving nucleases are activated specifically at the onset of mitosis. In case of budding yeast Mus81-Mms4, this cell cycle stage-specific activation is known to depend on phosphorylation by CDK and Cdc5 kinases. Here, we show that a third cell cycle kinase, Cdc7-Dbf4 (DDK), targets Mus81-Mms4 in conjunction with Cdc5—both kinases bind to as well as phosphorylate Mus81-Mms4 in an interdependent manner. Moreover, DDK-mediated phosphorylation of Mms4 is strictly required for Mus81 activation in mitosis, establishing DDK as a novel regulator of homologous recombination. The scaffold protein Rtt107, which binds the Mus81-Mms4 complex, interacts with Cdc7 and thereby targets DDK and Cdc5 to the complex enabling full Mus81 activation. Therefore, Mus81 activation in mitosis involves at least three cell cycle kinases, CDK, Cdc5 and DDK. Furthermore, tethering of the kinases in a stable complex with Mus81 is critical for efficient JM resolution.

**Keywords** cell cycle; genome stability; homologous recombination; joint molecule resolution; post-translational modification

**Subject Categories** Cell Cycle; DNA Replication, Repair & Recombination

**DOI** 10.15252/embj.201694831 | Received 22 May 2016 | Revised 15 December 2016 | Accepted 19 December 2016 | Published online 18 January 2017

**The EMBO Journal (2017) 36: 664–678**

## Introduction

Many DNA transactions are under cell cycle control to adjust them to cell cycle phase-specific features of chromosomes (Branzei & Foiani, 2008). Homologous recombination (HR) is cell cycle-regulated at several steps including the first, DNA end resection, and the

last, JM removal (Heyer *et al*, 2010; Ferretti *et al*, 2013; Mathiasen & Lisby, 2014; Matos & West, 2014). Given that JMs provide stable linkages between sister chromatids, they will interfere with chromosome segregation and therefore need to be disentangled before sister chromatid separation during mitosis. Accordingly, JM resolvases, such as budding yeast Mus81-Mms4 (Interthal & Heyer, 2000; Schwartz *et al*, 2012) or Yen1 (Ip *et al*, 2008), become activated during mitosis (Matos *et al*, 2011, 2013; Gallo-Fernández *et al*, 2012; Szakal & Branzei, 2013; Blanco *et al*, 2014; Eissler *et al*, 2014). In contrast, the alternative JM removal pathway, JM dissolution by the Sgs1-Top3-Rmi1 complex, is thought to be constantly active throughout the cell cycle (Mankouri *et al*, 2013; Bizard & Hickson, 2014). The activation of JM resolvases in mitosis therefore leads to a shift in the balance between JM removal pathways, with dissolution being preferred outside of mitosis, but JM resolution becoming increasingly important in mitosis (Matos *et al*, 2011, 2013; Gallo-Fernández *et al*, 2012; Dehé *et al*, 2013; Saugar *et al*, 2013; Szakal & Branzei, 2013; Wyatt *et al*, 2013). It has been hypothesized that JM resolvases are downregulated at cell cycle stages other than mitosis in order to counteract crossover-induced loss of heterozygosity or to prevent over-active resolvases from interfering with S phase by, for example, cleaving stalled replication forks (Gallo-Fernández *et al*, 2012; Szakal & Branzei, 2013; Blanco *et al*, 2014).

Budding yeast Mus81-Mms4 has previously been shown to be targeted by two cell cycle kinases, cyclin-dependent kinase Cdc28 (CDK) and the yeast polo-kinase Cdc5 (Matos *et al*, 2011, 2013; Gallo-Fernández *et al*, 2012; Szakal & Branzei, 2013). The corresponding Mms4 phosphorylation events were shown to correlate with and to be required for activation of Mus81-Mms4 in mitosis. In 2014, we showed that in mitosis Mus81-Mms4 also forms a complex with Slx4-Slx1 and the scaffold proteins Dpb11 and Rtt107 (Gritenaite *et al*, 2014). Interestingly, mass spectrometric analysis of this complex (Gritenaite *et al*, 2014) revealed that Cdc5 and a third cell cycle kinase Dbf4-Cdc7 (Dbf4-dependent kinase, DDK) are also a stable part of this protein assembly (see Appendix Fig S1A). Here,

<sup>1</sup> Max Planck Institute of Biochemistry, DNA Replication and Genome Integrity, Martinsried, Germany

<sup>2</sup> Institute of Biochemistry, Eidgenössische Technische Hochschule, Zürich, Switzerland

<sup>3</sup> Department of Biochemistry and Molecular Biology, Center for Research in Molecular Medicine and Chronic Diseases, Universidade de Santiago de Compostela, Santiago de Compostela, Spain

\*Corresponding author. Tel: +49 89 85783050; Fax: +49 89 85783022; E-mail: bpfander@biochem.mpg.de

we investigate the role of DDK in Mus81-Mms4 regulation and find that DDK can phosphorylate Mms4 and that DDK and Cdc5 target Mus81-Mms4 in an interdependent manner. Moreover, we show that Rtt107 promotes the association of both kinases with the Mus81-Mms4 complex. The DDK-dependent regulation of Mus81-Mms4 is critical for Mus81 activity thus revealing DDK as a novel regulator of homologous recombination.

## Results

### Mus81-Mms4 is a DDK phosphorylation target

The cell cycle regulation of JM resolution by Mus81-Mms4 is intricate and involves phosphorylation by the cell cycle kinases CDK

and Cdc5 (Matos *et al*, 2011, 2013; Gallo-Fernández *et al*, 2012; Szakal & Branzei, 2013) as well as complex formation with the scaffold proteins Dpb11, Slx4 and Rtt107 (Gritenaite *et al*, 2014). To study this protein complex, we performed an analysis of Mms4<sup>3FLAG</sup> interactors in mitosis by SILAC-based quantitative mass spectrometry (Gritenaite *et al*, 2014) and found in addition to Dpb11, Slx4, Rtt107 and Cdc5, also Cdc7 and Dbf4 as specific interactors of Mms4 (Appendix Fig S1A). We verified that Cdc7 binds to Mus81-Mms4 in an Mms4<sup>3FLAG</sup> pull down from mitotic cells analysed by Western blots (Fig 1A). The fact that Mus81-Mms4 binds to DDK suggested that it might be involved in the phosphorylation cascade that occurs on Mms4 and controls Mus81 activity in mitosis. Accordingly, we found that purified DDK was able to phosphorylate both subunits of purified Mus81-Mms4 *in vitro* (Fig 1B, lane 3). When we furthermore compared the DDK-dependent

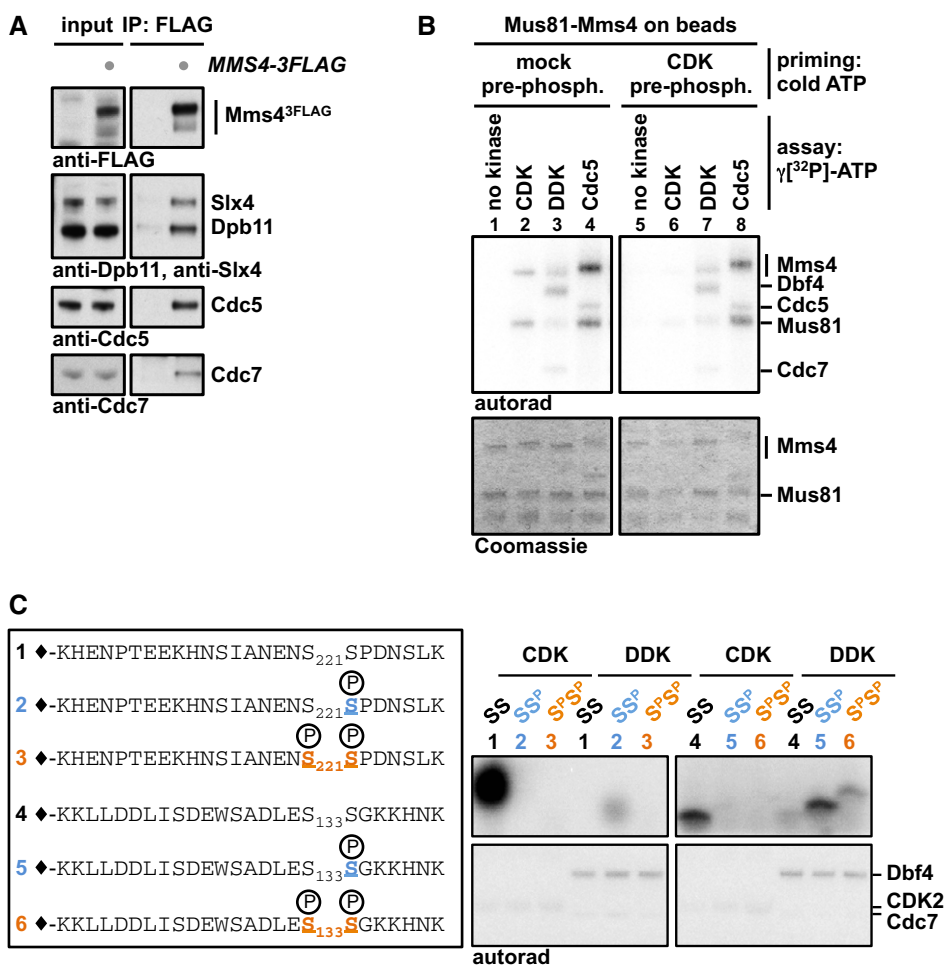


**Figure 1. Dbf4-dependent kinase (DDK) binds to the Mus81-Mms4 complex in mitosis and can phosphorylate Mms4 at (S/T)(S/T) motifs.**

A Cdc7 and Cdc5 are specifically enriched in Mms4<sup>3FLAG</sup> co-IPs from cells arrested in mitosis (with nocodazole). Under the same conditions, Mus81-Mms4 associates with scaffold proteins such as Dpb11 and Slx4 (Appendix Fig S1A and Gritenaite *et al*, 2014).

B DDK can phosphorylate Mus81-Mms4 *in vitro*. Purified, immobilized Mus81-Mms4 is incubated in an *in vitro* kinase assay with purified CDK2/cycA<sup>N170</sup> (a model CDK), DDK or Cdc5 (lanes 1–4). Additionally, Mus81-Mms4 is incubated with respective kinases after a non-radioactive priming step with CDK (lanes 5–8).

C DDK phosphorylates Mms4 peptides at (S/T)(S/T) motifs and is enhanced by priming phosphorylation. Mms4 peptides including (S/T)(S/T) motifs (221/222; 133/134) were synthesized in different phosphorylation states (depicted in left panel) and incubated in an *in vitro* kinase assay with either CDK or DDK. CDK targets unphosphorylated Mms4 peptides 1 and (to a weaker extent) 4 consistent with its substrate specificity (Mok *et al*, 2010), while DDK primarily targets Mms4 peptides 2 and 5, which harbour a priming phosphorylation at the C-terminal (S/T) site (see Appendix Fig S1B for in-gel running behaviour of peptides).

phosphorylation signal to Mms4 phosphorylation by CDK and Cdc5 (Fig 1B, lanes 2–4), we observed different degrees of phosphorylation shifts indicating that the three kinases phosphorylate Mms4 at distinct sites and/or to different degrees. DDK target sites on other proteins have been studied in detail, and in several cases, DDK was found to target (S/T)(S/T) motifs, where phosphorylation was stimulated by a priming phosphorylation usually on the second (S/T) (Masai *et al*, 2006; Montagnoli *et al*, 2006; Randell *et al*, 2010; Lyons *et al*, 2013). Intriguingly, Mms4 contains 15 of these motifs and we therefore tested whether these could be targeted by DDK and would depend on priming phosphorylation. We therefore turned to a peptide-based assay where Mms4 phosphorylation states are precisely defined. To this end, we synthesized peptides corresponding to two (S/T)(S/T) motifs of Mms4. We chose two representative motifs: S222, as it harbours a minimal CDK consensus motif (S/T)P, and S134, as it contains a non-(S/T)P consensus for CDK [(S/T)X(K/R)(K/R) (Suzuki *et al*, 2015)]. For each of these motifs, we generated peptides in three different phosphorylation states: non-phosphorylated, phosphorylated at the second serine and doubly phosphorylated (Fig 1C and Appendix Fig S1B). When using such peptides as substrates in *in vitro* kinase reactions, we saw that CDK targeted specifically only the second serine in each peptide, although much stronger for S222 than for S134, consistent with these residues matching CDK consensus motifs (Fig 1C). In contrast, DDK showed only little activity towards the non-phosphorylated peptides, but was strongly stimulated when the second residue in the (S/T)(S/T) motif was in a phosphorylated state (Fig 1C). DDK may thus be stimulated by priming phosphorylation in order to efficiently phosphorylate Mms4 on (S/T)(S/T) sites. However, using the full-length protein as a phosphorylation substrate, we did not obtain evidence for a stimulatory effect on DDK by prior CDK phosphorylation (Fig 1B and Appendix Fig S1C), perhaps because over the whole 15 (S/T)(S/T) motifs CDK phosphorylation plays a minor role. We also did not reveal any priming activity of either CDK or DDK for Mms4 phosphorylation by Cdc5 (Fig 1B and Appendix Fig S1D). Overall, the data in Fig 1 thus identify Mus81-Mms4 as an interaction partner and potential substrate of DDK.

### Mus81-Mms4 is phosphorylated by a mitotic Cdc5-DDK complex

DDK is present and active throughout S phase and mitosis until anaphase when the Dbf4 subunit is degraded by APC/C<sup>Cdc20</sup> (Cheng *et al*, 1999; Weinreich & Stillman, 1999; Ferreira *et al*, 2000). We therefore tested at which cell cycle stage DDK would associate with Mus81-Mms4 using cells synchronously progressing through the cell cycle. Figure 2A shows that DDK did not associate with Mus81-Mms4 in S phase, but only once cells had reached mitosis. Strikingly, DDK binding therefore coincided with binding of Cdc5, Slx4 and Dpb11 and most notably the appearance of the hyperphosphorylated form of Mms4<sup>3FLAG</sup> (Fig 2A).

Given this late timing of the association, we tested in co-immunoprecipitation (co-IP) experiments whether DDK binding to Mus81-Mms4 would depend on CDK or Cdc5 activity. Using analog-sensitive mutant yeast strains for CDK [*cdc28-as1* (Bishop *et al*, 2000)] and for Cdc5 [*cdc5-as1* (Snead *et al*, 2007)], we observed that inhibition of these kinases in mitotically arrested cells strongly reduced the hyperphosphorylation shift of Mms4 (see also Matos

*et al*, 2013) and compromised the association with DDK (Fig 2B and C, and Appendix Fig S2A–C). Notably, both conditions also interfered with Cdc5 binding (Fig 2B and C, and Appendix Fig S2A), suggesting that the association of DDK may follow a similar regulation as Cdc5.

Next, we tested whether conversely DDK is involved in Mms4 phosphorylation. To bypass the essential function of DDK in DNA replication, we used the *mcm5<sup>bob1-1</sup>* allele (Hardy *et al*, 1997), which allowed us to test a *cdc7Δ* mutant. Using Western blot and SILAC-based mass spectrometry as a read-out of Mms4<sup>3FLAG</sup> co-IPs from cells arrested in mitosis, we found that Cdc5 association with Mus81-Mms4 was strongly reduced in the *cdc7Δ* mutant strain (Fig 2D and E). Moreover, we observed that Mms4<sup>3FLAG</sup> phosphorylation as indicated by mobility shift was decreased in the absence of DDK, although not to the same extent as upon CDK or Cdc5 inhibition (Fig 2D and Appendix Fig S2C). Additionally, as an alternative way to deregulate DDK, we used the *cdc7-1* temperature-sensitive mutant. Even with WT cells, we observed that elevated temperature (38°C) leads to a slight reduction in Cdc5 binding to Mus81-Mms4. However, in *cdc7-1* mutant cells, incubation at 38°C leads to the complete disappearance of Cdc5 binding to Mus81-Mms4 (Appendix Fig S2D). Therefore, we conclude from these data that DDK and Cdc5 bind to Mus81-Mms4 in an interdependent fashion.

Interestingly, Cdc5 was previously shown to interact with DDK via a non-consensus polo-box binding site within Dbf4 (Miller *et al*, 2009; Chen & Weinreich, 2010). The proposed model based on genetic experiments suggested that DDK binding antagonizes mitotic functions of Cdc5. However, the catalytic activity of Cdc5 was not inhibited in this complex (Miller *et al*, 2009) and we reason that DDK may simply target Cdc5 to a specific set of substrates. Since the Cdc5 binding site was mapped to the N-terminal portion of Dbf4 (Miller *et al*, 2009), we tested whether N-terminal truncations of Dbf4 would affect DDK or Cdc5 association with Mus81-Mms4. While the *dbf4-ΔN66* truncation lacking the first 66 amino acids (including a D-box motif) did not influence DDK or Cdc5 binding to Mms4<sup>3FLAG</sup>, the *dbf4-ΔN109* truncation, which additionally lacks the Cdc5 binding motif (Miller *et al*, 2009), showed strongly decreased DDK and Cdc5 binding to Mus81-Mms4 (Fig 2F). Additionally, also mitotic hyperphosphorylation of Mms4 was diminished when DDK and Cdc5 could not interact with each other (Fig 2F). Overall, these data strongly suggest that Cdc5 and DDK interact with and target Mus81-Mms4 in an interdependent manner. Furthermore, it is currently unclear whether collaboration of DDK and Cdc5 is a widespread phenomenon that may affect other Cdc5 substrates as well, given that mitotic phosphorylation of two candidate Cdc5 substrates, Ulp2 and Scc1 (Alexandru *et al*, 2001), was affected to varying degree by the *cdc7Δ* mutation (Appendix Fig S2E).

Given the known cell cycle regulation of Cdc5 and DDK (Shirayama *et al*, 1998; Cheng *et al*, 1999; Weinreich & Stillman, 1999; Ferreira *et al*, 2000; Mortensen *et al*, 2005), the limiting factor for the temporal regulation of this complex and its restriction to mitosis is expected to be Cdc5 and not DDK, which is present already throughout S phase. Consistently, we observed that forced expression of Cdc5 (using the galactose-inducible GAL promoter) in cells that were arrested in S phase by hydroxyurea (HU) led to the premature occurrence of Mms4

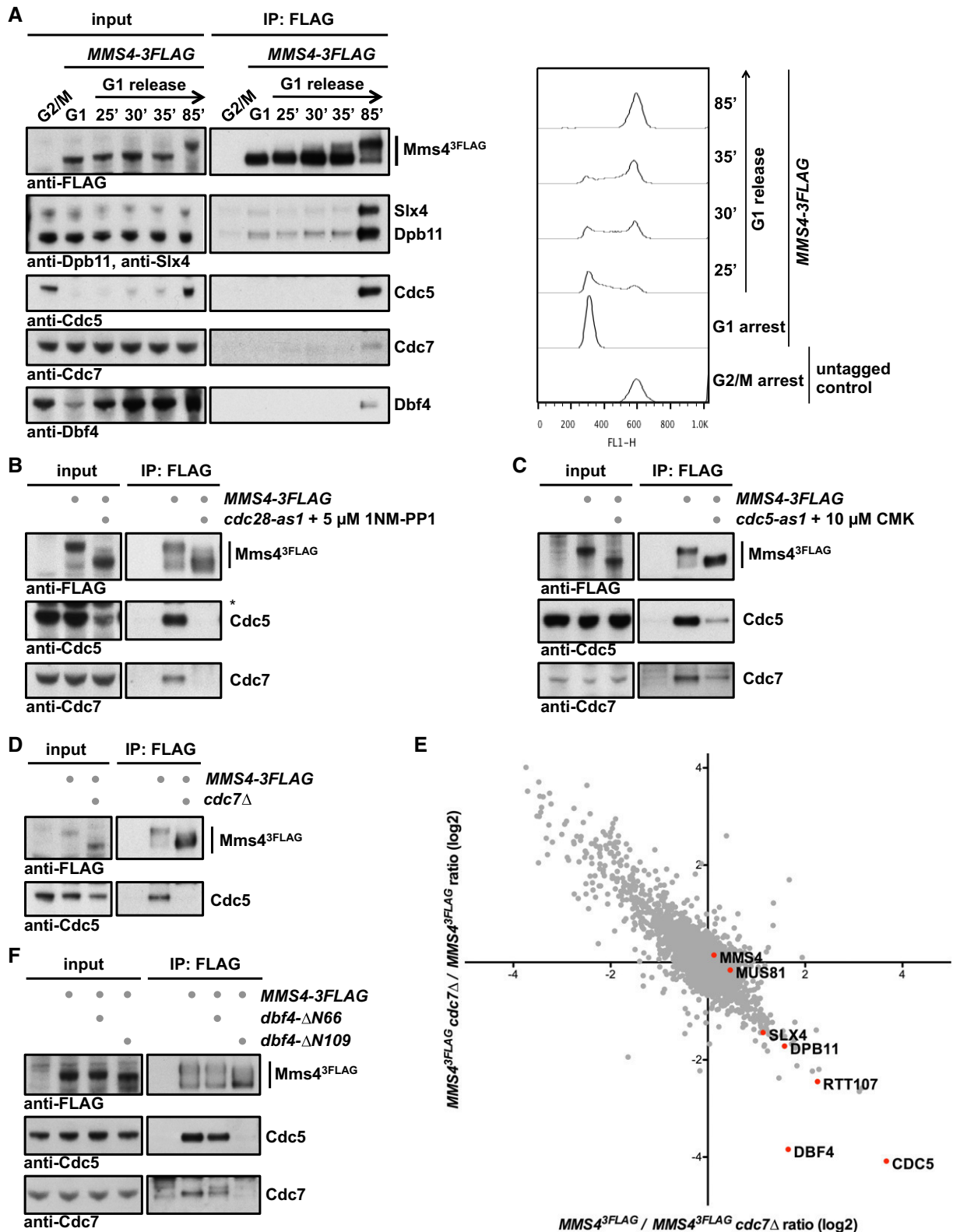


Figure 2.

hyperphosphorylation (Fig EV1A; Matos *et al*, 2013), suggesting that S-phase DDK is in principle competent for Cdc5 binding and joint substrate phosphorylation.

Furthermore, we performed additional experiments that addressed the regulation of Mus81-Mms4 by the DNA damage response. In M-phase-arrested cells, association of DDK and

**Figure 2. DDK and Cdc5 target Mus81-Mms4 in an interdependent manner.**

- A DDK stably associates with Mus81-Mms4 in mitosis, but not in S phase or G1. Mms4<sup>3FLAG</sup> pull down experiment (left panel, as in Fig 1A) from cells arrested in G1 (with alpha-factor) or in cells progressing synchronously through S phase until mitosis (arrest with nocodazole) reveals that DDK binds specifically in mitosis concomitant with the raise in Cdc5 levels and Cdc5 binding to Mus81-Mms4. A nocodazole-arrested untagged strain was used as a control. Right panel shows measurements of DNA content by FACS from the respective samples.
- B CDK activity is required for DDK and Cdc5 association with Mus81-Mms4. Mms4<sup>3FLAG</sup> pull down as in (A), but in mitotic WT or *cdc28-as1* mutant cells treated with 5 μM 1NM-PP1 for 1 h. Additional Western blots of this experiment are shown in Appendix Fig S5B, including as a control the identical anti-FLAG Western blot.
- C Cdc5 activity is required for DDK association with Mus81-Mms4. Mms4<sup>3FLAG</sup> pull down as in (A), but with mitotically arrested WT or *cdc5-as1* mutant cells treated with 10 μM CMK for 1 h.
- D, E DDK is required for Cdc5 binding to Mus81-Mms4 in mitosis and the mitotic Mms4 phospho-shift. (D) Mms4<sup>3FLAG</sup> pull down using mitotically arrested cells as in (A), but using a *bob1-1* background (all samples), where the DDK subunit Cdc7 could be deleted. (E) SILAC-based quantification of Mms4<sup>3FLAG</sup> pull downs in mitotically arrested *bob1-1* vs. *bob1-1 cdc7Δ* cells. Plotted are the H/L ratios of two independent experiments including label switch.
- F The Cdc5 binding region on Dbf4 is required for interaction of DDK and Cdc5 with Mus81-Mms4 and for efficient Mms4 phosphorylation. Mms4<sup>3FLAG</sup> pull down as in (A), but using mitotically arrested cells expressing N-terminal truncation mutants of Dbf4 lacking aa2–66 (including a D-box motif) or 2–109 [additionally including the Cdc5 binding site (Miller et al, 2009)].

Cdc5 with Mus81-Mms4 was reduced after induction of DNA damage with phleomycin (Appendix Fig S2F), but this treatment was not sufficient to induce a significant reduction in the Mms4 phosphorylation shift. Interestingly, when we forced Cdc5 expression in S-phase cells and compared normal S-phase cells to cells treated with hydroxyurea (HU), we observed that the Mms4 phosphorylation shift was less pronounced in the presence of hydroxyurea (HU) (Fig EV1B). These data are therefore consistent with the current view that DNA damage, specifically the DNA damage checkpoint, negatively influences Mus81 resolution activity (Szakal & Branzei, 2013; Gritenaite et al, 2014). Since DDK is known to be targeted and inhibited by the DNA damage checkpoint (Weinreich & Stillman, 1999; Lopez-Mosqueda et al, 2010; Zegerman & Diffley, 2010), it could become particularly critical to regulate Mms4 phosphorylation after DNA damage.

Even though DDK and Cdc5 seem to target Mus81-Mms4 in unison, we tested whether it was possible to resolve differences on the level of individual phosphorylation sites. Therefore, we analysed Mms4 phosphorylation sites in M-phase cells after Cdc5 inhibition (Fig 3A and C) or *CDC7* deletion (Fig 3B and D) by SILAC-based mass spectrometry. We also applied two different experimental set-ups that used either endogenously expressed Mus81-Mms4 (Fig 3A and B) or overexpressed Mus81-Mms4 (Fig 3C and D), as the latter set-up allowed much better coverage of Mms4 phosphopeptides in higher order phosphorylation states (peptides harbouring > 1 phosphorylated site). Cdc5 inhibition or lack of DDK led to overlapping, but distinct changes in Mms4 phosphorylation sites, suggesting that each kinase phosphorylates specific sites on Mms4. After Cdc5 inhibition, phosphorylation of many sites was reduced and among those were sites that match to a putative Cdc5 consensus [(D/E/N)X(S/T), blue, Fig 3A and C; Mok et al, 2010]. Overall, *CDC7* affected Mms4 phosphorylation less than Cdc5 inhibition, but nonetheless, we found widespread changes in the phosphorylation of (S/T)(S/T) motifs (Fig 3B and D). (S/T)(S/T) motifs were found less abundantly in the doubly phosphorylated state (Fig 3D, red), while conversely these motifs were found more abundantly in the state where only the second (S/T) was singly phosphorylated (Fig 3B and D, yellow), as expected for a substrate–product relation. These data are thus consistent with phosphorylation of the second (S/T) priming for phosphorylation at the preceding (S/T) (Appendix Table S1 and Appendix Fig S3).

### DDK phosphorylation is required for activation of Mus81-Mms4 during mitosis

Phosphorylation of Mms4 by CDK and Cdc5 has previously been shown to be required for the upregulation of Mus81-Mms4 activity during mitosis (Matos et al, 2011, 2013; Gallo-Fernández et al, 2012; Szakal & Branzei, 2013). Based on our finding that hyperphosphorylation of Mms4 was impaired in the absence of DDK (Fig 2D and Appendix Fig S2C), we predicted that also Mus81-Mms4 activity would be influenced. Therefore, we tested the activity of endogenous Mus81<sup>9myc</sup>-Mms4<sup>3FLAG</sup> immunopurified from G2/M arrested cells (approx. 5 fmol) on a nicked Holliday junction (nHJ) substrate (500 fmol) using an assay related to those in (Matos et al, 2011, 2013; Gritenaite et al, 2014). Notably, the activity of the endogenous purified Mus81-Mms4 from G2/M cells exceeded the activity of recombinant Mus81-Mms4 (subjected to a dephosphorylation step during the purification), indicating that it is the mitotically activated form (Appendix Fig S4A). Moreover, the activity of endogenous purified Mus81-Mms4 was not influenced by 350 mM NaCl salt washes. This indicates that the presence of accessory, salt-labile factors such as Rtt107 or Cdc5 in the reaction is unlikely to contribute to Mus81 activity (Appendix Fig S4B and C).

Importantly, when we used this assay to test immunopurified Mus81<sup>9myc</sup>-Mms4<sup>3FLAG</sup> from mitotic cells lacking DDK (*cdc7Δ* or *dbf4Δ*), we observed a reduced activity compared to Mus81<sup>9myc</sup>-Mms4<sup>3FLAG</sup> from WT cells (Fig 4A and Appendix Fig S4D; also observed with an RF substrate, Appendix Fig S4E). In order to exclude that indirect effects of the *CDC7* deletion may cause the reduction in Mus81 activity, we furthermore created an Mms4 mutant that specifically lacks candidate DDK phosphorylation sites. We chose to mutate (S/T)(S/T) motifs (SS motifs in particular) and created an *mms4-8A* mutant that harboured eight S to A exchanges at the N-terminal (S/T) of the motifs (see Appendix Fig S3A). This mutant appeared less phosphorylated in mitosis as judged by a less pronounced phosphorylation shift (Fig 4B). Furthermore, we observed a reduction in the association of DDK and Cdc5 with the Mus81-Mms4-8A complex in pull-down experiments (Fig 4B), suggesting that phosphorylation of Mms4 also plays a role in tethering these kinases. Notably, Mus81<sup>9myc</sup>-Mms4<sup>3FLAG</sup>-8A from mitotic cells showed a moderate but reproducible reduction in resolution activity on nHJ substrates compared to WT Mus81<sup>9myc</sup>-Mms4<sup>3FLAG</sup> (Fig 4C and Appendix Fig

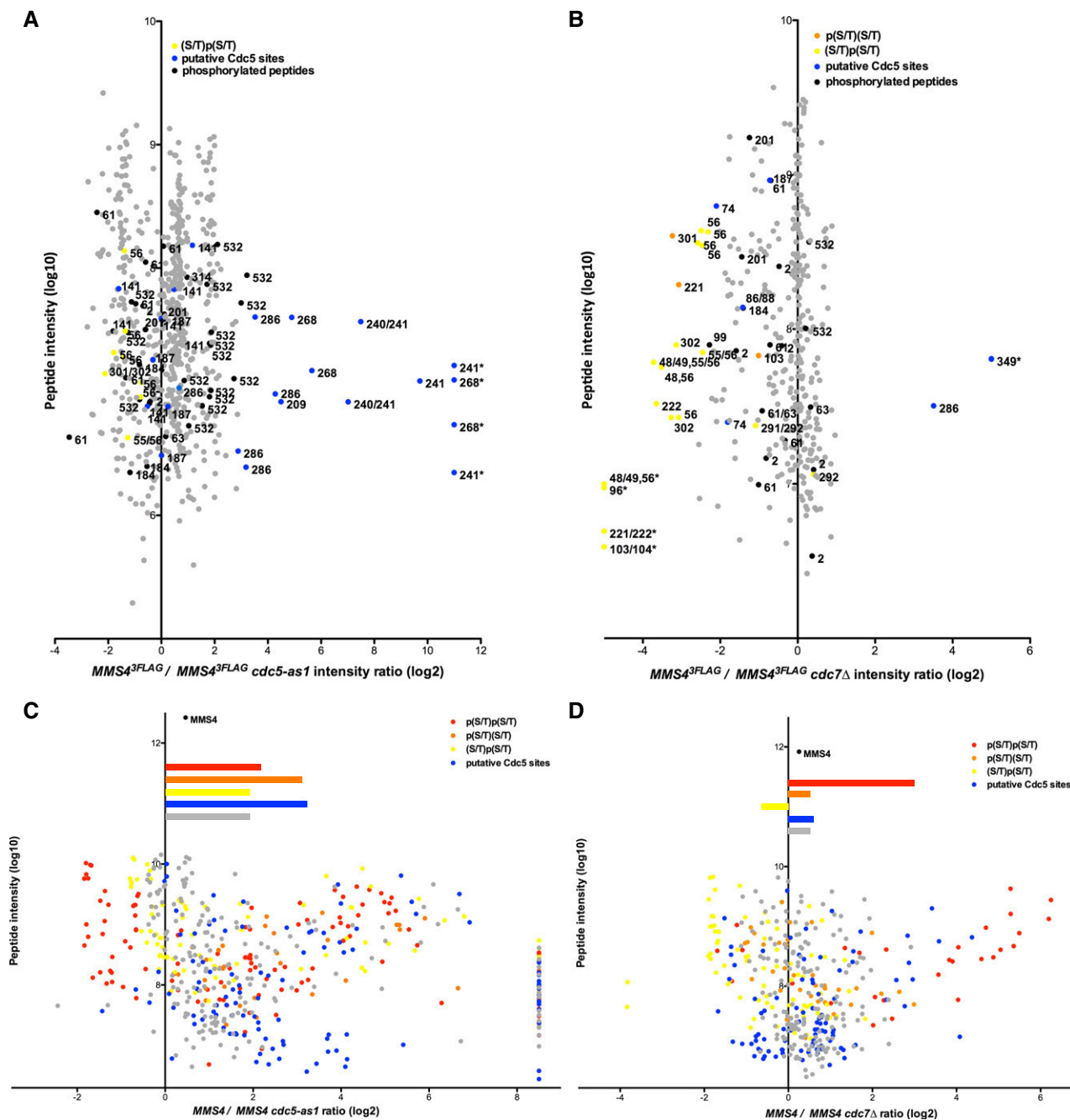


**Figure 3. Analysis of Mms4 phosphorylation sites reveals Cdc5 and DDK target sites, as well as the interdependence between the two.**

Changes of the abundance of phosphorylated Mms4 peptides after Cdc5 inhibition (as in Fig 2C) (A, C) or in the absence of Cdc7 (B, D) in mitotically arrested cells.

- A, B Depicted are SILAC-based intensity ratios of individual MS evidences for peptides of endogenously expressed Mms4. Evidences of non-phosphorylated Mms4 peptides are shown in grey; evidences of phosphorylated peptides are shown in black, yellow, orange or blue. Blue colour indicates putative Cdc5 phosphorylation as defined by the (D/E/N)X(S/T) consensus (and additionally S268, which was also very strongly deregulated upon Cdc5 inhibition). Yellow or orange colours mark singly phosphorylated (S/T)(S/T) motifs, with orange marking p(S/T)(S/T) and yellow marking (S/T)p(S/T). Numbers indicate the phosphorylated residue in the depicted peptide. An asterisk marks peptide evidences that contained measured intensity values exclusively in the heavy or light sample. For doubly phosphorylated peptides, the two phospho-sites are separated by a comma. For singly phosphorylated (S/T)(S/T) motifs, peptide ion fragmentation was in some cases unable to unambiguously identify the phosphorylated residue. In these cases, possible phosphorylation sites are indicated as “a/b”. Note that doubly phosphorylated (S/T)(S/T) sites were not reproducibly identified under conditions of endogenous Mus81-Mms4 expression.
- C, D As in panels (A, B) but using Mus81-Mms4 expressed from a high-copy promoter. Depicted are SILAC-based H/L ratios of individual MS evidences for phosphorylated peptides only. Peptides were sorted into categories according to their phosphorylation status: putative DDK target sites ((S/T)(S/T) motifs) were differentiated into the categories p(S/T)p(S/T) (red), p(S/T)(S/T) (orange) or (S/T)p(S/T) (yellow). Phosphorylated peptides matching the Cdc5 consensus site are coloured in blue. All other phosphorylated peptides are marked in grey. Bars depict the mean of the ratios of the respective category. Overall, Mms4 H/L ratio is shown on top.

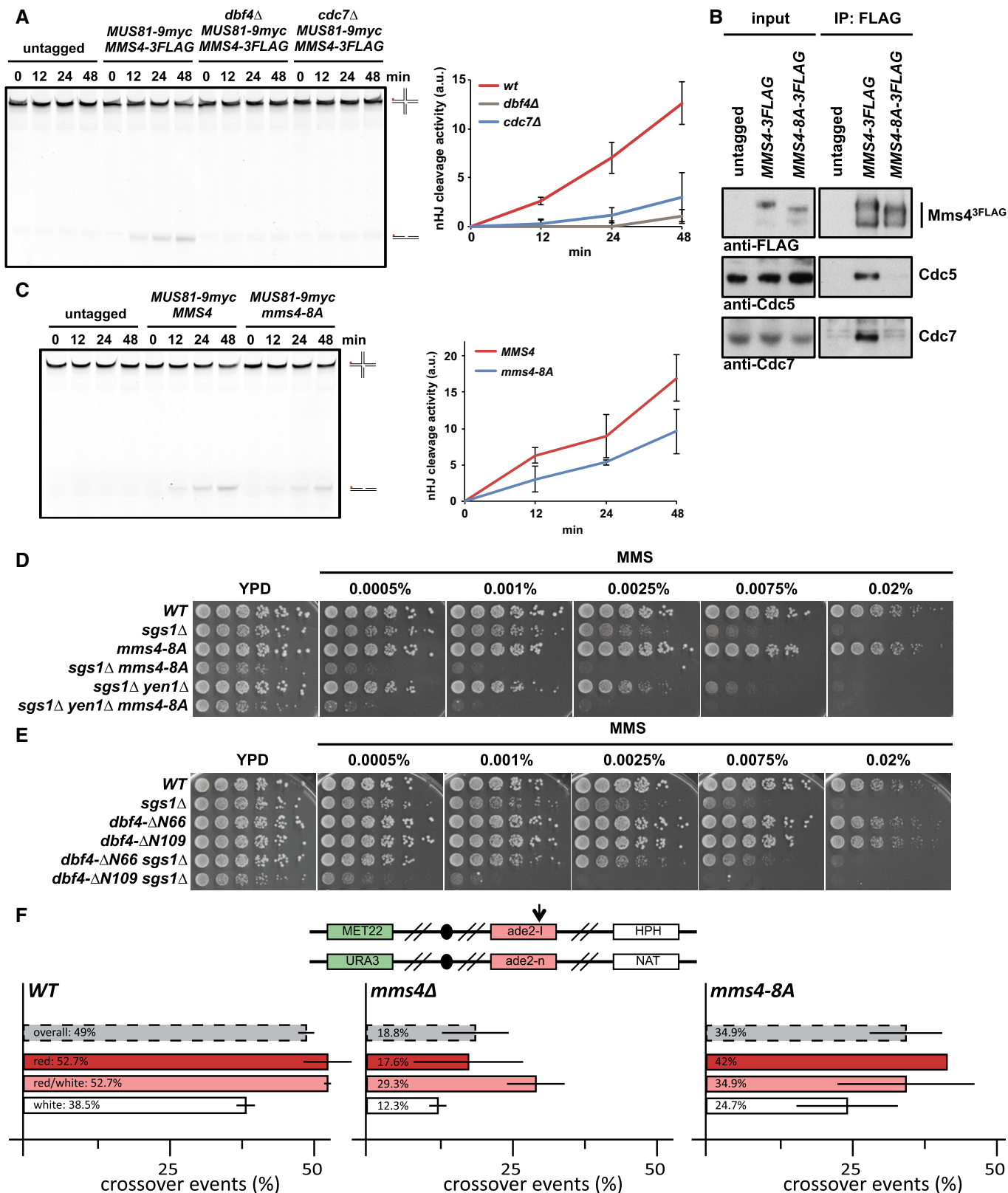


Figure 4.

S4F). These data thus indicate that DDK targets Mus81-Mms4 and that (S/T)(S/T) phosphorylation events are essential for full activation of Mus81 in mitosis.

Additionally, we investigated the relevance of the *mms4-8A* mutation *in vivo*. In comparison with *mus81Δ* or *mms4Δ* mutants, the *mms4-8A* mutant showed a hypomorphic phenotype. For

**Figure 4. DDK phosphorylation controls activation of Mus81-Mms4 resolvase activity in mitosis.**

- A DDK is required for mitotic activation of Mus81-Mms4. Resolution assay using a nicked Holliday junction (nHJ) substrate and Mus81<sup>9myc</sup>-Mms4<sup>3FLAG</sup> purified from mitotically arrested *bob1-1* (DDK-WT<sup>+</sup>), *bob1-1 dbf4Δ* and *bob1-1 cdc7Δ* strains or untagged control cells. Right panel: quantification of cleavage products. See Appendix Fig S4D for Western blots samples of anti-myc IPs. Left panel: representative gel image.
- B A defect in the phosphorylation of Mms4 (S/T)(S/T) sites causes reduced association of Cdc5 and DDK with Mus81-Mms4 and reduced phosphorylation of Mms4. Mms4<sup>3FLAG</sup> pull down as in Fig 1A, but using mitotically arrested WT and *mms4-8A* mutant cells, which harbour 8 serine to alanine exchanges at (S/T)(S/T) motifs (detailed in Appendix Fig S3).
- C Reduced (S/T)(S/T) phosphorylation of Mms4 generates a defect in Mus81-Mms4 activity. Resolution assay as in (A), but comparing mitotic Mus81-Mms4 from untagged, WT and *mms4-8A* strains (see Appendix Fig S4F for Western blot samples of anti-myc IPs).
- D, E The *mms4-8A* mutation and lack of the Cdc5-DDK interaction (*dbf4-ΔN109*) lead to hypersensitivity towards MMS specifically in the *sgs1Δ* background. Shown is the growth of indicated strains in fivefold serial dilution on plates containing MMS at indicated concentrations after 2 days at 30°C.
- F The *mms4-8A* mutant leads to a reduction in crossover formation. Recombination assay between heterologous *ade2* alleles in diploid cells as described in Ho et al (2010). The top panel indicates markers on both copies of chromosome XV that are used to determine genetic outcomes of DSB repair. Arrow indicates the I-SceI cut site. Bottom panel indicates rates of crossover events (%) overall (grey) and in the individual classes (red, red/white, white) that differ in gene conversion tract length. Error bars indicate standard deviation of two independent experiments, each scoring 400–600 colonies per strain.

Data information: (A, C) Depicted are means from three independent experiments, error bars correspond to standard deviation.

example, it did neither significantly increase the MMS hypersensitivity of a *yen1Δ* mutant, nor did it confer synthetic lethality with mutants defective in STR function, such as *sgs1Δ*, even though the *mms4-8A sgs1Δ* double mutant displayed a slow growth phenotype (Figs 4D and EV2A). Importantly, however, we did observe a strongly increased hypersensitivity towards MMS, when we tested an *mms4-8A sgs1Δ* double mutant and compared it to an *sgs1Δ* single mutant (Fig 4D). The *mms4-8A* mutation thus leads to a phenotype that is very similar to other activation-deficient *MMS4* mutants in budding and fission yeast (Gallo-Fernández et al, 2012; Dehé et al, 2013; Matos et al, 2013). Remarkably, the MMS hypersensitivity phenotype of the *mms4-8A* mutant was highly similar to that of the Cdc5 binding-deficient *dbf4-ΔN109* mutant (Figs 4E and EV2B), which also showed reduced survival when combined with *sgs1Δ* (Fig 4E). These data are therefore consistent with DDK functioning to stimulate JM resolution via Mms4 hyperphosphorylation.

It is likely that the *mms4-8A* mutant is only partially deficient in DDK phosphorylation, since Mms4 contains overall 15 (S/T)(S/T) sites and DDK may phosphorylate the protein on non-(S/T)(S/T) sites as well. We therefore note that an *mms4-12A* mutant, harbouring four additional S to A exchanges on (S/T)(S/T) motifs, showed further increased MMS sensitivity in the *mms4-12A sgs1Δ* mutant, when compared to the *mms4-8A sgs1Δ* mutant, even though there were only minor additional effects on either the Mms4 mitotic phosphorylation shift or JM resolution activity (Fig EV2C–E).

In order to directly assess whether DDK phosphorylation was required for Mus81 function during JM resolution, we tested the influence of the *mms4-8A* mutant in a genetic crossover assay (Ho et al, 2010). In this system, a site-specific DSB is induced in diploid cells and repair products can be measured by the arrangement of markers and colony sectoring (Fig 4F, upper panel). In this assay, *mus81Δ* and *mms4Δ* mutants show a reduction in CO products and a proportional increase in NCO products (Fig 4F; Ho et al, 2010), as would be expected from a defect in JM resolution and the accompanying shift of repair pathways towards JM dissolution. The *mms4-8A* mutant shows a similar, albeit weaker defect in the formation of CO products (Fig 4F), suggesting that the defect in Mus81 activation in mitosis results in an overall defect in JM resolution. We therefore conclude that DDK—in conjunction with Cdc5—acts directly on Mms4 and that these phosphorylation events are required for efficient Mus81-dependent JM resolution in mitosis.

**The Dpb11-Mms4 interaction is not required for DDK-Cdc5-dependent activation of Mus81-Mms4**

It is noteworthy that the association of DDK and Cdc5 with Mus81-Mms4 coincides with the formation of the Mus81-Mms4 complex with scaffold proteins such as Slx4, Dpb11 and Rtt107, which come together in mitosis (Fig 2A). Therefore, we asked whether the scaffold proteins Dpb11, Slx4 or Rtt107 would be required to target DDK and Cdc5 to Mus81-Mms4. In order to investigate the influence of Dpb11, we searched for an *MMS4* mutant that was deficient in the interaction with Dpb11. When we used a two-hybrid approach to map the Dpb11 interaction site on Mms4, we found that Mms4 constructs comprising aa 1–212 or 101–230 interacted with Dpb11, while constructs comprising aa 1–195 or 176–230 showed no or reduced interaction (Appendix Fig S5A). This suggested that the Dpb11 binding site may be located between aa 101–212 of Mms4. Consistently, we observed that the Mms4-S201A mutation abolished binding to Dpb11 in yeast two-hybrid and co-IP (Fig 5A and B), while the Mms4-S184A mutation reduced it (Fig 5A). Serine 201 and 184 are therefore likely candidates for phospho-sites bound and read by Dpb11. Serine 201 matches the full CDK consensus motif (S/T)PxK, while serine 184 matches the minimal CDK consensus motif (S/T)P. Indeed, we find that CDK inhibition reduced the Dpb11 interaction with Mus81-Mms4 (Appendix Fig S5B) consistent with a requirement of CDK phosphorylation for a robust interaction between Dpb11 and Mms4.

When we investigated the phenotype of the *mms4-SS184,201AA* mutant, we found that it showed enhanced hypersensitivity to MMS specifically in the *sgs1Δ* mutant background, consistent with a role of Dpb11 in JM resolution after MMS damage (Fig 5C). We also noted that the phenotype of this *MMS4* variant differed from that induced by Dpb11 binding-deficient version of Slx4 [*slx4-S486A* (Gritenaite et al, 2014; Ohouo et al, 2012)]. This could suggest that these mutants are able to separate different Dpb11 functions such as a mitotic function in conjunction with Mus81-Mms4 and an S-phase function, which Slx4 and Dpb11 might have independently of Mus81-Mms4 (Ohouo et al, 2012; Gritenaite et al, 2014; Cussiol et al, 2015; Princz et al, 2015). However, it also needs to be considered that Slx4 and Mus81-Mms4 may be connected by more than one scaffold protein (see below).

Importantly, however, we did not observe a defect in the association of DDK or Cdc5 with Mus81-Mms4, when we performed

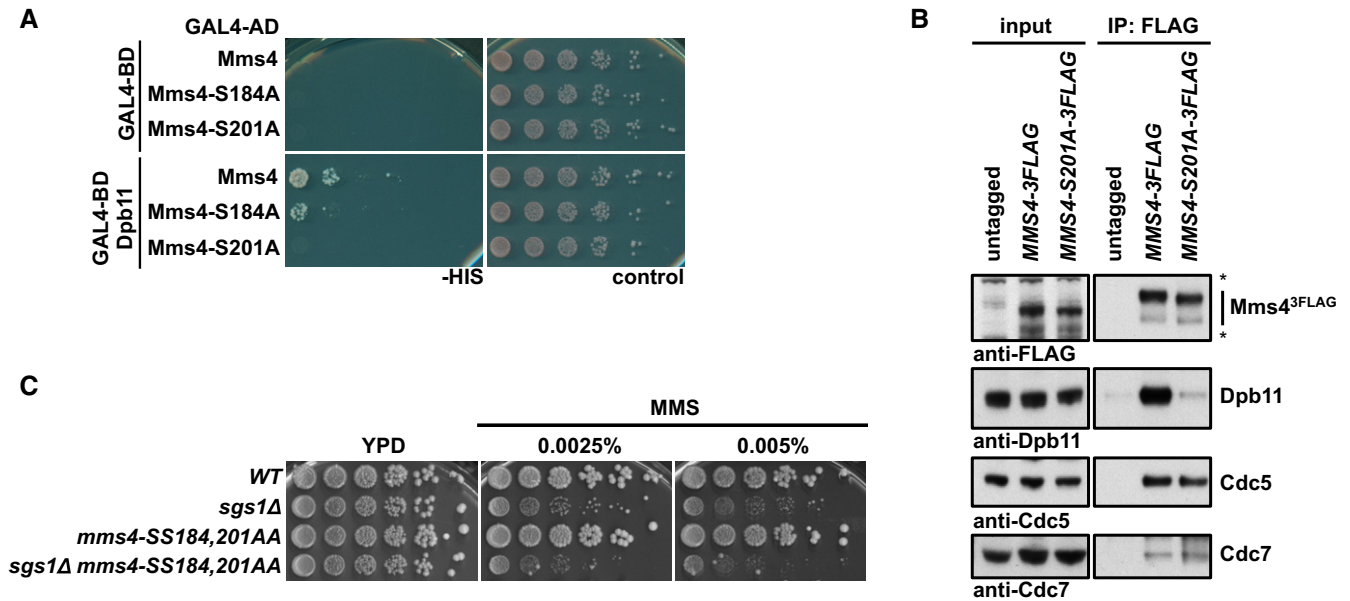


**Figure 5. The interaction between Mms4 and Dpb11 is dispensable for binding of Cdc5 and DDK and mitotic Mus81-Mms4 activation.**

A, B Serine 201 of Mms4 is required for Dpb11 binding, but not for interaction with DDK and Cdc5. (A) Two-hybrid interaction analysis using Gal4-BD-Dpb11 with Gal4-AD-Mms4, Gal4-AD-Mms4-S184A and Gal4-AD-Mms4-S201A constructs. (B) Mms4<sup>3FLAG</sup> pull downs from mitotically arrested cells as in Fig 1A, but using WT or S201A variants of Mms4<sup>3FLAG</sup>. Asterisks mark cross-reactive bands.

C The Dpb11 binding-deficient allele *mms4-SS184,201AA* leads to a MMS hypersensitivity specifically in the *sgs1Δ* background. Spotting assay as in Fig 4D.

Mms4-S201A<sup>3FLAG</sup> pull downs and compared them to a WT Mms4<sup>3FLAG</sup> pull down (Fig 5B). Furthermore, we only observed a very minor defect in the *in vitro* resolution of nHJ substrates, when we purified Mus81-Mms4 from mitotically arrested *mms4-S201A* cells (Appendix Fig S5C). We therefore reason that Dpb11 is most likely not involved in promoting Mms4 phosphorylation or DDK-Cdc5-dependent activation of Mus81-Mms4.

#### The Rtt107 scaffold recruits DDK and Cdc5 to Mus81-Mms4

Having excluded a role of Dpb11 in the recruitment of DDK and Cdc5, we next tested a possible involvement of the Rtt107 scaffold protein. Indeed, when we used an *rtt107Δ* mutant in IP and SILAC-based IP-MS experiments, we observed that DDK and Cdc5 binding to Mus81-Mms4 was strongly reduced (Fig 6A and Appendix Fig S6A). Interestingly, Rtt107 bound to DDK and Cdc5 even under conditions where Rtt107 binding to Mus81-Mms4 was abolished (*mus81Δ*, Appendix Fig S6B). This suggests that Rtt107 may form a subcomplex with DDK and Cdc5. Consistently, we found that Rtt107 bound to Cdc7 in a two-hybrid assay (Fig 6B). These data therefore suggest that Rtt107 mediates binding of DDK and Cdc5 to the Mus81-Mms4 complex, most likely via a Cdc7 interaction site on Rtt107.

During our co-IP studies, we furthermore found that the location of Rtt107 in the mitotic Mus81-Mms4 complex was different than expected. Given that Slx4 was required to bridge between Rtt107 and Dpb11 (Ohouo *et al*, 2010) and that Mms4 and Dpb11 seemingly interact directly (Gritenaite *et al*, 2014 and Fig 5A and B), we initially expected that Slx4 and Dpb11 would be required to mediate the interaction between Rtt107 and Mus81-Mms4. Surprisingly, we found that an *slx4Δ* mutant did not influence DDK or Cdc5 binding

to Mus81-Mms4 and thereby differed from *rtt107Δ* (Fig 6A). Therefore, we tested if Rtt107 could bind to Mus81-Mms4 independently of Slx4 or Dpb11. Indeed, we found that the Mus81-Mms4 interaction to Rtt107 was not influenced by the *slx4Δ* mutant (Fig 6C) or the Dpb11 binding-deficient *mms4-S201A* allele (Fig 6D), indicating that Rtt107 binding to the Mus81-Mms4 complex occurs independently of the other scaffold proteins. In contrast, our data also show that its binding is strongly dependent on kinases and Mms4 phosphorylation, since Rtt107 binding was strongly reduced in the absence of DDK (Fig 2E), after Cdc5 inhibition (Appendix Fig S2A) or in the *mms4-8A* phosphorylation site mutant (Fig EV3).

Therefore, these data provide novel insight into the role of Rtt107 in Mus81-Mms4 regulation. First, it shows that Rtt107 mediates the association of DDK and Cdc5 kinases with Mus81-Mms4. Second, it also suggests that Rtt107 may bind directly to Mus81-Mms4 and that this binding is dependent on Mms4 phosphorylation and the cell cycle kinases DDK and Cdc5, although an alternative model whereby Rtt107 indirectly promotes DDK and Cdc5 to tightly associate with Mus81-Mms4 cannot be ruled out entirely. The fact that Rtt107 promotes the interaction of Mus81-Mms4 with the kinases, yet in turn requires the kinases and Mms4 phosphorylation for interaction, suggests that Rtt107 may be acting after initial Mms4 phosphorylation has occurred and at this late stage tethers the kinases, thus promoting phosphorylation of otherwise inefficiently phosphorylated sites.

#### Rtt107 stimulates Mms4 hyperphosphorylation in order to enhance Mus81-Mms4 activity in mitosis

Given Rtt107's involvement in tethering DDK and Cdc5 to the Mus81-Mms4 complex, we asked whether Rtt107 would mediate

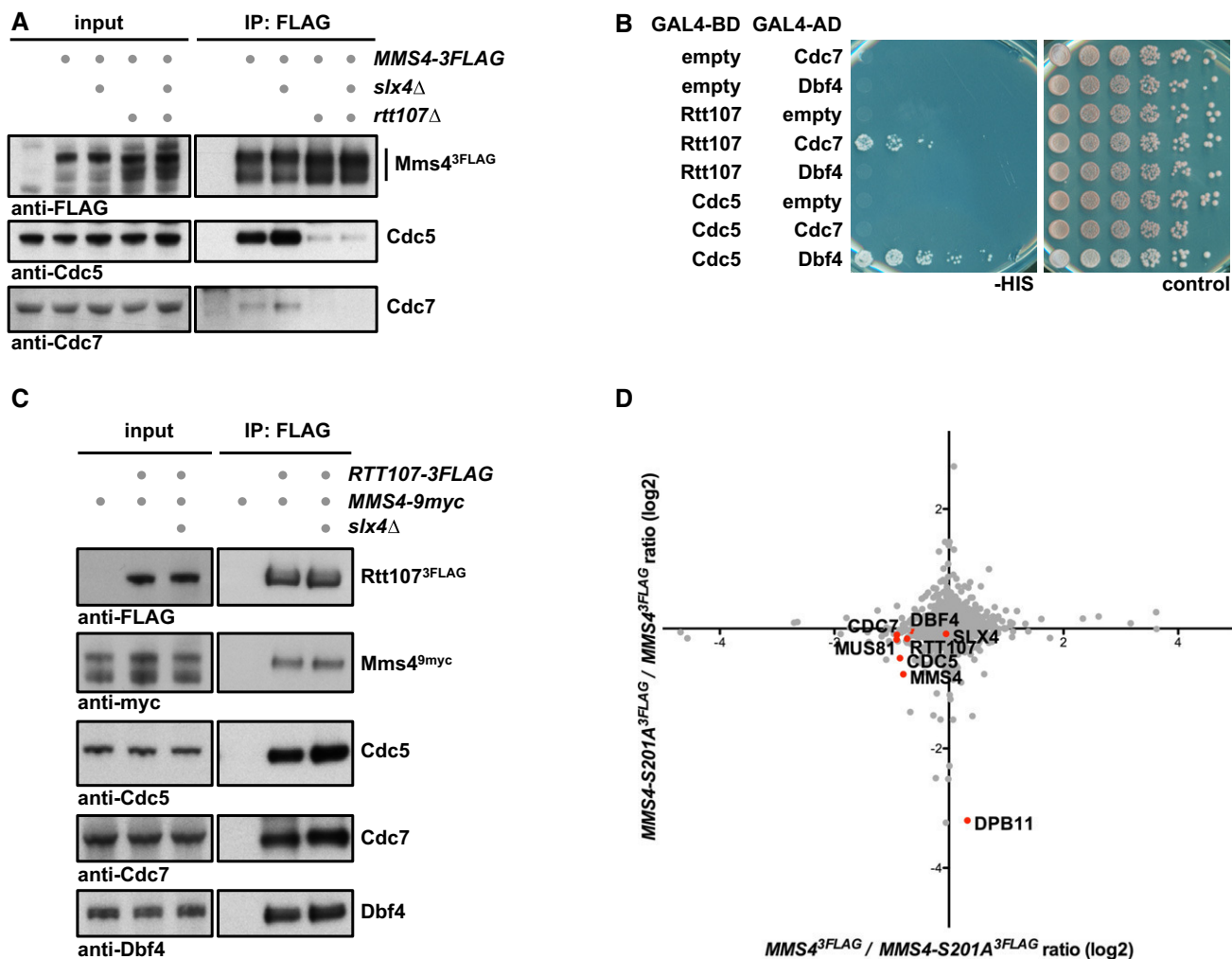


**Figure 6. The Rtt107 scaffold tethers DDK and Cdc5 to Mus81-Mms4 independently of Slx4 and Dpb11.**

- A Rtt107, but not Slx4, is required for DDK and Cdc5 interaction with Mus81-Mms4. Mms4<sup>3FLAG</sup> pull downs from mitotically arrested cells as in Fig 1A, but specifically comparing interactions of Mus81-Mms4 in WT, *slx4Δ*, *rtt107Δ* and *slx4Δ rtt107Δ* mutant backgrounds.
- B Rtt107 interacts with Cdc7. Two-hybrid interaction was tested using Gal4-BD-Rtt107 constructs and Gal4-AD-Cdc7 or Gal4-AD-Dbf4 constructs. Interaction between Gal4-BD-Cdc5 and Gal4-AD-Dbf4 serves as positive control.
- C Rtt107 interacts with Mus81-Mms4, DDK and Cdc5 independently of Slx4. Rtt107<sup>3FLAG</sup> co-IPs from untagged control, WT or *slx4Δ* cells arrested in mitosis were probed for indicated proteins.
- D Rtt107 interacts with Mus81-Mms4 independently of the Mms4-Dpb11 interaction. SILAC-based Mms4<sup>3FLAG</sup> pull down in WT and *mms4-S201A* cells reveals changes in the Dpb11 association, but not in Rtt107, Slx4, Cdc5 or DDK binding. Plotted are the H/L ratios of two experiments including label switch.

mitotic hyperphosphorylation of Mms4 and concomitant activation of the Mus81 nuclease. We observed only a minor effect on the mitotic phospho-shift of Mms4 when using *rtt107Δ* mutants (Fig 6A and Appendix Fig S2C). However, as it is still unclear which phosphorylation sites contribute to the Mms4 phospho-shift, we investigated the effect of *rtt107Δ* on individual phosphorylation sites in our mass spectrometry data. Appendix Fig S7A and B shows SILAC-based comparisons of Mms4 phosphorylation sites in WT and *rtt107Δ* cells, expressing Mus81-Mms4 from endogenous (Appendix Fig S7A) or high-copy promoters (Appendix Fig S7B). The overexpression set-up allowed us to quantify phosphorylation at (S/T)(S/T) motifs, and we found that double phosphorylation of several of these sites was reduced (Appendix Fig S7B), although the change was much smaller compared to cells lacking DDK. On the

other hand, while we could not detect higher order phosphorylated Mms4 peptides using endogenous Mus81-Mms4, we could detect an effect of Rtt107 on several other sites (T209, S241 and S268, and to a lesser extent S286; Appendix Fig S7A), which were also deregulated after Cdc5 inhibition (Fig 3A and C). These data are thus consistent with Rtt107 promoting efficient DDK and Cdc5 phosphorylation of Mms4.

Therefore, we tested whether Rtt107 would affect the mitotic activation of Mus81-Mms4. We immunopurified Mus81<sup>9myc</sup>-Mms4<sup>3FLAG</sup> from WT and *rtt107Δ* cells that were arrested in mitosis and found that Mus81-Mms4 activity on a nHJ substrate was reduced in the *rtt107Δ* background (Fig 7A and Appendix Fig S7C). Furthermore, in the background of deficient DDK (*cdc7Δ bob1-1*), additional mutation of *rtt107Δ* did not lead to a further defect in

Mus81-mediated cleavage (Appendix Fig S7D). Therefore, we conclude that Rtt107 is required for full mitotic activation of Mus81-Mms4 and that it works at least in part through cell cycle kinases such as DDK.

In order to test whether such a defect in Mus81-Mms4 activation would translate into a shifted balance of JM removal pathways, we measured rates of crossover and non-crossover formation in the absence of Rtt107. We observed a reduction in crossover rates in the *rtt107Δ* mutant indicating a shift in the balance of JM removal pathways (Fig 7B). The decrease was mostly visible in one class of recombinants (Fig 7B, “red”) and is smaller compared to the phenotype of a *mus81Δ* or a *mms4-8A* mutant (Ho et al, 2010; Fig 4F), consistent with a stimulatory but non-essential role of the Rtt107

scaffold in Mus81-Mms4 function. These data thus provide the first mechanistic insight of how the interaction of the mitotic Mus81-Mms4 complex with the scaffold proteins influences Mus81 function, as Rtt107 facilitates DDK and Cdc5 tethering, full mitotic phosphorylation of Mms4 and activation of Mus81-Mms4.

## Discussion

Activation of Mus81-Mms4 during mitosis is critical for the response to DNA damage, in particular to process repair intermediates that may arise from DSBs and stalled replication forks (Matos et al, 2011, 2013; Gallo-Fernández et al, 2012; Saugar et al, 2013; Szakal

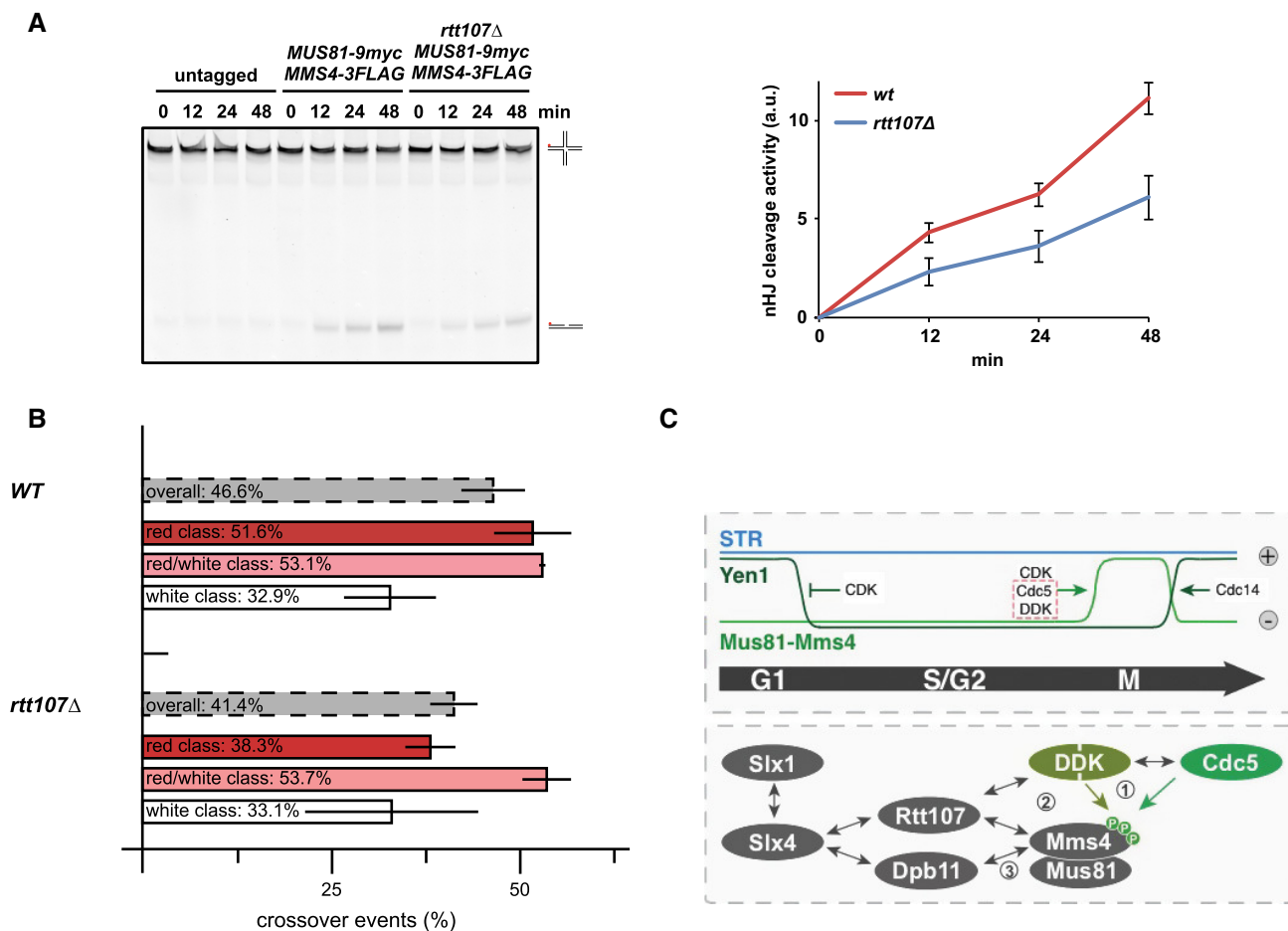


**Figure 7. Rtt107 is required for efficient Mus81-Mms4 activation in mitosis.**

**A** Mus81-Mms4 purified from mitotic *rtt107Δ* cells is less active compared to Mus81-Mms4 from WT cells. *In vitro* resolution activity of Mus81<sup>9myc</sup>-Mms4<sup>3FLAG</sup> purified from WT or *rtt107Δ* cells is tested on a nHJ substrate (see Appendix Fig S7C for control Western blot). Right panel: quantification of cleavage products from three independent experiments (mean ± SD). Left panel: representative gel picture.

**B** The *rtt107Δ* mutant leads to a reduction in crossover formation. Recombination assay as in Fig 4F. Note that the *rtt107Δ* mutant particularly affects crossover formation in the red class (long conversion tracts), while no significant defect could be observed in the red/white and white class (mean ± SD).

**C** Hypothetical model of Mus81-based JM resolution. Upper panel: cell cycle regulation of JM removal pathways, indicating Mus81 activation in mitosis. Lower panel: physical interactions of Mus81-Mms4 and its regulatory complex in mitotic cells. Grey arrows indicate physical interactions; green arrows specifically indicate kinase-substrate interactions. Genetic data indicate a hierarchy of molecular events leading to Mus81 activation. (1) DDK, Cdc5 and CDK (not shown) phosphorylate Mms4. (2) Rtt107 binds to DDK and Cdc5 and—in a phosphorylation-dependent manner—associates with Mus81-Mms4. This interaction is either direct or could potentially depend on bridging effects by DDK and Cdc5. Rtt107 promotes the stable interaction of DDK and Cdc5 with Mus81-Mms4 and thus full phosphorylation of Mms4 and Mus81 activation. (3) Upon Mms4 phosphorylation, two scaffold proteins, Rtt107 and Dpb11, bind independently to Mus81-Mms4. Both proteins can also bind to Slx4 enabling two alternative connections of Slx4 with Mus81-Mms4.

& Branzei, 2013). Previously, this regulation was shown to critically depend on phosphorylation by the cell cycle kinases CDK and Cdc5 (Matos *et al*, 2011, 2013; Gallo-Fernández *et al*, 2012; Saugar *et al*, 2013; Szakal & Branzei, 2013), but also involve the formation of a multi-protein complex comprising several scaffold proteins (Gritenaite *et al*, 2014). Here, we not only identify a new cell cycle kinase to be crucial for this regulation—DDK—but moreover show that the two regulatory pathways—cell cycle kinase phosphorylation and scaffold complex formation—are connected by Rtt107 (see Fig 7C for a hypothetical model). Rtt107 association depends on active cell cycle kinases and Mms4 phosphorylation, but in turn Rtt107 is required for stable DDK and Cdc5 association with the Mus81-Mms4 complex, as well as full phosphorylation of Mms4 and mitotic activation of Mus81. This study thus extends our mechanistic understanding of the regulatory framework that controls cell cycle-regulated JM resolution.

Interestingly, our work shows that for its function as a regulator of Mus81-Mms4 DDK must act interdependently and as a complex with Cdc5. DDK and Cdc5 have been shown to interact physically (Miller *et al*, 2009; Chen & Weinreich, 2010), but until now DDK was viewed to antagonize mitotic functions of Cdc5 (Miller *et al*, 2009). In contrast, in meiosis I DDK and Cdc5 are known to cooperate in order to promote chromosome segregation and jointly phosphorylate the monopolin and cohesin subunits Lrs4 and Rec8, respectively, as well as the meiotic regulator Spo13 (Matos *et al*, 2008). We now provide the first example for a joint DDK and Cdc5 substrate in the mitotic cell cycle, suggesting that cooperation between DDK and Cdc5 could be a more widespread phenomenon than previously anticipated. The apparent antagonism between DDK and Cdc5 in the regulation of mitotic exit (Miller *et al*, 2009), a canonical Cdc5 function, could be explained if DDK targeted Cdc5 to a specialized subset of substrates rather than to substrates involved in mitotic exit. It is also interesting to note that we could detect significant DDK binding to Mus81-Mms4 only after cells finished S phase (Fig 2A). Therefore, the role of DDK in Mms4 phosphorylation is clearly post-replicative and further challenges a simplified view of DDK as an S-phase kinase (Matos *et al*, 2008). It will therefore be interesting to see whether additional DDK substrates during mitosis can be identified and whether DDK collaborates with Cdc5 for their phosphorylation as well.

Mus81-Mms4 has previously been shown to be cell cycle-regulated and Mms4 to be a critical CDK and Cdc5 phosphorylation target (Matos *et al*, 2011; Gallo-Fernández *et al*, 2012). We add DDK to this already complex regulation. Our data clearly show that phosphorylation of (S/T)(S/T) motifs is critical for Mus81-Mms4 function. The hypomorphic phenotype of the *mms4-8A* mutant (Fig 4C, D and F) is likely due to additional DDK phosphorylation sites either on Mms4 or perhaps even on Mus81. Importantly, DDK does not appear to establish the timing of Mms4 phosphorylation in mitosis, as Cdc5 still seems to be the limiting factor for this temporal control in undisturbed cell cycles (Fig EV1B). However, the fact that activation of Mus81-Mms4 depends on the activity of several kinases makes it a coincidence detector that integrates the activity of several cell cycle regulators. Therefore, it can be envisioned that there are specific cellular conditions under which DDK activity becomes limiting for Mus81-Mms4 activation. Notably, DNA damage checkpoint kinases are known to phosphorylate DDK and counteract its function during S phase (Weinreich & Stillman, 1999; Lopez-Mosqueda *et al*, 2010; Zegerman & Diffley, 2010). Therefore,

it can be speculated that the checkpoint acts as a negative regulator of Mus81-Mms4 activation via inhibition of DDK. Such regulation could therefore explain how the presence of DNA damage restricts Mus81 activity towards replication intermediates (Matos *et al*, 2011, 2013; Saugar *et al*, 2013; Szakal & Branzei, 2013; Gritenaite *et al*, 2014), suggesting that cell cycle and checkpoint pathways converge in the regulation of Mus81.

A second layer of Mus81 regulation relies on the formation of a multi-protein complex, which assembles specifically in mitosis and contains Mus81-Mms4, DDK, Cdc5 and Slx4 as well as the scaffold proteins Dpb11 and Rtt107 (Gritenaite *et al*, 2014). We are only beginning to understand the mechanism whereby this scaffold complex influences Mus81 function. Here, we show that Rtt107, but not Dpb11 or Slx4, promotes the stable association of DDK and Cdc5 with Mus81-Mms4 (Fig 6), suggesting that one function of the multi-protein complex is to promote efficient Mus81-Mms4 phosphorylation. Conversely, our new data as well as our previous work (Gritenaite *et al*, 2014) show that phosphorylation by cell cycle kinases also regulates the formation of the multi-protein complex. In particular, Rtt107 association with Mus81-Mms4 depends strongly on DDK and Cdc5 (Fig 2E and Appendix Fig S2A). A direct interaction of Rtt107 with Mus81-Mms4 seems the most plausible interpretation of our data, although we currently cannot exclude that Rtt107 may facilitate the interaction of DDK and Cdc5 with Mus81-Mms4 without a direct interaction. A possible phosphorylation dependence of Rtt107 binding to the complex could thus originate from Mms4 phosphorylation generating a binding site for Rtt107 [e.g. for Rtt107 BRCT domains (Li *et al*, 2012)].

Importantly, Rtt107 is in turn required for stable binding of DDK and Cdc5 (Fig 6A and Appendix Fig S6A). Via tethering the kinases, Rtt107 regulates the phosphorylation of specific Mms4 sites and is required for full Mus81 activation (Fig 7A and Appendix Fig S7A and B). The interdependence between Rtt107 and Cdc5/DDK phosphorylation therefore suggests that Rtt107 may be part of a signal amplification mechanism, which ensures efficient Mus81-Mms4 phosphorylation and activation. Mechanistically, Rtt107-dependent stimulation of Mms4 phosphorylation thus resembles a kinase priming mechanism. It is entirely possible that other kinase priming mechanisms for either Cdc5 or DDK are at work in the Mms4 phosphorylation cascade, although the *in vitro* kinase assays with full-length proteins did not provide support for such a mechanism (Fig 1B, and Appendix Fig S1C and D). Altogether, it seems plausible to speculate that Rtt107-dependent and Rtt107-independent amplification mechanisms are involved in generating a switch-like activation of Mus81 in mitosis.

Furthermore, Rtt107 can also bind to Slx4 (Ohouo *et al*, 2010). There are thus two BRCT-containing scaffold proteins—Dpb11 (Gritenaite *et al*, 2014) and Rtt107—that could bridge between Mus81-Mms4 and Slx4. Interestingly, our data with different *mms4* mutants suggest that either one of these BRCT scaffold proteins is sufficient to connect Slx4 and Mus81-Mms4 [Figs 6D and EV3; note that the *rtt107Δ* mutant (Appendix Fig S6A) is difficult to interpret in this regard as it also leads to defects in Slx4 phosphorylation and the Slx4-Dpb11 interaction (Ohouo *et al*, 2010)]. This redundancy may thus explain the modest phenotype of the *mms4-S201A* mutant that is deficient in the Mms4-Dpb11 interaction (Fig 5C).

Several aspects of Mus81-Mms4 regulation are conserved throughout eukaryotic evolution. The HJ resolution activity of

Mus81-Eme1 in mammalian cells is cell cycle-regulated (Matos *et al*, 2011; Wyatt *et al*, 2013). Mus81-Eme1 furthermore binds to Slx4 and forms multi-protein complexes (Fekairi *et al*, 2009; Muñoz *et al*, 2009; Svendsen *et al*, 2009; Castor *et al*, 2013; Wyatt *et al*, 2013), albeit these complexes may have a different organization to that in yeast. Therefore, it will be interesting to explore in the future if in human cells DDK is also required for activation of Mus81-Eme1 and if this mechanism may contribute to the anti-tumorigenic activity of DDK inhibitors (Montagnoli *et al*, 2008).

## Materials and Methods

All yeast strains are based on W303 and were constructed using standard methods. Plasmids were constructed using the In-Fusion HD cloning kit (Clontech Laboratories), and mutations were introduced by site-directed mutagenesis. A summary of all yeast strains used in this study can be found in the Appendix Table S2.

Cell cycle synchronization was achieved using alpha-factor (G1), hydroxyurea (S), or nocodazole (mitosis). DNA content was measured by flow cytometry with a BD FACSCalibur system using SYTOX green to stain DNA.

Co-immunoprecipitations of yeast extracts were performed on anti-FLAG agarose resin (Sigma) for 2 h with head-over-tail rotation at 4°C as previously described (Gritenaite *et al*, 2014). After bead washing, proteins were eluted by 3X FLAG-peptide (Sigma), precipitated and separated on 4–12% Bis-Tris gels. For SILAC-based mass spectrometry, cells were labelled with heavy-isotope-labelled lysine (Lys6 or Lys8), and proteins were digested with Lys-C. Mass spectrometry data were analysed using MaxQuant (Cox & Mann, 2008).

Yeast two-hybrid assays, genetic interaction assays, *in vitro* kinase assays and peptide binding assays were performed as described previously (Pfander & Diffley, 2011; Gritenaite *et al*, 2014).

Nuclease assays were done as described (Matos *et al*, 2011, 2013). Briefly, Mus81<sup>9myc</sup> was immunopurified from mitotically arrested cells and mixed with 5'-Cy3-end-labelled nicked Holliday junctions. After incubation at 30°C for the indicated times, the reaction was stopped by proteinase K and SDS for 1 h at 37°C. Products were separated by 10% PAGE, and cleavage efficiency was normalized to the level of immunoprecipitated Mus81<sup>9myc</sup>. Unspecific nHJ cleavage in untagged controls was subtracted in the quantifications.

DSB-induced recombination assays were performed as described (Ho *et al*, 2010). Diploids harbouring I-SceI under the control of the GAL promoter were grown in adenine-rich raffinose medium and arrested in mitosis. Nuclease expression was induced by addition of galactose for 2.5 h. Cells were plated on YPAD and replica plated on YPAD + Hyg + Nat, YPAD + Hyg, YPAD + Nat, SC-Met, SC-Ura and SCR-ADE + Gal media after 3–4 days to classify recombination events.

Detailed experimental procedures are available in the Appendix.

### Data availability

Mass spectrometric datasets are available at EBI PRIDE. DDK and the Rtt107 scaffold promote Mus81-Mms4 resolvase activation during mitosis (2015). PXD005356.

**Expanded View** for this article is available online.

## Acknowledgements

We thank U. Kagerer for technical assistance, D. Gritenaite for early contributions to the project, N. Nagaraj and the proteomics laboratory of the MPIB core facility for proteomics analysis, the MPIB core facility for peptide synthesis and sequencing, J. Diffley and L. Symington for antibodies, plasmid constructs and strains, S. Jentsch, Z. Storchova, C. Biertümpfel and members of the Jentsch and Pfander labs for stimulating discussion and critical reading of the manuscript. Work in the Pfander laboratory is supported by the Max-Planck Society and the German Research Council (DFG). Work in the Matos laboratory is supported by ETH Zürich and the Swiss National Science Foundation (Grants 31003A\_153058 and 155823). Work in the Blanco laboratory is co-financed by Ministerio de Economía y Competitividad and FEDER (RYC-2012-10835 and BFU2013-41554-P). Philipp Wild is supported by an EMBO long-term fellowship (ALTF 475-2015). F. Javier Aguado is supported by a PhD fellowship from the I2C Program of Xunta de Galicia (ED481A-2015/011).

## Author contributions

PW and JM performed *in vitro* resolution assays of Figs 4A and C, 7A, and EV2E, and Appendix Figs S4A, C, E, and S7D and analysed the data. FJA and MGB provided recombinant purified Mus81-Mms4 used in Fig 1B, and Appendix Figs S1C and D, and S4A. All other experiments were performed and analysed by LNP, JB and BP. BP wrote the paper and all authors commented on the manuscript.

## Conflict of interest

The authors declare that they have no conflict of interest.

## References

- Alexandru G, Uhlmann F, Mechtler K, Poupard MA, Nasmyth K (2001) Phosphorylation of the cohesin subunit Scc1 by Polo/Cdc5 kinase regulates sister chromatid separation in yeast. *Cell* 105: 459–472
- Bishop AC, Ubersax JA, Petsch DT, Matheos DP, Gray NS, Blethrow J, Shimizu E, Tsien JZ, Schultz PG, Rose MD, Wood JL, Morgan DO, Shokat KM (2000) A chemical switch for inhibitor-sensitive alleles of any protein kinase. *Nature* 407: 395–401
- Bizard AH, Hickson ID (2014) The dissolution of double Holliday junctions. *Cold Spring Harb Perspect Biol* 6: a016477
- Blanco MG, Matos J, West SC (2014) Dual control of Yen1 nuclease activity and cellular localization by Cdk and Cdc14 prevents genome instability. *Mol Cell* 54: 94–106
- Branzei D, Foiani M (2008) Regulation of DNA repair throughout the cell cycle. *Nat Rev Mol Cell Biol* 9: 297–308
- Castor D, Nair N, Déclais A-C, Lachaud C, Toth R, Macartney TJ, Lilley DMJ, Arthur JSC, Rouse J (2013) Cooperative control of Holliday junction resolution and DNA repair by the SLX1 and MUS81-EME1 nucleases. *Mol Cell* 52: 221–233
- Chen YC, Weinreich M (2010) Dbf4 regulates the Cdc5 polo-like kinase through a distinct non-canonical binding interaction. *J Biol Chem* 285: 41244–41254
- Cheng L, Collyer T, Hardy CF (1999) Cell cycle regulation of DNA replication initiator factor Dbf4p. *Mol Cell Biol* 19: 4270–4278
- Cox J, Mann M (2008) MaxQuant enables high peptide identification rates, individualized p.p.b.-range mass accuracies and proteome-wide protein quantification. *Nat Biotechnol* 26: 1367–1372

- Cussiol JR, Jablonowski CM, Yimit A, Brown GW, Smolka MB (2015) Dampening DNA damage checkpoint signalling via coordinated BRCT domain interactions. *EMBO J* 34: 1704–1717
- Dehé P-M, Coulon S, Scaglione S, Shanahan P, Takedachi A, Wohlschlegel JA, Yates JR, Llorente B, Russell P, Gaillard P-HL (2013) Regulation of Mus81–Eme1 Holliday junction resolvase in response to DNA damage. *Nat Struct Mol Biol* 20: 598–603
- Eissler CL, Mazón G, Powers BL, Savinov SN, Symington LS, Hall MC (2014) The Cdk/Cdc14 module controls activation of the Yen1 Holliday junction resolvase to promote genome stability. *Mol Cell* 54: 80–93
- Fekairi S, Scaglione S, Chahwan C, Taylor ER, Tissier A, Coulon S, Dong M-Q, Ruse C, Yates JR, Russell P, Fuchs RP, McGowan CH, Gaillard P-HL (2009) Human SLX4 is a Holliday junction resolvase subunit that binds multiple DNA repair/recombination endonucleases. *Cell* 138: 78–89
- Ferreira MF, Santocanale C, Drury LS, Diffley JF (2000) Dbf4p, an essential S phase-promoting factor, is targeted for degradation by the anaphase-promoting complex. *Mol Cell Biol* 20: 242–248
- Ferretti LP, Lafranchi L, Sartori AA (2013) Controlling DNA-end resection: a new task for CDKs. *Front Genet* 4: 1–7
- Gallo-Fernández M, Saugar I, Ortiz-Bazán MÁ, Vázquez MV, Tercero JA (2012) Cell cycle-dependent regulation of the nuclease activity of Mus81–Eme1/Mms4. *Nucleic Acids Res* 40: 8325–8335
- Gritenaite D, Princz LN, Szakal B, Bantele SCS, Wendeler L, Schilbach S, Habermann BH, Matos J, Lisby M, Branzi D, Pfander B (2014) A cell cycle-regulated Slx4–Dpb11 complex promotes the resolution of DNA repair intermediates linked to stalled replication. *Genes Dev* 28: 1604–1619
- Hardy CF, Dryga O, Seematter S, Pahl PM, Sclafani RA (1997) mcm5/cdc46-bob1 bypasses the requirement for the S phase activator Cdc7p. *Proc Natl Acad Sci USA* 94: 3151–3155
- Heyer W-D, Ehmsen KT, Liu J (2010) Regulation of homologous recombination in eukaryotes. *Annu Rev Genet* 44: 113–139
- Ho CK, Mazón G, Lam AF, Symington LS (2010) Mus81 and Yen1 promote reciprocal exchange during mitotic recombination to maintain genome integrity in budding yeast. *Mol Cell* 40: 988–1000
- Interthal H, Heyer WD (2000) MUS81 encodes a novel helix-hairpin-helix protein involved in the response to UV- and methylation-induced DNA damage in *Saccharomyces cerevisiae*. *Mol Gen Genet* 263: 812–827
- Ip SCY, Rass U, Blanco MG, Flynn HR, Skehel JM, West SC (2008) Identification of Holliday junction resolvases from humans and yeast. *Nature* 456: 357–361
- Li X, Liu K, Li F, Wang J, Huang H, Wu J, Shi Y (2012) Structure of C-terminal tandem BRCT repeats of Rtt107 protein reveals critical role in interaction with phosphorylated histone H2A during DNA damage repair. *J Biol Chem* 287: 9137–9146
- Lopez-Mosqueda J, Maas NL, Jonsson ZO, DeFazio-Eli LG, Wohlschlegel J, Toczyski DP (2010) Damage-induced phosphorylation of Sld3 is important to block late origin firing. *Nature* 467: 479–483
- Lyons NA, Fonslow BR, Diedrich JK, Yates JR, Morgan DO (2013) Sequential primed kinases create a damage-responsive phosphodegron on Eco1. *Nat Struct Mol Biol* 20: 194–201
- Mankouri HW, Huttner D, Hickson ID (2013) How unfinished business from S-phase affects mitosis and beyond. *EMBO J* 32: 2661–2671
- Masai H, Taniyama C, Ogino K, Matsui E, Kakusho N, Matsumoto S, Kim JM, Ishii A, Tanaka T, Kobayashi T, Tamai K, Ohtani K, Arai K-I (2006) Phosphorylation of MCM4 by Cdc7 kinase facilitates its interaction with Cdc45 on the chromatin. *J Biol Chem* 281: 39249–39261
- Mathiasen DP, Lisby M (2014) Cell cycle regulation of homologous recombination in *Saccharomyces cerevisiae*. *FEMS Microbiol Rev* 38: 172–184
- Matos J, Lipp JJ, Bogdanova A, Guillot S, Okaz E, Junqueira M, Shevchenko A, Zachariae W (2008) Dbf4-dependent CDC7 kinase links DNA replication to the segregation of homologous chromosomes in meiosis I. *Cell* 135: 662–678
- Matos J, Blanco MG, Maslen S, Skehel JM, West SC (2011) Regulatory control of the resolution of DNA recombination intermediates during meiosis and mitosis. *Cell* 147: 158–172
- Matos J, Blanco MG, West SC (2013) Cell-cycle kinases coordinate the resolution of recombination intermediates with chromosome segregation. *Cell Rep* 4: 76–86
- Matos J, West SC (2014) Holliday junction resolution: regulation in space and time. *DNA Repair (Amst)* 19: 176–181
- Miller CT, Gabrielse C, Chen Y-C, Weinreich M (2009) Cdc7p-Dbf4p regulates mitotic exit by inhibiting polo kinase. *PLoS Genet* 5: 1–13
- Mok J, Kim PM, Lam HYK, Piccirillo S, Zhou X, Jeschke GR, Sheridan DL, Parker SA, Desai V, Jwa M, Cameroni E, Niu H, Good M, Remenyi A, Ma J-LN, Sheu Y-J, Sassi HE, Sopko R, Chan CSM, De Virgilio C et al (2010) Deciphering protein kinase specificity through large-scale analysis of yeast phosphorylation site motifs. *Sci Signal* 3: ra12
- Montagnoli A, Valsasina B, Brotherton D, Troiani S, Rainoldi S, Tenca P, Molinari A, Santocanale C (2006) Identification of Mcm2 phosphorylation sites by S-phase-regulating kinases. *J Biol Chem* 281: 10281–10290
- Montagnoli A, Valsasina B, Croci V, Menichincheri M, Rainoldi S, Marchesi V, Tibolla M, Tenca P, Brotherton D, Albanese C, Patton V, Alzani R, Ciavolella A, Sola F, Molinari A, Volpi D, Avanzi N, Fiorentini F, Cattoni M, Healy S et al (2008) A Cdc7 kinase inhibitor restricts initiation of DNA replication and has antitumor activity. *Nat Chem Biol* 4: 357–365
- Mortensen EM, Haas W, Gygi M, Gygi SP, Kellogg DR (2005) Cdc28-dependent regulation of the Cdc5/Polo kinase. *Curr Biol* 15: 2033–2037
- Muñoz IM, Hain K, Déclais A-C, Gardiner M, Toh GW, Sanchez-Pulido L, Heuckmann JM, Toth R, Macartney T, Eppink B, Kanaar R, Ponting CP, Lilley DMJ, Rouse J (2009) Coordination of structure-specific nucleases by human SLX4/BTBD12 is required for DNA repair. *Mol Cell* 35: 116–127
- Ohouo PY, de Oliveira FMB, Almeida BS, Smolka MB (2010) DNA damage signaling recruits the Rtt107-Slx4 scaffolds via Dpb11 to mediate replication stress response. *Mol Cell* 39: 300–306
- Ohouo PY, de Oliveira FMB, Liu Y, Ma CJ, Smolka MB (2012) DNA-repair scaffolds dampen checkpoint signalling by counteracting the adaptor Rad9. *Nature* 493: 120–124
- Pfander B, Diffley JFX (2011) Dpb11 coordinates Mec1 kinase activation with cell cycle-regulated Rad9 recruitment. *EMBO J* 30: 4897–4907
- Princz LN, Gritenaite D, Pfander B (2015) The Slx4–Dpb11 scaffold complex: coordinating the response to replication fork stalling in S-phase and the subsequent mitosis. *Cell Cycle* 14: 488–494
- Randell JCW, Fan A, Chan C, Francis LI, Heller RC, Galani K, Bell SP (2010) Mec1 is one of multiple kinases that prime the Mcm2-7 helicase for phosphorylation by Cdc7. *Mol Cell* 40: 353–363
- Saugar I, Vazquez MV, Gallo-Fernandez M, Ortiz-Bazan MA, Segurado M, Calzada A, Tercero JA (2013) Temporal regulation of the Mus81–Mms4 endonuclease ensures cell survival under conditions of DNA damage. *Nucleic Acids Res* 41: 8943–8958
- Schwartz EK, Wright WD, Ehmsen KT, Evans JE, Stahlberg H, Heyer WD (2012) Mus81–Mms4 functions as a single heterodimer to cleave nicked intermediates in recombinational DNA repair. *Mol Cell Biol* 32: 3065–3080

- Shirayama M, Zachariae W, Ciosk R, Nasmyth K (1998) The Polo-like kinase Cdc5p and the WD-repeat protein Cdc20p/fizzy are regulators and substrates of the anaphase promoting complex in *Saccharomyces cerevisiae*. *EMBO J* 17: 1336–1349
- Snead JL, Sullivan M, Lowery DM, Cohen MS, Zhang C, Randle DH, Taunton J, Yaffe MB, Morgan DO, Shokat KM (2007) A coupled chemical-genetic and bioinformatic approach to polo-like kinase pathway exploration. *Chem Biol* 14: 1261–1272
- Suzuki K, Sako K, Akiyama K, Isoda M, Senoo C, Nakajo N, Sagata N (2015) Identification of non-Ser/Thr-Pro consensus motifs for Cdk1 and their roles in mitotic regulation of C2H2 zinc finger proteins and Ect2. *Sci Rep* 5: 7929
- Svensden JM, Smogorzewska A, Sowa ME, O'Connell BC, Gygi SP, Elledge SJ, Harper JW (2009) Mammalian BTBD12/SLX4 assembles a Holliday junction resolvase and is required for DNA repair. *Cell* 138: 63–77
- Szakai B, Branzei D (2013) Premature Cdk1/Cdc5/Mus81 pathway activation induces aberrant replication and deleterious crossover. *EMBO J* 32: 1155–1167
- Weinreich M, Stillman B (1999) Cdc7p-Dbf4p kinase binds to chromatin during S phase and is regulated by both the APC and the RAD53 checkpoint pathway. *EMBO J* 18: 5334–5346
- Wyatt HDM, Sarbajna S, Matos J, West SC (2013) Coordinated actions of SLX1-SLX4 and MUS81-EME1 for Holliday junction resolution in human cells. *Mol Cell* 52: 234–247
- Zegerman P, Diffley JFX (2010) Checkpoint-dependent inhibition of DNA replication initiation by Sld3 and Dbf4 phosphorylation. *Nature* 467: 474–478



**License:** This is an open access article under the terms of the Creative Commons Attribution-NonCommercial-NoDerivs 4.0 License, which permits use and distribution in any medium, provided the original work is properly cited, the use is non-commercial and no modifications or adaptations are made.

## Expanded View Figures

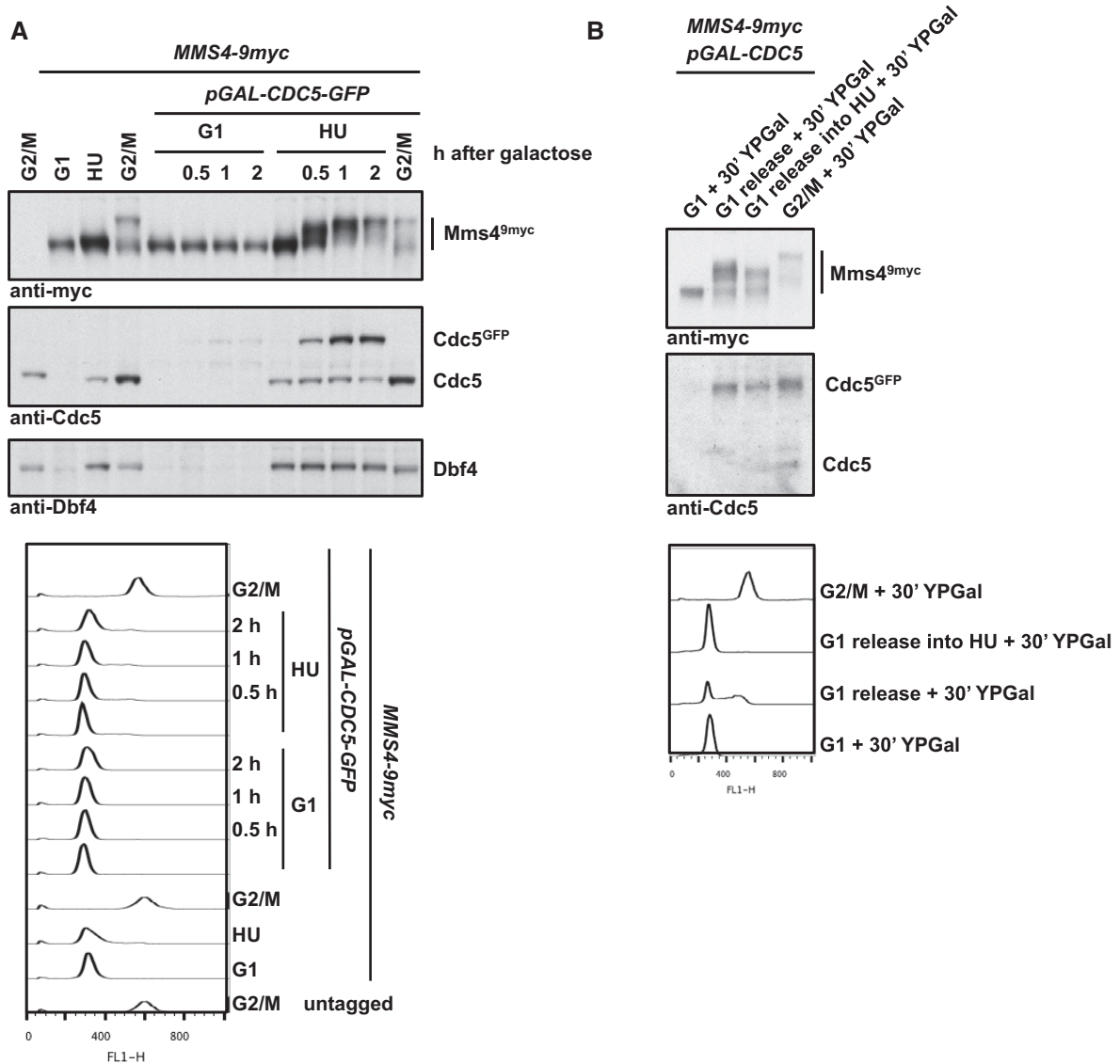


**Figure EV1. Cdc5 restricts Mms4 hyperphosphorylation to mitosis.**

- A Overexpression of *CDC5* in S phase results in premature Mms4 hyperphosphorylation. Western blot analysis of Mms4<sup>9myc</sup>, Cdc5 and Dbf4 from whole-cell extracts (upper panel) and FACS data (lower panel). Cells were arrested in G1 (with alpha-factor), S phase (with HU) or G2/M phase (with nocodazole). After arrest, *CDC5<sup>GFP</sup>* overexpression was induced by addition of 2% galactose for the indicated time to cells harbouring an additional copy of GFP-tagged *CDC5* under the *GAL1* promoter. Samples were run in 7% Tris-acetate gels.
- B Mms4 hyperphosphorylation by *CDC5* overexpression in S phase is reduced in HU-treated cells. Western blot analysis of Mms4<sup>9myc</sup> and Cdc5 from precipitated whole-cell extracts (upper panel) and FACS data (lower panel) of cells arrested in G1 (with alpha factor) or G2/M phase (with nocodazole), or released to S phase (with or without HU). *CDC5<sup>GFP</sup>* overexpression was induced for 30 min by addition of 2% galactose to cells harbouring an additional copy of GFP-tagged *CDC5* under the *GAL1* promoter. Note that upon *CDC5* overexpression cells are partially defective in bulk replication. Samples were run in 7% Tris-acetate gels.

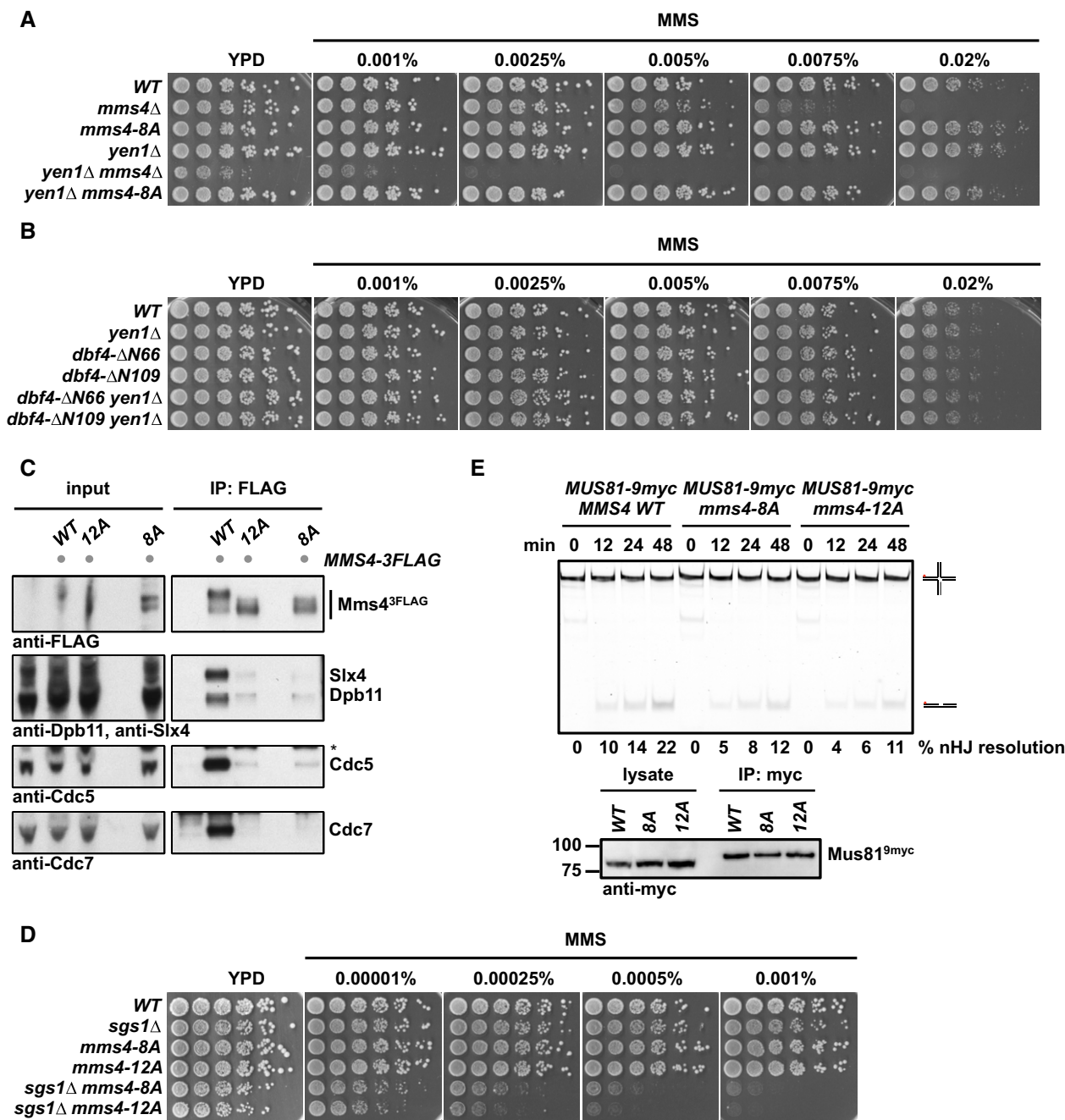


**Figure EV2. Phenotypic analysis of Mms4 variants deficient in (S/T)(S/T) phosphorylation sites.**

A, B The *mms4-8A* mutation or lack of Cdc5-DDK interaction does not lead to a synthetic hypersensitivity towards MMS in the *yen1* $\Delta$  background. Spotting assay as in Fig 4D and E.

C–E Additional mutation of 4 additional (S/T)(S/T) motifs in the background of the *mms4-8A* mutant (*mms4-12A*) leads to a reduction in the Mms4 phosphorylation shift (C), increases the hypersensitivity to MMS in the *sgs1* $\Delta$  background (D) and shows a slightly but not significantly decreased activity of Mus81–Mms4 (E). (C) Mms4<sup>3FLAG</sup> pull down as in Fig 1A, but in G2/M-arrested cells in untagged, WT, *mms4-12A* and *mms4-8A* backgrounds. Asterisk marks a cross-reactive band. (D) Spotting assay as in Fig 4D and E. (E) Resolution assay using a nHJ substrate and Mus81<sup>9myc</sup>–Mms4<sup>3FLAG</sup> purified from mitotically arrested WT, *mms4-8A* or *mms4-12A* cells. Lower panel: Western blot samples of anti-myc IPs.

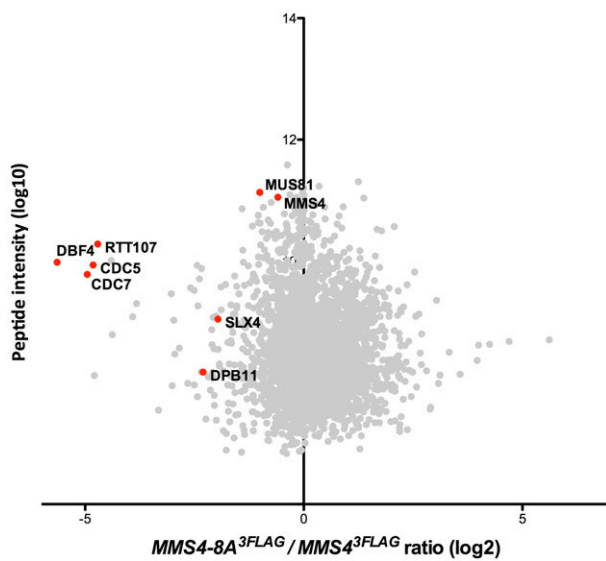


**Figure EV3.** A defect in the phosphorylation of Mms4 (S/T)(S/T) sites (*mms4-8A*) causes reduced association of Cdc5, DDK and Rtt107 with Mus81-Mms4.

SILAC-based quantification of Mms4<sup>3FLAG</sup> pull downs in WT vs. *mms4-8A* cells. Plotted are the H/L ratios against peptide intensity

## **Appendix – Table of Contents**

- **Appendix Figure Legends**
- **Appendix Figures**
- **Appendix Table S1**
- **Appendix Supplementary Materials and Methods (including Appendix Table S2)**
- **Appendix References**

## Appendix Figure Legends:

### Figure S1:

Mus81-Mms4 forms a complex in mitosis with kinases and scaffold proteins, and is a target to phosphorylation by these kinases.

**(A)** SILAC-based quantification of Mms4<sup>3FLAG</sup> pulldowns in untagged vs *MMS4*<sup>3FLAG</sup> cells after G2/M arrest with nocodazole. H/L ratios from two label-switch experiments without ratio count cut-off are plotted. #, as the only protein of the analysis Dpb11 displayed exclusively peptides that were derived from the Mms4<sup>3FLAG</sup> IP samples, but not the control samples. This experiment is already shown as Fig. S8A in Gritenaite *et al.*, 2014.

**(B)** Coomassie staining to show running behaviour of peptides used in Fig. 1C. Peptides 1-3 shift down upon increasing phosphorylation, whereas peptides 4-6 display an up-shift.

**(C)** Kinetic *in vitro* kinase assay. Purified, immobilized Mus81-Mms4 is either mock treated or treated with CDK in a non-radioactive priming step, and incubated with purified DDK (upper panel) or Cdc5 (lower panel). Samples were taken after indicated time points.

**(D)** Mus81-Mms4 *in vitro* phosphorylation is independent of DDK and/or CDK pre-phosphorylation. Purified, immobilized Mus81-Mms4 is incubated in an *in vitro* kinase assay with purified CDK2/cycA<sup>N170</sup> (a model CDK), DDK or Cdc5 (lanes 1-4). Additionally, Mus81-Mms4 is incubated with respective kinases after a non-radioactive priming step with DDK (lanes 5-8) or CDK and DDK (lanes 9-12).

### Figure S2:

DDK and Cdc5 target Mus81-Mms4 in an interdependent manner.

**(A)** Formation of the Mus81-Mms4 complex depends on Cdc5 activity. SILAC-based quantification of Mms4<sup>3FLAG</sup> pulldowns in *WT* vs *cdc5-as1* cells after mitotic arrest with nocodazole and additional treatment with 15  $\mu$ M CMK for 1 h. Plotted are the H/L ratios of two label-switch experiments.

**(B)** CDK activity is required for Mms4 hyperphosphorylation. Whole-cell extracts of *WT* and *cdc28-as1* cells arrested in mitosis, titrated with 1NM-PP1 as indicated.

**(C)** Phosphorylation shift of Mms4 in whole-cell extracts of mitotically arrested *WT* and mutant cells.

**(D)** Cdc5 association with Mus81-Mms4 is dependent on DDK activity. Mms4<sup>3FLAG</sup> pulldown as in Fig. 1A. Cells were cultivated and arrested in mitosis at RT. Inhibition of

DDK was achieved by using the *cdc7-1* allele and shifting cells to permissive temperature (38 °C) for the indicated time.

**(E)** Effect of DDK and Cdc5 mutants on Cdc5 substrates. Phosphorylation of Cdc5 substrates Ulp2 and Scc1 (and as control Mms4) was tested, indicated by their phosphorylation shift in 7% Tris-Acetate gels in untagged, *WT*, *cdc5-as1* and *cdc7Δ* backgrounds. Western blot analysis of Ulp2<sup>9myc</sup> and Scc1<sup>9myc</sup> whole-cell extracts from alpha-factor- (G1) or nocodazole-arrested (G2/M) cells. Cdc5 was inhibited by treatment with 15 μM CMK for 1 h.

**(F)** DDK and Cdc5 association to Mus81-Mms4 is reduced when the DNA damage checkpoint is triggered by DNA damage induction. Mms4<sup>3FLAG</sup> pulldown as in Fig. 1A, but in G2/M-arrested cells that were untreated or treated with 50 μg/ml phleomycin.

### **Figure S3:**

Summary of Mms4 phosphorylation sites. Shown is the Mms4 primary amino acid sequence. Colours indicate phosphorylation sites on endogenous Mms4 that were affected in SILAC-based mass spectrometry experiments (Fig. 3A-B) by Cdc5 inhibition (blue), *CDC7* deletion (red) or in both backgrounds (green). Serine to alanine exchanges in the *mms4-8A* mutant are boxed. Additional serine to alanine exchanges in the *mms4-12A* mutant are boxed with a dashed line.

### **Figure S4:**

DDK phosphorylation controls activation of Mus81-Mms4 resolvase activity in mitosis.

**(A)** Endogenous Mus81<sup>3FLAG</sup>-Mms4 purified from mitotically arrested cells shows increased activity compared to non-phosphorylated recombinant protein expressed in yeast. Left panel: Western blot analysis for quantification of bead-bound protein levels of Mus81 (endogenous and recombinant) compared to increasing amounts of soluble recombinant Mus81. Approx. 5 fmol Mus81<sup>3FLAG</sup>-Mms4 are used in the assay to cleave 500 fmol nHJ substrate. Right panel: Resolution assay using a nicked HJ substrate and comparing Mus81<sup>3FLAG</sup>-Mms4 purified from mitotically arrested cells with recombinant, dephosphorylated Mus81<sup>3FLAG</sup>-Mms4 in similar protein concentration.

**(B,C)** Interaction of Mus81-Mms4 with other complex factors such as Rtt107 and Cdc5 is salt-labile, but their absence does not influence Mus81-Mms4 activity.

**(B)** Mms4<sup>3FLAG</sup> pulldown as in Fig. 1A from mitotically arrested cells, but proteins were washed on beads with either low salt (150 mM NaCl) or high salt buffer (350 mM NaCl).

**(C)** Left panel: Resolution assay using a nHJ substrate and Mus81<sup>9myc</sup>-Mms4<sup>3FLAG</sup> purified from mitotically arrested cells under low salt (150 mM NaCl) or high salt (350 mM NaCl) conditions. Right panel: Western blots samples of anti-myc IPs.

**(D,F)** Western blot analysis of Mus81<sup>9myc</sup> IP samples that were used as inputs for the *in vitro* resolution assays of Fig. 4A and C, respectively.

**(E)** DDK is required for mitotic activation of Mus81-Mms4. Resolution assay using a replication fork (RF) substrate and Mus81<sup>9myc</sup>-Mms4<sup>3FLAG</sup> purified from mitotically arrested *bob1-1 (DDK+)* and *bob1-1 cdc7Δ* strains or untagged control cells. Lower panel: Western blots samples of anti-myc IPs.

### **Figure S5:**

Dpb11 interacts with the N-terminal region of Mms4 and its binding is dependent on CDK activity.

**(A)** Dpb11 binds to a minimal interacting fragment of Mms4 comprising the residues 101-230. Two-hybrid analysis of GAL4-BD fused to Dpb11 and GAL4-AD fusions with Mms4 or Mms4 fragment constructs (left panel). Expression of constructs was verified by western blot analysis (right panel).

**(B)** CDK activity is required for Dpb11 and Slx4 association with Mus81-Mms4. Mms4<sup>3FLAG</sup> pulldown as in Fig. 1A, but in G2/M-arrested *WT* and *cdc28-as1* mutant cells treated with 5 μM 1NM-PP1 for 1 h. This figure is from the same experiment as Fig. 2B and therefore as control includes the identical anti-Flag western.

**(C)** A defect in the Dpb11-Mms4 interaction introduces only a minor defect in Mus81 activation. Resolution assay using a nicked HJ substrate and Mus81<sup>9myc</sup>-Mms4<sup>3FLAG</sup> purified from mitotically arrested *WT* or *mms4-S201A* cells. Right panel: Western blots samples of anti-myc IPs.

### **Figure S6:**

The Rtt107 scaffold tethers DDK and Cdc5 to Mus81-Mms4.

**(A)** Formation of the Mus81-Mms4 complex depends on Rtt107. SILAC-based quantification of Mms4<sup>3FLAG</sup> pulldowns in *WT* vs *rtt107Δ* cells. Plotted are the H/L ratios of two experiments including label-switch.

**(B)** Rtt107 binding to Cdc5 and DDK is not affected by the presence of Mus81-Mms4. Rtt107<sup>3FLAG</sup> pulldown as in Fig. 1A, but in G2/M-arrested *WT* and *mus81Δ* cells.

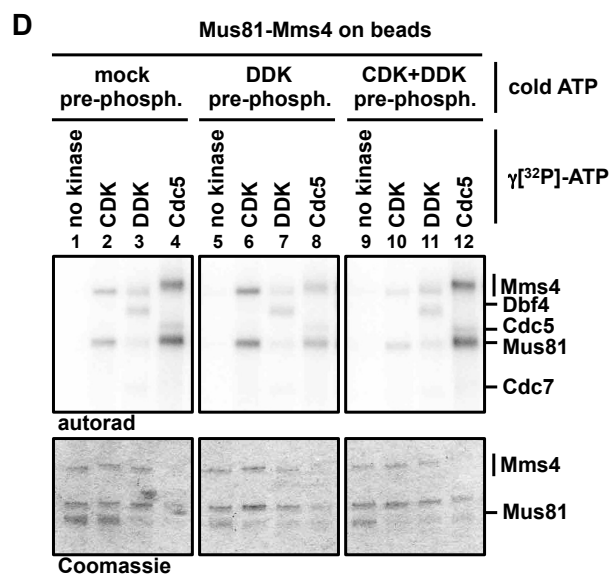
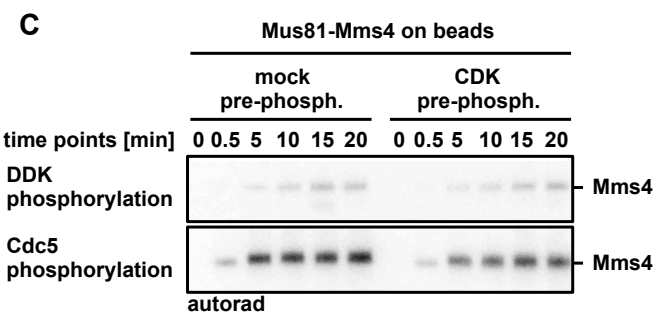
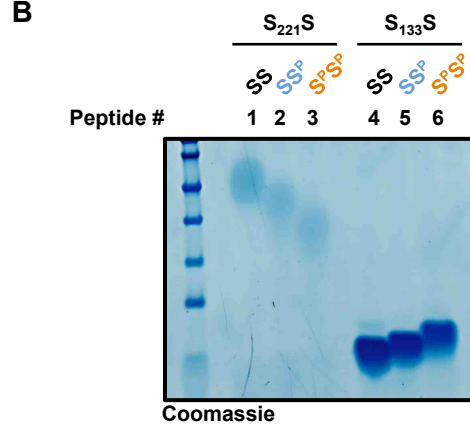
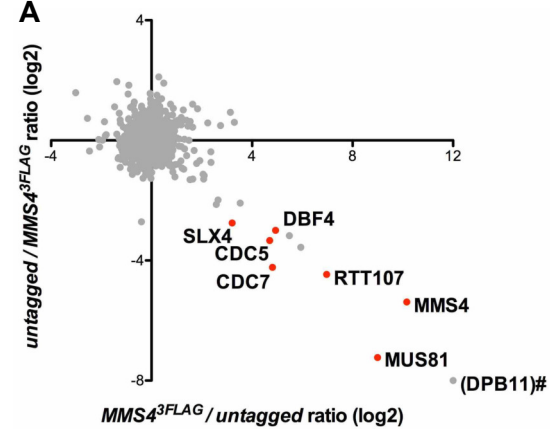
### **Figure S7:**

Rtt107 is required for efficient Mus81-Mms4 activation in mitosis.

**(A,B)** *Rtt107* influences the phosphorylation of specific Cdc5-dependent phosphorylation sites. SILAC-based MS analysis of Mms4 phosphorylation after purification of endogenously expressed Mus81-Mms4<sup>3FLAG</sup> **(A)** or of Mus81<sup>3FLAG</sup>-Mms4<sup>His10-Strep2</sup> expressed from the *pGAL1-10* promoter **(B)**.

**(C)** Western blot analysis of Mus81<sup>9myc</sup> IP samples that were used as inputs for the *in vitro* for resolution assay of Fig. 7A.

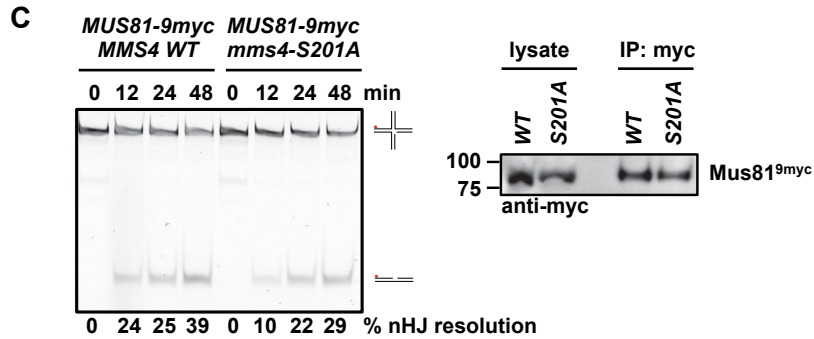
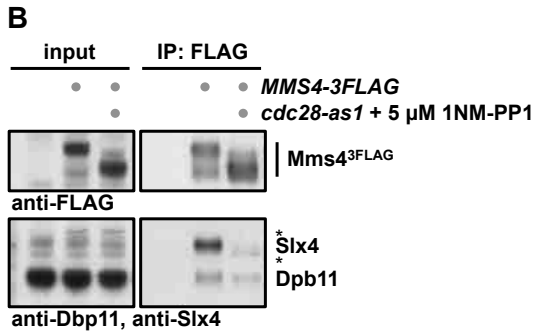
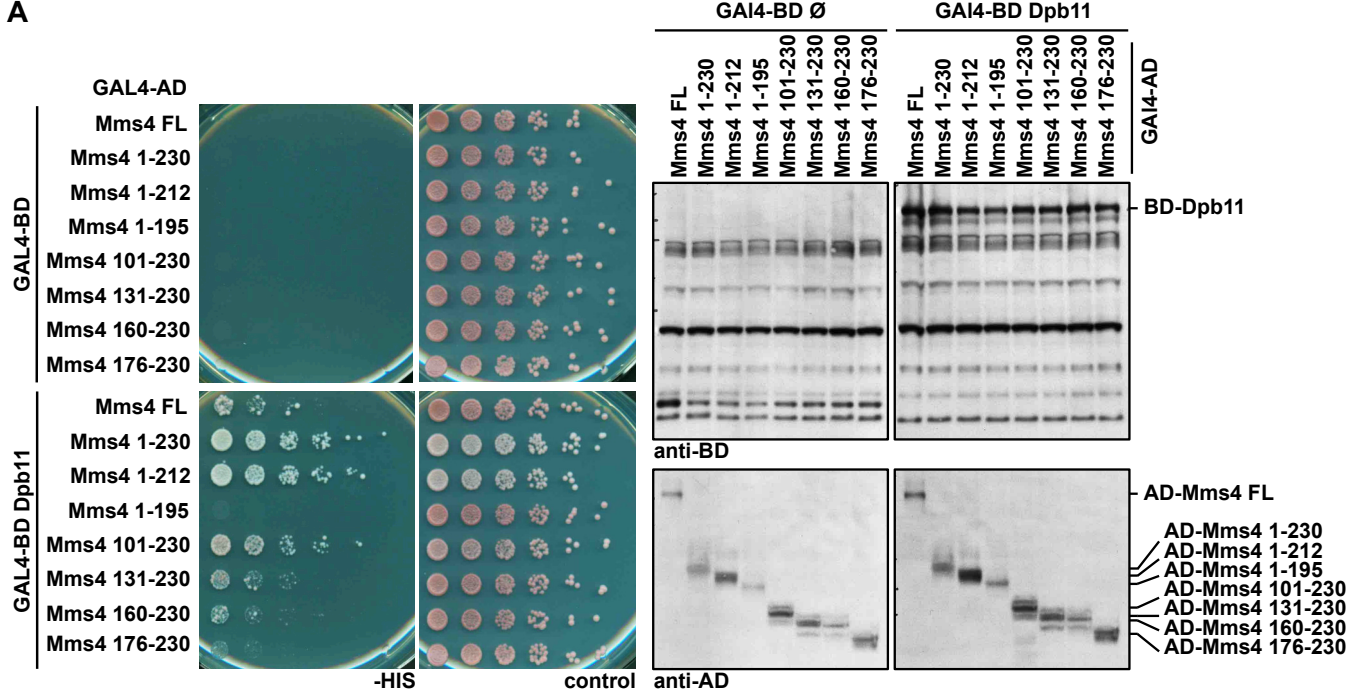
**(D)** *RTT107* deletion does not lead to a further reduction in Mus81 activity in the *cdc7Δ* background. Resolution assay using a nicked HJ substrate and Mus81<sup>9myc</sup>-Mms4<sup>3FLAG</sup> purified from mitotically arrested *bob1-1 cdc7Δ* or *bob1-1 cdc7Δ rtt107Δ* cells. Lower panel: Western blots samples of anti-myc IPs.

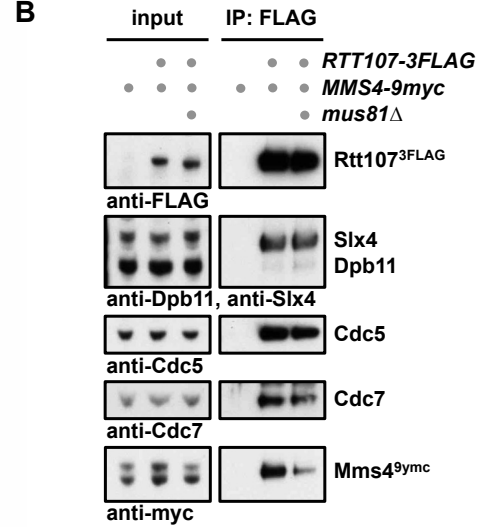
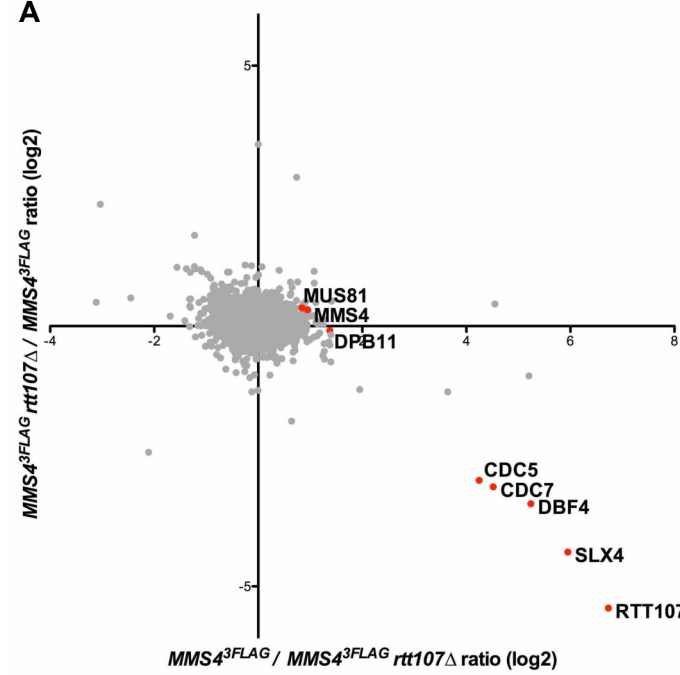


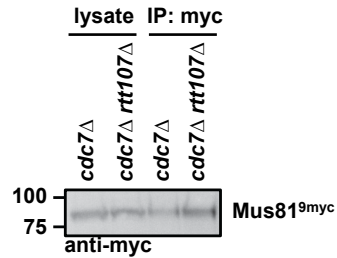
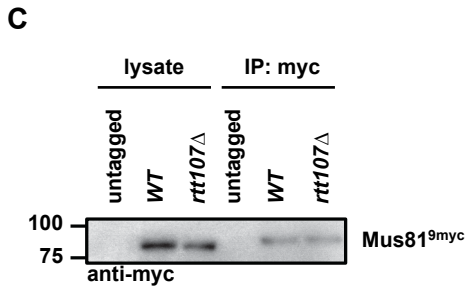
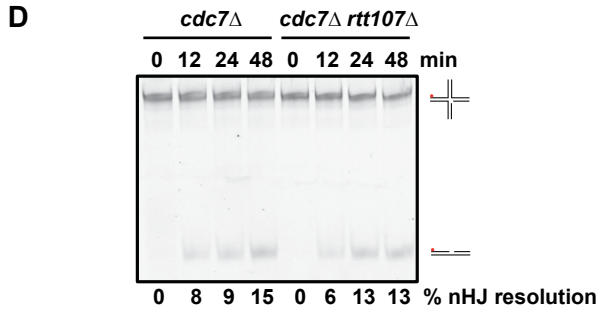
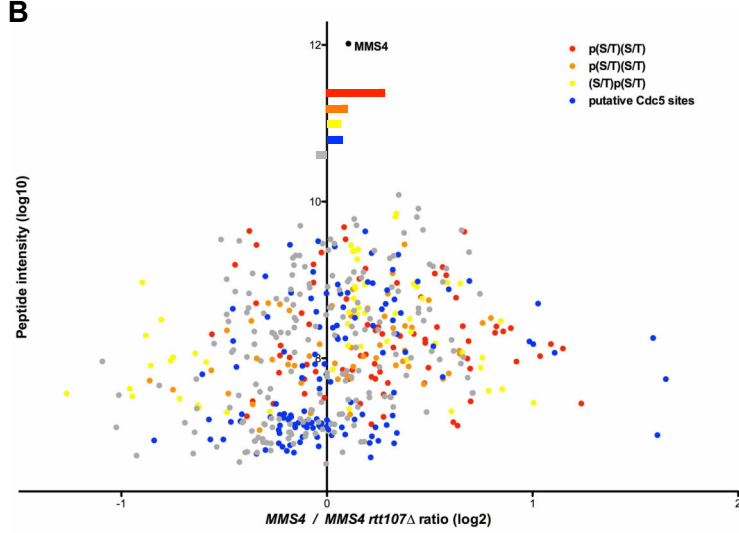
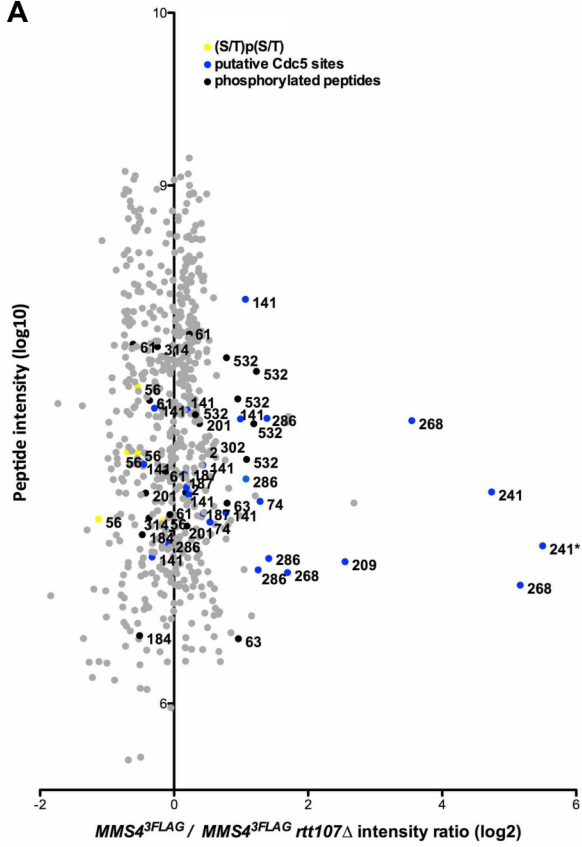


	10	20	30	40	50	60	70	80	90			
MSQIVDFVED	KDSRNDASIQ	IIDGSPSNVEI	IALSESMDQD	ECKRAHV	SA	EMIF	SPQRK	SVSNDVENVD	LNKSIELSAP	FFQDISISKL	DDFSTVNSI	100
IFSLRNENN	AKGNAKLLD	DLISDEWSAD	LESGKKHKN	SQYNLRDIAE	KWGVQSLKNP	EPIAVDCEYK	TQGIGKTNSD	ISDSPKSQIG	AADILDFDPL			200
SPVKHENPTE	EKHNSIANEN	SPDNSLKPA	GKQNHGEDGT	SMAKRVYKNG	EDEQEHLPGK	KKRTIALSRT	LINSTKLPDT	VELNLSKFLD	SDSITTDVL			300
TPAKGSNIV	RTGSQPIFSN	ANCFQEAQRS	KTLTAEDEPKC	TKNTAREVSO	LENYIAYGQY	YTREDSKNKI	RHLLKENKNA	FKRVNQIYRD	NIKARSQMII			400
EFSPSLLQLF	KKGSDSLQQQ	LAPAVVQSY	NDSMPLLRFL	RKCDSIYDFS	NDFYYPDDPK	IVEENVLILY	YDAQEFFEQY	TSQKKELYRK	IRFFSKNGKH			500
VILILSDINK	LKRAIFQLEN	EKYKARVEQR	LSGTEEALRP	RSKSSQVVGK	LGIKKFDLEQ	RLRFIDREWH	VKIHTVNSHM	EFINSLPNLV	SLIGQRMDP			600
AIRYMKY AHL	NVKSADSTE	TLKKTFFHQIG	RMPEMKANNV	VSLYPSFQSL	LEDIEKGRLO	SDNEGKYLMT	EAVEKRLYKL	FTCTDPNDTI	E.			700









**Appendix Table S1. Mms4 phosphorylation sites and their regulation by DDK or Cdc5 as detected by SILAC-based quantitative mass spectrometry (Fig. 3)**

Mus81-Mms4 endogenous	Mus81-Mms4 overexpressed
2	2
48	48
49	49
55	55
56	56
61	61
63	63
74	74
86	78**
88*	86
94**	88**
96	94
99	95
103	96
104	99
124**	103
128**	104
133**	124
134**	128
141**	133
156**	134
184*	141
187	156
201	187
209**	201
221*	222*
222*	264
240**	268
241**	274*
268**	280*
286	286
291	291
292	292
294	294
296**	297
297**	301
301	302
302	314
314**	330**
330**	349
349	366
366**	396**
396**	532
532	542

\* not measured in *cdc5-as1*

\*\* not measured in *cdc7Δ*

phosphorylation sites affected in *cdc5-as1*

phosphorylation sites affected in *cdc7Δ*

phosphorylation sites affected in *cdc5-as1* and *cdc7Δ* backgrounds

## Appendix Supplementary Materials and Methods

### Yeast strains and construction

All yeast strains are based on W303 (Thomas & Rothstein, 1989). Genotypes are listed below. All biochemical experiments were performed in a W303-1A *pep4*Δ background. The genetic experiments in Fig. 4D-E, 5C, and EV2A,B,D were performed in a W303 *RAD5+* background to exclude any effect from a partial defect of the *rad5-535* allele. Two-hybrid analyses were performed in the strain PJ69-7A (James *et al.*, 1996).

*S. cerevisiae* strains were prepared by genetic crosses and transformation techniques. Deletion of particular genes and endogenous protein tagging were performed as described (Knop *et al.*, 1999). Correct integrations were checked by genotyping PCR. Denaturing cell extracts were prepared by alkaline lysis and TCA precipitation. The *mms4* alleles were generated using site-directed mutagenesis and integrated as linear plasmids at the TRP1 locus.

**Appendix Table S2. Yeast strains used in this study**

Strain	Full genotype	Relevant genotype	Source
MGBY3294	MATa <i>ade2-1 his3-11 leu2-3,112 trp1Δ2 can1-100 pep4::KanMX bar1::hph-NT1 ura3-52::GAL1,10p-FLAG3-MUS81/GST-His10-Strep2-MMS4::URA3</i>	<i>pGAL-FLAG3-MUS81-GST-His10-Strep2-MMS4</i>	This study (Blanco lab)
YBP388	MATa <i>ade2-1 ura3-1 his3-11,15 trp1-1 can1-100 leu2-3,112::pep4::LEU2</i>	<i>pep4</i>	Klein lab
YDG208	MATa <i>RAD5+ ade2-1 ura3-1 leu2-3,112 his3-11,15 trp1-1 can1-100</i>		This study
YDG291	MATa <i>RAD5+ ade2-1 ura3-1 leu2-3,112 his3-11,15 trp1-1 can1-100 yen1::hph-NT1</i>	<i>yen1</i>	Gritenaite et al., 2014
YDG329	MATa <i>RAD5+ ade2-1 ura3-1 leu2-3,112 his3-11,15 trp1-1 can1-100 sgs1::hph-NT1</i>	<i>sgs1</i>	Gritenaite et al., 2014
YDG355	MATa <i>RAD5+ ade2-1 ura3-1 his3-11,15 trp1-1 can1-100 mms4::hph-NT1 leu2-3,112::mms4-SS184,201AA::LEU2</i>	<i>mms4-SS184,201AA</i>	Gritenaite et al., 2014
YDG356	MATa <i>RAD5+ ade2-1 ura3-1 trp1-1 can1-100 mms4::hph-NT1 leu2-3,112::mms4-SS184,201AA::LEU2 his3-11,15::sgs1::HIS3Mx4</i>	<i>mms4-SS184,201AA sgs1</i>	Gritenaite et al., 2014
YDG376	MATa <i>RAD5+ ade2-1 ura3-1 leu2-3,112 his3-11,15 trp1-1 can1-100 yen1::hph-NT1 sgs1::nat-NT2</i>	<i>yen1 sgs1</i>	Gritenaite et al., 2014

YJB82	Mata/Matalpha <i>ade2-1/ade2-1 ura3-1/ura3-1 leu2-3,112/leu2-3,112 his3-11,15/his3-11,15 trp1-1/trp1-1 can1-100/can1-100 ade2-n/ade2-I LYS2/lys2::Gal-ISceI his3::NATMX/his3::HPHMX4 met22::kIURA3/MET22</i>	<i>diploid</i>	This study
YJB84	Mata/Matalpha <i>ade2-1/ade2-1 ura3-1/ura3-1 leu2-3,112/leu2-3,112 his3-11,15/his3-11,15 trp1-1/trp1-1 can1-100/can1-100 ade2-n/ade2-I LYS2/lys2::Gal-ISceI his3::NATMX/his3::HPHMX4 met22::kIURA3/MET22 rtt107::KanMX/rtt107::KanMX</i>	<i>diploid rtt107</i>	This study
YJB86	Mata/Matalpha <i>ade2-1/ade2-1 ura3-1/ura3-1 leu2-3,112/leu2-3,112 his3-11,15/his3-11,15 trp1-1/trp1-1 can1-100/can1-100 ade2-n/ade2-I LYS2/lys2::Gal-ISceI his3::NATMX/his3::HPHMX4 met22::kIURA3/MET22 mms4::KanMX/mms4::KanMX trp1-1:pRS304-Mms4-SSSSSSS48,55,103,133,221,291,301,428AAA AAAAA:TRP1/trp1-1:pRS304-Mms4-SSSSSSS48,55,103,133,221,291,301,428AAA AAAAA:TRP1</i>	<i>diploid mms4-SSSSSSS48,55,103,133,221,291,301,428AAA AAAAA</i>	This study
YLP015	MATa <i>ade2-1 ura3-1 his3-11,15 can1-100 trp1-1::bar1::TRP1 leu2-3,112::pep4::LEU2 lys1::nat-NT2</i>	<i>lys1</i>	Gritenaite et al., 2014
YLP063	MATa <i>RAD5+ ade2-1 ura3-1 leu2-3,112 trp1-1 can1-100 cdc5-as1 his3-11,15::pep4::HIS3Mx4 MMS4-3FLAG::hph-NT1</i>	<i>MMS4-3FLAG cdc5-as1</i>	Gritenaite et al., 2014
YLP065	MATa <i>ade2-1 ura3-1 his3-11,15 can1-100 trp1-1::bar1::TRP1 leu2-3,112::pep4::LEU2 lys1::nat-NT2 MMS4-3FLAG::hph-NT1</i>	<i>lys1 MMS4-3FLAG</i>	This study
YLP070	MATa <i>ade2-1 ura3-1 leu2-3,112 can1-100 his3-11,15::pep4::HIS3Mx4 lys1::nat-NT2 mms4::KanMx trp1-1::mms4-S184A::TRP1 MMS4-3FLAG::hph-NT1</i>	<i>lys1 mms4-S184A-3FLAG</i>	This study
YLP074	MATa <i>ade2-1 ura3-1 leu2-3,112 can1-100 his3-11,15::pep4::HIS3Mx4 lys1::nat-NT2 mms4::KanMx trp1-1::mms4-S201A::TRP1 MMS4-3FLAG::hph-NT1</i>	<i>lys1 mms4-S201A-3FLAG</i>	This study
YLP078	MATa <i>ade2-1 ura3-1 leu2-3,112 trp1-1 can1-100 his3-11,15::pep4::HIS3Mx4 MMS4-3FLAG::hph-NT1 slx4::KanMx</i>	<i>MMS4-3FLAG slx4</i>	Gritenaite et al., 2014

YLP092	MATa <i>ade2-1 ura3-1 his3-11,15 trp1-1 can1-100 leu2-3,112::pep4::LEU2 RTT107-9myc::hph-NT1</i>	<i>RTT107-9myc</i>	This study
YLP100	MATa <i>ade2-1 ura3-1 trp1-1 leu2-3,112 can1-100 his3-11,15::bob1-1::HIS3Mx4 pep4::hph-NT1</i>	<i>bob1-1</i>	This study
YLP111	MATa <i>ade2-1 ura3-1 trp1-1 leu2-3,112 can1-100 his3-11,15::bob1-1::HIS3Mx4 pep4::hph-NT1 MMS4-3FLAG::KanMx4</i>	<i>bob1-1 MMS4-3FLAG</i>	This study
YLP113	MATa <i>ade2-1 ura3-1 trp1-1 leu2-3,112 can1-100 his3-11,15::bob1-1::HIS3Mx4 pep4::hph-NT1 cdc7::nat-NT2 MMS4-3FLAG::KanMx4</i>	<i>bob1-1 cdc7 MMS4-3FLAG</i>	This study
YLP121	MATa <i>RAD5+ ade2-1 ura3-1 leu2-3,112 trp1-1 can1-100 cdc5-as1 his3-11,15::pep4::HIS3Mx4 lys1::nat-NT2 MMS4-3FLAG::hph-NT1</i>	<i>lys1 MMS4-3FLAG cdc5-as1</i>	This study
YLP126	MATa <i>ade2-1 leu2-3,112 trp1-1 can1-100 his3-11,15::bob1-1::HIS3Mx4 pep4::hph-NT1 cdc7::nat-NT2 MMS4-3FLAG::KanMx4 ura3-1::lys1::URA3</i>	<i>lys1 bob1-1 cdc7 MMS4-3FLAG</i>	This study
YLP128	MATa <i>ade2-1 ura3-1 leu2-3,112 trp1-1 can1-100 his3-11,15::pep4::HIS3Mx4 cdc7-1</i>	<i>cdc7-1</i>	This study
YLP132	MATa <i>ade2-1 ura3-1 leu2-3,112 trp1-1 can1-100 his3-11,15::pep4::HIS3Mx4 cdc7-1 MMS4-3FLAG::KanMx</i>	<i>cdc7-1 MMS4-3FLAG</i>	This study
YLP156	MATa <i>ade2-1 ura3-1 leu2-3,112 trp1-1 can1-100 his3-11,15::pep4::HIS3Mx4 MMS4-3FLAG::hph-NT1 RTT107-9myc::nat-NT2</i>	<i>MMS4-3FLAG RTT107-9myc</i>	This study
YLP164	MATa <i>ade2-1 ura3-1 leu2-3,112 can1-100 MMS4-3FLAG::hph-NT1 his3-11,15::pep4::HIS3Mx4 rtt107::KanMx trp1-1::lys1::TRP1</i>	<i>lys1 MMS4-3FLAG rtt107</i>	This study
YLP277	MATa <i>ade2-1 ura3-1 trp1-1 leu2-3,112 can1-100 MMS4-3FLAG::hph-NT1 his3-11,15::pep4::HIS3Mx4 SCC1-9myc</i>	<i>MMS4-3FLAG SCC1-9myc</i>	This study
YLP279	MATa <i>RAD5+ ade2-1 ura3-1 trp1-1 leu2-3,112 can1-100 cdc5-as1 MMS4-3FLAG::hph-NT1 his3-11,15::pep4::HIS3 SCC1-9myc::KanMx</i>	<i>MMS4-3FLAG SCC1-9myc cdc5-as1</i>	This study
YLP287	MATa <i>ade2-1 ura3-1 leu2-3,112 can1-100 his3-11,15::pep4::HIS3Mx4 mms4::KanMx trp1-1::mms4-S201A::TRP1 MMS4-3FLAG::hph-NT1 RTT107-9myc::nat-NT2</i>	<i>mms4-S201A-3FLAG RTT107-9myc</i>	This study

YLP339	MATa <i>RAD5+ ade2-1 ura3-1 leu2-3,112 his3-11,15 can1-100 mms4::hph-NT1 trp1-1::mms4-SSSSSSSS48,55,103,133,221,291,301,428AAAAAAA::TRP1</i>	<i>mms4-SSSSSSSS48,55,103,133,221,291,301,428AAAAAAA</i>	This study
YLP341	MATa <i>RAD5+ ade2-1 ura3-1 leu2-3,112 his3-11,15 can1-100 mms4::hph-NT1 trp1-1::mms4-SSSSSSSS48,55,103,133,221,291,301,428AAAAAAA::TRP1 sgs1::nat-NT2</i>	<i>mms4-SSSSSSSS48,55,103,133,221,291,301,428AAAAAAA sgs1</i>	This study
YLP350	MATa <i>RAD5+ ade2-1 ura3-1 leu2-3,112 his3-11,15 can1-100 mms4::hph-NT1 trp1-1::mms4-SSSSSSSS48,55,103,133,221,291,301,428AAAAAAA::TRP1 yen1::KanMx</i>	<i>mms4-SSSSSSSS48,55,103,133,221,291,301,428AAAAAAA yen1</i>	This study
YLP351	MATa <i>RAD5+ ade2-1 ura3-1 leu2-3,112 his3-11,15 can1-100 mms4::hph-NT1 trp1-1::mms4-SSSSSSSS48,55,103,133,221,291,301,428AAAAAAA::TRP1 sgs1::nat-NT2 yen1::KanMx</i>	<i>mms4-SSSSSSSS48,55,103,133,221,291,301,428AAAAAAA sgs1 yen1</i>	This study
YLP344	MATa <i>ade2-1 ura3-1 leu2-3,112 trp1-1 can1-100 MMS4-3FLAG::hph-NT1 his3-11,15::pep4::HIS3Mx4 dbf4-ΔN66::KanMx</i>	<i>MMS4-3FLAG dbf4-ΔN66</i>	This study
YLP345	MATa <i>ade2-1 ura3-1 leu2-3,112 trp1-1 can1-100 MMS4-3FLAG::hph-NT1 his3-11,15::pep4::HIS3Mx4 dbf4-ΔN109::KanMx</i>	<i>MMS4-3FLAG dbf4-ΔN109</i>	This study
YLP356	MATa <i>ade2-1 ura3-1 leu2-3,112 can1-100 mms4::KanMx his3-11,15::pep4::HIS3 trp1-1::mms4-SSSSSSSS48,55,103,133,221,291,301,428AAAAAAA::TRP1 MMS4-3FLAG::hph-NT1</i>	<i>mms4-SSSSSSSS48,55,103,133,221,291,301,428AAAAAAA-3FLAG</i>	This study
YLP360	MATa <i>ade2-1 ura3-1 leu2-3,112 his3-11,15 trp1-1 can1-100 MMS4-3FLAG::hph-NT1 cdc28-as1</i>	<i>MMS4-3FLAG cdc28-as1</i>	This study
YLP367	MATa <i>ade2-1 ura3-1 leu2-3,112 can1-100 mms4::KanMx his3-11,15::pep4::HIS3Mx4 trp1-1:: MMS4::TRP1 MMS4-3FLAG::hph-NT1 MUS81-9myc::nat-NT2</i>	<i>MMS4-3FLAG MUS81-9myc</i>	This study

YLP368	MATa <i>ade2-1 ura3-1 leu2-3,112 can1-100 mms4::KanMx his3-11,15::pep4::HIS3Mx4 trp1-1::mms4-SSSSSSSS48,55,103,133,221,291,301,428AAAAAAA::TRP1 MMS4-3FLAG::hph-NT1 MUS81-9myc::nat-NT2</i>	<i>mms4-SSSSSSSS48,55,103,133,221,291,301,428AAAAAAA-3FLAG MUS81-9myc</i>	This study
YLP369	MATa <i>RAD5+ ade2-1 ura3-1 leu2-3,112 his3-11,15 trp1-1 can1-100 dbf4-ΔN66::KanMx</i>	<i>dbf4-ΔN66</i>	This study
YLP370	MATa <i>RAD5+ ade2-1 ura3-1 leu2-3,112 his3-11,15 trp1-1 can1-100 dbf4-ΔN109::KanMx</i>	<i>dbf4-ΔN109</i>	This study
YLP371	MATa <i>RAD5+ ade2-1 ura3-1 leu2-3,112 his3-11,15 trp1-1 can1-100 dbf4-ΔN66::KanMx sgs1::hph-NT1</i>	<i>dbf4-ΔN66 sgs1</i>	This study
YLP372	MATa <i>RAD5+ ade2-1 ura3-1 leu2-3,112 his3-11,15 trp1-1 can1-100 dbf4-ΔN109::KanMx sgs1::hph-NT1</i>	<i>dbf4-ΔN109 sgs1</i>	This study
YLP374	MATa <i>RAD5+ ade2-1 ura3-1 leu2-3,112 his3-11,15 trp1-1 can1-100 dbf4-ΔN66::KanMx yen1::hph-NT1</i>	<i>dbf4-ΔN66 yen1</i>	This study
YLP375	MATa <i>RAD5+ ade2-1 ura3-1 his3-11,15 trp1-1 leu2-3,112 can1-100 dbf4-ΔN109::KanMx yen1::hph-NT1</i>	<i>dbf4-ΔN109 yen1</i>	This study
YLP438	MATa <i>ade2-1 ura3-1 trp1-1 leu2-3,112 can1-100 MMS4-3FLAG::hph-NT1 his3-11,15::pep4::HIS3 ULP2-9myc::KanMx</i>	<i>MMS4-3FLAG ULP2-9myc</i>	This study
YLP439	MATa <i>RAD5+ ade2-1 ura3-1 trp1-1 leu2-3,112 can1-100 cdc5-as1 MMS4-3FLAG::hph-NT1 his3-11,15::pep4::HIS3 ULP2-9myc::KanMx</i>	<i>MMS4-3FLAG ULP2-9myc cdc5-as1</i>	This study
YLP442	MATa <i>ade2-1 ura3-1 leu2-3,112 can1-100 mms4::KanMx his3-11,15::pep4::HIS3 trp1-1::mms4-SSSSSSSS48,55,103,133,221,291,301,428AAAAAAA::TRP1 MMS4-3FLAG::hph-NT1 lys1::nat-NT2</i>	<i>lys1 mms4-SSSSSSSS48,55,103,133,221,291,301,428AAAAAAA-3FLAG</i>	This study
YLP444	MATa <i>ade2-1 ura3-1 leu2-3,112 can1-100 mms4::KanMx his3-11,15::pep4::HIS3 trp1-1::mms4- S201A::TRP1 MMS4-3FLAG::hph-NT1 MUS81-9myc::nat-NT2</i>	<i>mms4-S201A-3FLAG MUS81-9myc</i>	This study
YLP445	MATa <i>ade2-1 ura3-1 leu2-3,112 can1-100 trp1-1::MUS81-9myc::TRP1 his3-11,15::bob1-1::HIS3 pep4::hph-NT1 MMS4-3FLAG::KanMx cdc7::nat-NT2 rtt107::klURA</i>	<i>bob1-1 MUS81-9myc cdc7 rtt107</i>	This study
YLP458	MATa <i>ade2-1 his3-11,15 can1-100 trp1-1::bar1::TRP1 leu2-3,112::pep4::LEU2 lys1::nat-NT2 ura3-1::pRS306-pGAL1,10-FLAG3-MUS81-His-Strep-MMS4::URA3</i>	<i>lys1 pGAL-FLAG3-MUS81-His10-Strep2-MMS4</i>	This study

YLP459	MATa <i>ade2-1 trp1-1 leu2-3,112 can1-100 his3-11,15::bob1-1::HIS3 pep4::hph-NT1 lys1::nat-NT2 ura3-1::pRS306-pGAL1,10-FLAG3-MUS81-His-Strep-MMS4::URA3</i>	<i>lys1 pGAL-FLAG3-MUS81-His10-Strep2-MMS4</i>	This study
YLP461	MATa <i>ade2-1 ura3-1 leu2-3,112 can1-100 mms4::KanMx his3-11,15::pep4::HIS3 trp1-1::mms4-SSSSSSSSSSSS48,55,94,103,133,221,274,291,301,428,545,618AAAAAAAAAAAAA::TRP1 MMS4-3FLAG::hph-NT1</i>	<i>mms4-SSSSSSSSSSSS48,55,94,103,133,221,274,291,301,428,545,618AAAAAAAAAAAAA-3FLAG</i>	This study
YLP462	MATa <i>RAD5+ ade2-1 ura3-1 leu2-3,112 his3-11,15 can1-100 mms4::hph-NT1 trp1-1::mms4-SSSSSSSSSSSS48,55,94,103,133,221,274,291,301,428,545,618AAAAAAAAAAAAA::TRP1</i>	<i>mms4-SSSSSSSSSSSS48,55,94,103,133,221,274,291,301,428,545,618AAAAAAAAAAAAA</i>	This study
YLP463	MATa <i>RAD5+ ade2-1 ura3-1 leu2-3,112 his3-11,15 can1-100 mms4::hph-NT1 trp1-1::mms4-SSSSSSSS48,55,94,103,133,221,274,291,301,428,545,618AAAAAAAAA::TRP1 sgs1::nat-NT2</i>	<i>mms4-SSSSSSSSSSSS48,55,94,103,133,221,274,291,301,428,545,618AAAAAAAAAAAAA sgs1</i>	This study
YLP465	MATa <i>ade2-1 ura3-1 leu2-3,112 can1-100 his3-11,15::bob1-1::HIS3Mx4 pep4::hph-NT1 cdc7::nat-NT2 MMS4-3FLAG::KanMx4 trp1-1::ULP2-9myc::TRP1</i>	<i>bob1-1 cdc7 MMS4-3FLAG ULP2-9myc</i>	This study
YLP466	MATa <i>ade2-1 ura3-1 leu2-3,112 can1-100 his3-11,15::bob1-1::HIS3Mx4 pep4::hph-NT1 cdc7::nat-NT2 MMS4-3FLAG::KanMx4 trp1-1::SCC1-9myc::TRP1</i>	<i>bob1-1 cdc7 MMS4-3FLAG SCC1-9myc</i>	This study
YLP468	MATa <i>ade2-1 ura3-1 leu2-3,112 can1-100 mms4::KanMx his3-11,15::pep4::HIS3 trp1-1::mms4-SSSSSSSSSSSS48,55,94,103,133,221,274,291,301,428,545,618AAAAAAAAAAAAA::TRP1 MMS4-3FLAG::hph-NT1 MUS81-9myc::nat-NT2</i>	<i>mms4-SSSSSSSSSSSS48,55,94,103,133,221,274,291,301,428,545,618AAAAAAAAAAAAA-3FLAG MUS81-9myc</i>	This study
YLP469	MATa <i>RAD5+ ade2-1 leu2-3,112 trp1-1 can1-100 cdc5-as1 his3-11,15::pep4::HIS3Mx4 lys1::nat-NT2 ura3-1::GAL1,10p-FLAG3-MUS81/His10-Strep2-MMS4::URA3</i>	<i>lys1 cdc5-as1 pGAL-FLAG3-MUS81-His10-Strep2-MMS4</i>	This study
YLP470	MATa <i>ade2-1 leu2-3,112 trp1-1 can1-100 his3-11,15::bob1-1::HIS3Mx4 pep4::hph-NT1 cdc7::KanMx lys1::nat-NT2 ura3-1::GAL1,10p-FLAG3-MUS81/His10-Strep2-MMS4::URA3</i>	<i>lys1 bob1-1 cdc7 pGAL-FLAG3-MUS81-His10-Strep2-MMS4</i>	This study

YLP471	MATa <i>ade2-1 his3-11,15 trp1-1 can1-100 leu2-3,112::pep4::LEU2 rtt107::KanMx lys1::nat-NT2 ura3-1::GAL1,10p-FLAG3-MUS81/His10-Strep2-MMS4::URA3</i>	<i>lys1 rtt107 pGAL-FLAG3-MUS81-His10-Strep2-MMS4</i>	This study
YML1601	MATa <i>his3Δ1 leu2Δ0 met15Δ0 ura3Δ0 ADE2 MMS4-9myc::KanMx trp1-1::pGAL1-CDC5-GFP::TRP1</i>	<i>MMS4-9myc pGAL-CDC5-GFP</i>	Matos et al., 2013
YML3304	MATa <i>ade2-1 ura3-1 leu2-3,112 can1-100 trp1-1::MUS81-9myc::TRP1 his3-11,15::bob1-1::HIS3 pep4::hph-NT1 MMS4-3FLAG::KanMx dbf4::nat-NT2</i>	<i>bob1-1 MUS81-9myc dbf4</i>	This study (Matos lab)
YML3306	MATa <i>ade2-1 ura3-1 leu2-3,112 can1-100 trp1-1::MUS81-9myc::TRP1 his3-11,15::bob1-1::HIS3 pep4::hph-NT1 MMS4-3FLAG::KanMx cdc7::nat-NT2</i>	<i>bob1-1 MUS81-9myc cdc7</i>	This study (Matos lab)
YML3447	MATa <i>ade2-1 ura3-1 leu2-3,112 can1-100 trp1-1::MUS81-9myc::TRP1 his3-11,15::bob1-1::HIS3 pep4::hph-NT1 MMS4-3FLAG::nat-NT2 rtt107::KanMx</i>	<i>bob1-1 MUS81-9myc rtt107</i>	This study (Matos lab)
YSS3	MATa <i>ade2-1 ura3-1 trp1-1 leu2-3,112 can1-100 MMS4-3FLAG::hph-NT1 his3-11,15::pep4::HIS3Mx4</i>	<i>MMS4-3FLAG</i>	Gritenaite et al., 2014
YFZ020	MATa <i>ade2-1 ura3-1 trp1-1 can1-100 his3-11,15::pRS303-CDC5-3FLAG-pGAL1-GAL4::HIS3Mx4 leu2-3,112::pep4::LEU2</i>	<i>pGAL-CDC5-3FLAG</i>	This study
YFZ021	MATa <i>ade2-1 ura3-1 trp1-1 can1-100 his3-11,15::pRS303-DBF4-CDC7-pGAL1-GAL4::HIS3Mx4 pep4::hph-NT1 DBF4-3FLAG::KanMx leu2-3,112::CDC7-9myc::LEU2</i>	<i>pGAL-DBF4-3FLAG-CDC7-9myc</i>	This study

### Antibodies

Proteins were detected using specific antibodies: rabbit-anti-Dpb11 (BPF19, Pfander lab), rabbit-anti-Slx4 (2057, Pfander lab), goat-anti-Cdc5 (sc-6733, Santa Cruz), rabbit-anti-Cdc7 (Diffley lab), rabbit-anti-Clb2 (sc-9071, Santa Cruz), goat-anti-Dbf4 (sc-5705; Santa Cruz), rabbit-anti-FLAG (F7425, Sigma), mouse-anti-myc (05-724, clone 4A6; Millipore), mouse-anti-Gal4-AD (TA-C10; Santa Cruz), mouse-anti-Gal4-BD (RK5C1; Santa Cruz).

### FACS analysis

$1 \times 10^7$  -  $2 \times 10^7$  cells were harvested by centrifugation and resuspended in 70% ethanol + 50 mM Tris pH 7.8. After centrifugation cells were washed with 1 ml 50 mM Tris pH 7.8 (Tris buffer) followed by resuspending in 520  $\mu$ l RNase solution (500  $\mu$ l 50 mM Tris pH 7.8 + 20  $\mu$ l RNase A (10 mg/ml in 10 mM Tris pH 7.5, 10 mM MgCl<sub>2</sub>) and incubation for 4

h at 37 °C. Next, cells were treated with proteinase K (200 µl Tris buffer + 20 µl proteinase K (10 mg/ml in 50% glycerol, 10 mM Tris pH 7.5, 25 mM CaCl<sub>2</sub>) and incubated for 30' at 50 °C. After centrifugation cells were resuspended in 500 µl Tris buffer. Before measuring the DNA content, samples were sonified (5"; 50% CYCLE; minimum POWER) and stained by SYTOX solution (999 µl Tris buffer + 1 µl SYTOX). Measurement was performed using FL1 channel 520 for SYTOX-DNA by BD FACSCalibur system.

### **Acrylamide gel electrophoresis and western blot analysis**

Protein samples were separated by standard SDS-polyacrylamide gel electrophoresis in 4-12% Novex NuPAGE Bis-Tris precast gels (ThermoFisher) with MOPS buffer (50 mM MOPS, 50 mM Tris-base, 1.025 mM EDTA, 0.1% SDS, adjusted to pH 7.7). To resolve phosphorylation shifts of Mms4 in Fig. EV1, and of Ulp2<sup>9myc</sup> or Scc1<sup>9myc</sup> (Fig. S2E), protein samples were separated in 7% Novex NuPAGE Tris-Acetate precast gel (ThermoFisher) with Tris-Acetate buffer (50 mM Tris-base, 50 mM Tricine, 0.1% SDS, adjusted to pH 8.24).

After electrophoresis, proteins were transferred to a nitrocellulose membrane (Amersham Protran Premium 0.45 µm NC) using a tank blotting system. Membranes were incubated with primary antibodies at 4 °C overnight. Incubation with appropriate secondary antibodies coupled to horseradish peroxidase (HRP) was performed at room temperature for 3 h. Membranes were washed five times for 5 min with western wash buffer (50 mM Tris pH 7.5, 137 mM NaCl, 3 mM KCl, 0.2 % NP-40) and incubated with Pierce ECL western blotting substrate (ThermoFisher) according to the instructions of the manufacturer. Chemiluminescence was detected with a tabletop film processor (OPTMAX, Protec).

### **Yeast Two-Hybrid analysis**

The plasmids used for yeast two-hybrid analysis in this study were based on pGAD-C1 and pGBD-C1. To assay for an interaction between the proteins, respective plasmids were transformed into competent PJ69-7A cells. Transformants were spotted in serial dilution (1:5) either on SC-Leu-Trp plates (control) or on SC-Leu-Trp-His plates (selection) and incubated at 30 °C for 2-3 days. Cells from the control plates were then grown in SC-Leu-Trp to log-phase to take samples for subsequent analysis of the expression of the AD-/BD-fusion proteins by western blot.

### **Preparation of whole-cell extracts (alkaline lysis/TCA)**

Cell pellets were re-suspended in 1 ml pre-cooled H<sub>2</sub>O and incubated with 150 µl of freshly prepared lysis solution (1.85 M NaOH, 7.5% beta-mercaptoethanol) at 4 °C for 15 min. Then, the lysate was admixed with 150 µl 55% trichloroacetic acid (TCA) and incubated at 4 °C for 10 min. After centrifugation and careful aspiration of the supernatant, the precipitated proteins were re-suspended in 50 µl HU-buffer (8 M urea, 5% SDS, 200 mM Tris pH 6.8, 1.5% dithiothreitol, traces of bromophenol blue) and incubated at 65 °C for 10 min.

### **Synchronization of cells**

Logarithmic growing cells were synchronized in mitosis by nocodazole (5 µg/ml), in S-phase by HU (200 mM), or in G1-phase by  $\alpha$ -factor (5-10 µg/ml). Release from G1 synchronization into S-phase was performed by washing twice in pre-warmed YPD, and suspending cells in pre-warmed YPD with nocodazole, with HU or without chemical.

### **Drug treatment**

DNA damage in liquid cultures was induced by addition of phleomycin to a final concentration of 50 µg/ml.

For solid media, concentrations of methyl methanesulfonate (MMS) were as indicated in the figures. Cells from stationary grown ON cultures were spotted in serial dilution (1:5) and incubated at 30 °C for 2-3 days.

### **Interaction assays**

After cell growth under the indicated conditions, yeast extracts were obtained by freezer mill lysis (Spex Sample Prep) in lysis buffer (100 mM Hepes pH 7.6, 200 mM KOAc, 0.1% NP-40, 10% glycerol, 2 mM b-ME, 100 mM octadecanoic acid, 10 mM NaF, 20 mM b-glycerophosphate, 400 µM PMSF, 4 µM aprotinin, 4 mM benzamidin, 400 µM leupeptin, 300 µM pepstatin A). Co-IP was performed for 2 hours with head-over-tail rotation at 4 °C using anti-FLAG agarose resin (Sigma). Non-specific background was removed by six washes and bound proteins were eluted by incubation with 0.5 mg/ml 3X FLAG-peptide (Sigma). The TCA-precipitated eluates were resolved on 4-12% NuPAGE gradient gels (Invitrogen), and analyzed by standard Western blotting techniques.

### **SILAC-based quantitative mass-spectrometry**

For Co-IP experiments followed by mass spectrometry analysis, cells deficient in lysine biosynthesis were grown in synthetic complete (SC) medium supplemented with normal

lysine (“light” medium) or heavy-isotope-labeled lysine (Lys6 or Lys8; “heavy” medium) from Cambridge Isotope Laboratories and arrested in G2/M phase with nocodazole. In SILAC experiments with high-copy expression of *MUS81-MMS4*, overexpression was induced by addition of 2% galactose for 2 h after nocodazole arrest.

Lysates were prepared by harvesting cells in equal amounts after growth under the indicated conditions. After co-IP, eluted proteins from light and heavy cultures were pooled, TCA precipitated and separated on a 4-12% NuPAGE Bis-Tris gel (Invitrogen). The gel was stained with GelCode Blue (Thermo Scientific). The gel lane was excised into ten slices and peptides were analyzed by LC-MS/MS after in-gel Lys-C digestion. Samples were measured on an LTQ-Orbitrap and analyzed using MaxQuant (Cox & Mann, 2008).

For analysis of proteins (Fig. S1A, 2E, S2A, EV3A, 6D, S6A), log<sub>2</sub> values of H/L ratios from two label-switch experiments without ratio count cut-off were plotted against each other.

For analysis of phosphorylation sites from endogenous protein levels (Fig. 3A-B, S7A), H/L ratios for Mms4 peptides were calculated from the corresponding H and L intensities of MS evidences and plotted in their log<sub>2</sub> values against the log<sub>10</sub> values of the peptide’s overall intensity. Evidences of non-phosphorylated Mms4 peptides are shown in grey, evidences of phosphorylated peptides are shown in black. Phosphorylated peptides were sorted into categories according to their phosphorylation status. Putative DDK target sites were differentiated into the categories pSpS (red), pSS (orange) or SpS (yellow), in which the respective residues of the (S/T)(S/T) motif were phosphorylated (detected phosphorylation probability >0.7). Phosphorylated peptides matching the Cdc5 consensus site are coloured in blue. Numbers indicate the phosphorylated residue in the depicted peptide. An asterisk marks peptide evidences that contained measured intensity values exclusively in the H or L sample. Their ratio value was set to a fixed value.

For analysis of phosphorylation sites from overexpressed *MUS81-MMS4* (Fig. 3C-D, S7B), log<sub>2</sub> values of H/L ratios of Mms4 peptides were plotted against the log<sub>10</sub> values of the peptide’s intensity. Depicted are phosphorylated peptides only. Peptides were sorted into categories according to their phosphorylation status. Putative DDK target sites were differentiated into the categories pSpS (red), pSS (orange) or SpS (yellow), in which the respective residues of the (S/T)(S/T) motif were phosphorylated (detected phosphorylation probability >0.7). Phosphorylated peptides matching the Cdc5 consensus site are coloured in blue. All other phosphorylated peptides are marked in grey. Bars depict the mean of the ratios of the respective category.

## Protein purification

CDK was expressed in *E. coli* BL21 pRIL cells (Agilent). Mus81-Mms4, DDK and Cdc5 were overexpressed in *S. cerevisiae* from a galactose-inducible GAL1-10 promoter. All purification steps were performed on ice or at 4 °C.

### *Purification of Mus81-Mms4 from S. cerevisiae*

*FLAG3MUS81* and *GST-HIS10-STREP2MMS4* were cloned under the control of the *GAL1,10* bidirectional promoter in a pRS306 derivative plasmid. The resulting vector was linearized with *StuI* and integrated at the *ura3-1* locus of a W303 *pep4Δ* strain.

The resulting MGBY3294 strain was grown in YP+2% raffinose to mid-log phase at 25 °C and protein expression was induced by addition of 2% galactose. Cells (10 liters at ~2-4x10<sup>7</sup> cells/ml) were harvested, washed and resuspended in a small volume of A500 buffer (40 mM Tris-HCl pH 7.5, 500 mM NaCl, 20% glycerol, 0.1% NP-40, 1 mM DTT) containing phosphatase and protease inhibitors and mechanically disrupted. The frozen lysate was resuspended in 2 volumes of A500, cleared by ultracentrifugation and incubated with anti-FLAG M2 agarose beads (Sigma) for 1 h at 4 °C. After extensive washing of the beads in A500, Mus81-Mms4 was dephosphorylated by treatment with 10,000 units of lambda phosphatase (New England Biolabs) for 30 min at room temperature. Beads were washed in A500 buffer and Mus81-Mms4 was then eluted with 3 volumes of A500 supplemented with 0.5 mg/ml 3X FLAG-peptide (Sigma). The eluate was then adjusted to 5 mM imidazole and proteins were loaded onto a Ni-NTA column (Qiagen). The column was washed with A500 buffer containing increasing concentrations of imidazole up to 50 mM, and finally Mus81-Mms4 was eluted with A500 containing 300 mM imidazole. The eluate was dialyzed extensively against A500, and stored in aliquots at -80 °C. Protein concentrations were determined using the Bradford assay (BioRad) and on Coomassie-stained PAGE gels using BSA as the standard, which also confirmed absence of phosphorylation-dependent electrophoretic migration shifts. Control experiments confirmed the absence of non-specific endo- or exonuclease activities.

### *Purification of bacterially expressed CDK2/cycA<sup>ΔN170</sup>*

To generate CDK2/cycA<sup>ΔN170</sup> complex, *GSTCDK2* and *His6cycA<sup>ΔN170</sup>* were expressed separately. Bacteria with either expression plasmids were grown in 1 l LB medium supplemented with antibiotics to mid-log phase. Both cultures were cooled down on ice for 5 min to increase chaperone expression followed by addition of 1 mM IPTG and incubation for 20 h at 20 °C. Cells were pelleted and resuspended in 40 ml lysis buffer

(300 mM NaCl, 20 mM HEPES pH 7.6, 5 mM  $\beta$ -mercaptoethanol, 0.01% NP-40, 100  $\mu$ M AEBSF, 1x complete protease inhibitor cocktail EDTA-free) followed by lysis with an EmulsiFlex-C3 system for three rounds at 1,000 bar. Cell debris was spun down at 140,000 g for 45 min. To allow complex formation between both subunits, extracts were pooled and incubated for 45 min. For glutathione affinity chromatography, 1 ml bed volume of equilibrated Glutathione Sepharose beads were added to the extract and incubated for 2 h. Beads were then washed four times with 25 CV Wash Buffer B2 (300 mM NaCl, 20 mM HEPES pH 7.6, 5 mM  $\beta$ -mercaptoethanol, 0.01% NP-40) before elution was achieved by protease cleavage. For this purpose, beads were resuspended in 1 CV wash buffer (150 mM NaCl, 20 mM HEPES pH 7.6, 5 mM  $\beta$ -mercaptoethanol, 0.01% NP-40) and incubated together with 250 U GST-PreScission protease (MPIB Core Facility) for 18 h. The eluate was then adjusted to 300 mM NaCl and 6 mM imidazole for subsequent Ni-NTA affinity chromatography. Here, a bed volume of 1 ml equilibrated Ni-NTA Agarose (Qiagen) was added to the eluate and incubated for 1 h. Beads were subsequently washed four times with 15 CV wash buffer (300 mM NaCl) + 6 mM imidazole and five times with 2 CV wash buffer (300 mM NaCl) + 6 mM imidazole + 5% glycerol. Elution was then performed with wash buffer (300 mM NaCl) + 250 mM imidazole. Fractions containing CDK were pooled and dialyzed by stirring two times against 300 volumes of dialysis buffer (150 mM NaCl, 50 mM HEPES pH 7.6, 0.1% NP-40, 2 mM  $\beta$ -mercaptoethanol, 10% glycerol) for 4 h in a Slide-A-Lyzer Dialysis Cassette (Thermo Scientific). Dialysed material was recovered, aliquoted, snap-frozen and stored at -80 °C.

#### *Purification of Cdc5 from S. cerevisiae*

YFZ020 was grown in 10 l YP medium + 2% raffinose at 30 °C until mid-log phase before expression was induced by addition of 2% galactose. After 4 h of induction, yeast cells were harvested and washed twice with 250 ml 1 M Sorbitol + 25 mM HEPES pH 7.6. The pellet was resuspended in 1 volume of lysis buffer (500 mM NaCl, 100 mM HEPES pH 7.6, 0.1% NP-40, 10% glycerol, 2 mM  $\beta$ -mercaptoethanol, 400  $\mu$ M PMSF, 4  $\mu$ M aprotinin, 4 mM benzamidin, 400  $\mu$ M leupeptin, 300  $\mu$ M pepstatin A, 4x complete protease inhibitor cocktail, EDTA-free) and frozen drop-wise in liquid nitrogen. Frozen cell drops were crushed using a freezer/mill system (Spex Sample Prep). Cell powder was thawed on ice and centrifuged at >185,000 g for 1 h. The clear phase was recovered and incubated with 1 ml bed volume of anti-FLAG M2 resin (Sigma) equilibrated in lysis buffer. After 2 h of incubation, the resin was washed five times with 10 CV of wash buffer (500 mM NaCl, 100 mM HEPES pH 7.6, 0.1% NP-40, 10% glycerol, 2 mM  $\beta$ -

mercaptoethanol). Two elution steps were performed by adding 1 CV 0.5 mg/mL 3FLAG peptide in wash buffer and incubation for 30 min. Obtained fractions were pooled, brought to a conductivity of 10 mS/cm (100 mM salt) and subjected to anion exchange chromatography using a MonoQ 5/50 GL column with a salt gradient of 0.1-1 M NaCl over 20 CV. Cdc5<sup>3FLAG</sup> eluted at a conductivity of ~15 mS/cm. Kinase containing fractions were aliquoted, snap-frozen and stored at -80 °C.

#### *Purification of DDK from S. cerevisiae*

DDK was purified as described by Gros *et al.* with modifications (Gros *et al.* 2014). YFZ021 cells were grown in 10 l YP medium + 2% raffinose at 30 °C until mid-log phase before expression was induced by addition of 2% galactose. After 4 h of incubation, yeast cells were harvested and washed twice with 250 ml 1 M Sorbitol + 25 mM HEPES pH 7.6. The pellet was resuspended in 1 volume of lysis buffer (400 mM NaCl, 100 mM HEPES pH 7.6, 0.1% NP-40, 10% glycerol, 2 mM  $\beta$ -mercaptoethanol, 400  $\mu$ M PMSF, 4  $\mu$ M aprotinin, 4 mM benzamidin, 400  $\mu$ M leupeptin, 300  $\mu$ M pepstatin A, 4x complete protease inhibitor cocktail EDTA-free) and frozen drop-wise in liquid nitrogen. Frozen cell drops were crushed using a freezer/mill system. Cell powder was thawed on ice and centrifuged at >185,000 g for 1 h. The clear phase was recovered and incubated with 1 ml bed volume of anti-FLAG M2 resin (equilibrated in lysis buffer). After incubation for 2 h at 4 °C, the resin was washed six times with 2 CV wash buffer (400 mM NaCl, 100 mM HEPES pH 7.6, 0.1% NP-40, 10% glycerol, 2 mM  $\beta$ -mercaptoethanol). For  $\lambda$ -phosphatase treatment, beads were resuspended in 1 CV wash buffer + 2 mM MnCl<sub>2</sub> + 900 U  $\lambda$ -phosphatase (New England Biolabs) and incubated for 1 h at 30 °C in a tabletop thermoshaker. Beads were recovered and bound DDK was eluted twice with 1 CV 0.5 mg/ml 3FLAG peptide in wash buffer for 30 min. Elutions were pooled, concentrated using a Vivaspin 500 MWCO 50.000 (GE healthcare) and fractionated by size exclusion chromatography using a Superdex 200 GL 10/300 column (GE healthcare, equilibrated in wash buffer) over 1.2 CV. DDK containing fractions were pooled, brought to a conductivity of 10 mS/cm (100 mM salt) and fractionated by anion exchange chromatography using a MonoQ 5/50 GL column with a salt gradient of 0.1-1 M NaCl over 20 CV. DDK containing fractions eluted at ~24-26 mS/cm and were aliquoted, snap frozen and stored at -80 °C.

## ***In vitro* kinase assays**

### *Sequential kinase assays with purified Mus81-Mms4*

Kinase assays were performed as described previously (Pfander & Diffley, 2011; Mordes *et al.*, 2008) with minor modifications.

Per reaction 20 pmol Mus81-Mms4 were used as substrate for 10 pmol kinase (CDK2/cyclinA<sup>ΔN170</sup>, DDK and/or Cdc5) in a 50 μL reaction volume containing 5 μg BSA. For sequential phosphorylation reactions Mus81-Mms4 was immobilized to Glutathione Sepharose 4B resin (GE Healthcare) for 1 h at 4 °C shaking. Beads were washed twice with binding buffer-100 (100 mM Hepes pH 7.6, 100 mM KOAc, 10% glycerol, 0.02% NP-40, 2 mM β-mercaptoethanol) and once with kinase buffer (10 mM HEPES pH 7.6, 100 mM KOAc, 50 mM β-glycerophosphate, 10 mM MgCl<sub>2</sub>, 2 mM β-mercaptoethanol), and aliquoted. Residual buffer was removed.

Priming phosphorylation reactions were performed by addition of 10 pmol (of each) kinase and started by addition of 2 or 10 mM (Fig. 1B, S1C) ATP. For samples without priming reaction the equivalent volume of added kinase was substituted by kinase buffer. After 30 min at 30 °C in a tabletop shaker beads were washed twice with binding buffer-200 (100 mM Hepes pH 7.6, 200 mM KOAc, 10% glycerol, 0.02% NP-40, 2 mM β-mercaptoethanol), once with binding buffer-100 and once with kinase buffer.

The consecutive kinase reaction was performed by addition of 10 pmol kinase and started by addition of 1 mM ATP + 5 μCi γ[<sup>32</sup>P]-ATP (PerkinElmer). After incubation for 30 min shaking at 30 °C reactions were stopped by addition of Laemmli sample buffer followed by boiling at 95 °C.

For kinetic analysis of the phosphorylation reactions (Fig. S1C), the second kinase reaction was upscaled to 100 μl and 20 μl samples were taken at indicated time points. Proteins were separated on NuPAGE Novex 12% Bis-Tris gels (ThermoFisher) and analyzed by autoradiography using a Typhoon FLA 9500 imager (GE healthcare).

### *Kinase assays using synthetic Mms4 peptides*

Kinase reactions were performed with 25 μg desthiobiotin-labelled Mms4 peptide and 10 pmol kinase in kinase buffer (10 mM HEPES pH 7.6, 10 mM β-glycerophosphate, 10 mM MgCl<sub>2</sub>, 5 mM Mg(OAc)<sub>2</sub>, 2 mM β-mercaptoethanol) with 100 mM KOAc in a 50 μL reaction volume containing 5 μg BSA. Reactions were started by addition of 1 mM ATP + 5 μCi γ[<sup>32</sup>P]-ATP. After incubation for 30 min shaking at 30 °C reactions were stopped by addition of Laemmli sample buffer followed by boiling at 95 °C. Proteins were separated on NuPAGE Novex 12% Bis-Tris gels (ThermoFisher) in MES buffer and analyzed by autoradiography using a Typhoon FLA 9500 imager (GE healthcare).

### **Nuclease assays**

5'-Cy3-end-labelled oligonucleotides were used to prepare synthetic nicked Holliday Junctions (nHJ) as described (Rass & West, 2008). Nuclease assays were carried out with immunopurified Mus81<sup>9myc</sup> or Mus81<sup>3FLAG</sup> (Fig. S4A) from cells arrested in mitosis with nocodazole. The anti-myc/anti-FLAG immunoprecipitates were extensively washed and mixed with 10 µl reaction buffer (50 mM Tris-HCl pH 7.5, 3 mM MgCl<sub>2</sub>) containing 30 ng 5'-Cy3-end-labelled nHJs or RFs <sup>11</sup>. Reactions were incubated for the indicated times with gentle rotation at 30 °C and stopped by addition of 5 µl 10 mg/ml proteinase K and 2% SDS, and further incubation at 37 °C for 1 h. Loading buffer was added and fluorophore-labelled products were separated by 10% PAGE, and analyzed using a Typhoon scanner. Substrate cleavage was normalized using the level of immunoprecipitated Mus81<sup>9myc</sup> as reference.

### **DSB-induced recombination assay**

The DSB-induced recombination assay was performed as described previously (Ho *et al.*, 2010). In brief, diploids were grown in liquid YPAR (YPR + 40 mg/l Adenine) until the cultures reached an OD<sub>600</sub> of 0.5. Cells were arrested with nocodazole and I-SceI expression was induced by adding galactose to a final concentration of 2%. After 2.5 h cells were plated onto YPAD (YPD + 10 mg/l Adenine), incubated for 3-4 days and then replica plated onto YPAD+Hyg+Nat, YPAD+Hyg, YPAD+Nat, SC-Met, SC-Ura, and SCR-ADE+Gal media to classify recombination events. The different classes depicted arise from repair of DSBs by either short tract or long tract gene conversion which produces ade2-n or ADE+ recombinants, respectively (white class: two short tract conversions; red class: two long tract conversions; red/white class: one short and one long tract conversion). Within the distinct classes CO events are measured by the number of colonies that have rendered both daughter cells homozygous for the HPH and NAT marker.

## Appendix References

- Cox J & Mann M (2008) MaxQuant enables high peptide identification rates, individualized p.p.b.-range mass accuracies and proteome-wide protein quantification. *Nat Biotechnol* **26**(12): 1367-1372
- Gritenaite D, Princz LN, Szakal B, Bantele SCS, Wendeler L, Schilbach S, Habermann BH, Matos J, Lisby M, Branzei D & Pfander B (2014) A cell cycle-regulated Slx4-Dpb11 complex promotes the resolution of DNA repair intermediates linked to stalled replication. *Genes Dev* **28**: 1604–1619
- Gros J, Devbhandari S & Remus D (2014) Origin plasticity during budding yeast DNA replication *in vitro*. *EMBO J* **33**(6): 621-636
- Ho CK, Mazón G, Lam AF & Symington LS (2010) Mus81 and Yen1 promote reciprocal exchange during mitotic recombination to maintain genome integrity in budding yeast. *Mol Cell* **40**: 988–1000
- James P, Halladay J & Craig EA (1996) Genomic libraries and a host strain designed for highly efficient two-hybrid selection in yeast. *Genetics* **144**: 1425-1436
- Knop M, Siegers K, Pereira G, Zachariae W, Winsor B, Nasmyth K & Schiebel E (1999) Epitope Tagging of Yeast Genes using a PCR-based Strategy: More Tags and Improved Practical Routines. *Yeast* **15**: 963-972
- Mordes DA, Nam EA & Cortez D (2008) Dpb11 activated the Mec1-Ddc2 complex. *Proc Natl Acad Sci U S A* **105**(48): 18730-18734
- Pfander B & Diffley JFX (2011) Dpb11 coordinates Mec1 kinase activation with cell cycle-regulated Rad9 recruitment. *EMBO J*. **30**: 4897–4907
- Rass U & West SC (2006) Synthetic junctions as tools to identify and characterise Holliday junction resolvases. *Meth Enzymol* **408**: 485-501
- Thomas BJ & Rothstein R (1989) Elevated recombination rates in transcriptionally active DNA. *Cell* **56**: 619-630

# Human Holliday junction resolvase GEN1 uses a chromodomain for efficient DNA recognition and cleavage

Shun-Hsiao Lee<sup>1</sup>, Lissa Nicola Prinz<sup>2</sup>, Maren Felizitas Klügel<sup>1</sup>, Bianca Habermann<sup>3</sup>, Boris Pfander<sup>2</sup>, Christian Biertümpfel<sup>1\*</sup>

<sup>1</sup>Department of Structural Cell Biology, Molecular Mechanisms of DNA Repair, Max Planck Institute of Biochemistry, Martinsried, Germany; <sup>2</sup>Department of Molecular Cell Biology, DNA Replication and Genome Integrity, Max Planck Institute of Biochemistry, Martinsried, Germany; <sup>3</sup>Computational Biology, Max Planck Institute of Biochemistry, Martinsried, Germany

**Abstract** Holliday junctions (HJs) are key DNA intermediates in homologous recombination. They link homologous DNA strands and have to be faithfully removed for proper DNA segregation and genome integrity. Here, we present the crystal structure of human HJ resolvase GEN1 complexed with DNA at 3.0 Å resolution. The GEN1 core is similar to other Rad2/XPG nucleases. However, unlike other members of the superfamily, GEN1 contains a chromodomain as an additional DNA interaction site. Chromodomains are known for their chromatin-targeting function in chromatin remodelers and histone(de)acetylases but they have not previously been found in nucleases. The GEN1 chromodomain directly contacts DNA and its truncation severely hampers GEN1's catalytic activity. Structure-guided mutations *in vitro* and *in vivo* in yeast validated our mechanistic findings. Our study provides the missing structure in the Rad2/XPG family and insights how a well-conserved nuclease core acquires versatility in recognizing diverse substrates for DNA repair and maintenance.

DOI: [10.7554/eLife.12256.001](https://doi.org/10.7554/eLife.12256.001)

\*For correspondence:

[biertuempfel@biochem.mpg.de](mailto:biertuempfel@biochem.mpg.de)

**Competing interests:** The authors declare that no competing interests exist.

**Funding:** See page 20

**Received:** 12 October 2015

**Accepted:** 17 December 2015

**Published:** 18 December 2015

**Reviewing editor:** Volker Dötsch, Goethe University, Germany

© Copyright Lee et al. This article is distributed under the terms of the [Creative Commons Attribution License](https://creativecommons.org/licenses/by/4.0/), which permits unrestricted use and redistribution provided that the original author and source are credited.

## Introduction

Homologous recombination (HR) is a fundamental pathway ensuring genome integrity and genetic variability (Heyer, 2015). In mitotic cells, double-strand breaks (DSBs) can be repaired by HR using the sister chromatid as a template to restore the information in the complementary double strand. In meiosis, the repair of programmed DSBs by HR and the formation of crossovers are crucial to provide physical linkages between homologs and to segregate homologous chromosomes. Furthermore, HR during meiosis creates sequence diversity in the offspring through the exchange between homologs (Petronczki et al., 2003; Sarbajna and West, 2014).

HR proceeds by pathways that may lead to the formation of DNA four-way junctions or Holliday junctions (HJs) that physically link two homologous DNA duplexes (Heyer, 2015; Holliday, 1964; Schwacha and Kleckner, 1995; Szostak et al., 1983). Faithful removal of HJs is critical to avoid chromosome aberrations (Wechsler et al., 2011) and cells have evolved sophisticated measures to disentangle joint molecules. One basic mechanism is resolution mediated by HJ resolvases that introduce precise symmetrical nicks into the DNA at the branch point. Nicked DNA strands are then rejoined by endogenous ligases leading to fully restored or recombined DNA strands. This mechanism is well studied for bacterial and bacteriophage resolvases such as *Escherichia coli* RuvC, T7 endonuclease I, T4 endonuclease VII (Benson and West, 1994; Lilley and White, 2001). These resolvases operate as dimers and show a large degree of conformational flexibility in substrate

**eLife digest** Factors like ultraviolet radiation and harmful chemicals can damage DNA inside living cells, which can lead to breaks that form across both strands in the DNA double helix. “Homologous recombination” is one of the major mechanisms by which cells repair these double-strand breaks. During this process, the broken DNA interacts with another undamaged copy of the DNA to form a special four-way structure called a “Holliday junction”. The intact DNA strands are then used as templates to repair the broken strands. However, once this has occurred the Holliday junction needs to be ‘resolved’ so that the DNA strands can disentangle.

One way in which Holliday junctions are resolved is through the introduction of precise symmetrical cuts in the DNA at the junction by an enzyme that acts like a pair of molecular scissors. Re-joining these cut strands then fully restores the DNA. Enzymes that generate the cuts in DNA are called nucleases, and the nuclease GEN1 is crucial for resolving Holliday junctions in organisms such as fungi, plants and animals. GEN1 belongs to a family of enzymes that act on various types of DNA structures that are formed either during damage repair, DNA duplication or cell division. However, GEN1 is the only enzyme in the family that can also recognize a Holliday junction and it was unclear why this might be.

Lee et al. have now used a technique called X-ray crystallography to solve the three-dimensional structure of the human version of GEN1 bound to a Holliday junction. This analysis revealed that many features in GEN1 resemble those found in other members of the same nuclease family. These features include two surfaces of the protein that bind to DNA and are separated by a wedge, which introduces a sharp bend in the DNA. However, Lee et al. also found that GEN1 contains an additional region known as a “chromodomain” that further anchors the enzyme to the DNA. The chromodomain allows GEN1 to correctly position itself against DNA molecules, and without the chromodomain, GEN1’s ability to cut DNA in a test tube was severely impaired. Further experiments showed that the chromodomain was also important for GEN1’s activity in yeast cells growing under stressed conditions.

The discovery of a chromodomain in this human nuclease may provide many new insights into how GEN1 is regulated, and further work could investigate if this chromodomain is also involved in binding to other proteins.

DOI: [10.7554/eLife.12256.002](https://doi.org/10.7554/eLife.12256.002)

recognition and in aligning both active sites for coordinated cleavage. Interestingly, T4 endonuclease VII and RuvC reach into and widen the DNA junction point whereas T7 endonuclease I binds DNA by embracing HJs at the branch point (*Biertümpfel et al., 2007; Górecka et al., 2013; Hadden et al., 2007*).

In eukaryotes, HR is more complex and tightly regulated. In somatic cells, HJ dissolution by a combined action of a helicase and a topoisomerase (BLM-TOPIII $\alpha$ -RMI1-RMI2 complex in humans) is generally the favored pathway, possibly to restore the original (non-crossover) DNA arrangement (*Cejka et al., 2010, 2012; Ira et al., 2003; Putnam et al., 2009; Wu and Hickson, 2003*). In contrast, HJ resolution generates crossover and non-crossover arrangements depending on cleavage direction. Several endonucleases such as GEN1, MUS81-EME1, and SLX1-SLX4 have been implicated as HJ resolvases in eukaryotes (*Andersen et al., 2011; Castor et al., 2013; Fekairi et al., 2009; Garner et al., 2013; Ip et al., 2008; Muñoz et al., 2009; Svendsen and Harper, 2010; Svendsen et al., 2009; Wyatt et al., 2013*). Interestingly, these resolvases are not structurally related and have different domain architectures, giving rise to variable DNA recognition and regulation mechanisms. The interplay between resolution and dissolution mechanisms is not fully understood yet, however, cell cycle regulation of resolvases seems to play an important role (*Blanco et al., 2014; Chan and West, 2014; Eissler et al., 2014; Matos et al., 2011*).

GEN1 belongs to the Rad2/XPG family of structure-selective nucleases that are conserved from yeast to humans (*Ip et al., 2008; Lieber, 1997; Yang, 2011*). The Rad2/XPG family has four members with different substrate preferences that function in DNA maintenance (*Nishino et al., 2006; Tsutakawa et al., 2014*). They share a conserved N-terminal domain (XPG-N), an internal domain (XPG-I) and a 5’->3’ exonuclease C-terminal domain containing a conserved helix-hairpin-helix motif.

C-terminal to the nuclease core is a regulatory region that is diverse in sequence and predicted to be largely unstructured. Although the catalytic cores are well conserved in the superfamily, substrate recognition is highly diverse: XPG/Rad2/ERCC5 recognizes bubble/loop structures during nucleotide-excision repair (NER), FEN1 cleaves flap substrates during Okazaki fragment processing in DNA replication, EXO1 is a 5'→3' exonuclease that is involved in HR and DNA mismatch repair (MMR) and GEN1 recognizes Holliday junctions (*Grasby et al., 2012; Ip et al., 2008; Nishino et al., 2006; Tomlinson et al., 2010; Tsutakawa et al., 2014*). A common feature of the superfamily is their inherent ability to recognize flexible or bendable regions in the normally rather stiff DNA double helix. Interestingly, GEN1 shows versatile substrate recognition accommodating 5' flaps, gaps, replication fork intermediates and Holliday junctions (*Ip et al., 2008; Ishikawa et al., 2004; Kanai et al., 2007*). According to the current model, however, the primary function of GEN1 is HJ resolution (*Garner et al., 2013; Sarbajna and West, 2014; West et al., 2015*) and it is suggested to be a last resort for the removal of joint molecules before cytokinesis (*Matos et al., 2011*).

To date, structural information is available for all members of the family but GEN1 (*Miętus et al., 2014; Orans et al., 2011; Tsutakawa et al., 2011*). A unified feature of these structures is the presence of two DNA-binding interfaces separated by a hydrophobic wedge. This wedge is composed of two protruding helices that induce a sharp bend into flexible DNA substrates. Rad2/XPG family members also share a helix-two-turn-helix (H2TH) motif that binds and stabilizes the uncleaved DNA strand downstream of the catalytic center. However, the comparison of DNA recognition features within the Rad2/XPG family has been hampered because of the lack of structural information on GEN1.

To understand the molecular basis of GEN1's substrate recognition, we determined the crystal structure of human GEN1 in complex with HJ DNA. In combination with mutational and functional analysis using *in vitro* DNA cleavage assays and *in vivo* survival assays with mutant yeast strains, we highlight GEN1's sophisticated DNA recognition mechanism. We found that GEN1 does not only have the classical DNA recognition features of Rad2/XPG nucleases, but also contains an additional DNA interaction site mediated by a chromodomain. In the absence of the chromodomain, GEN1's catalytic activity was severely impaired. This is the first example showing the direct involvement of a chromodomain in a nuclease. Our structural analysis gives implications for a safety mechanism using an adjustable hatch for substrate discrimination and to ensure coordinated and precise cleavage of Holliday junctions.

## Results

### Structure determination and architecture of the GEN1-DNA complex

In order to structurally characterize human GEN1, we crystallized the catalytically inactive variant GEN1<sup>2-505 D30N</sup>, denoted GEN1 for simplicity, in complex with an immobile Holliday junction having arm lengths of 10 bp (*Figure 1*). The structure was determined experimentally and refined up to 3.0 Å resolution with an  $R_{\text{free}}$  of 0.25 (*Table 1*). The HJ crystallized bridging between two protein monomers in the asymmetric unit (*Figure 1—figure supplement 1*). The overall structure of GEN1 resembles the shape of a downwards-pointing right hand with a 'thumb' extending out from the 'palm' and the DNA is packed against the ball of the thumb (*Figure 1*). The palm contains the catalytic core, which is formed by intertwined XPG-N and XPG-I domains (*Figure 1A/B*, green). They consist of a seven-stranded  $\beta$ -sheet in the center surrounded by nine helices harboring the conserved active site (*Figure 1B/D*, orange). The catalytic residues form a cluster of negatively charged residues (D30, E75, E134, E136, D155, D157, D208) that were originally identified by mutational analysis (*Ip et al., 2008; Lee et al., 2002; Wakasugi et al., 1997*) and are conserved in other Rad2/XPG family members (*Figure 1B/C* and *Figure 2*). The XPG-I domain is followed by a 5'→3' exonuclease C-terminal domain (EXO; *Figure 1B/D*, blue). The EXO domain consists of a helix-two-turn-helix (H2TH) motif (helices  $\alpha$ 10- $\alpha$ 11) accompanied by several  $\alpha$ -hairpins ( $\alpha$ 12- $\alpha$ 13 and  $\alpha$ 14- $\alpha$ 15). A similar arrangement is also found in other proteins, which use a H2TH motif for non-sequence specific DNA recognition (*Tomlinson et al., 2010*). The EXO domain in GEN1 has a 78 amino acid insertion (residues 245–322), of which only helix  $\alpha$ 12b (residues 308–322) is ordered in the structure (*Figure 1A*, gray and *Figure 2*). Helix  $\alpha$ 12b packs loosely with the H2TH helices ( $\alpha$ 10- $\alpha$ 11) and helix  $\alpha$ 12 at the 'finger' part of GEN1. Yeast Rad2, a homolog of human XPG, also contains helix  $\alpha$ 12b,

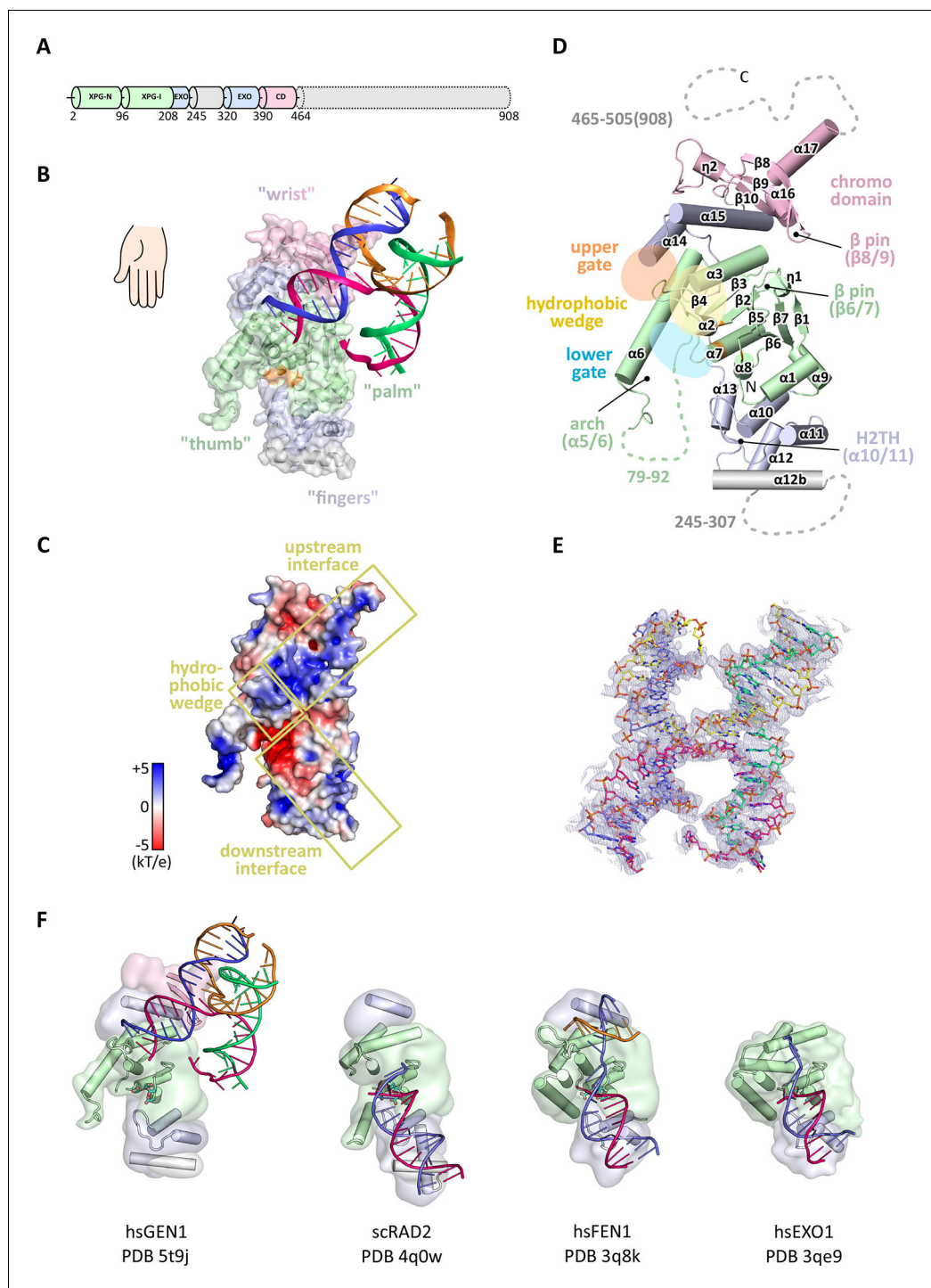


**Figure 1.** Architecture of human GEN1. (A) Domain architecture of human GEN1. The structurally unknown regulatory domain (residues 465–908) is shown with dotted lines. (B) Overview of the catalytic core of GEN1 in complex with HJ DNA. The protein resembles the shape of a downwards-pointing right hand with helix  $\alpha 6$  as the thumb. The protein is depicted in half transparent surface representation with secondary structure elements underneath. The DNA is shown in ladder representation with individual strands in different colors. The coloring of GEN1 follows domain boundaries: intertwining XPG-N and XPG-I in green, 5'→3' exonuclease C-terminal domain (EXO) in blue, chromodomain in pink, unassigned regions in gray. Active site residues (E134, E136, D155, D157) are highlighted in orange. (C) Electrostatic surface potential of GEN1. The coloring follows the potential from -5 (red) to +5 kT/e (blue). The DNA-binding interfaces and the position of the hydrophobic wedge are marked in yellow. (D) Secondary structure elements of the catalytic core of GEN1 in cartoon representation with the same coloring as in (B). (E) Alternative view of the catalytic core of GEN1. (F) Comparison of GEN1 with other proteins: hsGEN1 (PDB 5t9j), scRAD2 (PDB 4q0w), hsFEN1 (PDB 3q8k), and hsEXO1 (PDB 3qe9).

Figure 1 continued

colors as before. Dotted lines represent parts that are not resolved in the crystal structure. The numbering follows a unified scheme for the Rad2/XPG family (compare **Figure 2**) for  $\alpha$ -helices,  $\beta$ -sheets and  $3_{10}$ -helices ( $\eta$ ). (E) Experimental electron density map (autoSHARP, solvent flattened, contoured at  $1\sigma$ ) drawn around the HJ in the GEN1 complex. The DNA model is shown in ball-stick representation with carbon atoms of individual strands in different colors (yellow, light blue, magenta, green) and oxygen atoms in red, phosphor atoms in orange, nitrogen atoms in dark blue. (F) Structural comparison of Rad2/XPG family nucleases. Proteins are shown in a simplified surface representation with important structural elements in cartoon representation and DNA in ladder representation. The color scheme is the same as in **B. Figure 1—figure supplement 1** shows the content of the asymmetric unit.

DOI: [10.7554/eLife.12256.003](https://doi.org/10.7554/eLife.12256.003)

The following figure supplement is available for figure 1:

**Figure supplement 1.** Content of the asymmetric unit of the GEN1-HJ crystal.

DOI: [10.7554/eLife.12256.004](https://doi.org/10.7554/eLife.12256.004)

and it shows a similar arrangement as in GEN1 (**Figure 1F**). The EXO domain sandwiches the XPG-N/I domains with a long linker reaching from the bottom ‘fingers’ ( $\alpha 10$ - $\alpha 13$ ) along the backside of GEN1 to the top of the XPG-N/I domains at the ‘wrist’ ( $\alpha 14$ - $\alpha 15$ ). A structure-based sequence alignment of the nuclease core of human GEN1, FEN1, EXO1 and yeast Rad2 proteins with functional annotations relates sequence conservation to features in the Rad2/XPG family (**Figure 2**). The comparison with members in the Rad2/XPG identified two DNA binding interfaces and a hydrophobic wedge (ball of the thumb) that separates the upstream and the downstream interface (**Figure 1C/D** and compare **Figure 1F**). GEN1 has two prominent grooves close to the hydrophobic wedge, which we termed upper and lower gate or gateway for comparison (**Figure 1D**, orange and blue ellipses, respectively).

Notably, a small globular domain (residues 390–464) was found extending the GEN1 nuclease core at the wrist (**Figure 1**, pink). A DALI search (**Holm and Rosenström, 2010**) against the Protein Data Bank (PDB) identified this domain as a chromodomain (chromatin organization modifier domain). The domain has a chalice-shaped structure with three antiparallel  $\beta$ -strands packed against a C-terminal  $\alpha$ -helix and it forms a characteristic aromatic cage. The opening of the chalice abuts helix  $\alpha 15$  from the EXO domain.

### GEN1 has a conserved chromodomain with a closed aromatic cage

Chromodomains are found in many chromatin-associated proteins that bind modified histone tails for chromatin targeting (reviewed in **Blus et al., 2011; Eissenberg, 2012; Yap and Zhou, 2011**), but it has not previously been associated with nucleases. To understand the significance of the chromodomain for the function of GEN1, we first examined if the chromodomain is conserved in GEN1 homologs using HMM-HMM (Hidden Markov Models) comparisons in HHPRED (**Söding et al., 2005**). We found that the chromodomain in GEN1 is conserved from yeast (Yen1) to humans (**Figure 3A**). The only exception is *Caenorhabditis elegans* GEN1, which has a much smaller protein size of 443 amino acids compared to yeast Yen1 (759 aa) or human GEN1 (908 aa).

To further compare the structural arrangement of the aromatic cage in human GEN1 with other chromodomains, we analyzed the best matches from the DALI search (**Figure 3B**). We found many hits for different chromo- and chromo-shadow domains with root mean square deviations between 1.9 and 2.8 Å (compare **Figure 3—source data 1**). A superposition of the aromatic cage of the five structurally most similar proteins with GEN1 (**Figure 3C**) showed that residues W418, T438, and E440 are well conserved, whereas two residues at the rim of the canonical binding cleft are changed from phenylalanine/tyrosine to a leucine (L397) in one case and a proline (P421) in another (**Figure 3C**). Instead, Y424 occupies the space proximal to P421, which is about 1.5 Å outwards of the canonical cage and widens the GEN1 cage slightly. The substitution of phenylalanine/tyrosine to leucine is also found in CBX chromo-shadow domains (see below); however, the rest of the GEN1 aromatic cage resembles rather chromodomains.

Chromodomains often recognize modified lysines through their aromatic cage thus targeting proteins to chromatin (reviewed in **Blus et al., 2011; Eissenberg, 2012; Yap and Zhou, 2011**). Given the conserved aromatic cage in GEN1, we tested the binding to modified histone tail peptides

**Table 1.** Data collection and refinement statistics.

Data Set	G505-4w006native	G505-4w006Ta peak	G505-4w006SeMet peak
<b>Diffraction Data Statistics</b>			
Synchrotron Beamline	SLS PXII	SLS PXII	SLS PXII
Wavelength	0.99995	1.25473	0.97894
Resolution (Å)	75-3.0	75.4-3.8	43.6-4.4
Space Group	P 3 <sub>2</sub>	P 3 <sub>2</sub>	P 3 <sub>2</sub>
Cell dimensions			
a (Å)	86.94	87.06	87.11
b (Å)	86.94	87.06	87.11
c (Å)	200.72	201.30	199.69
α (°)	90	90	90
β (°)	90	90	90
γ (°)	120	120	120
I/σI*	18.4 (1.9)	27.49 (5.83)	16.58 (3.82)
Completeness (%)*	99.8 (98.8)	99.6 (97.3)	97.3 (83.3)
Redundancy*	6.3	10.2	5.1
R <sub>sym</sub> (%)*	6.2 (90.7)	7.7 (42.2)	6.9 (43.4)
<b>Refinement Statistics</b>			
Resolution (Å)	75-3.0		
Number of Reflections	33933		
R <sub>work</sub> /R <sub>free</sub>	0.199/0.241		
Number of Atoms			
Protein	6298		
DNA	1589		
Water/Solutes	27		
B-factors			
Protein	123.4		
DNA	150.2		
Water/Solutes	92.6		
R.M.S Deviations			
Bond lengths (Å)	0.010		
Bond Angles (°)	0.623		
Ramachandran Plot			
Preferred	753 (97.9 %)		
Allowed	16 (2.1%)		

\*Values for the highest resolution shell are shown in parenthesis

DOI: [10.7554/eLife.12256.005](https://doi.org/10.7554/eLife.12256.005)

(**Figure 3C/D**). However, we did not detect any binding despite extensive efforts using various histone tail peptides in pull-down assays, microscale-thermophoresis (MST) or fluorescence anisotropy measurements (compare **Figure 3—source data 2** and **Figure 3—figure supplement 2**). Our structure shows that the aromatic cage is closed by helix α15 (**Figure 3E** blue/pink), which has a hydrophobic interface towards the aromatic cage with residues L376, T380, and M384 reaching into it (compare **Figure 4F**). This potentially hampers the binding of the tested peptides in this conformation under physiological conditions.

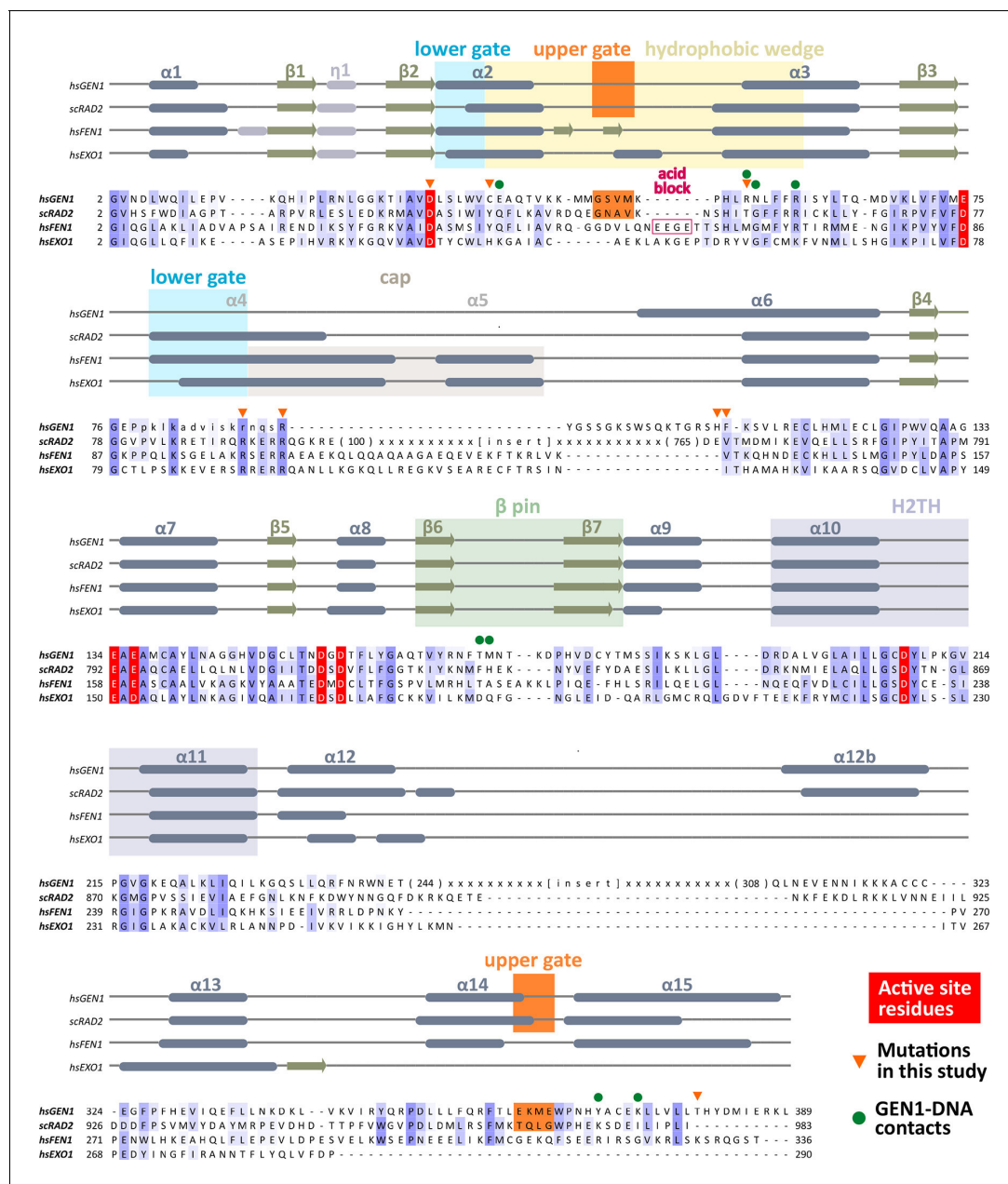


**Figure 2.** Alignment of the nuclease cores of Rad2/XPG-family proteins. The alignment is based on known crystal structures: human GEN1 (PDB 5t9j, this study), yeast Rad2 (PDB 4q0w), human FEN1 (PDB 3q8k), human EXO1 (3qe9). Secondary structure elements are depicted on top of the sequence with dark blue bars for  $\alpha$ -helices, light blue bars for  $3_{10}$ -helices and green arrows for  $\beta$ -sheets. The numbering follows a unified scheme for the superfamily. Functional elements are labeled and described in the main text. Sequences are colored by similarity (BLOSUM62 score) and active site residues are marked in red. Mutations analyzed in this study are marked with an orange triangle and DNA contacts found in the human GEN1-HJ structure have a dark green dot. Disordered or missing parts in the structures are labeled in small letters or with x.  
DOI: 10.7554/eLife.12256.006

## The GEN1 chromodomain is distantly related to CBX and CDY chromodomains

To explore the functional role of the GEN1 chromodomain, we evaluated its similarity to other chromodomains by comparing all of the 46 known human chromodomains from 34 different proteins. We made pairwise comparisons with HHPRED, PSIBLAST, combined the alignments and generated a phylogenetic tree (Figure 3F and Figure 3—figure supplement 1). The analysis showed a tree

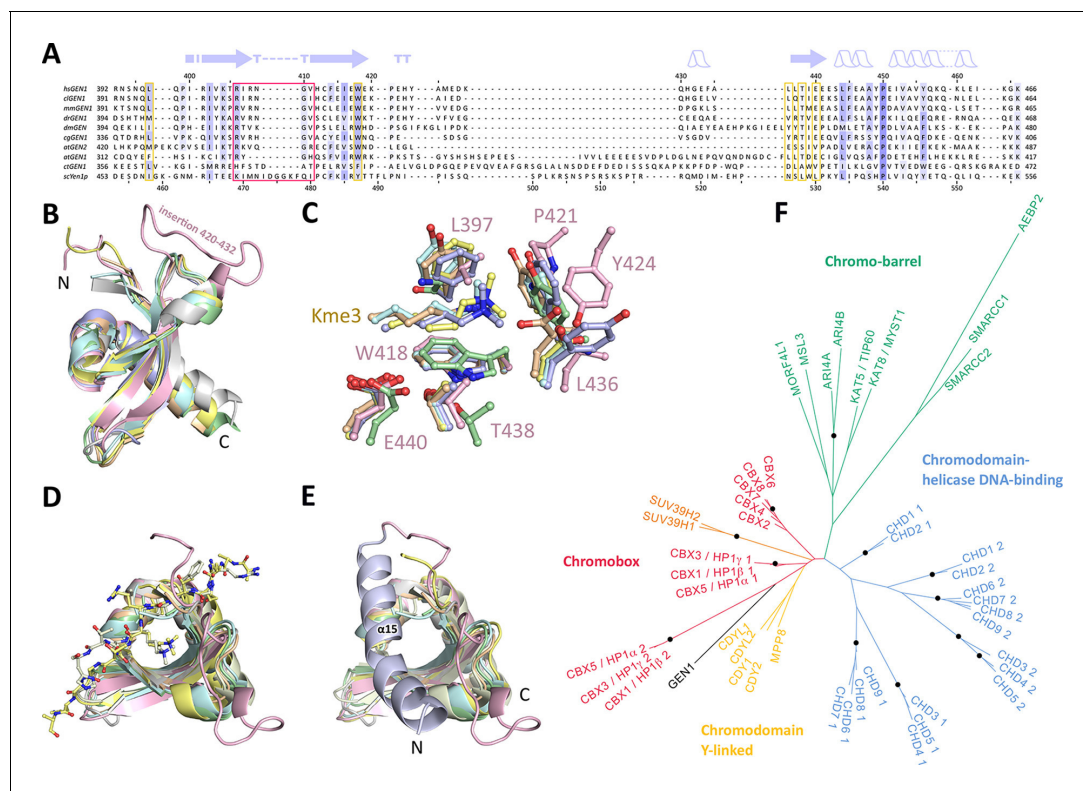


**Figure 3.** Chromodomain comparison. (A) Sequence alignment of GEN1 chromodomains from different organisms: hsGEN1 (*Homo sapiens*), clGEN1 (*Canis lupus*), mmGEN1 (*Mus musculus*), drGEN1 (*Danio rerio*), atGEN1/2 (*Arabidopsis thaliana*), cgGEN1 (*Crassostrea gigas*), scYEN1 (*Saccharomyces cerevisiae*). The presence of a chromodomain is conserved from yeast to human with *Caenorhabditis elegans* as an exception. Secondary structure elements of the GEN1 chromodomain are shown on top. The sequence coloring is based on a similarity matrix (BLOSUM62). The corresponding positions of the DNA-interaction site in human GEN1 is marked with a red box and residues of the aromatic cage are highlighted with a yellow box. (B) GEN1 has a canonical chromodomain fold of three antiparallel beta-sheets packed against an  $\alpha$ -helix. (C) The arrangement of the aromatic cage in GEN1 is comparable to other chromodomains but less aromatic and slightly larger. (D) The superposition of different chromodomains places cognate binding peptides of hsMPP8 and mmCBX7 (and others) into the aromatic cage. (E) The aromatic cage of GEN1 is closed by helix  $\alpha$ 15. Panels B–D show the chromodomains of hsGEN1 (pink, PDB 5t9j), hsCBX3 (gray, PDB 3kup), hsSUV39H1 (green, PDB 3mts), hsMPP8 (yellow, PDB 3lwe), dmHP1a (orange, chromo shadow PDB 3p7j), dmRHINO (cyan, PDB 4qvc/3r93), mmCBX7 (light blue, PDB 4x3s; compare **Figure 3—source data 1**). (F) Phylogenetic tree of all known human chromodomains. GEN1 is distantly related to the CBX chromo-shadow domains and CDY chromodomains. The corresponding alignment for calculating the phylogenetic tree is shown in **Figure 3—figure supplement 1**. GEN1 is colored in black, chromobox (CBX) proteins are colored in red, interspersed by SUV39H histone acetylases (orange) and chromodomain Y-linked (CDY) proteins (yellow). Chromo-barrel domain proteins are colored in green and chromodomain-helicase DNA-binding (CHD) proteins are in blue. Chromodomains and chromo-shadow domains from the same protein are labeled with 1 and 2, respectively. Stable branches with bootstrap values equal or higher than 0.8 are marked with a black dot. The binding of the GEN1 chromodomain to a set of histone peptides was tested but no interaction was detected (**Figure 3—source data 2** and **Figure 3—figure supplement 2**).

DOI: 10.7554/eLife.12256.007

The following source data and figure supplements are available for figure 3:

**Source data 1.** Proteins found in a DALI search.

DOI: 10.7554/eLife.12256.008

**Source data 2.** N-terminally fluorescein-labeled peptides used for chromodomain binding assays.

DOI: 10.7554/eLife.12256.009

**Figure supplement 1.** Sequence alignment of all known human chromodomains.

DOI: 10.7554/eLife.12256.010

**Figure supplement 2.** Histone peptide pull-down assay.

DOI: 10.7554/eLife.12256.011

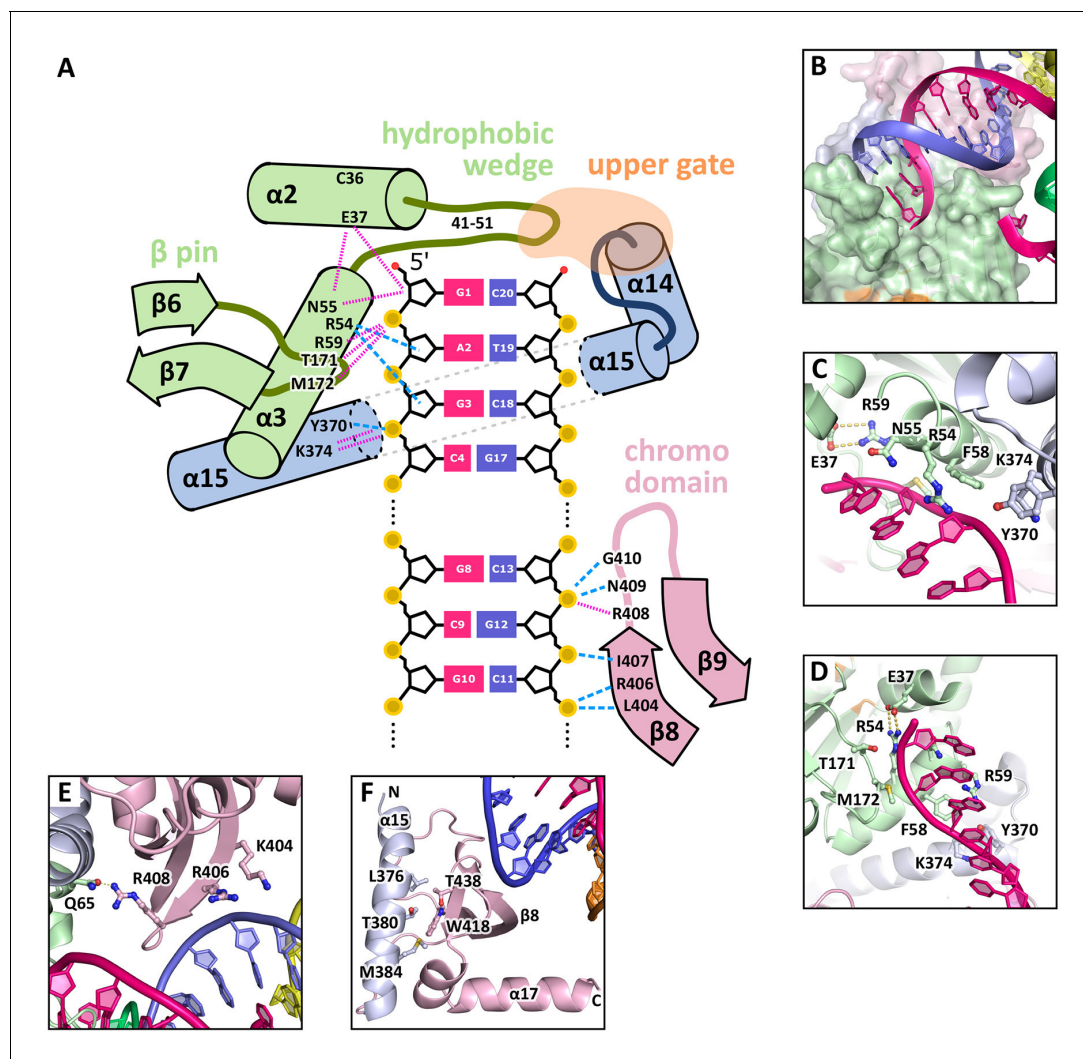


**Figure 4.** DNA interactions in the GEN1-DNA complex. (A) Schematic of the GEN1-DNA interactions at the upstream interface. The coloring is the same as in **Figure 1**. The nuclease core (green and blue) interacts with the uncleaved strand and the chromodomain (pink) contacts the complementary strand. Hydrogen bonds are shown with blue dashed lines and van-der-Waals contacts are in red dotted lines. (B) Interactions at the hydrophobic wedge. The end of the DNA double helix docks onto the hydrophobic wedge formed by helices  $\alpha 2$  and  $\alpha 3$ . (C/D) Interactions with the uncleaved strand in two views. All key residues form sequence-independent contacts to the DNA backbone. R54 reaches into the minor groove of the DNA. The complementary DNA strand has been removed for clarity (E/F) Interactions of the chromodomain with the complementary strand in two views. The backbone of residues 406–410 ( $\beta$ -hairpin  $\beta 8$ – $\beta 9$ ) abuts the DNA backbone. R406 has a supporting role in the interaction and R408 forms a polar interaction with Q65, which establishes a connection between the chromodomain and the nuclease core. Helix  $\alpha 15$  makes hydrophobic interactions with the aromatic cage and thus blocks it.

DOI: [10.7554/eLife.12256.012](https://doi.org/10.7554/eLife.12256.012)

branching into known subfamilies: chromobox proteins (CBX, red), chromodomain Y-linked proteins (CDY, yellow), chromodomain-helicase DNA-binding proteins (blue) and chromo-barrel domain proteins (green). The GEN1 chromodomain was found to be distantly related to the CDY chromodomains and chromobox proteins, particularly to the chromo-shadow domains of CBX1, CBX3 and CBX5. This agrees with the result from the DALI search, in which CBX chromo-shadow domains and homologs thereof were among the closest structural matches. Together with the observed differences in residues forming the aromatic cage, it indicates that the GEN1 chromodomain forms a new subgroup with features from chromo- and chromo-shadow domains that emerged from a common ancestor within CBX/CDY proteins.

## GEN1-DNA interactions

The GEN1-HJ structure revealed that the upstream DNA-binding interface acts as a docking site for double-stranded DNA and that the chromodomain secures its position. The DNA is bound at the upstream interface and the hydrophobic wedge but does not extend into the active site or to the downstream interface (**Figure 1B/C/D**). Comparison of the structure of GEN1 to related structures of FEN1, Rad2 and EXO1 (*Miqtus et al., 2014; Orans et al., 2011; Tsutakawa et al., 2011*) suggests that a DNA substrate has to extend to the downstream interface to position a DNA strand for cleavage by the active site of GEN1 (**Figure 1B/C** and **Figure 1F**). In the GEN1 structure, the end of the DNA arm attaches to the hydrophobic wedge provided by parts of helices  $\alpha 2$ - $\alpha 3$  and their connecting loop (**Figure 4A/B**), forming van-der-Waals contacts with the first base pair, which docks perfectly onto the protruding curb of residues 41–51 (**Figure 4B**). The uncleaved DNA strand is further stabilized and its geometrical arrangement is fixed by the upstream DNA-binding interface. Particularly, the DNA is contacted by a  $\beta$ -pin (strands  $\beta 6$ - $\beta 7$ ; **Figure 4A/C**) from one side and by R54 and F58 (**Figure 4A/D**) from helix  $\alpha 3$  together with Y370 and K374 (helix  $\alpha 15$ ) from the opposite side (**Figure 4A/C**). The key residues in the  $\beta$ -pin are T171 that forms a hydrogen bridge to the phosphate of the first base (**Figure 4A**, 'G1') and M172 that makes a van-der-Waals contact to the DNA backbone at the second base (**Figure 4A**, 'A2'). R54 reaches into the DNA minor groove and forms a hydrogen bond with the ribose ring oxygen at the third base of the uncleaved strand and F58 packs against the same ribose moiety (**Figure 4C/D**). Y370 and K374 in  $\alpha 15$  form hydrogen bonds to the backbone of the third base of the uncleaved DNA strand (**Figure 4D**, 'G3').

An additional interaction point is provided by a  $\beta$ -hairpin from the chromodomain (strands  $\beta 8$ - $\beta 9$ ), one DNA turn upstream of the hydrophobic wedge (**Figure 4A/E/F**). This  $\beta$ -hairpin interacts with the complementary DNA strand by matching the protein backbone (residues 406–411) to the contour of the DNA backbone in a sequence unspecific manner (**Figure 4A/E**). The side chains of K404 and R406 project out, and they are in hydrogen bonding distance to the DNA (**Figure 4E**). Remarkably, R408 forms a polar interaction with Q65, which establishes a connection between the DNA contact point at the chromodomain and the nuclease core (**Figure 4E**). The interactions at the chromodomain extend the upstream DNA-binding interface to cover a full DNA turn, reinforcing the binding.

The downstream binding interface can be inferred from other Rad2/XPG structures (**Figure 1C/F**) as the nuclease core is well conserved in GEN1, FEN1, Rad2 and EXO1 (root mean square deviations of 0.9–1.1 Å for 161 C $\alpha$  atoms, respectively). The residues corresponding to the tip of the thumb (residues 79–92), which are disordered in the GEN1 structure, likely form helix  $\alpha 4$  upon DNA binding to the downstream interface as seen in human FEN1 and EXO1 (*Orans et al., 2011; Tsutakawa et al., 2011*). The missing residues in GEN1 have 35.7% identity and 78.6% similarity (BLOSUM62 matrix) to the corresponding residues in FEN1 (90–103), which form helix  $\alpha 4$  in the FEN1-DNA complex (compare **Figure 2**). The same region is disordered in FEN1 when no DNA is bound (*Sakurai et al., 2005*). This indicates that also GEN1 undergoes such a disorder-to-order transition to form an arch with helices  $\alpha 4$  and  $\alpha 6$  upon substrate binding (*Patel et al., 2012*) and similar to the arrangement in T5 FEN (*Ceska et al., 1996*).

## The activity of GEN1 depends on correct DNA positioning

GEN1 has versatile substrate recognition features, ranging from gaps, flaps, replication fork intermediates to HJs (*Ip et al., 2008; Ishikawa et al., 2004; Kanai et al., 2007*). To understand the functional relevance of the GEN1 structure for DNA recognition we performed a series of mutagenesis studies with single point mutations and truncated protein variants (**Figure 5** and **Figure 5—figure supplement 1/2**) to investigate the effect on the active site (D30N), upstream DNA binding (R54E), downstream DNA binding (C36E), arch at the downstream interface (R89E, R93E, H109E, F110E), and chromodomain ( $\Delta$ chromo, K404E, R406E). We performed nuclease assays by titrating different amounts of GEN1 to a fixed DNA concentration of 40 nM for 15 min and DNA cleavage products were analyzed by native electrophoresis (**Figure 5A** and **Figure 5—figure supplement 1/2**). We used an immobile HJ and a 5' flap substrate side-by-side to facilitate the comparison of the effects on separate GEN1 functions. Notably, stoichiometric amounts of GEN1 were required to cleave HJ substrates whereas 5' flaps were readily processed with catalytic amounts (**Figure 5A**).

The active site modification D30N showed that the cleavage activity on both HJ and 5' flap substrates was lost in agreement with previously published data (*Ip et al., 2008*). According to our

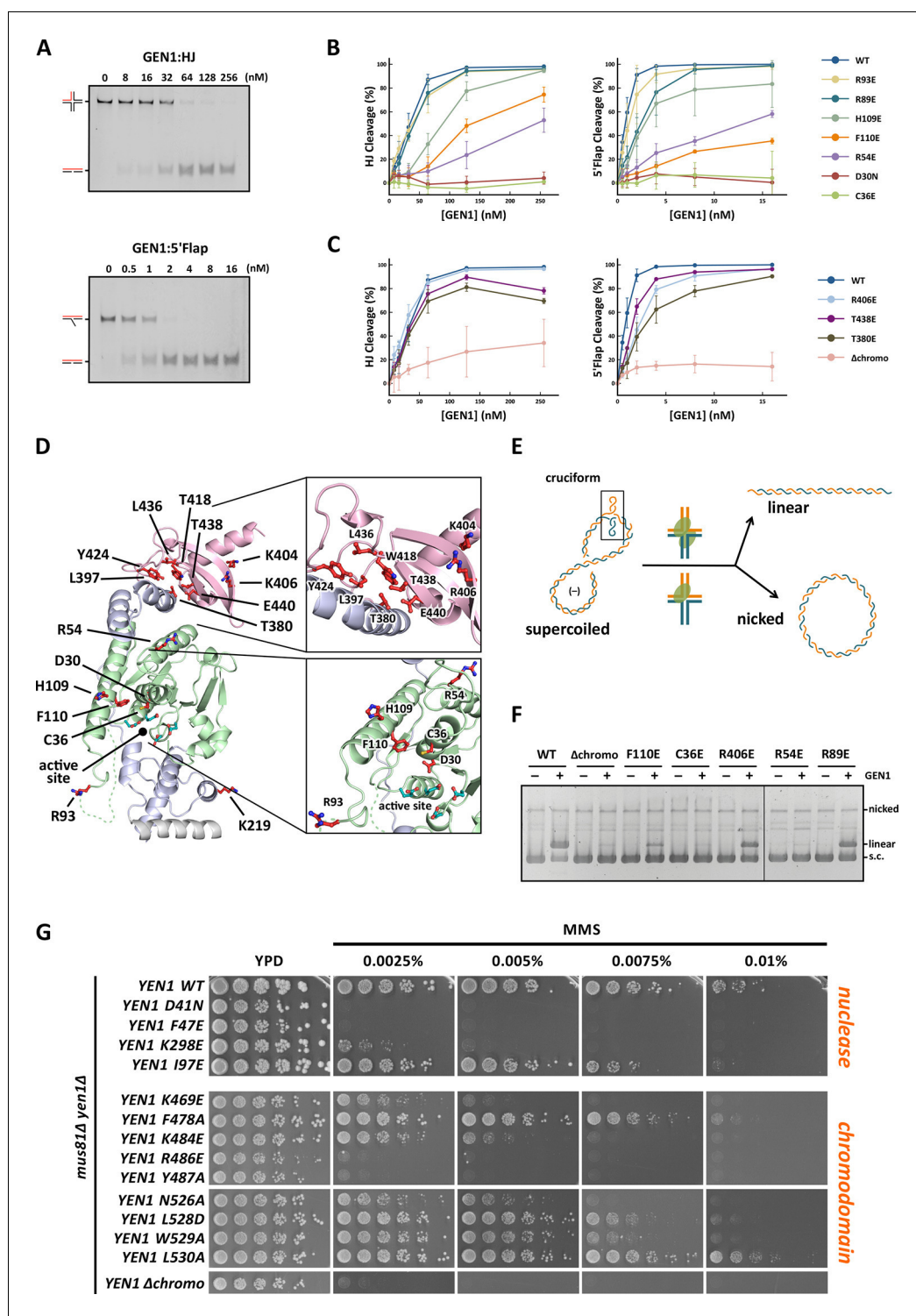


**Figure 5.** Functional analysis of GEN1. (A) Nuclease activity of GEN1 with HJ and 5' flap DNA. 40 nM 5' 6FAM-labeled substrates were mixed with indicated amounts of GEN1. Reactions were carried out at 37°C for 15 min, products were separated by native PAGE and analyzed with a phosphoimager. **Figure 5—source data 1** gives the sequences of DNA oligos used in biochemical assays and **Figure 5—source data 3** shows activity measurements. (B) Quantification of nuclease assays of wild type GEN1 and variants with mutated residues located at the protein-DNA interfaces. Percentage of cleavage was plotted against the enzyme concentration. Error bars depict the standard deviation calculated from at least three independent experiments. **Figure 5—figure supplement 1** shows representative gels from the PAGE analysis. (C) Quantification of nuclease assays of wild type GEN1 and **Figure 5 continued on next page**

Figure 5 continued

variants with mutated residues located at the chromodomain. Error bars depict the standard deviation calculated from at least three independent experiments. **Figure 5—figure supplement 2** shows representative gels from the PAGE analysis. (D) GEN1 mutations used in this study. Locations of human GEN1 mutations used in biochemical assays and corresponding residues in yeast MMS survival assays are highlighted in red. Active site residues E134, E136, D155, D157 are marked in turquoise. (E) Schematic of the cruciform plasmid cleavage assay. A cruciform structure can be formed in plasmid pIRbke8<sup>mut</sup>, which harbors an inverted-repeat sequence and is stabilized by negative supercoiling. Introducing two cuts across the junction point within the lifetime of the resolvase-junction complex yields linear products whereas sequential cleavage generates nicked products and the relaxed plasmid cannot be a substrate for the next cleavage. (F) Cruciform plasmid cleavage assay with different GEN1 variants. Plasmid pIRbke8<sup>mut</sup> was treated with 256 nM GEN1 each and reactions were carried out at 37°C for 15 min. Supercoiled, linear and nicked plasmids were separated by native agarose gel electrophoresis and visualized with SYBR safe under UV light. (G) MMS survival assays with yeast *yen1* variants. The survival of *yen1* mutants was tested under a *yen1Δ mus81Δ* background with indicated amounts of MMS. The top part shows mutations at GEN1-DNA interfaces and the bottom part mutations at the chromodomain (compare **Figure 5—figure supplement 3** for all controls and expression tests). **Figure 5—source data 2** gives a list of all yeast strains. DOI: [10.7554/eLife.12256.013](https://doi.org/10.7554/eLife.12256.013)

The following source data and figure supplements are available for figure 5:

**Source data 1.** Oligonucleotides used in biochemical assays.

DOI: [10.7554/eLife.12256.014](https://doi.org/10.7554/eLife.12256.014)

**Source data 2.** Yeast strains used for MMS survival assays.

DOI: [10.7554/eLife.12256.015](https://doi.org/10.7554/eLife.12256.015)

**Source data 3.** In vitro activity measurements of different GEN1<sup>2-505</sup> variants.

DOI: [10.7554/eLife.12256.016](https://doi.org/10.7554/eLife.12256.016)

**Figure supplement 1.** DNA cleavage assays of different GEN1 mutations.

DOI: [10.7554/eLife.12256.017](https://doi.org/10.7554/eLife.12256.017)

**Figure supplement 2.** DNA cleavage assays of different GEN1 fragments.

DOI: [10.7554/eLife.12256.018](https://doi.org/10.7554/eLife.12256.018)

**Figure supplement 3.** MMS survival assays with yeast *yen1* mutants.

DOI: [10.7554/eLife.12256.019](https://doi.org/10.7554/eLife.12256.019)

structure, R54 in helix  $\alpha 3$  at the upstream interface fixes the substrate position by reaching into the minor DNA groove and we observed that R54E had a strongly reduced cleavage activity (~50%; **Figure 5B**), indicating a key role in substrate positioning.

Residue C36 in helix  $\alpha 2$  points towards the downstream interface and likely contacts the DNA upon binding (compare **Figure 5D**). The corresponding FEN1 Y40, is a key residue stacking with the -1 base of the 5' flap at the FEN1 active site (*Tsutakawa et al., 2011*). Therefore, we tested the cleavage ability of a GEN1<sup>C36E</sup> and found that the mutant protein had completely lost its enzymatic activity for both, HJ and 5' flap cleavage, to the same degree as the active site modification D30N (**Figure 5B**). This effect is stronger than for FEN1<sup>Y40A</sup>, which showed only a partial loss in activity (*Tsutakawa et al., 2011*). Our results suggest that C36 provides a polar interface for orienting and guiding the cleaved strand towards the active site and the lower gateway.

We further tested a glutamate modification of the superfamily-conserved R89 and R93 located in the disordered part continuing to helix  $\alpha 6$ , presumably forming an arch (see above). The arch was shown to facilitate cleavage by clamping flap substrates in FEN1 and the modification R100A showed a strong decrease in the cleavage activity (*Patel et al., 2012*). The GEN1 R89E mutation, corresponding to residue R100 in FEN1, showed that the activity of GEN1 with a HJ substrate was not altered. In the case of a 5' flap substrate, cleavage was slightly reduced and it reached to the full level at enzyme concentrations higher than 10 nM. The effect of the R93E modification was even less pronounced compared to R89E. In contrast, the cleavage of both 5' flap and HJ substrates depended strongly on F110 at helix  $\alpha 6$  (thumb), which points towards the active site. An F110E modification showed a reduction in cleavage by 25% for HJ substrates, and the effect was even stronger for 5' flap substrates, where the activity is reduced by 65%. The equivalent position in FEN1 is V133 showing a critical involvement in stabilizing 5' flap DNA by orienting the -1 nucleotide for catalysis (*Tsutakawa et al., 2011*). We have also tested the effect of modifying H109, which neighbors the critical F110. Even though it points away from the active site, a glutamate at this

position reduced 5' flap cleavage to 83% and HJ cleavage recovered only at high substrate concentrations of 256 nM. Overall, the results suggest that F110 has a key position for DNA recognition and processing.

### Coordinated cleavage of HJs

Classical HJ resolvases introduce two symmetrical incisions across the junction point by coordinating the action of two active sites. The first nick is rate-limiting and the second one takes place near-simultaneously and within the lifetime of the resolvase-DNA complex. This mechanism has been well studied for bacterial and bacteriophage HJ resolvases (Fogg and Lilley, 2000; Giraud-Panis and Lilley, 1997; Pottmeyer and Kemper, 1992; Shah et al., 1997). Hence, it is thought that also GEN1 dimerizes upon binding to HJ substrates as indicated by coordinated cleavage and by an increase in hydrodynamic radius compared to protein alone (Chan and West, 2015; Rass et al., 2010). In order to further examine the effect of GEN1 modifications on HJ cleavage, we used a cruciform plasmid cleavage assay to evaluate GEN1's nicking function, as illustrated in Figure 5E. Here, the plasmid pIRbke8<sup>mut</sup> served as a substrate that contains an inverted-repeat sequence extruding a cruciform structure when supercoiled (Chan and West, 2015; Lilley, 1985; Rass et al., 2010). Coordinated dual incision of the cruciform (by a dimer) leads to linear duplex products with slow migration, whereas uncoordinated cleavage (by monomeric enzymes) results in nicked plasmids that migrate even slower (Figure 5F). Cruciform structures are reabsorbed when the superhelical stress is released upon single nicking and the DNA cannot serve as a substrate anymore.

We observed that wild type GEN1 resolved cruciform structures into linear products (Figure 5F) in agreement with previous reports (Chan and West, 2015; Rass et al., 2010). GEN1<sup>C36E</sup> (downstream interface) and GEN1<sup>R54E</sup> (upstream interface) showed only residual activity confirming their importance for HJ cleavage. The cruciform cleavage by F110E (thumb) was strongly reduced in line with our nuclease assays using small DNA substrates (Figure 5B). GEN1<sup>R89E</sup> (disordered part of the arch) did not show any appreciable effect, which suggests that this part of the arch is not directly involved in HJ recognition. Taken together, our results suggest that the positioning of HJ junction substrates both at the upper and the lower gateway is critical for productive cleavage. Furthermore, none of the tested modifications at the different DNA interaction interfaces was able to uncouple the coordinated HJ cleavage.

### The chromodomain of GEN1 facilitates efficient substrate cleavage

Agreeing with the structural significance for DNA binding, the truncation of the chromodomain ( $\Delta$ chromo, residues 2-389) showed a severe reduction (~3-fold) in HJ cleavage activity whereas all longer GEN1 fragments containing the chromodomain (2-464, 2-505 and 2-551) showed full activity (Figure 5—figure supplement 2). Interestingly, the effect of the chromodomain truncation is even more pronounced for 5' flap DNA cleavage than for HJs, showing a 7-fold reduction compared to wild type (Figure 5C). The activity of GEN1 in the plasmid-based cruciform cleavage assay was also severely hampered in the absence of the chromodomain (Figure 5F) showing only a weak band for linear products and no increase for nicked plasmid, emphasizing the importance of the chromodomain for GEN1 activity.

Further, to test the influence of the positively charged side chains K404 and R406 on DNA binding, we introduced charge-reversal mutations to glutamates and assessed their nuclease activities. Even though K404 and R406 are within hydrogen-bonding distance to the DNA, K404E, and R406E showed no appreciable influence on GEN1's nuclease activity. Only a slight reduction in cleavage of 5' flap substrates was observed for GEN1<sup>R406E</sup>, whereas the processing of HJ substrates was not altered significantly (Figure 5C). This reinforces the conclusion from our structural observations that the chromodomain and the DNA interact through their backbones via van-der-Waals interactions.

### Influence of phosphorylation-mimicking chromodomain modifications

PhosphoSitePlus (Hornbeck et al., 2014) lists two phosphorylation sites at residues T380 and T438 in GEN1 that were found in a T-cell leukemia and a glioblastoma cell line. These residues are located in helix  $\alpha$ 15 and at the rim of the aromatic cage, respectively. Both phosphorylation sites are positioned to interrupt hydrophobic interactions between helix  $\alpha$ 15 and the chromodomain (Figure 5D and Figure 4F). Therefore, we tested if the phosphorylation-mimicking modifications T380E and

T438E had an effect on GEN1's activity. At low enzyme concentrations (<50 nM) HJ cleavage was similar to that of wild-type protein but at high concentrations the activity declined to less than 80% (**Figure 5C**). For a 5' flap substrate, the assay showed consistently lower activity than wild type, recovering to about 80% cleavage at the highest enzyme concentration (**Figure 5C**). These results suggest that phosphorylation of GEN1 chromodomain residues may regulate DNA recognition and cleavage.

## Physiological relevance of GEN1 interactions

To test the physiological relevance of the identified GEN1-DNA interactions, we investigated the survival of *Saccharomyces cerevisiae* mutant strains expressing variants of Yen1 (GEN1 homolog) after treatment with the DNA-damaging agent MMS (**Figure 5G** and **Figure 5—figure supplement 3/source data 2**). All Yen1 variants were expressed to a similar degree as endogenous Yen1, which was confirmed by Western Blot analysis (**Figure 5—figure supplement 3**). Because of the functional overlap of Mus81 and Yen1 in HR (**Blanco et al., 2010**) a double knockout (*yen1Δ mus81Δ*) was used and complemented with different variants of Yen1.

The control strain, complemented with wild type Yen1, survived MMS concentrations of up to 0.01%, consistent with the described hypersensitivity of *mus81Δ* mutants (**Blanco et al., 2010; Interthal and Heyer, 2000**). In stark contrast, cells containing either the active site mutant Yen1-D41N (corresponding to GEN1<sup>D30N</sup>) or the downstream interface mutant Yen1-F47E (corresponding to GEN1<sup>C36E</sup>) did not grow even at an MMS concentration as low as 0.0025% (**Figure 5G**). After the expression of the upstream interface mutant Yen1-I97E (corresponding to GEN1<sup>R54E</sup>) cells showed a slight but significant growth defect at high MMS concentrations (see panels for 0.0075% and 0.01% MMS in **Figure 5G**). These results are therefore consistent with the in vitro cleavage results carried out with GEN1 mutants and showing a reduction in activity for R54E and no activity for C36E (see **Figure 5C**). As a last mutant in the nuclease core, we tested the K298E mutation which is located in helix  $\alpha$ 10 of the H2TH motif in the downstream DNA-binding interface, and for which we were unable to obtain the corresponding GEN1<sup>K219E</sup> modification for cleavage assays (compare **Figure 5D**). This mutant displayed a strong sensitivity towards MMS but lower than the one observed for the catalytic mutant, indicating that the mutant was partially functional in yeast (**Figure 5G**).

We next investigated the effect of mutations in the aromatic cage of Yen1's chromodomain (compare **Figure 3**) and found that their severity was strongly position dependent. Mutation of R486E and Y487A in Yen1, both of which are located near the base of the cage, corresponding to the W418 position in GEN1 (see **Figure 3C**), showed a strong effect on MMS sensitivity (see **Figure 5G**), similar to the one observed for the catalytic mutant, presumably due to a dysfunctional chromodomain. In contrast, mutations located further outside of the core (F478A and K484E) led to a less pronounced MMS sensitivity. The same was true for the K469E variant, which corresponds to position R406 at the chromodomain-DNA interface in GEN1 (see **Figure 3A** and **5F**), and for residues at the rim of the chromodomain (*yen1-N526A*, *yen1-L528D* and *yen1-W529A*), consistent with our in vitro observation for GEN1<sup>T438E</sup> (slightly reduced activity, **Figure 5C**). No effect on MMS sensitivity was detected for *yen1-L530A*, which corresponds to a conserved glutamate in chromodomains (E440 in GEN1). Lastly, we found that the deletion of the chromodomain (Yen1- $\Delta$ 452–560) lead to a severe phenotype comparable to the active site mutant Yen1-D41N (**Figure 5G** and **Figure 5—source data 2**). The Yen1 variant lacking the chromodomain was expressed to levels similar to the full-length protein and we therefore conclude that the chromodomain is crucial for the function of Yen1. Taken together, the functional data of Yen1 mutants in vivo and GEN1 mutants in vitro point towards an essential and evolutionary conserved role of the chromodomain in GEN1/Yen1 proteins.

## Discussion

### Implications of the chromodomain

The structure of the human GEN1 catalytic core provides the missing structural information in the Rad2/XPG family. The GEN1 structure complements recent reports on the structures of Rad2, EXO1 and FEN1, (**Miętus et al., 2014; Orans et al., 2011; Tsutakawa et al., 2011**). Thereby, it gives insights how relatively conserved nuclease domains recognize diverse substrates in a structure-

selective manner and act in different DNA maintenance pathways. In comparison with other Rad2/XPG nucleases, GEN1 shows many modifications on common structural themes that give the ability to recognize a diverse set of substrates including replication fork intermediates and HJs. The upstream DNA interface of GEN1 lacks the 'acid block' found in FEN1, instead it has a prominent groove at the same position (compare **Figure 1**, 'upper gate') with a strategically positioned R54 nearby. Furthermore, the helical arch in GEN1 misses helix  $\alpha 5$ , which forms a cap structure in FEN1 and EXO1 that stabilizes 5' overhangs for cleavage. These features have implications for the recognition and cleavage of HJ substrates (see below). The most striking difference to other Rad2/XPG family members is that the GEN1 nuclease core is extended by a chromodomain, which provides an additional DNA anchoring point for the upstream DNA-binding interface. The evolutionarily conserved chromodomain is important for efficient substrate cleavage as we showed using truncation and mutation analyses. This finding opens new perspectives for the regulation of GEN1 and for its interactions with other proteins. Chromodomains serve as chromatin-targeting modules (reviewed in **Blus et al., 2011; Eissenberg, 2012; Yap and Zhou, 2011**), general protein interaction elements (**Smother and Henikoff, 2000**) as well as dimerization sites (**Canzio et al., 2011; Cowieson et al., 2000; Li et al., 2011**). These possibilities are particularly interesting, as chromatin targeting of proteins via chromodomains has been implicated in the DNA damage response. The chromatin remodeler CHD4 is recruited in response to DNA damage to decondense chromatin (reviewed in **O'Shaughnessy and Hendrich, 2013; Stanley et al., 2013**). The chromodomains in CHD4 distinguish the histone modifications H3K9me3 and H3K9ac and determine the way how downstream DSB repair takes place (**Ayrapetov et al., 2014; Price and D'Andrea, 2013**). It is plausible that GEN1 uses its chromodomain not only as a structural module to securely bind DNA but also for targeting or regulatory purposes. Even though it was not possible to find any binding partner with a series of tested histone tail peptides, we cannot exclude that the chromodomain is used as an interaction motif or chromatin reader. It will therefore be interesting to extend our interaction analysis to a larger number of peptides and proteins. Interestingly, the modifications GEN1<sup>L397E</sup> and GEN1<sup>Y424A</sup> at the rim of the chromodomain did not alter DNA cleavage activity (**Figure 5—figure supplement 1**), however, mutations of residues at the rim of Yen1's chromodomain show a phenotype, suggesting an additional role like binding to an endogenous factor.

Another intriguing aspect of the chromodomain is that the conserved T438 at the rim of the aromatic cage and T380 at the closing helix  $\alpha 15$  are both part of a casein kinase II consensus sequence for phosphorylation (Ser/Thr-X-X-Asp/Glu). **Ayoub et al., 2008** showed that the analogous threonine in the chromodomain of CBX1 is phosphorylated in response to DNA damage and phosphorylation disrupts the binding to H3K9me. We observed a reduction in DNA cleavage activity for the phosphorylation mimicking mutations T380E and T438E, which may suggest a regulatory role. They might function together and in combination with other modifications to provide a way of functional switching at the chromodomain. Furthermore, **Blanco et al., 2014** and **Eissler et al., 2014** recently identified several CDK phosphorylation sites in an insertion in the Yen1 chromodomain which affects HJ cleavage and together with phosphorylation of a nuclear localization signal (NLS) in the regulatory domain restricts Yen1's activity to anaphase. The insertion is not found in other chromodomains and it is extended in Yen1 compared to GEN1, which is lacking these phosphorylation sites (compare **Figure 3A/B**). Notably, the activity of Yen1 is negatively regulated by CDK-dependent phosphorylation (**Blanco et al., 2014; Chan and West, 2014; Eissler et al., 2014; Matos et al., 2011**), suggesting that the chromodomain is targeted by cell cycle kinases. It also provides a likely explanation for the different regulatory mechanisms found in GEN1 and Yen1 (**Blanco and Matos, 2015; Chan and West, 2014; Matos and West, 2014**). Exploration of the regulatory function of the GEN1 chromodomain will be an important topic to follow up, and this may lead to the understanding of the precise regulation mechanism of GEN1 as well as its substrate recognition under physiological conditions.

It is noteworthy that our analysis also revealed that the human transcription modulator AEBP2, which is associated with the polycomb repression complex 2 (PRC2), contains a chromo-barrel domain, which, to our knowledge, has not been reported so far.

## Recognition of DNA substrates

The GEN1-DNA structure showed a considerable similarity to the other members of the Rad2/XPG family, and this facilitated the generation of a combined model to understand substrate recognition

of GEN1 (**Figure 6**). This was done by superimposing the protein part of the FEN1-DNA complex (PDB 3q8k) onto our GEN1 structure and extending the DNA accordingly (**Figure 6A/B**). Remarkably, the superimposition of the proteins aligns the DNA from the FEN1 structure in the same register as the DNA in the GEN1 complex at the upstream interface (**Figure 6A and 6B** insert). Furthermore, the free 5' and 3' ends of the double flap DNA from the FEN1 structure point towards the lower and the upper gateway in GEN1, respectively (**Figure 6B**). We extended the GEN1 structure by homology modeling of the disordered residues 79-92 (helix  $\alpha 4$ ) in GEN1 (**Figure 6B**). In addition to the similarity of this part to FEN1, the model readily showed the arrangement forming an arch structure. This would explain why GEN1 recognizes 5' flap substrates efficiently, analogous to FEN1, as the arch can clamp a single-stranded DNA overhang for productive cleavage. This also explains why the F110E modification in the arch at helix  $\alpha 6$  hampered 5' flap cleavage severely. The

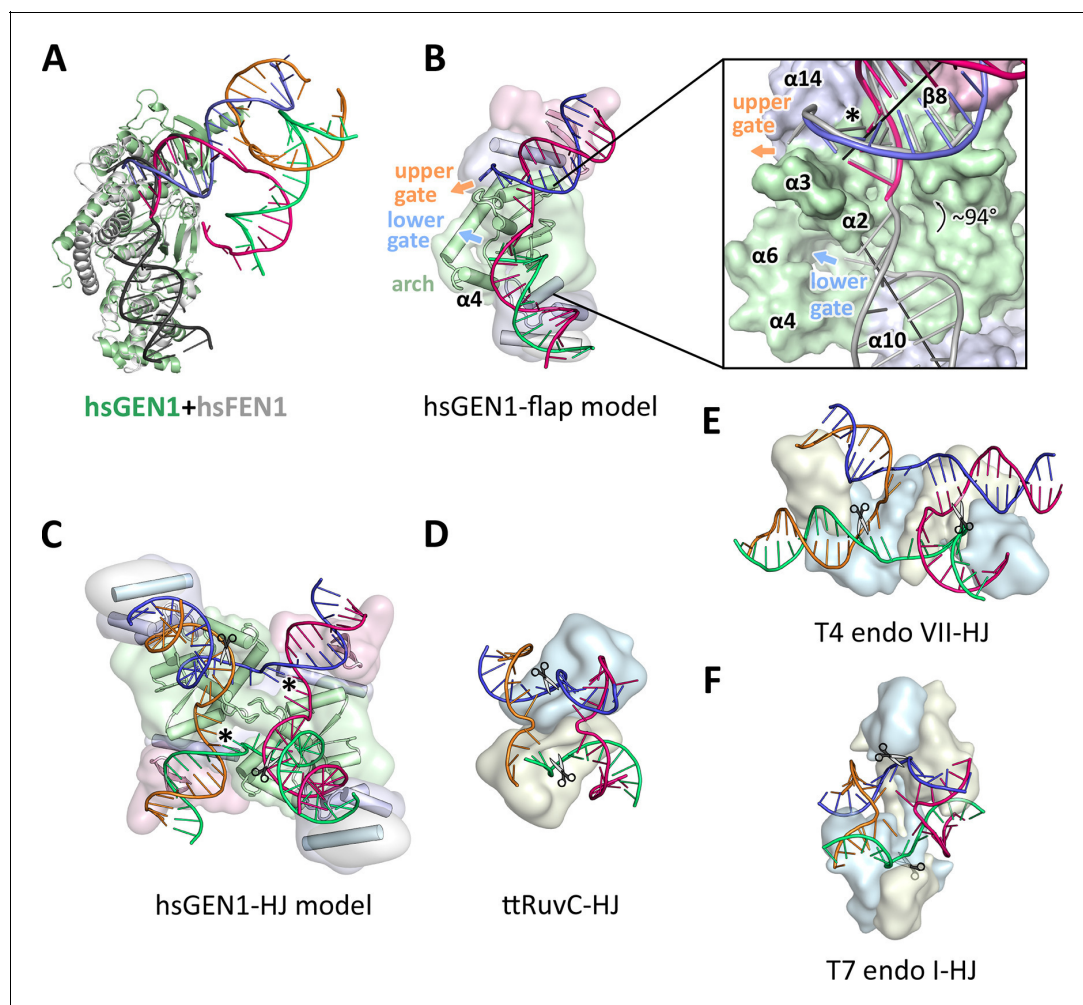


**Figure 6.** Substrate recognition features of GEN1. (A) Superposition of the protein part of the FEN1-DNA complex (PDB 3q8k, protein in gray, DNA in black) onto the GEN1-HJ complex (protein in green and the DNA strands in different colors). The FEN1-DNA aligns with the same register as the GEN1-DNA at the upstream interface. (B) Model for the recognition of a 5' flap substrate by GEN1. The DNA was extended using the superimposition from A. Homology modeling suggests an additional helix  $\alpha 4$  (disordered residues 79–92) forming an arch with helix  $\alpha 6$ . The protein is shown in a simplified surface representation with the same colors as in **Figure 1** and structural elements are highlighted. The insert shows a zoomed in view of the hydrophobic wedge with the modeled FEN1-DNA in gray. (C) Model for the dimerization of GEN1 upon binding to a HJ substrate based on the 5' flap model in B. The monomers interlock via both arches ( $\alpha 4$ - $\alpha 6$ ) and the hydrophobic wedges ( $\alpha 2$ - $\alpha 3$ ) contact each other. (D) Structure of the *Thermus thermophilus* RuvC-HJ complex (PDB 4ld0). (E) Structure of the T4 endonuclease VII-HJ complex (PDB 2qnc). (F) Structure of the T7 endonuclease I-HJ complex (PDB 2pfj). Individual monomers are in surface representation, colored in light blue and beige, respectively. DNA strands are shown as ladders in different colors.

DOI: 10.7554/eLife.12256.020

side chain points directly towards the active site and likely disturbs the stabilization of a 5' overhang for catalysis by charge repulsion. However, there are two features in GEN1 that vary from the arrangement in FEN1 and EXO1 considerably. Helix  $\alpha 6$  is longer (24 instead of 15 residues) and helix  $\alpha 5$  is missing in GEN1. As a result the arch points away from the DNA rather than forming a 'cap' structure as it is observed in FEN1 and EXO1 (Orans *et al.*, 2011; Tsutakawa *et al.*, 2011). Furthermore, the modified arch in GEN1 provides an opening, marked as 'lower gate' in **Figure 6B**. These differences are likely the basis for GEN1's versatile DNA recognition features.

### Implications of an adjustable hatch in GEN1 for substrate discrimination

The diverging orientation of the arch (helices  $\alpha 4$  and  $\alpha 6$ ) in GEN1 compared to the one in FEN1 and EXO1 (helices  $\alpha 4$ ,  $\alpha 5$ , and  $\alpha 6$ ) may have thus significance for the recognition of HJ substrates. By pointing away from the active site the arch provides an opening to accommodate unpaired, single-stranded DNA to pass along the arch at the lower gate (groove between  $\alpha 2$  and  $\alpha 4$ ) (**Figure 6B** 'lower gate') from one GEN1 monomer to the upper gate (groove between  $\alpha 2$ - $\alpha 3$  and  $\alpha 14$ ) (**Figure 6B** 'upper gate') of the other within a GEN1 dimer (**Figure 6B/C**). R54 is perfectly positioned at the minor groove to guide the second cleavage strand to pass through the upper gate (compare **Figure 4** and **Figure 6B/C**, marked with an asterisk). In FEN1, this position is occupied by the 'acid block', which stabilizes a single 3' flap of the unpaired substrate (Tsutakawa *et al.*, 2011) and it would not accommodate longer 3' DNA overhangs. In our model, two GEN1 monomers come together crosswise upon HJ binding (**Figure 6C**). The helical arches of both proteins likely provide additional protein-protein interactions as well as protein-DNA contacts by packing against the backbone of opposite DNA arms (**Figure 6C**). As a result, the GEN1 dimer orients both active sites symmetrically across the junction point resembling the situation in bacterial RuvC (**Figure 6D**; Bennett and West, 1995a; Górecka *et al.*, 2013). This arrangement would ensure that both incisions are introduced within the lifetime of the GEN1-HJ complex as observed biochemically by us and others (Chan and West, 2015; Rass *et al.*, 2010). The mechanism likely works in a coordinated nick-and-counter-nick fashion, as shown for bacterial or bacteriophage HJ resolvases (Fogg and Lilley, 2000; Giraud-Panis and Lilley, 1997; Pottmeyer and Kemper, 1992; Shah *et al.*, 1997) and recently for GEN1 (Chan and West, 2015).

The distance between both gates is bridged by unpaired bases in our GEN1-HJ model. This view is supported by the observation that FEN1 unpairs two bases near the active site through interactions with the hydrophobic wedge leading to strongly bent DNA arms between the upstream and downstream DNA interfaces. This mechanism seems to be a common feature of Rad2/XPG nucleases (Finger *et al.*, 2013; Grasby *et al.*, 2012; Tsutakawa *et al.*, 2011). Consistent with this view, the bacterial RuvC resolvase (**Figure 6D**) has also been shown to unfold HJ junctions (Bennett and West, 1995b; Górecka *et al.*, 2013). In the case of GEN1, the critical step would be the assembly of the dimer around the junction point in a highly restraint way and the introduction of the first nick. This releases the tension on the complex like a spring leading to an immediate second cut and subsequent disassembly of the GEN1-HJ complex. Furthermore, a HJ does not provide free DNA ends and adopts a structure that intrinsically restrains its degrees of freedom, thus inhibiting cleavage by a single GEN1 monomer. Altogether we speculate that the arch (helix  $\alpha 4$ - $\alpha 6$ ) acts like a lever or hatch switching between flap and HJ recognition modes. When a free 5' end is available it closes and clamps the flap, thus positions the DNA for cleavage. For the case of a HJ substrate, the arch adopts an open conformation, allowing unpaired, single-stranded DNA to pass, while preventing the correct positioning of the DNA for catalysis at first. HJ cleavage is inhibited until a second GEN1 monomer binds. This mechanism differs from the one used by bacterial or bacteriophage HJ resolvases, which act as obligate dimers binding to DNA substrates in a concerted way (compare **Figure 6D-F**). Our model for DNA cleavage by GEN1 describes a conformational switch provided by a flexible arch that can discriminate between substrates containing free 5' ends or those with a restraint structure like HJs. This aspect may explain our observation that GEN1 cleaves 5' flap DNA catalytically while stoichiometric amounts are required for HJ substrates (**Figure 5A-C**). Using a switchable hatch in a spring-loaded mechanism would be an efficient way of preventing a single cut at a HJ junction while allowing GEN1 to adapt to recognize various DNA substrates and perform different functional roles. Thus, GEN1 may have an intrinsic safety mechanism that ensures symmetrical dual incision across a branch point. Further studies have to address the exact engagement mechanism.

## GEN1 in a biological context

GEN1's biological role is not fully understood yet. Yeast cells are viable without the GEN1 homolog Yen1 even in the presence of DNA damaging agents as the Mus81-Eme1 complex can complement the defect (compare **Figure 5—figure supplement 3**; [Blanco et al., 2010](#)). Consistently, both proteins can cleave 5' flaps and HJ substrates in vitro. However, GEN1 can cleave intact HJs symmetrically whereas MUS81-EME1 is much more efficient with nicked DNA four-way junctions ([Castor et al., 2013](#); [Wyatt et al., 2013](#)). [Matos et al., 2011](#) suggested that Yen1/GEN1 might serve as a backup enzyme to resolve persistent HJs that have eluded other mechanisms of joint molecule removal before cytokinesis.

Our analysis infers that HJ cleavage is slower than 5' flap cleavage (**Figure 5B/C**), bringing interesting implications for a safety control of GEN1's activity. GEN1 may have to assemble in an accurate way before it can cleave a HJ. Likewise, it increases GEN1's persistence time on HJs and opens a window for branch migration for extending the length of recombined stretches of DNA. Moreover, GEN1 recognizes various DNA substrates, which may point towards a general role in processing substrates in different DNA maintenance pathways. GEN1 has been shown to cleave replication fork intermediates, and it is implicated in the resolution of replication-induced HJs ([Garner et al., 2013](#); [Sarbjana et al., 2014](#)). Like MUS81-EME1, it might also be important for the processing of fragile sites to ensure proper chromosome segregation ([Ying et al., 2013](#)). These functions have to be tested systematically to understand GEN1's biological role. In this context, the regulation of GEN1 is an important factor and needs to be explored. Our study identified a chromodomain extending the GEN1 nuclease core that might have a role in regulating the enzyme. An open question is the function and architecture of the remaining 444 amino acids at the C-terminus of GEN1. They are thought to regulate the nuclease activity and control subcellular localization ([Blanco et al., 2014](#); [Chan and West, 2014](#); [García-Luis et al., 2014](#)). It is very likely that new interaction sites and post-translational modifications in this region will be discovered in future. The presented structure together with additional studies will help to unravel these questions and to obtain a comprehensive view of the functions of the Rad2/XPG nucleases.

## Materials and methods

### Experimental procedures

#### Protein expression and purification

Wild type human GEN1 and truncations thereof (residues 2-551, 2-505, 2-464, 2-389) were amplified by PCR from IMAGE clone 40125755 (Mammalian Gene collection, natural variant S92T, S310N, UniProtID Q17RS7) and cloned into a self-made ligation-independent cloning vector with various C-terminal tags followed by His8. Truncated versions were designed based on limited proteolysis in combination with domain prediction and functional assays to determine the smallest yet active fragment. The N-terminal methionine was cleaved by cellular methionyl-aminopeptidase, which is an essential requirement in the Rad2/XPG family as the N-terminus (conserved residue G2) folds towards the active site. Mutations were introduced by site-directed mutagenesis using Phusion Polymerase (NEB, Frankfurt/Main, Germany). All recombinant proteins were expressed in the *E. coli* BL21(DE3) pRIL strain (MerckMillipore, Darmstadt, Germany). Cells were grown at 37°C until mid-log phase and induced overnight with 0.2 mM IPTG at 16°C. Cells were harvested by centrifugation and resuspended in lysis buffer containing 1x phosphate buffered saline (PBS) with additional 500 mM NaCl, 10% (v/v) glycerol, 2 mM DTT, 1 mM EDTA, 1 μM leupeptin, 1 μM pepstatin A, 0.1 mM AEBSF and 2 μM aprotinin and lysed by sonication. Cell debris was removed by centrifugation (75 600 g for 45 min), the clarified lysate was applied onto Complete HisTag Nickel resin (Roche Diagnostics, Mannheim, Germany) and washed with buffer A consisting of 20 mM Tris-HCl pH 7.5, 500 mM NaCl, 10% (v/v) glycerol, 2 mM DTT and followed by a chaperone wash step with 20 mM Tris-HCl pH 7.5, 500 mM NaCl, 2 mM ATP, 5 mM MgCl<sub>2</sub>, 10% (v/v) glycerol and 2 mM DTT. The protein was eluted with buffer A containing 300 mM imidazole. The tag was cleaved, followed by cation exchange chromatography using a HiTrap SP HP column (GE Healthcare, Freiburg, Germany) with a linear gradient from 150 mM to 450 mM NaCl. Peak fractions were pooled and further purified by size-exclusion chromatography on a HiLoad 16/60 Superdex 200 (GE Healthcare) equilibrated with 20 mM Tris-HCl

pH 7.5, 100 mM NaCl, 5%(v/v) glycerol, 0.1 mM EDTA and 2 mM TCEP. Peak fractions were pooled, concentrated, flash-frozen in liquid nitrogen and stored at  $-80^{\circ}\text{C}$ .

### Crystallization and data collection

GEN1<sup>2-505 D30N</sup> and DNA (4w1010-1 GAATTCGGATTAGGGATGC, 4w1010-2 GCATCCCTAAGC TCCATCGT, 4w1010-3 ACGATGGAGCCGCTAGGCTC, 4w1010-4 GAGCCTAGCGTCCGGAATTC) were mixed at a molar ratio of 2:1.1 at a final protein concentration of 14 mg/ml including 1 mM  $\text{MgCl}_2$  and co-crystallized by sitting drop vapor diffusion. Drops were set up by mixing sample with mother liquor consisting of 100 mM MES-NaOH pH 6.5 and 200 mM NaCl at a 2:1 ratio at room temperature. Crystals grew within 2 days, and several iterations of streak seeding were needed for obtaining diffraction quality crystals. For data collection, crystals were stepwise soaked in 10%, 20%, and 30% (v/v) glycerol in 100 mM MES-NaOH pH 6.5, 200 mM NaCl and 5% PEG 8000 and flash-frozen in liquid nitrogen. Diffraction data were collected at beamline PXII of the Swiss Light Source (SLS, Villigen, Switzerland) at 100 K with a Pilatus 6M detector. In order to obtain phase information, crystals were soaked for 10–30 min in 1 mM  $[\text{Ta}_6\text{Br}_{12}]\text{Br}_2$ , flash-frozen and data were collected at the Ta L(III)-edge. In addition, seleno-methionine (SeMet)-substituted protein was expressed in M9 media supplemented with SeMet, purified, and crystallized according to the protocol above and data were collected at the Se K-edge.

### Structure determination and refinement

All data were processed with XDS (Table 1, Kabsch, 2010). HKL2MAP (Pape and Schneider, 2004) found 12 tantalum and 8 selenium positions, which were used in a combined MIRAS strategy (multiple isomorphous replacement with anomalous scattering) in autoSHARP (Vonrhein, et al., 2007) to determine the structure of the GEN1-HJ complex. The obtained solvent-flattened experimental map was used to build a model with PHENIX (Adams et al., 2010) combined with manual building. The structure was then further refined by iterative rounds of manual building in COOT (Emsley and Cowtan, 2004), refinement with PHENIX and assisted by the PDB\_REDO server (Joosten, et al., 2014). The structure was visualized and analyzed in PYMOL (Delano, 2002). Electrostatic surface potentials were calculated with PDB2PQR (Dolinsky et al., 2004) and APBS (Baker et al., 2001).

### Nuclease assay

All DNA substrates (Figure 5—source data 1) were synthesized by Eurofins/MWG (Ebersberg, Germany), resuspended in annealing buffer (20 mM Tris-HCl pH 8.0, 50 mM NaCl, 0.1 mM EDTA), annealed by heating to  $85^{\circ}\text{C}$  for 5 min and slow-cooling to room temperature. Different amounts of GEN1 proteins (as indicated) were mixed with 40 nM 6FAM-labeled DNA substrates in 20 mM Tris-HCl pH 8.0, 50 ng/ $\mu\text{l}$  bovine serum albumin (BSA) and 1 mM DTT. Reactions were initiated by adding 5 mM  $\text{MgCl}_2$ , incubated at  $37^{\circ}\text{C}$  for 15 min and terminated by adding 15 mM EDTA, 0.3% SDS and further, DNA substrates were deproteinized using 1 mg/ml proteinase K at  $37^{\circ}\text{C}$  for 15 min. Products were separated by 8% 1x TBE native polyacrylamide gel electrophoresis, the fluorescence signal detected with a Typhoon FLA 7000 phosphorimager (GE Healthcare), quantified with IMAGEJ (GE Healthcare) and visualized by GNU PLOT (Williams et al., 2015).

### Cruciform plasmid cleavage assay

The cruciform plasmid pIRbke8<sup>mut</sup> was a gift from Stephen West's lab (Rass et al., 2010), and it was originally prepared by David Lilley's lab (Lilley, 1985). 50 ng/ $\mu\text{l}$  plasmid were mixed with 20 mM Tris-HCl pH 8.0, 50 mM potassium glutamate, 5 mM  $\text{MgCl}_2$ , 50 ng/ $\mu\text{l}$  BSA and 1 mM DTT and pre-warmed at  $37^{\circ}\text{C}$  for 1 hr to induce the formation of a cruciform structure. Reactions were initiated by adding indicated amounts of GEN1, incubated at  $37^{\circ}\text{C}$  for 15 min and stopped as for DNA cleavage assays. The products were separated by 1% 1xTBE native agarose gel electrophoresis, stained with SYBR safe (Life Technologies, Darmstadt, Germany) and visualized under UV light.

### Sequence alignments and phylogenetic analysis

Sequences of GEN1 proteins from different organisms as well as all human chromodomain proteins were aligned to the human GEN1 sequence using the programs HHPRED (Söding et al., 2005), PSI-BLAST and further by manual adjustments. Alignments were tested by back-searches against RefSeq

or HMM databases. A phylogenetic tree was calculated by the program PHYML with 100 bootstraps using the alignment in **Figure 3—figure supplement 1** and a BLOSUM62 substitution model. The tree was displayed with DENDROSCOPE (*Huson and Scornavacca, 2012*).

### Histone peptide pull-down assay

The GEN1 chromodomain with a C-terminal His8-tag was immobilized on complete HisTag Nickel resin and washed twice with binding buffer consisting of 20 mM Tris-HCl pH 7.5, 200 mM NaCl, 5% glycerol, 0.1 mM EDTA, 0.05% (v/v) Tween-20 and 2 mM TCEP. Peptide mixtures containing 0.4  $\mu$ M fluorescein labeled histone peptides were incubated with beads at 4°C for 1 hr and washed twice with binding buffer. Immobilized proteins were eluted with binding buffer supplemented with 300 mM imidazole and separated on 20% SDS-PAGE. Fluorescein-labeled peptides were visualized by detecting the fluorescence signal with a Typhoon FLA 7000 phosphoimager (GE Healthcare).

### Yeast genetics and MMS survival assay in *Saccharomyces cerevisiae*

All yeast strains are based on W303 Rad5+ (see **Figure 5—source data 2** for a complete list). *yen1 $\Delta$*  or *yen1 $\Delta$  mus81 $\Delta$*  strains were transformed with an integrative plasmid expressing mutant versions of *YEN1*. Freshly grown over-night cultures were diluted to  $1 \times 10^7$  cells/ml. 5-fold serial dilutions were spotted on YPD plates with/without MMS (methyl methanesulphonate, concentrations as indicated) and incubated for 2 days at 30°C. The expression of 3FLAG-tagged Yen1 constructs was verified by SDS-PAGE and Western Blot analysis. Proteins were detected using a mouse monoclonal anti-FLAG M2-peroxidase (HRP) antibody (Sigma-Aldrich, München, Germany).

### Database entry

The coordinates of the human GEN1-Holliday junction complex have been deposited in the Protein Data Bank (PDB code 5t9j).

## Acknowledgements

We would like to thank Naoko Mizuno, Michael J. Taschner and Esben Lorentzen for many scientific discussions and critical reading of the manuscript. We are grateful for the support by the Department of Structural Cell Biology at the MPI of Biochemistry (MPIB), particularly for the help with screening by the Crystallization Facility and Claire Basquin for assistance with biophysical analysis. The Microchemistry Core Facility of the MPIB provided mass spectrometry analysis. We would like to thank Jürg Müller for providing histone tail peptides for binding tests and Stephen C. West for providing the plasmid pIRbke8<sup>mut</sup> for functional assays. Furthermore, we would like to acknowledge the professional assistance of the beamline staff at the Swiss Light Source, Villigen, Switzerland, during data collection. The Max Planck Society for the Advancement of Science supported this research through the Otto Hahn Program (BP) and the Max Planck Research Group Leader Program (CB).

## Additional information

### Funding

Funder	Grant reference number	Author
Max-Planck-Gesellschaft	Max Planck Research Group Leader Program	Shun-Hsiao Lee Maren Felizitas Klügel Christian Biertümpfel
Max-Planck-Gesellschaft	Otto Hahn Program	Lissa Nicola Princz Boris Pfander
Max-Planck-Gesellschaft	MPI of Biochemistry	Bianca Habermann

The funders had no role in study design, data collection and interpretation, or the decision to submit the work for publication.

**Author contributions**

S-HL, CB, Conception and design, Acquisition of data, Analysis and interpretation of data, Drafting or revising the article, Contributed unpublished essential data or reagents; LNP, MFK, Acquisition of data, Contributed unpublished essential data or reagents; BH, Acquisition of data, Analysis and interpretation of data; BP, Acquisition of data, Analysis and interpretation of data, Drafting or revising the article

**Additional files****Major datasets**

The following dataset was generated:

Author(s)	Year	Dataset title	Dataset URL	Database, license, and accessibility information
Lee S-H, Biertumpfel C	2016	Crystal Structure of human GEN1 in complex with Holliday junction DNA in the upper interface	<a href="http://www.rcsb.org/pdb/explore/explore.do?structureId=5T9J">http://www.rcsb.org/pdb/explore/explore.do?structureId=5T9J</a>	Publicly available at the RCSB Protein Data Bank (accession no. 5T9J)

**References**

- Adams PD**, Afonine PV, Bunkóczi G, Chen VB, Davis IW, Echols N, Headd JJ, Hung LW, Kapral GJ, Grosse-Kunstleve RW, McCoy AJ, Moriarty NW, Oeffner R, Read RJ, Richardson DC, Richardson JS, Terwilliger TC, Zwart PH. 2010. PHENIX: a comprehensive Python-based system for macromolecular structure solution. *Acta Crystallographica Section D Biological Crystallography* **66**:213–221. doi: [10.1107/S0907444909052925](https://doi.org/10.1107/S0907444909052925)
- Andersen SL**, Kuo HK, Savukoski D, Brodsky MH, Sekelsky J, Lichten M. 2011. Three structure-selective endonucleases are essential in the absence of BLM helicase in *Drosophila*. *PLoS Genetics* **7**:e1002315. doi: [10.1371/journal.pgen.1002315](https://doi.org/10.1371/journal.pgen.1002315)
- Ayoub N**, Jeyasekharan AD, Bernal JA, Venkitaraman AR. 2008. HP1-beta mobilization promotes chromatin changes that initiate the DNA damage response. *Nature* **453**:682–686. doi: [10.1038/nature06875](https://doi.org/10.1038/nature06875)
- Ayrapetov MK**, Gursoy-Yuzugullu O, Xu C, Xu Y, Price BD. 2014. DNA double-strand breaks promote methylation of histone H3 on lysine 9 and transient formation of repressive chromatin. *Proceedings of the National Academy of Sciences* **111**:9169–9174. doi: [10.1073/pnas.1403565111](https://doi.org/10.1073/pnas.1403565111)
- Baker NA**, Sept D, Joseph S, Holst MJ, McCammon JA. 2001. Electrostatics of nanosystems: application to microtubules and the ribosome. *Proceedings of the National Academy of Sciences* **98**:10037–10041. doi: [10.1073/pnas.181342398](https://doi.org/10.1073/pnas.181342398)
- Bennett RJ**, West SC. 1995a. RuvC protein resolves Holliday junctions via cleavage of the continuous (noncrossover) strands. *Proceedings of the National Academy of Sciences* **92**:5635–5639. doi: [10.1073/pnas.92.12.5635](https://doi.org/10.1073/pnas.92.12.5635)
- Bennett RJ**, West SC. 1995b. Structural analysis of the RuvC-Holliday junction complex reveals an unfolded junction. *Journal of Molecular Biology* **252**:213–226. doi: [10.1006/jmbi.1995.0489](https://doi.org/10.1006/jmbi.1995.0489)
- Benson FE**, West SC. 1994. Substrate specificity of the *Escherichia coli* RuvC protein. Resolution of three- and four-stranded recombination intermediates. *The Journal of Biological Chemistry* **269**:5195–5201.
- Biertumpfel C**, Yang W, Suck D. 2007. Crystal structure of T4 endonuclease VII resolving a Holliday junction. *Nature* **449**:616–620. doi: [10.1038/nature06152](https://doi.org/10.1038/nature06152)
- Blanco MG**, Matos J, Rass U, Ip SC, West SC. 2010. Functional overlap between the structure-specific nucleases Yen1 and Mus81-Mms4 for DNA-damage repair in *S. cerevisiae*. *DNA Repair* **9**:394–402. doi: [10.1016/j.dnarep.2009.12.017](https://doi.org/10.1016/j.dnarep.2009.12.017)
- Blanco MG**, Matos J, West SC. 2014. Dual control of Yen1 nuclease activity and cellular localization by Cdk and Cdc14 prevents genome instability. *Molecular Cell* **54**:94–106. doi: [10.1016/j.molcel.2014.02.011](https://doi.org/10.1016/j.molcel.2014.02.011)
- Blanco MG**, Matos J. 2015. Hold your horSSEs: controlling structure-selective endonucleases MUS81 and Yen1/GEN1. *Frontiers in Genetics* **6**:1–11. doi: [10.3389/fgene.2015.00253](https://doi.org/10.3389/fgene.2015.00253)
- Blus BJ**, Wiggins K, Khorasanizadeh S. 2011. Epigenetic virtues of chromodomains. *Critical Reviews in Biochemistry and Molecular Biology* **46**:507–526. doi: [10.3109/10409238.2011.619164](https://doi.org/10.3109/10409238.2011.619164)
- Canzio D**, Chang EY, Shankar S, Kuchenbecker KM, Simon MD, Madhani HD, Narlikar GJ, Al-Sady B. 2011. Chromodomain-mediated oligomerization of HP1 suggests a nucleosome-bridging mechanism for heterochromatin assembly. *Molecular Cell* **41**:67–81. doi: [10.1016/j.molcel.2010.12.016](https://doi.org/10.1016/j.molcel.2010.12.016)
- Castor D**, Nair N, Déclais AC, Lachaud C, Toth R, Macartney TJ, Lilley DM, Arthur JS, Rouse J. 2013. Cooperative control of holliday junction resolution and DNA repair by the SLX1 and MUS81-EME1 nucleases. *Molecular Cell* **52**:221–233. doi: [10.1016/j.molcel.2013.08.036](https://doi.org/10.1016/j.molcel.2013.08.036)
- Cejka P**, Plank JL, Bachrati CZ, Hickson ID, Kowalczykowski SC. 2010. Rmi1 stimulates decatenation of double Holliday junctions during dissolution by Sgs1-Top3. *Nature Structural & Molecular Biology* **17**:1377–1382. doi: [10.1038/nsmb.1919](https://doi.org/10.1038/nsmb.1919)

- Cejka P, Plank JL, Dombrowski CC, Kowalczykowski SC. 2012. Decatenation of DNA by the *S. cerevisiae* Sgs1-Top3-Rmi1 and RPA complex: a mechanism for disentangling chromosomes. *Molecular Cell* **47**:886–896. doi: [10.1016/j.molcel.2012.06.032](https://doi.org/10.1016/j.molcel.2012.06.032)
- Ceska TA, Sayers JR, Stier G, Suck D. 1996. A helical arch allowing single-stranded DNA to thread through T5 5'-exonuclease. *Nature* **382**:90–93. doi: [10.1038/382090a0](https://doi.org/10.1038/382090a0)
- Chan YW, West S. 2015. GEN1 promotes Holliday junction resolution by a coordinated nick and counter-nick mechanism. *Nucleic Acids Research* **43**:10882–10892. doi: [10.1093/nar/gkv1207](https://doi.org/10.1093/nar/gkv1207)
- Chan YW, West SC. 2014. Spatial control of the GEN1 Holliday junction resolvase ensures genome stability. *Nature Communications* **5**:4844. doi: [10.1038/ncomms5844](https://doi.org/10.1038/ncomms5844)
- Cowieson NP, Partridge JF, Allshire RC, McLaughlin PJ. 2000. Dimerisation of a chromo shadow domain and distinctions from the chromodomain as revealed by structural analysis. *Current Biology* **10**:517–525. doi: [10.1016/S0960-9822\(00\)00467-X](https://doi.org/10.1016/S0960-9822(00)00467-X)
- Delano WL. *The PyMOL molecular graphics system*. 2002.
- Dolinsky TJ, Nielsen JE, McCammon JA, Baker NA. 2004. PDB2PQR: an automated pipeline for the setup of Poisson-Boltzmann electrostatics calculations. *Nucleic Acids Research* **32**:W665–W667. doi: [10.1093/nar/gkh381](https://doi.org/10.1093/nar/gkh381)
- Eissenberg JC. 2012. Structural biology of the chromodomain: form and function. *Gene* **496**:69–78. doi: [10.1016/j.gene.2012.01.003](https://doi.org/10.1016/j.gene.2012.01.003)
- Eissler CL, Mazón G, Powers BL, Savinov SN, Symington LS, Hall MC. 2014. The Cdk/cDc14 module controls activation of the Yen1 holliday junction resolvase to promote genome stability. *Molecular Cell* **54**:80–93. doi: [10.1016/j.molcel.2014.02.012](https://doi.org/10.1016/j.molcel.2014.02.012)
- Emsley P, Cowtan K. 2004. Coot: model-building tools for molecular graphics. *Acta Crystallographica Section D Biological Crystallography* **60**:2126–2132. doi: [10.1107/S0907444904019158](https://doi.org/10.1107/S0907444904019158)
- Fekairi S, Scaglione S, Chahwan C, Taylor ER, Tissier A, Coulon S, Dong MQ, Ruse C, Yates JR, Russell P, Fuchs RP, McGowan CH, Gaillard PH. 2009. Human SLX4 is a Holliday junction resolvase subunit that binds multiple DNA repair/recombination endonucleases. *Cell* **138**:78–89. doi: [10.1016/j.cell.2009.06.029](https://doi.org/10.1016/j.cell.2009.06.029)
- Finger LD, Patel N, Beddows A, Ma L, Exell JC, Jardine E, Jones AC, Grasby JA. 2013. Observation of unpaired substrate DNA in the flap endonuclease-1 active site. *Nucleic Acids Research* **41**:9839–9847. doi: [10.1093/nar/gkt737](https://doi.org/10.1093/nar/gkt737)
- Fogg JM, Lilley DM. 2000. Ensuring productive resolution by the junction-resolving enzyme RuvC: large enhancement of the second-strand cleavage rate. *Biochemistry* **39**:16125–16134. doi: [10.1021/bi001886m](https://doi.org/10.1021/bi001886m)
- García-Luis J, Clemente-Blanco A, Aragón L, Machín F. 2014. Cdc14 targets the Holliday junction resolvase Yen1 to the nucleus in early anaphase. *Cell Cycle* **13**:1392–1399. doi: [10.4161/cc.28370](https://doi.org/10.4161/cc.28370)
- Garner E, Kim Y, Lach FP, Kottemann MC, Smogorzewska A. 2013. Human GEN1 and the SLX4-associated nucleases MUS81 and SLX1 are essential for the resolution of replication-induced Holliday junctions. *Cell Reports* **5**:207–215. doi: [10.1016/j.celrep.2013.08.041](https://doi.org/10.1016/j.celrep.2013.08.041)
- Giraud-Panis MJ, Lilley DM. 1997. Near-simultaneous DNA cleavage by the subunits of the junction-resolving enzyme T4 endonuclease VII. *The EMBO Journal* **16**:2528–2534. doi: [10.1093/emboj/16.9.2528](https://doi.org/10.1093/emboj/16.9.2528)
- Górecka KM, Komorowska W, Nowotny M. 2013. Crystal structure of RuvC resolvase in complex with Holliday junction substrate. *Nucleic Acids Research* **41**:9945–9955. doi: [10.1093/nar/gkt769](https://doi.org/10.1093/nar/gkt769)
- Grasby JA, Finger LD, Tsutakawa SE, Atack JM, Tainer JA. 2012. Unpairing and gating: sequence-independent substrate recognition by FEN superfamily nucleases. *Trends in Biochemical Sciences* **37**:74–84. doi: [10.1016/j.tibs.2011.10.003](https://doi.org/10.1016/j.tibs.2011.10.003)
- Hadden JM, Déclais AC, Carr SB, Lilley DM, Phillips SE. 2007. The structural basis of Holliday junction resolution by T7 endonuclease I. *Nature* **449**:621–624. doi: [10.1038/nature06158](https://doi.org/10.1038/nature06158)
- Heyer WD. 2015. Regulation of recombination and genomic maintenance. *Cold Spring Harbor Perspectives in Biology* **7**:a016501. doi: [10.1101/cshperspect.a016501](https://doi.org/10.1101/cshperspect.a016501)
- Holliday R. 1964. A mechanism for gene conversion in fungi. *Genetical Research* **5**:282–304. doi: [10.1017/S0016672300001233](https://doi.org/10.1017/S0016672300001233)
- Holm L, Rosenström P. 2010. Dali server: conservation mapping in 3D. *Nucleic Acids Research* **38**:W545–W549. doi: [10.1093/nar/gkq366](https://doi.org/10.1093/nar/gkq366)
- Hornbeck PV, Zhang B, Murray B, Kornhauser JM, Latham V, Skrzypek E. 2014. PhosphoSitePlus, 2014: mutations, PTMs and recalibrations. *Nucleic Acids Research* **43**:D512–D520. doi: [10.1093/nar/gku1267](https://doi.org/10.1093/nar/gku1267)
- Huson DH, Scornavacca C. 2012. Dendroscope 3: an interactive tool for rooted phylogenetic trees and networks. *Systematic Biology* **61**:1061–1067. doi: [10.1093/sysbio/sys062](https://doi.org/10.1093/sysbio/sys062)
- Interthal H, Heyer WD. 2000. MUS81 encodes a novel helix-hairpin-helix protein involved in the response to UV- and methylation-induced DNA damage in *Saccharomyces cerevisiae*. *Molecular and General Genetics MGG* **263**:812–827. doi: [10.1007/s004380000241](https://doi.org/10.1007/s004380000241)
- Ip SC, Rass U, Blanco MG, Flynn HR, Skehel JM, West SC. 2008. Identification of Holliday junction resolvases from humans and yeast. *Nature* **456**:357–361. doi: [10.1038/nature07470](https://doi.org/10.1038/nature07470)
- Ira G, Malkova A, Liberi G, Foiani M, Haber JE. 2003. Srs2 and Sgs1-Top3 suppress crossovers during double-strand break repair in yeast. *Cell* **115**:401–411. doi: [10.1016/S0092-8674\(03\)00886-9](https://doi.org/10.1016/S0092-8674(03)00886-9)
- Ishikawa G, Kanai Y, Takata K, Takeuchi R, Shimanouchi K, Ruike T, Furukawa T, Kimura S, Sakaguchi K. 2004. DmGEN, a novel RAD2 family endo-exonuclease from *Drosophila melanogaster*. *Nucleic Acids Research* **32**:6251–6259. doi: [10.1093/nar/gkh962](https://doi.org/10.1093/nar/gkh962)
- Joosten RP, Long F, Murshudov GN, Perrakis A. 2014. The PDB\_REDO server for macromolecular structure model optimization. *IUCrJ* **1**:213–220. doi: [10.1107/S2052252514009324](https://doi.org/10.1107/S2052252514009324)

- Kabsch W.** 2010. Integration, scaling, space-group assignment and post-refinement. *Acta Crystallographica Section D Biological Crystallography* **66**:133–144. doi: [10.1107/S0907444909047374](https://doi.org/10.1107/S0907444909047374)
- Kanai Y, Ishikawa G, Takeuchi R, Ruike T, Nakamura R, Ihara A, Ohashi T, Takata K, Kimura S, Sakaguchi K, Nakamura Ryo-ichi, Takata Kei-ichi.** 2007. DmGEN shows a flap endonuclease activity, cleaving the blocked-flap structure and model replication fork. *FEBS Journal* **274**:3914–3927. doi: [10.1111/j.1742-4658.2007.05924.x](https://doi.org/10.1111/j.1742-4658.2007.05924.x)
- Lee Bi BI, Nguyen LH, Barsky D, Fernandes M, Wilson DM.** 2002. Molecular interactions of human Exo1 with DNA. *Nucleic Acids Research* **30**:942–949. doi: [10.1093/nar/30.4.942](https://doi.org/10.1093/nar/30.4.942)
- Li J, Li Z, Ruan J, Xu C, Tong Y, Pan PW, Tempel W, Crombet L, Min J, Zang J, Gay N.** 2011. Structural basis for specific binding of human MPP8 chromodomain to histone H3 methylated at lysine 9. *PLoS ONE* **6**:e25104. doi: [10.1371/journal.pone.0025104](https://doi.org/10.1371/journal.pone.0025104)
- Lieber MR.** 1997. The FEN-1 family of structure-specific nucleases in eukaryotic DNA replication, recombination and repair. *BioEssays* **19**:233–240. doi: [10.1002/bies.950190309](https://doi.org/10.1002/bies.950190309)
- Lilley DM, White MF.** 2001. The junction-resolving enzymes. *Nature Reviews Molecular Cell Biology* **2**:433–443. doi: [10.1038/35073057](https://doi.org/10.1038/35073057)
- Lilley DM.** 1985. The kinetic properties of cruciform extrusion are determined by DNA base-sequence. *Nucleic Acids Research* **13**:1443–1465. doi: [10.1093/nar/13.5.1443](https://doi.org/10.1093/nar/13.5.1443)
- Matos J, Blanco MG, Maslen S, Skehel JM, West SC.** 2011. Regulatory control of the resolution of DNA recombination intermediates during meiosis and mitosis. *Cell* **147**:158–172. doi: [10.1016/j.cell.2011.08.032](https://doi.org/10.1016/j.cell.2011.08.032)
- Matos J, West SC.** 2014. Holliday junction resolution: regulation in space and time. *DNA Repair* **19**:176–181. doi: [10.1016/j.dnarep.2014.03.013](https://doi.org/10.1016/j.dnarep.2014.03.013)
- Miętus M, Nowak E, Jaciuk M, Kustos P, Studnicka J, Nowotny M.** 2014. Crystal structure of the catalytic core of Rad2: insights into the mechanism of substrate binding. *Nucleic Acids Research* **42**:10762–10775. doi: [10.1093/nar/gku729](https://doi.org/10.1093/nar/gku729)
- Muñoz IM, Hain K, Déclais AC, Gardiner M, Toh GW, Sanchez-Pulido L, Heuckmann JM, Toth R, Macartney T, Eppink B, Kanaar R, Ponting CP, Lilley DM, Rouse J.** 2009. Coordination of structure-specific nucleases by human SLX4/BTBD12 is required for DNA repair. *Molecular Cell* **35**:116–127. doi: [10.1016/j.molcel.2009.06.020](https://doi.org/10.1016/j.molcel.2009.06.020)
- Nishino T, Ishino Y, Morikawa K.** 2006. Structure-specific DNA nucleases: structural basis for 3D-scissors. *Current Opinion in Structural Biology* **16**:60–67. doi: [10.1016/j.sbi.2006.01.009](https://doi.org/10.1016/j.sbi.2006.01.009)
- Orans J, McSweeney EA, Iyer RR, Hast MA, Hellinga HW, Modrich P, Beese LS.** 2011. Structures of human exonuclease 1 DNA complexes suggest a unified mechanism for nuclease family. *Cell* **145**:212–223. doi: [10.1016/j.cell.2011.03.005](https://doi.org/10.1016/j.cell.2011.03.005)
- O'Shaughnessy A, Hendrich B.** 2013. CHD4 in the DNA-damage response and cell cycle progression: not so NuRDy now. *Biochemical Society Transactions* **41**:777–782. doi: [10.1042/BST20130027](https://doi.org/10.1042/BST20130027)
- Pape T, Schneider TR.** 2004. HKL2MAP: a graphical user interface for macromolecular phasing with SHELX programs. *Journal of Applied Crystallography* **37**:843–844. doi: [10.1107/S0021889804018047](https://doi.org/10.1107/S0021889804018047)
- Patel N, Atack JM, Finger LD, Exell JC, Thompson P, Tsutakawa S, Tainer JA, Williams DM, Grasby JA.** 2012. Flap endonucleases pass 5'-flaps through a flexible arch using a disorder-thread-order mechanism to confer specificity for free 5'-ends. *Nucleic Acids Research* **40**:4507–4519. doi: [10.1093/nar/gks051](https://doi.org/10.1093/nar/gks051)
- Petronczki M, Siomos MF, Nasmyth K.** 2003. Un ménage à quatre: the molecular biology of chromosome segregation in meiosis. *Cell* **112**:423–440. doi: [10.1016/S0092-8674\(03\)00083-7](https://doi.org/10.1016/S0092-8674(03)00083-7)
- Pottmeyer S, Kemper B.** 1992. T4 endonuclease VII resolves cruciform DNA with nick and counter-nick and its activity is directed by local nucleotide sequence. *Journal of Molecular Biology* **223**:607–615. doi: [10.1016/0022-2836\(92\)90977-R](https://doi.org/10.1016/0022-2836(92)90977-R)
- Price BD, D'Andrea AD.** 2013. Chromatin remodeling at DNA double-strand breaks. *Cell* **152**:1344–1354. doi: [10.1016/j.cell.2013.02.011](https://doi.org/10.1016/j.cell.2013.02.011)
- Putnam CD, Hayes TK, Kolodner RD.** 2009. Specific pathways prevent duplication-mediated genome rearrangements. *Nature* **460**:984–989. doi: [10.1038/nature08217](https://doi.org/10.1038/nature08217)
- Rass U, Compton SA, Matos J, Singleton MR, Ip SC, Blanco MG, Griffith JD, West SC.** 2010. Mechanism of Holliday junction resolution by the human GEN1 protein. *Genes & Development* **24**:1559–1569. doi: [10.1101/gad.585310](https://doi.org/10.1101/gad.585310)
- Sakurai S, Kitano K, Yamaguchi H, Hamada K, Okada K, Fukuda K, Uchida M, Ohtsuka E, Morioka H, Hakoshima T.** 2005. Structural basis for recruitment of human flap endonuclease 1 to PCNA. *The EMBO Journal* **24**:683–693. doi: [10.1038/sj.emboj.7600519](https://doi.org/10.1038/sj.emboj.7600519)
- Sarbajna S, Davies D, West SC.** 2014. Roles of SLX1-SLX4, MUS81-EME1, and GEN1 in avoiding genome instability and mitotic catastrophe. *Genes & Development* **28**:1124–1136. doi: [10.1101/gad.238303.114](https://doi.org/10.1101/gad.238303.114)
- Sarbajna S, West SC.** 2014. Holliday junction processing enzymes as guardians of genome stability. *Trends in Biochemical Sciences* **39**:409–419. doi: [10.1016/j.tibs.2014.07.003](https://doi.org/10.1016/j.tibs.2014.07.003)
- Schwacha A, Kleckner N.** 1995. Identification of double Holliday junctions as intermediates in meiotic recombination. *Cell* **83**:783–791. doi: [10.1016/0092-8674\(95\)90191-4](https://doi.org/10.1016/0092-8674(95)90191-4)
- Shah R, Cosstick R, West SC.** 1997. The RuvC protein dimer resolves Holliday junctions by a dual incision mechanism that involves base-specific contacts. *The EMBO Journal* **16**:1464–1472. doi: [10.1093/emboj/16.6.1464](https://doi.org/10.1093/emboj/16.6.1464)
- Smothers JF, Henikoff S.** 2000. The HP1 chromo shadow domain binds a consensus peptide pentamer. *Current Biology* **10**:27–30. doi: [10.1016/S0960-9822\(99\)00260-2](https://doi.org/10.1016/S0960-9822(99)00260-2)
- Söding J, Biegert A, Lupas AN.** 2005. The HHpred interactive server for protein homology detection and structure prediction. *Nucleic Acids Research* **33**:W244–W248. doi: [10.1093/nar/gki408](https://doi.org/10.1093/nar/gki408)

- Stanley FKT**, Moore S, Goodarzi AA. 2013. CHD chromatin remodelling enzymes and the DNA damage response. *Mutation Research/Fundamental and Molecular Mechanisms of Mutagenesis* **750**:31–44. doi: [10.1016/j.mrfmmm.2013.07.008](https://doi.org/10.1016/j.mrfmmm.2013.07.008)
- Svendsen JM**, Harper JW. 2010. GEN1/Yen1 and the SLX4 complex: Solutions to the problem of Holliday junction resolution. *Genes & Development* **24**:521–536. doi: [10.1101/gad.1903510](https://doi.org/10.1101/gad.1903510)
- Svendsen JM**, Smogorzewska A, Sowa ME, O'Connell BC, Gygi SP, Elledge SJ, Harper JW. 2009. Mammalian BTBD12/SLX4 assembles a Holliday junction resolvase and is required for DNA repair. *Cell* **138**:63–77. doi: [10.1016/j.cell.2009.06.030](https://doi.org/10.1016/j.cell.2009.06.030)
- Szostak JW**, Orr-Weaver TL, Rothstein RJ, Stahl FW. 1983. The double-strand-break repair model for recombination. *Cell* **33**:25–35. doi: [10.1016/0092-8674\(83\)90331-8](https://doi.org/10.1016/0092-8674(83)90331-8)
- Tomlinson CG**, Atack JM, Chapados B, Tainer JA, Grasby JA. 2010. Substrate recognition and catalysis by flap endonucleases and related enzymes. *Biochemical Society Transactions* **38**:433–437. doi: [10.1042/BST0380433](https://doi.org/10.1042/BST0380433)
- Tsutakawa SE**, Classen S, Chapados BR, Arvai AS, Finger LD, Guenther G, Tomlinson CG, Thompson P, Sarker AH, Shen B, Cooper PK, Grasby JA, Tainer JA. 2011. Human flap endonuclease structures, DNA double-base flipping, and a unified understanding of the FEN1 superfamily. *Cell* **145**:198–211. doi: [10.1016/j.cell.2011.03.004](https://doi.org/10.1016/j.cell.2011.03.004)
- Tsutakawa SE**, Lafrance-Vanasse J, Tainer JA. 2014. The cutting edges in DNA repair, licensing, and fidelity: DNA and RNA repair nucleases sculpt DNA to measure twice, cut once. *DNA Repair* **19**:95–107. doi: [10.1016/j.dnarep.2014.03.022](https://doi.org/10.1016/j.dnarep.2014.03.022)
- Vonrhein C**, Blanc E, Roversi P, Bricogne G. 2007. Automated structure solution with autoSHARP. *Methods in Molecular Biology* **364**:215–245. doi: [10.1385/1-59745-266-1:215](https://doi.org/10.1385/1-59745-266-1:215)
- Wakasugi M**, Reardon JT, Sancar A. 1997. The non-catalytic function of XPG protein during dual incision in human nucleotide excision repair. *Journal of Biological Chemistry* **272**:16030–16034. doi: [10.1074/jbc.272.25.16030](https://doi.org/10.1074/jbc.272.25.16030)
- Wechsler T**, Newman S, West SC. 2011. Aberrant chromosome morphology in human cells defective for Holliday junction resolution. *Nature* **471**:642–646. doi: [10.1038/nature09790](https://doi.org/10.1038/nature09790)
- West SC**, Blanco MG, Chan YW, Matos J, Sarbajna S, Wyatt HDM. 2015. Resolution of Recombination Intermediates: Mechanisms and Regulation. *Cold Spring Harbor Symposia on Quantitative Biology* **80**:103–109. doi: [10.1101/sqb.2015.80.027649](https://doi.org/10.1101/sqb.2015.80.027649)
- Williams T**, Kelley C, Campbell J, Cunningham R, Denholm D, Elber G, Fearick R, Grammes C, Hart L, Hecking L. *Gnuplot 5.0.0*. 2015.
- Wu L**, Hickson ID. 2003. The Bloom's syndrome helicase suppresses crossing over during homologous recombination. *Nature* **426**:870–874. doi: [10.1038/nature02253](https://doi.org/10.1038/nature02253)
- Wyatt HDM**, Sarbajna S, Matos J, West SC. 2013. Coordinated Actions of SLX1-SLX4 and MUS81-EME1 for Holliday Junction Resolution in Human Cells. *Molecular Cell* **52**:234–247. doi: [10.1016/j.molcel.2013.08.035](https://doi.org/10.1016/j.molcel.2013.08.035)
- Yang W**. 2011. Nucleases: diversity of structure, function and mechanism. *Quarterly Reviews of Biophysics* **44**:1–93. doi: [10.1017/S0033583510000181](https://doi.org/10.1017/S0033583510000181)
- Yap KL**, Zhou MM. 2011. Structure and mechanisms of lysine methylation recognition by the chromodomain in gene transcription. *Biochemistry* **50**:1966–1980. doi: [10.1021/bi101885m](https://doi.org/10.1021/bi101885m)
- Ying S**, Minocherhomji S, Chan KL, Palmal-Pallag T, Chu WK, Wass T, Mankouri HW, Liu Y, Hickson ID. 2013. MUS81 promotes common fragile site expression. *Nature Cell Biology* **15**:1001–1007. doi: [10.1038/ncb2773](https://doi.org/10.1038/ncb2773)



---

## Figures and figure supplements

Human Holliday junction resolvase GEN1 uses a chromodomain for efficient DNA recognition and cleavage

**Shun-Hsiao Lee et al**

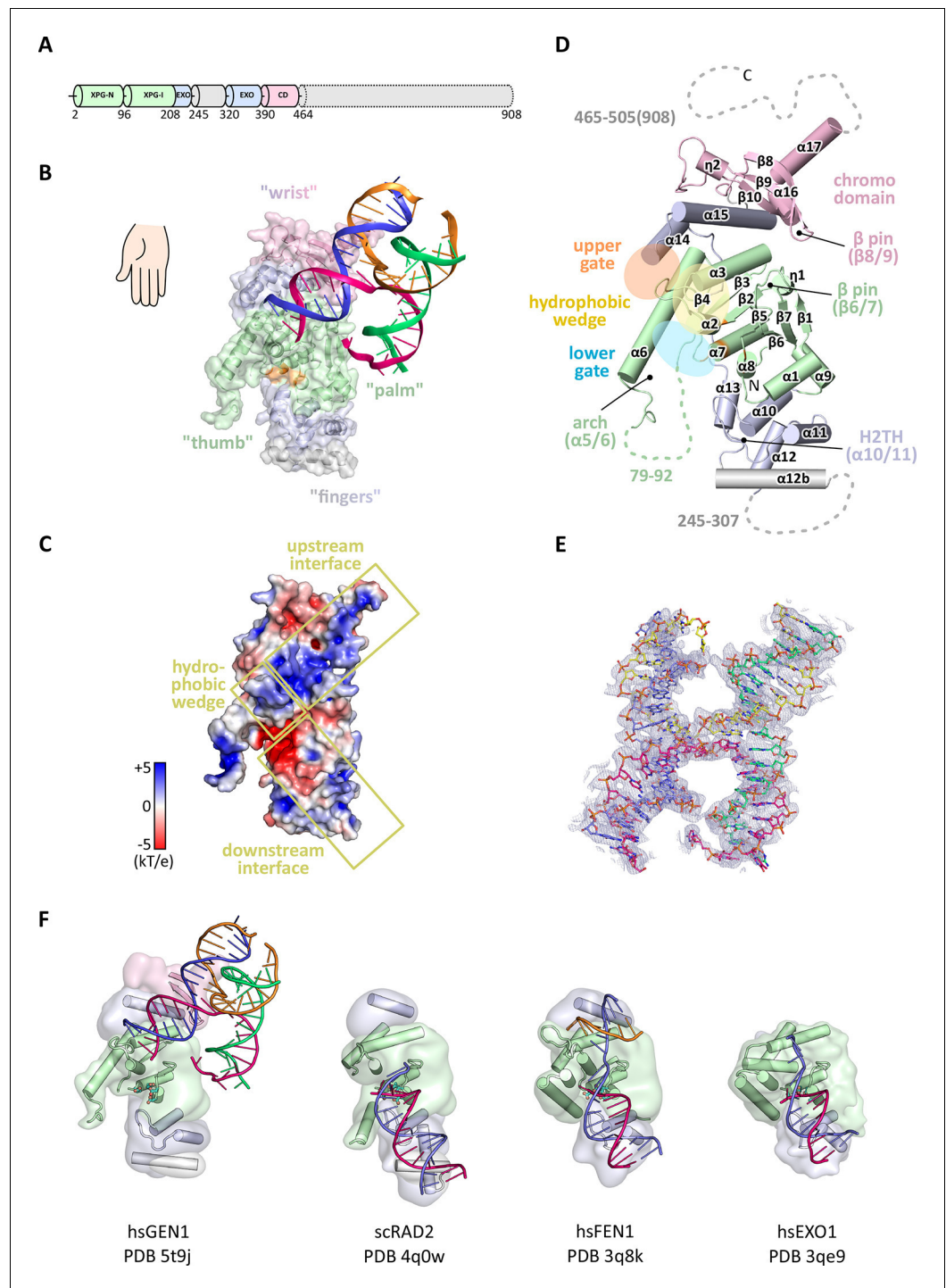


**Figure 1.** Architecture of human GEN1. (A) Domain architecture of human GEN1. The structurally unknown regulatory domain (residues 465–908) is shown with dotted lines. (B) Overview of the catalytic core of GEN1 in complex with HJ DNA. The protein resembles the shape of a downwards-pointing right hand with helix  $\alpha_6$  as the thumb. The protein is depicted in half transparent surface representation with secondary structure elements underneath. The DNA is shown in ladder representation with individual strands in different colors. The coloring of GEN1 follows domain boundaries: intertwining XPG-N and XPG-I in green, 5'→3' exonuclease C-terminal domain (EXO) in blue, chromodomain in pink, unassigned regions in gray. Active site residues (E134, E136, D155, D157) are highlighted in orange. (C) Electrostatic surface potential of GEN1. The coloring follows the potential from -5 (red) to +5 kT/e (blue). The DNA-binding interfaces and the position of the hydrophobic wedge are marked in Figure 1 continued on next page

*Figure 1 continued*

yellow. (D) Secondary structure elements of the catalytic core of GEN1 in cartoon representation with the same colors as before. Dotted lines represent parts that are not resolved in the crystal structure. The numbering follows a unified scheme for the Rad2/XPG family (compare **Figure 2**) for  $\alpha$ -helices,  $\beta$ -sheets and  $3_{10}$ -helices ( $\eta$ ). (E) Experimental electron density map (autoSHARP, solvent flattened, contoured at  $1\sigma$ ) drawn around the HJ in the GEN1 complex. The DNA model is shown in ball-stick representation with carbon atoms of individual strands in different colors (yellow, light blue, magenta, green) and oxygen atoms in red, phosphor atoms in orange, nitrogen atoms in dark blue. (F) Structural comparison of Rad2/XPG family nucleases. Proteins are shown in a simplified surface representation with important structural elements in cartoon representation and DNA in ladder representation. The color scheme is the same as in **B. Figure 1—figure supplement 1** shows the content of the asymmetric unit.

DOI: [10.7554/eLife.12256.003](https://doi.org/10.7554/eLife.12256.003)

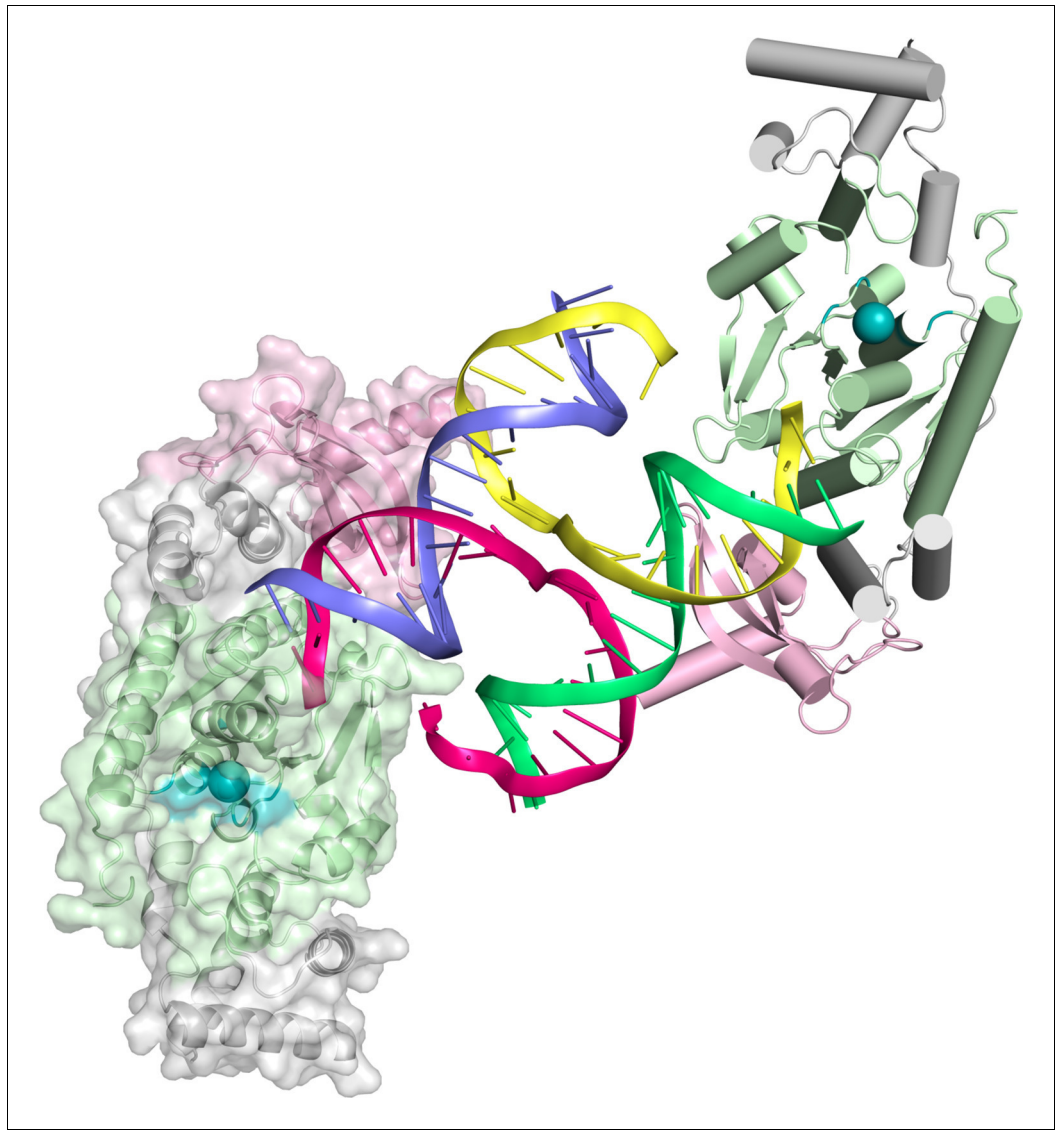


**Figure 1—figure supplement 1.** Content of the asymmetric unit of the GEN1-HJ crystal. One protein monomer is shown in surface representation with secondary structure cartoons underneath, the other one only in cartoon representation with  $\alpha$ -helices as cylinders and  $\beta$ -strands as arrows. The HJ DNA bridges between two protein monomers in the asymmetric unit. The active sites are labeled with a turquoise ball each.

DOI: [10.7554/eLife.12256.004](https://doi.org/10.7554/eLife.12256.004)

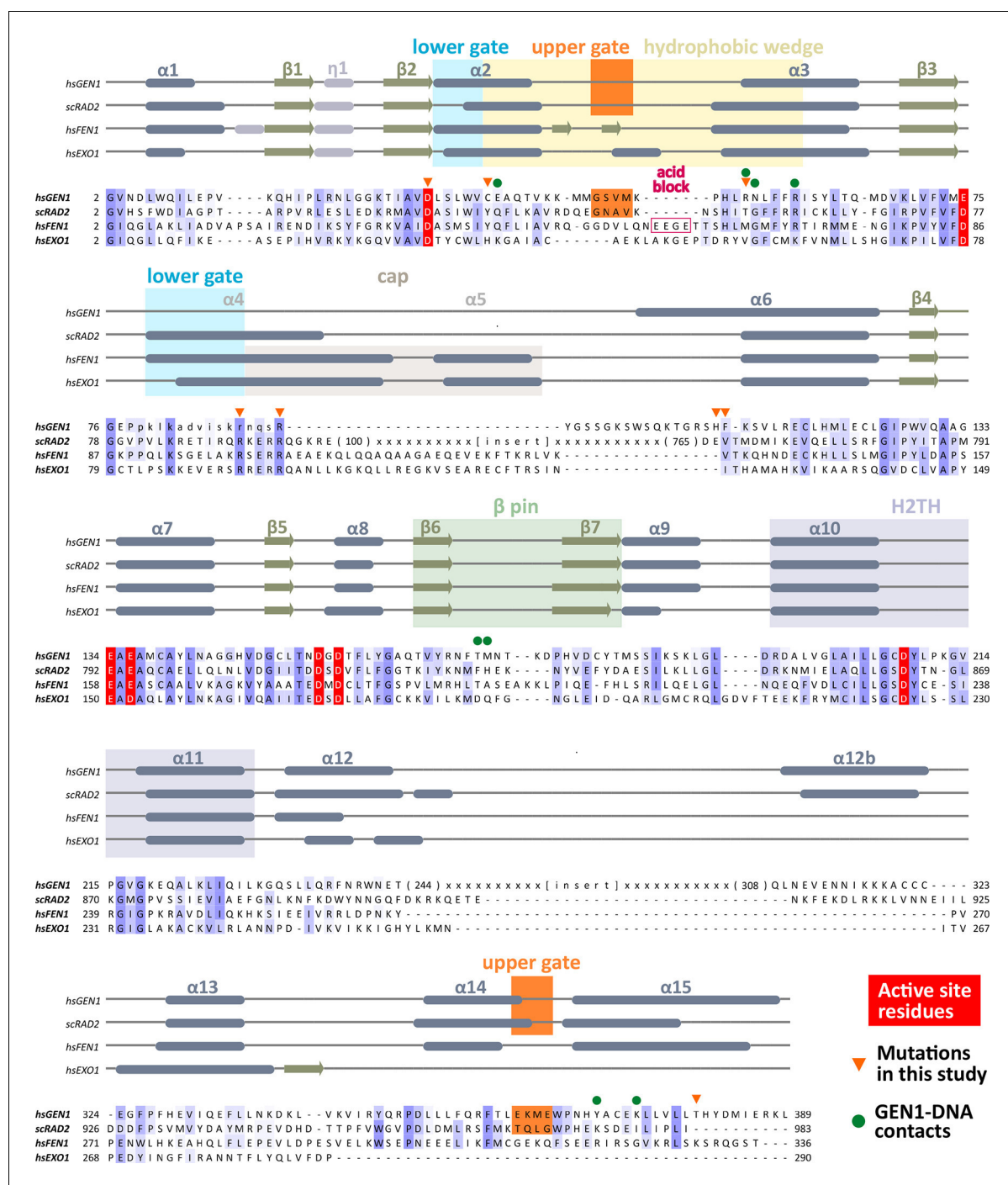


**Figure 2.** Alignment of the nuclease cores of Rad2/XPG-family proteins. The alignment is based on known crystal structures: human GEN1 (PDB 5t9j, this study), yeast Rad2 (PDB 4q0w), human FEN1 (PDB 3q8k), human EXO1 (3qe9). Secondary structure elements are depicted on top of the sequence with dark blue bars for  $\alpha$ -helices, light blue bars for  $3_{10}$ -helices and green arrows for  $\beta$ -sheets. The numbering follows a unified scheme for the superfamily. Functional elements are labeled and described in the main text. Sequences are colored by similarity (BLOSUM62 score) and active site residues are marked in red. Mutations analyzed in this study are marked with an orange triangle and DNA contacts found in the human GEN1-HJ structure have a dark green dot. Disordered or missing parts in the structures are labeled in small letters or with x.

DOI: [10.7554/eLife.12256.006](https://doi.org/10.7554/eLife.12256.006)

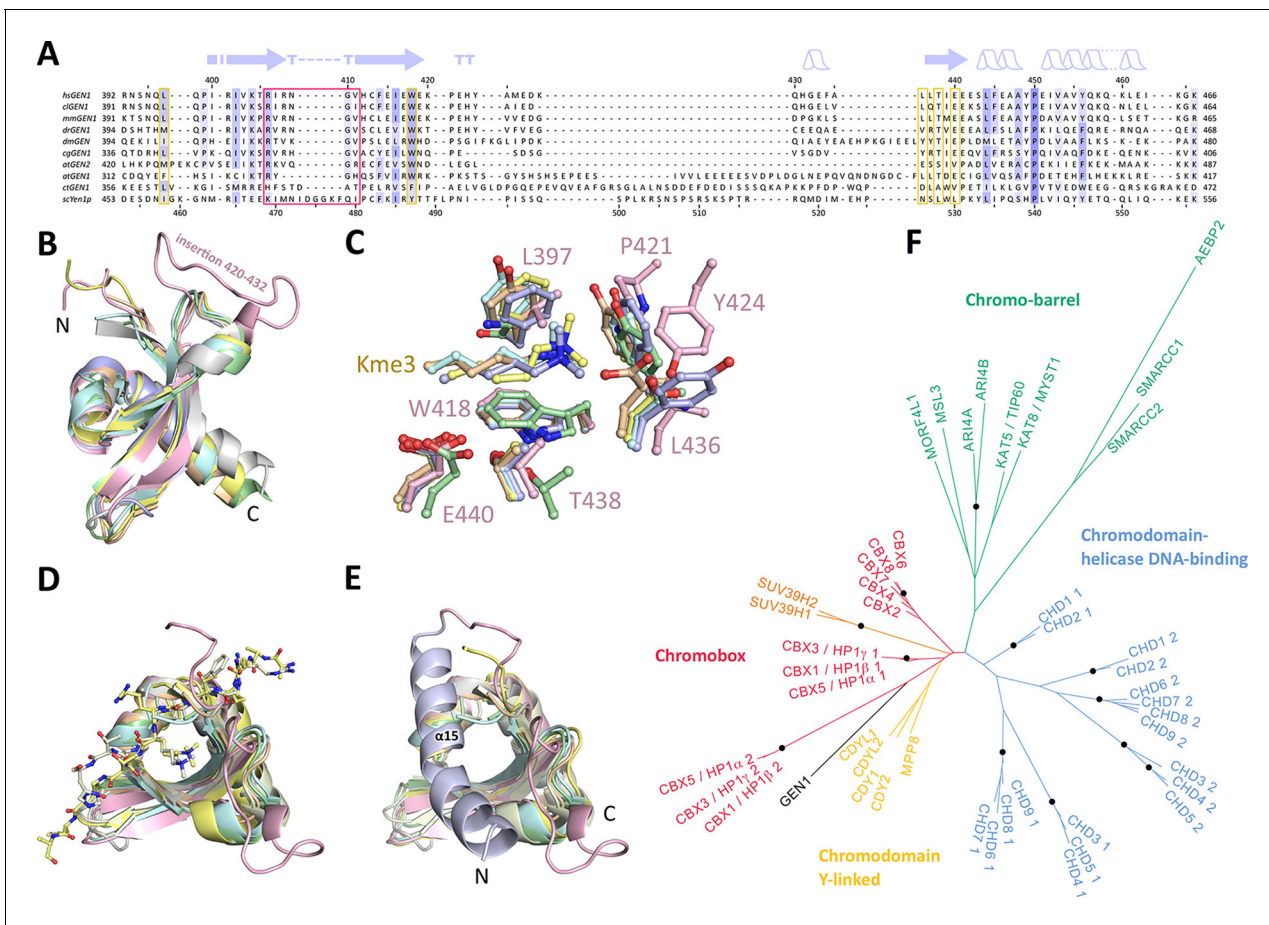


**Figure 3.** Chromodomain comparison. (A) Sequence alignment of GEN1 chromodomains from different organisms: hsGEN1 (*Homo sapiens*), cGEN1 (*Canis lupus*), mmGEN1 (*Mus musculus*), drGEN1 (*Danio rerio*), atGEN1/2 (*Arabidopsis thaliana*), cgGEN1 (*Crassostrea gigas*), scYEN1 (*Saccharomyces cerevisiae*). The presence of a chromodomain is conserved from yeast to human with *Caenorhabditis elegans* as an exception. Secondary structure elements of the GEN1 chromodomain are shown on top. The sequence coloring is based on a similarity matrix (BLOSUM62). The corresponding positions of the DNA-interaction site in human GEN1 is marked with a red box and residues of the aromatic cage are highlighted with a yellow box. (B) GEN1 has a canonical chromodomain fold of three antiparallel beta-sheets packed against an  $\alpha$ -helix. (C) The arrangement of the aromatic cage in GEN1 is comparable to other chromodomains but less aromatic and slightly larger. (D) The superposition of different chromodomains places cognate binding peptides of hsMPP8 and mmCBX7 (and others) into the aromatic cage. (E) The aromatic cage of GEN1 is closed by helix  $\alpha$ 15. Panels B–D show the chromodomains of hsGEN1 (pink, PDB 5t9j), hsCBX3 (gray, PDB 3kup), hsSUV39H1 (green, PDB 3mts), hsMPP8 (yellow, PDB 3lwe), dmHP1 $\alpha$  (orange, chromo shadow PDB 3p7j), dmRHINO (cyan, PDB 4quc/3r93), mmCBX7 (light blue, PDB 4x3s; compare **Figure 3—source data 1**). (F) Phylogenetic tree of all known human chromodomains. GEN1 is distantly related to the CBX chromo-shadow domains and CDY chromodomains. The corresponding alignment for calculating the phylogenetic tree is shown in **Figure 3—figure supplement 1**. GEN1 is colored in black, chromobox (CBX) proteins are colored in red, interspersed by SUV39H histone acetylases (orange) and chromodomain Y-linked (CDY) proteins (yellow). Chromo-barrel domain proteins are colored in green and chromodomain-helicase DNA-binding (CHD) proteins are in blue. Chromodomains and chromo-shadow domains from the same protein are labeled with 1 and 2, respectively. Stable branches with bootstrap values equal or higher than 0.8 are marked with a black dot. The binding of the GEN1 chromodomain to a set of histone peptides was tested but no interaction was detected (**Figure 3—source data 2** and **Figure 3—figure supplement 2**).

DOI: 10.7554/eLife.12256.007

The following source data is available for figure 3:

**Source data 1.** Proteins found in a DALI search.

DOI: 10.7554/eLife.12256.008

**Source data 2.** N-terminally fluorescein-labeled peptides used for chromodomain binding assays.

DOI: 10.7554/eLife.12256.009

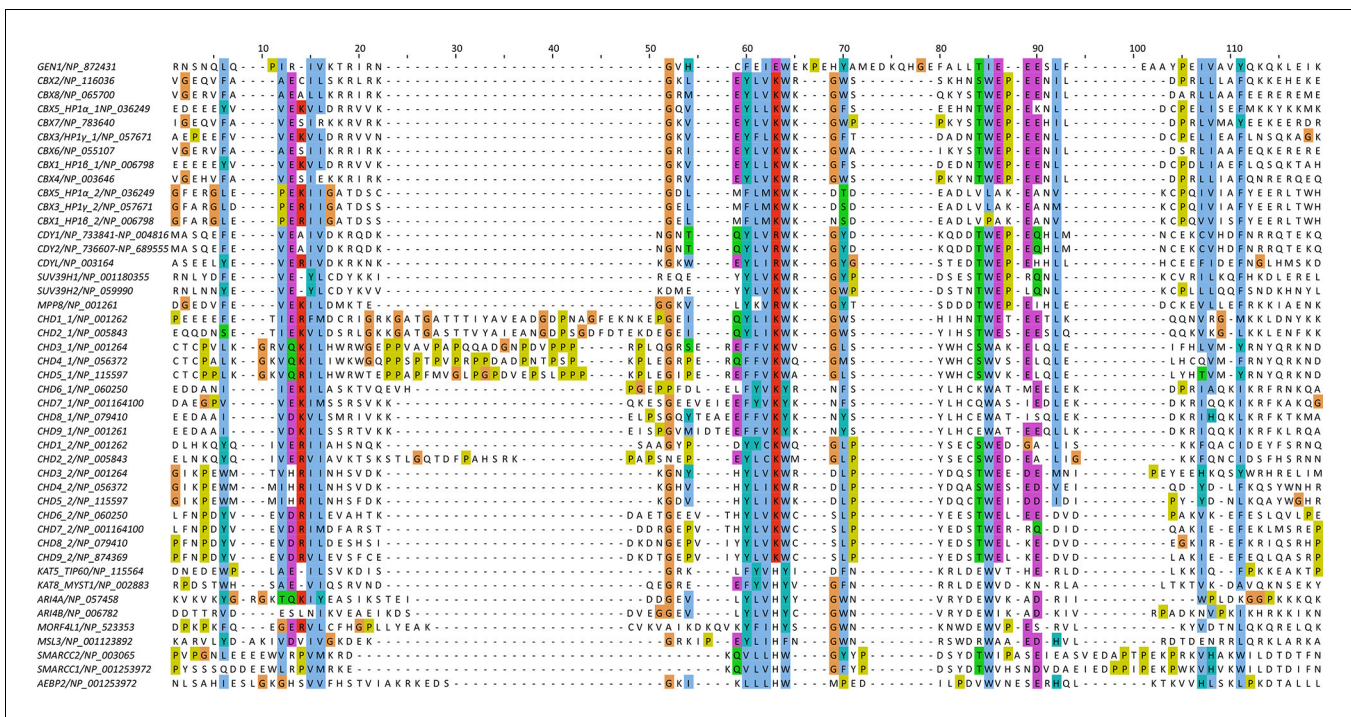


**Figure 3—figure supplement 1.** Sequence alignment of all known human chromodomains. The alignment was used to calculate the phylogenetic tree in Figure 3F. Colors follow the CLUSTAL X coloring scheme.

DOI: 10.7554/eLife.12256.010

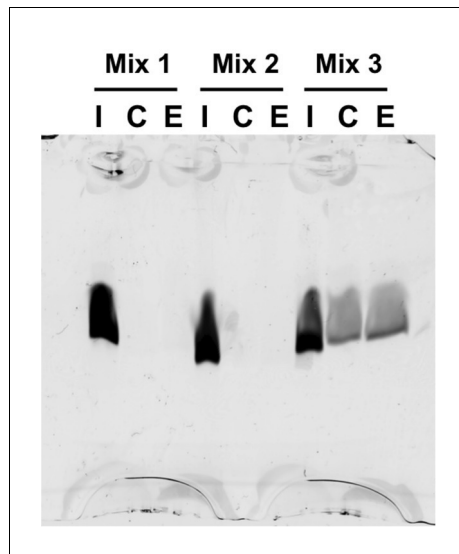


**Figure 3—figure supplement 2.** Histone peptide pull-down assay. Nickel resin-immobilized GEN1 chromodomain was incubated with the mixtures of fluorescein-labeled histone peptides, washed, bound peptides eluted and separated by 20% SDS-PAGE. Mix 1 and 2 did not show any binding, and non-specific binding to the resin was found with Mix 3. The smearing of the bands is due to the small size of the peptides (~1.5 kDa). I, C and E represent input, resin control and elution, respectively. Mix 1: H3K9, H3K9me1, H3K9me2, and H3K9me3. Mix 2: H3K27, H3K27me1, H3K27me2, and H3K27me3. Mix 3: H3K36me1, H3K36me2, H3K36me3, and H3K36Ac. DOI: [10.7554/eLife.12256.011](https://doi.org/10.7554/eLife.12256.011)

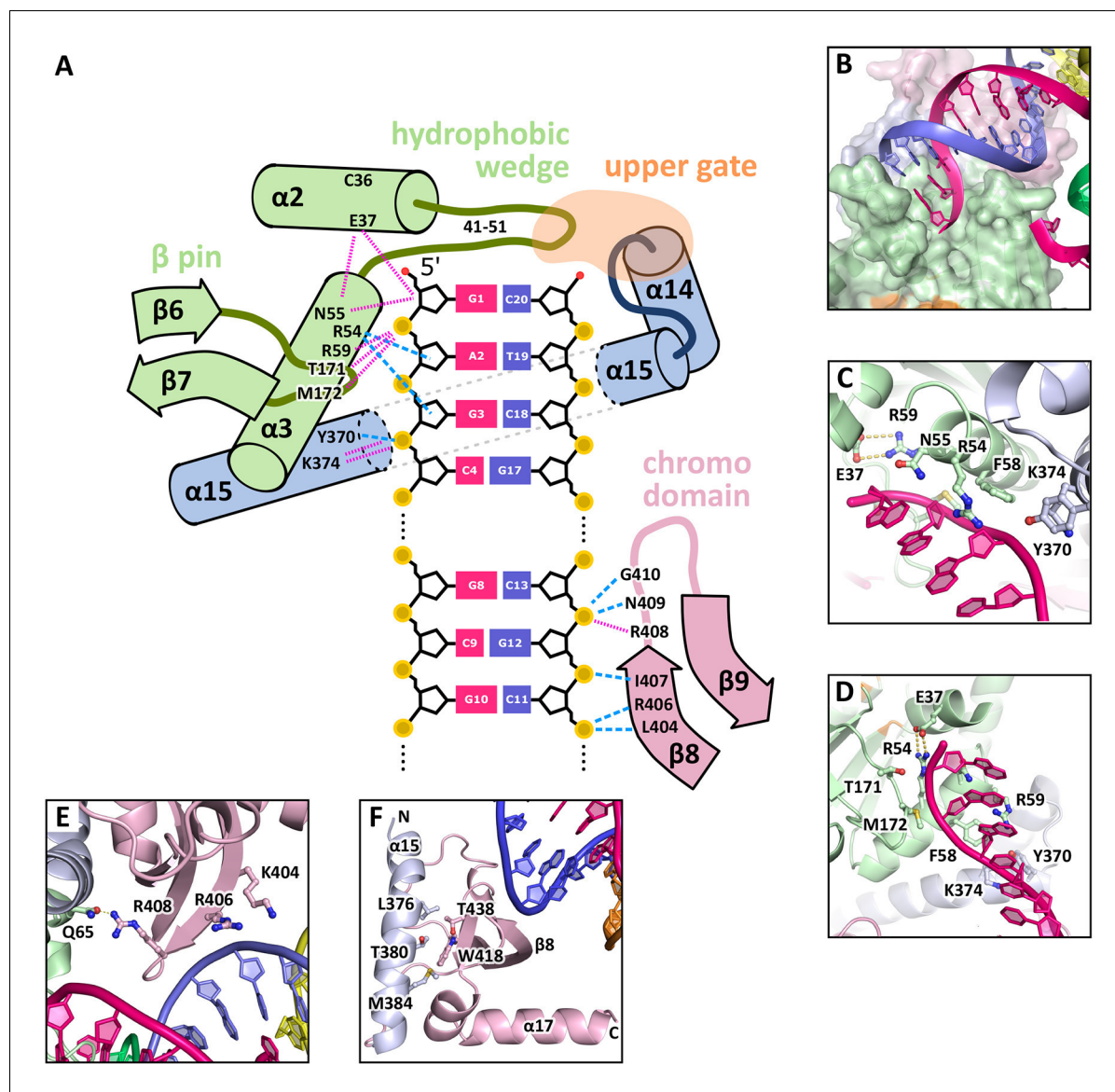


**Figure 4.** DNA interactions in the GEN1-DNA complex. (A) Schematic of the GEN1-DNA interactions at the upstream interface. The coloring is the same as in **Figure 1**. The nuclease core (green and blue) interacts with the uncleaved strand and the chromodomain (pink) contacts the complementary strand. Hydrogen bonds are shown with blue dashed lines and van-der-Waals contacts are in red dotted lines. (B) Interactions at the hydrophobic wedge. The end of the DNA double helix docks onto the hydrophobic wedge formed by helices  $\alpha 2$  and  $\alpha 3$ . (C/D) Interactions with the uncleaved strand in two views. All key residues form sequence-independent contacts to the DNA backbone. R54 reaches into the minor groove of the DNA. The complementary DNA strand has been removed for clarity (E/F) Interactions of the chromo domain with the complementary strand in two views. The backbone of residues 406–410 ( $\beta$ -hairpin  $\beta 8$ - $\beta 9$ ) abuts the DNA backbone. R406 has a supporting role in the interaction and R408 forms a polar interaction with Q65, which establishes a connection between the chromodomain and the nuclease core. Helix  $\alpha 15$  makes hydrophobic interactions with the aromatic cage and thus blocks it.

DOI: [10.7554/eLife.12256.012](https://doi.org/10.7554/eLife.12256.012)

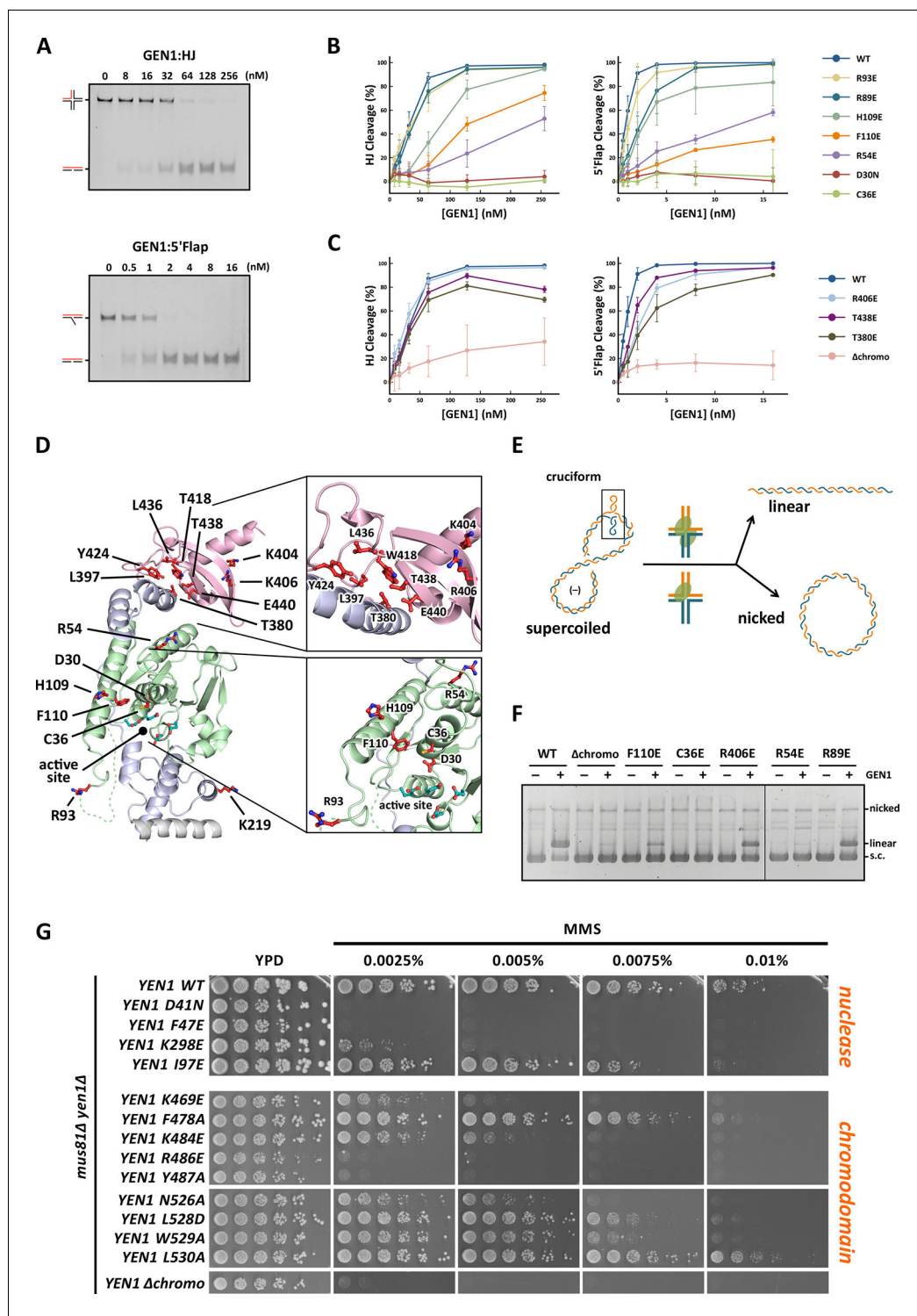


**Figure 5.** Functional analysis of GEN1. (A) Nuclease activity of GEN1 with HJ and 5' flap DNA. 40 nM 5' 6FAM-labeled substrates were mixed with indicated amounts of GEN1. Reactions were carried out at 37°C for 15 min, products were separated by native PAGE and analyzed with a phosphoimager. **Figure 5—source data 1** gives the sequences of DNA oligos used in biochemical assays and **Figure 5—source data 3** shows activity measurements. (B) Quantification of nuclease assays of wild type GEN1 and variants with mutated residues located at the protein-DNA interfaces. Percentage of cleavage was plotted against the enzyme concentration. Error bars depict the standard deviation calculated from at least three independent experiments. **Figure 5—figure supplement 1**

Figure 5 continued on next page

*Figure 5 continued*

shows representative gels from the PAGE analysis. (C) Quantification of nuclease assays of wild type GEN1 and variants with mutated residues located at the chromodomain. Error bars depict the standard deviation calculated from at least three independent experiments. **Figure 5—figure supplement 2** shows representative gels from the PAGE analysis. (D) GEN1 mutations used in this study. Locations of human GEN1 mutations used in biochemical assays and corresponding residues in yeast MMS survival assays are highlighted in red. Active site residues E134, E136, D155, D157 are marked in turquoise. (E) Schematic of the cruciform plasmid cleavage assay. A cruciform structure can be formed in plasmid pIRbke8<sup>mut</sup>, which harbors an inverted-repeat sequence and is stabilized by negative supercoiling. Introducing two cuts across the junction point within the lifetime of the resolvase-junction complex yields linear products whereas sequential cleavage generates nicked products and the relaxed plasmid cannot be a substrate for the next cleavage. (F) Cruciform plasmid cleavage assay with different GEN1 variants. Plasmid pIRbke8<sup>mut</sup> was treated with 256 nM GEN1 each and reactions were carried out at 37°C for 15 min. Supercoiled, linear and nicked plasmids were separated by native agarose gel electrophoresis and visualized with SYBR safe under UV light. (G) MMS survival assays with yeast *yen1* variants. The survival of *yen1* mutants was tested under a *yen1Δ mus81Δ* background with indicated amounts of MMS. The top part shows mutations at GEN1-DNA interfaces and the bottom part mutations at the chromodomain (compare **Figure 5—figure supplement 3** for all controls and expression tests). **Figure 5—source data 2** gives a list of all yeast strains.

DOI: [10.7554/eLife.12256.013](https://doi.org/10.7554/eLife.12256.013)

The following source data is available for figure 5:

**Source data 1.** Oligonucleotides used in biochemical assays.

DOI: [10.7554/eLife.12256.014](https://doi.org/10.7554/eLife.12256.014)

**Source data 2.** Yeast strains used for MMS survival assays.

DOI: [10.7554/eLife.12256.015](https://doi.org/10.7554/eLife.12256.015)

**Source data 3.** In vitro activity measurements of different GEN1<sup>2-505</sup> variants.

DOI: [10.7554/eLife.12256.016](https://doi.org/10.7554/eLife.12256.016)

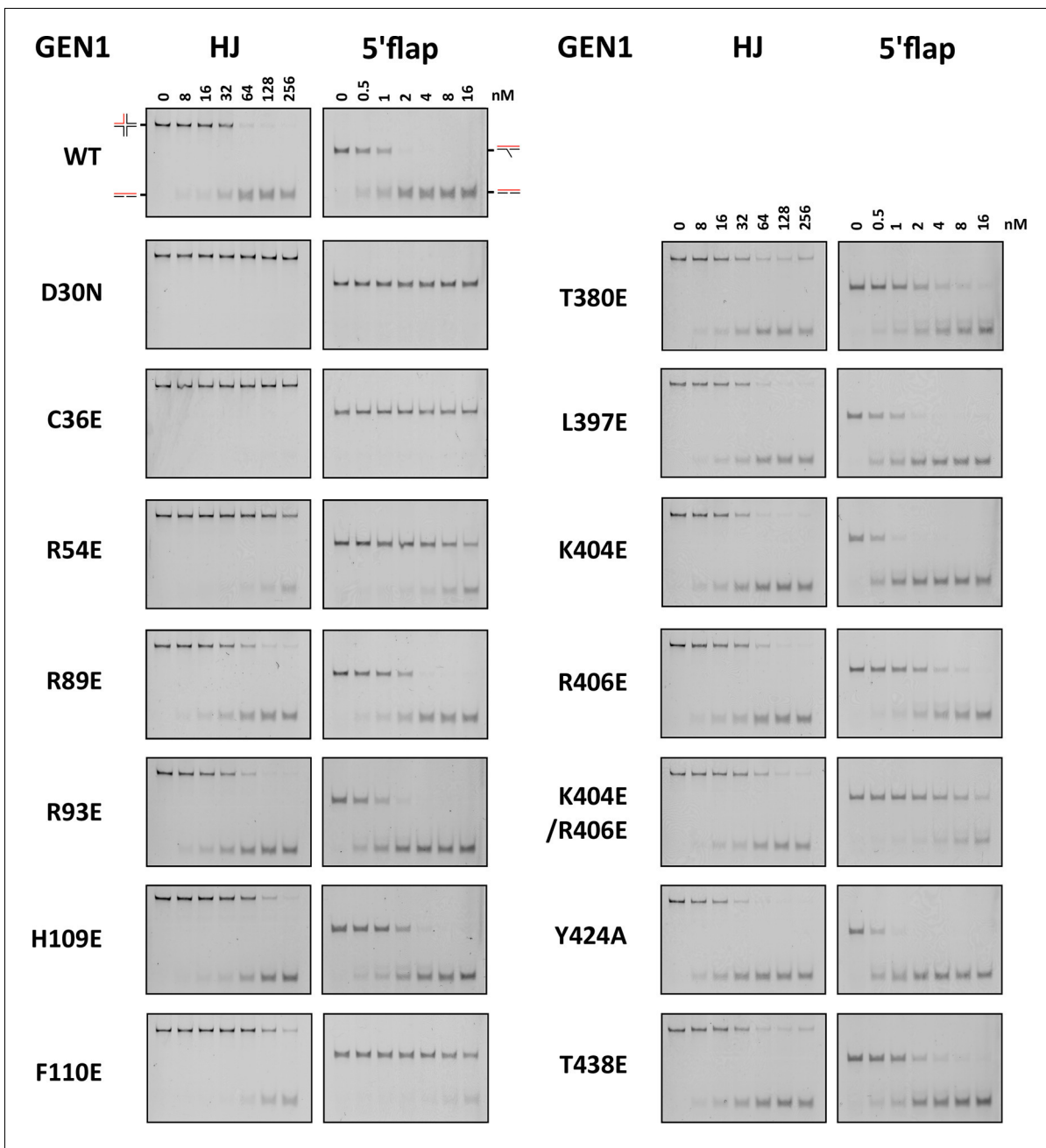


**Figure 5—figure supplement 1.** DNA cleavage assays of different GEN1 mutations. All GEN1<sup>2-505</sup> mutations were generated by site-directed mutagenesis and purified with the same procedure. Experiments were repeated three times and a representative gel picture is shown for each protein variant in **Figure 5**.

DOI: [10.7554/eLife.12256.017](https://doi.org/10.7554/eLife.12256.017)

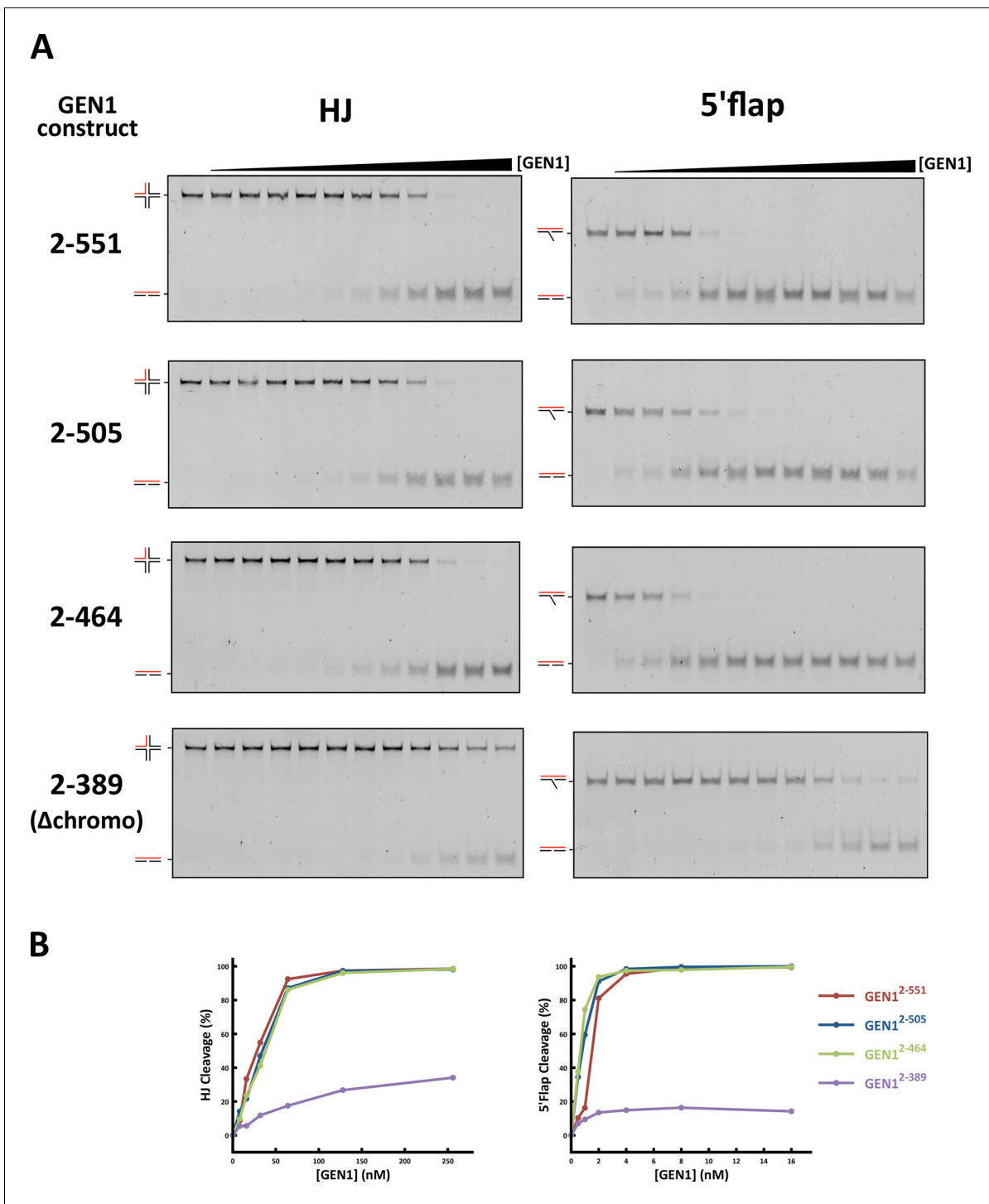


**Figure 5—figure supplement 2.** DNA cleavage assays of different GEN1 fragments. (A) 5' 6FAM labeled four-way junction or 5'flap DNA (40 nM) were mixed with varying concentrations of GEN1 truncations (0.25, 0.5, 1, 2, 4, 8, 16, 32, 64, 128, 256 nM, respectively). (B) Quantification of activity assays.

DOI: [10.7554/eLife.12256.018](https://doi.org/10.7554/eLife.12256.018)

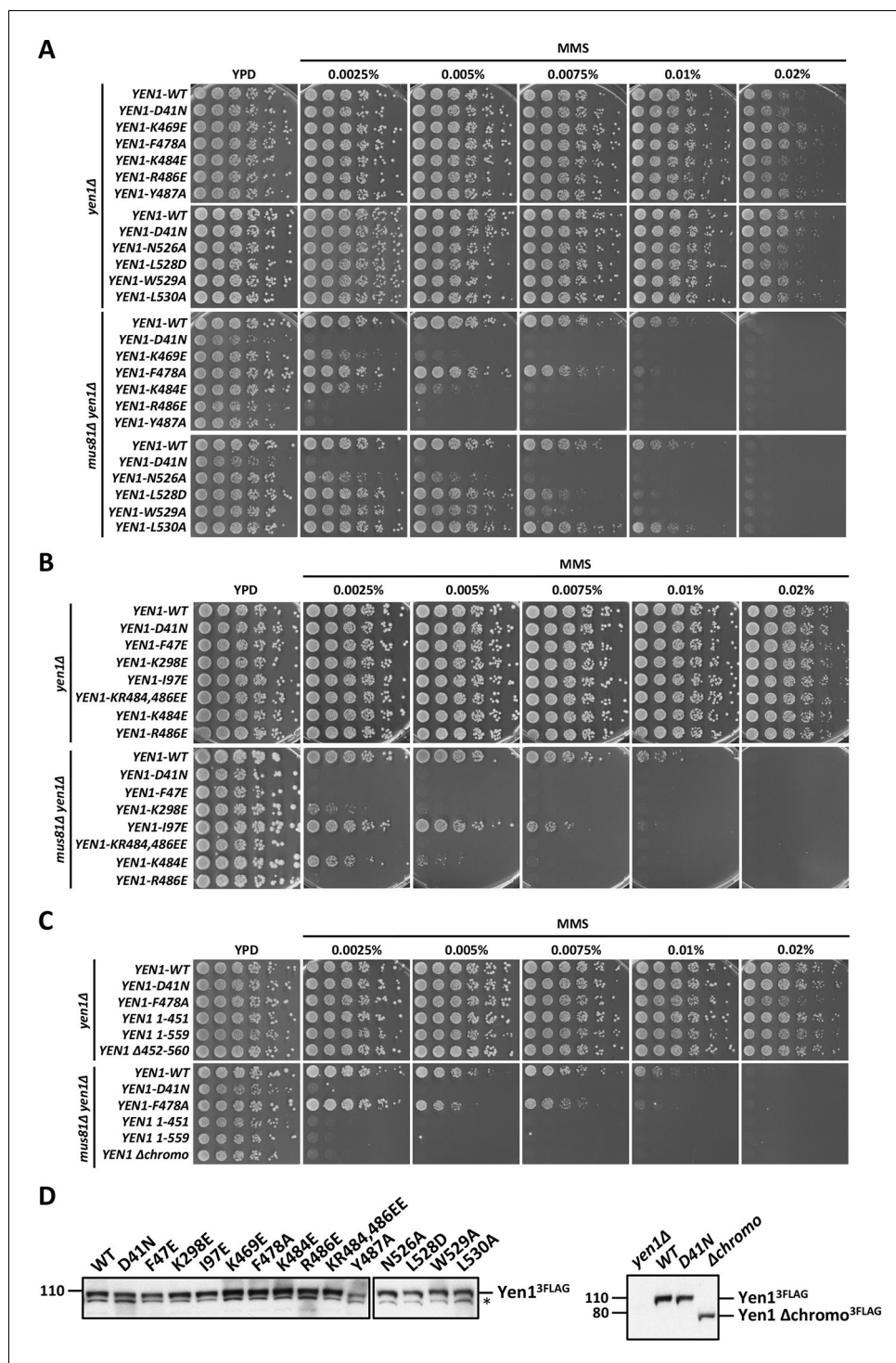


**Figure 5—figure supplement 3.** MMS survival assays with yeast *yen1* mutants. The survival of *yen1* mutants was tested in a *yen1Δ* or *yen1Δ mus81Δ* background with indicated amounts of MMS (compare **Figure 5** and **Figure 5—source data 2**). Mus81 overlaps with Yen1 functionally, therefore *yen1Δ* knock-out strains are fully viable even in the presence of MMS, and hypersensitivity is only seen in the double knock-out. (A) Mutations in the chromodomain. (B) Mutations at protein-DNA interfaces. (C) *Yen1* truncations and chromodomain deletion. (D) Protein expression test (Western Blot analysis) of 3FLAG tagged *Yen1* variants. Asterisk denotes a cross-reactive band.

DOI: [10.7554/eLife.12256.019](https://doi.org/10.7554/eLife.12256.019)

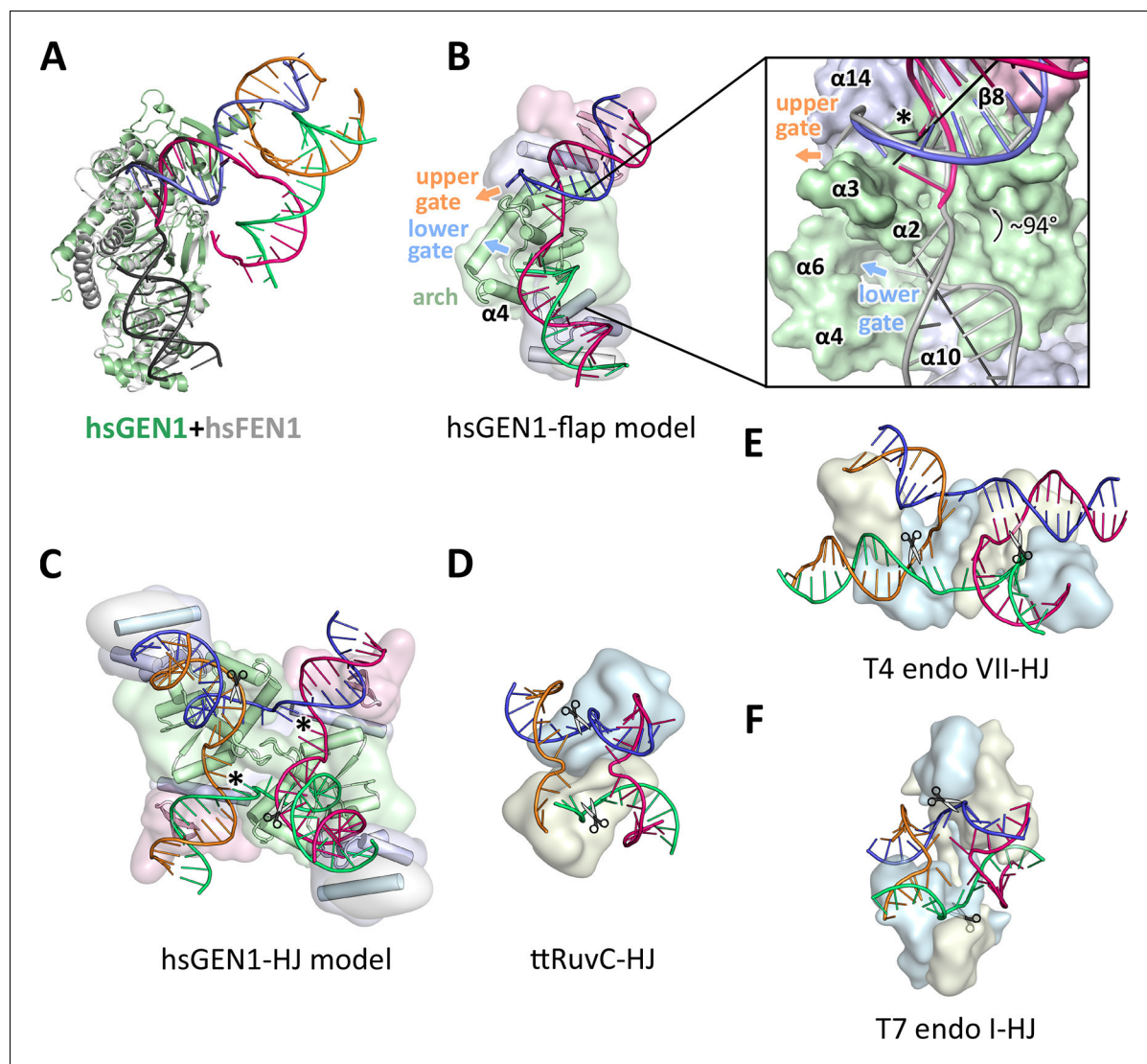


**Figure 6.** Substrate recognition features of GEN1. (A) Superposition of the protein part of the FEN1-DNA complex (PDB 3q8k, protein in gray, DNA in black) onto the GEN1-HJ complex (protein in green and the DNA strands in different colors). The FEN1-DNA aligns with the same register as the GEN1-DNA at the upstream interface. (B) Model for the recognition of a 5' flap substrate by GEN1. The DNA was extended using the superimposition from A. Homology modeling suggests an additional helix  $\alpha 4$  (disordered residues 79–92) forming an arch with helix  $\alpha 6$ . The protein is shown in a simplified surface representation with the same colors as in **Figure 1** and structural elements are highlighted. The insert shows a zoomed in view of the hydrophobic wedge with the modeled FEN1-DNA in gray. (C) Model for the dimerization of GEN1 upon binding to a HJ substrate based on the 5' flap model in B. The monomers interlock via both arches ( $\alpha 4$ - $\alpha 6$ ) and the hydrophobic wedges ( $\alpha 2$ - $\alpha 3$ ) contact each other. (D) Structure of the *Thermus thermophilus* RuvC-HJ complex (PDB 4ld0). (E) Structure of the T4 endonuclease VII-HJ complex (PDB 2qnc). (F) Structure of the T7 endonuclease I-HJ complex (PDB 2pfj). Individual monomers are in surface representation, colored in light blue and beige, respectively. DNA strands are shown as ladders in different colors.

DOI: [10.7554/eLife.12256.020](https://doi.org/10.7554/eLife.12256.020)

# The Slx4-Dpb11 scaffold complex: coordinating the response to replication fork stalling in S-phase and the subsequent mitosis

Lissa N Prinz<sup>†</sup>, Dalia Gritenaite<sup>†</sup>, and Boris Pfander\*

Max-Planck Institute of Biochemistry; DNA Replication and Genome Integrity; Martinsried, Germany

<sup>†</sup>These authors equally contributed to this work.

**R**eplication fork stalling at DNA lesions is a common problem during the process of DNA replication. One way to allow the bypass of these lesions is via specific recombination-based mechanisms that involve switching of the replication template to the sister chromatid. Inherent to these mechanisms is the formation of DNA joint molecules (JMs) between sister chromatids. Such JMs need to be disentangled before chromatid separation in mitosis and the activity of JM resolution enzymes, which is under stringent cell cycle control, is therefore up-regulated in mitosis. An additional layer of control is facilitated by scaffold proteins. In budding yeast, specifically during mitosis, Slx4 and Dpb11 form a cell cycle kinase-dependent complex with the Mus81-Mms4 structure-selective endonuclease, which allows efficient JM resolution by Mus81. Furthermore, Slx4 and Dpb11 interact even prior to joining Mus81 and respond to replication fork stalling in S-phase. This S-phase complex is involved in the regulation of the DNA damage checkpoint as well as in early steps of template switch recombination. Similar interactions and regulatory principles are found in human cells suggesting that Slx4 and Dpb11 may have an evolutionary conserved role organizing the cellular response to replication fork stalling.

critically dependent on the integrity of the DNA template, which is, however, constantly compromised by DNA lesions arising from intrinsic and extrinsic sources. It has been estimated that a human cell acquires between 15,000 and 100,000 DNA lesions per day.<sup>1,2</sup> A large fraction of DNA lesions are modifications of individual bases, which affect only one DNA strand. To detect these lesions in the vast genomic landscape is challenging for cellular DNA repair pathways. Hence, the number of such base damages is estimated to be high at steady-state. Importantly, these base damages may present obstacles for replicative polymerases during DNA replication and eukaryotic cells are frequently confronted with polymerase stalling. This block needs to be overcome in order to complete replication and to avoid replication fork collapse, which causes chromosome breaks and genome instability.<sup>3</sup>

In order to bypass polymerase-stalling DNA lesions, two fundamentally different mechanisms can be utilized: translesion synthesis (TLS) and template switching (TS). In TLS, the stalled replicative polymerase is exchanged by one of several specialized translesion polymerases. These polymerases are characterized by a higher tolerance for structurally distorted DNA in their active site. This attribute allows translesion polymerases to read and synthesize across certain DNA lesions, but because of their reduced fidelity this pathway is also potentially mutagenic (see<sup>4</sup> for a recent summary about TLS). Alternatively, cells can avoid the damaged DNA template, but utilize the already replicated sister chromatid as a template instead. Several recombination-based mechanisms

**Keywords:** cell cycle, DNA damage response, homologous recombination, joint molecule resolution, post-replicative repair

\*Correspondence to: Boris Pfander; E-mail: bpfander@biochem.mpg.de

Submitted: 10/07/2014

Accepted: 11/14/2014

<http://dx.doi.org/10.4161/15384101.2014.989126>

## Template Switch Recombination – from Initiation to Disentanglement of DNA Joint Molecules

Accurate inheritance of the genetic information is a fundamental requirement of life. DNA replication accuracy is

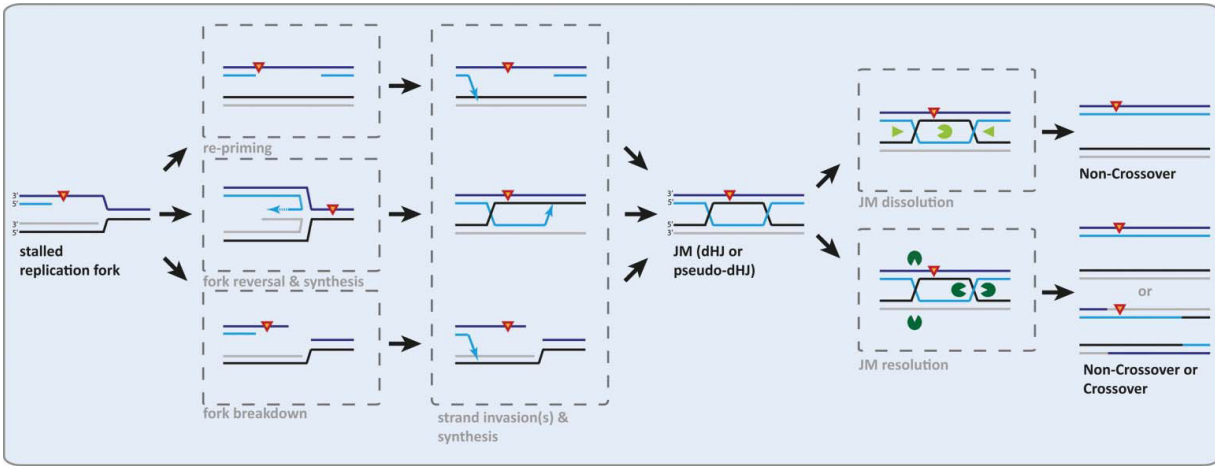


**Figure 1.** Overview of recombination-based pathways to replication fork stalling. Parental DNA strands are shown in black and dark blue; newly synthesized DNA strands are shown in gray and light blue. In order to facilitate the bypass of a fork stalling DNA lesion (red triangle) template switch recombination can be initialized by different mechanisms. First, after replication fork stalling is circumvented by a re-priming event downstream of the DNA lesion, the gapped DNA may engage in a strand invasion (arrow) with the fully replicated sister chromatid behind the replication fork (post-replicative). Second, fork reversal and synthesis across the lesion (dotted arrow) may lead to the formation of JMs. Third, stalled replication fork structures may be cleaved leading to a one-ended DSBs, which may initialize strand invasion. Bypass synthesis and a second strand invasion leads to the formation of a JM, most likely in the shape of a double Holliday-Junction or pseudo Holliday-Junction (containing single-stranded DNA). These JMs can be disentangled by dissolution mechanisms yielding Non-Crossover products or by resolution mechanisms yielding a mixture of Non-Crossover and Crossover products. Alternative bypass mechanisms such as recombination-dependent restart of reversed forks/stalled replication forks leading to single Holliday junctions and requiring processing specifically by resolution enzymes are not shown.

have been suggested to mediate TS (Fig. 1). These include: (A) repriming and strand invasion by a gapped DNA substrate behind the replication fork, (B) controlled fork reversal and (C) fork breakdown and recombination-dependent restart. Whether all 3 mechanisms universally operate in eukaryotic cells and what the molecular determinants are is a matter of active research (see Refs.<sup>5,6</sup> for recent summaries about TS).

Common to all TS mechanisms is the formation of covalent linkages between sister chromatids termed joint molecules (JMs, Fig. 1). Importantly, JMs need to be disentangled before sister chromatid separation in mitosis in order to avoid chromosome breakage. Two mechanistically distinct pathways—termed dissolution and resolution—allow JM processing (Fig. 1, Refs.<sup>7-9</sup>).

Dissolution is mediated by the yeast Sgs1-Top3-Rmi1 complex (STR complex; BLM-TopoIII $\alpha$ -RMI1-RMI2 (BTR complex) in vertebrates). Here, JMs (most likely having the form of double-Holliday junctions or pseudo double-Holliday junctions) are first converted to hemicatenanes by the action of the Sgs1/BLM helicase and the Top3 topoisomerase.<sup>10-12</sup>

The hemicatenanes are subsequently dissociated by the action of the Top3 topoisomerase and possibly other type IA topoisomerases.<sup>10,11,13</sup>

Resolution occurs through the action of structure-selective endonucleases. So far Slx4-Slx1, Mus81-Mms4 and Yen1 in budding yeast (SLX4-SLX1, MUS81-EME1, GEN1 in vertebrates) have been implicated in this process.<sup>8,9,14</sup> These nucleases belong to different families and are thought to resolve Holliday junctions by different mechanisms. The XPG family nuclease Yen1 cleaves HJs by introducing two symmetrical cuts.<sup>15</sup> In contrast, the XPF family nuclease Mus81 has a broad substrate specificity and cleaves HJs relatively poorly.<sup>16,17</sup> Specifically in mammalian cells, it has been shown that MUS81-EME1 and SLX1-SLX4 functionally cooperate in HJ resolution.<sup>17-19</sup> The four proteins can form a complex (SLX-MUS), which displays enhanced activity, enabling HJ resolution via a nick and counter-nick mechanism.<sup>17</sup> Until recently however, it remained questionable whether a complex similar to SLX-MUS existed outside of the vertebrate system.<sup>20,21</sup> It is furthermore still unclear, whether Slx1 has a general, evolutionary conserved role in

processing JMs arising from stalled replication.

The last years have brought significant progress in our understanding of the regulation of dissolution and resolution mechanisms. In budding yeast, JM resolution by both Mus81 and Yen1 is tightly regulated by the cell cycle and restricted up until mitosis,<sup>22-26</sup> while JM dissolution by the STR complex is cell cycle-independent (Fig. 2). Mus81-Mms4 is targeted by the cell cycle kinases Cdk1 and Cdc5 (Polo-like kinase) and these phosphorylation events strongly up-regulate the catalytic activity upon entry into mitosis (Fig. 2,<sup>24,25</sup>). Yen1 activation occurs even later in the cell cycle as it is inhibited by Cdk1 phosphorylation, and only becomes active once these phosphorylation marks are removed by the Cdc14 phosphatase in anaphase (Fig. 2,<sup>22</sup>). One reason for restriction of the resolution enzymes to mitosis may be that these nucleases need to be restrained from acting on stalled replication forks or other S-phase intermediates in order to avoid interference with the template switch reaction.<sup>27</sup> Additionally, this cell cycle regulation creates a hierarchy in the dissolution-resolution system, enabling the STR complex to dissolve JMs

before the resolution enzymes are activated. This hierarchy favors dissolution, which exclusively generates Non-Crossover products, and disfavors resolution, which results in a mixture of Crossover and Non-Crossover products. Therefore, this hierarchy may be a mechanism to protect mitotically dividing diploid cells from loss-of-heterozygosity.

Recently, we described an additional layer of control in the response to stalled replication forks and in JM resolution.<sup>28</sup> This regulation depends on the formation of a protein complex containing several scaffold proteins (Slx4, Dpb11 and Rtt107), which is exquisitely regulated by cell cycle- and DNA damage-dependent kinases. This complex can first be observed in S-phase cells and an *slx4* mutation, which impairs the formation of this complex, causes defects in the response to replication fork stalling drugs, persistent DNA lesions/repair intermediates and a misregulated DNA damage checkpoint. Importantly, later in the cell cycle, in mitosis, Mus81-Mms4 joins the Slx4-Dpb11 complex thereby promoting its ability to resolve JMs.

### The Slx4 and Dpb11 Scaffold Proteins Organize the Response to Replication Fork Stalling

Scaffold proteins, even though devoid of catalytic activity, have important regulatory functions in almost every cellular process. Prominent examples are Rad9 (53BP1), a mediator of the DNA damage checkpoint, and the sliding clamp PCNA, which serves as a docking site for many proteins at replication forks.<sup>29,30</sup> In both cases, protein-protein interactions are dependent on post-translational modifications enabling a fine-tuned regulation.

The Slx4 scaffold protein has important functions in response to replication fork stalling, but also in the repair of DSBs and inter-strand crosslinks, as well

as in the regulation of the DNA damage checkpoint.<sup>31-35</sup> Accordingly, studies in mammalian cells and yeasts have identified several Slx4 binding partners and phosphorylation of Slx4 was found to be crucial for the differential regulation of the different Slx4 functions.<sup>33,35-37</sup> However, many important questions regarding Slx4 remain unanswered. Are there distinct Slx4 complexes? How do these complexes influence each other? How similar are Slx4 functions between different organisms?

Our recent work provides new insights into the formation and the function of one Slx4-containing complex in budding yeast. This complex consists of at least three scaffold proteins—Slx4, Dpb11 and Rtt107 (Fig. 3A, Refs.<sup>28,37</sup>). In agreement with previous work<sup>37</sup> we noticed that the formation of this complex is stimulated by replication fork stalling. The formation of the Slx4-Dpb11 complex is heavily regulated by post-translational modifications and the scaffold complex integrates at least two cellular signals: the cell cycle phase through Cdk1-dependent phosphorylation of Slx4 serine 486 and the presence of DNA lesions or repair intermediates in a DNA damage checkpoint-dependent manner.<sup>28,34,37</sup>

Importantly, we additionally observed that the structure-selective endonuclease Mus81-Mms4 interacts with the Slx4-

Dpb11 complex (Fig. 3A). While the other core subunits (Slx4, Dpb11, Rtt107, Slx1) interact during S, G2 and M-phases of the cell cycle (ref.<sup>28</sup> and LNP and BP, unpublished), Mus81-Mms4 joins the complex specifically in M-phase.<sup>28</sup> The association with Mus81-Mms4 is restricted to mitosis, because it is dependent on the mitotic kinase Cdc5 (Polo-like kinase). These findings immediately suggest that the composition of the Slx4-Dpb11 complex changes throughout the cell cycle and that at least two different types of complexes exist—one specific for mitosis, one found already in S/G2-phases (Fig. 3B and see below). Given the dynamic nature of the two Slx4-Dpb11 containing complexes, we cannot assess currently, whether in mitosis the S-phase complex is completely converted into the Mus81-containing M-phase complex or whether both complexes may coexist in mitotic cells.

To investigate the function of these complexes we have used a phosphorylation-site mutant in Slx4 (*slx4-S486A*), which shows reduced binding to Dpb11, both in the context of the S-phase Slx4-Dpb11 complex as well as in the context of the M-phase Slx4-Dpb11-Mms4-Mus81 complex.<sup>28,34</sup> Importantly, this mutant is specifically defective in binding to Dpb11 and does not influence binding to other proteins (for example Slx1 or

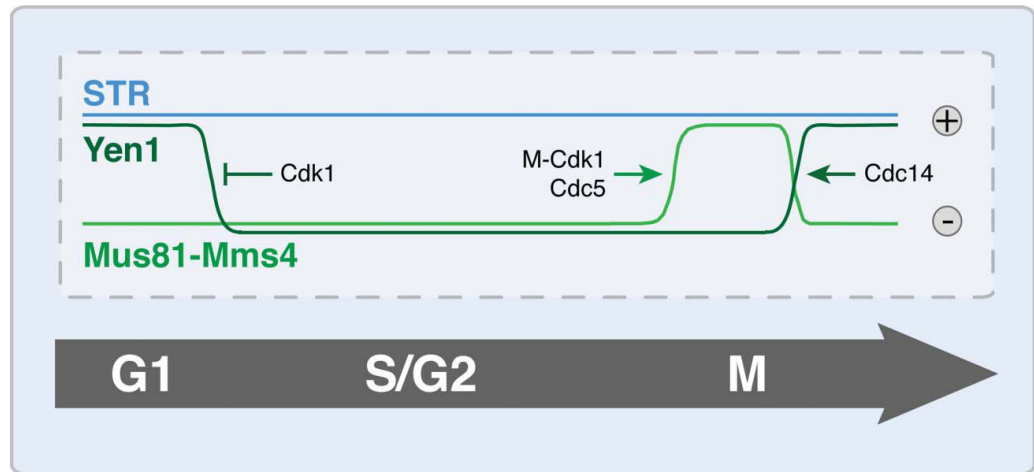


**Figure 2.** Activity profiles of JM processing protein complexes in *S. cerevisiae* throughout the cell cycle. While the Sgs1-Top3-Rmi1 complex (STR) is active at all cell cycle stages, the resolution activities of Mus81-Mms4 and Yen1 are cell cycle-regulated. Mus81-Mms4 is stimulated at the G2/M transition by M-Cdk1 and Cdc5-dependent phosphorylation. Concurrently, Cdk1 targets Yen1 by phosphorylation to inhibit its action. Upon metaphase to anaphase transition, Yen1 dephosphorylation by Cdc14 relieves this inhibition.

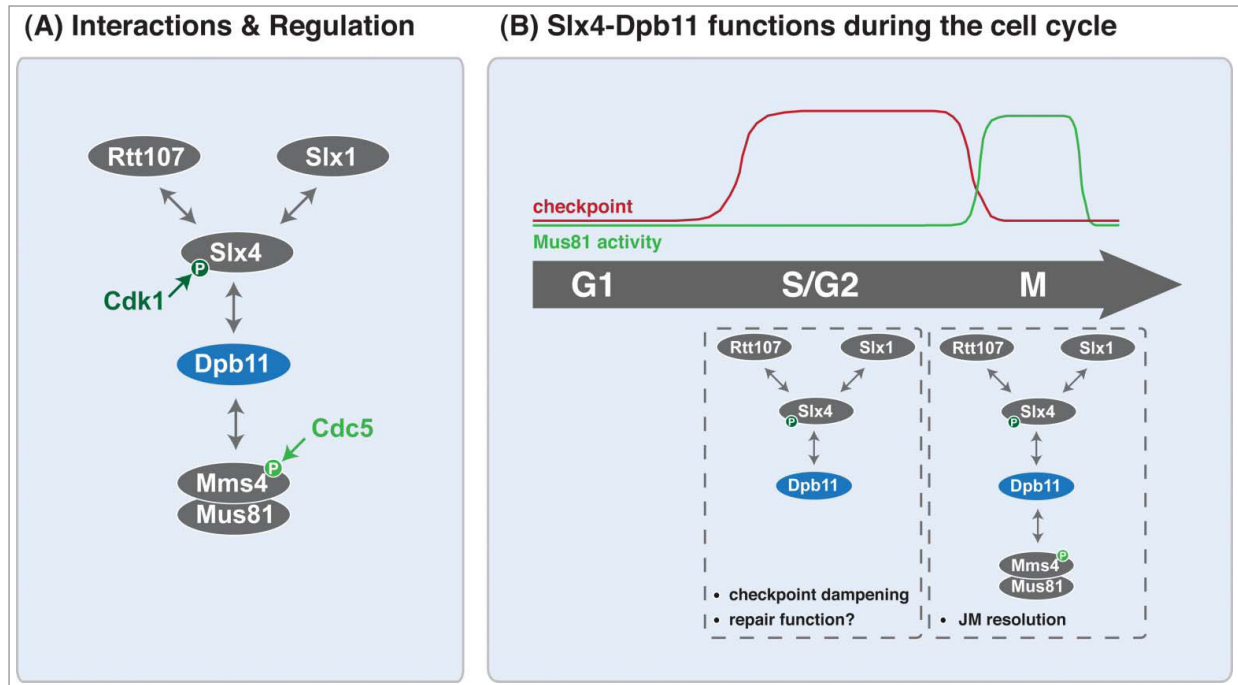


**Figure 3.** Schematic model of the S-phase- and M-phase-specific Slx4-Dpb11 complexes and their regulation throughout the cell cycle (adapted from<sup>28</sup>). **(A)** Interactions and regulations. Upon Cdk1 phosphorylation of Slx4, interaction with Dpb11 is established. Slx4 also binds to Rtt107 and Slx1. Phosphorylation of Mms4 by Cdc5 facilitates binding of Mus81-Mms4 to Dpb11. **(B)** The Slx4-Dpb11 complex functions during the cell cycle. Different proteins are found in the Slx4-Dpb11 complex at different cell cycle stages suggesting distinct cell cycle phase-specific functions. The S-phase-specific complex consisting of Slx4, Dpb11, Slx1 and Rtt107 has a role in dampening the DNA damage checkpoint, but possibly also a role in repairing stalled replication forks. The M-phase-specific complex consisting of Slx4, Dpb11, Slx1, Rtt107, Mus81 and Mms4 promotes the resolution of DNA joint molecules.

Rtt107). The *slx4-S486A* mutant phenotypes are also highly specific: mutant cells are specifically hypersensitive to the DNA alkylating agent MMS and the cellular response to MMS-induced replication fork stalling appears to be particularly affected.<sup>28</sup> The observed phenotypes can be subdivided into two categories. The first defects manifest already in S-phase: upon MMS treatment this mutant accumulates Replication Protein A (RPA) nuclear foci compared to WT cells. These foci also dissolve more slowly compared to RPA foci of WT cells, suggesting that single-stranded DNA containing structures, potentially stalled replication forks or their repair intermediates, persist in *slx4-S486A* cells. Accordingly, S-phase progression is slower in MMS-treated *slx4-S486A* than in WT cells and the reappearance of fully replicated chromosomes is delayed, as is the switching off of the DNA damage checkpoint. Currently, the only proposed function of the S-phase Slx4-Dpb11 complex is to regulate the DNA

damage checkpoint<sup>34</sup> (and see below), but an additional repair function is possible as well.

The second class of defects can be attributed to inefficient JM resolution by the structure-selective endonuclease Mus81-Mms4 and these are therefore likely to arise from defects in the M-phase-specific Slx4-Dpb11-Mms4-Mus81 complex.<sup>28</sup> These phenotypes become apparent in the JM dissolution-defective *sgs1Δ* mutant, where cells are exclusively dependent on JM resolution mechanisms in order to cope with MMS-induced replication fork stalling. Indeed, mutation of *slx4-S486A* causes a delay to the disappearance of JM structures in the *sgs1Δ* background as judged by 2D gel electrophoresis. Such persistent JMs are expected to interfere with sister chromatid separation in mitosis. Consistently, an increase in the occurrence of chromosome bridges<sup>38</sup> is apparent in mitotic *sgs1Δ slx4-S486A* cells. Moreover, the *slx4-S486A* mutant shows reduced rates of Crossover

formation in an ectopic (direct repeat) recombination assay. This finding supports the idea that the Slx4-Dpb11 complex is specifically important for JM resolution mechanisms and that *slx4-S486A* mutant cells rely strongly on JM dissolution by the STR complex. Notably, the JM resolution defect can be pinpointed to a defect in Mus81 function, since the *slx4-S486A* mutant and *mus81Δ* or *mms4Δ* show epistasis with regard to MMS hypersensitivity and turnover of JM structures. Collectively, these findings therefore suggest that the Slx4-Dpb11 complex is a regulator of Mus81-Mms4-dependent JM resolution.<sup>28</sup>

### Cell Cycle Regulation of Slx4-Dpb11 Complex Formation and JM Resolution

Dpb11, and its human homolog TopBP1, specifically recognize phosphorylated proteins.<sup>39</sup> The phosphorylation

marks that are “read” by Dpb11 have been shown in several cases to depend on cell cycle kinases, in particular Cdk1. Also in the case of Slx4, phosphorylation of the critical serine 486 (a putative Cdk1 target site) is cell cycle-regulated and dependent on Cdk1 (Fig. 3A,<sup>28</sup>). In contrast, binding of Mms4 to Dpb11 (in context of the Slx4-Dpb11 complex) additionally requires phosphorylation by the mitotic kinase Cdc5, thereby restricting the formation of the Slx4-Dpb11-Mms4-Mus81 complex to mitosis (Fig. 3A).

Interestingly, Slx4-Dpb11-Mms4-Mus81 complex formation thereby underlies the same temporal regulation as the catalytic activity of Mus81<sup>23-26,28</sup>). This finding thus substantiates current models of the temporal regulation of JM resolution/dissolution (Fig. 2) providing further support for mitotic restriction of JM resolution pathways. Formation of the Slx4-Dpb11-Mms4-Mus81 complex is not responsible for the previously demonstrated enhanced catalytic activity of mitotic Mus81 in *in vitro* resolution assays.<sup>28</sup> The current data therefore suggests that at least two mechanisms exist, by which cell cycle kinases control Mus81 action upon entry into mitosis: direct up-regulation of the catalytic activity and stimulation of complex formation with Slx4 and Dpb11.

It remains an open question by which mechanism the Slx4-Dpb11-Mms4-Mus81 complex enhances JM resolution by Mus81. The finding that Mus81-Mms4 is physically coupled to the Slx4-Dpb11 complex opens up the possibility that Slx4 and Dpb11 are involved in targeting to damaged chromosomes. Interestingly, the formation of the S-phase Slx4-Dpb11 complex directly responds to replication stalling. Together, these findings may suggest a speculative model, whereby the Slx4-Dpb11 complex is first recruited to sites of replication fork stalling and may subsequently escort these sites through different steps of repair. The Slx4-Dpb11 complex may thus act as a platform at sites of replication fork stalling, potentially by targeting specific repair enzymes, such as Mus81, which would catalyze the final step in the reaction.

## Evolutionary Conserved Features of JM Resolution and its Regulation by Multiprotein Complexes

Mammalian cells have a temporal program of JM dissolution/resolution that is highly similar to the one found in budding yeast. JM resolution is commonly investigated in cells from Bloom’s syndrome patients that are deficient in BLM-TopoIII $\alpha$ -RMI1-RMI2 (BTR)-mediated JM dissolution and therefore show an increased number of crossover events/sister chromatid exchanges (SCEs,<sup>40</sup>). Mammalian JM resolution can be executed by one of three structure-selective endonucleases: MUS81-EME1, GEN1 or SLX1-SLX4. Interestingly, depletion of SLX4, SLX1 or MUS81 in cells lacking BTR exhibits a comparable reduction of SCEs as the combination of MUS81 with SLX4 or SLX1, whereas additional depletion of GEN1 leads to a more severe phenotype.<sup>17,18</sup> These data suggest a cooperative activity of the SLX1-SLX4 and MUS81-EME1 nucleases and intriguingly, the two nucleases also physically interact with each other (SLX-MUS complex,<sup>17</sup>). The resolution of a Holliday Junction requires two cuts in order to disentangle the DNA strands and it has been suggested that SLX1 and MUS81 may cooperate as two nicking endonucleases.<sup>17</sup>

Despite conservation of the MUS81-binding SAP domain in eukaryotic Slx4 proteins,<sup>32</sup> so far, a direct association of budding yeast Slx4 and Mus81 has not been described.<sup>21</sup> However, both proteins are part of the Slx4-Dpb11-Mms4-Mus81 complex. Moreover, the formation of the two complexes from yeast and human is subject to a similar regulation: also the interaction between SLX1-SLX4 and MUS81-EME1 nucleases is only established at the G2/M transition involving phosphorylation by CDK1 and, to a lesser extent, PLK1.<sup>17</sup>

It is currently unclear whether the yeast Slx4-Dpb11-Mms4-Mus81 complex acts by bringing together the Mus81 and Slx1 nucleases. In fact it remains to be determined if Slx1 has an active role in this complex. A physical interaction of Slx1 with the Slx4-Dpb11 complex was

detected after MMS treatment as well as in mitosis<sup>28</sup> (L.N.P. and B.P., unpublished data), but no defects were observed in response to MMS treatment of *slx1 $\Delta$*  deletion mutants.<sup>28,36</sup> This suggests that either Slx1 does not play any role in JM resolution after MMS-induced replication fork stalling, or that a redundant factor may take over in the absence of Slx1.

Interestingly, also the mammalian homolog of Dpb11, TopBP1, interacts with SLX4 in a CDK phosphorylation-dependent manner.<sup>28</sup> Whether TopBP1 also binds to MUS81-EME1, and whether SLX4-TopBP1 has a role in JM resolution in mammals needs further investigation. Intuitively, Dpb11’s bridging function in yeast seems to be unnecessary in the context of the mammalian SLX-MUS complex as MUS81 directly binds to SLX4. Nevertheless, TopBP1 could be important for stabilization of the complex or for the recruitment of additional factors. On the other hand, following the observation of two cell cycle-regulated Slx4-Dpb11 complexes in yeast (S-phase- and M-phase-specific), it appears possible that TopBP1 could be involved in a function of SLX4, which is independent of MUS81, presumably in S-phase, while it may be dispensable for the mitotic function in JM resolution carried out by SLX-MUS. In other words, mammalian SLX4-TopBP1 may represent the S-phase-specific SLX4 complex, while SLX-MUS may represent the M-phase-specific SLX4 complex.

## The Slx4-Dpb11 Complex and the DNA Damage Checkpoint Counteract Each Other

At least in budding yeast the Slx4-Dpb11 complex forms already in response to replication fork stalling in S-phase. One function of this S-phase complex is connected to the DNA damage checkpoint.<sup>34</sup> The central finding of the study by Ohouo et al. is that the Slx4-Dpb11 complex regulates DNA damage checkpoint signaling. Interestingly, they found that after MMS damage the DNA damage checkpoint is hyperactivated in the *slx4 $\Delta$*  deletion mutant. This hyperactivation can be suppressed by mutations in the

checkpoint proteins Rad9 or Rad53. Importantly, also cellular viability of *slx4*Δ deletion mutants after MMS treatment can be improved by partially inhibiting checkpoint signaling suggesting that Slx4 acts as dampener of the DNA damage checkpoint.<sup>34</sup>

Mechanistically, checkpoint dampening may likely involve the competition between checkpoint proteins and Slx4 for Dpb11 binding. Dpb11 itself is an agonist of checkpoint signaling as it binds several checkpoint proteins, such as Rad9, the Ddc1 subunit of the 9–1–1 complex and Mec1-Ddc2.<sup>41</sup> Here, Dpb11 functions as an activator of Mec1 and as adaptor that brings together the different checkpoint factors. Given that Dpb11 expression levels are low, it is therefore possible that by competing with checkpoint proteins Slx4 may be limiting the amounts of how much Dpb11 checkpoint complex can form. Indeed, it was shown that more Rad9 binds to Dpb11 in the absence of Slx4, suggesting that Slx4 might be a competitive inhibitor of Rad9.<sup>34</sup>

On the other hand, persistent DNA lesions/repair intermediates can be observed in MMS-treated cells deficient in Slx4-Dpb11 complex formation (see above,<sup>28</sup>). These DNA structures could be visualized as persistent RPA foci, which are expected to trigger an enhanced checkpoint activation. Indeed, checkpoint hyperactivation has been shown for other mutants with defects in the response to replication fork stalling.<sup>42,43</sup> Thus, an underlying repair defect could be in part responsible for the checkpoint hyperactivation of *slx4* mutant cells.

Is checkpoint dampening the sole function of the Slx4-Dpb11 complex in the response to replication fork stalling? Currently, we favor the idea that the Slx4-Dpb11 complex has an additional repair function in response to replication fork stalling. First, the *slx4-S486A* mutant is specifically sensitive to MMS but not to other kinds of DNA damaging agents, while the checkpoint responds universally to different kinds of DNA damage.<sup>28,34</sup> Second, this sensitivity is rescued by expression of an artificial covalent fusion of Dpb11 and Slx4.<sup>28</sup> In these experiments the Dpb11-Slx4 fusion is expressed as a second copy of Dpb11. Due to the

high levels of Dpb11 this mutant should be deficient in checkpoint dampening, but the hypersensitivity to MMS is rescued nonetheless. Until today, however, no repair enzyme was found to interact with the S-phase Slx4-Dpb11 complex and it therefore remains to be determined what this additional repair function of the Slx4-Dpb11 complex may be.

Interestingly, not only does the S-phase Slx4-Dpb11 complex counteract the DNA damage checkpoint, but the DNA damage checkpoint also counteracts the M-phase Slx4-Dpb11 complex. After its activation by MMS damage the checkpoint appears to delay Mms4 phosphorylation by Cdc5 and thereby Mus81-Mms4 activation thereby creating a second layer of temporal regulation that is in addition to the cell cycle control<sup>26,28</sup> (Fig. 3B).

Do the early functions of the Slx4-Dpb11 complex in S-phase therefore have an influence on the later stages of the cell cycle? Strikingly, in addition to directly promoting Mus81 function in JM resolution, the Slx4-Dpb11 complex may promote Mus81 activity indirectly by checkpoint regulation. Notably, the partial inactivation of the checkpoint by the *ddc1-T602A* mutant promotes earlier Mms4 phosphorylation by Cdc5 in cells that have an impaired Dpb11-Slx4 interaction.<sup>28</sup> Moreover, also the rescue of *slx4* mutant sensitivity by partial checkpoint inactivation strictly depends on Mus81-Mms4. This suggests that the checkpoint dampening function in S-phase may be connected to the later JM resolution function of the Slx4-Dpb11 complex in M-phase.

## Conclusion

The response to replication fork stalling is strictly regulated during the cell cycle. A means of integrating these cell cycle signals appears to be the formation of multiprotein complexes containing scaffold proteins. At least two Slx4-Dpb11 complexes act during the response to stalled replication forks: an S-phase complex, which regulates the DNA damage checkpoint and possibly has a DNA repair function as well, and an M-phase

complex, which additionally contains Mus81-Mms4 and promotes JM resolution. Future research will need to identify additional repair factors in the S-phase complex and to investigate the crosstalk between the two complexes in order to shed light on the rather enigmatic cellular response to replication fork stalling.

## Acknowledgments

We are grateful to Dana Branzei, Stefan Jentsch, Michael Lisby, Joao Matos and members of the Pfander and Jentsch labs for helpful discussion and critical reading of the manuscript.

## Funding

Work in the Pfander lab is supported by the Max-Planck Society and the German Research Council (DFG). The authors declare that they have no competing financial interest.

## References

1. Hoeijmakers JHJ. DNA damage, aging, and cancer. *N Engl J Med* 2009; 361:1475-85; PMID:19812404; <http://dx.doi.org/10.1056/NEJMra0804615>
2. Lindahl T, Barnes DE. Repair of endogenous DNA damage. *Cold Spring Harb Symp Quant Biol* 2000; 65:127-33; PMID:12760027; <http://dx.doi.org/10.1101/sqb.2000.65.127>
3. Branzei D, Foiani M. Maintaining genome stability at the replication fork. *Nat Rev Mol Cell Biol* 2010; 11:208-19; PMID:20177396; <http://dx.doi.org/10.1038/nrm2852>
4. Sale JE. Translesion DNA synthesis and mutagenesis in eukaryotes. *Cold Spring Harbor Perspectives in Biology* 2013; 5:a012708; PMID:23457261; <http://dx.doi.org/10.1101/cshperspect.a012708>
5. Branzei D. Ubiquitin family modifications and template switching. *FEBS Letters* 2011; 585:2810-2817; PMID:21539841; <http://dx.doi.org/10.1016/j.febslet.2011.04.053>
6. Ulrich HD. Timing and spacing of ubiquitin-dependent DNA damage bypass. *FEBS Letters* 2011; 585:2861-7; PMID:21605556; <http://dx.doi.org/10.1016/j.febslet.2011.05.028>
7. Mankouri HW, Huttner D, Hickson ID. How unfinished business from S-phase affects mitosis and beyond. *Embo J* 2013; 32:2661-71; PMID:24065128; <http://dx.doi.org/10.1038/emboj.2013.211>
8. Matos J, West SC. Holliday junction resolution: regulation in space and time. *DNA Repair (Amst.)* 2014; 19:176-81; PMID:24767945; <http://dx.doi.org/10.1016/j.dnarep.2014.03.013>
9. Sarbjana S, West SC. Holliday junction processing enzymes as guardians of genome stability. *Trends in Biochemical Sciences* 2014; 39:409-19; PMID:25131815; <http://dx.doi.org/10.1016/j.tibs.2014.07.003>
10. Cejka P, Plank JL, Bachrati CZ, Hickson ID, Kowalczykowski SC. Rrm1 stimulates decatenation of double Holliday junctions during dissolution by sgs1-top3. *Nat Struct Mol Biol* 2010; 17:1377-82; PMID:20935631; <http://dx.doi.org/10.1038/nsmb.1919>

11. Cejka P, Plank JL, Dombrowski CC, Kowalczykowski SC. Decatenation of DNA by the *S. cerevisiae* sgs1-Top3-rmi1 and RPA complex: a mechanism for disentangling chromosomes. *Mol Cell* 2012; 47:886-96; PMID:22885009; <http://dx.doi.org/10.1016/j.molcel.2012.06.032>
12. Giannattasio M, Zwicky K, Follonier C, Foiani M, Lopes M, Branzei D. Visualization of recombination-mediated damage bypass by template switching. *Nat Struct Mol Biol* 2014; 10:884-92; PMID:25195051; <http://dx.doi.org/10.1038/nsmb.2888>
13. Bizard AH, Hickson ID. The dissolution of double Holliday junctions. *Cold Spring Harb Perspect Biol* 2014; 6:a016477; PMID:24984776; <http://dx.doi.org/10.1101/cshperspect.a016477>
14. Mankouri HW, Ashton TM, Hickson ID. Holliday junction-containing DNA structures persist in cells lacking sgs1 or top3 following exposure to DNA damage. *Proc Natl Acad Sci USA* 2011; 108:4944-9; PMID:21383164; <http://dx.doi.org/10.1073/pnas.1014240108>
15. Ip SCY, Rass U, Blanco MG, Flynn HR, Skehel JM, West SC. Identification of Holliday junction resolvases from humans and yeast. *Nature* 2008; 456:357-61; PMID:19020614; <http://dx.doi.org/10.1038/nature07470>
16. Boddy MN, Gaillard PH, McDonald WH, Shanahan P, Yates JR, Russell P. Mus81-eme1 are essential components of a Holliday junction resolvase. *Cell* 2001; 107:537-48; PMID:11719193; [http://dx.doi.org/10.1016/S0092-8674\(01\)00536-0](http://dx.doi.org/10.1016/S0092-8674(01)00536-0)
17. Wyatt HDM, Sarbajna S, Matos J, West SC. Coordinated actions of SLX1-SLX4 and MUS81-EME1 for Holliday junction resolution in human cells. *Mol Cell* 2013; 52:234-47; PMID:24076221; <http://dx.doi.org/10.1016/j.molcel.2013.08.035>
18. Castor D, Nair N, Déclaux A-C, Lachaud C, Toth R, Macartney TJ, Lilley DMJ, Arthur JSC, Rouse J. Cooperative control of Holliday junction resolution and DNA repair by the SLX1 and MUS81-EME1 nucleases. *Mol Cell* 2013; 52(2), 221-33; PMID:24076219; <http://dx.doi.org/10.1016/j.molcel.2013.08.036>
19. Sarbajna S, Davies D, West SC. Roles of SLX1-SLX4, MUS81-EME1, and GEN1 in avoiding genome instability and mitotic catastrophe. *Genes Dev* 2014; 28:1124-36; PMID:24831703; <http://dx.doi.org/10.1101/gad.238303.114>
20. Mukherjee S, Wright WD, Ehmsen KT, Heyer WD. The mus81-mms4 structure-selective endonuclease requires nicked DNA junctions to undergo conformational changes and bend its DNA substrates for cleavage. *Nucleic Acids Res* 2014; 42:6511-22; PMID:24744239; <http://dx.doi.org/10.1093/nar/gku265>
21. Schwartz EK, Wright WD, Ehmsen KT, Evans JE, Stahlberg H, Heyer WD. Mus81-Mms4 functions as a single heterodimer to cleave nicked intermediates in recombinational DNA repair. *Mol Cell Biol* 2012; 32:3065-80; PMID:22645308; <http://dx.doi.org/10.1128/MCB.00547-12>
22. Blanco MG, Matos J, West SC. Dual control of Yen1 nuclease activity and cellular localization by cdk and cdc14 prevents genome instability. *Mol Cell* 2014; 54:94-106; PMID:24631285; <http://dx.doi.org/10.1016/j.molcel.2014.02.011>
23. Gallo-Fernández M, Saugar I, Ortiz-Bazán MÁ, Vázquez MV, Tercero JA. Cell cycle-dependent regulation of the nuclease activity of mus81-eme1/mms4. *Nucleic Acids Res* 2012; 40:8325-35; PMID:22730299; <http://dx.doi.org/10.1093/nar/gks599>
24. Matos J, Blanco MG, West SC. Cell-cycle kinases coordinate the resolution of recombination intermediates with chromosome segregation. *Cell Rep* 2013; 4:76-86; PMID:23810555; <http://dx.doi.org/10.1016/j.celrep.2013.05.039>
25. Matos J, Blanco MG, Maslen S, Skehel JM, West SC. Regulatory control of the resolution of DNA recombination intermediates during meiosis and mitosis. *Cell* 2011; 147:158-72; PMID:21962513; <http://dx.doi.org/10.1016/j.cell.2011.08.032>
26. Szakal B, Branzei D. Premature cdk1/cdc5/mus81 pathway activation induces aberrant replication and deleterious crossover. *Embo J* 2013; 32:1155-67; PMID:23531881; <http://dx.doi.org/10.1038/emboj.2013.67>
27. Saugar I, Vazquez MV, Gallo-Fernandez M, Ortiz-Bazan MA, Segurado M, Calzada A, Tercero JA. Temporal regulation of the mus81-mms4 endonuclease ensures cell survival under conditions of DNA damage. *Nucleic Acids Res* 2013; 41:894358; PMID:23901010; <http://dx.doi.org/10.1093/nar/gkt645>
28. Gritenaite D, Prinz LN, Szakal B, Bantele SCS, Wendeler L, Schilbach S, Habermann BH, Matos J, Lisby M, Branzei D, et al. A cell cycle-regulated slx4-dpb11 complex promotes the resolution of DNA repair intermediates linked to stalled replication. *Genes Dev* 2014; 28:1604-19; PMID:25030699; <http://dx.doi.org/10.1101/gad.240515.114>
29. Finn K, Lowndes NF, Grenon M. Eukaryotic DNA damage checkpoint activation in response to double-strand breaks. *Cell Mol Life Sci* 2011; 69:1447-73; PMID:22083606; <http://dx.doi.org/10.1007/s00018-011-0875-3>
30. Moldovan G-L, Pfander B, Jentsch S. PCNA, the maestro of the replication fork. *Cell* 2007; 129:665-79; PMID:17512402; <http://dx.doi.org/10.1016/j.cell.2007.05.003>
31. Douwel DK, Boonen RACM, Long DT, Szybowska AA., Räschle M, Walter JC, Knipscheer P. XPF-ERCC1 Acts in unhooking DNA interstrand crosslinks in cooperation with FANCD2 and FANCP/SLX4. *Mol Cell* 2014; 54:460-71; PMID:24726325; <http://dx.doi.org/10.1016/j.molcel.2014.03.015>
32. Fekairi S, Scaglione S, Chahwan C, Taylor ER, Tissier A, Coulon S, Dong M-Q, Ruse C, Yates JR, Russell P, et al. Human SLX4 is a Holliday junction resolvase subunit that binds multiple DNA repair/recombination endonucleases. *Cell* 2009; 138:78-89; PMID:19596236; <http://dx.doi.org/10.1016/j.cell.2009.06.029>
33. Kim Y, Spitz GS, Veturi U, Lach FP, Auerbach AD, Smogorzewska A. Regulation of multiple DNA repair pathways by the Fanconi anemia protein SLX4. *Blood* 2013; 121:54-63; PMID:23093618; <http://dx.doi.org/10.1182/blood-2012-07-441212>
34. Ohouo, PY, de Oliveira FMB, Liu Y, Ma CJ, Smolka MB. DNA-repair scaffolds dampen checkpoint signaling by counteracting the adaptor rad9. *Nature* 2012; 493:120-4; PMID:23160493; <http://dx.doi.org/10.1038/nature11658>
35. Svendsen JM, Smogorzewska A, Sowa ME, O'Connell BC, Gygi SP, Elledge SJ, Harper JW. Mammalian BTBD12/SLX4 assembles a Holliday junction resolvase and is required for DNA repair. *Cell* 2009; 138:63-77; PMID:19596235; <http://dx.doi.org/10.1016/j.cell.2009.06.030>
36. Flott S, Alabert C, Toh GW, Toth R, Sugawara N, Campbell DG, Haber JE, Pasero P, Rouse J. Phosphorylation of Slx4 by Mec1 and Tel1 regulates the single-strand annealing mode of DNA repair in budding yeast. *Mol Cell Biol* 2007; 27:6433-45; PMID:17636031; <http://dx.doi.org/10.1128/MCB.00135-07>
37. Ohouo PY, de Oliveira FMB, Almeida BS, Smolka MB. DNA Damage signaling recruits the rtt107-slx4 scaffolds via dpb11 to mediate replication stress response. *Mol Cell* 2010; 39:3006; PMID:20670896; <http://dx.doi.org/10.1016/j.molcel.2010.06.019>
38. Germann SM, Schramke V, Pedersen RT, Gallina I, Eckert-Boulet N, Oestergaard VH, Lisby M. TopBP1/dpb11 binds DNA anaphase bridges to prevent genome instability. *J Cell Biol* 2014; 204:45-59; PMID:24379413; <http://dx.doi.org/10.1083/jcb.201305157>
39. Wardlaw CP, Carr AM, Oliver AW. TopBP1: A BRCT-scaffold protein functioning in multiple cellular pathways. *DNA Repair (Amst.)* 2014; 22:165-174; PMID:25087188; <http://dx.doi.org/10.1016/j.dnarep.2014.06.004>
40. Ray JH, German J. Bloom's syndrome and EM9 cells in BrdU-containing medium exhibit similarly elevated frequencies of sister chromatid exchange but dissimilar amounts of cellular proliferation and chromosome disruption. *Chromosoma* 1984; 90:383-8; PMID:6510115; <http://dx.doi.org/10.1007/BF00294165>
41. Pfander B, Diffley JFX. Dpb11 coordinates Mec1 kinase activation with cell cycle-regulated rad9 recruitment. *Embo J* 2011; 30:4897-907; PMID:21946560; <http://dx.doi.org/10.1038/emboj.2011.345>
42. Chen Y-H, Szakal B, Castellucci F, Branzei D, Zhao X. DNA damage checkpoint and recombinational repair differentially affect the replication stress tolerance of smc6 mutants. *Mol Biol Cell* 2013; 24:2431-41; PMID:23783034; <http://dx.doi.org/10.1091/mbc.E12-11-0836>
43. Karras GI, Jentsch S. The RAD6 DNA damage tolerance pathway operates uncoupled from the replication fork and is functional beyond S phase. *Cell* 2010; 141:255-67; PMID:20403322; <http://dx.doi.org/10.1016/j.cell.2010.02.028>